UNIVERSITY OF CRETE

SCHOOL OF MEDICINE

PhD Thesis

Identification of novel genes implicated in habituation of *D. melanogaster,* using *Minos* transposable element.

Iliana-Georgia Roussou

Biologist, MSc

Heraklion, 2019

ΠΑΝΕΠΙΣΤΗΜΙΟ ΚΡΗΤΗΣ

ΙΑΤΡΙΚΗ ΣΧΟΛΗ

Διδακτορική Διατριβή

Ανίχνευση νέων γονιδίων που σχετίζονται με την εξοικείωση στη *D. melanogaster*, με την βοήθεια του *Minos* μεταθέσιμου γενετικού στοιχείου.

Ηλιάνα-Γεωργία Ρούσσου

Βιολόγος, MSc

Ηράκλειο Κρήτης, 2019

Principal Supervisor: Charalambos Savakis, Emeritus Professor of Medical School of Crete

Co-Supervisors:

Efthimios Skoulakis, Researcher A', B.S.R.C. Alexander Fleming, Athens

Christos Delidakis, Professor of Biology Department of Crete

Seven members committee:

Charalambos Savakis, Emeritus Professor of Molecular Biology and Molecular Medicine, Medical School of Crete

Efthimios Skoulakis, Researcher A', B.S.R.C. Alexander Fleming, Athens

Christos Delidakis, Professor of Genetics and Developmental Biology, Biology Department of Crete

Christos Consoulas, Assistant Professor of Experimental Physiology, Medical School of Athens

Domna Karagogeos, Professor of Molecular Biology and Developmental Neurobiology, Medical School of Crete

Kiriaki Sidiropoulou, Assistant Professor of neurophysiology and Behavior, Biology Department of Crete

Nektarios Tavernarakis, Professor of Molecular Systems Biology, Medical School of Crete

Acknowledgements

This thesis is based on research held in the Institute of Fundamental Biomedical Research (I.F.B.R) of B.S.R.C. Alexander Fleming, Greece, during the years 2012-2019. Firstly, I would like to express my sincere gratitude to my advisor, Professor Charalambos Savakis for the valuable support during my Ph.D studies. He was always shielding me as a student, holding the difficult part of finding financial resources and grants for the continuation of my thesis. This study would have never been accomplished though, if the other member of the team, Researcher A' Efthimios Skoulakis had not always been the main contributor to my everyday research. I must express my profound appreciation to him, not only for his motivation, ideas, immense knowledge and patience but for his belief and trust in me. His guidance helped me during all the time of my research and of the writing of this thesis. This explorative journey would have been completely different without the good and the intense times we encountered in Skoulakis lab.

Next, I would like to thank Professor Christos Delidakis, for being a part of the three-member committee and for his very constructive remarks during this study. Moreover, I would like to thank Professor Nektarios Tavernarakis, Professor Domna Karagogeos and Dr. Georgia Tsikala for the collaboration, as well as Christos Consoulas and Kiriaki Sidiropoulou for being part of the seven-member committee.

Words cannot describe how grateful I am, to Researcher Katerina Papanikolopoulou. I had the chance of being close to her since the first day of my Ph.D., while collaborating with her was beyond comparison. She was always encouraging me to proceed and advising me on how to find the way out of the obstacles. She taught me, not only things related to research but plentiful other features concerning how to carry out difficulties. Her morals and integrity serve as a great example to follow. Her support was fundamental for accomplishing my thesis while her friendship is a blessing to me.

Also, I would like to express my deepest gratitude to Dr. Jean Y. Gouzi, who showed me how beautiful Behavioral Neurobiology is, through endless scientific conversations and by his great deal of patience. He managed to fill in every scientific gap I was encountering as a beginner, through his treasure trove of knowledge and his boundless love for science. He taught me that every bad situation has a positive perspective that shouldn't be forgotten and he was always there to listen and to give advice. Our collaboration hence flourished and his help proved to be immense. His friendship is a precious gift to me, in and out of the lab.

In addition, I would like to thank Dr. Thanos Metaxakis for giving me the opportunity to work with him and having a wonderful collaboration while studying starvation.

Special thanks to our collaborator Luca Turin, for such inspiring and motivating conversations as well as for his incredible knowledge and ingenious sense of humor.

Furthermore, I would like to acknowledge the members of the Skoulakis lab, for sharing the same everyday challenges and worries. Eirini Georganta, for her serenity and composure even during the tough days, Rania Semelidou for sharing part of the habituation project, Ergina Vourkou for being always willing to help no matter how occupied she was, as well as the undergraduate students Vasia Alexandri, Anna Papadopoulou, Aggeliki Kontopoulou and Rania Christodoulou, who performed their bachelor thesis under my supervision and who gave me the opportunity to teach and being reciprocally taught by them. Especially, I am very thankful to my very talented girl, Rania Christodoulou for all her help, support and friendship. I would also like to thank Maria Loizou, for making my life easier by providing me with fresh-made fly food whenever I solicited her. Besides them, I would like to thank the past and current members of the lab, Maria Anezaki, Klio Maniati, Efi Drimili, Alexandros Gaitanidis, Anna Bourouliti and Kiriaki Foka for the joyful moments we shared in the fly room.

Finally, I feel the pressing need to thank here all my own people. First, I would like to express my very profound gratitude to my parents Giorgos and Panagiota, for providing me with unceasing support and everlasting encouragement throughout all the years of my studies. This accomplishment would not have been possible without them, who are constantly supporting me in all my pursuits, by any means and with great self-denial. They are the ultimate role models for me. Then, I would like to thank my sisters, Katerina and Eleni for being there whenever I needed them. Most importantly, I would like to thank my husband Vasilis, for being patient, loving and supportive throughout all the stages of my Ph.D, especially the hardest ones. Last but not least, I would like to thank my son, Dimitris, for showing me the true meaning of life and motivating me to finish my thesis.

Thank you.

Iliana G. Roussou

To my mother,

who has been always encouraging me

to set and reach even higher goals.

Στην μητέρα μου,

που πάντα με παροτρύνει να θέτω

αλλά και να πετυχαίνω ολοένα υψηλότερους στόχους.

Table of Contents

Tables and figures

Fig.4. dBtk is acutely required within α'/β' MB neurons to inhibit premature habituation to footshock.
Fig.5. Differential roles for dBtk in latency and habituation in α/β and α'/β' MB neurons.
Fig.6. Antipsychotics selectively rescue the defective habituation of btk mutants.

4. Drosophila Tau negatively regulates translation and olfactory Long-Term Memory, but facilitates footshock habituation and cytoskeletal homeostasis.
Fig.1. dTau loss precipitates changes in microtubule cytoskeleton.
Table 1. Selected proteins, p values, and average log2 fold differences from three biological and two technical replicas.
Fig.2. dTau loss affects the actin cytoskeleton.
Fig.3. dTau abrogation affects long term memory.
Fig.4. dTau is not required for forgetting of olfactory memories, and its abrogation increases protein synthesis levels.
Table 2. Upregulation of proteins that function in translation upon dTau loss.
Table 3. Differentially regulated proteins upon dTau deletion that affect memory formation.
Table 4. Differentially regulated proteins involved in cytoskeleton organization and translation upon acute pan-neuronal dTau downregulation.
Table 5. Differentially regulated proteins upon acute dTau loss that affect memory.
Fig.5. dTau abrogation impairs habituation.
Fig.6. dTau elevation within the adult MBs leads to premature habituation and LTM deficits with a concomitant decrease in protein synthesis levels.

5. Drosophila adenylate cyclase rutabaga is implicated in footshock habituation.
Fig.1. Rut mutants fail to habituate.
Fig.2. Rut abrogation in elav, leo and dnc neurons respectively results in elimination of habituation response.
Fig.3. Reinstating rut specifically within the adult MBs of adult rut flies, using the UAS-rut transgene fully reversed their deficient habituation.
Fig.4. Clozapine and Risperidone rescue the defective habituation of Mirut flies.
Fig.5. Clozapine and Risperidone rescue the defective habituation of rut^{2080} flies.
Fig.6. Rut^{2080} flies show learning deficit and risperidone treatment does not restore the deficient learning phenotype.

III. Appendix

1. Stage dependent nutritional regulation of transgenerational longevity
Fig.1. Starvation-induced transgenerational effect on longevity is evolutionarily conserved in *Drosophila melanogaster*.
Fig.2. Nutritional regulation of transgenerational longevity in w^{Dah} strain is sex-specific.
Fig.3. Dietary restriction during adulthood induces transgenerational effects on longevity.

2. The Drosophila Receptor Tyrosine Kinase Alk Constrains Long-Term Memory Formation

Fig.1. Pharmacological inhibition of dAlk activity enhances STM and LTM.

Fig.2. Downregulation of dAlk in intrinsic α/β MB neurons enhances PSD-LTM.

Fig.3. Downregulation of dAlk in the MBs enhances PSD-LTM specifically.

Fig.4. dAlk levels in the adult MBs during conditioning enhance or constrain LTM performance.

Fig.5. dAlk and its ligand Jeb are enriched in synapses of projection neurons and Kenyon cells.

Fig. 6. The dAlk-activating ligand Jeb is not involved in LTM.

Fig. 7. Dendritic dAlk levels in the MBs increase rapidly upon conditioning to constrain LTM.

Περίληψη

Η παρούσα διδακτορική διατριβή πραγματοποιήθηκε στο Ε.ΚΕ.Β.Ε. «Αλέξανδρος Φλέμιγκ» στη Βάρη, υπό την επίβλεψη του Καθηγητή Ιατρικής Χαράλαμπου Σαββάκη σε συνεργασία με τον Ερευνητή Α' Ευθύμιο Σκουλάκη.

Η εργασία πραγματεύεται γενετική σάρωση με τη βοήθεια του MiMIC, ενός τροποποιημένου *Minos* μεταθέσιμου γενετικού στοιχείου. Σκοπός της σάρωσης ήταν η εύρεση γονιδίων που σχετίζονται με το φαινόμενο της εξοικείωσης στο πειραματόζωο *Drosophila melanogaster*.

Η εξοικείωση αποτελεί μια πολύ συντηρημένη μορφή συμπεριφορικής πλαστικότητας που δίνει τη δυνατότητα στα ζώα να αγνοούν επαναλαμβανόμενα ερεθίσματα χαμηλής σημαντικότητας, προκειμένου να εστιάζουν την προσοχή τους σε άλλα, σημαντικά για την επιβίωση τους. Αποτελεί τη βάση της επιλεκτικής προσοχής, οι μηχανισμοί όμως που διέπουν την εξοικείωση δεν έχουν ακόμη εξακριβωθεί. Η αδυναμία εξοικείωσης σχετίζεται με διάφορες ασθένειες στον άνθρωπο, μεταξύ αυτών και η σχιζοφρένεια. Είναι γνωστό ότι δυσλειτουργίες προσοχής και επεξεργασίας πληροφοριών είναι κύρια συμπτώματα στις διαταραχές σχιζοφρένειας που οφείλονται στην μειωμένη ικανότητα για το φιλτράρισμα άσχετων ερεθισμάτων.

Στην παρούσα μελέτη, χρησιμοποιήθηκαν ενθέσεις του MiMIC μεταθέσιμου γενετικού στοιχείου σε διάφορες θέσεις του γονιδιώματος της *Drosophila melanogaster*, προκειμένου να εντοπιστούν γονίδια που σχετίζονται με την εξοικείωση. Το συγκεκριμένο πειραματόζωο, παρουσιάζει ιδιαίτερα πλεονεκτήματα που οφείλονται στην ευκολία και το χαμηλό κόστος συντήρησης καθώς και στην ύπαρξη πολλών εργαλείων που επιτρέπουν μοριακή και γενετική ανάλυση. Τα στελέχη που έφεραν τις αντίστοιχες ενθέσεις ελέγχονταν συμπεριφορικά ως προς την αποφυγή επαναλαμβανόμενων ηλεκτρικών ερεθισμάτων. Από τα στελέχη που ελέγχθηκαν, προέκυψαν διάφορα γονίδια, εκ των οποίων, τα γονίδια *Btk*, *Tau* και *rut* που μελετήθηκαν περαιτέρω.

Σχετικά με το γονίδιο Btk, η μελέτη κατέδειξε ότι η εξοικείωση σε επαναλαμβανόμενα ηλεκτρικά ερεθίσματα περιλαμβάνει δύο φάσεις που ελέγχονται από διαφορετικούς νευρώνες των μισχοειδών σωματίων και στις οποίες συμμετέχει η πρωτεΐνη BTK. Συγκεκριμένα, το γονίδιο Btk κωδικοποιεί μια κινάση τυροσίνης, που σύμφωνα με την παρούσα μελέτη, εκφράζεται στα μισχοειδή σωμάτια του κεντρικού νευρικού συστήματος της *Drosophila melanogaster* -δομές που όπως έχει αποδειχτεί προστατεύουν από την πρώιμη εξοικείωση. Η συγκεκριμένη πρωτεΐνη δρα με διαφορετικό τρόπο σε ξεχωριστούς νευρώνες. Πιο συγκεκριμένα, στους α και β λοβούς λειτουργεί αποτρέποντας την πρώιμη εξοικείωση, ενώ

στους α′ και β′ λοβούς συμμετέχει στην εξοικείωση μετά από επαναλαμβανόμενα ηλεκτρικά ερεθίσματα. Συνεπώς, η έλλειψη της πρωτεΐνης BTK στους νευρώνες α και β οδηγεί σε πρώιμη εξοικείωση, ενώ στους νευρώνες α′ και β′ οδηγεί σε ελλειμματική εξοικείωση. Ο τελευταίος φαινότυπος, βρέθηκε να αναστρέφεται μετά από χορήγηση των αντιψυχωσικών φαρμάκων κλοζαπίνη και ρισπεριδόνη. Έτσι, καταφέραμε να συνδέσουμε την ελαττωματική εξοικείωση στη Δροσόφιλα με συγκεκριμένα συμπτώματα της σχιζοφρένειας.

Από την άλλη, το γονίδιο Tau κωδικοποιεί πρωτεΐνη που συμμετέχει στη σταθεροποίηση των μικροσωληνίσκων του κυττάρου κι εντοπίζεται κυρίως στους άξονες. Η πρωτεΐνη αυτή σχετίζεται με νευροεκφυλιστικές νόσους στον άνθρωπο. Σύμφωνα με την παρούσα έρευνα, έλλειψη της δροσοφιλικής Tau πρωτεΐνης (μεταξύ άλλων φαινοτύπων) στους α′ και β′ λοβούς των μισχοειδών σωματίων οδηγεί σε ελλειμματική εξοικείωση, ενώ υπερέκφραση της ίδιας πρωτεΐνης στα μισχοειδή σωμάτια οδηγεί σε πρόωρη εξοικείωση.

Σχετικά με το γονίδιο *rut*, τα πειράματα κατέδειξαν πως η δράση του απαιτείται μέσα στα μισχοειδή σωμάτια προκειμένου το πειραματόζωο να καταφέρει να αγνοήσει τα επαναλαμβανόμενα ηλεκτρικά ερεθίσματα, καθώς η έλλειψη της πρωτεΐνης αδενυλικής κυκλάσης rut στους νευρώνες αυτούς οδηγεί σε ελλειμματική εξοικείωση. Όπως και στην περίπτωση της πρωτεΐνης BTK, η ελλειμματική εξοικείωση των μεταλλαγμάτων αναστρέφεται μετά από χορήγηση του αντιψυχωσικού φαρμάκου ρισπεριδόνη. Επιπλέον πειράματα απαιτούνται για την μελέτη της δράσης του γονιδίου *rut*.

Συμπερασματικά λοιπόν, η παρούσα μελέτη συντέλεσε στην εύρεση νέων γονιδίων που με τη σειρά τους ρίχνουν φως στην αποκάλυψη μηχανισμών εξοικείωσης, γεγονός που συμβάλλει στην κατανόηση διαταραχών εξοικείωσης, όπως η σχιζοφρένεια. Έτσι, δείχνουμε πως η *Drosophila melanogaster* μπορεί να αποτελέσει ικανό μοντέλο όχι μόνο για την μελέτη της εξοικείωσης ως ενδοφαινοτύπου της σχιζοφρένειας και για την εύρεση νέων σχετικών γονιδίων αλλά και για την επαλήθευση και την περαιτέρω μελέτη ήδη γνωστών γονιδίων που σχετίζονται με ανθρώπινες διαταραχές.

Abstract

This doctoral thesis was performed at the B.S.R.C. "Alexander Fleming" in Vari, Athens under the supervision of Professor Charalambos Savakis together with Researcher A', Efthimios M.C. Skoulakis. The research study involves a genetic screen employing MiMIC transposable element. The aim was to identify new genes implicated in habituation of *Drosophila melanogaster*.

Habituation is a highly conserved, yet little understood form of behavioral plasticity that enables salience filtering, by precipitating perceptual changes that attenuate the value of environmental stimuli. Normal habituation allows animals to ignore/devalue repetitive or prolonged non-reinforced stimuli and does not involve sensory adaptation or fatigue. It likely underlies selective attention. Defective habituation is the retention of the value of an inconsequential stimulus beyond the time typical for the onset of the attenuated response and is thought to underlie Schizophrenia (SD) as SD patients present characteristic deficits in devaluing and attenuating responses to repeated stimulation.

Here, we used MiMIC insertions within different genetic loci of *Drosophila melanogaster*, to identify genes involved in habituation. Drosophila, as an experimental animal model, exhibits multiple assets such as its ease of handling, low cost of breeding and availability of scientific tools that allow molecular and genetic analysis. MiMIC mutants were tested using the shock habituation experimental paradigm. Several insertion lines that exhibited abnormal responses were identified. Among them, insertions within the genes *Btk*, *Tau* and *rut* were further analyzed.

The Btk gene encodes a non-receptor tyrosine kinase. This study showed that footshock habituation consists of two distinct phases, which both depend on different mushroom body neurons and Btk is necessary for both of them. Btk is expressed in the mushroom bodies of *Drosophila melanogaster* and has distinct roles in different neurons. In the α/β neurons, it protects from premature habituation, while in the α'/β' neurons promotes habituation after repetitive electric footshocks. Thus, elimination of Btk protein in the α/β neurons results in premature habituation whereas in the α'/β' neurons it results in defective habituation. Defective habituation can be restored after administration of the antipsychotic drugs clozapine and risperidone. Hence, we propose a link between defective habituation and schizophrenia.

A second identified gene, Tau, encodes a protein involved in microtubule stabilization and is found mainly in axons. It is implicated in human neurodegenerative diseases. According to our study, elimination of drosophila Tau protein from the α'/ β' mushroom body neurons results in defective habituation while its overexpression leads to premature habituation.

The third identified gene examined in this thesis is *rut*, which codes for an adenylate cyclase. Experiments showed that *rut* is required within the mushroom bodies for the fly to ignore the repetitive stimuli during the footshock habituation assay. As for Btk, defective habituation of *rut* mutants can be restored after administration of risperidone. Further experiments are required to clarify *rut* function.

In conclusion, this study contributed to the identification of new genes implicated in habituation and shed light on yet poorly known mechanisms. These genes and their mechanisms of action will certainly lead to a better understanding of the habituation related diseases of great complexity, such as schizophrenia. Thus the study demonstrated that *Drosophila melanogaster* can be a potent model not only for studying habituation as an endophenotype of schizophrenia and the identification of new implicated genes, but also for the verification and further study of already known genes related to human diseases.

I. Introduction

1. The fruit fly

Drosophila melanogaster, also known as fruit fly or vinegar fly, belongs to the family Drosophilidae. The complete scientific classification is the following:

Kingdom	Animalia	**Infraorder**	Cyclorrhapha
Infrakingdom	Protostomia	**Superfamily**	Ephydroidea
Superphylum	Ecdysozoa	**Family**	Drosophilidae
Phylum	Arthropoda	**Subfamily**	Drosophilinae
Subphylum	Hexapoda	**Tribe**	Drosophilini
Class	Insecta	**Subtribe**	Drosophilina
Subclass	Pterygota	**Genus**	*Drosophila*
Superorder	Holometabola	**Subgenus**	*Sophophora*
Order	Diptera	**Species group**	*Drosophila melanogaster*
Suborder	Brachycera		

Table 1. *Drosophila melanogaster* complete classification

Fruit flies have a simple life cycle, summarized in **Fig. 1** Their karyotype consists of four chromosomes, the X and Y sex chromosomes (first), two larger autosomal chromosomes, named 2 and 3, and a small fourth chromosome. Females bear two X chromosomes, while males a single X and the Y chromosome. Both sexes have two sets of the second, third, and fourth autosomal chromosomes. Sex is determined by the X : autosome balance, as following: if X:A = 1 then it is female, while if X:A = 0.5 it is male. The whole genome is 175.000.000 kb long while annotation of the Drosophila genome identified 17,728 genes, of which 13,907 are protein coding and encode 21,953 unique polypeptides. The remaining 3821 identified genes encode various types of RNA noncoding genes (1).

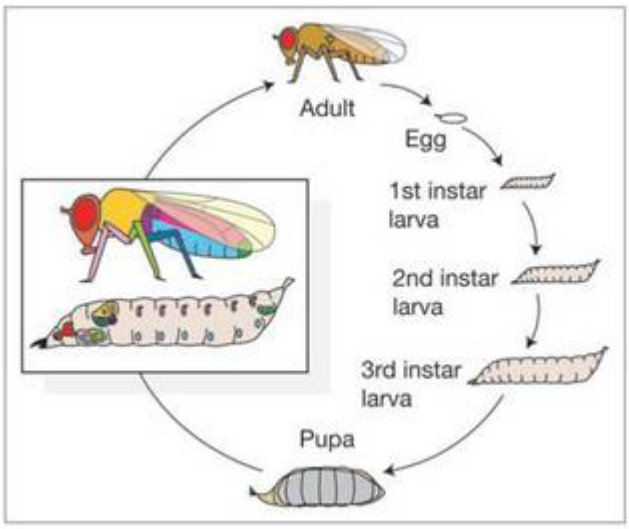

Fig. 1. *Drosophila melanogaster* life cycle. *Drosophila* is a holometabolous insect and its adult organs develop from larval imaginal discs. Larvae include three larval instar stages before metamorphosing into their adult form. Inset shows imaginal discs, while colors associate imaginal discs to matching adult organ. Copy from (2).

2. Contribution of Drosophila in research

At the beginning of the 20th century Thomas Hunt Morgan published the most influential work in the field of genetics, since Gregor Mendel's work in 1866. It established the Drosophila research field by unraveling the chromosomal basis of heredity. "The chromosomes are the bearers of the hereditary characters; and the known chromosomal behavior suffices as a mechanism to explain Mendel's law" (3). This dogma of genetics offered Morgan a Nobel Prize in 1933.

Since then, an immense number of tools has been developed and used to analyze subjects other than heredity in Drosophila. An enormous amount of data has been generated and this is the reason why the humble *Drosophila melanogaster*, became the premier research system for genetics. The contribution of the fruitfly is flourishing in many scientific fields. Milestone publications refer to immunology and genetics, development and cancer, neurobiology and neurological diseases. Since Morgan, studies on *Drosophila melanogaster* have paved the way for elucidating many basic biological processes, while the fact that more than 60% of the protein-coding fly genes have human homologs is indicative of the pivotal role of flies in understanding human biology.

Yet, it was only during the sixties that the field of behavioral neurogenetics emerged. Seymour Benzer reasoned that if genetics could be used to dissect the principles of inheritance and development, a systematic genetic analysis of fly behavior should thus yield genes that control neuronal function. He inaugurated this field by revealing mutants with defective phototaxis (4) and then persuaded the scientific community that the study of the molecular basis of behavior could be achieved. In 1971 he performed a forward

genetic screen and identified mutant flies for the daily rhythm of eclosion and for locomotor activity (5). However, the most significant contribution of Benzer's lab was the development of the olfactory shock-avoidance learning assay in 1974 (6), which allowed the identification of the first learning mutant *dunce* (*dnc*) (7). After a while, another learning gene was brought to light, *rutabaga* (8). Along with another scientific landmark, the establishment of the powerful P-element mediated transformation (9), Benzer's work laid the ground for the subsequent discovery of many other genes implicated in learning and memory in flies.

Drosophila melanogaster serves as a very tempting experimental organism because of its important assets, such as accelerated generation time and easy handling in the laboratory. Moreover, it offers multiple special features that ensure that Drosophila will continue to be a leading research model organism for the following years. The fly genome has been fully sequenced (10). The accurate and delicate manipulations that Drosophila allows cannot be easily found in other organisms. Available tools can help scientists ask very specific questions in many different fields. For example, removal or addition of genes, - two very important experimental approaches used in every model organism, can be easily achieved in flies. Drosophilists can easily remove genes using transposable elements or lower gene expression by RNAi interference (11). Conversely, adding genes or gene constructs is available through P -element –mediated mutagenesis since 1982 (9). The transformation process has been improved since then by using the FRT recombination (12) and the ectopic expression GAL4/UAS systems (13) thus extending the arsenal of Drosophila available tools. Furthermore, transposons provide the possibility of creating single-gene or multi-gene mutations or chromosomal aberrations (14), insertions and deletions while the expansion of this system using the φC31 bacteriophage (15) offers even more potential applications.

The ability to manipulate the fly genome has enabled significant contributions to many distinct areas of biology, including genetics, developmental biology, cell biology, neuroscience, physiology and metabolism, disease mechanisms, population genetics, and evolution. This broad toolkit allows scientists to study the function of specific cells in a sophisticated manner and unparalleled level of resolution. At the same time, many other methods are currently being developed, warranting that Drosophila will continue being at the forefront of research for many years to come.

Nonetheless, it is obvious that flies do not have the potential of addressing vertebrate specific issues, such as the development of specific brain structures, regulation of neural crest migration, the function and properties of hippocampal neurons, or to assess how the cerebellum controls motor outputs. However, flies still have the ability to provide crucial information about the fundamental characteristics of nervous system organization and function, the implication of specific genes in neurodegeneration, the processing of information, the way in which different brain areas are wired together and which gene products and genetic cascades control behavior.

3. Drosophila as a model to study behavior and human neurological diseases

Given the high degree of evolutionary conservation among genes that control basic developmental processes, Drosophila is as an excellent model for studying not only a variety of human diseases, such as cancer and heart diseases but also behavioral disorders such as Alzheimer's or Huntington's disease.

3.A. Studying behavior with *Drosophila melanogaster*

Behavior, arguably one of the most complicated phenotypes, has long been considered to be the action of an animal in response to its internal and external environment (16). Yet, although the idea that genes may contribute to behavior seemed extreme then, nowadays it has become a fact. Since 1961, when the first article on behavioral genetics was published (17), not only behavioral studies have been well established but they have also led to the identification of large number of genes involved in behavior.

Studying behavior is a challenging task because of the many steps that intervene between gene expression and the manifestation of a behavior, the colossal variation between behaviors, the distinct genes that are involved, the complexity of the nervous system and the environmental conditions that affect behavior. Moreover, behavior is characterized by polymorphic traits since many genetic loci interact in order to influence the activity of neural circuits. When performing a behavioral experiment, animals of the same age, reproductive condition and experience should be used in order to reduce developmental contributions. In addition, as in every experiment, accurate controls should be included to demonstrate that it is the behavior of interest itself that has been specifically modified by genetic intervention (18).

Drosophila melanogaster is at the cutting edge of behavioral genetics and has been providing research with substantial insight about the molecular, cellular and evolutionary basis of behavior. Besides, the fly genome was one of the first to be completely sequenced, paving the way for direct comparisons with human genes implicated in a variety of disease phenotypes. Although the mechanisms that rule mammalian behavior are more complex than those in the fly, the basic characteristics of such mechanisms are often conserved. The fact that many fly genes have homologs in vertebrates, strongly suggests that genetic discoveries in fruit flies can provide valuable insights into evolutionarily conserved processes. Drosophila however, is not just a gene-finding tool for those studying mammalian genes. It is also an exceptionally useful genetic model to study both simple and complex behaviors. Drosophila research has given rise to an important

amount of literature, concerning the molecular, cellular and evolutionary features of behavior (18).

Drosophila exhibits a large repertoire of behaviors including courtship, circadian rhythmicity, olfaction, gustation, learning and memory, aggression, addiction, etc. This is the reason why Drosophila is a valuable model to study the neurobiology of behavior. For instance, the discovery of the cellular mechanisms that control the circadian clock is widely considered as a major contribution of fruit flies to the field. The discovery began with the isolation of *long-day*, *short-day* and *arrhythmic* fly mutants, all of which finally proved to be alleles of the gene *period* (5). With the subsequent isolation and cloning of additional mutants in flies, fungi and mice, the cellular mechanisms of circadian clock were identified and found to be nearly universal in the animal kingdom (19),(20). Many of the actual genes involved, such as *period*, are conserved between flies and mammals (**Fig. 2**). The fundamental biological principles that emerged from the genetic studies of learning and memory in fruit flies have proved to be broad, if not universal, in the animal kingdom. Importantly, they have set the way for understanding the human biology underlying these behavioral phenotypes. This is an indisputable argument for the importance of flies as models for humans.

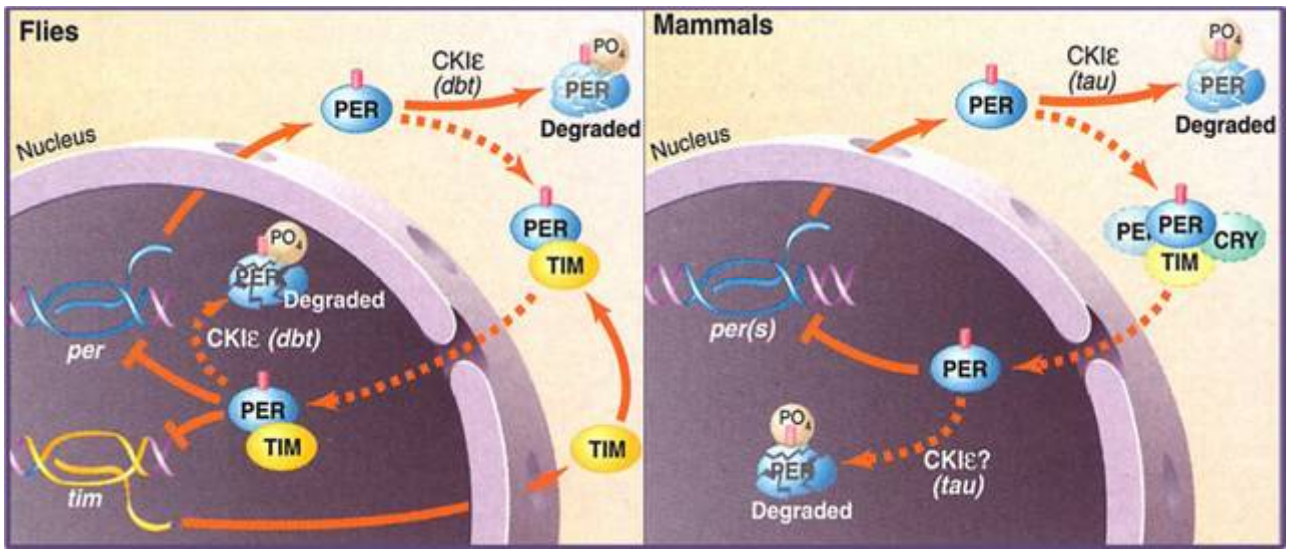

Fig.2. Conservation of molecular mechanisms of the circadian clock between flies and mammals. PER: period gene, TIM: timeless gene, CKIε: casein kinase gene. Copy from (21)

3.B. Studying human neurological diseases with *D. melanogaster*

Human diseases are often of high complexity. The fact that the Drosophila genome is completely sequenced, gives the possibility to identify fly genes that are homologous to human disease genes (22). Almost 60% of the known human disease genes have related sequences in flies (666 of 911 genes) (23) , and roughly 10% of these genes, are involved in neurological diseases. Consequently, Drosophila can be used as an efficient model

system in which powerful genetic tools can be employed to understand the neurobiological basis of disconcerning behaviors. Drosophila and humans separated a hundred million years ago, following hence different evolutionary paths. Nevertheless, despite their apparent dissimilarities, they share common fundamental cellular and neurobiological processes. These similar processes involve brain architecture (gross subdivisions of the brain into forebrain, midbrain and hindbrain), the main neurotransmitter systems, as well as common behavioral traits including learning, circadian behavior and some social behaviors (24).

It is known that neuropsychiatric diseases affect human social behavior. Compared to humans, Drosophila is obviously a less social animal. Nevertheless, flies do exhibit conspicuous social behaviors from simple ones like aggregation, to complex ones like courtship and aggression. While Seymour Benzer performing genetic screens to identify mutants with abnormal behavior, he isolated the *drop dead* (*drd*) mutant which exhibited shortened lifespan and degenerating brain. He therefore proposed for the first time that the fly could model human late-onset degenerative disorders (25).

Further studies led to the isolation of additional mutants with features similar to human brain disease pathology thus demonstrating the usefulness of Drosophila as a model to study brain genes involved in human diseases: *spongecake* and *eggroll* develop membranous vacuoles and multilamellar structures reminiscent of the pathological structures that form in Creutzfeldt-Jakob disease and Tay-Sachs disease (26). The *swiss cheese* mutant (*sws*), which exhibits an age-dependent loss in motor activity and brain degeneration shows homology to the human gene encoding the neuropathy target esterase. Moreover, mutations in the PNPLA6 gene cause motor neuron disease as well as the rare neurodegenerative Boucher-Neuhauser and Gordon-Holmes syndromes (27).

Since then, researchers have added to their arsenal, a compelling tool, genome information, which allowed them to use more sophisticated approaches to study human diseases. For instance, reverse genetics has made possible to express pathological forms of human genes in flies. A detailed analysis of the general strategy used to assess the pathways and mechanisms involved in the disease is described below (**Fig.3**). In other words, creating a simplified version of human neurological disease by expressing (or knocking down) the human mutant gene in the fly has now become the state-of-the-art approach for modelling features of distinct neurological and neurodegenerative disorders such as Parkinson's disease, Alzheimer's disease, fragile X syndrome, fragile X tremor/ataxia syndrome and additional spinocerebellar ataxias (28);(29);(30);(31). Data obtained from such fly models, combined with those available from human patient pathology or human population genetics have provided mechanistic insights into the molecular pathways of disease. Considering the list of the 2,309 human disease-associated genes, ~700 human disease genes are estimated to have well-conserved homologues in *D. melanogaster.*

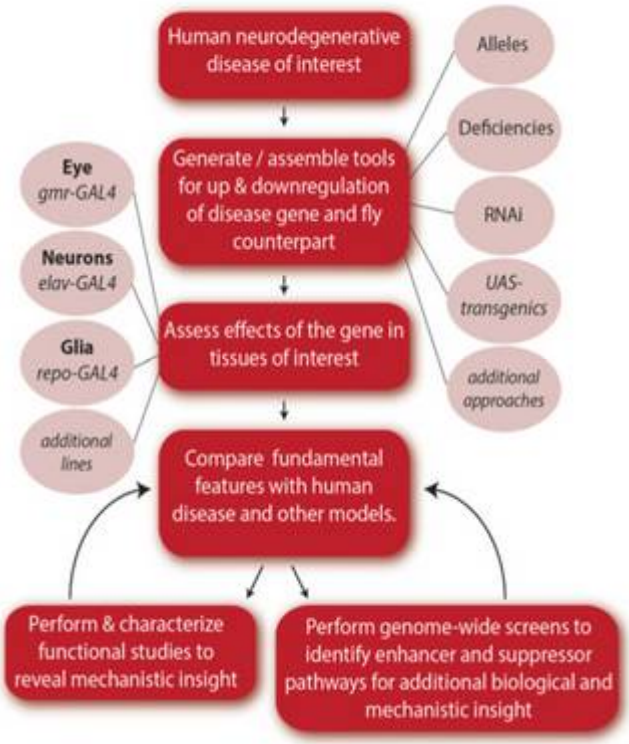

Fig. 3. Creating a Drosophila model for a human neurodegenerative disease. Beginning with genes known to be involved in disease, Drosophila orthologs are identified to enable loss-of-function and gain of- function gene manipulation. Alternatively, or in addition, the human gene or the genetic lesion associated with the disease can be expressed in the fly. Upon establishment of the model, the effects of the disease gene are examined and compared to known manifestations and features of the human disease. Detailed functional studies of the fly model may reveal new insight into the disease process. Functional characterization and genome-wide screens in the fly can allow additional information on disease pathways and mechanisms. Genes and processes identified through these studies can then be examined in human samples or mammalian models to identify novel disease-associated genes, risk factors and pathological hallmarks. Fly models can also be used to screen pharmacological compounds. Copy from (32).

Moreover, the arsenal of Drosophila tools grows fast, providing us the ability of expanding our knowledge. After the establishment of the Gal4/UAS system (33) and split Gal4 drivers (34), the Minos mediated integration cassette (MiMIC) (35), in combination with clustered regularly interspaced short palindromic repeats (CRISPR)/Cas9 methods in flies (36), a totally different horizon has been unfolded.

Finally, because of the high evolutionary conservation among genes of basic developmental processes and the availability of genome sequences of human and flies, as well as the extensive Drosophila toolkit, new approaches on studying heritable diseases in humans have emerged. All of the above data indicate that *D. melanogaster* can serve as a complex multicellular system for analyzing the function of a wide array of gene functions involved in human disease (37).

4. Drosophila brain

As in mammals, the Drosophila brain consists of two basic cellular components, neurons and glia. Fly neurons share a similar functional and molecular organization with mammalian neurons: axons with their transport machinery, pumps and voltage-gated channels that underlie action potential transmission, presynaptic terminals with all the machinery for synaptic vesicle release and recycling, dendrites, postsynapses with localized receptor fields and active zones etc. Glial cells are intimately associated with neurons and often surround defined axon bundles to form a blood–brain barrier (38).

The Drosophila central nervous system (CNS) is subdivided into the brain and the ventral nerve cord that innervates the thorax and abdomen. These tissues are functionally equivalent to the mammalian brain and spinal cord, respectively. *Drosophila* brain is a bilaterally symmetrical structure that contains approximately 10^5 neurons, one millionth of humans neurons. The developing fly brain divides into protocerebrum, deutocerebrum, and tritocerebrum, areas which appear evolutionarily homologous to the forebrain, midbrain and hindbrain regions of vertebrates (39).

Other similarities between fly and human nervous systems include the main neurotransmitter systems and channels, which are the targets of many pharmacological approaches for neuropsychiatric diseases. However, unlike glutamate in humans, it is acetylcholine that is the main excitatory neurotransmitter in Drosophila CNS, glutamate being the main excitatory neurotransmitter only at the fly neuromuscular junction (NMJ). As in vertebrates, GABA (gamma-aminobutyric acid) is the principal inhibitory neurotransmitter in flies and is found widely throughout the brain. The pharmacology of these is broadly similar but not identical to that of vertebrate receptors (40).

In humans, the dopaminergic system is the target of many addictive substances. Drosophila also has a dopaminergic system, comprising over a hundred neurons per adult brain hemisphere (41). However, the cannabinoid system, another important neurotransmitter system of psychiatric importance, does not exist in Drosophila. Pharmacological and sequence analysis indeed revealed the absence of the CB1 or CB2 cannabinoid receptor families in flies (42).

4.A. Mushroom bodies

The mushroom bodies (MBs) or *corpora pedunculata*, are two of the most clearly distinguishable neuropil structures in the insect brain. They form a pair of characteristic mirror-symmetrical neuro-anatomical structures in the protocerebrum of the fly brain (**Fig.4** left). Most of them are contributed by the Kenyon Cells (KCs) whose densely packed cell bodies are located in the dorsocaudal brain cortex, where their dendrites arborize in a dense structure called calyx. Their long and thin axons form a bundle (the

pedunculus) that extends from the dorsocaudal to the rostroventral area of the midbrain and bifurcate frontally into a vertical and two horizontal lobes (43). Mushroom bodies are comprised of ~2500 neurons per hemisphere and subdivided into α/β, α′/β′ and γ subtypes (**Fig.4** right). These distinct neuron types exhibit differential expression levels of a number of specific mushroom body genes, suggesting that they may have corresponding functional differences (44).

Kenyon cells (KCs) are produced in each hemisphere of the brain by the division of four neuroblasts born during early embryonic stage. The sequential division of these neuroblasts produces three morphologically and spatially distinct subtypes of KCs, which apear in the following order: γ, α′/β′ and α/β (45). The γ neurons are generated up to the mid-third instar larval stage and their axons form the larval dorsal and medial horizontal lobe (46). Then, α′/β′ neurons are generated and continue to be produced until puparium formation. Lastly, α/β neurons are generated from puparium formation until adult eclosion. Their axons are organized in concentric layers within the α/β lobe. The youngest axonal processes situated in the inner layer are successively displaced outwards as they differentiate and newer α/β processes are added to the structure from the most recently born KCs. This inner part, the α/β core (α/β c) into which the last-born axons grow contains densely packed and extremely thin fibers that are rich in actin filaments (47). Mushroom bodies are well-known for being implicated in the regulation of behavioral activity and particularly olfactory learning and memory (48). Genes such as *dunce* and *rutabaga*, whose mutations disrupt olfactory learning and memory, are highly expressed in the MBs (49),(44), while chemical ablation of the MB abolishes olfactory learning and memory (48). Behavioral studies suggest functional differences between the MB lobes. The γ lobe has been reported to support short-term memory (50) while the α/β lobes have been shown to play important roles in long-term memory (51). In addition, outputs from α/β neurons are necessary for olfactory memory retrieval but not for memory formation and storage (52);(53).

Moreover, it has been claimed that neural transmission from α′/β′ neurons is required for acquisition and stabilization of odor memory but is dispensable for memory retrieval (54). Recent studies also support a role for mushroom body neurons in footshock habituation (55),(56). Finally, MBs have been suggested to mediate various other functions, such as locomotor activity control, sleep, complex forms of visual learning, courtship conditioning, place preference in an arena, place memory, context-dependent association, odor perception, and experience-dependent nonassociative osmotactic responses (57).

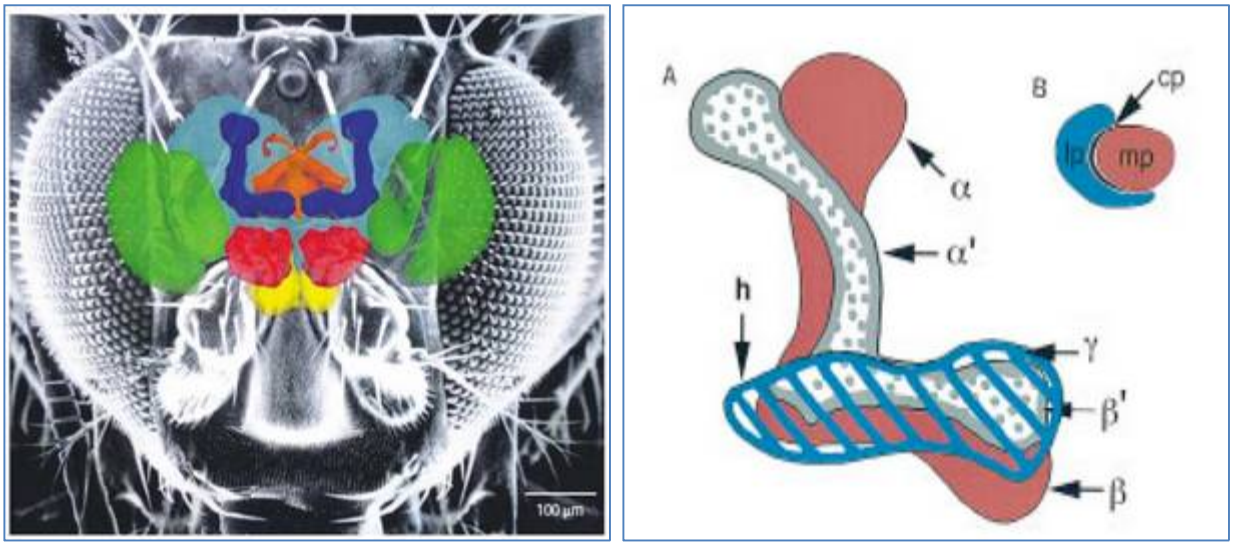

Fig. 4. Left: Drosophila brain inside the head capsule. Green: optic lobes; yellow: suboesophageal ganglion, red: antennal lobes, blue: mushroom bodies, orange: central complex. Copy from (43). Right: Cartoon of the mushroom body lobes depicting only the left lobe structure. Dorsal is up, medial is to the right. The peduncle would extend behind the plane of paper toward the Kenyon cells. The most anterior lobe, γ, is shown striped in blue, and is continuous with the heel (h). Posterior to the γ lobe are the α′ and β′ collateral lobes, stippled in gray. The β lobe, ventral to the β′ lobe, and its collateral α, are in brown. (B) Cartoon of a cross section through the peduncle at the level of the fanshaped body. The lateral peduncle is in blue, the central peduncle in black and the medial peduncle in brown, corresponding to the coloration of the lobes to which they project. Copy from (58).

5. The MiMIC transposable element as a genetic tool

Transposable elements (TEs), also known as transposons or "jumping genes," are mobile repeated DNA sequences that are able to move from one location in the genome to another, thus altering its identity and size. They were first discovered by Barbara McClintock in 1950.They are found in almost all organisms, prokaryotic and eukaryotic, and typically in large numbers. TEs have been "domesticated" by molecular scientists to manipulate the genome and have been extensively used as genetic tools for genomic studies in several living organisms including Drosophila.

Different types of transposons have been used in Drosophila but in each case, each transposon is designed for a specific purpose and none is truly multi-facetted. The most commonly used transposons are *P*-elements, *piggyBac* and *Minos* (59). *P*-elements mobilize efficiently and often excise imprecisely, yet they exhibit a strong insertional bias for the 5' ends of genes. *piggyBac* elements show less bias, excise precisely but mobilize less efficiently than *P*-elements.

Nontheless, Minos elements exhibit a number of different advantages. They have very little insertional bias (59), transpose stably and efficiently in numerous organisms, and excise imprecisely at a useful frequency (60). This is the reason why they have been used in a broad range of organisms. MiMIC is a modified Minos element (**Mi**nos **M**ediated **I**ntegration **C**assette) (35) that contains a gene-trap cassette and the yellow+ marker flanked by two inverted bacteriophage ΦC31 attP sites (**Fig. 5**). MiMIC integrates almost randomly in the genome to create sites for DNA manipulation. The attP sites allow the MiMIC insertions that function as gene traps and cause mutant phenotypes to be reverted to wild type by RMCE (Recombinase-mediated cassette exchange) and insertions can be modified to control *GAL4* or *QF* overexpression systems or perform lineage analysis using the Flp system. Moreover, insertions within coding introns can be exchanged with protein-tag cassettes to create fusion proteins to follow protein expression and perform biochemical experiments. The applications of MiMIC vastly extend the *Drosophila melanogaster* toolkit offering unprecedented potentials of gene manipulations.

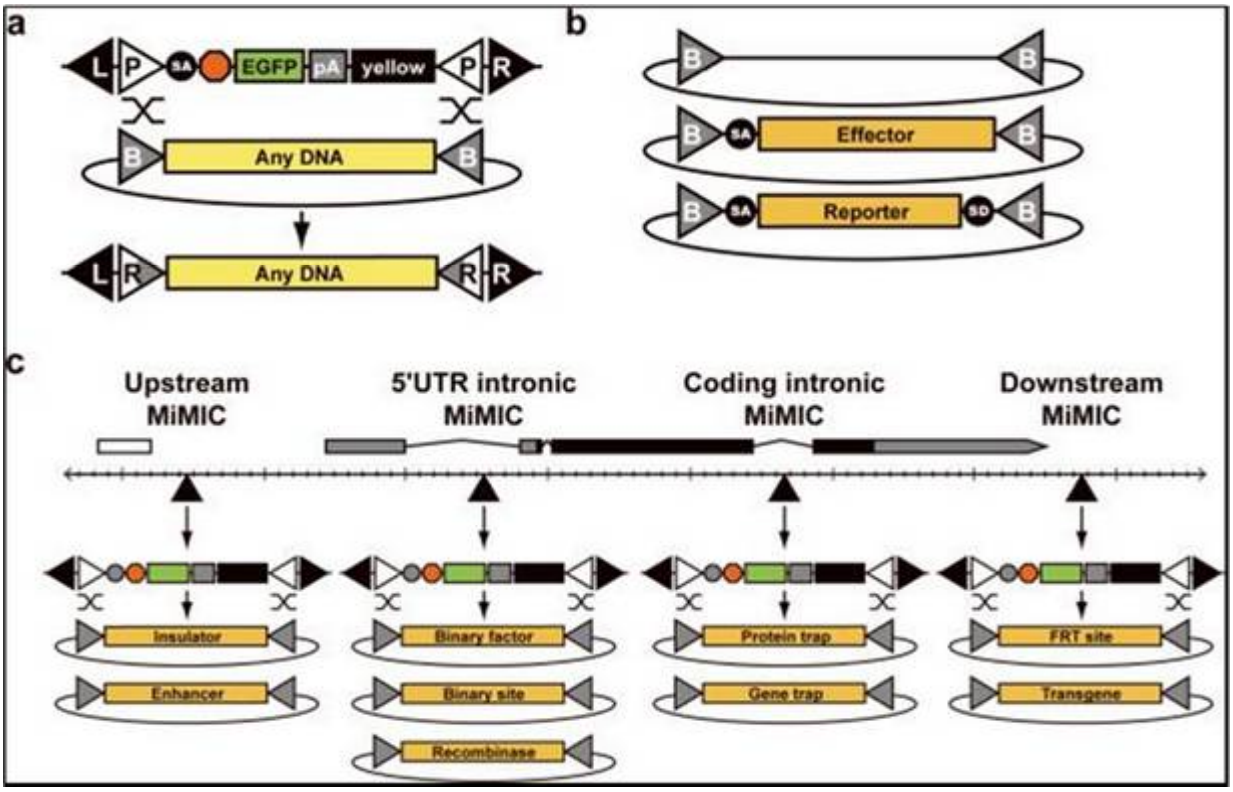

Fig.5. The MiMIC transposon system. (a) MiMIC consists of two Minos inverted repeats (L and R), two inverted ΦC31 attP sites (P), a gene trap cassette consisting of a splice acceptor site (SA) followed by stop codons in all three reading frames, and the EGFP coding sequence with a polyadenylation signal (pA), and the yellow+ marker. The sequence between the attP sites can be replaced via RMCE, resulting in two attR sites (R). (b) Three attB plasmids for RMCE: a correction plasmid consisting of a multiple cloning site, a gene-trap plasmid consisting of a SA fused to a downstream effector, and a protein-trap plasmid consisting of a reporter flanked by SA and SD sites. (c) Various MiMIC insertions in a hypothetical gene with regulatory element (white), 5' and 3' untranslated regions (grey), and coding regions (black), that can be used for several applications as indicated. Copy from (35).

6. Habituation

"People must be able to filter out information in order to maintain perceptual constancy in a world of otherwise chaotic over-stimulation".

Geyer and Braff, 1987

(60)

Habituation is a highly conserved, but little understood form of non-associative plasticity manifested as a response attenuation to repetitive inconsequential stimuli (61). All animals exploit this fundamental mechanism to filter irrelevant input and prioritize attention. Normal habituation permits animals to devalue and therefore to ignore repetitive or prolonged non-reinforced stimuli, while it does not involve sensory adaptation, sensory or motor fatigue and likely underlies selective attention (62). Moreover, animals need to be able to change their behavior because of experience. Habituation is characterized by progressive response decline to repeatedly experienced yet inconsequential stimuli (63),(64). Even though it is considered as a simple form of learning, habituation nevertheless provides a quantifiable form of neuroplasticity (65). In humans, deficits in habituation represent hallmark features of cognitive and behavioral disorders, including schizophrenia, addiction, attention deficit hyperactivity disorder (ADHD) and other disorders marked by "intellectual disability" (66),(67),(68). Despite its biological conservation, our understanding of the genetic mechanisms governing habituation is limited. Identifying the genes that govern how neural circuits regulate habituation is therefore fundamental to understanding disorders manifesting habituation deficits. Besides, because habituation allows animals to filter out irrelevant stimuli and focus selectively on important stimuli, it is a prerequisite for other forms of learning. Therefore, to fully understand the mechanisms of more complex forms of learning and cognition it is important to understand the basic building blocks of habituation.

6.A. Characteristics of habituation

According to the revised description of habituation characteristics (64), habituation is defined as a behavioral response decrement that results from repeated stimulation and that does not involve sensory adaptation/sensory fatigue, or motor fatigue. Traditionally, habituation has been distinguished from sensory adaptation and motor fatigue by the process of dishabituation; however this distinction can also be made by demonstrating stimulus specificity (the response still occurs to other stimuli) and/or frequency-dependent spontaneous recovery (more rapid recovery following stimulation delivered at a high frequency than to stimulation delivered at a lower frequency).

Based on the fundamental study of Thomson and Spencer (69) as well as the revised study of Rankin (64), the characteristics of habituation are the following:

1. Progressive decrease

Repeated application of a stimulus results in a progressive decrease in some parameters (response frequency, magnitude, duration) of a response to an asymptotic level. This change may include decrease in frequency and/or magnitude of the response. In many cases, the decrement is exponential, but it may also be linear; in addition, a response may show facilitation prior to decrementing because of (or presumably derived from) a simultaneous process of sensitization.

2. Spontaneous recovery

If the stimulus is withheld after response decrement, the response recovers at least partially (or even completely) over the observation time.

3. Potentiation of habituation

After multiple series of stimulus repetitions and spontaneous recoveries, the response decrement becomes successively more rapid and/or more pronounced.

4. Frequency (The **I**nter**S**timulus **I**nterval Effect)

Other things being equal, more frequent stimulation results in more rapid and/or more pronounced response decrement, and more rapid spontaneous recovery (if the decrement has reached asymptotic levels).

5. Intensity effect

Within a stimulus modality, the less intense the stimulus, the more rapid and/or more pronounced the behavioral response decrement. Very intense stimuli may yield no significant observable response decrement.

6. Below-zero habituation

The effects of repeated stimulation may continue to accumulate even after the response has reached an asymptotic level (which may or may not be zero, or no response). This effect of stimulation beyond asymptotic levels can alter subsequent behavior, for example, by delaying the onset of spontaneous recovery.

7. Stimulus specificity

Within the same stimulus modality, the response decrement shows some stimulus specificity. To test for stimulus specificity/stimulus generalization, a second, novel stimulus is presented and a comparison is made between the changes in the responses to the habituated stimulus and the novel stimulus. In many paradigms (e.g. developmental studies of language acquisition) this test has been improperly termed a dishabituation test rather than a stimulus generalization test, its proper name.

8. Dishabituation

Presentation of a different stimulus results in an increase of the decremented response to the original stimulus. This phenomenon is termed "dishabituation." It is important to note that the proper test for dishabituation is an increase in response to the original stimulus and not an increase in response to the dishabituating stimulus. Indeed, the dishabituating stimulus by itself need not even trigger the response on its own.

9. Habituation of dishabituation

If a response is repeatedly habituated and dishabituated, the magnitude of the dishabituation decreases.

10. Long term habituation

Some stimulus repetition protocols may result in properties of the response decrement (e.g. more rapid rehabituation than baseline, smaller initial responses than baseline, smaller mean responses than baseline, less frequent responses than baseline) that last hours, days or weeks. This persistence of aspects of habituation is termed long-term habituation.

6.B. Distinct habituation paradigms

The theoretical basis of habituation has been established since Thompson and Spencer introduced the characteristics of the phenomenon (69). Since then, habituation has been studied in different organisms, using different paradigms. A notable piece of information derived from studies in A. Californica (72) as well as C. elegans (76). Interestingly, Drosophila has given a great deal of insight to the field.

Organism	Habituation paradigm	Important References
A. californica	gill/siphon withdrawal reflex	(70), (71),(72),(73)
C. elegans	tap- withdrawal reflex	(74),(75),(76),(77)
Danio rerio	novel tank test	(78)
	light/dark locomotion	(79)
	startle reflex	(80)
D. melanogaster	giant fiber	(81),(82),(83)
	landing response	(84),(85)
	cleaning reflex	(86)
	olfactory jump response	(87),(88)
	olfactory startle response	(89),(90)
	olfactory habituation	(91),(92),(93)
	gustatory habituation	(94),(95)
	footshock habituation	(96),(56)
	other types of habituation	(97),(98),(99)
rodents	startle response	(100),(101),(102),(103)
	olfactory habituation	(104),(105),(106),(107)
primates	orienting response	(108)
humans	olfactory habituation	(109), (110),(111),(112)
	auditory habituation	(113)
	visual habituation	(114),(115)

Table 2. Habituation paradigms studied in different organisms.

Aplysia exhibits a reflexive withdrawal of its gill and siphon in response to weak or moderate tactile stimulation of its skin. Repeated tactile stimulation causes this defensive withdrawal reflex to habituate (70). *C. elegans* responds to the mechanical stimulus of a tap delivered to the side of the Petri dish it inhabits by swimming backwards. This backward swimming has been called the tap withdrawal response and it can habituate (74). Habituation in Zebra fish (*Danio rerio*) is mainly studied using the novel tank paradigm (78), where freezing behavior after exploration of a novel tank is assessed. In mice and rats the acoustic startle reflex (ASR) has been used in habituation studies. When animals are surprised by a loud noise their facial and skeletal muscles rapidly contract so they close their eyes and stiffen their neck and body. Repetition of the startle stimulus eventually leads to a weaker ASR (100),(101). As far as Drosophila is concerned, numerous habituation paradigms have been established. Among them, visual (giant fiber,

landing response), chemical (gustatory/ odor habituation) or mechanical (footshock habituation) stimuli have been used to evoke habituation. In **Table 2**, we summarize different habituation paradigms, studied in a variety of organisms, as well as the landmark bibliography pertinent to them, emphasizing in Drosophila research.

6.B.1.Footshock Habituation in *D. melanogaster*

During this thesis, I studied Drosophila habituation using the footshock habituation assay as it has been established in (55). For this paradigm, a special apparatus is needed, called T-maze (**Fig. 6**). The experiments were performed in an appropriately designed behavior room with strictly controlled conditions. Briefly, for the electric footshock avoidance part of the experiment, ~70 flies were placed at the choice point of a T-maze (**Fig. 6C**) to choose for 90 s between an electrified and an otherwise identical inert standard copper grid (**Fig.6E,D** respectively). In the electrified grid, 45 V shocks were delivered every 5.15 s, each lasting 1.2 s. The avoiding fraction (AF) was calculated by dividing the number of flies avoiding the shock by the total number of flies. Habituation to electric shock experiments were performed as described in (55). For the training phase ~70 flies were sequestered in the upper arm of a standard T-maze lined with an electrifiable grid (**Fig.6A**). They were exposed to 15 1.2 s electric shocks at 45 V with a 5.15 s interstimulus interval. Air was not drawn through the tube during training to avoid association of the shocks with air. After a 30 s rest and 30 s for transfer to the lower part of the maze, the flies were tested by choosing between an electrified and an inert grid. Therefore, the earliest measures of post-training responses are 1 min after the flies received the last training stimulus. Testing was performed at the same voltage (45 V) as for training. During the 90 s choice period, 17–18 1.2 s stimuli were delivered to the electrified arm of the maze. At the end of the choice period, the flies in each arm were trapped and counted, and the habituation fraction (HF) was calculated.

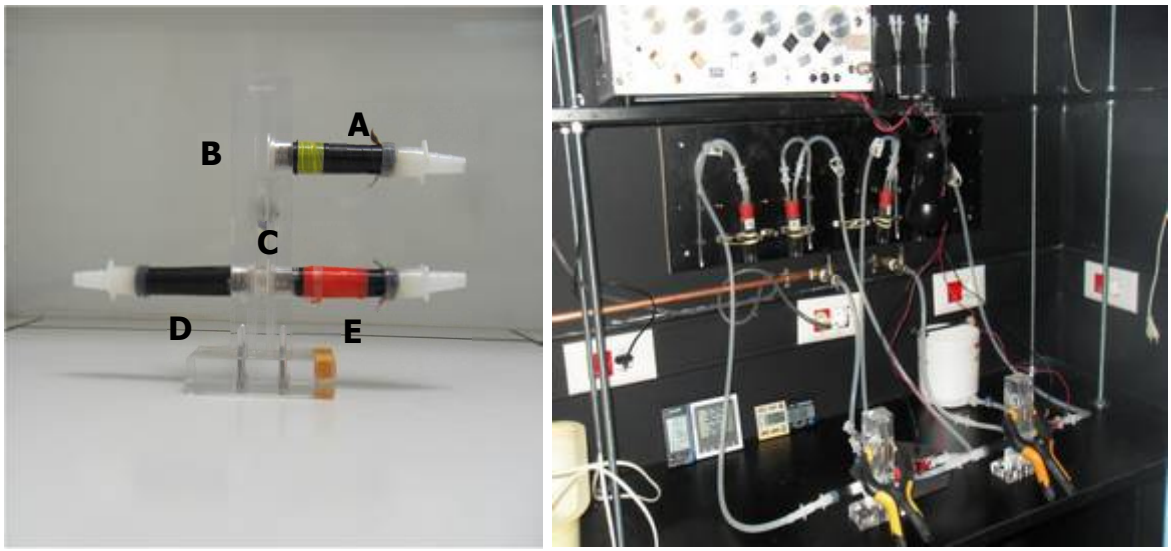

Fig. 6. (Left) T-maze description. A: Training arm containing an electrifying grid. B. Fly entrance point C. Choice point D. Testing arm without an electrifying grid E. Testing arm with an electrifying grid (Right). Experimental set up as it is installed in the behavior room.

Normal flies attenuate their response after 10-11 electric shocks, after presenting a period of habituation latency. Mutant flies may yield two distinct phenotypes of premature or defective habituation (**Fig. 7**). In the first case, animals devaluate stimuli early than expected while in the second case, animals fail to habituate after repetitive electric shocks, exhibiting continuous responsiveness.

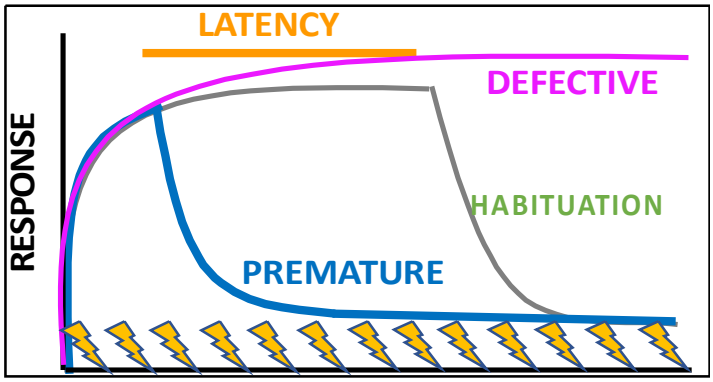

Fig. 7. Experimentally-based model of responses to repetitive non-reinforced stimuli (bolts). Initially, animals respond normally to the stimulation (latency to habituate-orange bar). Additional stimuli are devalued relatively rapidly and responses decline to baseline(habituation). Animals with premature devaluation of the stimulus are expected to reach baseline responses much faster (blue line) as obtained from animals with blocked MB α/β neuron neurotransmission. In contrast, defective habituation yields continuous responsiveness (defective habituation- magenta line).

6.C. Mechanisms of habituation

The selection of dissimilar signals to focus on depends on a neural mechanism that filters or gates familiar or predicted incidents. Despite the ubiquity of habituation, and its vital importance as a "building block for cognition", its mechanisms remain largely unknown (62).

Habituation characteristics mentioned before, are quite well conserved throughout evolution. This is the reason why it has been hypothesized that there must be a well-conserved mechanism underlying habituation. Studying a great variety of organisms and paradigms, various mechanisms have been proposed in the current and past literature to interpret habituation. Most of them culminate in either homosynaptic depression of excitatory neurotransmission or network-level potentiation of inhibitory neurotransmission. Nevertheless, evidence from *C. elegans* support that habituation consists of multiple behaviorally and molecularly distinct mechanisms that mediate shifts in behavioral strategy (116),(117). The prevailing mechanisms proposed to explain habituation are being discussed here.

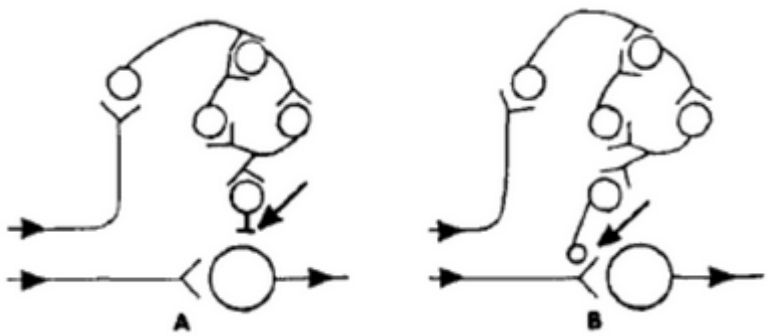

Fig.8. Possible habituation mechanisms. A. Postsynaptic inhibition B. Presynaptic inhibition as proposed in (63)

<u>Stimulus-model comparator theory</u>

Sokolov proposed the stimulus-model comparator theory while studying the orienting response, who defined it as EEG (electroencephalogram) activity. Orienting responses arouse when an organism is exposed to a new or changing stimulus and result in observable behaviors and EEG activity. This behavior may undergo habituation after repeated presentation of the eliciting stimulus (118). Sokolov suggested that after experienced a stimulus for several times, the nervous system creates a model of the expected stimulus (stimulus model). As the brain keeps encountering the stimulus, it compares the experienced stimulus with the stimulus model. If the experienced stimulus matches the stimulus model, responding is constrained. In the beginning, the stimulus model is not so alike the presented stimulus, so the animal continues responding due to this incongruity. Further presentations result in improvement the stimulus model, so there is no longer a mismatch, thus responding is inhibited causing habituation. On the other

hand, if the stimulus is changed so that it no longer resembles the stimulus model, the orienting response is no longer inhibited.

The dual process theory

Groves and Thomson proposed (63) that response plasticity after repetitive stimulation involves two distinct processes. The first one (habituation) is decremental while the second one (sensitization, increased responsiveness after repeated stimulation) is incremental. The two processes are supposed to develop independently (separate neuronal mechanisms) within the brain and interplay to generate the final behavioral outcome. Finally, "the strength of the behavioral response elicited by a repeated stimulus is the net outcome of the two independent processes of habituation and sensitization" (63).

Homosynaptic depression of excitatory neurotransmission

Early habituation studies in *Aplysia californica* revealed that synaptic depression of the sensorimotor connection is a mechanism of habituation of the withdrawal reflex (70),(71). During habituation training the siphon skin was repeatedly stimulated with a weak mechanical or electrical stimulus. This weak stimulus evoked an excitatory postsynaptic potential (EPSP) in the gill motor neuron, and this EPSP, decremented with repeated stimulation of the siphon skin. After impaling the sensory neurons with sharp electrodes and fired them repeatedly with brief injections of positive current, the EPSP evoked in the motor neuron depressed, just as had the EPSP produced by the mechanical/electrical stimuli applied to the siphon skin. A Following study (119), came to the conclusion that depression was due to a decrease in the number of quanta of presynaptic transmitter released per action potential in the sensory neuron, and not to a change in the sensitivity or number of postsynaptic receptors (**Fig. 8**). Finally, Bailey and Chen revealed that the number of terminal varicosities—the sites of presynaptic release—on the axonal branches of sensory neurons in habituated animals were significantly reduced. Moreover, the number and area of the active zones, as well as the number of presynaptic vesicles associated with each active zone, were significantly reduced in habituated animals (120). Homosynaptic depression is supported by a considerable amount of studies in different organisms (72),(121),(77),(122) and it is the predominant model explanation for habituation.

Network-level potentiation of inhibitory neurotransmission

Ramaswami suggests the "negative image model" based on the potentiation of inhibition of active neurons (62) to explain habituation. According to this model, habituation may be driven by enhanced recurrent inhibition rather than depression. Evidence from flies show that olfactory habituation results from selective potentiation of recurrent GABAergic inhibition in projection neurons that have been previously activated by the familiar odor (92),(123, 124). At a systems level, this can be summarized in "the negative-image model"

where central idea is "*the ability of any repeated and unreinforced excitatory stimulus to create an inhibitory (or negative) image of itself, which then acts as a selective filter for the familiar stimulus pattern*". The negative-image model offers an explanation for habituation across different structures of the nervous system and different species (62). Pieces of evidence from flies support this model (124), (105).

6.C.1 Molecular mechanisms linked to habituation

Different ISIs exert differential effects on habituation

Directly opposing effects on short-term habituation of the same response component can be exerted by the same molecules, when trained at different ISIs. A recent study (125) revealed that different molecules mediate different effects on habituation at different ISIs. The *C. elegans* homologs of calcium/calmodulin-dependent protein kinases (*cmk-1*) and O-linked *N*-aketylglucosamine transferase *ogt-1* both function to promote habituation of response distance (reversal response to repeated non-localized mechanosensory stimuli-tap- withdrawal reflex, (74)) at a longer 60 s ISIs and impede habituation of response distance to shorter 10 s ISIs stimulation.

Dopamine mediates reversal reflex response in *C. elegans* after mechanosensory tap stimuli

Nonlocalised mechanosensory tap stimuli (or vibration of the growth substrate) elicit a reversal—a switch from forward to backward locomotion in *C. elegans.* With repeated stimulation, the response habituates and the worm no longer moves backwards (escape reflex or tap habituation) (74). Studies from Sanyal et al., (117) revealed that dopamine acted through the G protein-coupled dopamine receptor DOP-1 on the mechanosensory neurons to trigger a downstream G_q/phospholipase C second-messenger signal transduction pathway that mediates habituation. Dopamine G_q signaling affected habituation of the likelihood of eliciting a response (response probability). Moreover Kindt et al., (116) revealed a more specific role for dopamine in regulating habituation. Dopamine only affected habituation of the tap reflex response probability in the presence of food. They showed that the worms' food source is physically detected by a transient receptor potential channel in dopamine neurons of the animal and dopamine release from these neurons mediated the context specificity. Further, the dopamine neurons could in turn be excited by the touch receptor neurons during habituation training, forming a positive feedback loop capable of integrating context and experience into ongoing behavior. Dopamine implication in habituation is supported by other studies, in different habituation paradigms as well (126), (99).

Calcium as a modulator of habituation

Using the calcium sensitive protein cameleon in *C. elegans*, (116) Kindt et al., demonstrated that calcium serves as another habituation modulator. More specifically, worms expressing a high calcium affinity version of cameleon (YC2.12) in their touch cells habituated faster than animals expressing a low calcium affinity version (YC3.12). YC3.12 is identical to YC2.12, except one of the four conserved Ca^{2+}-binding sites in the calmodulin domain is mutated, which leads to faster calcium release. In line with the above, a recent study demonstrated that calcium activated potassium channels (BK channels) affect habituation of the acoustic startle reflex and of the exploratory locomotor behavior in the open field box in mice (107).

Stimulus modality but not context, affects habituation

According to recent evidence from mice, context cues are not important for habituation of the acoustic reflex, since changing in context did not disrupt the process (102). On the other hand, habituation is stimulus modality dependent, as it differs for different types of stimuli.

Other parameters that can affect habituation include stressors (127), or the distance of the stimulus to the body (128), as well as the physiological state of the animal (129).

In conclusion, it is clear that habituation of different response components is mediated by different molecular mechanisms and that the nervous system recruits different mechanisms for optimal habituation in different external and internal contexts. Moreover, the "simplest form of learning" is actually very complicated, maybe because ignoring a stimulus is critical both for survival and for complex forms of learning and memory so that nervous system has evolved multiple independent mechanisms. Another explanation could be that multiple habituation mechanisms facilitate shifts in behavioral strategy. For this reason, it would be extremely important to enhance all of these mechanisms with the identification of genes implicated in habituation.

6.D. Habituation impairments and schizophrenia

Schizophrenia (SD) is a poorly understood psychiatric disease presenting multiple manifestations. Approximately 0.5% of the general population or over 24 million globally, suffer from different manifestations of Schizophrenia. The disease apparently involves both genetic and environmental components, with the genetic component thought to represent about 80% of the risk to develop the condition (130).

As mentioned before, defective habituation, is the retention of the value of an inconsequential stimulus beyond the time typical for the onset of the attenuated response

and is thought to underlie SD (131),(132),(133),(134). Since habituation underlies gated selective attention and discrimination between novel and pre-experienced stimuli (63, 131), it represents a form of adaptive behavioral flexibility. This adaptive behavioral flexibility is defective in SD individuals as pre-experienced stimuli retain their value illustrated by PPI test results (135-139). More specifically, SD patients present characteristic deficits in devaluing and attenuating responses to repeated stimulation including the startle response in the PrePulse inhibition (PPI) test (132),(140),(66),(138). PPI characterizes and measures the adaptive ability of the nervous system of humans and animals (141) to suppress the startle response to any sudden intense stimulus if it was preceded by a similar, albeit of lower intensity stimulus (prepulse) and is detected in numerous species including humans (141).

In Drosophila, habituation to repetitive inconsequential electric footshocks (55) engages and occurs in particular higher brain structures of the fly and therefore represents habituation of Central Nervous System (CNS) circuits rather than peripheral sensory neurons in a manner akin to circuits thought to be involved in PPI responses in humans (141). Studying footshock habituation in Drosophila is thus reminiscent of the PPI assays used in SD patients.

Apart from SD, recent studies indicate that habituation deficits are linked to intellectual disability (142), (143-145), autism (146),(147) and AHDH (Attention Deficit Hyperactive Disorder) (148). Because of that the need to decipher habituation mechanisms is imperative.

6.F. Modelling Schizophrenia in flies

Schizophrenia (SD) is a perplexing and heterogeneous psychiatric disease presenting various manifestations, the best known symptoms of which include hallucinations and illusions, and which may overlap with other disorders. The disease involves genetic as well as environmental factors, with the genetic ones representing about 80% of the risk to develop the disease (130). Despite the fact that a great amount of genetic evidence comes from disease-associated polymorphisms from Genome-wide Association studies (GWAS), the genetic contribution is not well understood, because the condition is apparently multigenic and has many manifestations (149).

At present, it is impossible to establish such behavioral phenomena in flies and this is the reason why modeling these features of the disease in *Drosophila* is unfeasible. Yet, these higher level behavioral phenomena must-at least to some degree- underlie elemental neurobiological processes. In agreement with this, SD has a strong genetic component. At the same time, an amount of interesting genetic loci has started to emerge, thus providing the opportunity to use flies for understanding the functions of the affected genes (150). Therefore, since implicated loci are being identified, *Drosophila* has

the potential to shed light on how these genes might underlie the cellular and neurobiological mechanisms of the disease. Unfortunately, one of the strongest schizophrenia candidate genes, DISC1 does not have an ortholog in flies (151). Therefore, either DISC1 is specific to the deuterostome lineage of animals (including humans), or protostomes along with *Drosophila* might have a different DISC1 ortholog, laborious to be found by sequence homology searches. However, flies do have well studied homologs of some known DISC1 binding partners, as the cAMP phosphodiesterase PDE4B, also implicated in psychiatric diseases (152). Interestingly, *Drosophila* PDE4B ortholog, dunce, is a learning and memory mutant (7).

A different gene implicated in SD is *dysbindin* (153). Fortunately, *Drosophila* has provided a great deal of functional information on *dysbindin* that may be pertinent to a causative role in SD. Encoded by the DTNBP1 locus, *dysbindin*, is a binding partner of *dystrobrevin* and a component of the BLOC-1 complex that it is implicated in trafficking in the endosomal–lysosomal pathway (154). *Dysbindin* mutations showed moderate effects on baseline neurotransmission, but serious impairment of this homeostatic regulation, which is likely to be a key process in regulating the strength of synaptic transmission. This data provide a valid model of how *dysbindin* mutations might be implicated in neurobiological defects that lead to the behavioral symptoms of SD (155).

Conclusively, the usefulness of Drosophila as a model to gain mechanistic insights into SD has just started to grow. Expecting flies to be an accurate but simple model for SD is too naive. Nonetheless, as more susceptibility genes are identified, the need to understand their role is getting bigger. Drosophila provides great possibilities for this. In addition, as the neurobiological knowledge concerning SD and related diseases emerges, Drosophila does offer the opportunity to study the pertinent neurobiological processes in a model with powerful genetic and cell biological tools (156). Finally, because schizophrenia patients, as well as other neuropsychiatric disorder patients (migraines, autism spectrum disorder, Parkinson's disease), often show habituation impairments (60),(157),(158),(159), understanding habituation mechanisms will provide important insight to understanding these perplexing diseases.

Aim of this thesis

The aim of this thesis was the discovery of new genes implicated in footshock habituation, by performing a genetic screen using the Minos transposable element in *Drosophila melanogaster*.

Results

1. Transposition of the Minos element

The initial goal of this thesis was to generate a considerably large number of Minos insertions and consequently to screen them in order to identify genes implicated in footshock habituation. For this reason, we initially used the modified Minos element, MiExT (Metaxakis, unpublished data) which serves as a gene trap system, shown in **Fig.1.** In order to transpose the MiExT transposable element, we performed crosses according to Metaxakis et al.,(160) using the Minos transposase.

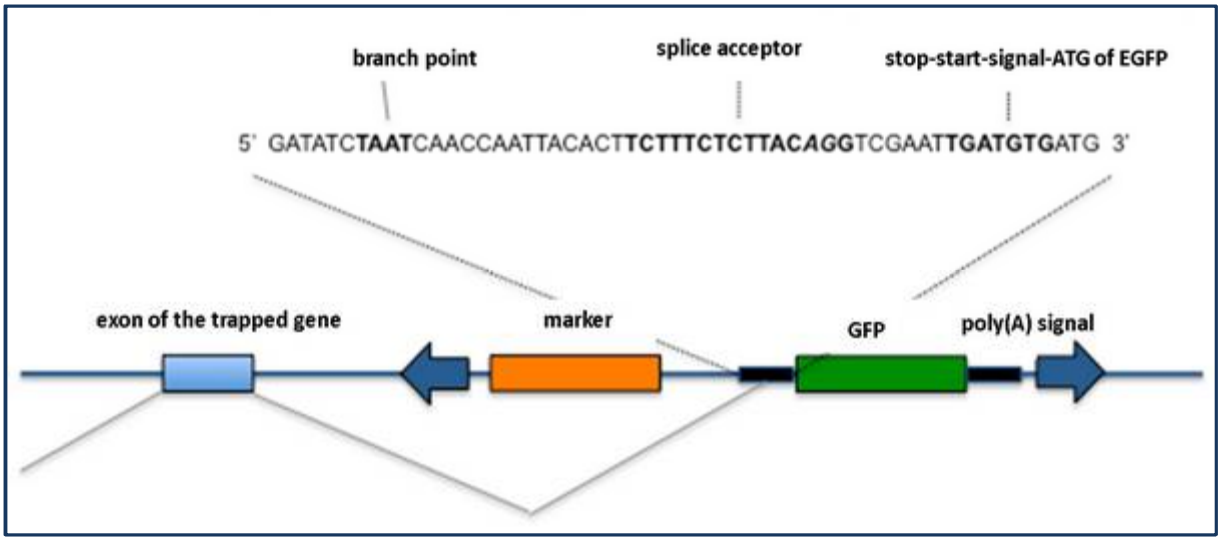

Fig.1. Schematic insertion of the MiExT1 into an intron. The w gene of *Drosophila melanogaster* serves as a marker to identify the transposon into the genome. The insertion of MiExT1 leads after splicing to GFP production and early termination of transcription of the trapped gene.

Unexpectedly, the transposition rates where too low. Since the MiExT transposon did not provide us the insertions needed for our screen, we sought alternative sources of transposition-mediated mutants to perform the screen. We wanted to keep the Minos-based transposons because of its non-biased insertional preference and because of the fact that the transposase can provide precise integration as well as stable transposition effects with great efficiency (161),(160). Since Venken et al., (35) detailed its use and advantages, we decided to use the highly versatile MiMIC transposon (**Fig.5**, Introduction). After ordering and expanding all the necessary stocks, we performed

crosses as described in **Fig. 2**. Hence, we created a great number of new potential insertion lines which were afterwards analyzed by inverse PCR. After sequencing the i-PCR products, we found that all the insertions were in the vicinity of the initial one (local jumps). In order to perform a genetic screen, we needed insertions all over the genome and unfortunately the MiMIC transposon system could not provide them. Therefore, instead of *de novo* transposing MiMIC and thus creating new insertions, we opted for the use of already existing insertions, made by Venken et al. (35).

The next step included a thorough look through the bibliography in order to search for genes expressed in the CNS and potentially implicated in habituation/learning, or for genes interacting with known genes associated with different types of habituation in *Drosophila melanogaster*. Moreover, we looked for genes implicated in habituation in other organisms, as well as genes found to be involved in human schizophrenia and used FlyBase (the online bioinformatics database and primary repository of genetic and molecular data for Drosophila) to identify the genes from this initial list that have available MiMIC insertion lines. This resulted in the genes and MiMIC lines listed in **Table 1.**

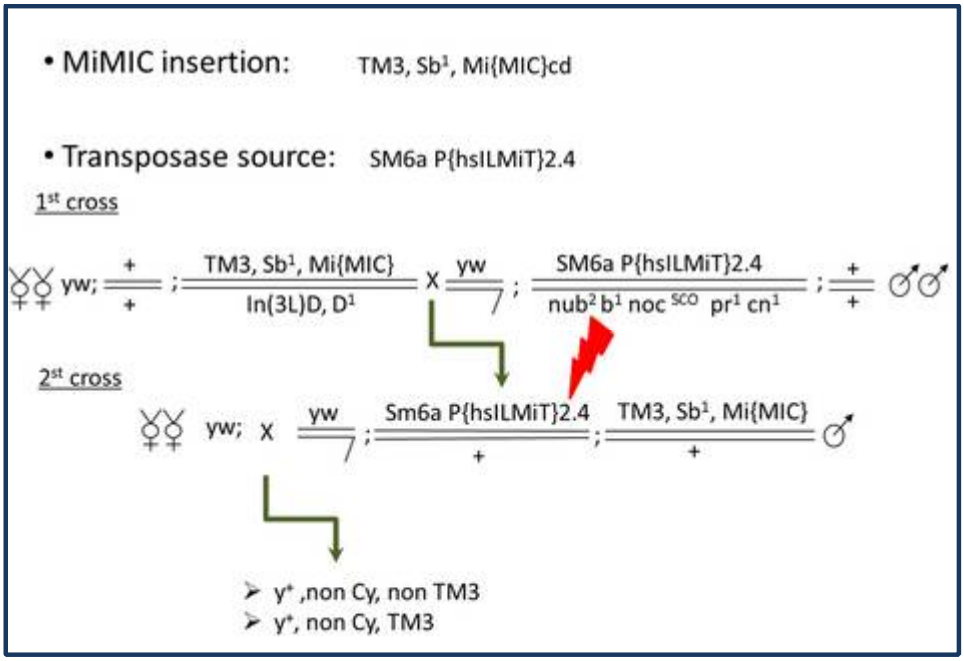

Fig.2. Crosses made for transposing the MiMIC transposon. At the first cross, females bearing a MiMIC insertion on the TM3 chromosome are crossed to males bearing the construct that produces transposase under a heat shock promoter. The female progeny is called "jumpstarter" because embryos or larvae are heat-shocked in order to move the transposon in their germ line cells. Jumpstarters are then crossed to yw flies and the progeny of this cross is scanned for a) y+, non Cy, non TM3 flies (jumps in chromosomes different than TM3, b) y+, non Cy, TM3 flies (local jumps).

Genes		MiMIC insertions
aos	argos	36267, 36995
arm	armadillo	44994
bab1	bric a brac 1	44736
Btk	Bruton's Tyrosine Kinase	34172, 36444, 37042, 34284
Cf2	Chorion factor 2	37710
cindr	CIN85 and CD2AP orthologue	40244
Csk	C-terminal Src kinase	44884
csw	corkscrew	41405
CtBp	C-terminal Binding Protein	44916
DAAM	Dishevelled Associated Activator of Morphogenesis	38567
Dg	Dystroglycan	42067, 42406
Dys	dystrophin	36944, 37029, 37037, 37109, 42464, 51243
Egfr	Epidermal growth factor receptor	36152
for	foraging	37776, 37926, 38112
Fur1	Furin 1	36401,51078, 42180, 60536
futsch	futsch	53073, 53409
gig	gigas	59563
Kah	Kahuli	34187
kel	kelch	41484
Khc	Kinesin heavy chain 73	34271, 59086
Kr	Kruppel	42077
Mef2	Myocyte enhancer factor 2	36201, 37229, 51069
mGluR	metabotropic Glutamate Receptor	32830
mim	missing-in-metastasis	41450
msn	misshapen	53778
Nedd4	Nedd4	44709
neur	neuralized	35950, 36196, 37345
nub	nubbin	37920, 42336
pcs	parcas	56709
Pkc53E	Protein C kinase 53E	42309
PKD	Protein Kinase D	37604
ptc	patched	32811
Ptp61F	Protein tyrosine phosphatase 61F	37014,37132, 42128,43037
Pvr	PDGF- and VEGF-receptor	37275

	related	
Ras85D	Ras oncogene at 85D	38026
rau	rau	52096, 53136
rut	rutabaga	54509
sno	strawberry notch	42190
sns	sticks and stones	35916, 36164
Src42A	Src oncogene at 42A	35877, 35990
Src64B	Src oncogene at 64B	37952
sty	sprouty	37183, 53064
sxc	super sex combs	34307
tau	tau	37602,56122
Trl	Trithorax-like	36041, 52049
wasp	wasp	42088

Table 1. Genes and their MiMIC insertions used in the screen for habituation mutants.

In conclusion, as it was not possible to create new MiMIC insertions that cover the whole genome, we finally confined our screen, using the already existing and available in FlyBase MiMIC insertions and focused on genes expressed in the Central Nervous System.

2. Behavioral screen using MiMIC insertions

After expanding all the stocks listed in **Table 1**, we used the shock habituation assay (55) to test if these mutants could habituate after 15 electric shocks or failed to do so. As a control line we used yw flies, since the MiMIC construct has been inserted in the yw background (they are mentioned as Mibg flies which corresponds to MiMIC background). Different lines were tested concurrently, but when a positive result was obtained, these putative mutant lines were tested separately in order to confirm the results. As illustrated in the example of **Fig.3**, our initial results suggested that insertions in *PKD*, *for* and *Src* were interesting.

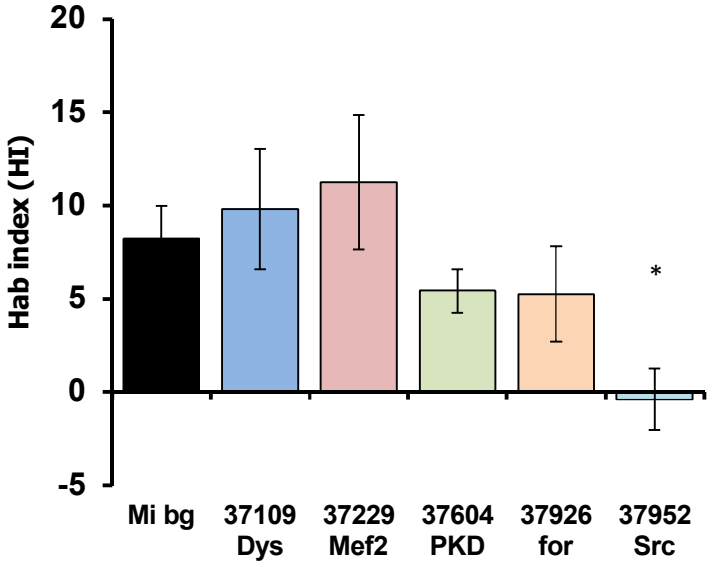

Fig.3. First behavioral output concerning MiMIC insertions in the following genes: *Dys*, *Mef2*, *PKD*, *for* and *Src*. Control flies exhibit a habituation index of 8,22 while the insertions of PKD, for and Src show habituation index of 5,4 , 5,3 and – 0.39 respectively. ANOVA $F_{(5,54)}$ = 3.5728, p=0.0078*.

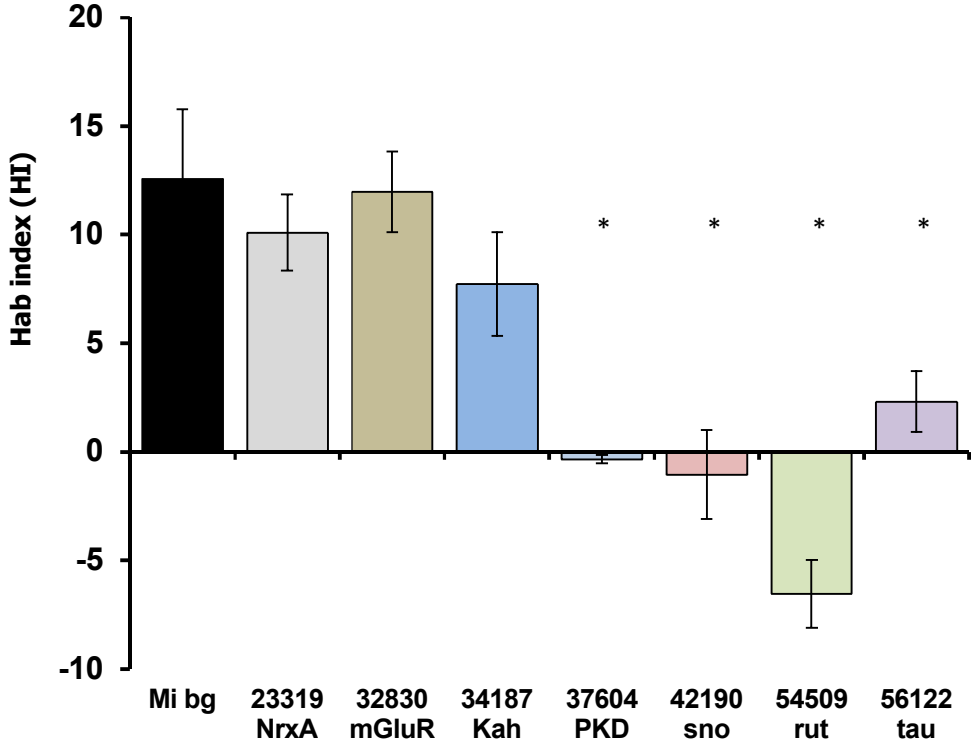

Fig.4. Second set of experiments. Insertion lines within the genes NrxA, mGluR and Kah habituate normally after 15 shocks while insertions into the PKD, sno, rut and tau loci are resistant to habituation after 15 shocks. ANOVA $F_{(7,61)}$ = 7.6613, p<0.0001*

In a different set of experiments, we verified that the PKD insertion failed to habituate and this was the case for the *sno*, *rut* and *tau* insertions as well, as illustrated in **Fig. 4**.

Finally, after testing many insertions in different loci, the screen culminated as presented in **Table 2**.

Gene	BDRC Stock #	verification by different mutants	verification by RNAi
arm	44994		
Btk29A	34172	#34284	#25791, #35159
for	38112		
Fur1	36401		
futsch	53409		
Ibm	34173		
kel	41484		
Pvr	37275		
rut	54509	*rut*^{2080}	#27035
Src64B	37952		
tau	37602	#56122, *tau*^{KO}	*tau*^{IR}
Wasp	42088		

Table 2. Genes emerging from the screen, which exhibit habituation failure after pre-exposure to 15 electric foot shocks. Some of the insertions mentioned were analyzed further. Moreover, mutations other than MiMIC insertions, as well as RNAi driven by pan-neuronal drivers were tested in order to validate the results.

3. Drosophila Bruton's Tyrosine Kinase Regulates Habituation Latency and Facilitation in Distinct Mushroom Body Neurons

Ilianna G. Roussou, Katerina Papanikolopoulou, Charalambos Savakis, and Efthimios M. C. Skoulakis

Introduction

Habituation is a form of adaptive behavioral plasticity that permits animals to ignore repetitive or prolonged non-reinforced stimuli (69);(64). Timely devaluation of such stimuli is the behavioral output of largely undefined molecular processes, apparently engaging multiple cellular systems (62). Because habituation underlies gated selective attention and discrimination between novel and pre-experienced stimuli (131), it represents a form of adaptive behavioral flexibility, reported defective in patients with migraines (162);(163), attention deficit hyperactivity disorder (67);(148), schizophrenia (SD),(138);(133) and autism spectrum disorders (ASD), (164);(165). Hence, defining molecular mechanisms that govern habituation is likely to contribute toward understanding the molecular etiology of these conditions.

To explore habituation mechanisms of CNS circuits in *Drosophila*, we developed a novel habituation paradigm to repetitive mild electric footshock (55). Habituation to repetitive footshock requires structurally and functionally intact mushroom bodies (MBs), neurons also essential for associative learning and memory (166). The MBs are comprised by ~2500 neurons per hemisphere subdivided into α/β, α′/β′ and γ subtypes (58). Because neurotransmission from α/β MB neurons is required to suppress premature habituation, we proposed that physiologically, it blocks devaluation of the repetitive footshock stimuli, hence required for habituation latency (55). However, whether other intrinsic or extrinsic MB neurons are required to facilitate habituation remained unclear.

To address this question and to identify proteins governing habituation within the MBs, we have conducted a genetic screen for mutants that present defective habituation. Here we report on the role of one of the proteins identified in the screen, Bruton's tyrosine kinase (dBtk), which belongs to the Src non-receptor kinase superfamily and is associated with agammaglobulinemia in humans (167). The *Drosophila dBtk29A* (dBtk) gene encodes two proteins by alternative splicing, dBtk type 1 and dBtk type 2, with the latter considered orthologous to the human protein (168). dBtk consists of conserved SH2, SH3 and kinase domains, whereas an N-terminal plekstrin homology (PH) domain characterizes the larger type 2 protein (169). dBtk is implicated in many essential functions in *Drosophila* (168);(170);(171);(172), including regulation of the actin cytoskeleton (169). Although dBtk is highly expressed in the fly CNS, there is limited information regarding its functional role(s) therein (87); (173). Here we demonstrate acute differential roles for this kinase within distinct MB neuronal populations in the regulation of habituation dynamics to repeated footshock stimuli.

Materials and Methods

Drosophila *culture and strains*

Drosophila were cultured in standard wheat-flour-sugar food supplemented with soy flour and CaCl2 (55) at 18°C or 25°C. All MiMIC insertions were from the Bloomington Stock Center (BDRC; Indiana University; (35)) and they were backcrossed to y^1w^1 for at least seven generations before use in behavioral experiments. MBGal80 (54) was obtained from Ron Davis (Scripps Florida). The Btk-Gal4 (49182), dncGal4 (48571), and Btk RNAi stocks (35159 and 25791) were from BDRC. To generate the driver heterozygote controls for experiments with the RNAi-encoding transgenes, driver-bearing strains were crossed to their y^1v^1 (BDSC, 36303) background. The UAS-Btk lines (109-093 and 109-095) were from the Kyoto Stock Center (Kyoto Institute of Technology). VT44966-Gal4 (γ-driver) was from the Vienna *Drosophila* Resource Center (VDRC; Vienna Biocenter Core Facilities, 203571). The α′/β′ Gal4 drivers VT030604 (VDRC, 200228) and c305a were a kind gift from S. Waddell (University of Oxford). The glial driver repo-Gal4, the pan-neuronal drivers elav-Gal4 and Ras2Gal4, and the mushroom body specific drivers 247-Gal4, leo-Gal4, c739-Gal4, c772-Gal4 were described previously (174); (175). The $Gal80^{ts}$ transgene was added to the driver-bearing chromosomes by recombination or standard crosses as indicated.

Description of Gal4 expression patterns used in this work.

Elav: pan-neuronal expression in all developmental stages (FlyBase ID: FBrf0237128)

Ras2: throughout the larval and adult CNS, enriched in the adult MBs (175)

repo: all glia (FlyBase ID: FBrf0237128)

leo: adult α, α′, β, β′, γ MB neurons (176)

247: adult α, α′, β, β′, γ MB neurons (RRID:BDSC_50742)

dnc: adult α, α′, β, β′, γ MB neurons, scattered neurons in subesophageal ganglion and ventral optic lobes (177)

c772: adult α,β,γ MB neurons, antennal lobe, medulla, tritocerebrum (174)

c739: adult α, β MB neurons, antennal lobe, medulla, restricted protocerebral neurons, inferior neuropils (174)

VT44966: γ MB neurons, wedge neurons, superior lateral protocerebrum, gnathal neurons, medial bundle (178)

c305a: adult α′, β′ MB neurons, antennal nerve, medulla, restricted protocerebral neurons, inferior neuropil, gnathal neurons (174)

VT030604: adult α′, β′ MB neurons, gnathal neurons (178)

Behavioral assays

All flies used in behavioral experiments were tested 3–5 d after emergence. All experiments were performed under dim red light at 25°C and 65–75% relative humidity. To obtain animals for behavioral experiments Gal4 driver homozygotes were crossed *en masse* to strains carrying either UAS-btk, UAS-btk-RNAi, or UAS-shi^{ts} transgenes. Animals

expressing Gal80^{ts} (179) were raised at 18°C until hatching and then placed at 30°C for 2 d before testing. Flies carrying UAS-shi^{ts} were reared at 18°C and the dynamin was inactivated by incubation at 32°C for 30 min before the behavioral experiment.

Electric footshock avoidance. Experiments were performed as described before (55). Briefly, ~70 flies were placed at the choice point of a T-maze to choose for 90 s between an electrified and an otherwise identical inert standard copper grid. In the electrified grid, 45 V shocks were delivered every 5.15 s, each lasting 1.2 s. The avoiding fraction (AF) was calculated by dividing the number of flies avoiding the shock by the total number of flies.

Habituation to electric footshock. Habituation to electric shock experiments were performed as described before (55). Briefly, for the training phase ~70 flies were sequestered in the upper arm of a standard T-maze lined with an electrifiable grid. They were exposed to 15 1.2 s electric shocks at 45 V with a 5.15 s interstimulus interval. Air was not drawn through the tube during training to avoid association of the shocks with air. After a 30 s rest and 30 s for transfer to the lower part of the maze, the flies were tested by choosing between an electrified and an inert grid. Therefore, the earliest measures of post-training responses are 1 min after the flies received the last training stimulus. Testing was performed at the same voltage (45 V) as for training. During the 90 s choice period, 17–18 1.2 s stimuli were delivered to the electrified arm of the maze. At the end of the choice period, the flies in each arm were trapped and counted, and the habituation fraction (HF) was calculated by dividing the number of flies preferring the shock by the total number of flies, as above. Finally, the habituation index (HI) was calculated as (HF-AF) X 100% and therefore represents the change in footshock avoidance contingent upon prior footshock experience (habituation). Although the absolute avoidance score is variable, even for the same genotypes (Table 1), as expected for behavioral experiments performed over a significant time period, because the HI measures the relative change in avoidance within each genotype, it is not affected by such variability. In fact, failure to habituate, which is the primary phenotype reported herein, is a manifestation of maintained avoidance relative to that of naive flies of the same genotype.

Dishabituation. To distinguish habituation from fatigue or sensory adaptation, flies were dishabituated post-training with an 8 s puff [yeast odor (YO)] of air drawn at 500 ml/min over a 30% (w/v) aqueous solution of Brewer's yeast (Acros Organics) and then were submitted to testing.

Olfactory habituation. Olfactory habituation experiments were performed as detailed in (93). Avoidance of the aversive odorant 3-octanol (OCT) carried in an airstream of 500 ml/min in one arm of a standard T-maze versus air was assessed and an index (AF) was calculated. For the "training phase", ~70 flies were exposed in the upper arm of a standard T-maze to OCT for 4 min. After a 30 s rest period, the flies were lowered to the center of the maze for testing their osmotactic response by a choice of air versus OCT. At

the end of the 90 s choice period the flies in each arm were trapped counted and HF and HI were calculated as described.

Pharmaceutical treatments

The Btk inhibitor Ibrutinib (Selleck Chemicals) and the antipsychotic drugs clozapine (Sigma-Aldrich) and risperidone (Tocris Bioscience) were diluted in DMSO and mixed at the indicated final concentrations in Brewer's yeast (Acros Organics) aqueous paste. The concentration ranges used bracketed analogous concentrations as used for humans. Ibrutinib was used at 0.1, 1, and 10 μM; clozapine at 5 and 10 μM; and risperidone at 0.1, 1, and 10 μM. Flies were starved for 5 h in empty vials at 25°C before exposure to drug or vehicle-only containing yeast paste for 14–16 h. The following day, flies were transferred in normal food vials, trained, and tested as detailed for footshock habituation.

Western blots

Five adult female heads 1–3 d post-eclosion were homogenized in 1 X Laemmli buffer (50 mM Tris, pH 6.8, 100 mM DTT, 5% 2-mercaptoethanol, 2% SDS, 10% glycerol, and 0,01% bromophenol blue). The lysates were boiled for 5 min at 95°C, centrifuged at 10,000 X *g* for 5 min and separated by SDS-PAGE. Proteins were transferred to a PVDF membrane at 120 V for 80 min and probed with anti-dBtk antibody (169) at 1:4000 and anti-syntaxin (Syn) antibody (8C3; Developmental Studies Hybridoma Bank) at 1:3000. Rat and mouse HRP-conjugated antibodies were applied at 1:5000 and proteins were visualized with chemiluminescence (ECL Plus, GE Healthcare). Signals were measured with Bio-Rad Molecular Imager Chemidoc XRS+.

Confocal microscopy

BtkGal4 flies were crossed to UAS-mCD8-GFP (180) and progeny were used to examine the expression pattern of dBtk in the adult brain. Flies were dissected in cold PBS, fixed in 4% paraformaldehyde for 15 min, and imaged by laser-scanning confocal microscopy (Leica, TCS SP8). Images were captured using a 40 X /1.3 NA oil objective after 488 nm excitation and digital image resolution was set at 1024 X 1024. Image stacks were collected at 0.75 μm intervals to cover the entire brain. The images were converted to grayscale, inverted in Adobe Photoshop 3, and shown as maximum intensity projections derived from confocal stacks.

Statistical analysis and experimental design

For all experiments, controls and genetically matched experimental genotypes were tested in the same session in a balanced experimental design. The order of training and testing was randomized. When two genetic controls were used, we required an experimental result to be significantly different from both genetic controls. Untransformed (raw) data were analyzed parametrically with the JMP 7 statistical software package (SAS Institute). If significant, initial ANOVA tests were followed by planned comparisons [least square mean (LSM) contrast analyses] if they indicated significant differences among the genotypes and the level of significance was adjusted for the experiment-wise error rate as suggested by (181).

Results

dBtk mutants are defective in footshock habituation

In the footshock habituation paradigm (55), flies avoid the initial 2–8 repetitive stimuli, but their response declines rapidly to an asymptotic baseline as predicted (64), after 10–11 stimuli. This pre-exposure dependent attenuated avoidance after 15 footshocks relative to that of naive animals is quantified as a positive change in the HI of control flies in Figure 1*C* (open bar). Failure to establish habituation does not attenuate shock avoidance after shock pre-exposure and therefore yields the zero or negative difference from the naive response reported by the HI. Because the HI measures the relative change in avoidance within each genotype, it is not dependent on absolute 45 V avoidance levels, which can be variable (Table 1). Viable MiMIC (35) insertion mutants (34172-*dBtkM1*) in intron 2 of the *dBtk* gene (Fig. 1*A*), resulting in reduction of both protein isoforms in adult heads (Fig. 1*B*), did not attenuate shock avoidance following exposure to 15 stimuli, in contrast to controls and heterozygotes, indicating failure to habituate (Fig. 1*C*, $btk^{M1/M1}$; ANOVA: $F_{(2,58)}$=16.7450, p<0.0001; subsequent LSM: p=1.2X10^{-6} vs control). Mutants for a different insertion (34284-*btkM2*) in intron 4 (Fig. 1*A*), which has a milder effect on dBtk levels (Fig. 1*B*), habituated to the footshocks, albeit not to the same degree as controls (Fig. 1*D*, $btk^{M2/M2}$; ANOVA: $F_{(5,68)}$ = 13.3566, p<0.0001; subsequent LSM: p = 0.0144 vs control). In agreement with the behavior of $dBtk^{M1}$/+ (Fig. 1*C*, $dBtk^{M1}$/+; ANOVA: $F_{(2,58)}$=16.7450, p<0.0001; subsequent LSM: p = 0.4960 vs control), heterozygotes for a lethal insertion (37042-*btkL*) in intron 4 (Fig. 1*A*) presented normal habituation (Fig. 1D, btk^{L}/+; ANOVA: $F_{(5,68)}$ = 13.3566, p< 0.0001; subsequent LSM: p = 0.4495 vs control). It should be noted that although the shock AF is intrinsic to calculation of the HI, AFs for all genotypes used herein are collectively presented on Table 1.

To ascertain that the habituation defect is indeed consequent of reduction in dBtk levels and not unrelated mutations on the chromosome, we examined heteroallelic combinations of these independently isolated mutations. Significantly, hetero-allelics of the lethal btk^{L} with both viable btk^{M1} and btk^{M2} insertions failed to habituate to 15 footshocks (Fig. 1*D*; ANOVA: $F_{(5,68)}$ =13.3566, p <0.0001; subsequent LSM: p = 1.2 X 10^{-7} $btk^{M1/L}$ vs control and p<1.1X 10^{-6} $btk^{M2/L}$ vs control), indicating that indeed reduced dBtk in the CNS does not support normal footshock habituation.

Table 1. Collective avoidance indices and statistics

Genotype	Mean ± SEM	*t* Ratio	*p*
Fig. 1*C*. ANOVA: $F_{(2,58)} = 1.6020, p = 0.2106$			
c (control)	0.76 ± 0.03		
$btk^{M1}/+$	0.77 ± 0.05	0.106	0.9158
btk^{M1}/btk^{M1}	0.66 ± 0.07	1.5444	0.1281
Fig. 1*D*. ANOVA: $F_{(5,68)} = 0.8807, p = 0.4993$			
c (control)	0.61 ± 0.02		
$btk^{M2/M2}$	0.62 ± 0.04	−0.007	0.9945
$btk^{M1/M1}$	0.59 ± 0.05	0.4748	0.6365
$btk^{M1/ML}$	0.55 ± 0.05	1.0243	0.310
$btk^{M2/ML}$	0.53 ± 0.05	1.4211	0.1602
$btk^{ML}/+$	0.63 ± 0.03	−0.192	0.848
Fig. 1*E*. ANOVA: $F_{(3,60)} = 0.8603, p = 0.4670$			
0 μM	0.53 ± 0.03		
0.1 μM	0.49 ± 0.03	1.2032	0.2339
1 μM	0.55 ± 0.03	−0.291	0.7722
10 μM	0.49 ± 0.04	0.9707	0.3358
Fig. 1*F*. ANOVA: $F_{(3,62)} = 1.9514, p = 0.1312$			
c (control)	0.54 ± 0.04		
$btk^{M1/M1}$	0.67 ± 0.05	−1.737	0.0877
$btk^{M2/M2}$	0.51 ± 0.06	0.3651	0.7163
$btk^{ML}/+$	0.62 ± 0.06	−1.031	0.3066
Fig. 2*A*. ANOVA: $F_{(2,44)} = 1.3353, p = 0.2740$			
elavGAL4/+;UAS-btk^{RNAi7}/$GAL80^{ts}$	0.59 ± 0.05		
elavGAL4/+;$GAL80^{ts}$/+	0.61 ± 0.04	−0.237	0.8139
UASbtk^{RNAi7}/+	0.49 ± 0.07	1.3101	0.1973
Fig. 2*B*. ANOVA: $F_{(2,35)} = 2.0785, p = 0.1412$			
elavGAL4/+;UAS-btk^{RNAi2}/$GAL80^{ts}$	0.66 ± 0.04		
elavGAL4/+;$GAL80^{ts}$/+	0.72 ± 0.03	−1.105	0.2771
UASbtk^{RNAi2}/+	0.78 ± 0.03	−2.006	0.0531
Fig. 2*C*. ANOVA: $F_{(2,30)} = 1.100\ p = 0.3468$			
elavGAL4/+;UAS-btk^{RNAi7}/$GAL80^{ts}$	0.73 ± 0.05		
elavGAL4/+;$GAL80^{ts}$/+	0.63 ± 0.03	1.4796	1.1502
UASbtk^{RNAi-1}/+	0.68 ± 0.05	0.7939	0.4340
Fig. 2*D*. ANOVA: $F_{(2,27)} = 0.1719, p = 0.8431$			
Ras2GAL4,$GAL80^{ts}$/+; UASbtk^{RNAi}	0.67 ± 0.08		
Ras2GAL4, $GAL80^{ts}$/+	0.65 ± 0.05	0.1811	0.8578
UASBTK^{RNAi7}/+	0.70 ± 0.04	−0.386	0.703
Fig. 2*E*. ANOVA: $F_{(2,46)} = 2.1609, p = 0.1273$			
repoGAL4,$GAL80^{ts}$/UAS-btk^{RNAi}	0.63 ± 0.05		
repoGAL4,$GAL80^{ts}$/+	0.73 ± 0.03	−2.075	0.044
UASbtk^{RNAi7}/+	0.67 ± 0.03	−0.955	0.3449
Fig. 2*F*. ANOVA: $F_{(2,47)} = 3.2093, p = 0.0498$			
elavGAL4/+;MBG80,$GAL80^{ts}$/UASbtk^{RNAi}	0.71 ± 0.02		
elavGAL4/+; MBG80, $GAL80^{ts}$/+	0.63 ± 0.02	2.2266	0.031
UASbtk^{RNAi7}/+	0.71 ± 0.03	−0.085	0.932
Fig. 3*A*. ANOVA: $F_{(2,34)} = 0.5313, p = 0.5929$			
leoMBGAL4,$GAL80^{ts}$;UAS-btk^{RNAi7}/+	0.46 ± 0.09		
leoMB-GAL4, $GAL80^{ts}$/+	0.56 ± 0.07	−0.905	0.3723
UAS-btk^{RNAi7}/+	0.56 ± 0.07	−0.892	0.3788
Fig. 3*B*. ANOVA: $F_{(5,66)} = 2.7712, p = 0.0255$			
leoMBGAL4,btk^{M1}/+; GAL80ts/+ UN	0.65 ± 0.03		
leoMBGAL4,btk^{M1}/ btk^{M1}; GAL80ts/+ UN	0.50 ± 0.03	2.205	0.031
leoMBGAL4,btk^{M1}/ btk^{M1};GAL80ts,UASbtk^{5} UN	0.59 ± 0.05	0.9337	0.3541
leoMBGAL4,btk^{M1}/+; GAL80ts/+ IN	0.56 ± 0.04		
leoMBGAL4,btk^{M1}/ btk^{M1}; GAL80ts/+ IN	0.45 ± 0.04	−1.265	0.211
leoMBGAL4,btk^{M1}/btk^{M1};GAL80ts,UASbtk^{5} IN	0.62 ± 0.04	−0.914	0.364
Fig. 3*C*. ANOVA: $F_{(2,39)} = 0.5892, p = 0.5599$			
leoMBGAL4/+;UASbtk^{RNAi2}/$GAL80^{ts}$	0.65 ± 0.05		
leoMBGAL4/+;$GAL80^{ts}$/+	0.68 ± 0.03	−0.471	0.640
UAS-btk^{RNAi2}/+	0.61 ± 0.06	0.6403	0.5260
Fig. 3*D*. ANOVA: $F_{(2,42)} = 0.4747, p = 0.6256$			
247MBGAL4,$GAL80^{ts}$/UAS-btk^{RNAi7}	0.63 ± 0.03		
247MBGAL4,$GAL80^{ts}$/+	0.60 ± 0.02	0.9688	0.3385
UASbtk^{RNAi7}/+	0.61 ± 0.03	0.5817	0.5640

(*Table continues.*)

Table 1. Continued

Genotype	Mean ± SEM	*t* Ratio	*p*
Fig. 3*E*. ANOVA: $F_{(2,30)} = 0.2194, p = 0.8044$			
dncGAL4,$GAL80^{ts}$/ UASbtk^{RNAi7}	0.53 ± 0.02		
dncGAL4,$GAL80^{ts}$/+	0.51 ± 0.02	0.4624	0.6474
UASbtk^{RNAi7}/+	0.54 ± 0.03	−0.198	0.8443
Fig. 3*F*. ANOVA: $F_{(2,44)} = 1.1638, p = 0.3222$			
c772GAL4,$GAL80^{ts}$/ UASbtk^{RNAi7}	0.63 ± 0.03		
c772GAL4,$GAL80^{ts}$/+	0.54 ± 0.06	1.451	0.1542
UASbtk^{RNAi7}/+	0.57 ± 0.03	1.1173	0.2702
Fig. 3*G*. ANOVA: $F_{(2,43)} = 1.891, p = 0.1766$			
UASbtk^{RNAi-1}/c739GAL4,$GAL80^{ts}$	0.57 ± 0.05		
c739GAL4,$GAL80^{ts}$/+	0.46 ± 0.04	1.8657	0.0692
UASbtk^{RNAi7}/+	0.53 ± 0.04	0.6998	0.488
Fig. 3*H*. ANOVA: $F_{(2,47)} = 3.0762, p = 0.0559$			
γ lobeGAL4/+;UASbtk^{RNAi7}/$GAL80^{ts}$	0.58 ± 0.03		
γ lobe GAL4/+;$GAL80^{ts}$/+	0.49 ± 0.03	2.0924	0.0421
UASbtk^{RNAi7}/+	0.59 ± 0.03	−0.238	0.8133
Fig. 3*I*. ANOVA: $F_{(2,28)} = 1.0786, p = 0.3548$			
c305aGAL4/+;UASbtk^{RNAi7}/$GAL80^{ts}$	0.77 ± 0.03		
c305a GAL4/+;$GAL80^{ts}$/+	0.71 ± 0.02	1.3002	0.2049
UASbtk^{RNAi7}/+	0.77 ± 0.04	0.0361	0.9715
Fig. 3*J*. ANOVA: $F_{(2,49)} = 2.5477, p = 0.0156$			
VT030604GAL4/+, UASbtk^{RNAi7} 18°C	0.74 ± 0.03		
VT030604GAL4/+, UASbtk^{RNAi7} 25°C	0.67 ± 0.02	1.9623	0.0557
VT030604-GAL4/+, UAS-btk^{RNAi7} 18 > 30°C	0.78 ± 0.03	−0.972	0.3361
Fig. 3*K*. ANOVA: $F_{(1,25)} = 9.7589, p = 0.0046$			
c305aGAL4-UAS shi^{ts} UN	0.85 ± 0.03		
c305aGAL4-UAS shi^{ts} IN	0.75 ± 0.01	−3.124	**0.0046**
Fig. 4*A*. ANOVA: $F_{(5,104)} = 4.7413, p = 0.0006$			
control 6 sh	0.79 ± 0.04		
$btk^{M1/M1}$ 6 sh	0.63 ± 0.04	2.9535	**0.0039**
control 10 sh	0.69 ± 0.03		
$btk^{M1/M1}$ 10 sh	0.60 ± 0.04	1.6587	0.1003
control 15 sh	0.73 ± 0.02		
$btk^{M1/M1}$ 15 sh	0.58 ± 0.04	2.9818	**0.0036**
Fig. 4*B*. ANOVA: $F_{(8,156)} = 2.8880, p = 0.0051$			
UASbtk^{RNAi7}/elavGAL4;$GAL80^{ts}$ 6 sh	0.82 ± 0.02		
elavGAL4;$GAL80^{ts}$/+ 6 sh	0.66 ± 0.03	3.7031	**0.0003**
UAS-btk^{RNAi-1}/+ 6 sh	0.71 ± 0.04	2.5227	0.0127
UASbtk^{RNAi7}/elavGAL4;$GAL80^{ts}$ 10 sh	0.77 ± 0.02		
elavGAL4;$GAL80^{ts}$/+ 10 sh	0.66 ± 0.03	2.2533	0.0257
UAS btk^{RNAi7}/+ 10 sh	0.66 ± 0.06	2.0069	0.0466
UASbtk^{RNAi7}/elavGAL4;$GAL80^{ts}$ 15 sh	0.73 ± 0.04		
elavGAL4;$GAL80^{ts}$/+ 15 sh	0.74 ± 0.03	−0.171	0.8644
UASbtk^{RNAi-1}/+ 15 sh	0.70 ± 0.03	0.6554	0.5132
Fig. 4*C*. ANOVA: $F_{(2,28)} = 1.2620, p = 0.2999$			
0 μM	0.58 ± 0.05		
0.1 μM	0.64 ± 0.04	−0.832	0.4129
1 μM	0.68 ± 0.04	−1.588	0.1245
Fig. 4*D*. ANOVA: $F_{(2,30)} = 0.0147, p = 0.9854$			
Habituation,15 shocks	0.76 ± 0.02		
YO dishabituation	0.77 ± 0.02	−0.147	0.8839
AVD after yeast puff	0.77 ± 0.02	−0.147	0.8839
Fig. 4*E*. ANOVA: $F_{(2,30)} = 0.0147, p = 0.9854$			
$btk^{M1/M1}$ habituation 6 sh	0.68 ± 0.03		
$btk^{M1/M1}$ Dishabituation 6 sh	0.68 ± 0.03	0	1
$btk^{M1/M1}$ habituation 10 sh	0.73 ± 0.04		
$btk^{M1/M1}$ Dishabituation 10 sh	0.73 ± 0.03	0.0617	0.9511
$btk^{M1/M1}$ AVD after yeast puff	0.73 ± 0.04	−1.102	0.2772
Fig. 5*A*. ANOVA: $F_{(5,119)} = 3.8885\ p = 0.0027$			
leoGAL4/+;UASbtk^{RNAi7}/$GAL80^{ts}$ UN 6 sh	0.81 ± 0.02		
leoMBGAL4/+; UASbtk^{RNAi7}/$GAL80^{ts}$ IN 6 sh	0.78 ± 0.02	1.2528	0.2128
leoMBGAL4/+; UASbtk^{RNAi7}/$GAL80^{ts}$ IN 10 sh	0.82 ± 0.01		
leoMBGAL4/+; UASbtk^{RNAi7}/$GAL80^{ts}$ UN 10 sh	0.75 ± 0.02	3.053	**0.0052**
leoMBGAL4/+; UASbtk^{RNAi7}/$GAL80^{ts}$ IN 15 sh	0.82 ± 0.01		
leoMB-GAL4/+; UASbtk^{RNAi7}/$GAL80^{ts}$ UN 15 sh	0.75 ± 0.02	3.053	**0.0028**

(*Table continues.*)

Table 1. Continued

Genotype	Mean ± SEM	*t* Ratio	*p*
Fig. 5B. ANOVA: $F_{(5,77)} = 0.2798$, $p = 0.9227$			
leoG4,btk^{M1}/btk^{M1},G80ts,UASbtk^{5} UN 6 sh	0.69 ± 0.03		
leoG4,btk^{M1}/btk^{M1},G80ts, UASbtk^{5} IN 6 sh	0.71 ± 0.03	−0.391	0.6966
leoG4,btk^{M1}/btk^{M1},G80ts,UAS-btk^{5} UN 10 sh	0.69 ± 0.03		
leoG4,btk^{M1}/btk^{M1},G80ts,UAS-btk^{5} IN 10 sh	0.72 ± 0.03	−0.759	0.4505
leoG4,btk^{M1}/btk^{M1},G80ts,UAS-btk^{5} UN 15 sh	0.69 ± 0.03		
leoG4,btk^{M1}/btk^{M1},G80ts,UAS-btk^{5} IN 15 sh	0.72 ± 0.03	−0.759	0.4505
Fig. 5C. ANOVA: $F_{(5,77)} = 1.1341$, $p = 0.3503$			
UAS-btk^{RNAi7}/c739-GAL4,GAL80^{ts} UN 6 sh	0.73 ± 0.02		
UAS-btk^{RNAi7}/c739-GAL4,GAL80^{ts} IN 6 sh	0.72 ± 0.02	0.4393	0.6617
UAS-btk^{RNAi7}/c739-GAL4,GAL80^{ts} UN 10 sh	0.74 ± 1.01		
UAS-btk^{RNAi7}/c739-GAL4,GAL80^{ts} IN 10 sh	0.70 ± 0.02	1.2977	0.1985
UAS-btk^{RNAi7}/c739-GAL4,GAL80^{ts} UN 15 sh	0.74 ± 1.01		
UAS-btk^{RNAi7}/c739-GAL4,GAL80^{ts} IN 15 sh	0.70 ± 0.02	1.2977	0.1985
Fig. 5D. ANOVA: $F_{(5,82)} = 1.3274$ $p = 0.2614$			
c305aGAL4,GAL80^{ts}/UAS-btk^{RNAi7} UN 6 sh	0.78 ± 0.02		
c305aGAL4,GAL80^{ts}/UAS-btk^{RNAi7} IN 6 sh	0.74 ± 0.02	1.3687	0.1751
c305aGAL4,GAL80^{ts}/UAS-btk^{RNAi7} UN 10 sh	0.78 ± 0.02		
c305aGAL4,GAL80^{ts}/UAS-btk^{RNAi7} IN 10 sh	0.74 ± 0.02	1.5464	0.1261
c305aGAL4,GAL80^{ts}/UAS-btk^{RNAi7} UN 15 sh	0.78 ± 0.02		
c305aGAL4,GAL80^{ts}/UAS-btk^{RNAi7} IN 15 sh	0.74 ± 0.02	1.5222	1.1321
Fig. 6A. ANOVA: $F_{(2,28)} = 1.1989$, $p = 0.3176$			
0 μM	0.37 ± 0.04		
5 μM	0.45 ± 0.04	−1.45	0.1591
10 μM	0.43 ± 0.03	−1.139	0.2652
Fig. 6B. ANOVA: $F_{(2,30)} = 0.8493$, $p = 0.4384$			
0 μM	0.50 ± 0.05		
5 μM	0.54 ± 0.05	−0.624	0.5376
10 μM	0.46 ± 0.03	0.5694	0.5736
Fig. 6C. ANOVA: $F_{(3,44)} = 1.3657$, $p = 0.2667$			
0 μM	0.50 ± 0.03		
0.1 μM	0.57 ± 0.06	−1.432	0.1598
1 μM	0.56 ± 0.02	−1.373	0.1772
10 μM	0.50 ± 0.03	−0.063	0.9502
Fig. 6D. ANOVA: $F_{(2,26)} = 8.8963$, $p = 0.0013$*			
0 μM	0.71 ± 0.03		
5 μM	0.53 ± 0.07	2.7508	**0.0111**
10 μM	0.78 ± 0.03	−1.216	0.0243
Fig. 6E. ANOVA: $F_{(2,27)} = 1.3673$, $p = 0.2732$			
c305aGAL4/+;UAS-btk^{RNAi7}/GAL80^{ts}	0.66 ± 0.04		
c305aGAL4/+;UAS-btk^{RNAi7}/GAL80^{ts} Clz	0.73 ± 0.03	−1.54	0.1361
c305-GAL4/+;UAS-btk^{RNAi-7}/GAL80^{ts} Ris	0.72 ± 0.03	−1.26	0.2193
Fig. 6F. ANOVA: $F_{(2,26)} = 2.2671$, $p = 0.1254$			
c739GAL4/+;UAS-btk^{RNAi7}/GAL80^{ts}	0.66 ± 0.04		
c739GAL4/+;UAS-btk^{RNAi7}/GAL80^{ts} Clz	0.73 ± 0.03	1.6255	0.1171
c739GAL4/+;UAS-btk^{RNAi7}/GAL80^{ts} Ris	0.72 ± 0.03	−0.378	0.7085
Fig. 6G. ANOVA: $F_{(5,95)} = 1.8751$, $p = 0.1065$			
$btk^{M1/M1}$ 6 sh	0.44 ± 0.05		
$btk^{M1/M1}$ Clz 6 sh	0.43 ± 0.02	0.3073	0.7593
$btk^{M1/M1}$ 10 sh	0.43 ± 0.05		
$btk^{M1/M1}$ Clz 10 sh	0.45 ± 0.03	−0.352	0.726
$btk^{M1/M1}$ 15 sh	0.20 ± 0.04		
$btk^{M1/M1}$ Clz 15 sh	0.43 ± 0.03	−2.527	0.0133
Fig. 6H. ANOVA: $F_{(5,73)} = 28.6620$, $p < 0.0001$*			
$btk^{M1/M1}$ 6 sh	0.35 ± 0.03		
$btk^{M1/M1}$ Ris 6 sh	0.63 ± 0.03	−6.509	**1.1×10^{-8}**
$btk^{M1/M1}$ 10 sh	0.36 ± 0.02		
$btk^{M1/M1}$ Ris 10 sh	0.64 ± 0.04	−6.91	**2.1×10^{-9}**
$btk^{M1/M1}$ 15 sh	0.38 ± 0.03		
$btk^{M1/M1}$ Ris 15 sh	0.68 ± 0.04	−6.64	**6.3×10^{-9}**
Fig. 6I. ANOVA: $F_{(3,52)} = 0.5727$, $p = 0.6356$			
0 μM 6 sh	0.76 ± 0.03		
10 μM 6 sh	0.72 ± 0.03	0.952	0.3458
0 μM 15 sh	0.78 ± 0.0.02		
10 μM 15 sh	0.73 ± 0.04	0.8233	0.4143

(Table continues.)

Table 1. Continued

Genotype	Mean ± SEM	*t* Ratio	*p*
Fig. 6J. ANOVA: $F_{(3,53)} = 65.5164$, $p < 0.0001$*			
0 μM 6 sh	0.78 ± 0.01		
10 μM 6 sh	0.85 ± 0.00	−10.26	**7×10^{-14}**
0 μM 15 sh	0.79 ± 0.01		
10 μM 15 sh	0.84 ± 0.00	−9.555	**7×10^{-13}**

Table 1. Avoidance of 45 V footshocks are shown for all genotypes per figure as indicated. Initial ANOVA: values are shown as well as individual statistical comparisons with the respective controls. Significant differences uncovered are highlighted in bold.

Because the human ortholog is implicated in cancers (182) and the kinase domain is highly conserved (168), covalent Btk inhibitors have been developed (183) and are available. Hence, dBtk activity was inhibited by feeding the commonly used inhibitor Ibrutinib to control flies. Compared with vehicle treated animals, Ibrutinib treatment resulted in strong abrogation of footshock habituation at low (Fig. 1*E*; 0.1 μM, ANOVA: $F_{(3,60)}$ = 5.4217, p= 0.0024; subsequent LSM: p =0.0012 vs 0 μM), but not high concentrations (Fig. 1*E*; ANOVA: $F_{(3,60)}$=5.4217, p=0.0024; subsequent LSM: p= 0.5368, 1 vs 0 μM, and p= 0.7965 10 vs 0 μM). The reason for this sharp concentration optimum is unclear at the moment, but at higher concentrations it may affect activities of potentially related proteins with opposing effects on habituation to footshock. Nevertheless, the results are consistent with the genetic evidence and strengthen the conclusion that dBtk kinase activity is required for habituation to repeated footshocks.

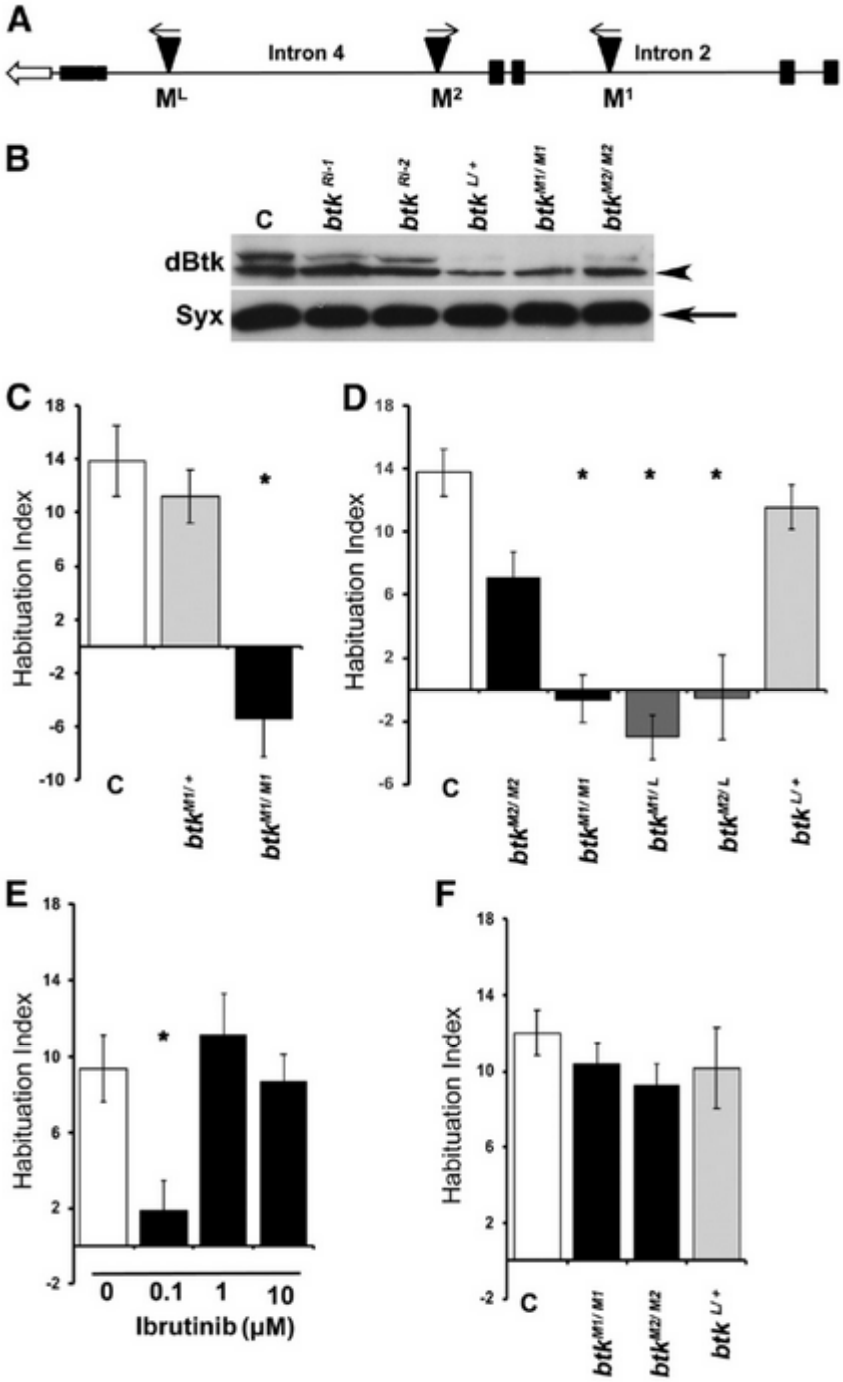

Fig 1. dBtk is essential for footshock habituation. ***A***, A schematic of the *Btk29A* (*dBtk*) genomic area where the transposon insertions used in this study, reside. The open arrow demonstrates the direction of transcription. Filled boxes correspond to exons, whereas lines correspond to the indicated introns. The triangles show the MiMIC insertions.M^1, The homozygous viable MI01270; M^2, the homozygous viable MI02160;M^L, the lethal insertion MI02966. ***B***, Western blot analysis of head lysates from five 3- to 5-d-old female *btk* mutants and pan-neuronally expressing RNAis as indicated. The arrowhead points to a band which migrates as predicted for the long (type 2) dBtk protein, whereas the arrow points to the apparent short (type 1) isoform (184). The following strains were used: C, Control (y^1w^*); btk^{Ri-1}, pan-neuronal expression under Elav-Gal4 of the BDSC 35159 RNAi-encoding transgene; btk^{Ri-2}, pan-neuronal expression under Elav-Gal4 of the BDSC

25791 RNAi-encoding transgene; *btk* ^{L}/+, heterozygotes for the lethal (MI02966) insertion; *btk* $^{M1/M1}$, homozygotes for the M^1 (MI01270) insertion; *btk* $^{M2/M2}$, homozygotes for the M^2 MI02160) insertion. The anti-dBtk antibody (Btk) recognizes two bands, the upper one of which is reduced the most in all mutants and RNAi-expressing animals, with the lower one also reduced, albeit to a lesser degree. Syntaxin 1 (Syx) is used as a loading control. ***C–F***, Habituation indices quantify the difference in footshock avoidance following exposure to 15 stimuli from that of same genotype naive flies and are shown as the mean $\pm$ SEM for the indicated number of repetitions (*n*). Stars indicate significant differences from controls as indicated in the text. ***C***, Homozygous *btk*$^{M1/M1}$ mutants perform significantly different from mutant heterozygotes and y^1w^* controls (***C***). $n \geq 16$ for all groups. ***D***, Complementation of the habituation failure among *dBtk* insertion mutants. Although the performance of *btk*^{L} heterozygotes was not significantly different from that of the y^1w^*controls (***C***), heteroallelics of this lethal insertion over both viable M^1 and M^2 insertions presented significant habituation deficits. $n \geq 9$ for all groups. ***E***, The Btk inhibitor Ibrutinib induces habituation deficits in y^1w^* control flies in a dose-specific manner. 0 represents y^1w^* animals fed the DMSO vehicle and compared with their performance; 0.1μM Ibrutinib induced a significant deficit, but higher doses did not. $n \geq 9$ for all groups. ***F***, *dBtk* mutants do not present habituation deficits to 4 min exposure of the aversive odorant OCT. $n \geq 12$ for all groups.

Because *dBtk* mutants were found to habituate prematurely in an olfactory jump reflex assay (87), we tested whether dBtk reduction resulted in deficient olfactory avoidance habituation. However, dBtk abrogation did not affect habituation to aversive odor (OCT) exposure (93), suggesting that the protein is specifically required for habituation to footshocks (Fig. 1*F*; ANOVA: $F_{(3,62)} = 0.8339$, $p = 0.4806$).

To independently validate these results, we used the TARGET system (179) to abrogate the protein in adult animals by transgene-mediated RNA-interference (RNAi). In fact, adult-specific pan-neuronal (Fig. 2A; ANOVA: $F_{(2,44)} = 6.1651$, p=0.0045; subsequent LSM: p=0.0016 and p=0.018 vs controls, respectively), dBtk attenuation recapitulated the footshock habituation failure of the mutants and also did not compromise habituation to the aversive odorant octanol (Fig. 2C; ANOVA: $F_{(2,30)} = 1.3588$, p = 0.2734). The latter supports the notion that dBtk functions specifically in footshock habituation. Identical results were obtained with the second RNAi-mediating transgene (Fig. 2B; ANOVA: $F_{(2,35)} =11.8202$, p<0.0001; subsequent LSM: p = 0.00068 and p= 0.00014 vs controls, respectively) and a different pan-neuronal driver (185), Ras2Gal4 (Fig. 2D; ANOVA: $F_{(2,27)} =11.2630$, p = 0.0003; subsequent LSM: p=0.0002 and p= 0.0008 vs controls, respectively).

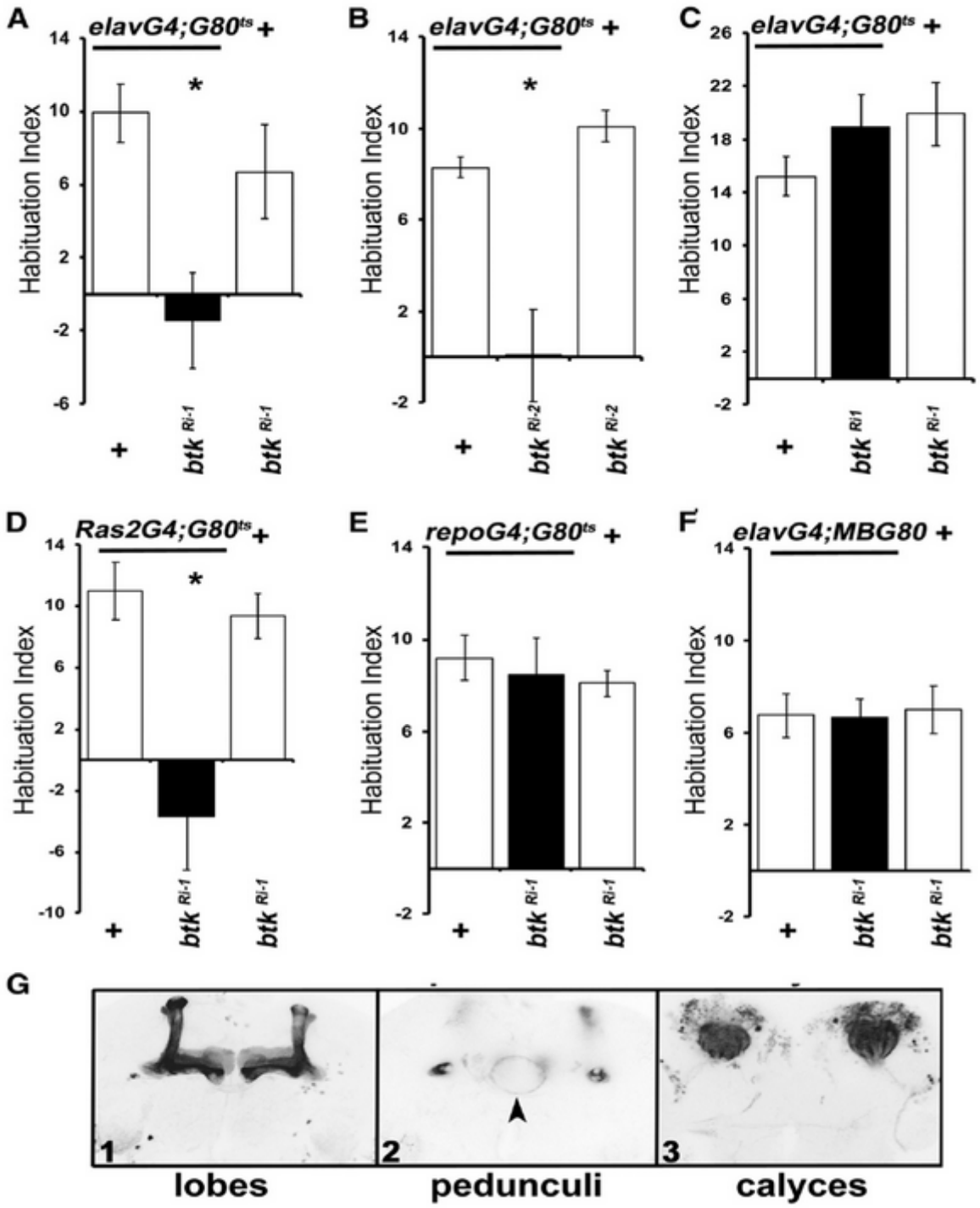

Figure 2. Adult-specific abrogation of dBtk results in deficient footshock habituation. HIs quantifying the difference in footshock avoidance following exposure to 15 stimuli from that of same genotype naive flies are shown as the mean±SEM for the indicated number of repetitions (*n*). All panels show the performance of animals expressing a *dbtk* RNAi-encoding transgene (btk^{Ri-1}/+) under the indicated driver (black bar), the driver heterozygotes (left open bars), and the RNAi-mediating transgene heterozygotes (+, right open bars). driver/+, Progeny from the cross of the w^{1118} background driver with 36303 y^1v^1, whereas for the btk^{Ri-1}/+, the y^1v^1 background of

btk^{Ri-1} was crossed to*w*^{1118} so that the two controls have equivalent backgrounds as the experimentals. Asterisks indicate significant differences from controls as detailed in the text. ***A***, Adult limited pan-neuronal expression of *btk*$^{Ri-1}$ eliminates habituation to 15 footshocks. $n \geq 11$ for all groups. ***B***, Adult-limited pan-neuronal expression of an independent RNAi-mediating transgene (*btk*$^{Ri-2}$), also results in habituation defects. $n \geq 9$ for all groups. ***C***, Adult-limited pan-neuronal expression of *btk*$^{Ri-1}$ does not yield defects in habituation to 4 min of OCT exposure. $n \geq 9$ for all groups.***D***, Flies expressing *btk*$^{Ri-1}$ under the pan-neuronal Ras2Gal4,Gal80^{ts} driver present adult-specific habituation defects compared with controls. $n \geq 9$ for all groups. ***E***, Adult limited *btk*$^{Ri-1}$ expression in glia did not precipitate deficits. $n \geq 14$ for all groups. ***F***, Pan-neuronal expression of *btk*$^{Ri-1}$, but at the exclusion of the MBs did not yield deficits in shock habituation. $n \geq 12$ for all groups. ***G***, dBtk is preferentially distributed within the MBs evidenced by mcD8-GFP expression under the control of the BtkG4 driver (BDSC, 49182). The arrowhead indicates faint expression in the ring neurons of the ellipsoid body at the level of the pedunculi.

Therefore, the failed habituation phenotype of dBtk mutants is not developmental in origin, but reflects an acute requirement for dBtk activity to facilitate habituation. Significantly, its abrogation in glia (Fig. 2E; ANOVA: $F_{(2,46)} = 0.2643$, p=0.7690), or constitutively sparing the MBs from dBtk attenuation under MBGal80 (Fig. 2F; ANOVA: $F_{(2,47)} = 0.0326$, p= 0.9679; (54)), did not affect habituation, suggesting that activity of the kinase is required within these neurons. Therefore, the habituation failure is not a consequence merely of the presence of the RNAi encoding transgenes, or drivers, but their induction not in glia, but within MB neurons, as suggested by Figure 2F and reported (Fig. 2G) expression of dBtk in these neurons.

dBtk functions within α′/β′ mushroom body neurons to facilitate footshock habituation

Neurotransmission from the α/β MB neurons is essential to prevent premature footshock habituation (55), but apparently not to facilitate its onset. So, we wondered where within the adult CNS is dBtk activity required for facilitation of footshock habituation. Initially, to unequivocally establish that dBtk activity solely within the MBs is essential for facilitation of footshock habituation, we attenuated it therein with the strong pan-MB driver Leo-Gal4 (176). This abolished footshock habituation (Fig. 3*A*; ANOVA: $F_{(2,34)} = 12.6248$, $p<0.0001$; subsequent LSM: $p= 0.0001$ and $p = 0.0002$ vs controls, respectively) and the result was independently validated with another RNAi transgene (Fig. 3*C*; ANOVA: $F_{(2,39)}= 60,9160$, $p<0.0001$; subsequent LSM: $p=1.76X10^{-12}$ and $p=6.55X10^{-10}$ vs controls, respectively), establishing the necessity of dBtk within the MBs for the process. This conclusion was strengthened by reinstating dBtk specifically within the MBs of adult *btk*^{M1} homozygotes, which fully reversed their deficient habituation (Fig. 3*B*; ANOVA: $F_{(5,66)} = 18.3727$, $p<0.0001$; subsequent LSM: $p = 6 X 10^{-6}$ leoMB-GAL4, btk^{M1}/ btk^{M1}; GAL80ts/+ induced vs leoMB-GAL4,btk^{M1}/+; GAL80ts/+ induced and $p=0.1918$ leoMB-GAL4,btk^{M1}/ btk^{M1}; GAL80ts,UAS-btk$^{short\ isoform}$ induced vs leoMB-GAL4,btk^{M1}/+; GAL80ts/+ induced). The transgene encodes the predominately neuronal type 1 short dBtk isoform (169), containing all conserved domains except the N-terminal PH. However, if the UAS-btk$^{short\ isoform}$ was not induced in adult animals the mutant

phenotype persisted (Fig. 3*B*; uninduced LSM: uninduced leoG4,btk^{M1}/btk^{M1}; G80ts/ UASbtk p=0.0367 vs leoG4,btk^{M1}/btk^{M1}; G80ts/+ and $p<$ 0.0001 with leoG4,btk^{M1}/+; G80ts/+controls, respectively). The acute requirement for dBtk within adult MBs for footshock habituation was further supported by attenuating its levels under the pan-MB drivers 247-Gal4 (Fig. 3*D*; ANOVA: $F_{(2,42)}$ =11.0752, p= 0.0001; subsequent LSM: p= 0.0032 and p = 4 X 10^{-5} vs controls, respectively) and dnc-Gal4 (Fig. 3*E*; ANOVA: $F_{(2,30)}$ = 12.4333, p = 0.0001; subsequent LSM: p = 0.0012 and p = 0.0001 vs controls, respectively), both of which precipitated pronounced habituation defects.

Given the role of neurotransmission from MB α/β neurons in preventing premature habituation (55), we wondered whether dBtk acts within these neurons to inhibit this process and consequently facilitate habituation. Thus, dBtk was attenuated within α/β neurons under the c772 (Fig. 3*F*; ANOVA: $F_{(2,44)}$ = 0.6731, p = 0.5156) and c739 (Fig. 3*G*; ANOVA: $F_{(2,43)}$ = 1.1146, p = 0.3378) drivers in αβ cortex or core neurons, respectively (186), but habituation was not altered, eliminating this hypothesis. In addition, dBtk attenuation within γ neurons also did not affect footshock habituation (Fig. 3*H*; ANOVA: $F_{(2,47)}$ =0.0266, p = 0.9737). Significantly however, dBtk abrogation within α'/β' MB neurons [Fig. 3*I*; ANOVA: $F_{(3,44)}$= 22.5186, p<0.0001; subsequent LSM: induced (IN) p<0.0001 vs both controls] abolished footshock habituation. In contrast, if the RNAi-mediating transgene remained uninduced, habituation was indistinguishable from controls (Fig. 3*I*; LSM: uninduced (UN) p= 0.0891 and p= 0.3397 vs the controls, respectively). Therefore, dBtk is not developmentally, but rather acutely required within α'/β' MB neurons to facilitate footshock habituation.

To verify this conclusion independently, we used a "split- Gal4" driver expressed specifically in α'/β' MB neurons and varied the expression of the RNAi-mediating transgene (btkRi-1) based on the optimum temperature for Gal4-mediated transcription (187). Raising and maintaining the flies at 18°C, should not yield appreciable btkRi-1 expression and presented normal habituation within the range of controls (**Fig. 1**).

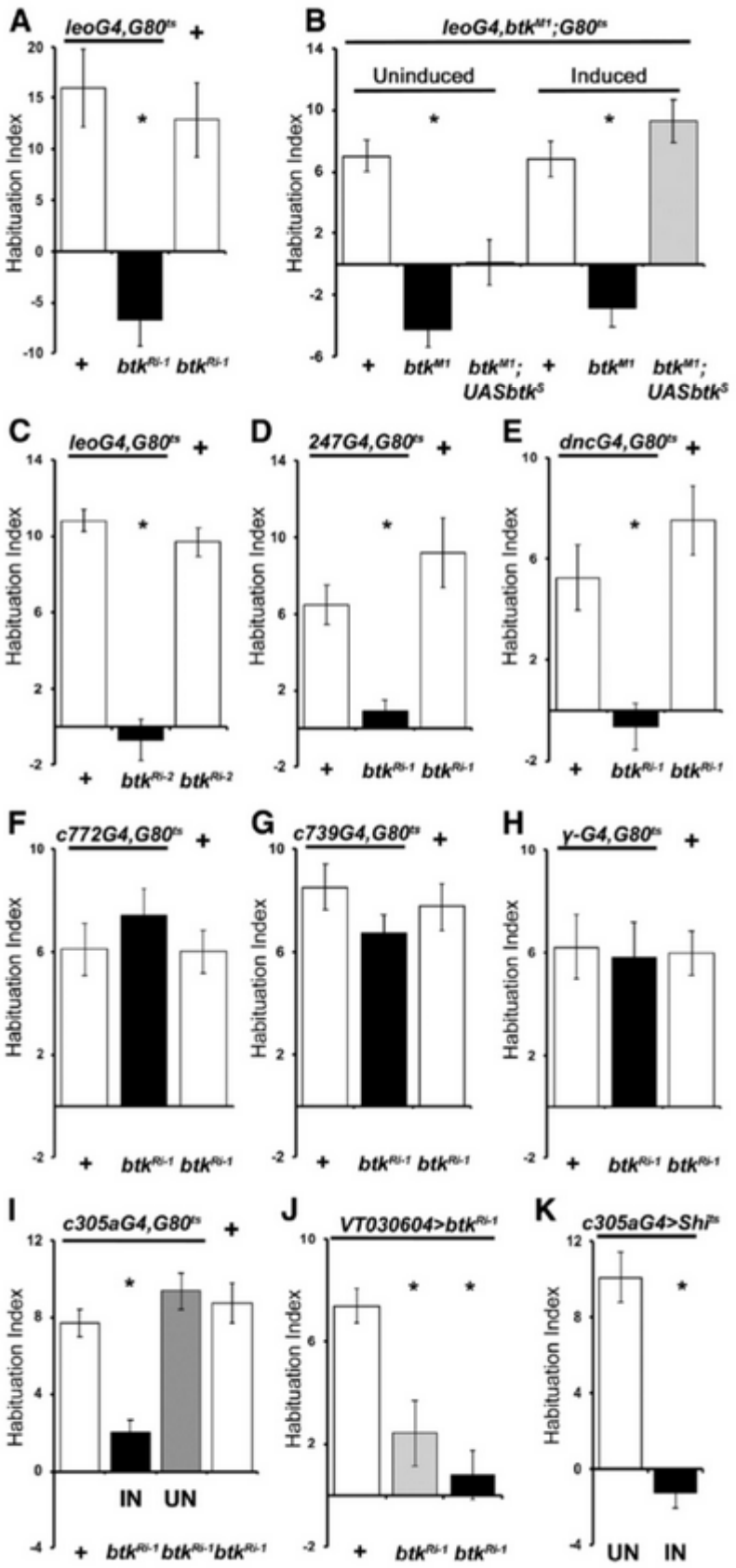
A
leoG4,G80ts
Habituation Index
+
btkRi-1 btkRi-1
B
leoG4,btkM1;G80ts
Uninduced
Induced
Habituation Index
+ btkM1 btkM1; UASbtkS + btkM1 btkM1; UASbtkS
C
leoG4,G80ts
Habituation Index
+ btkRi-2 btkRi-2
D
247G4,G80ts
Habituation Index
+ btkRi-1 btkRi-1
E
dncG4,G80ts
Habituation Index
+ btkRi-1 btkRi-1
F
c772G4,G80ts
Habituation Index
+ btkRi-1 btkRi-1
G
c739G4,G80ts
Habituation Index
+ btkRi-1 btkRi-1
H
γ-G4,G80ts
Habituation Index
+ btkRi-1 btkRi-1
I
c305aG4,G80ts
Habituation Index
IN UN
+ btkRi-1 btkRi-1 btkRi-1
J
VT030604>btkRi-1
Habituation Index
+ btkRi-1 btkRi-1
K
c305aG4>Shits
Habituation Index
UN IN

Figure 3. dBtk is acutely required within the α'/β mushroom body neurons to facilitate habituation to footshock. Habituation indices quantifying the difference in footshock avoidance following exposure to 15 stimuli from that of same genotype naïve flies are shown as the mean ± SEM for the indicated number of repetitions (*n*). All panels show the performance of animals expressing a *dbtk* RNAi-encoding transgene (btk^{Ri-1}/+) under the indicated driver (black bar), the driver heterozygotes (left open bars), and the RNAi-mediating transgene heterozygotes (+, right open bars). driver/+, Progeny from the cross of the w^{1118} background driver with 36303 y^1v^1, whereas for the btk^{Ri-1}/+, the y^1v^1 background btk^{Ri-1} was crossed to w^{1118} so that the two controls have equivalent backgrounds as the experimental. Asterisks indicate significant differences from controls as detailed in the text. ***A***, Adult limited pan-MB expression of btk^{Ri-1} eliminates habituation to 15 footshocks. $n \geq 11$ for all groups. ***B***, Rescue of the habituation deficit of $btk^{M1/M1}$ by adult-limited expression of a dBtk transgene in the MBs. Uninduced transgene-bearing flies (gray bar) behave significantly different from controls, much like non-transgene bearing mutants homozygotes (p = 0.0014 and p = 2.2 X 10^{-6}, respectively). In contrast, a 2 d induction of the transgene (gray bar right side) completely reversed the deficient habituation (p= 0.1918 vs p=6X10^{-6} for mutant homozygotes compare to controls; open bar). $n \geq 8$ for all groups. ***C***, Adult limited pan-MB expression of the independent btk^{Ri-2} transgene precipitates defective shock habituation compared with both controls. $n \geq 10$ for all groups. ***D***, Adult specific expression of btk^{Ri-1} under the independent pan-MB 247Gal4 driver results in abrogated shock habituation compared with controls. $n \geq 14$ for all groups. ***E***, A third MB-restricted driver (dncGal4) yields adult-specific shock habituation deficits when driving UAS-btk^{Ri-1}. $n \geq 9$ for all groups. ***F***, Adult-limited btk^{Ri-1} expression in α/β MB neurons does not precipitate habituation deficits. $n \geq 11$ for all groups. ***G***, Adult-specific btk^{Ri-1} expression in α/β MB neurons under the independent c739Gal4 driver does not compromise shock habituation. $n \geq 13$ for all groups. ***H***, Adult-specific btk^{Ri-1} expression in γ MB neurons under VT030604 also does not compromise shock habituation. $n \geq 14$ for all groups. ***I***, Adult-specific IN of btk^{Ri-1} expression in α'/β'MB neurons abrogates shock habituation, whereas the uninduced transgene (UN) does not. $n \geq 9$ for all groups. ***J***, Expression of btk^{Ri-1} driven by the α'/β'-specific VT030604 driver present aberrant habituation (black bar) when induced for 2 d compared to their uninduced siblings. However, when flies were raised at 25°C (gray bar), they presented an ameliorated deficit compared with those raised at 18°C and uninduced. $n \geq 14$ for all groups. ***K***, Expression of shi^{ts} in α'/β' MB neurons compromises habituation under the restrictive conditions (black bar) compared with animals kept under permissive temperature (p = 9 X 10^{-8}). $n \geq 11$ for all groups.

In contrast, animals raised at 18°C, but kept at 30°C for 48 h before training to achieve maximal btk^{Ri-1} expression failed to habituate (Fig. 3*J*; ANOVA: $F_{(2,55)}$ =4.8324, p = 0.0118; subsequent LSM: p= 0.0032 vs 18°C). Footshock habituation in animals raised and kept at 25°C was not abolished, but was highly suppressed compared with the performance of animals kept at 18°C (Fig. 3*J*; ANOVA: $F_{(2,55)}$ = 4.8324, p = 0.0118; subsequent LSM: p = 0.0546 vs 18°C). These results demonstrate that dBtk function in α'/β' neurons is indeed essential to facilitate footshock habituation. This is not specific to dBtk, as conditionally blocking neurotransmission from α'/β' neurons with the thermosensitive transgenic dynamin Shi^{ts} (187), under c305a-Gal4 completely blocked habituation (Fig. 3*K*; ANOVA: $F_{(1,25)}$ =56.7690, p<0.0001; subsequent LSM: p = 9 X10^{-8}). This is despite the small but significant shock avoidance reduction in the "induced" (IN)

versus the "uninduced" (UN) state (Table 1), which does not contribute to the phenotype because of the normalization afforded by the calculation of the HI.

The collective results demonstrate two important points. Neurotransmission from α'/β' MB neurons facilitates footshock habituation, whereas activation of their α/β counterparts suppresses it (55).

dBtk is also required within α/β neurons to maintain stimulus responsiveness

Three main reasons prompted us to investigate dBtk function in α/β neurons. The protein appears present in these neurons (Fig. 2*G*), *dbtk* mutants habituate prematurely their olfactory jump reflex (87) and neurotransmission from α/β neurons is essential for mediating responsiveness to footshocks and prevent premature habituation (55). Therefore, we wondered whether dBtk is also involved in maintenance of stimulus responsiveness within α/β neurons. Surprisingly, in contrast to controls subjected to the same number of stimuli, btk^{M1} mutants habituated prematurely after 6 and 10 footshocks (Fig. 4*A*; ANOVA: $F_{(5,104)}$ =34.9318, p<0.0001; subsequent LSM: 6 shocks p = 4 X 10^{-10}, 10 shocks p = 0.0027 vs controls), but failed to habituate to 15 shocks (LSM: p = 9 X 10^{-16} vs controls). The deficits were phenocopied by acute panneuronal dBtk abrogation (Fig. 4*B*; ANOVA: $F_{(8,156)}$= 3.8010, p = 0.0004; subsequent LSM: 6 shocks p = 0.0088 and p = 0.0193, 10 shocks p = 0.0121 and p = 0.0259, 15 shocks p = 0.0057 and p = 0.0125 vs controls, respectively) and induced upon inhibition of dBtk activity with Ibrutinib in control flies with a similar dose–response as for failed habituation to 15 stimuli (Fig. 4*C*; ANOVA: $F_{(2,28)}$ = 10.1984, p = 0.0005; subsequent LSM: p = 0.0002, 0.1 vs 0 μM and p = 0.2240, 1 vs 0 μM). Therefore, as for habituation failure to 15 shocks, the premature avoidance attenuation of the mutants is also not developmental in origin. If the attenuated avoidance is indeed habituation, it should be dishabituated (64). We used an 8 s puff of YO, which has been shown effective for habituation to aversive odors (125). In fact, the premature footshock avoidance attenuation was reversed by post-training exposure to YO (Fig. 4E; ANOVA: $F_{(4,43)}$ = 45.5267, p<0.0001; subsequent LSM: 6 shocks p = 1.1 X 10-11, 10 shocks p = 1.5 X 10^{-9}, AVD after YO p=1.9X10-9), which also suffices to dishabituate control flies after typical habituation to 15 shock stimuli (Fig. 4D; ANOVA: $F_{(2,30)}$=84.8182, p<0.0001; subsequent LSM:YO dishabituation, p=9.28X10^{-12}; AVD, p= 6.27 X 10^{-12}). Because control flies do not habituate to six shocks (Fig. 4A,B), dishabituation after six shocks was not performed as unnecessary.

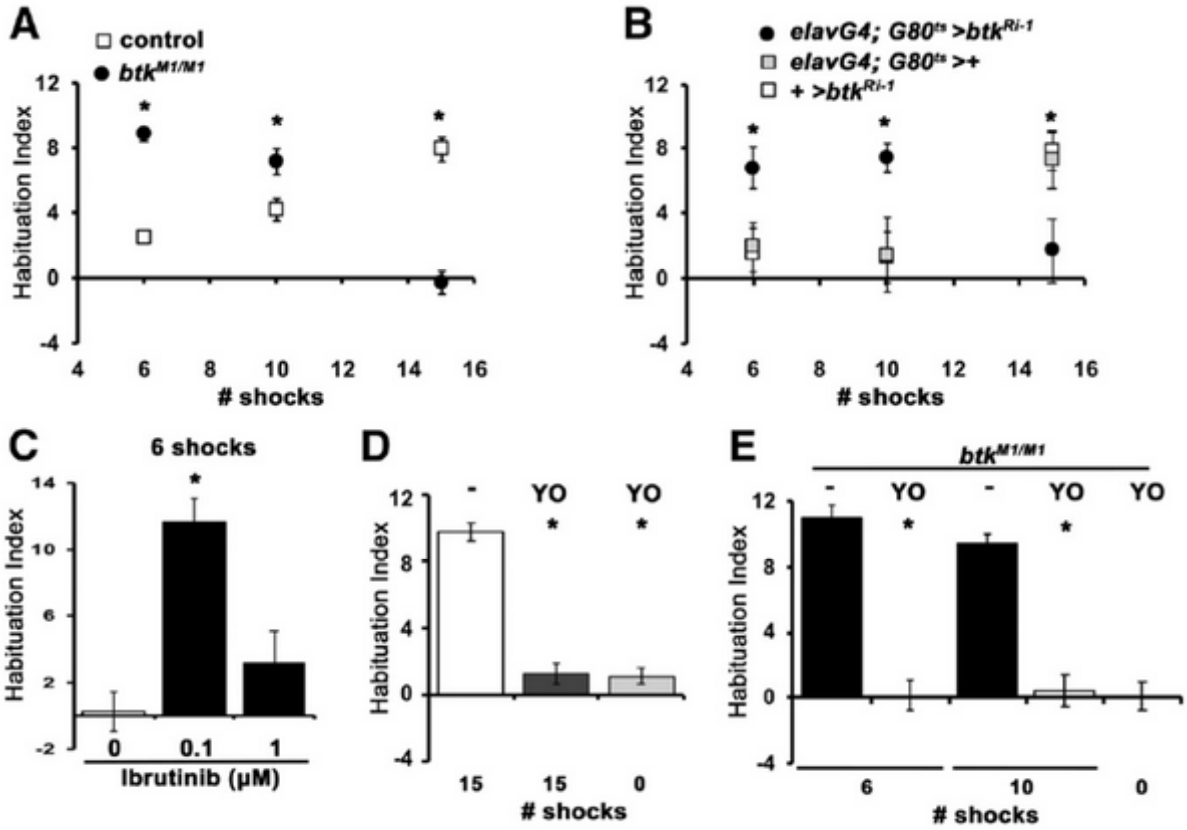

Figure 4. dBtk is acutely required within α/β MB neurons to inhibit premature habituation to footshock. Habituation indices quantifying the difference in footshock avoidance following exposure to the indicated number of stimuli from that of same genotype naive flies are shown as the mean±SEM for the indicated number of repetitions (*n*). Filled circles represent the mean performance of animals with abrogated dBtk, whole open squares the respective controls. Stars indicate significant differences from controls as detailed in the text. ***A***, Footshock habituation of controls (y^1w^*) and $btk^{M1/M1}$ mutants after prior experience of 6, 10, and 15 shocks. The performance of controls is significantly different from that of the mutants after 6, 10, and 15 footshocks. $n \geq 13$ for all groups. ***B***, Adult-limited pan-neuronal expression of btk^{Ri-1} recapitulates both the premature habituation after 6 and 10 shocks and the habituation failure after 15 stimuli. So that the controls have similar genetic backgrounds, progeny from the cross of the w^{1118} background ElavGal4;Gal80^{ts} with 36303 y^1v^1, whereas for the btk^{Ri-1} /+, the y^1v^1 background btk^{Ri-1} was crossed to w^{1118}. $n \geq 11$ for all groups. ***C***, Ibrutinib promotes premature habituation after 6 shocks at 0.1µM, but not at 1µM relative to the performance of vehicle-treated y^1w^* animals. $n \geq 8$ for all groups. ***D***, Dishabituation in y^1w^* flies after 8 s of YO puff. White bar, Habituation after 15 shocks; dark gray bar, dishabituation with YO after experiencing 15 shocks; light gray bar, the effect on avoidance of YO on naive flies before testing their shock avoidance. YO exposure has significant effects on reversing the habituated response, but YO exposure of naive flies does not affect their shock avoidance (0). $n \geq 10$ for all groups. ***E***, The reduced avoidance of $btk^{M1/M1}$ mutants after 6 and 10 footshocks is *bona fide* premature habituation because it is reversible (dishabituated) by a single puff of YO after the respective footshocks as indicated. Black bars denote habituation without YO and the open bars after odor presentation. 0 denotes shock avoidance of naive flies after YO exposure. YO exposure results in significant dishabituation after 6 and 10 shocks. $n \geq 8$ for all groups.

Further confirmation that both aberrant habituation phenotypes result from dBtk attenuation and not another mutation on the *btk*^{M1} chromosome was obtained by adult-specific pan-MB abrogation of the protein under Leo-Gal4. This also yielded both premature habituation to 6 and 10 footshocks and failure to habituate to 15 stimuli and significantly both deficits were absent if the attenuating transgene was uninduced (Fig. 5*A*; ANOVA: $F_{(5,119)}$ = 8.6993 p <0.0001; subsequent LSM, 6 shocks, p = 0.0002; 10 shocks, p = 0.0304; 15 shocks, p = 1 X 10^{-5} vs uninduced). Importantly, expression of the dBtk-encoding transgene (UAS-*btk*^{S}) under Leo-Gal4 in *btk*^{M1} homozygotes fully restored both, the ability to prevent premature habituation to 6 and 10 footshocks and to facilitate habituation after 15 stimuli, but not if the transgene remained uninduced (Fig. 5*B*; ANOVA: $F_{(5,77)}$=13.3452 p<0.0001; subsequent LSM, 6 shocks, p=0.0036; 10 shocks, p=0.0161; 15 shocks, p=6X10^{-10} vs uninduced). This is consistent with the notion that dBtk functions to maintain habituation latency within α/β MB neurons and to facilitate footshock habituation within their α′/β′ counterparts.

To confirm the independent function of dBtk in both preventing premature habituation in α/β and facilitating it in α˙/β˙neurons, the protein was selectively abrogated therein. Significantly, animals with abrogated dBtk in adult α/β neurons under c739Gal4 habituated prematurely to 6 and 10 stimuli (Fig. 5*C*; ANOVA: $F_{(5,77)}$ = 17.1806, p <0.0001; subsequent LSM: 6 shocks p=8.9X10^{-6}, 10 shocks p=2.9X10^{-8}, 15 shocks p= 0.9504 vs control), whereas attenuation in α˙/β˙ neurons under c305aGal4 did not affect habituation latency, but blocked habituation to 15 shocks (Fig. 5*D*; ANOVA: $F_{(5.82)}$ = 12.2529, p<0.0001; subsequent LSM: 6 shocks p = 0.3433, 10 shocks p =0.777, 15 shocks p = 3.7 X 10^{-7} vs control).

Therefore, dBtk has two functionally distinct and apparently independent neuronal type-specific roles. It engages mechanisms that maintain latency, thus preventing premature habituation within α/β neurons and potentially distinct mechanisms that facilitate habituation in their α˙/β˙ counterparts. Alternatively, upon activation of these neurons by the footshock stimuli, dBtk may mediate neurotransmission from both types, which in the case of α/β neurons is required to maintain the value of the stimulus and prevent premature habituation (55) and α˙/β′ neurons to facilitate it (Fig. 3*I*,*K*). Moreover, since *btk* mutants present habituation deficits specifically to footshock, but not odor stimuli, it is possible that the kinase is involved in second messenger pathways transducing dopaminergic signals that apparently communicate footshock information to the MBs and result in their activation (189); (190).

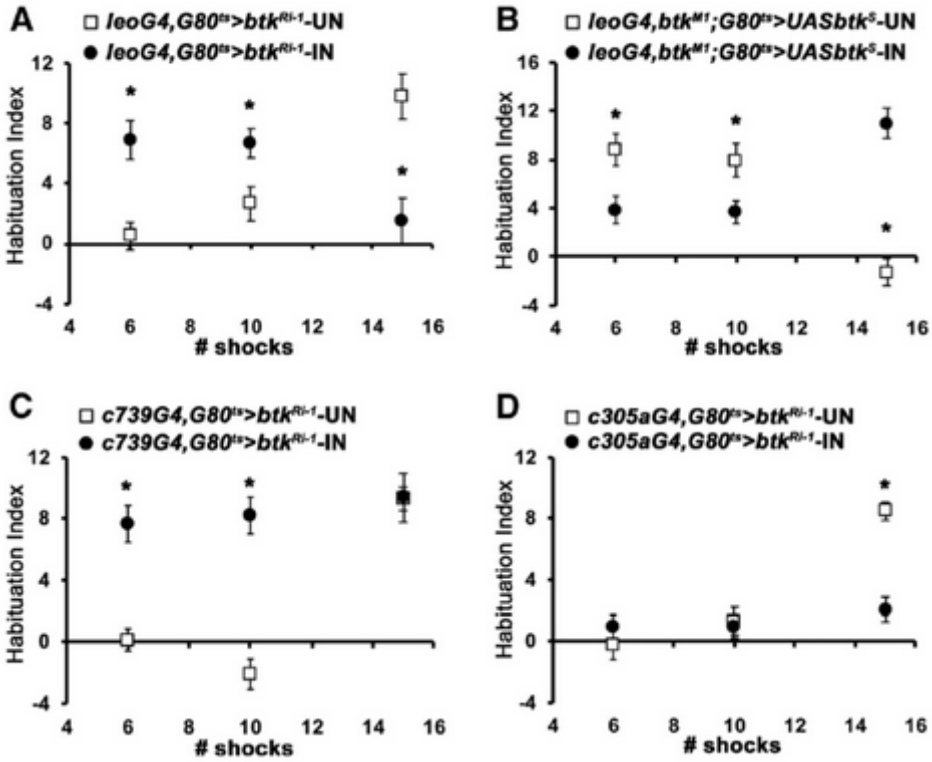

Figure 5. Differential roles for dBtk in latency and habituation in α/β and α'/β' MB neurons. Habituation indices quantifying the difference in footshock avoidance following exposure to the indicated number of stimuli from that of same genotype naive flies are shown as the mean±SEM for the indicated number of repetitions (*n*). Filled circles represent the mean performance of animals with abrogated dBtk; whole open squares, the respective controls. Asterisks indicate significant differences from controls as detailed in the text. ***A***, Adult-limited pan-MB expression of btk^{Ri-1} (IN) yields premature habituation after 6 and 10 stimuli and failed habituation after 15 shocks compared to in-genotype controls of siblings with the transgene silent (UN). $n \geq 18$ for all groups. ***B***, The complementary experiment of adult-limited pan-MB expression of UAS-btk^{S} rescued (IN) the premature habituation after 6 and 10 stimuli, as well as the habituation deficit after 15 footshocks compared to siblings not expressing the transgene (UN). $n \geq 12$ for all groups. ***C***, Adult-limited expression of btk^{Ri-1} in α/β MB neurons (IN) recapitulates the premature habituation after 6 and 10 shocks but not the failed habituation after 15 stimuli, compared to siblings not expressing the transgene (UN). $n \geq 10$ for all groups. ***D***, Adult-limited expression of btk^{Ri-1} in α'/β' MB neurons (IN) recapitulates the failed habituation to 15 footshocks, but not the premature habituation to 6 or 10 stimuli compared to siblings not expressing the transgene (UN). $n \geq 11$ for all groups.

Antipsychotics rescue the deficient habituation of dBtk mutants

We assumed that the inability to habituate upon dBtk attenuation may result from persistent neurotransmission from α'/β'. This could be due to excess dopaminergic signaling or inability of the mutants to downregulate the response to dopaminergic input. To differentiate between these possibilities, we initially sought to inhibit dopaminergic inputs pharmacologically. Interestingly, excess dopaminergic signaling has been linked with schizophrenia in humans (188); (189), a condition also associated with habituation failures and defects (131); (132); (136); (157) . In fact, pharmaceuticals used to treat this

condition are thought to act mostly as monoamine receptor antagonists including dopaminergic ones (190); (191).

Therefore, to investigate whether monoamine receptors are involved, we sought to antagonize them in the *btk* mutants, with the typical tricyclic antipsychotic clozapine, thought to primarily address dopamine, but also serotonin receptors and the atypical benzisothiazole risperidone, which is thought to be a more pronounced serotonergic antagonist, but also efficaciously antagonizes additional monoamine receptors (191). Interestingly, administration of clozapine for 16–18 h before habituation training reversed in a dose-dependent manner the inability of btk^{M1} homozygotes (Fig. 6*A*; ANOVA: $F_{(2,28)}$=11.6054, p=0.0002; subsequent LSM: 5μM p=0.0041, 10μM p=0.0001 vs 0 μM) and $btk^{M1/M2}$ hetero-allelics (Fig. 6*B*; ANOVA: $F_{(2,30)}$ = 4.7128, p=0.0172; subsequent LSM: 5μM p=0.0648, 10μM p=0.0048 vs 0μM) to habituate to 15 footshocks. A similar treatment with risperidone also reversed the defective habituation of btk^{M1} homozygotes, although at the high concentration of 10 μM, the effect of the drug appeared reduced (Fig. 6*C*; ANOVA: $F_{(3,44)}$ = 9.0647, p = 0.0001; subsequent LSM: 0.1 μM p = 0.0005, 1 μM p = 1.2 X 10^{-5}, 10 μM p = 0.0066 vs 0 μM). Assuming that clozapine antagonizes dopamine receptors, dBtk loss appears to affect their levels or activity. Since phenotypic reversal was elicited by risperidone, at least at the lower concentrations and serotonergic neurotransmission has not been reported to mediate footshock information to the MBs, it is likely that this drug also addresses dopaminergic receptors.

Importantly, clozapine treatment also reversed the defective footshock habituation of animals with pan-MB RNAi-mediated dBtk abrogation (Fig. 6*D*; ANOVA: $F_{(2,26)}$ = 5.2147, p = 0.0132; subsequent LSM: 5 μM p =0.0531, 10 μM p = 0.0038 vs 0 μM) suggesting that the drug reaches these neurons and mediates the observed phenotypic reversal upon acute dBtk attenuation therein. Significantly, both pharmaceuticals reversed the habituation defect to 15 shocks in animals with dBtk abrogation specifically in α'/β'MB neurons (Fig. 6*E*; ANOVA: $F_{(2,27)}$ = 19.1763, p<0.0001; subsequent LSM: 10μM clozapine p<0.0001, 10μM risperidone p<0.0001 vs untreated-0). As expected, dBtk attenuation in α/β neurons did not yield deficient habituation, and the drugs did not affect normal habituation to 15 footshocks (Fig. 6*F*; ANOVA: $F_{(2,26)}$=1.5268, p=0.2376). These results confirm that the habituation failure is specifically driven by dBtk attenuation within the α'/β' neurons and likely results from consequent excess or elevated signaling from one or more monoamine receptors within these neurons. In fact, Dop1R2 (58) and 5HT1B have been reported to be expressed in these neurons (192). Moreover, dBtk abrogation in α/β neurons did not affect habituation to 15 shocks, further suggesting that the drugs specifically address consequences of dBtk abrogation within theirα'/β' counterparts.

As *btk* mutants present both impaired latency and failed habituation, we wondered whether the antipsychotics can reverse both phenotypes. Interestingly, 10 μM clozapine did not alter the premature habituation of btk^{M1} homozygotes, but potently reversed their failure to habituate (Fig. 6*G*; ANOVA: $F_{(5,95)}$ = 7.8245, p <0.0001; subsequent LSM: 6 shocks p = 0.8085, 10 shocks p =0.1382, 15 shocks p= 7.3X10^{-7} vs control). Risperidone

also potently suppressed the habituation failure in the mutants (Fig. 6*H*; ANOVA: $F_{(5,73)}$= 39.2195, p <0.0001; subsequent LSM: 6 shocks p=0.00014, 10 shocks p= 0.0017, 15 shocks p =1X10^{-19} vs control), but interestingly it increased significantly the shock avoidance of the mutants (Table 1), suggesting that it may actually induce hyperactivity, increased locomotion or enhance the aversion of the 45 V shock. In agreement, whereas 10 μM clozapine did not affect avoidance (Table 1), or habituation to 6 or 15 stimuli in control flies (Fig. 6*I*; ANOVA: $F_{(3,52)}$ =14.7186, p <0.0001; subsequent LSM: 6 shocks p = 0.3096, 15 shocks p = 0.3398 vs control), risperidone (10 μM) consistently elevated 45 V avoidance in control flies (Table 1). However, this did not affect habituation to 6 shocks in control animals, but appeared to mildly enhance habituation after 15 stimuli (Fig. 6*F*; ANOVA: $F_{(3,53)}$ =16.9637, p <0.0001; subsequent LSM: 6 shocks p = 0.5796, 15 shocks p =0.0205 vs control). Collectively these results suggest distinct mechanisms of action for the two antipsychotics in *Drosophila*, in agreement with their proposed activities in vertebrates. In fact, risperidone is a potent serotonin and dopamine antagonist, but unlike clozapine presents measurable activities against adrenergic and histamine receptors (PDSD Ki database; (193), which may underlie the increase in avoidance or locomotion upon its administration.

Discussion

The response dynamics to repeated footshocks define two phases. Avoidance is initially maintained for 8–10 stimuli, followed by its rapid attenuation to an apparently asymptotic habituated response by the 15th stimulus (55) (Figs. 4*A*,*B*, 5*A*,*B*, controls). Neurotransmission from α/β MB neurons is required to maintain stimulus responsiveness in the initial latency phase (55) and significantly we now demonstrate that synaptic activity from their α'/β' counterparts is essential to facilitate the subsequent habituation phase (Fig. 2*K*). Therefore, the two habituation phases are mediated by distinct MB neurons.

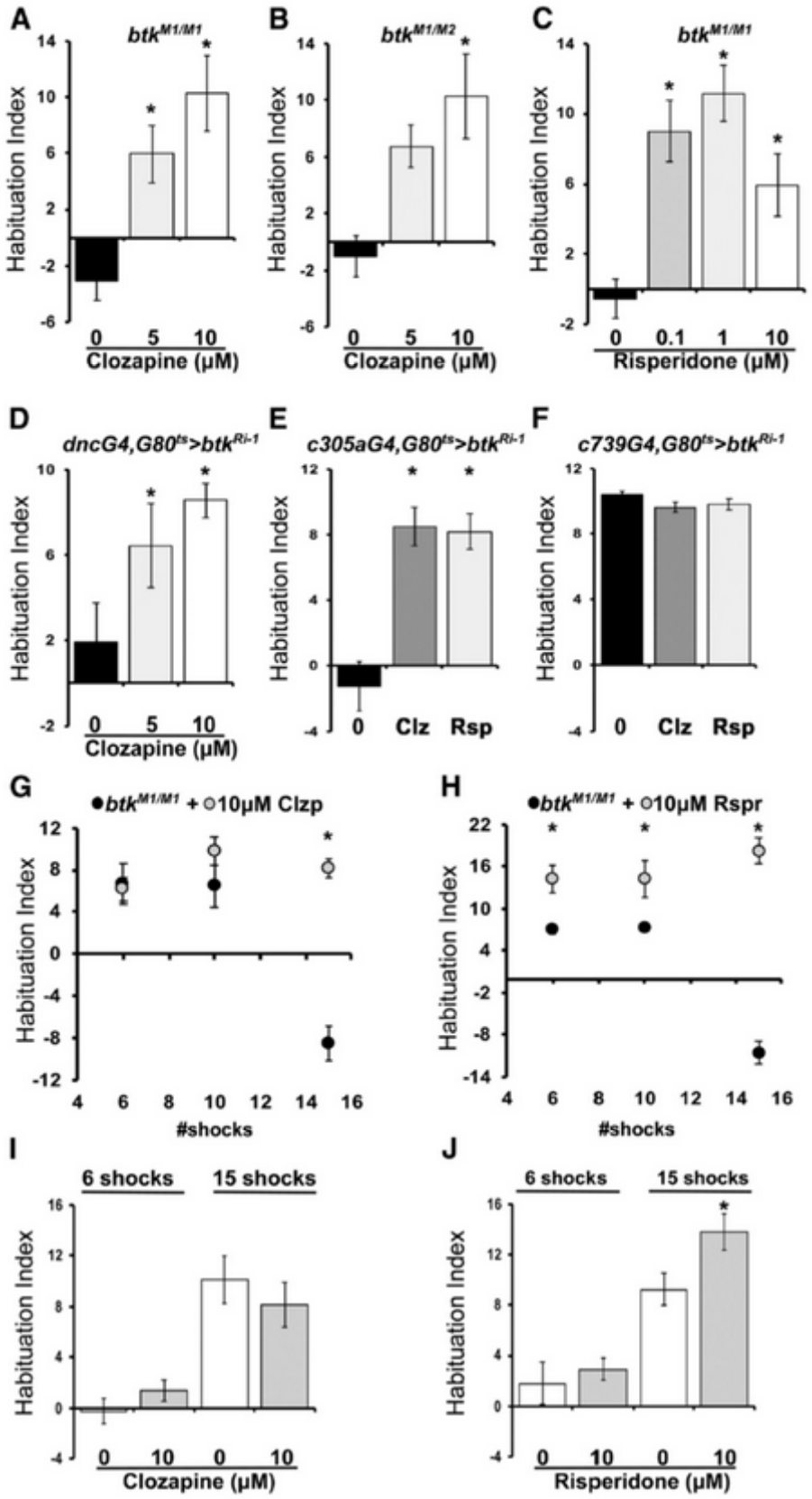

Figure 6. Antipsychotics selectively rescue the defective habituation of *btk* mutants. Habituation indices quantifying the difference in footshock avoidance following exposure to the indicated

number of stimuli from that of same genotype naive flies are shown as the mean±SEM for the indicated number of repetitions (*n*). Asterisks indicate significant differences from controls as detailed in the text. ***A***, Clozapine restores the defective habituation of btk^{M1} homozygotes. Compared with vehicle-treated mutants that do not habituate to 15 footshocks (0), habituation was significantly improved after treatment with 5 and 10μM clozapine. $n \geq 9$.***B***, Clozapine restores the defective habituation of $btk^{M1/M2}$ hetero-allelics, which present a strong habituation defect if treated only with vehicle (0). Clozapine at 5 and 10 μM restored habituation to 15 footshocks. $n \geq 8$ for all groups. ***C***, Risperidone restores the defective habituation of btk^{M1} homozygotes. The strong habituation defect to 15 shocks of vehicle-treated mutant homozygotes was reversed after treatment with 0.1, 1, and 10 μM risperidone. $n \geq 9$ for all groups. ***D***, The habituation defect precipitated by adult limited pan-MB abrogation of dBtk is barely reversible by 5 μM, but restored with 10 μM clozapine compared with vehicle-treated animals (0). $n \geq 8$ for all groups. ***E***, Clozapine (10μM) and risperidone (10μM) restore the defective habituation phenotype precipitated by adult-limited abrogation of dBtk in α'/β' neurons. $n \geq 9$ for all groups. ***F***, Clozapine (10 μM) and risperidone (10μM) do not affect the performance of flies where adult-limited abrogation of dBtk in α/β neurons. $n \geq 9$ for all groups. ***I***, Clozapine (10μM) in control flies does not induce premature habituation after 6 shocks, or a change in habituation after 15 such stimuli relative to vehicle (0)-treated controls. $n \geq 9$ for all groups. ***J***, Risperidone (10μM) in control flies does not induce premature habituation after 6 shocks, but yields elevated habituation after 15 such stimuli relative to vehicle (0)-treated controls. $n \geq 9$ for all groups. ***G***, Clozapine selectively restores the defective, but not the premature habituation of btk^{M1} homozygotes. Clozapine did not change the premature habituation to 6 or 10 stimuli, but reversed the habituation failure after 15 footshocks. $n \geq 10$ for all groups. ***H***, Risperidone restores the defective habituation, but also enhances the premature habituation of btk^{M1} homozygotes. Risperidone rescued the habituation defect after 15 stimuli, but also resulted in significantly higher habituation scores after 6 and 10 footshocks. $n \geq 10$ for all groups.

Because neurotransmission from different MB neurons is required both to prevent and to induce the habituated response, it is likely that it engages distinct α/β and α'/β' MB output neurons (MBONs; (194)). We hypothesize that these potentially antagonistic signals are relayed to neurons driving the choice to avoid or ignore the footshocks in a manner akin to neurons toggling attractive and aversive odor responses in *Drosophila* (195). It is unclear at the moment how the activities of the two types of MB neurons are coordinated upon repeated stimulation as indicated by the response dynamics ((55); Fig. 3*A*,*C*–*F*). However, the current data predict that synaptic transmission from α/β neurons requisite for maintenance of habituation latency precedes α'/β' activation, which facilitates habituation onset. Nevertheless, how neurotransmission from α/β neurons is attenuated after a relatively set number of stimuli and why it precedes activation of α'/β' neurons is unclear at the moment. Significantly, abrogation of dBtk in adult α/β neurons yielded strong latency attenuation (Fig. 3*E*), whereas loss from α'/β' neurons did not affect latency, but eliminated habituation (Fig. 3*F*). Therefore, although α/β and α'/β' activities may be coordinated, they appear independent.

Importantly, we describe the first mutant with specific defects in footshock habituation and demonstrate that dBtk activity is acutely required in adult MBs for both

phases (Figs. 1*B*,*C*, 3*A*), in accord with its apparent expression within α/β and α'/β' neurons. The premature habituation upon dBtk abrogation suggests reduced or dysregulated neurotransmission from α/β neurons ((55); Fig. 2*K*), whereas the habituation defect is consistent with attenuated neurotransmission from their α'/β' counterparts. As Btk is involved in regulation of actin cytoskeleton dynamics (196) and given the involvement of cortical actin in neurotransmitter release (197), the kinase may modulate directly or indirectly the responsiveness to afferent signaling and subsequent neurotransmission to MBONs from both types of MB neurons. In agreement with this notion, dBtk loss specifically from α/β and α'/β neurons phenotypically mimics Shibire^{ts}-dependent silencing of their synaptic output (Figs. 3*I*–*K*, 5*C*,*D*).

Alternatively, dBtk may be involved in footshock signal reception at least by the α'/β neurons, which specifically respond to the dopamine and serotonin receptor antagonists clozapine and risperidone upon attenuation of the kinase. Given that footshock signals are relayed to the MBs by dopamine (198) and these neurons contain at least one dopamine (58) and serotonin (192) receptors, dBtk loss may alter the number or activity of these receptors within these neurons. Interestingly, mammalian Btk is implicated in regulation of G-protein-coupled receptor (GPCR) signaling (196) and importantly, clozapine and risperidone address and antagonize primarily the typical serotonin and dopamine GPCRs ((199); (191)). This is in accord with the notion that in α'/β'neurons dBtk negatively regulates dopamine and/or serotonin receptor signaling or levels. It follows that dBtk loss would increase the levels or activity of one or more of these receptors, altering MB activation threshold and reducing synaptic transmission to efferents mediating the habituated response. Clozapine and risperidone-mediated antagonism of this putative α'/β' overactivation upon repetitive footshock may restore regulated neurotransmission mediating normal habituation. In contrast, in α/β neurons, which do not appear to respond to dopamine or serotonin receptor antagonism, dBtk may regulate neurotransmitter release via its modulation of actin dynamics (196). Impaired neurotransmission from α/β neurons may also underlie the reduced latency to suppress the olfactory jump response of *btk* mutants (87).

Therefore, we propose that dBtk may differentially regulate neuronal activities in α/β and α'/β' neurons. In α/β by positively regulating neurotransmitter release, which is impaired upon dBtk loss, leading to shortened latency and premature habituation. In contrast, in α'/β' neurons dBtk could have primarily a postsynaptic role, by negatively regulating the number or downstream signaling of dopamine and/or serotonin receptors. Elevated intra- α'/β' monoamine receptor signaling upon dBtk loss may lead to dysregulation of downstream synaptic activity and functional silencing of neurotransmission required to facilitate footshock habituation onset. Ongoing experiments aim to test these hypotheses.

It is intriguing that schizophrenia patients also present habituation defects manifested as failures in prepulse inhibition (138); (135); (132); (133); (130), where a weak prestimulus inhibits the reaction to a following strong startling stimulus. These

defects are thought to reflect inability to devalue inconsequential stimuli (138); (140) and can be reversed with antipsychotics including clozapine and risperidone implicating excessive or dysregulated dopaminergic and/or serotonergic signaling similar to *btk* mutants. Recent genome-wide association studies (GWASs) suggested linkage of polymorphisms in a number of genes to schizophrenia and other neuropsychiatricdisorders (149);(200);(201), but human Btk was not among them. Nevertheless, given that habituation deficits in flies and humans are reversible with antipsychotics, it is possible that mutations in *Drosophila* orthologs of genes linked to schizophrenia by GWAS may also present defective footshock habituation and provide expedient experimental validation of their effects on signaling within and between CNS neurons.

4. Drosophila Tau negatively regulates translation and olfactory Long-Term Memory, but facilitates footshock habituation and cytoskeletal homeostasis.

Katerina Papanikolopoulou1#, **Ilianna G Roussou**#, Jean Y Gouzi1#, Martina Samiotaki, George Panayotou, Luca Turin and Efthimios MC Skoulakis.

Author Contributions:

# Authors contributed equally to this work

K.P. and E.M.C.S. wrote the manuscript with input from all authors.

K.P., I.R., J.G., L.T., G.P. and E.M.C.S. designed research.

K.P., I.R., J.G., E.M.C.S. performed research.

K.P., I.R., J.G., M.S. and E.M.C.S. analyzed data.

Introduction

Tau is a microtubule-associated (MAP), neuronal protein enriched in axons. Through its interaction with Tubulin, Tau is involved in the regulation of neuronal polarity, axon outgrowth and axonal transport mediated by kinesin and dynein motor proteins. Apart from its axonal function, several studies indicate alternative cellular functions of Tau proteins at the synapse and in the nucleus, as well as interactions with the plasma membrane and the actin cytoskeleton (202).

Under pathological conditions, Tau undergoes post-translational modifications that trigger its pathogenicity (203). The prevalence of Tauopathies and current lack of prevention or treatment mandate elucidation of the physiological functions of Tau, requisite to understand the molecular aetiology of its pathogenicity. Transgenic expression of human Tau isoforms in *Drosophila* has contributed to identification of novel Tau phosphorylation sites (204);(205);(206) and molecular pathways contributing to neuronal dysfunction and toxicity (207);(208). However, the physiological function of the endogenous *Drosophila* protein has not been fully elucidated.

Drosophila possesses a single *tau* gene encoding multiple transcripts and potential protein isoforms ostensibly via alternative splicing (http://flybase.org/reports/FBgn0266579). It contains the characteristic conserved tubulin binding repeats with 46% identity and 66% similarity to the corresponding human Tau sequences (209). Despite the similarity, the presence of unique and divergent sequences outside the repeats, and the presence of an apparent 5th repeat (210) have led to questions as to whether the fly protein functions as a physiological Tau ortholog (211).

Drosophila Tau (dTau) is expressed in the developing and adult Central Nervous System (CNS), prominently in photoreceptors (209), cell bodies and neuropils of the visual system and the central brain (212). Functional regulation by phosphorylation seems conserved in flies, since dTau possesses multiple SKXGS motifs and has been shown to be phosphorylated (213);(214). Examination of its physiological functions was attempted with the generation of a knock-out (tau^{KO}) mutant lacking exons 2 to 6 including the tubulin-binding repeats (214). However, obvious phenotypes were not reported for these mutants and apparently this was not consequent of up-regulation of other microtubule-associated proteins as in mice (215), furthering the notion that dTau may not be an ortholog of the vertebrate protein. This prompted us to determine whether dTau loss affects the neuronal cytoskeleton as would be expected if functionally conserved with its vertebrate homolog.

Reduced Tau characterizes humans with variants of Frontotemporal Lobar Degeneration with Granulin (*GRN*) mutations (216);(217);(218);(219). In addition, a deletion encompassing the *tau* gene is linked to mental retardation, although it also removes adjacent genes (220);(221), making assignment of the pathological phenotype to Tau loss difficult. Therefore, we also investigated whether dTau loss also precipitates phenotypes in learning and memory as upon human Tau expression in the fly CNS (222); (206); (223).

Materials and Methods

Drosophila Culture and Strains. Flies were cultured on standard wheat-flour-sugar food supplemented with soy flour and CaCl2, at 25°C in 50–70% relative humidity in a 12 h light/dark cycle. tau^{KO} mutant flies (214)were a kind gift from Dr. L. Partridge (Max Planck Institute for Biology of Ageing, Cologne, Germany). The mutant was backcrossed into the resident Cantonised-w^{1118} control isogenic background for six generations. The transposon insertion mutant Mi(216) tau[MI03440] was obtained from the Bloomington Stock Center (#BL37602) and Mi{PT-GFSTF.0}tau[MI03440-GFSTF.0] (#BL60199) was a gift from Dr. Carla Sofia Lopes, Universidade do Porto. Gal4 driver lines used in this work were: elav[C155]-Gal4 (224), LeoMB-Gal4 (225), dnc-Gal4 (BL48571) (174), MB247-Gal4 and c739-Gal4 (50). The Gal4 α'/β' c305a driver was a kind gift of Dr. S. Waddell (University of Oxford). The c739-Gal4;TubGal80^{ts} line was from Dr. G. Roman (University of Mississippi, Oxford, MS). The TubGal80^{ts} transgene (226) was introduced into all other Gal4 strains through standard genetic crosses.

To generate UAS-Flag-dtau a NotI/XbaI fragment containing the RA *dtau* cDNA (227) was subcloned into pUAST-FLAG vector (228). The dtau RNAi target region was selected to be a 632bp BglII-BamHI fragment from the entire *dtau* cDNA to target all Tau splice forms. UAS-dTauRNAi was designed as a genomic-cDNA hybrid consisting of the BglII-BamHI fragment cloned into pUAST vector in forward and reverse orientations. Germline transformants were obtained in the Canton S-w^{1118} genetic background using

standard methods. A second *dtau* RNAi line was obtained from the Bloomington Stock Center (BDSC-40875).

Proteomic analysis. Three to four biological and two technical replicas from each genotype (w^{1118} versus backcrossed tau^{KO} and Elav-Gal4;TubGal80^{ts} >+ versus Elav-Gal4; TubGal80^{ts} >dtauRNAi induced for three days at 30°C) were used for this experiment. Briefly, 10 fly brains per genotype were dissected in PBS and after removal of the optic lobes, were lysed by boiling for 3 min in 50 µl of a solution containing 4% SDS, 100 mM fresh DTT and 10mM Tris pH 7.6. The lysates were processed according to the filter aided sample preparation (FASP) protocol using spin filter devices with 10kDa cut-off (Sartorius, VN01H02) (229). Proteins were subsequently subjected to alkylation and trypsin digestion (1 µg trypsin/ LysC mix mass spec grade, Promega). Peptide products were analyzed by nano-LC–MS/MS using a LTQ Orbitrap XL mass spectrometer (Thermo Fisher Scientific, Waltham, MA, USA) coupled to a nano-LC HPLC (RSLCnano, Thermo Scientific) as described in (230).

The raw files were analyzed using MaxQuant 1.5.3.30 (231) against the complete Uniprot proteome of *Drosophila melanogaster* (Downloaded 1 April 2016/ 42.456 entries) and a common contaminants database by the Andromeda search engine. Protein abundance was calculated on the basis of the normalized spectral protein intensity as label free quantitation (LFQ intensity). The statistical analysis was performed with Perseus (version 1.5.3.2) using a two samples *t*-test with a false discovery rate (FDR) value of 0.05 (232).

Western Blot Analyses. Single female fly heads at 1-3 days post-eclosion were homogenized in 1x Laemmli buffer (50mM Tris pH 6.8, 100mM DTT, 5% 2-mercaptoethanol, 2% SDS, 10% glycerol and 0,01% bromophenol blue). Proteins were transferred to PVDF membrane and probed with the following monoclonal antibodies: N2 7A1 Armadillo (Developmental Studies Hybridoma Bank, DSHB) at 1:200, E7 beta-tubulin 97EF (DSHB) at 1:250, ADL84.12 Lamin Dm0 (DSHB) at 1:100, Acetyl-α-Tubulin (Cell Signalling) at 1:2000, FLAGM2 (Sigma) at 1:1000 and 8C3 syntaxin (DSHB) at 1:3000. Anti-αTub84B+D guinea pig polyclonal antibody (1:300) was a kind gift from Stefan Baumgartner (233), rabbit polyclonal anti-βTub56D (1:1000) was from Dr. Detlev Buttgereit (234) and rabbit polyclonal anti-dTau was from Dr. Nick Lowe (1:2000). Appropriate HRP-conjugated secondary antibodies were applied at 1:5000. Proteins were visualized with chemiluminescence (ECL Plus, Amersham) and signals were quantified by densitometry with the Image Lab 5.2 program (BioRad). Results were plotted as means ± SEM from two or three independent experiments. The data were analyzed by standard parametric statistics (*t* tests) as indicated in the text.

Confocal Microscopy. The protein-trap Drosophila strain Mi{PT-GFSTF.0}tau[MI03440-GFSTF.0] was used to examine the expression pattern of dTau in the adult brain. Flies were dissected in cold PBS, fixed in 4% paraformaldehyde for 15 min and imaged by laser-scanning confocal microscopy (Leica TCS SP8). F-actin levels were determined in adult fly brains from three independent experiments as described before (235).

F-actin and Microtubule precipitation assay. Total F-actin has been isolated as in (235). Briefly 4 brains from each genotype (1-3 day-old flies) were dissected in cold PBS and transferred in 25 µl homogenization buffer (100 mM Na_2HPO_4–NaH_2PO_4 at pH 7.2, 2 mM ATP, 2 mM $MgCl_2$), supplemented with phosphatase- (Sigma) and protease- (Thermo Scientific) inhibitor cocktails. After homogenization, biotinylated phalloidin (Invitrogen, Molecular Probes) was added to a final concentration of 0.15 units per brain followed by precipitation with streptavidin-coupled Dynabeads (Invitrogen). The precipitated material and supernatant were probed for dTau (1:2000) and actin (1:1000, Sigma). To control for non-specific binding, the same protocol was followed without the addition of biotinylated phalloidin to the lysate. Microtubule-binding experiments were based on established methods ((236); (237)). Briefly, Taxol-stabilized microtubules have been isolated from head extracts by ultracentrifugation at 100,000 g for one hour. Soluble and insoluble fractions were probed with E7 and Acetyl-α-Tubulin.

Puromycin assay. The protocol was adapted from (Belozerov et al., 2014) and (Deliu et al., 2017). Briefly, flies were starved for 4h and transferred onto 5% sucrose-1% low-melting agarose supplemented with 600 µM puromycin (Santacruz) for 16 h. Six female fly heads were homogenized in 20 µl of buffer containing 20 mM Tris-HCl pH 8.0, 137 mM NaCl, 1 mM EDTA, 25% glycerol, 1% NP-40 and a protease inhibitor cocktail (Thermo Scientific). Samples were run on SDS 10% PAGE gels, proteins were transferred to PVDF membrane and probed sequentially with anti-puromycin (Millipore) at 1:2000 and anti-syntaxin (8C3, DSHB) at 1:3000. Anti-mouse HRP-conjugated secondary antibody was applied at 1:5000. Proteins were visualized with chemiluminescence (ECL Plus, Amersham) and signals corresponding to molecular weight region 30-125 KDa were quantified by densitometry with Image Lab 5.2 (BioRad). Results were plotted as means $\pm$ SEM from two independent experiments. The data were analyzed by standard parametric statistics (*t* tests) as indicated in the text.

Behavioural Analyses. All experiments were performed in mixed sex populations. Animals bearing $Gal80^{ts}$ were raised at 18C until adulthood and transgenes were induced maximally by placing 2–5-day old flies at 30C for 72 h. Flies were kept at the training temperature (25C) for 30 min before the behavioral assays. Other flies or mutants were raised at 25C throughout development, adulthood and behavioral testing. Olfactory memory in the negatively reinforced paradigm coupling aversive odors as conditioned stimuli (CS) with the electric shock unconditioned stimulus (US) (238) was performed essentially as described previously (239). The aversive odors used were benzaldehyde and 3-octanol, diluted in isopropylmyristate (Fluka). Electric foot shock avoidance and habituation to electric shock experiments were performed under the conditions described in (55). Each genotype was tested in yoked experiments whereby estimation of the avoidance was immediately followed by habituation training and testing of the same genotype. Hence, all data consist of yoked pairs per genotype. The avoidance fraction was calculated by dividing the number of naïve flies preferring shock by the total number of flies. After exposure of the flies to several 1.2-sec electric shocks at 45 V, the habituation

fraction was calculated by dividing the number of flies preferring shock by the total number of flies. Finally, the habituation index (HI) was calculated by subtracting the avoidance fraction from the habituation fraction and multiplying by 100. Cycloheximide treatment has been performed as in (240). Briefly, flies were treated with 35 mM CXM, 5% sucrose for 16 h before training at 30 C. After training and until memory test, flies were kept on regular food.

Learning experiments described in Figure 4 were performed as in (241). Briefly, training for 3 min-learning experiments consisted of 1 single session of 12 US/CS pairings of 90 V electric shocks (US) with one odor (CS^+) over 1 min, followed after a 30 s purge with air, by the presentation of the second odor (CS^-) without shocks for 1min. Training for reversal learning consisted of a standard conditioning protocol (CS^+ =OCT, CS^- =BNZ; reciprocal CS^+ =BNZ, CS^- =OCT) followed by 1 min of air and then the reverse odor-shock contingency (CS^+ =BNZ, CS^- =OCT; reciprocal CS^+ =OCT, CS^- =BNZ). Testing was performed immediately after reversal training.

Experimental design and Statistical Analysis. For all experiments, controls and experimental genotypes were tested in the same session in balanced design. The order of training and testing these genotypes was randomized. We required an experimental result to be significantly different from both genetic controls. Data are shown as mean $\pm$SEM. Data were analyzed parametrically with the JMP 7.1 statistical software package (SAS Institute Inc.) as described previously (175). Following initial ANOVA, planned multiple comparisons were performed, using p-value=0.05. The level of significance was adjusted for the experiment wise error rate. Detailed results of all ANOVA and planned comparisons are reported in the text.

Results

dTau loss alters Microtubule polymerization and stability

Because the Drosophila genome contains only one homologue of the Tau/MAP2/MAP4 family (209) and given the involvement of Tau in multiple vital functions (202), it was highly surprising that null mutants of the protein were viable in *Drosophila* (214). Potential explanations for this could be that unlike its apparent vertebrate homologs, dTau is not involved in essential cytoskeletal functions, or that like in mice, its activities are compensated at least in part by other Microtubule Associated Proteins -MAPs (215);(242);(243). If dTau acted like its vertebrate homolog, then its absence should affect the cytoskeleton and /or the levels of other microtubule-associated proteins, perhaps in compensation for its absence.

To address this hypothesis, we adopted a comparative proteomic approach using LC-MS/MS and label free quantitation in protein extracts from the brains of null tau^{KO} (**Fig. 1A**) (214) versus control (WT) flies (**Table 1**). As expected, dTau was present in the CNS of WT flies and absent in the mutants. In agreement with a previous report (214), dTau loss did not affect the levels of Futsch and Ensconsin, the known fly homologues of MAP1

and MAP7 respectively, neither those of Map205 (**Table 1**). Since Drosophila does not contain a MAP2 homologue, these are the MAPs that could presumably compensate dTau loss and account for the viability of the mutants as suggested for Tau loss in mice (215);(242);(243). Furthermore, although the centrosomal MAP60 was elevated, previous studies suggested that it cannot functionally replace dTau (215). The atypical MAP Jupiter (244), was found significantly reduced in tauKO animals.

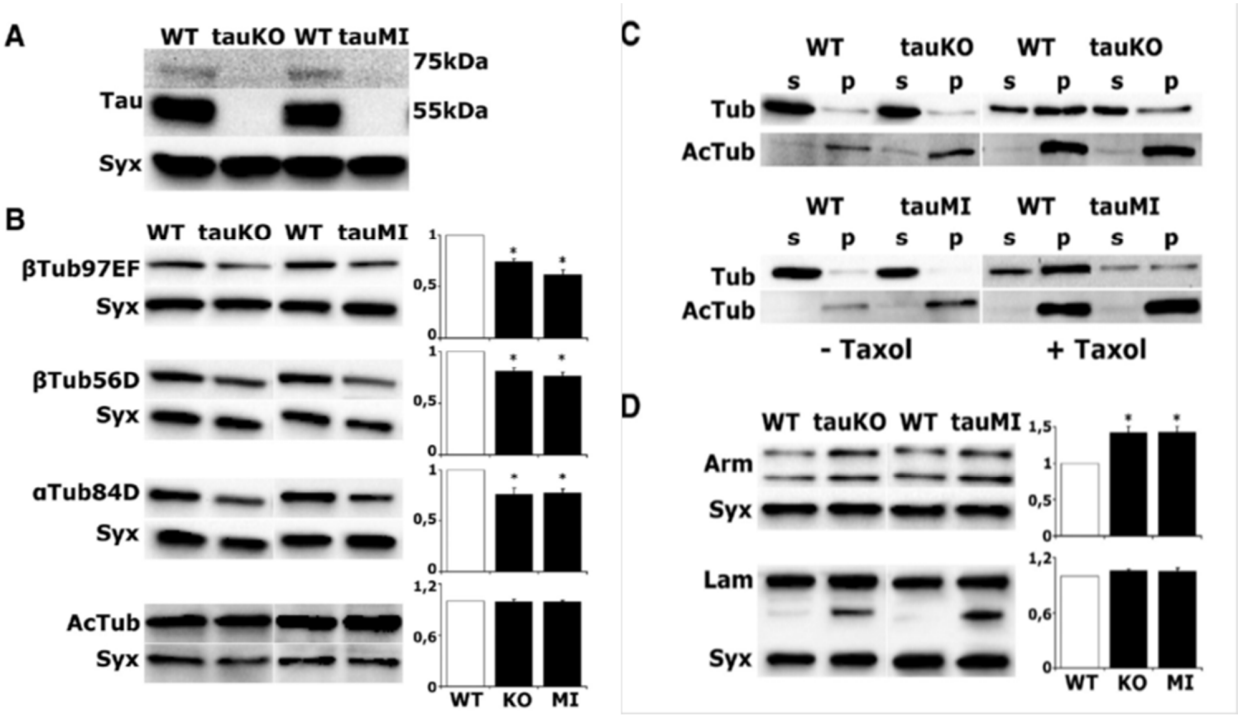

Figure 1. dTau loss precipitates changes in microtubule cytoskeleton. ***A***, Western blot analysis of head lysates from WT, *tau*^{KO}, and *tau*^{MI} flies probed with anti-dTau. ***B***, ***D***, Representative blots of head lysates probed with the indicated antibodies. For quantifications, levels of the indicated protein in the mutants were normalized using the syntaxin (Syx) loading control and are shown as a ratio of their mean±SEM values relative to their respective level in WT flies, which is arbitrarily set to 1. Stars indicate significant differences (p<0.05) from control (open bars) for *tau*^{KO} and *tau*^{MI}. ***C***, Endogenous microtubules were purified from fly head lysates in the absence or presence of Taxol. p, Pellet fraction; s, supernatant fraction. Fractions were analyzed by Western blotting using antibodies against total tubulin (Tub) and acetylated tubulin (AcTub).

In addition, the spectraplakin Short Stop (Shot), a large actin-microtubule linker molecule, which could in principle functionally overlap Tau for microtubule stabilisation (Alves-Silva et al., 2012), remained unaltered upon dTau deletion (**Table 1**). Only the highly divergent Mapmodulin (245) was highly upregulated in the mutant. However, Mapmodulin is leucine–rich, unlike the proline rich-dTau and this along with its divergent sequence strongly suggests that it is rather unlikely to functionally compensate for loss of the latter. Hence, there is no obvious upregulation of one of the major Drosophila MAPs under chronic dTau loss (**Table 1**), similar to that reported to account for the viability and lack of gross mutant phenotypes in *tau*^{KO} mice (215). Therefore, functional compensation of

Tau loss by MAP upregulation may characterize vertebrates, but divergent molecular mechanisms appear able to overcome the deficit in *Drosophila*.

However, dTau depletion resulted in significant reductions in both α and β Tubulin and interestingly, elevation in the major microtubule-associated motor proteins (**Table 1**). We aimed to validate independently the reduction of Tubulins in tau^{KO} and a second MiMIC transposon insertion mutant (tau^{MI}) by western blots. Both mutants are null as they lack the 50 and 75 kDa dTau isoforms (**Fig. 1A**) and both harboured reduced levels of both Tubulin (Tub) isoforms in head lysates (Fig. 1B, for tau^{KO} and tau^{MI} respectively βTub97EF $p=0.004$, $p=0.009$, $n=4$, βTub56D $p<0.0001$, $n=6$ and $n=8$, αTub84D $p=0.0003$, $n=5$ and $n=7$), in agreement with the results in Table 1. Given the lack of obvious phenotypes despite the significant reduction, we wondered whether Tubulin attenuation affected its partitioning between monomer and polymer pools. Neuronal-specific dTau reduction has been reported to affect microtubule morphology and density, resulting in fewer, but larger axonal microtubules (212). A hallmark of long-lived, stably polymerized microtubules is Tubulin acetylation, which is negatively regulated by the Tubulin-deacetylase, HDAC6 (246). Importantly, HDAC6 levels were reduced in tau^{KO} flies (**Table 1**), suggesting that Tubulin acetylation could be elevated in the mutants. As total Tubulin acetylation did not differ among genotypes (**Fig. 1B**, for tau^{KO} and tau^{MI} respectively AcTub $p=0.678$, $p=0.875$, $n=4$), it raised the possibility that it is the non-acetylated Tubulin which is lower in the mutants and is reflected in the reduced α and β Tubulin isoforms (**Fig. 1B**).

To validate this notion, we extracted intact microtubules from the same number of *Drosophila* heads in the presence of the microtubule-stabilizing paclitaxel (Taxol) (236). Microtubules were then sedimented by ultracentrifugation and the pellet and supernatant fractions were probed for total and acetylated Tubulin. In the absence of the microtubule stabilizing Taxol, polymerized acetylated Tubulin appeared more abundant in the mutants. However, Taxol addition revealed a significant increase in pelleted Tubulin in control, but

Table 1. Differentially regulated cytoskeletal proteins upon dTau deletion

Gene	Identifier	Log 2 fold change	*p* Value
tau	FBgn0266579	−7.66922013	0*
futsch	FBgn0259108	−0.098929167	0.23816
Map205	FBgn0002645	0.172052622	0.163753
Map60	FBgn0010342	0.447441737	0.012972*
Jupiter	FBgn0051363	−0.281016827	0.013477*
ens	FBgn0264693	−0.176790555	0.411188
Mapmodulin	FBgn0034282	0.385273457	0.00035*
βTub56D	FBgn0003887	−0.467973868	0.000265*
βTub97EF	FBgn0003890	−0,399647633	0.004722*
αTub84D	FBgn0003885	−0.209974686	0.01011*
HDAC6	FBgn0026428	−0.393520594	0.014513*
Dhc64C	FBgn0261797	0.173733711	0.00421*
Dlic	FBgn0030276	0.268746932	0.001894*
BicD	FBgn0000183	0.389154911	0.013152*
Klc	FBgn0010235	0.258972645	0.008748*
Khc	FBgn0001308	0.284088135	0.000915*
Klp10A	FBgn0030268	0.30295078	0.000371*
Mtor	FBgn0013756	0.234465	0.000624*
CLIP-190	FBgn0020503	0.197493394	0.001698*
shot	FBgn0013733	0.026000439	0.729461
Actin-5C	FBgn0000042	0.101068815	0.097274
Arm	FBgn0000117	0.287528	0.005765*
α-Cat	FBgn0010215	0.194383144	0.008364*
sqh	FBgn0003514	0.302096923	0.011639*
sn	FBgn0003447	0.478138049	0.000003*
cpb	FBgn0011570	0.188986699	0.013467*
tsr	FBgn0011726	0.160349607	0.000611*
cpa	FBgn0034577	0.211062511	0.00578*
zip	FBgn0265434	0.229537	0.018528*
vib	FBgn0267975	−0.180737	0.015157*
flr	FBgn0260049	0.207514842	0.000992*
Lam	FBgn0002525	0.170005878	0.016684*

Table 1. Selected proteins, *p* values, and average log2 fold differences from three biological and two technical replicas have been calculated as described in Materials and Methods. The log2 fold change becomes positive when mutant> control and negative when control > mutant. The *t* test was performed with a permutation-based FDR (0.05) calculation, and the *p* value determines the statistical significance (**p*<0.05). Proteins are functionally grouped into Drosophila MAP family proteins, tubulin and microtubule-associated proteins, actin, and actin associated proteins.

not the mutant lysates, while the fraction of acetylated Tubulin remained equivalent (**Fig. 1C**). Taken together the data indicate that whereas total polymerized Tubulin is reduced in the mutants, its acetylation appears unaltered. Because acetylation enhances flexibility and confers resilience against mechanical stresses (247), the data suggest that the microtubule lattice in dTau mutants is likely less rigid. Collectively, the results underscore the essential role of dTau in microtubule cytoskeleton dynamics, supporting its functional role as a true ortholog of its vertebrate counterpart.

Loss of dTau destabilizes F-actin.

Although significant changes in the ubiquitous Actin 5C levels were not detected, dTau loss resulted in elevation of both α (α-cat) and β-catenin (Armadillo-Arm) and a number of other major Actin-binding proteins, as well as the nucleoskeletal protein Lamin (**Table 1**). These results were selectively verified for Arm and Lamin due to reagent availability (**Fig. 1D**, for *tau*^{KO} and *tau*^{MI} respectively Arm p=0.007, p=0.001, n=5, Lam p=0.231, p=0.817, n=4). Notably, although the full-length 75 kDa Lamin was present in equal quantities in both mutants and controls, a 45-50 kDa band, representing a cleavage product (248), was detected only in the *tau*^{KO} and *tau*^{MI} flies, suggestive of excess Lamin degradation. In accord with these results, transgenic Tau elevation by expression of human Tau in the fly CNS promotes F-actin stabilization leading to disruption of the Lamin nucleoskeleton and reduction of Lamin levels in flies (235); (249).

Given the broad upregulation of Actin-binding proteins (**Table 1**) and its interaction with Tau (250);(251), we investigated whether the Actin cytoskeleton is altered upon dTau loss. We capitalized on a protein-trap fly strain expressing a GFP::dTau fusion protein, which recapitulated the distribution of dTau in the visual system and central brain, including the MBs (**Fig. 2A**). The MBs are bilateral clusters of neurons in the dorsal posterior cortex of the brain, essential for olfactory learning and memory in *Drosophila* (252). Notably, the GFP-marked dTau co-localized with rhodamine-phalloidin within these neurons (**Fig. 2B**). In accord, total F-actin isolated from brain lysates with biotinylated phalloidin, co-precipitated a significant amount of dTau (**Fig. 2C**). Because dTau was absent from the pellet if phalloidin was omitted, this validates specificity of dTau interaction with polymerised filamentous actin.

Furthermore, immunofluorescence microscopy of *tau*^{KO} mutant brains revealed a substantial decrease in total F-actin levels (**Fig. 2D**, p<0.0001, n=10). This was independently verified in *tau*^{MI} flies, where pelleted, phalloidin-bound F-actin levels were also significantly reduced (p=0.01, n=3), while total actin was unaltered (**Fig. 2E** and **Table 1**). Collectively therefore, dTau promotes actin polymerization and cytoskeletal dynamics in vivo. It follows that the upregulation of Actin-binding proteins upon dTau loss (**Table 1**), is likely a reflection of homeostatic compensatory responses consequent to decreased F-Actin levels (**Figs. 2D, 2E**).

dTau is a negative regulator of translation and PSD-LTM.

Because cytoskeletal proteins are essential for multiple neuronal properties including plasticity and metabolism (253), in conjunction with its presence within the MBs, neurons

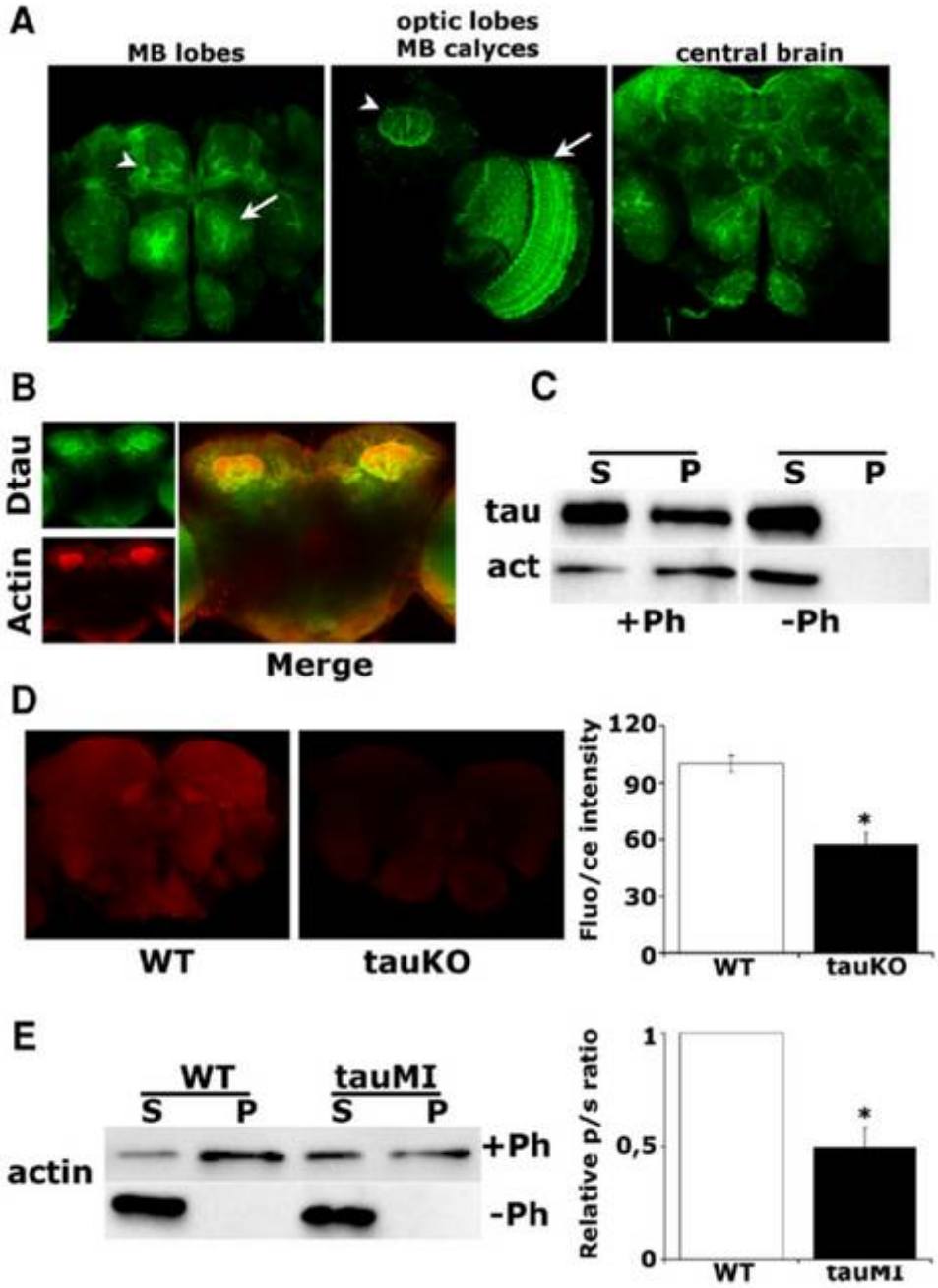

Figure 2. dTau loss affects the actin cytoskeleton. ***A***, Expression pattern of a GFP::dTau protein-trap in the adult brain at the level of the MB lobes (arrowhead) and antennal lobe (arrow; left), MB calyx (arrowhead) and optic lobe (arrow), (middle), and the central brain (right). ***B***, Prominent colocalization of rhodamine-phalloidin-stained F-actin with the GFP::dTau fusion protein in adult MBs. ***C***, Coprecipitation of phalloidin-bound F-actin and dTau from WT fly brains. ***D***, Confocal images in the central fly brain following rhodamine-phalloidin staining of whole-mount brains from WT and *tau*^{KO} flies (arrow, ellipsoid body). The mean relative fluorescence intensities $\pm$SEM are shown as a percentage of control. ***E***, Phalloidin-bound F-actin was isolated from fresh brain extracts Of WT and *tau*^{MI} mutants, and its levels were assessed by probing for actin. The ratio of precipitated actin in the pellet (p) to the actin in the supernatant (s) was used for quantification and was significantly different in the mutant, as indicated by the star.

essential for learning and memory in the fly, prompted us to investigate whether dTau loss affects behavioral plasticity.

To examine whether dTau is involved in associative learning and memory we used the olfactory classical conditioning paradigm and examined controls and mutants immediately after training to assess 3-minute memory/learning and 24 hours later to probe consolidated memories (**Figs. 3A, 3B**). Two forms of consolidated memories can be assayed in Drosophila, the Protein Synthesis Dependent Long-Term Memory (PSD-LTM), induced after multiple rounds of spaced training and the protein synthesis independent Anesthesia Resistant Memory (ARM), elicited after repeated massed training cycles (254). Whereas 3-minute memory was not affected (*tau*^{KO}, ANOVA: $F_{(2,29)}$= 0.1721, p=0.8428; *tau*^{MI}, ANOVA: $F_{(2,31)}$= 0.7133, p=0.4984), both mutants surprisingly presented enhanced LTM (*tau*^{KO}, ANOVA: $F_{(2,31)}$= 11.2031 p=0.0002; subsequent LSM: p=7.4x10^{-5} vs WT, *tau*^{MI} , ANOVA: $F_{(2,31)}$= 23.8424 p<0.0001; subsequent LSM: p=9.6 x10^{-7} vs WT). In contrast, ARM remained at control levels (*tau*^{KO}, ANOVA: $F_{(2,29)}$= 1.9692, p=0.1591; *tau*^{MI}, ANOVA: $F_{(2,31)}$= 1.7708, p=0.1881).

To determine whether the enhanced 24 hr performance is indeed PSD-LTM, we took advantage of its requirement for de novo protein-synthesis (254) and fed control and mutant flies with the protein synthesis inhibitor cycloheximide (CXM). CXM-fed mutants did not present elevated 24 hr spaced training-induced memory (ANOVA: $F_{(3,31)}$= 35.9177, p<0.0001; subsequent LSM: p=0.2981, *tau*^{MI} +CXM vs WT+CXM), but their performance was reduced equally with the expected (255) PSD-LTM reduction of drug fed controls (**Fig. 3C**). Therefore, the enhanced memory of the mutants (ANOVA: $F_{(3,31)}$=35.9177, p<0.0001; subsequent LSM: p=1.6x10^{-4}, *tau*^{MI}-CXM vs WT-CXM) is the PSD-LTM form of consolidated memory.

To confirm these surprising results independently and to determine whether they are consequent of altered development upon dTau loss, we used RNA interference (RNAi) and the TARGET system (226). Adult-specific pan-neuronal RNAi-mediated abrogation of dTau in the CNS reduced its level by ~65% (**Fig. 3D**, p<0.0001, n=4). As shown in **Fig. 3E**, this did not alter learning, but resulted in strong PSD-LTM enhancement (Fig. 3F, Elav: ANOVA: $F_{(2,31)}$=23.2665, p<0.0001; subsequent LSM: p=6.4x10^{-5} and p=2.5x10^{-7} vs controls respectively). Hence, the elevated memory is not developmental in origin, but reflects an acute requirement for dTau-engaging processes to limit negatively reinforced olfactory PSD-LTM.

Given their essential role for LTM (252), we limited dTau abrogation to adult MBs (**Fig. 3F**). The LeoMB and dnc-Gal4 are pan-mushroom body drivers (256);(225), MB247-Gal4 drives expression mainly in α/β and γ neurons whereas c305α and c739 are restricted to α'/β' and α/β respectively (256). To verify that pan-MB dTau attenuation under dnc-Gal4 did not result in enhanced learning, we limited the number of odor/shock pairings from 6 to 3, conditions conducive to revealing such properties (239);(257).

However, enhanced learning was not detectable even under such limited training (**Fig. 3E**, ANOVA: $F_{(2,30)}$=1.9220, p=0.1651) but in contrast, PSD-LTM was significantly enhanced (LeoMB: ANOVA: $F_{(2,31)}$=14.6273, p<0.0001; subsequent LSM: p=0.0027 and p=9.5x10^{-6} vs controls respectively; dnc: ANOVA: $F_{(2,30)}$=12.8673, p<0.0001; subsequent LSM: p=0.0001 and p=0.0002 vs controls respectively; MB247: ANOVA: $F_{(2,31)}$=14.8900, p<0.0001; subsequent LSM: p=0.0199 and p=7.2x10^{-6} vs controls respectively) under these drivers (**Fig. 3F**). These results were confirmed with an independent RNAi-mediating transgene (dTau levels for control set to 1, pan-neuronally expressed dtauRNAi40875 =0.674± 0.0497, p<0.0001, n=6), which also yielded elevated PSD-LTM (dnc >+ =23.32±1.51; dtauRNAi40875 >+ =27.72±1.10; dnc >dtauRNAi40875 =32.36 ±1.26; n=9, ANOVA: $F_{(2,23)}$=12.4614, p=0.0003; subsequent LSM: p=6.2x10^{-5} and p=0.0224 vs controls respectively) under dncGal4, $Gal80^{ts}$.

Significantly, attenuation of dTau within α'/β' and α/β MB neurons (**Fig. 3F**, c305α and c739 respectively), yielded strong PSD-LTM memory improvement (c305α: ANOVA: F(2,23)=18.8052, p<0.0001; subsequent LSM: p=0.00001 and p=0.00011 vs controls respectively; c739: ANOVA: F(2,31)=20.0470, p<0.0001; subsequent LSM: p=0.0005 and p=8x10-7 vs controls respectively). Both subtypes of neurons are known to be essential for 24-hour memory with apparently distinct roles in olfactory memory processing (258);(259);(54);(175). Output from the α'/β' neurons is required for olfactory memory acquisition and stabilization (54), whereas neurotransmission from the α/β neurons is required for its retrieval (52);(51);(259). Collectively, the data strongly indicate that dTau acts as a negative regulator of PSD-LTM within MB neurons in accord with cumulative evidence on the role of these neurons in the process (53); (54).

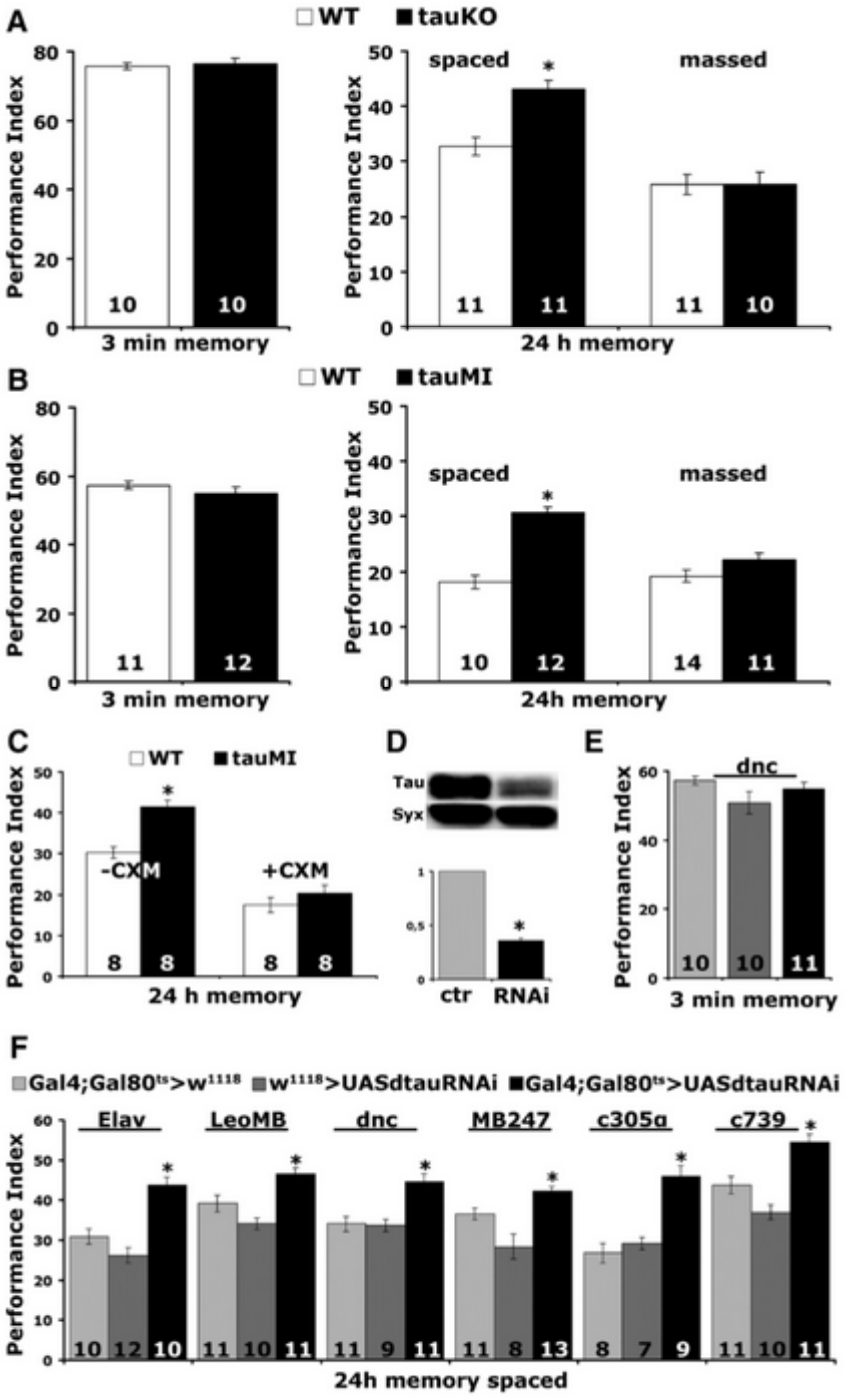

Figure 3. dTau abrogation affects long term memory. ***A***, ***B***, *tau*^{KO} and *tau*^{MI} mutants present enhanced LTM (**p* <0.0001), whereas 3 min memory and ARM are not affected (*p* > 0.05). The number of experimental replicates (*n*) is indicated within the bars. ***C***, CXM administration eliminated the enhanced LTM of *tau*^{MI} flies (**p* <0.0001). ***D***, Representative Western blot of head lysates from flies expressing UAS-dtauRNAi with Elav-Gal4 using an anti-dTau antibody. The genotype of control animals was Elav-Gal4/+. Compared with its levels in control animals, dTau was significantly reduced. For the quantification, tau levels were normalized using the syntaxin (Syx) loading control and shown as a ratio of their mean ± SEM values relative to its respective

levels in control flies, which was set to 1. The star indicates significant differences from the control indicative of reduced dTau levels (**p*<0.0001). ***E***, Three minute memory is not affected after the downregulation of dTau in the adult MBs using dnc compared with driver and transgene heterozygotes. ***F***, Enhanced LTM performance upon abrogation of dTau during adulthood using Elav (**p* <0.0001), LeoMB (**p*= 0.0027), MB247 (**p*=0.0199), dnc (**p*=0.0001), c305a (**p*=0.00001), and c739 (**p*=0.0005).

The CXM treatment experiment in **Fig. 3C** suggested that elevated memory upon dTau loss could be due to improved consolidation, whereas the equivalent performance of control and dTauRNAi flies immediately after training with limited number of US/CS pairings (**Fig. 3E**) indicated that the increased memory observed at later time points was not due to improved acquisition. However, the enhanced memory observed upon attenuation of dTau could also arise from decreased forgetting (241). To test whether forgetting is defective upon dTau attenuation, we performed reversal learning in which we trained flies to associate an aversive odor to footschock and one minute later to the opposite contingency. Control flies typically avoid the odor most-recently associated with shock, whereas flies with decreased forgetting keep the memory of the initial contingency (241). As shown in **Fig. 4A**, dTau attenuation within αβ MB neurons yielded equal learning as the in-genotype controls both in the typical learning paradigm (learning, ANOVA: $F_{(1,17)}$= 0.7532, p=0.3983) and upon reverse training (reversal, ANOVA: $F_{(1,17)}$ = 0.0067, p=0.9356). The reversal PIs are negative because the performance was scored as if the initial contingency was the correct choice. This would be expected to be positive if dTau loss impaired forgetting, in essence eliminating the effect of the second contingency in favor of the initial odor shock pairing. Therefore, the increased memory upon dTau loss is unlikely to be due to impaired forgetting.

The proteomic results suggested elevation of proteins essential for translation in the mutant (**Table 2**) and this included a number of proteins involved in memory formation or recall (**Table 3**), in accord with the PSD-LTM dependence on translation. To independently confirm that protein synthesis is in fact elevated upon dTau loss, we used a functional assay, that of puromycin incorporation. Puromycin acts as an aminoacyl-tRNA analog becoming incorporated into nascent peptides causing termination, but also labeling newly synthesized proteins, whose levels are readily measured with an anti-puromycin antibody.

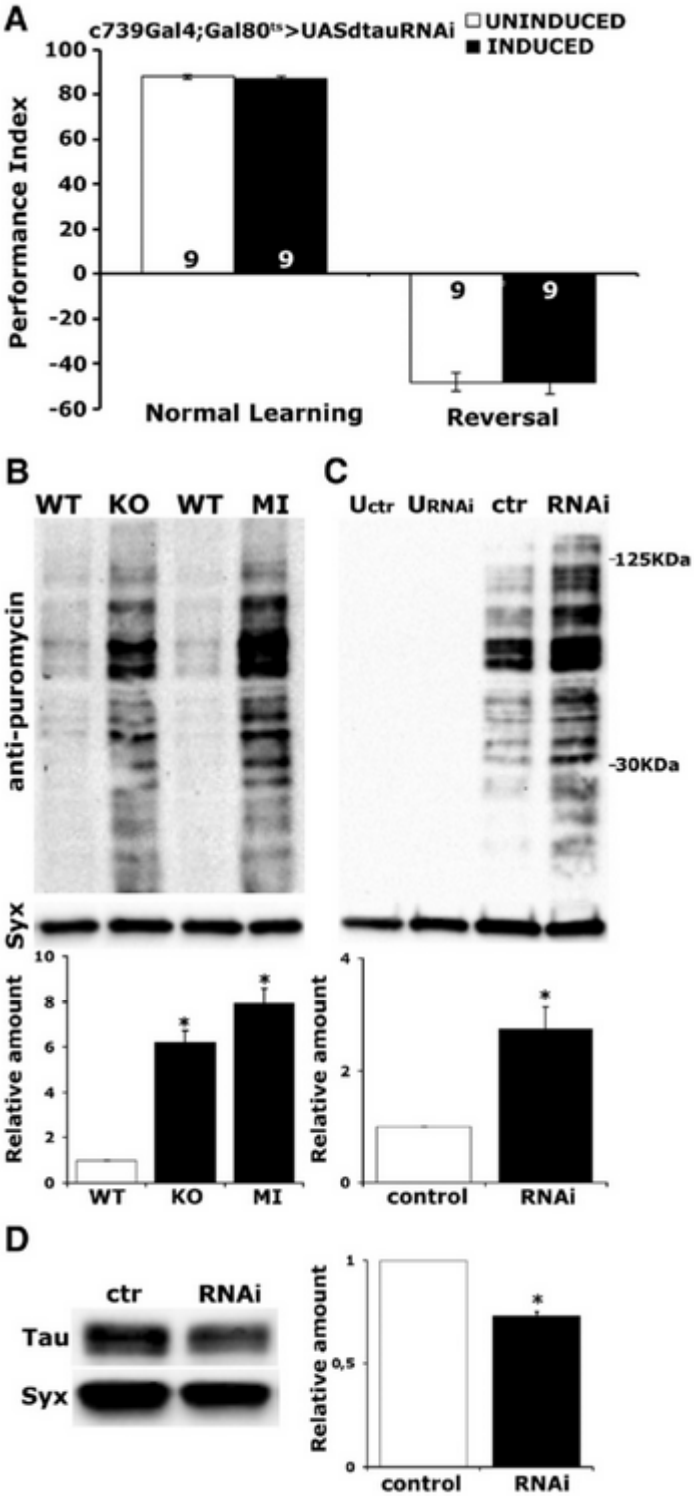

Figure 4. dTau is not required for forgetting of olfactory memories, and its abrogation increases protein synthesis levels. ***A***, Flies expressing dTauRNAi within αβ MB neurons under c739-Gal4;TubGal80ts performed at levels similar to the control group when they were trained with a reversed contingency. Both groups expressed considerable memory to the more recent learning event. No significant difference in 3 min memory was observed between the experimental and control groups when using the typical learning protocol. Animals were raised at 18°C and shifted

to 30°C for 3 d, while uninduced animals were kept at 18°C for these 3 d and were used as controls. The number of experimental replicates (*n*) is indicated within the bars. ***B***, To measure protein synthesis levels flies were treated with 600μM puromycin for 16 h. Representative blots of head lysates from WT, tau^{KO}, and tau^{MI} flies probed with either antipuromycin or anti-syntaxin (Syx). For quantifications, levels of the signal corresponding to molecular weight region 30 –125 Da in the mutants were normalized using the Syx loading control and are shown as a ratio of their mean±SEM values relative to their respective level in WT flies, which is arbitrarily set to 1. Stars indicate significant differences ($p<0.0001$) from control (open bars) for *tauKO* and *tauMI*. ***C***, Representative Western blot of head lysates from flies expressing UAS-dtauRNAi using Elav-Gal4;TubG80ts and probed with anti-puromycin antibody. Animals were raised at 18°C and shifted to 30°C for 3 d, while uninduced animals (U) were kept at 18°C for these 3 d. The genotype of control animals was Elav-Gal4;TubG80 ts/+. For the quantification, levels of the signal corresponding to molecular weight region 30 –125 kDa were normalized using the Syx loading control and are shown as a ratio of their mean±SEM values relative to their respective level in control flies, which is arbitrarily set to 1. The star indicates significant differences ($p= 0.0044$) from control (open bar), indicative of increased protein synthesis upon dTau loss. ***D***, Representative Western blot of head lysates from flies expressing UAS-dtauRNAi with Elav-Gal4;TubG80ts using an anti-dTau antibody. The genotype of control animals was Elav-Gal4;TubG80 ts/+ shifted to 30°C for 3 d. Compared with its levels in control animals, dTau was significantly reduced. For the quantification, tau levels were normalized using the Syx loading control and are shown as a ratio of their mean±SEM values relative to respective levels in control flies, which was set to 1. The star indicates significant differences from the control indicative of reduced dTau levels (*$p<0.0001$).

In agreement with the proteomic results, protein synthesis levels were significantly elevated in both mutants relative to control (WT) flies (**Fig. 4B**, for tau^{KO} and tau^{MI} respectively p=0.00004, p=0.00002, n=4). Moreover, qualitatively similar elevation of puromycin incorporation was obtained upon adult-specific pan-neuronal dTau abrogation (**Fig. 4C**, p=0.0044, n=4), suggesting rather acute effects on translation. It is also worth noting that protein synthesis increases in response to temperature elevation as expected (**Fig. 4C**, uninduced control –lane 1- versus control induced flies –lane 3). Given the dependence of PSD-LTM on translation, this protein synthesis up-regulation could account, at least in part, for the enhanced memory in the mutants. The collective results on **Tables 2** and **3** and **Fig. 4** support a role for dTau as an acute negative regulator of protein synthesis in the CNS.

Interestingly, acute abrogation of dTau yielded a similar memory enhancement as in the null mutants. Therefore, we wondered whether the proteomic profiles would be similar or diverge, an indication of compensatory mechanisms dynamics in these situations of acute, or chronic dTau attenuation. Therefore, proteomic profiling was performed after acute panneuronal dTau attenuation, which as shown in **Fig. 4D** leads to 30% reduction of dTau expression levels (p<0.0001, n=6).

Table 2. Upregulation of proteins that function in translation upon dTau loss

Gene	Identifier	Log 2 fold change	*p* Value
RpL3	FBgn0020910	0.29769754	0.015227*
RpL4	FBgn0003279	0.28274552	0.017456*
RpL10	FBgn0024733	0.38811628	0.019366*
RpL10Ab	FBgn0036213	0.41334375	0.010486*
RpL11	FBgn0013325	0.47628427	0.008492*
RpL12	FBgn0034968	0.22205798	0.008651*
RpL13	FBgn0011272	0.42983913	0.005514*
RpL18A	FBgn0010409	0.46355637	0.000564*
RpL23	FBgn0010078	0.44537226	0.022022*
RpL26	FBgn0036825	0.33991647	0.020167*
RpL30	FBgn0086710	0.33723116	0.011247*
RpLP2	FBgn0003274	0.38862832	0.005669*
RpS2	FBgn0004867	0.32947826	0.000604*
RpS3	FBgn0002622	0.33969498	0.002684*
RpS3A	FBgn0017545	0.29286544	0.014919*
RpS4	FBgn0011284	0.44215218	0.000334*
RpS6	FBgn0261592	0.35850573	0.013199*
RpS7	FBgn0039757	0.34377821	0.008244*
RpS8	FBgn0039713	0.28432178	0.007677*
RpS10b	FBgn0261593	0.30869754	0.020561*
RpS11	FBgn0033699	0.47895050	0.001293*
RpS12	FBgn0260441	0.45860616	0.005995*
RpS13	FBgn0010265	0.35336463	0.012484*
RpS14b	FBgn0004404	0.37592173	0.000738*
RpS15Aa	FBgn0010198	0.3678902	0.00019*
RpS16	FBgn0034743	0.36565614	0.00736*
RpS17	FBgn0005533	0.34326967	0.011799*
RpS18	FBgn0010411	0.34453487	0.003018*
RpS23	FBgn0033912	0.30110852	0.005235*
RpS27	FBgn0039300	0.3223815	0.010737*
Rbp2	FBgn0262734	0.26778308	0.002853*
sta	FBgn0003517	0.32786949	0.005807*
Ef1beta	FBgn0028737	0.23767066	0.015910*
Elf	FBgn0020443	0.31957237	0.002937*
eEF1delta	FBgn0032198	0.20101547	0.007045*
eIF2gamma	FBgn0263740	0.33932988	0.009390*
eIF-3p66	FBgn0040227	0.36954904	0.005558*
eIF3-S5–1	FBgn0037270	0.43084621	0.005214*
eIF3-S8	FBgn0034258	0.38344447	0.000346*
eIF3-S9	FBgn0034237	0.25910266	0.005049*
eIF3-S10	FBgn0037249	0.37967841	0.001322*
eIF4G	FBgn0023213	0.31082757	0.011195*
eRF1	FBgn0036974	0.34124954	0.002162*
bel	FBgn0263231	0.37415822	0.000987*
bol	FBgn0011206	0.36492339	0.000232*
glo	FBgn0259139	0.31756496	0.002210*
Trip1	FBgn0015834	0.41510550	0.000583*
Tango7	FBgn0033902	0.37924329	0.003916*
AGO1	FBgn0262739	0.20476087	0.011386*
U2af50	FBgn0005411	0.25440500	0.017200*
Dp1	FBgn0027835	0.27406081	0.009374*
Fmr1	FBgn0028734	0.32938814	0.000069*
Hrb27C	FBgn0004838	0.29338336	0.000018*
Hrb98DE	FBgn0001215	0.18872627	0.002404*
kra	FBgn0250753	0.36629526	0.005815*
Not1	FBgn0085436	0.27462665	0.002692*
Not3	FBgn0033029	0.33431784	0.011705*
pAbp	FBgn0265297	0.32483967	0.000818*
tyf	FBgn0026083	1.42353360	0.000399*

Table 2. Upregulation of proteins that function in translation upon dTau loss. Average log2 fold differences and *p* values for the indicated proteins calculated from three biological and two technical replicas. As the log2 fold changes denote, all listed proteins were upregulated in the *tauKO* mutant. The *t* tests were performed with a permutation-based FDR (0.05) calculation, and the *p* value determines the statistical significance of the difference (*significant *p* value 0.05).

In accord to the results from chronic dTau reduction in the mutants, proteomic changes were also uncovered upon acute dTau attenuation. Although they represented the three main protein groups, cytoskeletal (**Table 1**), translation-linked (**Table 2**) and neuronal function-linked (**Table 3**), which were also altered in the mutants, few were in common (**Table 4** and **Table 5**). For example, although Tubulin levels and HDAC6 appeared unaltered upon acute attenuation, nevertheless proteins critical for the dynamics and function of the microtubule cytoskeleton were altered. These include the microtubule tip-localizing protein Eb1, critical for accelerating their dynamics (260), the synaptic microtubule stabilization protein Ank2 (261), downregulated upon acute dTau loss and Arp2, an actin-related protein within the Arp2/3 complex, which is the basic actin nucleator in eukaryotes (262). In support of these results, Ank2 was recently suggested to interact with human Tau expressed in Drosophila (263).

Similarly, few of the proteins involved in translation and memory formation such as Fmr1, lig and CG4612 (**Table 5**) are shared between chronic and acute dTau attenuation. These similarities, but also the intriguing differences suggest dynamic proteostatic adjustments of cytoskeletal and translation-linked proteins upon acute dTau loss, which evolve into steady state long-term compensatory changes to support neuronal structure and function in the mutant. It is interesting that proteins such as 14-3-3ζ and the catalytic and regulatory subunits of Protein Kinase A, known to be involved in *Drosophila* learning and memory (264), are significantly changed upon acute but not chronic dTau attenuation (**Table 3** and **Table 5**). 14-3-3ζ has recently been reported to interact with human Tau expressed pan-neuronally in *Drosophila* in support of this (265). This suggests that the molecular mechanisms underlying PSD-LTM enhancement upon acute and chronic dTau loss are also dynamically proteostatically adjusted although the net effect may be similar. This is in accord with the notion that PSD-LTM formation or attenuation may result from engagement of distinct possibly parallel molecular pathways.

dTau is required for footshock habituation.

Apart from their established roles in olfactory learning and memory (43), MBs are also involved in habituation to repeated footshocks (55). Habituation is a form of non-associative plasticity manifested as response attenuation to repetitive inconsequential stimuli. To investigate whether dTau is involved in mechanisms underlying habituation,

Table 3. Differentially regulated proteins upon dTau deletion that affect memory formation

Gene	Identifier	Log2 fold change	*p* Value	References
A2bp1	FBgn0052062	0.242381	0.01749*	1
arm	FBgn0000117	0.287528	0.00576*	2
cer	FBgn0034443	0.352768	0.0016*	3
emb	FBgn0020497	0.187307	0.005865*	4
Fmr1	FBgn0028734	0.329388	0.00007*	5
Hop	FBgn0024352	0.358213	0.0002*	6
lig	FBgn0020279	0.360493	0.0066*	4
Pdk	FBgn0017558	0.392657	0000001*	4
Pkc53E	FBgn0003091	0.207134	0.0022*	7
CG4612	FBgn0035016	0.332883	0.00988*	8
Ugt	FBgn0014075	0.248749	0.0097*	4
Ugt35b	FBgn0026314	4.02456	0*	4

Table 3. Differentially regulated proteins upon dTau deletion that affect memory formation. Selected proteins, *p* values, and average log2 fold differencess (four biological and three technical replicas) have been calculated as described in Materials and Methods. As the log2 fold change denotes all proteins are upregulated in the *tauKO* mutant. The *t* test was performed with a permutation-based FDR (0.05) calculation, and the *p* value determines the statistical significance (**p* value<0.05). References: 1, (166); 2, (266); 3, (267); 4, (268); 5, (269); 6, (270); 7, (271); and 8, (272). The two proteins highlighted in gray are family members of a protein identified in 4.

both tauKO and tauMI mutants and their genetic background controls (w^{1118} and y^1w^1 respectively) were subjected to the established footshock habituation protocol (55) to repeated 45V electric shocks (**Figs. 5A, 5B**).

All genotypes avoided electric shock normally when naïve (tau^{KO} ANOVA: $F_{(2,34)}$= 5.5093, p=0.0088; tau^{MI} ANOVA: $F_{(2,40)}$ = 1.8286, p<0.1745) and the controls presented habituated responses after exposure to 15 such stimuli (**Figs. 5A, 5B**) as expected (55). In contrast, both dTau mutants failed to habituate to 15, 45V shocks (tau^{KO}, ANOVA: $F_{(2,34)}$= 58.5474, p<0.0001; subsequent LSM: p=3x10^{-10} vs WT, tau^{MI}, ANOVA: $F_{(2,40)}$= 11.0184, p=0.0002; subsequent LSM: p=7.9x10^{-5} vs WT), indicating inability to devalue inconsequential stimuli. The habituation deficit was not sensitive to CXM in the mutants (**Fig. 5C**, ANOVA: $F_{(3,68)}$ = 30.4059, p<0.0001; subsequent LSM: p=5x10^{-7}, tau^{MI} -CXM vs WT-CXM and ANOVA: $F_{(3,68)}$ = 30.4059, p<0.0001; subsequent LSM: p=8x10^{-11}, tau^{MI} +CXM vs WT+CXM), indicating that failure to habituate is not the result the elevated protein synthesis. Hence, dTau appears to physiologically engage neuronal mechanisms necessary to devalue the repeated footshock stimulation and facilitate habituation.

Table 4. Differentially regulated proteins involved in cytoskeleton organization and translation upon acute pan-neuronal dTau downregulation

	Identifier	Log 2 fold change	*p* Value
14-3-3ζ	FBgn0004907	−0.250421	0.023824*
Ank2	FBgn0261788	−0.16070	0.040059*
Eb1	FBgn0027066	−0.269836	0.038913*
dgt3	FBgn0034569	1.62118	0.031084*
Klp35D	FBgn0267002	−0.490059	0.016159*
Mtor	FBgn0013756	−0.376771	0.040521*
mud	FBgn0002873	2.61944	0.010824*
Pka-C1	FBgn0000273	−0.229651	0.009899*
Pka-R1	FBgn0259243	−0.217834	0.006967*
Rab11	FBgn0015790	−0.172639	0.018478*
Rbp	FBgn0262483	−0.173228	0.012758*
Strip	FBgn0035437	−0.457799	0.016759*
Arp2	FBgn0011742	−0.410359	0.009826*
bt	FBgn0005666	0.361831	0.034574*
btsz	FBgn0266756	−1.04969	0.049232*
didum	FBgn0261397	1.17976	0.001963*
mtm	FBgn0025742	−1.24456	0.034627*
SelR	FBgn0267376	−0.198595	0.039084*
vib	FBgn0267975	2.51317	0.001071*
WASp	FBgn0024273	−0.415598	0.003013*
zip	FBgn0265434	−0.16072	0.019419*
RpLP2	FBgn0003274	−0.22082	0.016296*
RpL9	FBgn0015756	0.363787	0.014304*
Ef1β	FBgn0028737	−0.18861	0.025385*
eIF-4B	FBgn0020660	1.22347	0.017551*
Elf	FBgn0020443	0.783829	0.029138*
EF2	FBgn0000559	−0.36835	0.001801*
eIF-2α	FBgn0261609	−0.16968	0.027685*
LeuRs	FBgn0053123	−1.95364	0.016296*
Fmr1	FBgn0028734	−0.8741	0.028043*
Dp1	FBgn0027835	−0.19861	0.03618*
U2af50	FBgn0005411	0.37609	0.024622*
qkr54B	FBgn0022987	0.619797	0.049061*
nito	FBgn0027548	−0.99659	0.045671*
La	FBgn0011638	0.505715	0.028674*
CG4612	FBgn0035016	−0.32493	0.011309*

Table 4. Differentially regulated proteins involved in cytoskeleton organization and translation upon acute pan-neuronal dTau downregulation. Selected proteins, *p* values, and average log2 fold differences from four biological and two technical replicas have been calculated as described in Materials and Methods. Control animals are Elav-Gal4;TubG80ts>+ vs Elav-Gal4;TubG80ts>dtauRNAi induced for 3 d at 30°C. The log2 fold change becomes positive when RNAi>control and negative when control>RNAi. The *t* test was performed with a permutation-based FDR (0.05) calculation, and the *p* value determines the statistical significance (**p*<0.05). In bold are proteins whose levels were also found to be changed in the mutant (Tables 1, 2).

Table 5. Differentially regulated proteins upon acute dTau loss that affect memory formation

Gene	Identifier	Log 2 fold change	*p* Value	References
Fmr1	FBgn0028734	−0.874096	0.028043*	1
lig	FBgn0020279	−1.006	0.032011*	2
14-3-3zeta	FBgn0004907	−0.250421	0.023824*	3
Ank2	FBgn0261788	−0.1607	0.040059*	4
CG4612	FBgn0035016	−0.324925	0.011309*	5
SLC22A	FBgn0037140	−0.850807	0.006731*	6
Fdh	FBgn0011768	0.29288	0.007593*	7
Pka-C1	FBgn0000273	−0.229651	0.009899*	8
Pka-R1	FBgn0259243	−0.217834	0.006967*	9
Sap47	FBgn0013334	−0.802852	0.003545*	10
Syn	FBgn0004575	−0.150291	0.005463*	11

Table 5. Differentially regulated proteins upon acute dTau loss that affect memory formation. Selected proteins, *p* value, and average log2 fold differences (four biological and three technical replicas) have been calculated as described in Materials and Methods. Control animals are Elav-Gal4;TubGal80ts>+ vs Elav-Gal4; TubGal80ts>dtauRNAi induced for 3 d at 30°C. The log2 fold change becomes positive when RNAi>control and negative when control>RNAi. The *t* test was performed with a permutation-based FDR (0.05) calculation, and the *p* value determines the statistical significance (**p*<0.05). In bold are proteins whose levels were also found to be changed in the mutant (Table 3). References: 1, (269); 2, (268); 3, (273); 4, (274); 5, (272); 6, (177); 7, (275); 8, (276); 9, (277); 10, (278) and 11, (279)

To confirm that the habituation defect maps to the adult MBs, we used the same Gal4 drivers as above to conditionally attenuate dTau via RNAi (**Fig. 5D**). Habituation deficits were uncovered upon pan-neuronal (Elav: ANOVA: $F_{(2,39)}$= 18.8294, p<0.0001; subsequent LSM: p=1.3x10^{-5} and p=2.2x10^{-6} vs controls respectively) and adult MB limited attenuation (LeoMB: ANOVA: $F_{(2,39)}$= 8.0835, p=0.0012; subsequent LSM: (280) p=0.0004 and p=0.0058 vs controls respectively; dnc: ANOVA: $F_{(2,29)}$= 16.7159, p<0.0001; subsequent LSM: p=2.2x10^{-5} and p=4.3x10^{-5} vs controls respectively; MB247: ANOVA: $F_{(2,30)}$=11.5623, p=0.0002; subsequent LSM: p=0.0004 and p=0.0002 vs controls respectively). These results were recapitulated with an independent RNAi-mediating transgene driven pan-MB under dncGal4 (dnc-Gal4;TubGal80^{ts} >+ =12.23±1.34; dtauRNAi40875 >+ =8.71±1.88; dnc-Gal4; TubGal80^{ts} >dtauRNAi40875 =1.99±1.65; n=14, ANOVA: $F_{(2,42)}$=9.8512, p=0.0003; subsequent LSM: p=0.0001 and p=0.0056 vs controls respectively).

Interestingly, dTau attenuation restricted to α'β' neurons precipitated pronounced habituation defects (c305α: ANOVA: $F(_{2,28})$=72.8606, p<0.0001; subsequent LSM: p=1.16x10^{-10} and p=2.63x10^{-11} vs controls respectively), in agreement with an accompanying report (56). In contrast, habituation was normal if abrogation was limited to 739-Gal4-marked neurons (c739: ANOVA: $F_{(2,43)}$= 0.5378, p=0.5881). Collectively the results indicate a distinct role for dTau specifically within the α'/β' neurons in molecular

mechanisms that facilitate footshock habituation, in addition to its role in limiting PSD-LTM within these and their α/β counterparts.

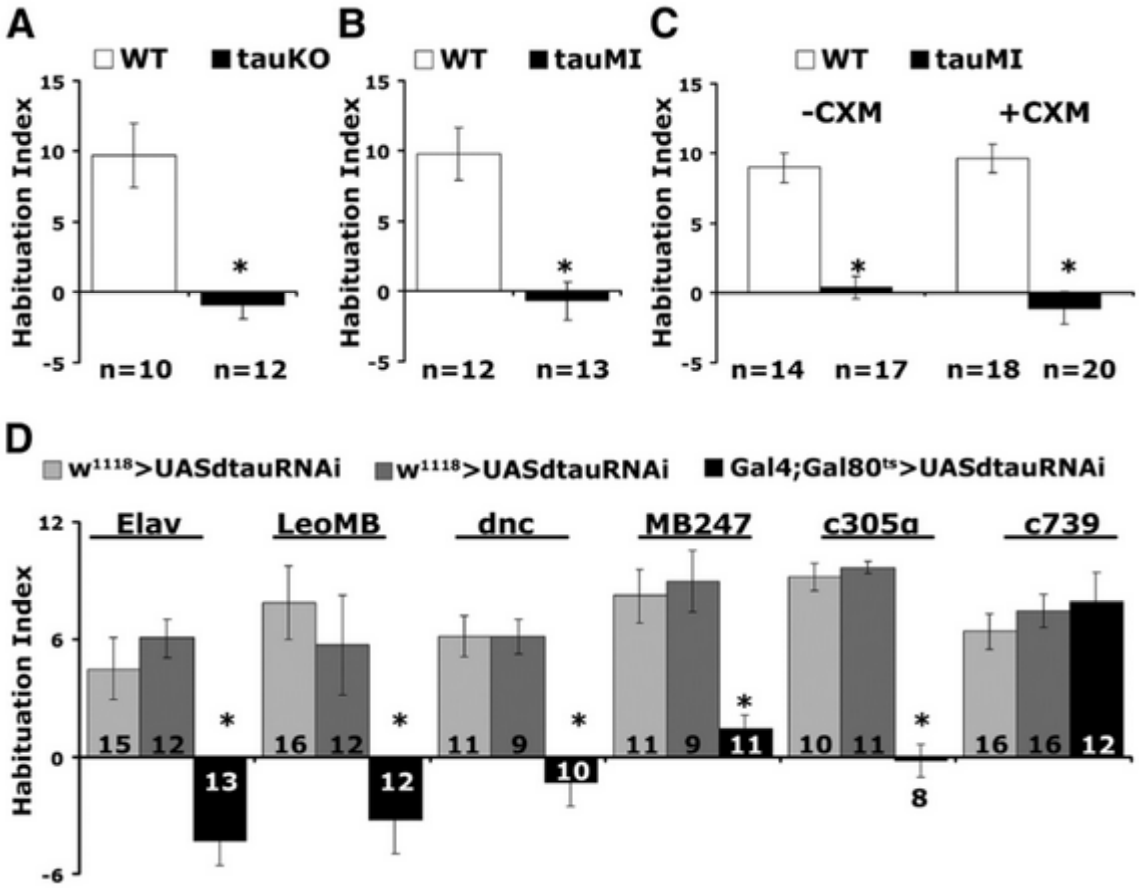

Figure 5. dTau abrogation impairs habituation. ***A***, ***B***, *tauMI* and *tauKO* mutants present strong habituation deficits (**p* <0.0001). The number of experimental replicates (*n*) is indicated below the graphs. ***C***, CXM administration did not affect the defective habituation of *tauMI* flies. ***D***, Deficient habituation upon dTau abrogation in adult animals using Elav (**p*<0.0001), LeoMB (**p*=0.0004), MB247 (**p*_0.0004), dnc (**p* 0.0001), and c305α (**p*<0.0001) drivers, but not under c739 (*p*= 0.3269). The number of experimental replicates (*n*) is indicated within the bars.

dTau elevation in adult MBs suppresses memory and results in premature habituation.

Because LTM and footshock habituation appear sensitive to dTau levels within the MBs, we hypothesized that its elevation within these neurons may lead to the opposite phenotypes akin to those observed upon overexpression of human Tau (223). In humans, duplication of the tau gene and hence presumably elevation the protein, causes prominent neurofibrillary tangle pathology leading to early-onset dementia with an AD clinical phenotype (281).

To elevate dTau, a UAS-Flag-dTau transgene was expressed specifically throughout the adult MBs under the pan-mushroom body driver dnc-Gal4;TubGal80^{ts} (**Fig. 6E**). The

increase in dTau within the MBs did not affect learning (**Fig. 6A**, ANOVA: $F_{(2,33)}$ = 0.9706, p=0.3901), or the protein synthesis-independent ARM (**Fig. 6B** massed, ANOVA $F_{(2,23)}$= 1.9193, p=0.1716), but PSD-LTM (**Fig. 6B** spaced) was deficient (ANOVA: $F_{(2,28)}$= 13.7758, p<0.0001; subsequent LSM: p=$4.1x10^{-5}$ and p=0.0003 vs controls respectively). In accord with the hypothesis that elevated translation is in part at least, responsible for the increased PSD-LTM, adult-specific pan-neuronal accumulation of dTau resulted in an acute translation decrease (**Fig. 6I**, p=0.0026, n=4). Therefore, processes required for PSD-LTM are sensitive to dTau levels in a manner akin to that recently described for dAlk (175) and in accord with the interpretation that dTau participates in processes that limit LTM formation, storage or recall.

Interestingly, dTau elevation did not affect habituation (**Fig. 6C**) to 15 footshocks (ANOVA: $F_{(2,27)}$ = 0.7958, p=0.4623), but onset of the habituated response was premature (**Fig. 6D**), as it occurred after only two stimuli (ANOVA: $F_{(2,39)}$ = 33.1018, p<0.0001; subsequent LSM: p=$3.2x10^{-6}$ and p=$1.9x10^{-9}$ vs controls respectively). Because silencing neurotransmission from α/β MB neurons results in premature habituation (55), we overexpressed dTau specifically in these neurons under c739-Gal4. Although this resulted in deficient (**Fig. 6F**) PSD-LTM (ANOVA: $F_{(2,31)}$= 18.0720, p<0.0001; subsequent LSM: p=$8.9x10^{-6}$ and p=$4x10^{-5}$ vs controls respectively), it yielded normal habituation to 15 footshocks (ANOVA: $F_{(2,43)}$= 0.5105, p=0.6040) and did not result in premature habituation after two footshocks (ANOVA: $F_{(2,43)}$ = 0.9059, p=0.4121) (**Figs. 6G, 6H**). This suggests that its over-accumulation does not inhibit neurotransmission and dTau is strongly implicated in a dosage-dependent manner in processes mediating footshock habituation within the MBs.

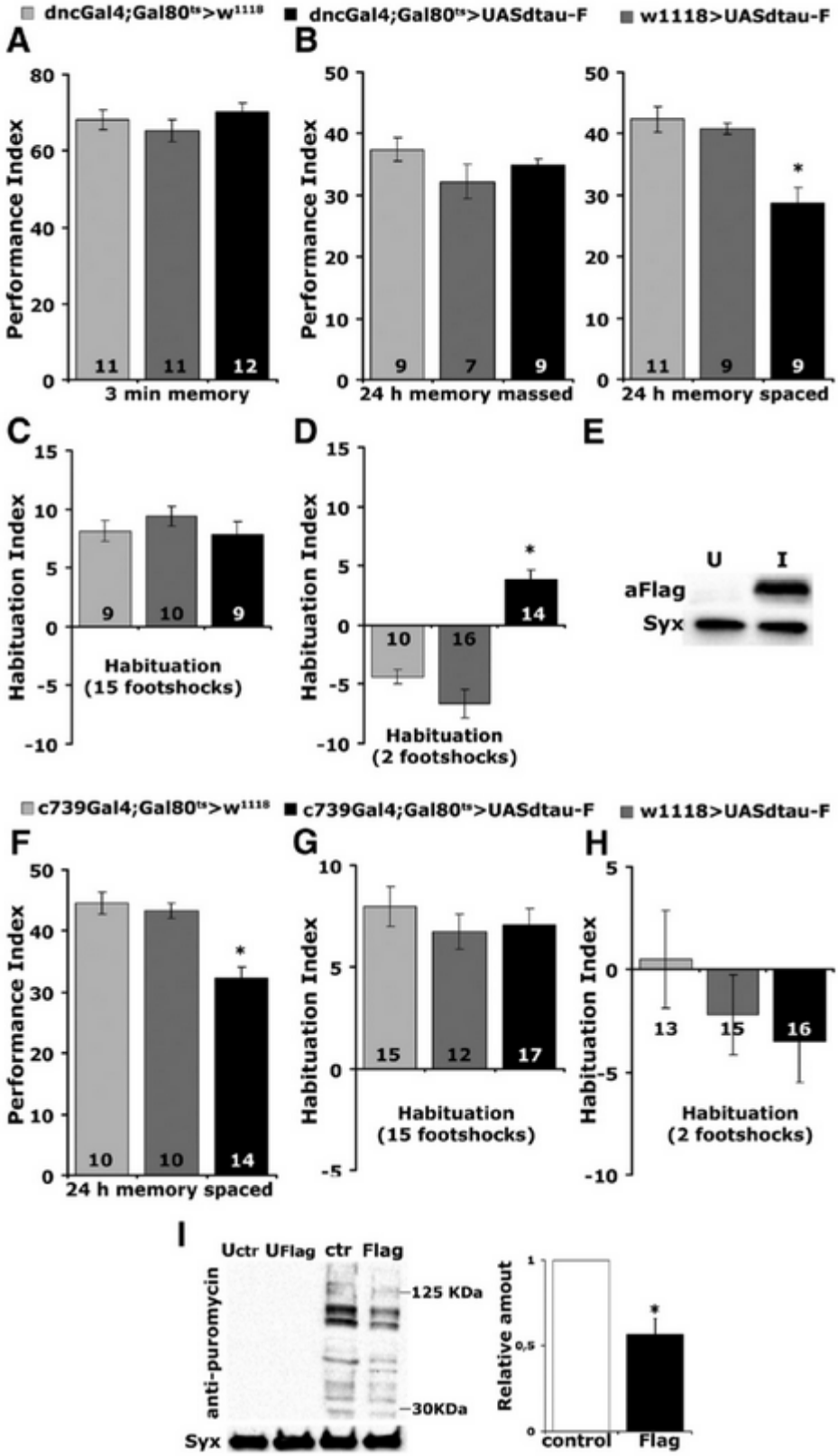

Figure 6. dTau elevation within the adult MBs leads to premature habituation and LTM deficits with a concomitant decrease in protein synthesis levels. ***A***, ***A–D***, Adult-specific expression of UAS-

Flag dTau within the MBs under dnc-Gal4 results (***A***), normal 3 min memory (***B***), normal ARM after massed training but LTM deficits after spaced training (*p<0.0001), normal habituation following 15-stimulus training (***C***), and premature habituation (*p<0.0001) following 2-stimulus training (***D***). The number of experimental replicates (n) is indicated within the bars. ***E***, Representative Western blot demonstrating accumulation of Flag-dTau in adult MBs using LeoMB-Gal4;TubG80ts of animals raised at 18°C and shifted to 30°C for 2 d (I), while uninduced animals (U) were kept at 18°C for these 2 d. dTau was revealed with an anti-Flag antibody. Syntaxin (Syx) was used as a loading control. ***F–H***, Adult-specific expression of UAS-Flag dTau within αβ neurons under c739 yields significant LTM deficits (*p<0.0001) compared with controls (***F***), and results in normal habituation following 15-stimuli (***G***) or 2-stimuli (***H***) training. The number of experimental replicates (n) is indicated within the bars. ***I***, Representative Western blot of head lysates from flies expressing UAS-Flag-dTau using Elav-Gal4;TubG80ts and probed with anti-puromycin antibody. Animals were raised at 18°C and shifted to 30°C for 3 d, while uninduced animals (U) were kept at 18°C for these 3 d. The genotype of control animals was Elav-Gal4;Gal80ts/+. Flies were treated with 600μM puromycin for 16 h. For the quantification, levels of the signal corresponding to molecular weight region 30 –125 kDa were normalized using the Syx loading control and are shown as a ratio of their mean_SEM values relative to their respective level in control flies, which is arbitrarily set to 1. The star indicates significant differences (p=0.0026) from control (open bar), indicative of decreased protein synthesis upon dTau loss.

Discussion

Although our phenotypic search was not exhaustive, our results demonstrate robust mutant phenotypes upon dTau loss for the first time to our knowledge. In agreement with prior reports we also find that both tau^{KO} and tau^{MI} mutants are viable and fertile (not shown).

Proteostatic changes upon chronic and acute dTau loss.

Significant changes in the adult CNS cytoskeletal proteome were uncovered by comparative proteomics and appear to underlie a global proteostatic adjustment to dTau abrogation. We have modelled two scenarios of dTau abrogation, chronic dTau loss as in the mutants and a milder acute attenuation in the adult CNS. Although both situations elicited broad changes with certain proteins altered in common, they yielded differential proteomic signatures (**Tables 1-5**). Chronic changes appear to have resolved into a proteostatic steady state, presumably to minimize the effects of dTau loss. This is reflected by compensatory changes in HDAC levels for example, which stabilize the microtubule cytoskeleton, despite the ostensibly chronic reduction in Tubulin (**Fig 1B**, **Table 1**). On the other hand, acute dTau attenuation revealed the initial response of the CNS proteome to the insult, which included downregulation of many Tau interacting proteins (**Table 4**). We suggest that with time, this acute proteostatic flux resolves to a steady state reflective of the level of dTau attenuation, and ongoing experiments are addressing this hypothesis.

Interestingly, the steady state levels of all three tubulins were significantly reduced (**Table 1**), in accord with the notion that Tau is essential for maintenance of long labile domains of microtubules (282), and may also be reflected in the acute downregulation of

proteins such as labile end-organizing protein Eb1 (260). dTau loss-dependent reduction of labile domain length is in effect reducing microtubule mass and hence the amount of tubulins. The relative increase in acetylated tubulin (**Fig. 1B, C**) is consistent with the reduction in labile domains, which are expected to be under-acetylated (282). A potential consequence of the increased microtubule stability is the significant elevation in the subunits of both anterograde and retrograde moving motor proteins (**Table 1**).

Cytoskeletal homeostasis upon chronic dTau loss also benefits from the reduction in the deacetylace HDAC (**Table 1**), which may mediate the increase in acetylated tubulin and also account for the proposed reduction in the labile domains. Although how dTau loss affects HDAC levels is unclear at the moment, levels of the deacetylase are sensitive to Tau dosage as HDAC6 is elevated in Alzheimer's disease (AD) brains and tubulin acetylation is reduced in neurofibrillary tangle-bearing neurons (283). Consistent with these observations, increased tubulin acetylation rescues human Tau overexpression-induced defects in Drosophila (284);(41).

The functional role for dTau as a major regulator of cytoskeletal dynamics in vivo is also illustrated by the upregulation of the steady state levels of actin binding proteins (**Table 1**), likely in response to the negative effects on actin polymerization upon dTau loss. Our data demonstrate that F-actin interacts directly with and is stabilized by dTau within the fly CNS (**Fig 2 B-E**). In congruence, perturbation of actin dynamics has also been reported upon pan-neuronal expression of human Tau isoforms in *Drosophila* (235) and may underlie some of the resultant neuropathologies. Therefore, our collective data strongly support the notion that dTau is a true MAP impacting the microtubule and actin cytoskeleton and despite the sequence diversity an apparent ortholog of its vertebrate counterpart.

dTau translation regulation and neuroplasticity.

Chronic, but surprisingly, also acute dTau abrogation resulted in upregulation of translation-linked proteins (**Table 2, Table 4**) strongly indicating that dTau is a negative regulator of translation (**Fig 4B**). Congruently, vertebrate Tau is a negative regulator of translation (285) and was also recently reported to act as a negative regulator of ribosomal protein levels in mouse brains (286). Importantly, the fly brain comparative proteomics provide further validation of these results in a different system, as clearly dTau loss results in broad elevation of proteins involved in regulation, initiation and termination of translation, as well as most cellular ribosomal proteins (**Table 2, Table 4**). In addition, Tau is known to bind to ribosomes in the brain and impair their function reducing protein synthesis (287), an effect also observed in human Tauopathy brains (288). Finally, this agrees with quantitative proteomics in a mouse model of Tauopathy, which revealed a decrease in protein synthesis specifically in neurons with high levels of pathological Tau (289). This effect was recapitulated by acute dTau overexpression (**Fig 6I**), demonstrating the sensitivity of translation to Tau levels.

Interestingly, translational upregulation may be partially selective, because under chronic, or acute dTau attenuation most MAPs, Tubulins, HDAC and other abundant proteins were not elevated, but rather reduced (**Table 1, Table 4**). Consistent with this notion, the translational regulator dFmr1, whose loss results in LTM deficits (290), is also elevated (**Table 2**), suggesting that dTau may be implicated in translational selectivity mechanisms. Elevation of proteins potentially involved in PSD-LTM in mutant brains (**Table 3, Table 5**) and probably within MB neurons, likely underlies, at least in part, the enhanced memory in agreement with its CXM sensitivity (**Fig. 3C**). The enhanced 24 hr memory is not ARM (**Fig 3A, B**), or impaired forgetting (**Fig 4A**). Furthermore, dTau is required within α/β and a'/β'neurons involved in recall and memory consolidation respectively (52);(53);(51);(291);(54). Collectively then, the enhanced 24hr memory upon dTau abrogation is most likely due to enhanced consolidation of true PSD-LTM.

In contrast to PSD-LTM, the defective footshock habituation upon dTau loss is CXM insensitive, arguing that it is not consequent of excessive protein synthesis (**Fig 5**). Is it possible that failure to devalue the electric footshock US results in better acquisition resulting in better learning that eventually forms enhanced memory? This is unlikely because abrogation of dTau in the MBs did not result in better performance after limited training with 3 odor/shock pairings (**Fig 3E**). Moreover, limiting dTau abrogation to the α'/β' MB neurons resulted in enhanced PSD-LTM, as well as failure to devalue the shock stimulus, demonstrating that these effects are cell-autonomous. Neurotransmission from these neurons is required for olfactory memory acquisition and stabilization (54), but also to facilitate shock habituation (56). Therefore, it is unlikely that dTau is implicated in a common mechanism affecting both processes, because enhanced PSD-LTM mediated by these neurons (**Fig 3F**) suggests increased neurotransmission, whereas failure to habituate its impairment.

A parsimonious explanation for this paradox would be that dTau functions in distinct mechanisms regulating conditional neurotransmitter traffic and release within these neurons, in line with the changes in actin binding proteins, microtubule motor and associated proteins uncovered by the proteomics (**Table 1, Table 4**). Changes upon dTau abrogation may selectively deregulate neurotransmitter levels and their regulated release, known to depend on presynaptic microtubule and cortical actin dynamics (197). This may selectively enhance neurotransmission upon associative (memory), but not upon non-associative (habituation) stimulation. This is in line with the observation that dTau abrogation in αβ neurons, where neurotransmission is essential for LTM retrieval (52);(53);(51);(291), also enhances LTM (**Fig 3F**). Interestingly, Tau null mice were also recently reported to perform better than WT littermates in a spatial navigation task (292) and showed enhanced exploration and recognition memory (293). Given these collective results, the effects of dTau loss on Drosophila PSD-LTM and the molecular targets offered by our comparative proteomic data, potential physiological roles for dTau in these processes are currently under investigation.

Overexpression of human Tau in the adult Drosophila CNS precipitates significant impairment in LTM, but not ARM (223). This effect was recapitulated by adult-specific pan-neuronal, or MB limited overexpression of dTau (**Fig. 6**). Again, relatively acute dTau elevation precipitated the complementary phenotype of premature habituation. Blocked neurotransmission from the MBs results in premature footshock habituation (55) similar to that observed upon dTau overexpression. Therefore, we hypothesize that excess dTau in the MBs might reduce neurotransmitter availability in accord with data from the larval neuromuscular junction (294).

In conclusion, it is apparent that dTau contributes in a dosage-dependent manner to a broad number of distinct processes involved in CNS function. Although it is a challenge of future work to understand how dTau can alter neuronal plasticity, the emerging insights on its physiological functions are expected to enhance our understanding of the molecular and cellular pathways perturbed in the various Tauopathies.

5. *Drosophila* adenylate cyclase *rutabaga* is implicated in footshock habituation.

Ilianna G. Roussou, Rania Christodoulou, Aggeliki Kontopoulou and Efthimios M. C. Skoulakis

Introduction

Rutabaga (*rut*) encodes an adenylate cyclase in fruit flies, similar in properties to the Type I AC characterized from vertebrate brain. The enzyme is activated by G-protein and Ca^{++} and has the potential of integrating incoming signals. The gene has been implicated in learning and memory (8);(295) and together with *dunce* (*dnc*) which encodes a cAMP phosphodiesterase, play a critical role in olfactory learning of *Drosophila* (296). Both genes are expressed in the mushroom bodies, neuroanatomical sites that mediate olfactory learning (297). *Rut* is thought to be a coincidence detector during learning and memory consolidation (298), while *rut* mutants show decreased basal cAMP levels and thus are not able to temporally increase cAMP in response to acute stimulation.

Furthermore, *rut* is implicated in non-associative learning. Rut mutants demonstrate divergent responses when studied in distinct behavioral assays. In Proboscis extension Reflex (PER), *rut* mutants show poor habituation while habituation of the landing response is fast compare to control flies. In addition, habituation of the cleaning reflex is characterized as short lived (reviewed in (299)) while a recent study demonstrates the necessity of *rut* in maintenance of olfactory habituation latency (93).

Here, we investigate the role of *rut* in footshock habituation. *Rut* was included in the genes to be screened because of its implication in various forms of habituation as described above. In addition, human orthologs ADCY2 and ADCY3 have been found in genome-wide association studies (GWAS) being implicated in schizophrenia (300);(301). Despite the fact that GWAS do not provide functional proofs, they can supply valid indication of a gene involvement in schizophrenia.

Materials and Methods

Drosophila *culture and strains. Drosophila* were cultured in standard wheat-flour-sugar food supplemented with soy flour and CaCl2 (55) at 18°C or 25°C. The MiMIC *rut* insertion (54509) was from the Bloomington Stock Center (BDRC; Indiana University; (35)). *The rut* RNAi encoding stock (27035), as well as the UAS-*rut* line (9405) was also from BDRC. To generate the driver heterozygote controls for experiments with the RNAi-encoding transgene, driver-bearing strains were crossed to their y^1v^1 (BDSC, 36303) background. The pan-neuronal drivers elav-Gal4, and the mushroom body specific drivers leo-Gal4,

were described previously (174); (175). The Gal80^{ts} transgene was added to the driver-bearing chromosomes by recombination or standard crosses as indicated.

Behavioral assays. All flies used in behavioral experiments were tested 3–5 d after emergence. All experiments were performed under dim red light at 25°C and 65–75% relative humidity. To obtain animals for behavioral experiments Gal4 driver homozygotes were crossed *en masse* to strains carrying the UAS-*rut*-RNAi transgene. Animals expressing Gal80^{ts} (179) were raised at 18°C until hatching and then placed at 30°C for 2 d before testing.

Electric footshock avoidance. Experiments were performed as described before (55). Briefly, ~70 flies were placed at the choice point of a T-maze to choose for 90 s between an electrified and an otherwise identical inert standard copper grid. In the electrified grid, 45 V shocks were delivered every 5.15 s, each lasting 1.2 s. The avoiding fraction (AF) was calculated by dividing the number of flies avoiding the shock by the total number of flies.

Habituation to electric footshock. Habituation to electric shock experiments were performed as described before (55). Briefly, for the training phase ~70 flies were sequestered in the upper arm of a standard T-maze lined with an electrifiable grid. They were exposed to 15 1.2 s electric shocks at 45 V with a 5.15 s interstimulus interval. Air was not drawn through the tube during training to avoid association of the shocks with air. After a 30 s rest and 30 s for transfer to the lower part of the maze, the flies were tested by choosing between an electrified and an inert grid. Therefore, the earliest measures of post-training responses are 1 min after the flies received the last training stimulus. Testing was performed at the same voltage (45 V) as for training. During the 90 s choice period, 17–18 1.2 s stimuli were delivered to the electrified arm of the maze. At the end of the choice period, the flies in each arm were trapped and counted, and the habituation fraction (HF) was calculated by dividing the number of flies preferring the shock by the total number of flies, as above. Finally, the habituation index (HI) was calculated as (HF-AF) X 100% and therefore represents the change in footshock avoidance contingent upon prior footshock experience (habituation). Although the absolute avoidance score is variable, even for the same genotypes (Table 1), as expected for behavioral experiments performed over a significant time period, because the HI measures the relative change in avoidance within each genotype, it is not affected by such variability. In fact, failure to habituate, which is the primary phenotype reported herein, is a manifestation of maintained avoidance relative to that of naive flies of the same genotype.

Olfactory Learning. Olfactory learning in the Pavlovian negatively reinforced conditioning paradigm, coupling aversive odors as conditioned stimuli (CS^+ and CS^-) with the electric shock unconditioned stimulus (US), were performed essentially as described previously, for 3 min/learning (257). Briefly, all experiments were performed in a genotype-balanced manner, with the experimenter blind to genotype and under dim red light, at 25°C and

70% humidity. Groups of ~75, 2- to 3-d-old flies were transferred to fresh vials 1 h before training and then trained in a T-maze apparatus. The aversive odors used were benzaldehyde and 3-octanol, diluted in isopropyl myristate (Fluka). Training for 3 min/learning or 3 h/mid-term memory experiments consisted of 1 single session of 12 US/CS pairings of 90 V electric shocks (US) with one odor (CS^+) over 1 min, followed after a 30 s purge with air, by the presentation of the second odor (CS^-) without shocks for 1 min. For testing, flies were allowed to choose between the two odors presented in the two arms of the T-maze apparatus for 1.5 min. Performance was measured by calculating a performance index (PI) as follows: the fraction of flies that avoided the shock-associated odor (CS^+) minus the fraction that avoided the control odor (CS^-) represented half of the PI. One PI was calculated as the average of the half-learning indexes for each of the two groups of flies trained to complementary conditioning stimuli.

Pharmaceutical treatments. The antipsychotic drugs clozapine (Sigma-Aldrich) and risperidone (Tocris Bioscience) were diluted in DMSO and mixed at the indicated final concentrations in Brewer's yeast (Acros Organics) aqueous paste. The concentration ranges used bracketed analogous concentrations as used for humans. Clozapine at 1, 5 and 10 μM; and risperidone at 1, 5 and 10 μM. Flies were starved for 5 h in empty vials at 25°C before exposure to drug or vehicle-only containing yeast paste for 14–16 h. The following day, flies were transferred in normal food vials, trained, and tested as detailed for footshock habituation.

Results

Rut functions within the MBs to promote footshock habituation

In the footshock habituation paradigm (55), flies avoid the initial 2–8 repetitive stimuli, but their response declines rapidly to an asymptotic baseline as predicted (64), after 10–11 stimuli. This pre-exposure dependent attenuated avoidance after 15 footshocks relative to that of naïve animals is quantified as a positive change in the HI of control flies. Failure to establish habituation does not attenuate shock avoidance after shock pre-exposure and therefore yields the zero or negative difference from the naïve response reported by the HI. The viable MiMIC (35) insertion mutant in *rut* (54509-Mirut), did not attenuate shock avoidance following exposure to 15 stimuli, in contrast to controls as shown in **Fig. 1**. This was verified by retesting the Mi*rut* insertion alone (**Fig. 1 left**).

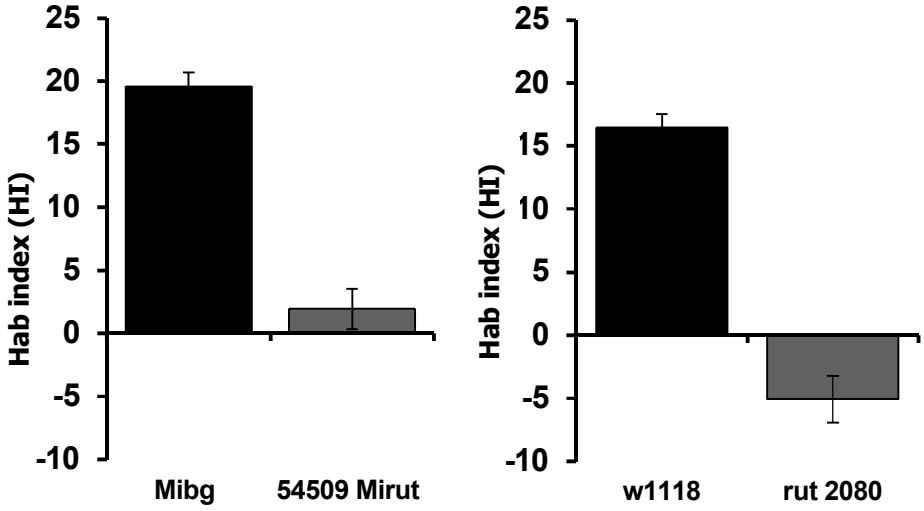

Fig.1. Mirut mutants (54509) fail to habituate (left), ANOVA $F_{(1,22)}=68.3610$ $p<0.0001$*. The same phenotype is exhibited by another P-element insertion mutant (right), ANOVA $F_{(1,21)}=76.1077$ $p<0.0001$*

The same outcome resulted from a P element insertion within the *rut* locus (rut2080). These mutants also do not habituate after pre exposure to 15 shocks (**Fig.1**, right). This data demonstrate that the Rut Adenylyl Cyclase activity is required for footshock habituation. Next, we wondered where *Rutabaga* is required within the adult CNS to facilitate footshock habituation. Hence, we abrogated Rut using a UAS-rut^{RNAi}-encoding transgene. As expected, Rut attenuation under the pan-neuronal elav driver resulted in failed habituation after 15 footshocks (**Fig.2**). The necessity of *Rut* within the MBs for facilitation of habituation was strongly established using two independent MB drivers, leo and dnc (**Fig.2**). This conclusion was strengthened by reinstating Rut specifically within the adult MBs, using the UAS-rut transgene (**Fig.3**) which fully reversed their deficient habituation. However if the UAS-rut transgene was not induced in adult animals the mutant phenotype persisted.

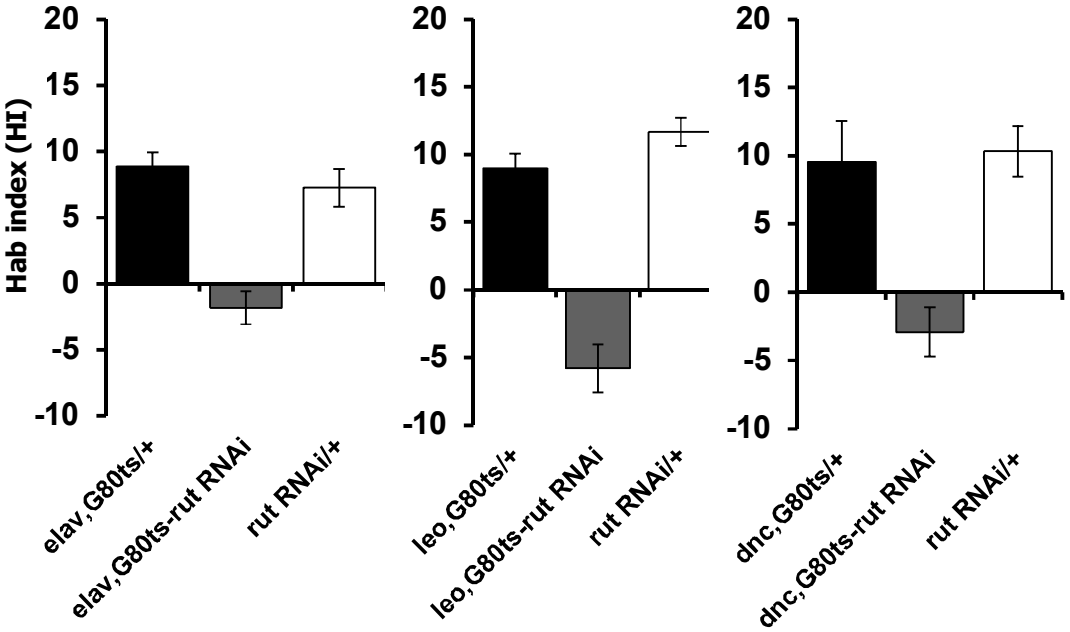

Fig.2. Rut abrogation in elav, leo and dnc neurons respectively results in elimination of habituation response. Elav: ANOVA $F_{(2,48)}=15.9679$ $p<0.0001$*. Leo: ANOVA $F_{(2,40)}=44.2619$ $p<0.0001$*. Dnc: ANOVA $F_{(2,30)}=11.5279$ $p<0.0001$*

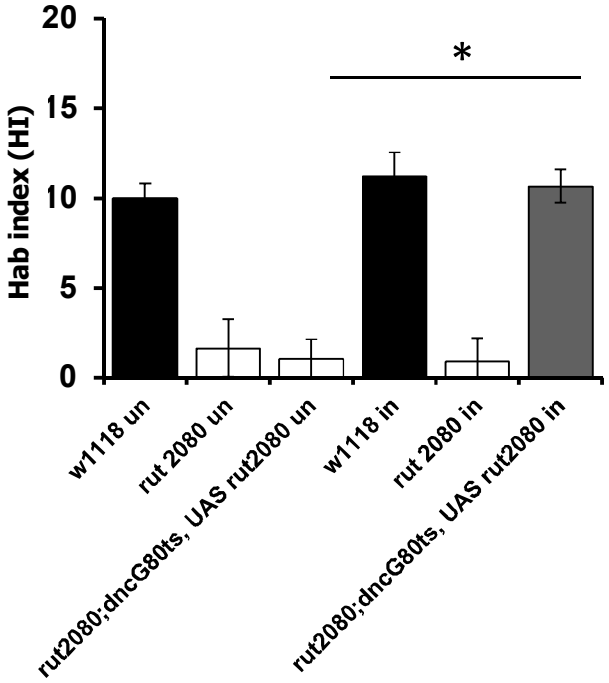

Fig.3. Reinstating rut specifically within the adult MBs of adult rut flies, using the UAS-rut transgene fully reversed their deficient habituation ANOVA $F_{(5,92)}=17.2398$ $p<0.0001$*

Antipsychotics rescue the deficient habituation of rut mutants

In accord with published results from the Btk gene (56), we sought to determine whether the typical antipsychotic clozapine and the atypical risperidone could restore the inability of rut mutants (both *Mirut* and *rut*^{2080}) to habituate after 15 shocks. Interestingly, administration of clozapine for16–18 h before habituation training reversed the inability of

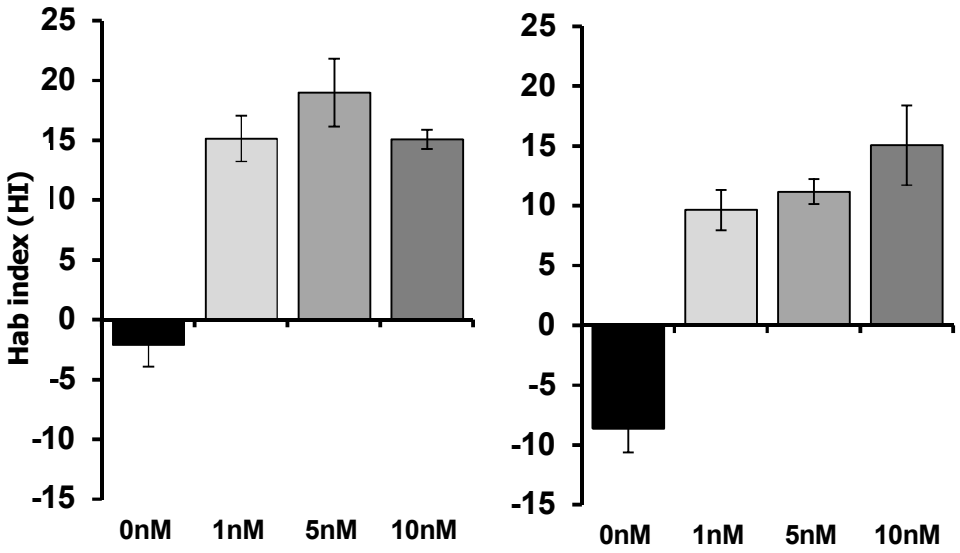

Fig.4. Clozapine rescues the defective habituation of Mirut flies (left). ANOVA $F_{(3,36)}$=27.7501, p<0.0001* . Risperidone restores the inability to habituate in Mirut flies (right). ANOVA $F_{(3,42)}$=26.2958, p<0.0001*

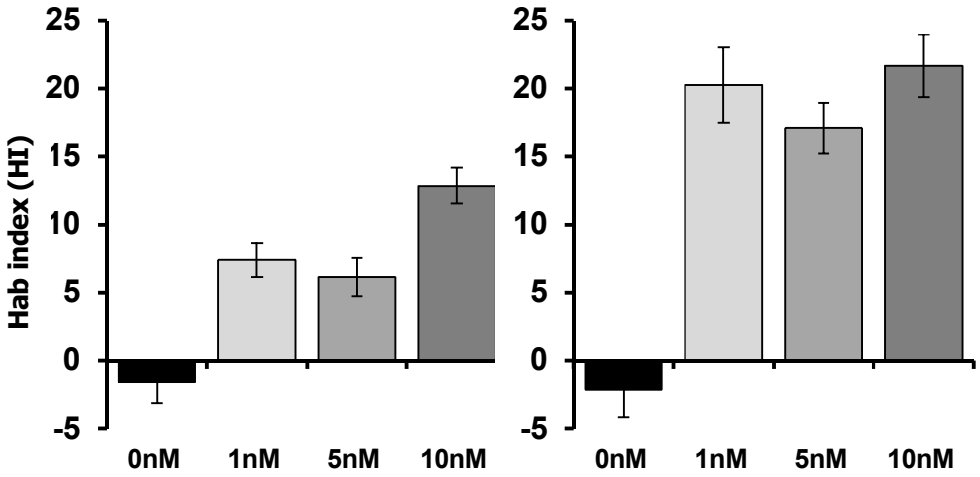

Fig.5. Clozapine rescues the defective habituation of rut2080 flies (left). ANOVA $F_{(3,40)}$= 16.9095, p<0.0001* . Risperidone restores the inability to habituate in rut2080 flies (right). ANOVA $F_{(3,43)}$= 19,9738, p<0.0001*

rut mutants to habituate to 15 footshocks (**Fig.4, left, Fig.5, left**). A similar treatment with risperidone also reversed the defective habituation of rut flies (**Fig.4 right, Fig.5 right**).

Since it is known that *rut* mutants are learning deficient, we aimed to determine whether their failed habituation could underlie their learning deficit, by testing initially whether both deficits of the mutant flies could be reversed by risperidone.

Interestingly, although able to reverse their deficient habituation, risperidone could not restore the learning deficit of rut mutants (**Fig.6**).

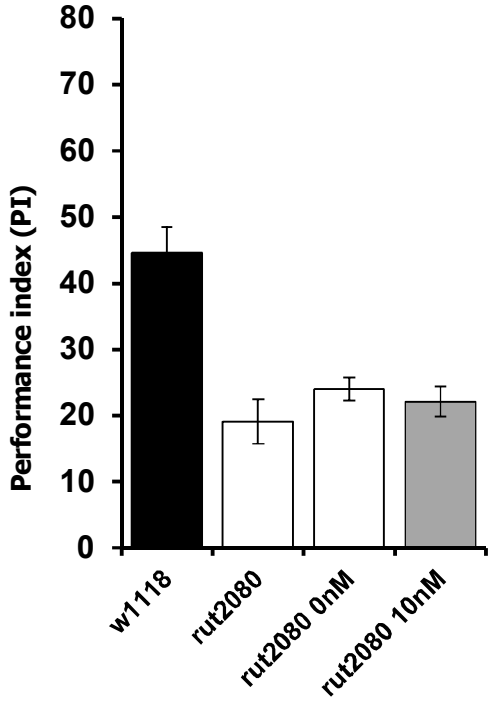

Fig.6. *Rut*^{2080} flies show learning deficit compared to *w*^{1118} flies. Risperidone treatment does not restore the deficient learning phenotype of *rut*^{2080} flies ANOVA $F_{(4,47)}$= 11.1976 p<0.0001*.

Discussion

In this study, we describe a footshock habituation mutant that derived from the screen mentioned in (56). Rutabaga encodes an adenylate cyclase that plays an important role in learning and memory. Here, we demonstrate that rutabaga regulates footshock habituation and that it is required within the MBs to promote the response attenuation. However, more experiments have to be done to further analyze the specific neurons in which r*utabaga* is necessary to promote habituation.

Moreover, it is very intriguing that schizophrenia patients also present habituation defects manifested as failures in prepulse inhibition (138);(135), where a weak prestimulus inhibits the reaction to a following strong startling stimulus. These defects are thought to reflect inability to devalue inconsequential stimuli (138) and can be reversed with antipsychotics including clozapine and risperidone similar to *rut* and *Btk* (56) mutants. Nevertheless, the common antipsychotic risperidone, does not restore the learning deficit.

Given that habituation deficits in flies and humans are reversible with antipsychotics, it is possible that mutations in *Drosophila* orthologs of genes linked to schizophrenia by GWAS may also present defective footshock habituation and provide expedient experimental validation of their effects on signaling within and between CNS neurons.

III. Appendix

Concurrent projects

1. Stage dependent nutritional regulation of transgenerational longevity

Ilianna G. Roussou, Charalambos Savakis, Nektarios Tavernarakis and Athanasios Metaxakis

Introduction

Discovery of single genetic mutations that increase lifespan in animal model systems established aging research as one of the most fascinating and rapidly evolving scientific fields. Such mutations were rapidly linked to reduced insulin-insulin like signaling pathway (IIS) (302),(303),(304) and since then, several genes, signaling pathways, dietary interventions and drugs, often converging into common lifespan-extending mechanisms, have been shown to affect aging (305). Importantly, most of these lifespan-extending factors seem to have an evolutionarily conserved anti-aging role, thus making their manipulation a promising method to delay aging and increase healthy lifespan in humans. However, recent findings offer new insights on longevity regulation; nutritional state can have a transgenerational impact on future generations' longevity.

As such, statistical analyses of human famines indicate food availability as a transgenerational regulator of longevity. Historical data analyses linking food availability and mortality of several generations (Overkalix study), revealed a strong association of longevity with ancestors' diet during the slow growth period (SGP) in mid childhood (9–12 years) (306);(307). Specifically, the grandsons, but not the granddaughters, of paternal grandfathers who had experienced low food supply during the SGP exhibited lower mortality rates. Similarly, paternal grandmother's food supply had some tendency to be linked with reduced granddaughters', but not grandsons', mortality. In summary, this study showed for the first time that food supply during a specific period of human development can affect mortality of next generations. Importantly, recent findings have associated starvation with transgenerational longevity in *Caenorhabditis elegans* (308), thus showing for the first time experimentally that nutrition can regulate longevity of future generations.

Materials and Methods

We used two laboratory-adapted strains, Canton Special (CS) and white Dahomey (wDah), maintained on a 12 hours lights on/12 hours dark cycle at 25◦C. Standard food contained: 65 gram/lt cornmeal, 23 gram/lt sugar, 10 gram/lt agar, 56 gram/lt dry yeast, 16 ml/lt nipagin (10% in ethanol), 4 ml/lt propionic acid. Larvae were reared in food with different yeast concentrations as follows: Flies laid eggs in sugaragar petri dishes (5 gram agar, 40ml apple juice and 5ml propionic acid per 100 ml). Eggs were washed in PBS and 100 ul of eggs were placed in bottles with varying concentrations of yeast. These corresponded to 10% (starvation conditions), 50%, 100% and 200% of standard yeast concentration used in our laboratory (0.1, 0.5, 1.0 and 2.0 food respectively). Adult males (F0) were selected from each bottle and were massively crossed with virgin females reared under standard food (normally fed females). From their progeny we selected both virgin males (F1 males) and females (F1 females). These were separately crossed with normally fed females or males respectively. We then selected virgin males (F2 males) of these crosses and performed lifespan analysis under standard food.

First, we analyzed lifespans of F2 males, derived from the male offspring of F0 males that were reared under different yeast concentrations (*F2 parental males*) and secondly we analyzed lifespans of F2 males derived from the daughters of these F0 males (*F2 maternal males*). F2 males were put in plastic vials in groups of twenty. For each food condition we analyzed at least 13 plastic vials and totally at least 260 flies. To measure lifespan, flies were transferred to new vials three times per week at which time deaths were scored.

Lifespan data were analyzed using ANOVA, with Graph Pad Prism 5.03 software (Graph Pad Prism Software Inc.). Multiple comparisons among strains were performed with one-way ANOVA with Dunnett's Multiple Comparison test. Regression analysis was performed in Graph Pad Prism 5.03 software (Graph Pad Prism Software Inc.). Survivorship data were analyzed in Excel using the Log Rank test.

Results and discussion

To test whether nutritional regulation of transgenerational longevity is a general, evolutionarily conserved rule underlying aging regulation in animals, we simulated the Overkalix study in flies, a powerful model organism for aging research. We reared larvae of a *Drosophila melanogaster* control, laboratory-adapted Canton Special (CS) strain under food conditions containing four yeast concentrations, 10%, 50%, 100% and 200% of standard fly food used in our laboratory (0.1, 0.5, 1.0 and 2.0). Yeast concentration alone sufficiently recapitulates the effect of food availability on flies' lifespan (309) and lifespan of wild derived *Drosophila* strains is shown to respond to these yeast concentrations with a typical tentshaped response, with the lowest one (0.1) representing starvation

conditions. F0 males were classified in four groups based on rearing food conditions (groups F0 0.1, 0.5, 1.0 and 2.0) and massively crossed with females reared under standard food (1.0- normally fed). F1 males and females were crossed with normally fed flies and lifespan analysis was carried out in F2 virgin males. These were named as F2 (paternal) or F2 (maternal) depending on whether they derived from male or female offspring of the F0 males reared under different food conditions. They were also categorized as groups F2 0.1, 0.5, 1.0 and 2.0, based on the food rearing conditions of their ancestors.

First, we measured lifespan of F2 males whose paternal grandfathers had experienced starvation through larval stages. *F2 (paternal) 0.1* flies had the longest and *2.0 flies* the shortest lifespan (**Fig. 1A**).Mean, median and maximum lifespan values were significantly influenced by paternal grandparents' diet (for mean lifespan: $p = 0.0008$, F = 6.52, R2 = 0.2736, for median lifespan: $p = 0.022$, F = 5.53, R2= 0.2421, for maximum lifespan: $p = 0.019$, F = 3.6, R2 = 0.172, one-way ANOVA) and *F2 (paternal) 0.1* group had significantly higher mean and median lifespan values compared to the *F2 parental 2.0 males* (**Fig. 1B**). To test if the above observations are caused by sex specific transgenerational mechanisms we performed similar analysis on maternal grandsons. The effects of ancestor's diet during larval stages were even more robust on longevity of maternal grandsons (Fig. 1A and 1B). *F2 (maternal) 0.1* flies had the longest and *2.0 flies* the shortest lifespan. Again, mean, median and maximum lifespan values were significantly influenced by maternal grandparents' diet and significantly correlated with shortage of food during development (for mean lifespan: $p = 0.0001$, F = 21.72, R2 = 0.5422, for median lifespan: $p = 0.0001$, F = 22.06, R2 = 0.5461, for maximum lifespan: $p = 0.0011$, F = 6.143, R2 = 0.2510, one-way ANOVA). Concluding, the poorest feeding conditions that we used (10% of standard yeast concentration, which corresponds to starvation conditions) to rear larvae of F0 males induced a significant lengthening of lifespan in F2 male offspring. Conversely, rich nutrients conditions had a robust shortening effect on longevity.

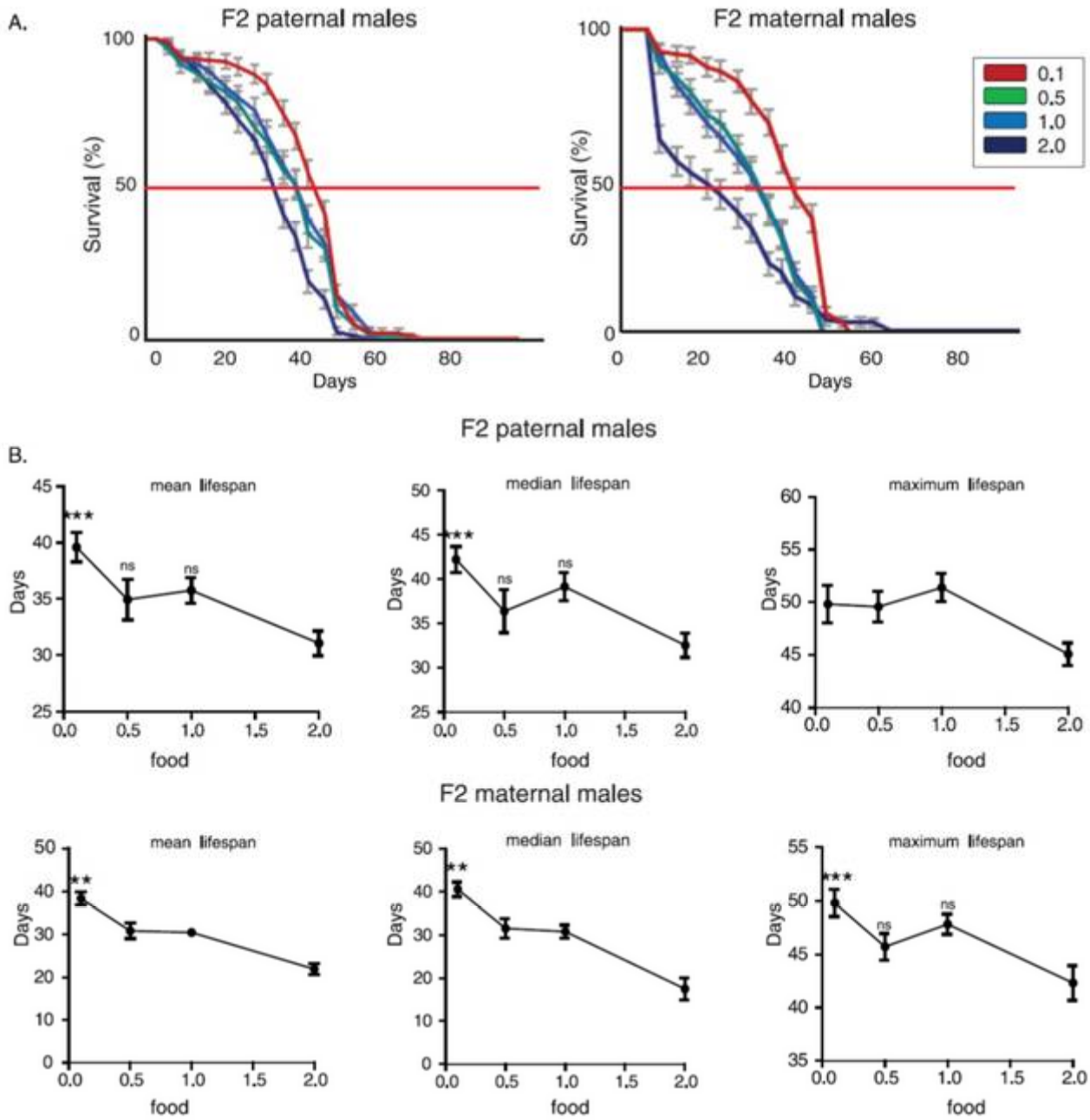

Fig. 1. Starvation-induced transgenerational effect on longevity is evolutionarily conserved in *Drosophila melanogaster*. A) Lifespan curves of F2 males (CS strain) from paternal and maternal grandfathers exposed to different dietary conditions. F2 virgin males whose paternal grandfathers had experienced starvation through larval stages (*F2 paternal 0.1 males*) were long-lived compared to the other groups. *F2 (paternal) 0.1 vs. 0.5*: $p < 1.2\times10–4$, *F2 (paternal) 0.1 vs. 1.0*: $p < 0.014$ and *F2 (paternal) 0.1 vs. 2.0*: $p < 1.7\times10–21$, log rank test. Also, F2 virgin males whose paternal grandfathers were fed under the richest conditions through larval stages (*F2 paternal 2.0 males*) were the shortest lived compared to the other groups. *F2 (paternal) 2.0 vs. 1.0:* $p < 1.7\times10–9$, *F2 (paternal) 2.0 vs. 0.5*: $p < 5.7\times10–7$, log rank test. F2 virgin males whose maternal grandfathers had experienced starvation through larval stages (*F2 maternal 0.1 males*) were also long-lived compared to the other groups. *F2 (maternal) 0.1 vs. 0.5*: $p<7\times10–14$, *F2 (maternal) 0.1 vs. 1.0*: $p < 1.6\times10–14$ and *F2 (paternal) 0.1 vs. 2.0*: $p<1\times10–40$, log rank test. On the contrary, the richest conditions of larval feeding (*F2 maternal 2.0 males*) led to significant lifespan reduction. *F2 (paternal) 2.0 vs. 1.0:* $p < 1.3\times10–11$, *F2 (paternal) 2.0 vs. 0.5*: $p < 7\times10–12$, log rank test.

Lifespan data shown are from a single trial. For each lifespan experiment $n > 260$. Error bars indicate SEM. B) Mean, median and maximum lifespan of F2 males from paternal and maternal grandfathers exposed to different dietary conditions. Grandparents' feeding affected mean, median but not maximum lifespan in F2 paternal flies (the mean lifespan of the longest-lived 10% of flies); *F2 (paternal) 0.1 vs. 2.0*: $p < 0.001$, $q = 4{,}404$ and $p < 0.001$, $q = 3.912$, for mean and median lifespan respectively. Ancestor's feeding affected more pronouncedly lifespan values in maternal grandsons (*F2 maternal 0.1 vs. 0.5*: $p < 0.01$, $q = 3{,}739$ and $p < 0.01$, $q = 3{,}204$ for mean and median lifespan respectively, *F2 maternal 0.1 vs. 1.0*: $p < 0.001$, $q = 3{,}929$ and $p < 0.01$, $q = 3{,}465$ for mean and median lifespan respectively, *F2 maternal 0.1 vs. 2.0*: $p < 0.001$, $q = 8{,}067$, $p < 0.001$, $q = 8.081$ and $p < 0.001$, $q = 4.100$ for mean, median and maximum lifespan. One-way ANOVA with Dunnett's multiple comparison against *F2 0.1 flies*. For each lifespan experiment $n > 13$, $^{**}p < 0.01$, $^{***}p < 0.001$. Error bars indicate SEM.

To further verify the nutritional effect on transgenerational longevity we repeated lifespan analysis in another laboratory adapted *Drosophila* strain, whiteDahomey (wDah). *F2 (paternal) 0.1* flies lived longer compared to the other three F2 (paternal) groups (**Fig. 2A**). No statistically significant differences were observed among lifespans of F2 (paternal) 0.5, 1.0 and 2.0 flies ($p > 0.05$, log rank test). Feeding through larval stages significantly affected mean and median, but not maximum lifespan (for mean lifespan: $p = 0.0189$, F = 3.611, R2 = 0.1671, for median lifespan: $p = 0.0279$, F = 3.275, R2 = 0.1539, for maximum lifespan: $p = 0.0898$, F = 2.28, R2 = 0.1124, one-way ANOVA) and *F2 (paternal) 0.1* group had significantly higher mean and median lifespan values (**Fig. 2B**). Interestingly though, feeding through larval stages did not exert lifespan effects on F2 maternal grandsons ($p > 0.05$, log rank test, for mean lifespan: $p = 0.84$, F = 0.2785, R2 = 0.014, for median lifespan: $p = 0.87$, F = 0.2263, R2 = 0.011980, for maximum lifespan: $p = 0.8307$, F = 0.2924, R2 = 0.0154, one-way ANOVA). Thus, we conclude that starvation-induced transgenerational effects on longevity passed only through male line in wDah strain (**Fig. 2A and B**).

We then subjected adult F0 males belonging to the CS strain into different food regimes, to test if nutritional effects on transgenerational longevity are exclusively generated through larval developmental stages. As depicted in **Fig. 3A**, in both experiments with F2 paternal and maternal grandsons, dietary restriction induced the highest lifespan-extending effect on males grandsons' longevity ($p < 0.05$, log rank test).

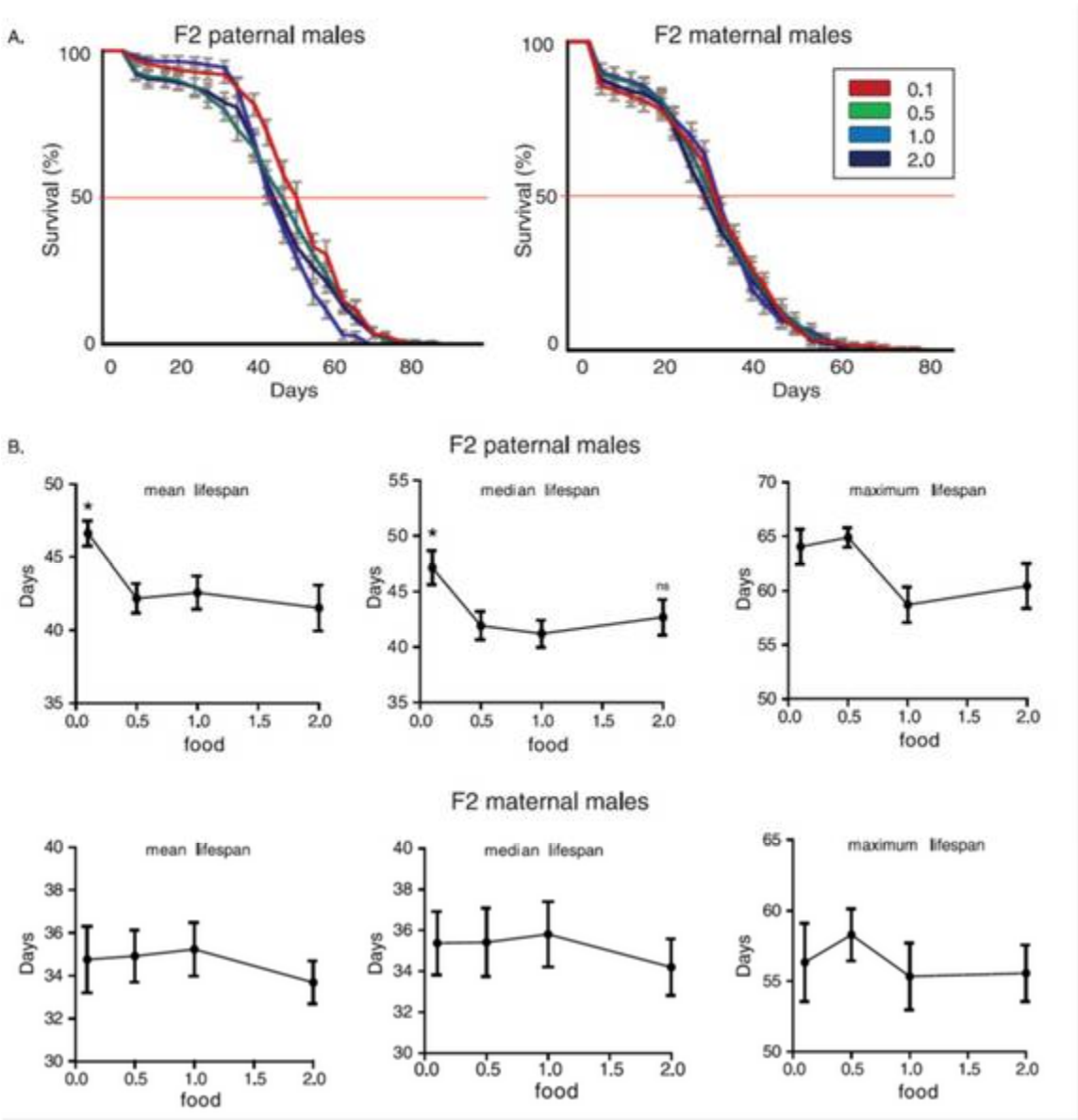

Fig. 2. Nutritional regulation of transgenerational longevity in wDah strain is sex-specific. A) Lifespan curves of F2 males from paternal and maternal grandfathers subjected to different dietary regimes through larval stages. F2 virgin males whose paternal grandfathers had experienced starvation through larval stages (*F2 paternal 0.1 males*) were long-lived compared to the other groups. *F2 (paternal) 0.1 vs. 0.5*: $p < 0.042$, *F2 (paternal) 0.1 vs. 1.0*: $p<4\times10–6$ and *F2 (paternal) 0.1 vs. 2.0*: $p < 0.0025$, log rank test. Lifespan curves did not differ significantly in F2 virgin males whose maternal grandfathers were reared under different food conditions (*F2 maternal males*) ($p > 0.05$, log rank test). Lifespan data shown are from a single trial. For each lifespan experiment $n > 260$. Error bars indicate SEM. B) Mean, median and maximum lifespan of F2 males from paternal and maternal grandfathers exposed to different dietary conditions. Mean and median, but not maximum, lifespans were significantly increased in *F2 parental males*. *F2 (paternal) 0.1 vs. 0.5*: $p < 0.05$, $q = 2.54$, $p < 0.05$, $q = 2.49$ and $p > 0.05$, $q = 0.356$, *F2 (paternal) 0.1 vs. 1.0*: $p < 0.05$, $q = 2.54$, $p < 0.05$, $q = 2.89$ and $p > 0.05$, $q = 1.696$, *F2 (paternal) 0.1 vs. 2.0*: $p < 0.05$, $q=3$, $p > 0.05$, $q = 2.203$ and $p > 0.05$, $q = 1.548$, for mean, median and maximum lifespan respectively. However, ancestor's diet during larval stages did not significantly affect lifespan of *F2 maternal males*. One-way ANOVA with Dunnett's multiple comparison against *F2 0.1 flies*. For each lifespan experiment $n > 13$, $*p < 0.05$. Error bars indicate SEM.

Although *F2 (maternal) 0.1* flies were equally long lived as *F2 (maternal) 0.5* flies (*F2 maternal 0.1 vs. 0.5* flies $p > 0.05$, log rank test), in F2 paternal flies only dietary restriction induced enhanced longevity in F2 (*F2 paternal 0.1 vs. 0.5* flies $p < 1.48\times10–9$, log rank test). Nutrition through adulthood significantly affected lifespan values (For F2 paternal males, median lifespan: $p = 0.0105$, F = 4.05, R2 = 0.1555, for maximum lifespan: p=10–4, F = 9.668, R2 = 0.3053. For F2 maternal males, mean lifespan: $p = 0.0247$, F = 3.397, R2 = 0.1665, median lifespan: $p = 0.089$, F = 2.295, R2 = 0.1189, maximum lifespan: $p = 0.0742$, F = 2.449, R2 = 0.1259, one-way ANOVA) (**Fig. 3B**). Hence, adult specific nutritional effects can also induce enhanced transgenerational longevity; however, it is dietary restriction and not starvation that has the major impact on future generations' lifespan.

Lifespan response to dietary restriction fits in a polynomial equation, but response of F2 males' lifespan to F0 larval feeding conditions did not fit in such a model. The former has been previously shown to fit a third-order polynomial (cubic) model, described by the equation: Y=B0 + B1*X + B2*X2+ B3*X 3 (310). Non-linear regression analysis showed that goodness of fit was low for all models tested (For wDah strain; first order polynomial: $R^2 = 0.08639$ and 0.03723, second order polynomial: $R^2 = 0.1234$ and 0.1403, third order polynomial: $R^2 = 0.1556$ and 0.1539, fourth order polynomial: $R^2 = 0.1556$ and 0.1539, for mean and median lifespans respectively). Hence, transgenerational influence of larval feeding on F2 male offspring's lifespan does not fit a polynomial equation and does not mimic the pattern of lifespan response to dietary restriction.

Nutritional state can affect future generations through specific mechanisms; diet can generate transgenerationally heritable rDNA rearrangements in flies (311), caloric restriction can induce histone modification, as also DNA methylation (311),(312),(313) and parental diet can affect cholesterol and lipid metabolism in offspring, through DNA methylation in mammals (312) . Interestingly, IIS pathway and nutritional alterations have similar effects on rDNA in flies, thus making IIS pathway a putative mediator of starvation-induced transgenerational phenomena. In support, insulin growth

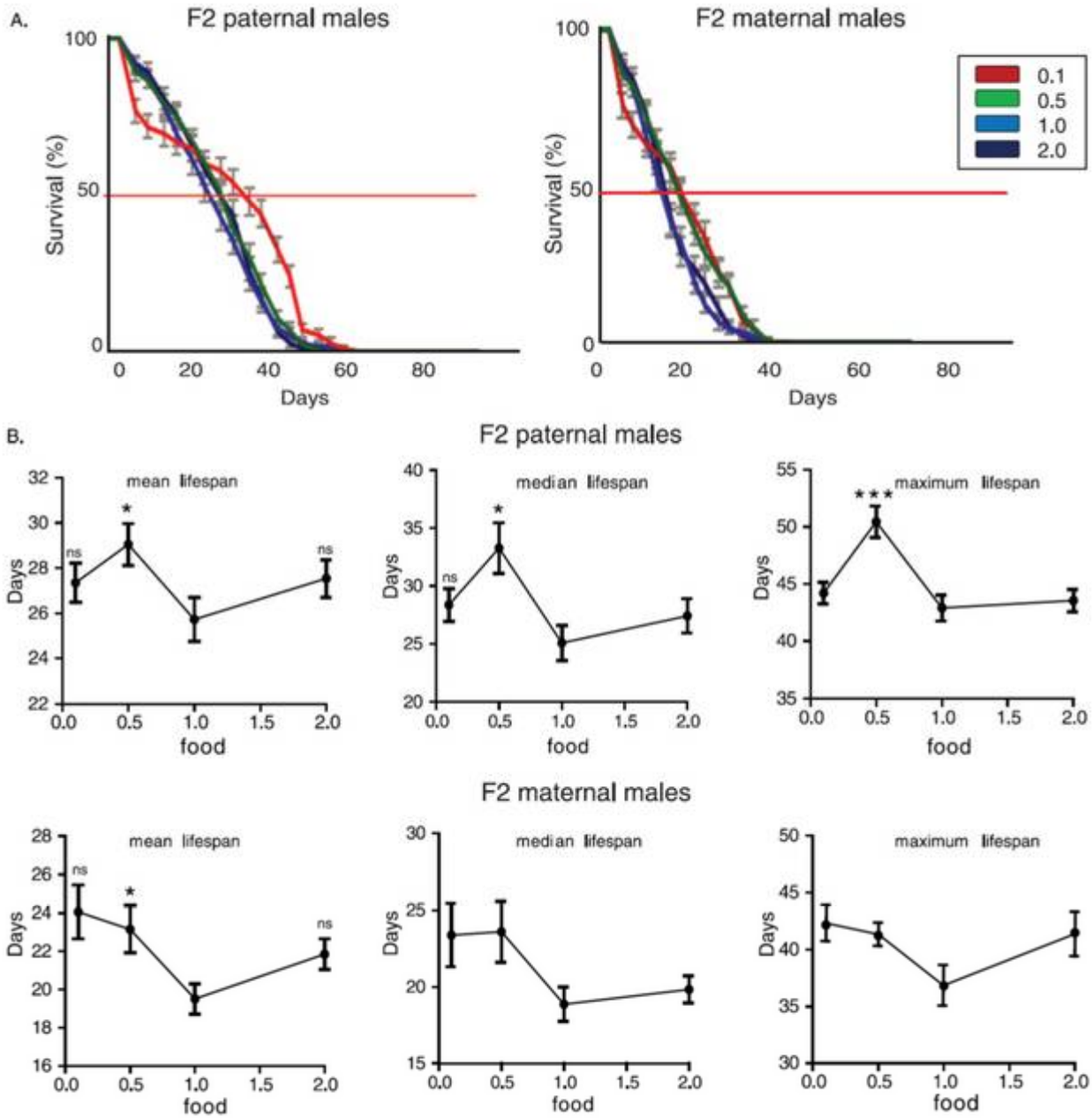

Fig. 3. Dietary restriction during adulthood induces transgenerational effects on longevity. A) Lifespan curves of F2 males from paternal and maternal grandfathers subjected to different dietary regimes through adult stages. F2 virgin males whose paternal grandfathers had experienced starvation through adult stages lived longer; *F2 (paternal) 0.1 vs.. 0.5*: p <1.47×10–9, *F2 (paternal) 0.1 vs.. 1.0*: p < 3.6×10–10 and *F2 (paternal) 0.1 vs.. 2.0*: p<3×10–12, log rank test. In F2 maternal males, dietary restriction and starvation of F0 males induced similar effects; *F2 (maternal) 0.5 vs. 0.1*: p > 0.9, *F2 (maternal) 0.5 vs. 1.0*: p<8×10–7, *F2 (maternal) 0.5 vs. 2.0*: p < 0.0049, *F2 (maternal) 0.1 vs. 1.0*: p<1×10–6, *F2 (maternal) 0.1 vs. 2.0*: p < 0.0049, log rank test. Lifespan data shown are from a single trial. For each lifespan experiment n > 260. Error bars indicate SEM. B) Mean, median and maximum lifespan of F2 males from paternal and maternal grandfathers exposed to different dietary conditions during adulthood. *F2 (paternal) 0.5 vs. 0.1*: p < 0.001, q = 4.097, for maximum lifespan, *F2 (paternal) 0.5 vs. 1.0*: p < 0.05, q = 2.512, p < 0.01, q = 3.326, p < 0.001, q = 4.6 for mean, median and maximum lifespan, *F2 (paternal) 0.5 vs. 2.0*: p < 0.05, q = 2.456 and p < 0.001, q = 4.34, for median and maximum lifespan. *F2 (maternal) 0.5 vs. 1.0*: p < 0.05, q = 2.457 for mean lifespan, *F2 (maternal) 0.1 vs. 1.0*: p < 0.05, q = 2.95, for mean lifespan, one-way ANOVA with

Dunnett's multiple comparison against *F2 0.5 flies*. For each lifespan experiment $n > 13$, $*p < 0.05$, $***p < 0.001$. Error bars indicate SEM.

factor (Igf) gene can be regulated by DNA methylation and parental imprinting (314), (315). IIS pathway downregulation and dietary restriction are the most reliable ways to extend lifespan in yeast, worms, flies and mammals, but also to improve health, even in aged humans (316),(317). For this, we predict that nutritional effects at specific developmental stages in flies and humans might change activity of genes affecting nutrient-sensing pathways, such as IIS, which, in turn, affect lifespan in future generations.

It has been suggested that Y- and X-chromosomes might control epigenetic effects by altering the chromatin structure on other chromosomes (317),(318). *Drosophila* genes can be methylated (319) and imprinted (320). Moreover, the Y chromosome alters expression of several X-linked and autosomal genes affecting, among others, lipid and mitochondrial metabolism (321). Such trans-chromosomal epigenetic effects imposed by the Y chromosome could explain the sex-specific lifespan increase observed in F2 males of the *wDah*. However, in CS flies transgenerational lifespan increase was not affected by female interference in F1. *Drosophila* strains, including *wDah* and CS, have been previously reported to differ regarding the nutritional range affecting longevity and sex-specific factors differentially influence lifespan extending factorsXgenotype interactions among strains (322),(323). Identification of the molecular mechanisms underlying nutritional effects on transgenerational longevity in flies is a prerequisite to understand sex-specific transgenerational lifespan increase of *wDah*.

In worms, specific heritable chromatin modifications, affecting epigenetics, are shown to induce transgenerational inheritance of longevity (324). Furthermore, a recent study showed that starvation can transgenerationally increase longevity through expression and transmittance of small RNAs. Interestingly, these RNA molecules target metabolism-related genes (325). In conclusion, dietary conditions seem to alter activity of metabolic pathways through DNA methylation, histone modifications or small regulatory RNAs molecules production. We hypothesize that such alterations underlie transgenerational longevity effects of starvation.

Interestingly, despite starvation during larval stages being the effector of transgenerational lifespan increase in F2, dietary restriction seem to be the equivalent effector during adulthood. In the case of F2 maternal males, starvation had a similar lifespan effect to dietary restriction. Hence, we could presume that, during adulthood, the range of nutrients shortage, which suffices for generation of transgenerational longevity effects, differs through development. In adults, a narrower reduction in nutrients might be necessary for generation of longevity effects in future generations.

Here for the first time we show that *Drosophila* lifespan can be transgenerationally regulated. We found that starvation during development can transgenerationally increase lifespan in flies, as it has been previously reported in humans and worms. We assume that

this is an evolutionarily conserved mechanism of lifespan regulation in animals. Moreover, our findings revealed a sex-specific mode for this regulation in one of the strains tested, similarly to what has been observed in humans. This implicates common mechanisms underlying lifespan extension in flies and humans. Therefore, we believe that *Drosophila* is suitable as an experimental platform to study epigenetic alterations that increase life expectancy and identify genes that regulate human aging. Reversibility and chemical manipulation of epigenetic alterations make them promising tools for the development of anti-aging treatments in humans. Our findings pave the way for further studies towards elucidating the molecular mechanisms by which limited nutrition increases transgenerational longevity, and assessing whether it enhances healthspan in addition to lifespan.

2. The *Drosophila* Receptor Tyrosine Kinase Alk Constrains Long-Term Memory Formation

Jean Y. Gouzi, Mikela Bouraimi, **Ilianna G. Roussou**, Anastasios Moressis, and Efthimios M.C. Skoulakis

Author contributions:
J.Y.G. and E.M.C.S. edited the paper.
J.Y.G., A.M., and E.M.C.S. designed research.
J.Y.G.,M.B., I.G.R., and A.M. performed research.
J.Y.G., A.M., and E.M.C.S. analyzed data.
J.Y.G. and E.M.C.S. wrote the paper.

Introduction

Since its identification, the receptor tyrosine kinase (RTK) anaplastic lymphoma kinase (ALK) has emerged as a key player in the physiology and pathology of the CNS (326). ALK belongs to the insulin receptor subfamily of monomeric RTKs. It features a large extracellular ligand-binding domain, a short transmembrane-spanning region, and an intracellular tyrosine kinase (TK) domain. Upon activation by its recently identified ALKAL ligands (327);(328), ALK initiates the activation of several intracellular signaling pathways, including the canonical Ras/ERK cascade. Unsurprisingly, ALK has been linked to multiple human cancers (326) characterized by constitutive kinase activation due to point mutations, chromosomal translocations, or overexpression by gene amplification, which confer ligand independence. However, the normal role of ALK in the CNS remains poorly documented.

ALK is highly conserved in vertebrates, *Caenorhabditis elegans* and *Drosophila melanogaster* (329);(326). *Drosophila* Alk (dAlk) and its secreted activating ligand Jelly Belly (Jeb) are essential for gut muscle differentiation, axon targeting in the retina, organ and body size growth control, and synapse growth at the larval neuromuscular junction (326). Recent studies indicate that dAlk activity regulates ethanol sensitivity (330), sleep (331), and learning/short-term memory (STM) (185) in adult flies. Jeb or dAlk overexpression precipitates associative olfactory learning deficits, whereas genetic or pharmacological inhibition of dAlk kinase activity enhances learning performance (185). dAlk-dependent learning, spatial memory, and novel object recognition inhibition were subsequently confirmed in mice also (332).

dAlk is widely expressed in the adult brain (185), accumulating preferentially in the dendrites of the mushroom bodies (MBs), neuroanatomical structures essential for olfactory learning and memory (333), sleep (334);(335), and ethanol sensitivity (336). However, whereas dAlk-dependent regulation of sleep and ethanol sensitivity require its expression within the MBs (330);(331), regulation of learning does not (185). However, dAlk is present within MBs; and because these neurons are also essential for

intermediate/middle-term memory (MTM), anesthesia-resistant memory (ARM), and protein-synthesis-dependent long-term memory (PSD-LTM) (337);(166), we hypothesized that dAlk could serve one or more of these forms of labile and consolidated olfactory memories.

Materials and Methods

Drosophila culture and strains. Drosophila were cultured on standard wheatflour-sugar food supplemented with soy flour and $CaCl_2$, at 25°C in 50%– 70% relative humidity in a 12 h light/dark cycle (185). *Alk*^{1} mutants (338) were a kind gift from R. H. Palmer (University of Gothenburg, Gothenburg, Sweden). *Alk*^{MB06458} flies were obtained from the Bloomington Stock Center (BL25509). Transgenic fly strains used in this work were as follows: UAS-*Alk*^{WT} (338), UAS-*Alk*^{RNAi} (v11446 and v107083, Vienna Drosophila Resource Centre), UAS-*Jeb* (339), UAS-*Jeb*^{RNAi} (v30799 and v103047, Vienna Drosophila Resource Centre), UAS-*mCD8::GFP* (180), and TubGal80^{ts} (340). The Gal4 driver lines used in this work were as follows: Alk(38)-Gal4 (185), repo-Gal4 (BL715), nSyb-Gal4, Ras2-Gal4, Elav[C155]-Gal4 (BL458), TH-Gal4, MB247-Gal4, c739-Gal4, OK107-Gal4 (BL854), LeoMB-Gal4 (176), 17d-Gal4 (BL51631), NP1131-Gal4, and 1471-Gal4 (BL9465; (341)). The c739-Gal4,TubGal80^{ts} line was obtained from G. Roman (University of Mississippi, Oxford, MS). The GH146-Gal4, TubGal80^{ts} line was from M. Ramaswami (Trinity College Dublin, Dublin, Ireland). The MB-specific Gal80 (MBGal80), which drives expression predominantly in the MBs, was introduced into the Elav- Gal4 strain through standard genetic crosses. All strains were backcrossed into the resident Cantonised-*w*^{1118} control isogenic strain for six generations to normalize their genetic background.

Drug feeding. The selective Alk inhibitor NPV-TAE684 (342) was dissolved in DMSO, and serial dilutions of stock solutions were prepared following the previously described method (185). Briefly, the solution was mixed into 10 ml Brewers-yeast paste and was fed for 16 h to flies previously starved for 6–8 h and transferred into normal fly-food vials 1 h before behavioral conditioning.

Western blot analysis. For detection of Jeb levels, 10 adult heads or 5 larval CNSs were homogenized in standard Laemmli buffer supplemented with protease and phosphatase inhibitors. Extract equivalent to one adult head was loaded per lane on 10% acrylamide gels, transferred to PVDF membranes, and probed with primary antibodies, which were used at 1:1000 for guinea-pig anti-JEB (343) and at 1:2000 for mouse anti-Syntaxin (8C3, Developmental Studies Hybridoma Bank), which was used to normalize sample loading.

Immunohistochemical analysis and confocal imaging. Whole-mount adult brains were dissected in cold PBS, fixed in 4% PFA for 20 min, and permeabilized using 1% Triton X-100 in PBS. The primary antibodies used were as follows: rabbit anti-dALK (1:1000) (329), guinea-pig anti-JEB (1:1000) (339) , mouse anti-DLG1 (1:1000) (4F3), and mouse anti-ChAT (1:1000) (4B1) (both from the Developmental Studies Hybridoma Bank, University

of Iowa). The following secondary antibodies were used: goat anti-mouse, or anti-rabbit conjugated with AlexaFluor secondary antibodies (1:400, all from Invitrogen). Confocal laser microscopy was performed using a TCS SP5 Confocal system (Leica Microsystems) equipped with the LAS AF image acquisition analysis software suite (Leica Microsystems). To quantify dAlk expression levels in the MBs, we used an adapted semiquantitative immunofluorescence protocol detailed previously (344). Whole-mount brains were dissected and prepared as described above and were stained with a rabbit anti-dALK antibody and counterstained with rhodamine-conjugated phalloidin (Invitrogen; 1:100) to mark the neuropil. Single confocal plane images ofMBcalyces were captured at the same section level corresponding to the middle part of the calyx and using constant optical acquisition settings (laser power, gain, pinhole, offset, zoom) and examined within a single session to allow comparison between control and experimental samples. dAlk expression levels in the calyces were estimated by subtracting from the measured mean grayscale intensity of a ROI (delimited by hand around a calyx), the measured mean grayscale intensity of an identical area adjacent to the calyx (background region). Fluorescence intensities were measured with ImageJ 1.51k software (National Institutes of Health).

Behavioral analyses and conditioning. Olfactory learning and memory in the Pavlovian negatively reinforced conditioning paradigm, coupling aversive odors as conditioned stimuli (CS^+ and CS^-) with the electric shock unconditioned stimulus (US), were performed essentially as described previously, for 3 min/learning (185) and for 24 h memory/LTM (345). Briefly, all experiments were performed in a genotype-balanced manner, with the experimenter blind to genotype and under dim red light, at 25°C and 70% humidity. Groups of ~75, 2- to 3-d-old flies were transferred to fresh vials 1 h before training and then trained in a T-maze apparatus. The aversive odors used were benzaldehyde and 3-octanol, diluted in isopropyl myristate (Fluka). Training for 3 min/learning or 3 h/mid-term memory experiments consisted of 1 single session of 12 US/CS pairings of 90 V electric shocks (US) with one odor (CS^+) over 1 min, followed after a 30 s purge with air, by the presentation of the second odor (CS^-) without shocks for 1 min. For 24 h memory, animals were subjected to five such training sessions, either massed together or spaced by a 15 min rest interval. For testing, flies were allowed to choose between the two odors presented in the two arms of the T-maze apparatus for 1.5 min. Performance was measured by calculating a performance index (PI) as follows: the fraction of flies that avoided the shock-associated odor (CS^+) minus the fraction that avoided the control odor (CS^-) represented half of the PI. One PI was calculated as the average of the half-learning indexes for each of the two groups of flies trained to complementary conditioning stimuli. To validate consolidated LTM, flies were placed for 16 h at 25°C in empty vials containing a piece of Whatman filter paper (2 X 2 cm) soaked with 200 µl of 5% sucrose solution (Fisher Scientific) containing 35 mM cycloheximide (Sigma-Aldrich). Flies were then transferred to standard food vials 30 min before training. After training, flies were kept in standard food vials for 24 h at 18°C until testing. To

assess 10 min and 3 h ARMs, flies were cold-shocked in prechilled glass vials on ice for 2 min after a single round of training. Complete anesthesia and recovery were controlled. After a 2 min recovery, they were transferred back to vials at 25°C in the dark and maintained until testing. For 10 min short-term ARM (ST-ARM), trained flies were cold-shocked immediately after training as described previously ((346), (347)). For 3 h middle-term ARM (MT-ARM), trained flies were cold-shocked 2 h after training, as described by Bouzaiane et al. (2015). Task-relevant sensory behavioral responses, such as odor avoidance and electric shock avoidance, were controlled and performed as described previously in detail (185).

Experimental design and statistical analysis. For all experiments, controls and experimental genotypes were tested in the same session in balanced design. The order of training and testing these genotypes was randomized. We required an experimental result to be significantly different from both genetic controls. Data are shown as mean $\pm$ SEM. The final number of experiments per genotype is listed on the bars in all figures and represents data collected from at least two broods of the given genotypes.

Untransformed (raw) data were analyzed parametrically with the JMP 7.1 statistical software package (SAS Institute) as described previously (185). Following initial ANOVA, planned comparison con-trast analyses (LSM) were performed between the experimental group (in black throughout all figures) and its genetic or treatment controls, using α=0.05. The level of significance was adjusted for the experimentwise error rate. Detailed results of all ANOVA and planned comparisons are reported in the text.

Results

Pharmacological inhibition of dAlk enhances both STM and LTM

To investigate whether dAlk plays a role in negatively reinforced associative olfactory memory, we administered the dAlk selective kinase inhibitor TAE684 (342) to control (w^{1118}) flies (**Fig. 1**). In agreement with published data (185), 100 nM and 1 μM TAE684 enhanced 3 min memory by ~12% and 20%, respectively, (STM: ANOVA $F_{(2,26)}$ = 8.3362, p=0.0018; subsequent LSM: p=0.0208 and p=0.0005 for 100 nM and 1 μM, respectively, vs vehicle-fed w^{1118} controls), but significantly it also precipitated a very robust increase in 24 h memory of ~20% and 36% (LTM: ANOVA $F_{(2,31)}$= 11.6696, p=0.0002; subsequent LSM: p=0.0194 and p=4.2X10^{-5} for 100 nM and 1 μM, respectively, vs vehicle). Together, these initial pharmacological results strongly suggest that dAlk inhibits olfactory memory in *Drosophila* in

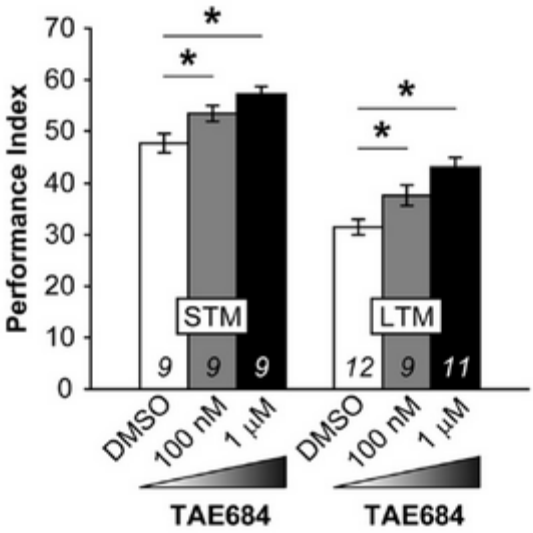

Figure 1. Pharmacological inhibition of dAlk activity enhances STM and LTM. Mean PIs (bars) ±SEMs (error bars) are shown. The number of experimental replicates (*n*) are indicated within the bars. *Significant differences denoted by horizontal line pairs. Left, TAE684 administration 100 nM or 1 µM to w^{1118} flies enhanced their learning/3 min STM performance in a high-resolution limited training protocol (1 cycle of 3 CS/US pairings). Right, TAE684 administration to w^{1118} flies enhanced their 24 h LTM performance. LTM performance was obtained using the typical spaced training protocol of 5 cycles of 12 CS/US pairings, each cycle separated (spaced) by a 15 min rest interval.

addition to its established role in inhibition of learning/3 min memory in the context of Nf1-regulated pathway(s) (185).

Downregulation of dAlk specifically within MB neurons enhances LTM

To validate this memory enhancement genetically, we attenuated dAlk in cells endogenously expressing the RTK by RNAi mediated abrogation with $AlkR^{NAi\ (11446)}$ under Alk(38)-Gal4 (185). Consistent with the TAE684 results, dAlk abrogation in Alk-expressing cells (**Fig. 2*A***) elevated 24 h memory (Alk(38)-Gal4: ANOVA: $F_{(2,31)}$ = 12.8918, p = 0.0001; subsequent LSM vs controls: p = 0.0011 and p = 4.5 X 10^{-5}, respectively), suggesting that the RTK mediates long-term memory attenuation. Task-relevant sensory responses were known to be normal (185).

To determine the neurons requiring dAlk function to constrain 24 h memory, we abrogated the RTK in defined brain cell types (**Fig. 2*A***, top). Attenuating dAlk in glia did not affect 24 h memory (Repo-Gal4: ANOVA: $F_{(2,23)}$ =1.9385, p = 1688). In contrast, pan-neuronal dAlk abrogation (nSyb-Gal4: ANOVA: $F_{(2,31)}$ =12.9304, p = 0.0001; subsequent LSM vs controls: p = 0.0026 and p = 3 X 10^{-5}, respectively; and Elav-Gal4: ANOVA: $F_{(2,39)}$ =19.9132, p =0.0001; subsequent LSM vs controls: p = 0.0003 and p= 3.8 X 10^{-7}) enhanced 24 h memory, mimicking the results with Alk(38)-Gal4, but not

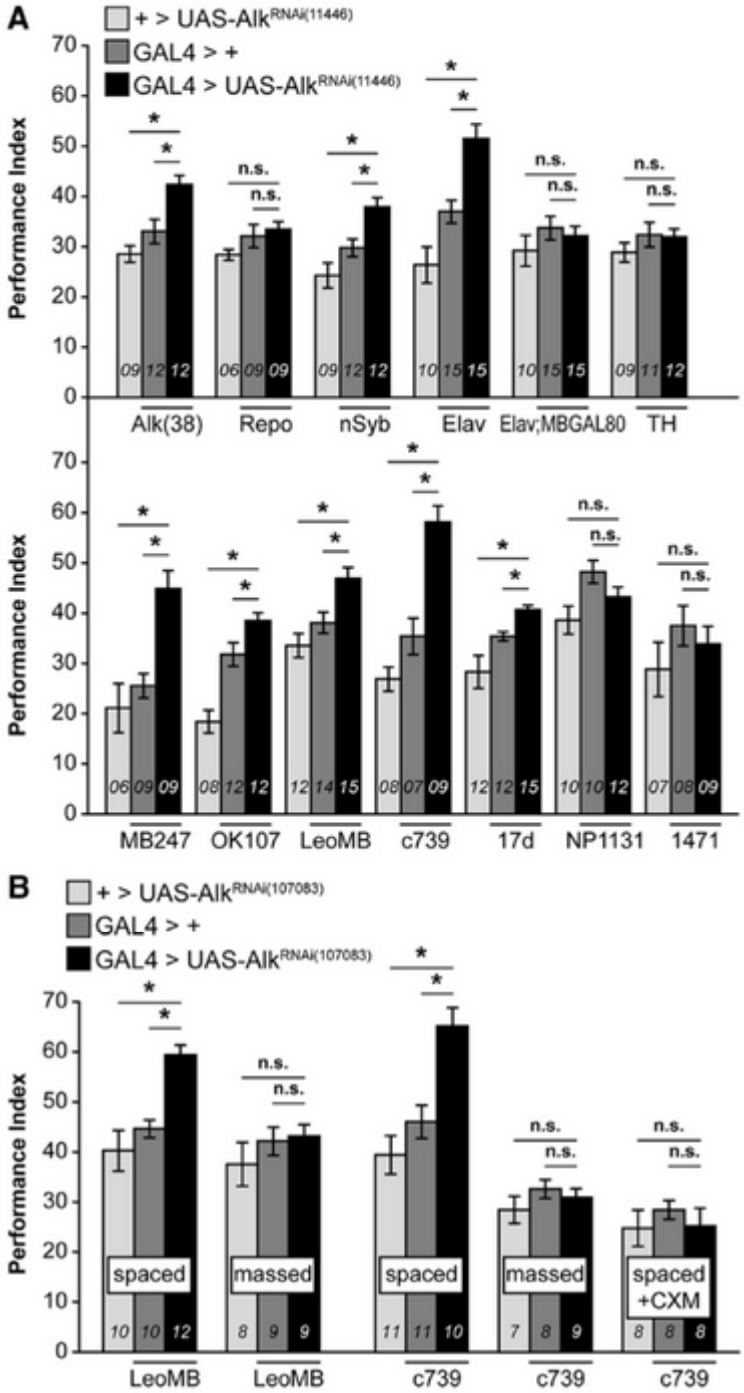

Figure 2. Downregulation of dAlk in intrinsic α/β MB neurons enhances PSD-LTM. Mean PIs (bars) ±SEMs (error bars) are shown. The number of experimental replicates (*n*) are indicated within the bars. Mean PIs are shown after typical spaced training of 5 cycles of 12 CS/US pairings, unless indicated otherwise. *Significant differences denoted by horizontal line pairs. n.s. means not significant. ***A***, GAL4 screen performed with expression of a UAS-*AlkRNAi* transgene in defined GAL4-marked neuronal subsets of the fly brain. Neuronal and glial GAL4 drivers (top) and MB GAL4 drivers (bottom) represent LTM PI of flies expressing the UAS*AlkRNAi(11446)* transgene driven by the indicated GAL4 (dark bars) and relevant genetic controls (light and dark gray bars). SignificantLTM enhancement was revealed for Alk(38), nSyb, Elav, MB247, OK107, LeoMB, c739,

and 17d driven dAlk abrogation. ***B***, Validation of the specificity of the 24 h memory enhancement with the independent RNAi-mediating transgene UAS*AlkRNAi(107083)*. Attenuation of dAlk specifically in LeoMB and c739 marked MB neurons (black bars) improved 24 h memoryperformance after spaced training (spaced) and phenocopied the effect previously observed with *AlkRNAi(11446)*. In contrast, 24 h memory performance observed after massed training (massed) or cycloheximide treatment (35 mM, spaced +CXM) was not enhanced, demonstrating that the enhanced memory consists entirely of bona fide PSD-LTM.

if MB neurons were spared (Elav-Gal4; MBGal80: ANOVA: $F_{(2,39)}$ = 0.9212, p = 0.4070). Hence, dAlk within MB neurons appears necessary for the 24 h memory enhancement. Dopaminergic neurons (TH-Gal4: ANOVA: $F_{(2,31)}$ = 0.9152, p= 0.4117) were not required, minimizing the possibility that enhanced memory is the consequence of attenuated forgetting (348).

To determine which MB neurons require dAlk for memory suppression, several specific drivers were used (**Fig. 2*A***, bottom). dAlk abrogation under the panMB drivers MB247-Gal4, OK107-Gal4, and LeoMB-Gal4 (176), and c739-Gal4, 17d-Gal4 marking α/β neurons, yielded significantly elevated 24 h memory (MB247-Gal4: ANOVA: $F_{(2,23)}$ = 13.9858, p = 0.0001; subsequent LSM vs controls: p=3.4X10^{-4} and p=1.2X10^{-4}, respectively; OK107-Gal4: ANOVA: $F_{(2,31)}$ = 23.3012, p = 0.0001; subsequent LSM: p=0.0172 and p = 1.8 X10^{-7} vs controls, respectively; LeoMB-Gal4: ANOVA: $F_{(2,39)}$ = 10.9654, p = 0.0002; subsequent LSM: p = 0.0034 and p = 6.1 X 10^{-5} vs controls, respectively; c739-Gal4:ANOVA:$F_{(2,23)}$=31.3183, p=0.0001; subsequent LSM: p=2.6X10^{-5} and p=1.8X10^{-7} vs controls, respectively; 17d-Gal4: ANOVA: $F_{(2,38)}$=11.7483, p=0.0001; subsequent LSM: p=0.0257 and p= 2.4 X 10^{-5} vs controls, respectively). In contrast, attenuation within γ neurons did not affect memory (NP1131-Gal4: ANOVA:$F_{(2,31)}$=4.4173, p=0.0212; 1471-Gal4:ANOVA:$F_{(2,23)}$=1.0385, p = 0.3715). The stronger memory improvement yielded by c739-Gal4 compared with 17d-Gal4 is consistent with previous reports (291) that, although both mark MB α/β lobes, c739-Gal4 is expressed higher and in more than twice the number of Kenyon cells compared with 17d-GAL4. These results demonstrate that dAlk is required specifically in α/β neurons, known to be essential for 24 h memory (341) (345). These results were further validated (Fig. 2*B*, spaced) with an independent RNAi-mediating transgene (UAS*Alk*$^{RNAi(107083)}$) (185), which also yielded elevated 24 h memory after spaced conditioning under LeoMB-Gal4 and c739-Gal4 (LeoMB-Gal4 spaced: ANOVA: $F_{(2,31)}$=14.6651, p=0.0001; subsequent LSM vs controls: p=0.0005 and p = 1.9 X 10^{-5}, respectively; and c739-Gal4 spaced: ANOVA: $F_{(2,31)}$ =13.8101, p<0.0001; subsequent LSM vs controls: p = 0.0007 and p= 2 X 10^{-5}).

Two forms of consolidated memory are detectable 24 h after training: PSD-LTM, formed after spaced training; and ARM, formed after massed training, which does not depend on *de novo* protein synthesis (337),(341). Significantly, MB-specific dAlk downregulation did not affect ARM (**Fig. 2*B***, massed), suggesting that the 24 h memory enhancement is PSD-LTM-specific (LeoMB-Gal4 massed: ANOVA: $F_{(2,25)}$ = 0.8317, p =

0.4480; and c739-Gal4 massed: ANOVA: $F_{(2,23)}$ = 0.9291, p=0.4105). Consistently, inhibition of protein synthesis before spaced training with cycloheximide (337) eliminated the 24 h memory enhancement (Fig. 2*B*, spaced + CXM:c739-Gal4:ANOVA:$F_{(2,23)}$=0.4472, p= 0.6454), demonstrating that it consists entirely of bona fide PSD-LTM.

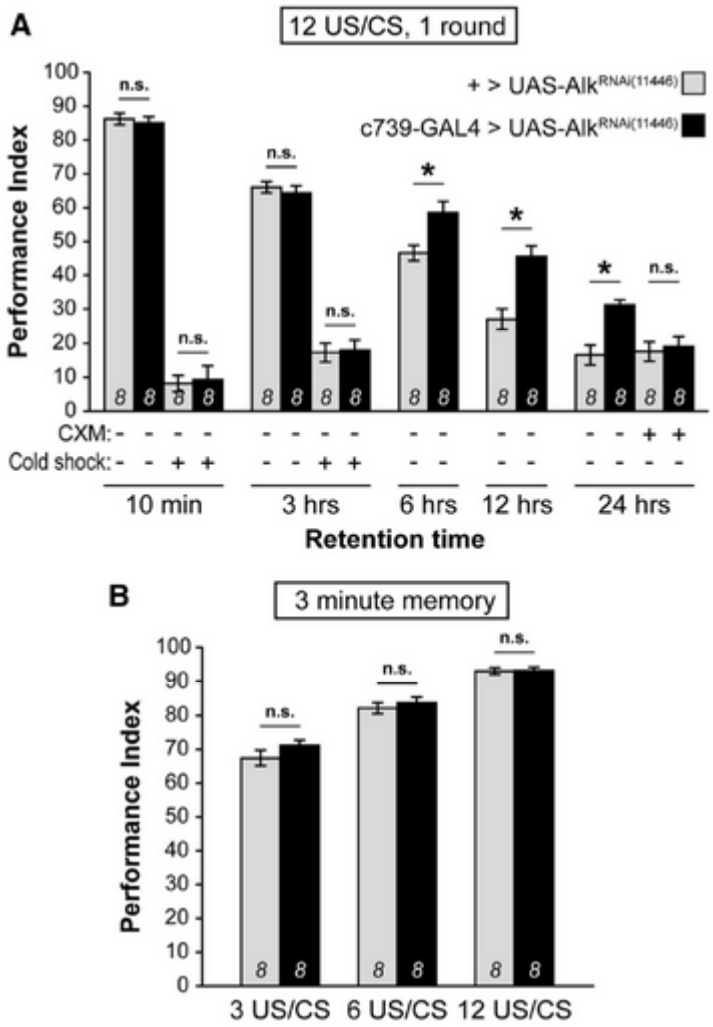

Figure 3. Downregulation of dAlk in the MBs enhances PSD-LTM specifically. Mean PIs (bars) ±SEMs (error bars) are shown. The number of experimental replicates (*n*) are indicated within the bars. *Significant differences denoted by horizontal line pairs. n.s. means not significant. ***A***, After a single round of 12 US/CS conditioning, memory retention was significantly enhanced at 6, 12, and 24 h upon attenuation of dAlk levels within c739-marked MB neurons (black bars) compared with the indicated relevant control (light gray bars). The improvement of 24 hmemoryconsisted of bona fide PSD-LTM, as treatment with the protein synthesis inhibitor CXM totally eliminated the improvement. In contrast, 10 min and 3 h memories were not improved upon dAlk attenuation. ARM immediately after training (10 min+cold shock) and ARM after 3 h (3 h+cold shock) were also not elevated. ***B***, Learning (3 min memory) was not significantly improved in flies with attenuated dAlk expression in c739-marked MB neurons (black bars) compared with control (light gray bars) under any US/CS pairing protocol (3, 6, 12 US/CS)

Downregulation of dAlk in the MBs enhances PSD-LTM specifically

Are earlier memories affected by dAlk attenuation in α/β MB neurons? To increase resolution and assess all memory forms concurrently, we used 1 training cycle of 12 US/CS pairings. Under these conditions (**Fig. 3*A***), dAlk abrogation did not affect 10 min memory (STM, 10 min cold shock: ANOVA: $F_{(1,15)}$ =0.2659, p=0.6142) as expected (185), or labile short-term ARM (346) (10 min cold shock: ANOVA: $F_{(1,15)}$=0.0717, p=0.7928). Moreover, 3 h middle-term memory (MTM) (3 h - cold shock: ANOVA: $F_{(1,15)}$ = 0.3578, p = 0.5593) and labile middle-term ARM (3 h + cold shock :ANOVA: $F_{(1,15)}$ = 0.0313, p = 0.8622) remained unaffected (**Fig. 3*A***). However, a mild enhancement was detectable at 6 h after training (ANOVA: $F_{(1,15)}$ =8.6609, p = 0.0107), which was striking at 12 h (ANOVA: $F_{(1,15)}$ = 17.1629, p =0.0010) and 24 h (24 h-CXM: ANOVA:$F_{(1,15)}$ =19.2126, p = 0.0006). Even after one training cycle, the resultant 24 h memory was also bona fide PSD-LTM and not long-term ARM (347), as it was eliminated by cycloheximide treatment (24 h + CXM: ANOVA: $F_{(1,15)}$= 0.1461, p= 0.7081) (**Fig. 3*A***).

Because 10 min memory was maximal under the intense 12 US/CS training conditions, enhanced learning may not have been visible due to ceiling effect. Hence, to verify that dAlk attenuation within the MBs did not result in enhanced learning, we limited the number of US/CS pairings from 12 to 3 (**Fig. 3*B***). Nevertheless, enhanced learning was not detectable even under limited training (3 US/CS: ANOVA: $F_{(1,15)}$ = 1.9861, p = 0.1806; 6 US/CS: ANOVA: $F_{(1,15)}$ = 0.5248, p = 0.4808; 12 US/CS: ANOVA: $F_{(1,15)}$ = 0.0428, p =0.8392). In conclusion, a single training cycle upon dAlk abrogation in α/βMB lobes elicits bona fide PSD-LTM, which is not consequent of enhanced learning per se.

dAlk levels constrain PSD-LTM in adult MBs

To ascertain that dAlk plays an acute role in PSD-LTM, we modulated dAlk levels specifically in the adult CNS (340). Adult-restricted dAlk abrogation (**Fig. 4*A***) yielded significant memory elevation whether it was pan-neuronal (Elav;Gal80^{ts}: ANOVA: $F_{(2,31)}$=35.5212, p=0.0001; LSM vs controls: p = 8 X 10^{-7} and p =1.1 X 10^{-8}, respectively), pan-MB (Leo;Gal80ts: ANOVA: $F^{(2,38)}$ = 8.1033, p =0.0012; subsequent LSM vs controls: p = 0.0038 and p= 0.0008), or specifically in α/β neurons (c739;Gal80^{ts}: ANOVA: $F_{(2,31)}$ =15.7468, p <0.0001; LSM vs controls: p = 0.0005 and p=1X10^{-5}). Hence, dAlk attenuation within α/β MB neurons appears sufficient for the 24 h PSD-LTM elevation, and developmental alterations within MBs cannot account for the enhancement. Although still formally possible, it is highly unlikely that adult-specific attenuation of dAlk outside of the MBs could lead to LTM enhancement as constitutive attenuation of dAlk under Elav-Gal4; MB-Gal80 did not elevate it (**Fig. 2*A***).

Collectively, dAlk appears to constrain PSD-LTM formation and its abrogation enhances it, even after minimal training. It follows then that acute dAlk elevation within α/β neurons could suppress PSD-LTM. Notably, increasing the levels of dAlk in adult neurons marked by commonly used drivers resulted in lethality within 24 h but was circumvented by reducing transgene induction to 8 h. Acute adult-specific overexpression

of dAlk precipitated a highly significant LTM deficit (**Fig. 4*B***), whether pan-neuronal (Elav;Gal80^{ts}: ANOVA: $F_{(2,23)}$ = 19.2806, p = 0.0001; subsequent LSM vs controls: p = 3.9 X 10^{-6} and p = 0.0031), pan-MB (LeoMB; Gal80^{ts}: ANOVA: $F_{(2,23)}$ = 6.6558, p = 0.0058; LSM vs controls: p = 0.0037 and p = 0.0048, respectively), or only in α/β neurons (c739;Gal80^{ts}: ANOVA: $F_{(2,23)}$=30.1603, p<0.0001; LSM vs controls: p= 1.3X10^{-7} and p=0.0021). This deficit seems specific to LTM as sensory responses under Elav were normal (185), the flies were viable, normal externally, without apparent locomotor deficits (data not shown), and both their ARM after massed training and 3 min memory (Fig. 4*B*, massed and STM) were normal (massed: ANOVA: $F_{(2,23)}$ = 0.7627, p=0.4789;STM:ANOVA:$F_{(2,23)}$=0.6109, p =0.5522). Thus, the deficit is not consequent of disabled or unfit flies, and increased dAlk levels impair LTM, whereas its attenuation improves it.

We used the fact that 8 h of *dAlk^{WT}* induction suffice to yield deficits, to dissect the requirement for this RTK in PSD-LTM formation, consolidation, or retrieval (337) (**Fig. 4*C***). Inducing *dAlk^{WT}* in adult MB neurons 8 h before conditioning manifested in deficient LTM ([t_{-8h}-t_0]: ANOVA: $F_{(2,23)}$ = 30.1603, p<0.0001; LSM vs controls: p= 1.3X10^{-7} and p = 0.0021, respectively). However, elevating dAlk for 8 h post-training or 8h pre-testing did not result in LTM deficits ([t_0-$t_{+8\ h}$]: ANOVA: $F_{(2,31)}$= 3.8911, p= 0.0318; [$t_{+16\ h}$-$t_{+24\ h}$]: ANOVA: $F_{(2,23)}$= 4.6712, p= 0.0210). Therefore, to constrain PSD-LTM formation, dAlk activity is required during conditioning; therefore, it acts specifically as a negative regulator of its formation, not of its consolidation or retrieval.

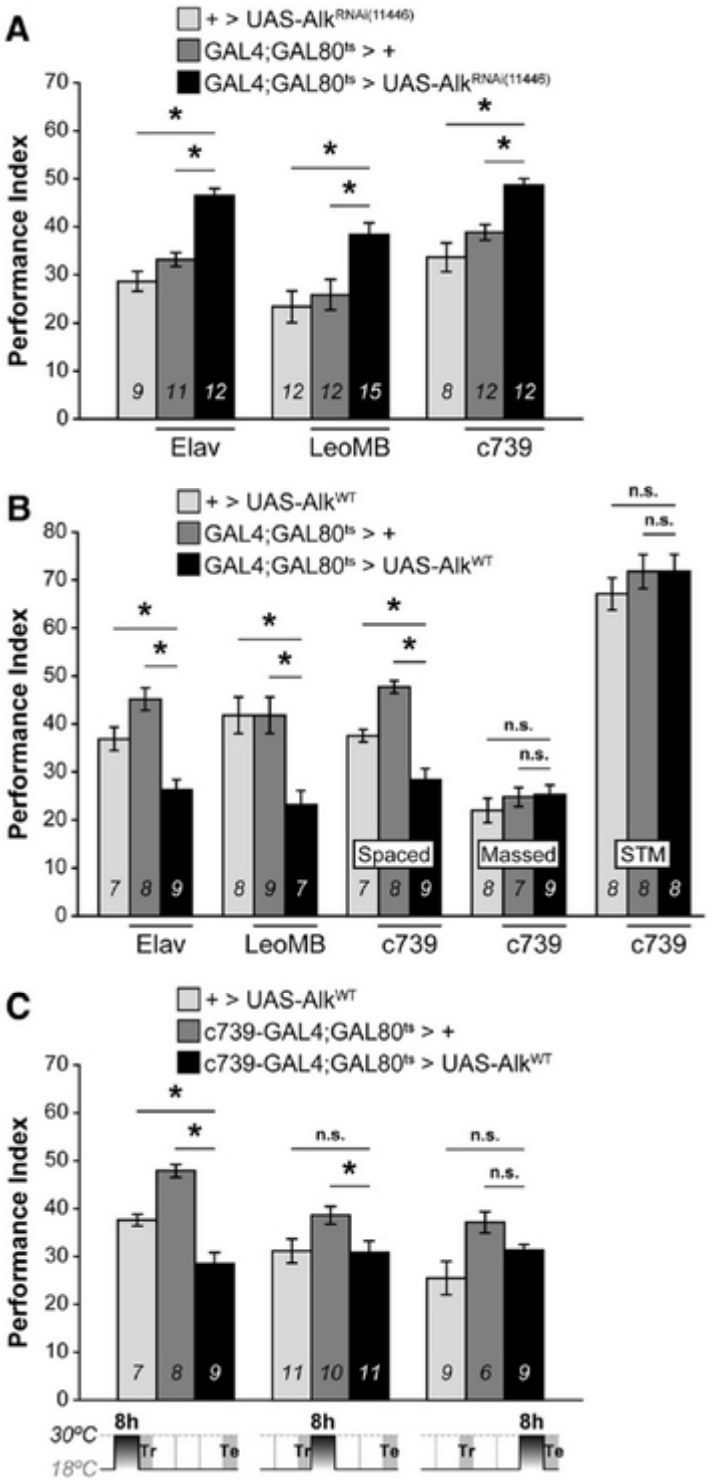

Figure 4. dAlk levels in the adult MBs during conditioning enhance or constrain LTM performance. Mean PIs (bars)±SEMs (error bars) are shown. The number of experimental replicates (*n*) are indicated within the bars. *Significant differences denoted by horizontal line pairs. n.s. means not significant. ***A***, Attenuation of dAlk expression levels with the *dAlkRNAi(11446)* transgene restricted specifically to the adult CNS for 48 h before training yielded significant LTM increase (black bars) compared with controls (light and dark gray bars) when the transgene was expressed pan-neuronally (Elav;G80ts), in all MB neurons (LeoMB;G80ts) and more specifically in α/β MB neurons

(c739;G80ts). ***B***, Conversely, adult-specific overexpression of the wild-type dAlk WT transgene using the same indicated G80ts drivers elicited significant LTM deficits. In contrast, ARM and learning/3 min memory (Massed and STM) were not affected. ***C***, Induction of dAlk WT expression in adult c739;G80ts MB neurons for 8 h before conditioning (t_{-8h}-t_0) resulted in deficient LTM; but in contrast, it left LTM intact if the transgene was induced for 8 h immediately following conditioning (t_0-t_{+8h}), or 8 h before testing (t_{+16h}-t_{+24h}), as indicated in the diagram below.

dAlk is confined to the dendritic postsynaptic active zones of Kenyon cells

Is the distribution of dAlk within the MBs consistent with its proposed role in LTM inhibition? As shown in Figure 5*A1*, intense anti-dAlk staining was observed in the calyces and absent in other parts of MB neurons, such as the pedunculus and the lobes (**Fig. 5*A2–A4***) in a manner reminiscent of another memory suppressor protein in *Drosophila*, SLC22A (177).

Further examination at higher magnification and single optical sections revealed that dAlk is broadly distributed throughout the calyces (**Fig. 5*B2***) in contrast to its ligand Jeb, whose distribution appeared discrete, punctate, and granular (**Fig. 5*B1***), proximal to dAlk, but without obvious colocalization (**Fig. 5*B3***). Indeed, dAlk appeared to surround areas of Jeb immunoreactivity (**Fig.5*B4***), whose size and morphology are characteristic of MB calycal microglomeruli (349). These postsynaptic microstructures are formed by the claw-like dendritic specializations of the KCs, and presynaptically by the enlarged terminal specializations/boutons of projection neurons (PNs). This notion was validated with typical presynaptic and postsynaptic MB markers (**Fig. 5*C***). dAlk is extensively colocalized with the postsynaptic active zone marker DLG (discs large), whereas Jeb colocalized within characteristic large puncta with ChAT (Choline Acetyl Transferase), a PN presynaptic marker (349). Thus, dAlk and Jeb are components of the calycal PN-MB synapses, sites of structural plasticity underlying olfactory learning and memory.

The dAlk-activating ligand Jeb does not affect LTM

Based on the complementarity of dAlk and Jeb patterns in MB calyces, we predicted that reducing Jeb levels would phenocopy dAlk attenuation and enhance PSD-LTM. However, developmental (**Fig. 6*A***) or adult-specific (**Fig. 6*B***) downregulation of Jeb by pan-neuronal (Elav, Ras2, and nSyb), glial (Repo), or PN specific (GH146) expression of two different Jeb^{RNAi} transgenes did not enhance LTM (**Fig. 6*A***; $Jeb^{RNAi\ (103047)}$·Elav-Gal4: ANOVA: $F_{(2,29)}$ = 6.6866, p = 0.0044; LSM vs controls: p = 0.0011 and p = 0.0988, respectively; Ras2-Gal4: ANOVA: $F_{(2,30)}$=8.7923, p=0.0011; LSM vs controls: p=0.0002 and p=0.0563, respectively; nSyb-Gal4: ANOVA: $F_{(2,30)}$ = 0.3647, p =0.6976; Repo-Gal4: ANOVA: $F_{(2,31)}$ = 2.1992, p = 0.1291; Fig. 6*B*; $Jeb^{RNAi(103047)}$: Elav-Gal80^{ts}: ANOVA: $F_{(2,37)}$ = 0.1693, p = 0.8449; Repo-Gal80^{ts}: ANOVA: $F_{(2,55)}$ =2.5336, p =0.0890; GH146-Gal80^{ts}: ANOVA: $F_{(2,31)}$ = 0.4709, p= 0.6291; Fig. 6*B*; $Jeb^{RNAi(30799)}$: Elav-Gal80^{ts}: ANOVA: $F_{(2,68)}$

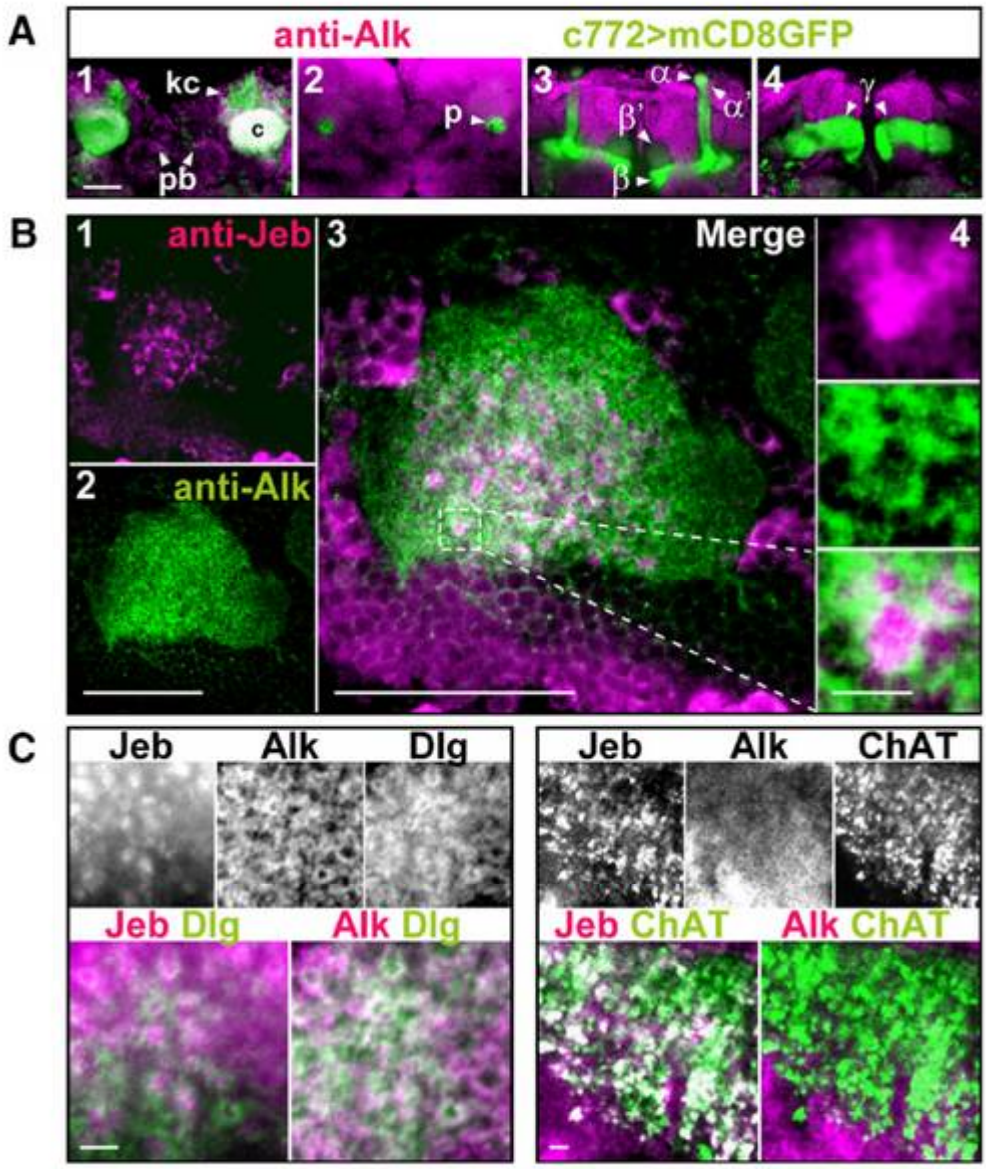

Figure 5. dAlk and its ligand Jeb are enriched in synapses of projection neurons and Kenyon cells. ***A***, dAlk is enriched in MB calyces but is absent in the MB lobes. Confocal images of single optical sections of the fly brain from posterior to anterior (***A1–A4***) were acquired at the level of MB calyces (***A1***), pedunculus (***A2***), α/β lobes (***A3***), and γ lobe (***A4***). Confocal images were acquired at the same section levels with identical settings. dAlk was visualized with an anti-dAlk antibody (purple). Fly brain structures were marked with a membrane GFP (green) encoded by the mCD8:GFP transgene expressed with the neuronal c772-GAL4 driver. White represents colocalization of dAlk and GFP immunofluorescence. dAlk protein accumulates within the dendrites (***A1***: calyces, c) and cell bodies (***A1***: Kenyon cells, kc, arrowhead) of MB neurons and in the protocerebral bridge (***A1***: pb, arrowheads). It is also expressed widely in the neuropil, above background. In contrast,MBaxons (***A2***: pedunculus, p, arrowhead) (***A3***: α/α'/β, and β' lobes, arrowheads) (***A4***: γ lobes, arrowheads) are devoid of dAlk staining. Scale bar, 50μm. ***B***, dAlk and Jeb display a complementary pattern of expression within MB calyces. Confocal images of a single optical transverse section of an MB calyx were acquired using identical settings and at the

same section level corresponding approximately to its middle section (***B1–B3***). Jeb protein was visualized with an anti-Jeb antibody (***B1***, purple), and dAlk protein was visualized with an anti-dAlk antibody (***B2***, green). Scale bar, 50µm. Colocalization of Jeb and dAlk immunofluorescence (***B3***, merge, white) is shown at the same magnification. Scale bar, 50µm. Inset, Higher magnification of the hatched box, showing in a single synaptic microglomerulus (***B4***), from top to bottom, Jeb, dAlk, and their complementary pattern. Scale bar, 10µm. ***C***, dAlk is expressed at the postsynaptic dendritic active zones of the MB calyces, whereas Jeb is expressed presynaptically in the synaptic buttons of apparent projection neurons. Confocal images of single optical sections of MB calyces were acquired at similar levels, using identical settings and displaying triple staining of Jeb, dAlk, and membrane GFP. Scale bars, 10µm. Left, White represents signals of anti-Jeb, anti-dAlk, and anti-Dlg, a marker of the postsynaptic active zones. Colored images represent lack of colocalization of Jeb (purple) and Dlg (green), and colocalization (white) of dAlk (purple) and Dlg (green). Right, White represents signals of anti-Jeb, anti-dAlk, and anti-ChAT, a marker of presynaptic terminal buttons. Colored images represent complete colocalization of Jeb (purple) and ChAT (green), and lack of colocalization (white) between dAlk (purple) and ChAT (green).

=0.5738, p= 0.5662). Jeb overexpression also did not alter LTM (**Fig. 6*B***, *Jeb*^{WT}: GH146-Gal80^{ts}: ANOVA: $F_{(2,31)}$= 1.1982, p= 0.3162). We are certain that the tools used for Jeb abrogation are functional because they dramatically reduce its level (**Fig. 6*D***) and recapitulated established Jeb-dependent phenotypes (Gouzi et al., 2011) of increased pupal size (Elav-Gal80^{ts}: ANOVA: F(2,103)= 85.3173, p< 0.0001; LSM vs controls: p= 5.9X 10^{-17} and p= 1.3X 10^{-20}, respectively) and enhanced 3 min memory (Elav-Gal80^{ts}: ANOVA: $F_{(2,35)}$=13.0861, p<0.0001; LSM vs controls: p=0.0026 and p=1.6X10^{-5}, respectively) (**Fig. 6*C***). Therefore, the dAlk-dependent LTM inhibition is Jeb independent.

dAlk levels increase rapidly in KC dendrites upon conditioning

Because excessive dAlk in the MBs suppressed LTM, we wondered whether, under physiological conditions, its levels change within these neurons consequent to conditioning. Therefore, we used a well-established quantification protocol (344) to monitor dAlk levels in MB calyces after conditioning with 1 round of 12 US/CS, which is sufficient to trigger elevated LTM upon its attenuation (**Fig. 3*A***). Given the time required to condition and sacrifice the flies, we monitored its levels at 20 min and 3 h after conditioning.

Significantly, dAlk levels were substantially elevated in conditioned flies (US/CS paired), in contrast to animals after sham conditioning (US/CS unpaired) with the US preceding the CS without coincidence (**Fig. 7*A***). Quantification of dAlk levels **(Fig. 7*B***, left) revealed that US/CS pairing resulted in a significant ~1.5-fold elevation (ANOVA: $F_{(3,50)}$=7.9802, p=0.0002; LSM 20′ paired vs 20′ unpaired: p= 0.005; and p= 0.0003 for 3 h paired vs 20′ unpaired). Because each group of flies experienced both stimuli, this result indicates that dendritic dAlk elevation emerges specifically upon stimulus pairing. In confirmation, dAlk levels after sham training were found equivalent to those in naive flies (LSM 20′ naive vs 20′ unpaired: p= 0.8114). This difference cannot be attributed to positioning or to the size of the flies because female flies of similar age were used for all

quantifications and the calycal areas quantified were statistically identical (ANOVA $F_{(3,50)}$= 0.3589, p= 0.7829) in the 51 individuals evaluated (**Fig. 7*E***, left). Finally, dAlk levels were not found further elevated upon increasing the number of conditioning rounds from 1X to 5X (spaced conditioning) (**Fig. 7*B***, right, ANOVA $F_{(1,31)}$=0.0000, p=0.9976). Therefore, the first round of conditioning appears sufficient for dAlk to attain maximal accumulation levels in the early phase of memory encoding. This is consistent with the notion that dAlk elevation attenuates or blocks PSD-LTM formation upon a single round of conditioning and congruent with PSD-LTM formation with a single round of conditioning when dAlk was abrogated (**Fig. 3*A***).

Importantly, dAlk elevation in MB dendrites was detected 20 min after conditioning and remained elevated for at least 3 h (**Fig. 7*B***; LSM 3 h paired vs 20′ paired: p= 0.3305). The short time required for a rather large transmembrane protein to increase its dendritic levels fits the temporal requirement for locally translated proteins (350). Considering the role of dAlk in PSD-LTM formation, its restricted dendritic distribution, and its rapid increase upon US/CS pairing, we suggest that its mRNA is likely transported to dendrites and translated upon conditioning. Furthermore, we hypothesized that dendritic targeting and local translation of dAlk mRNA may be conferred by sequences in its 3′UTR, as for several other synaptic proteins (350),(351). Inspection of the dAlk 3′UTR with TargetScanFly 6.2 (352) and RBPmap 1.1 (353) revealed that it contains numerous elements potentially controlling mRNA stability and translation, such as AU-rich elements and cytoplasmic polyadenylation elements, but also sites for RNA binding proteins (RBPs). Disruption of the spatial arrangement of such sequences could reduce or eliminate its translation and keep local dAlk levels low, in effect mimicking its attenuation.

To test this possibility, we capitalized on flies carrying a P-element insertion in the 3′UTR of *dAlk* (*Alk*^{MB06458}), which disrupts the spatial continuity of the putative translational control sequences. These mutants present increased responses to ethanol, are otherwise normal, and their total dAlk levels remain comparable with controls (330). Consistent with these observations, we did not detect differences in the steady-state levels of dendritic dAlk in mutants and controls (**Fig. 7*D***, unpaired) (ANOVA: $F_{(3,53)}$ =18.2206, p < 0.0001; LSM unpaired w^{1118} vs unpaired mutant: p= 0.9219). However, after

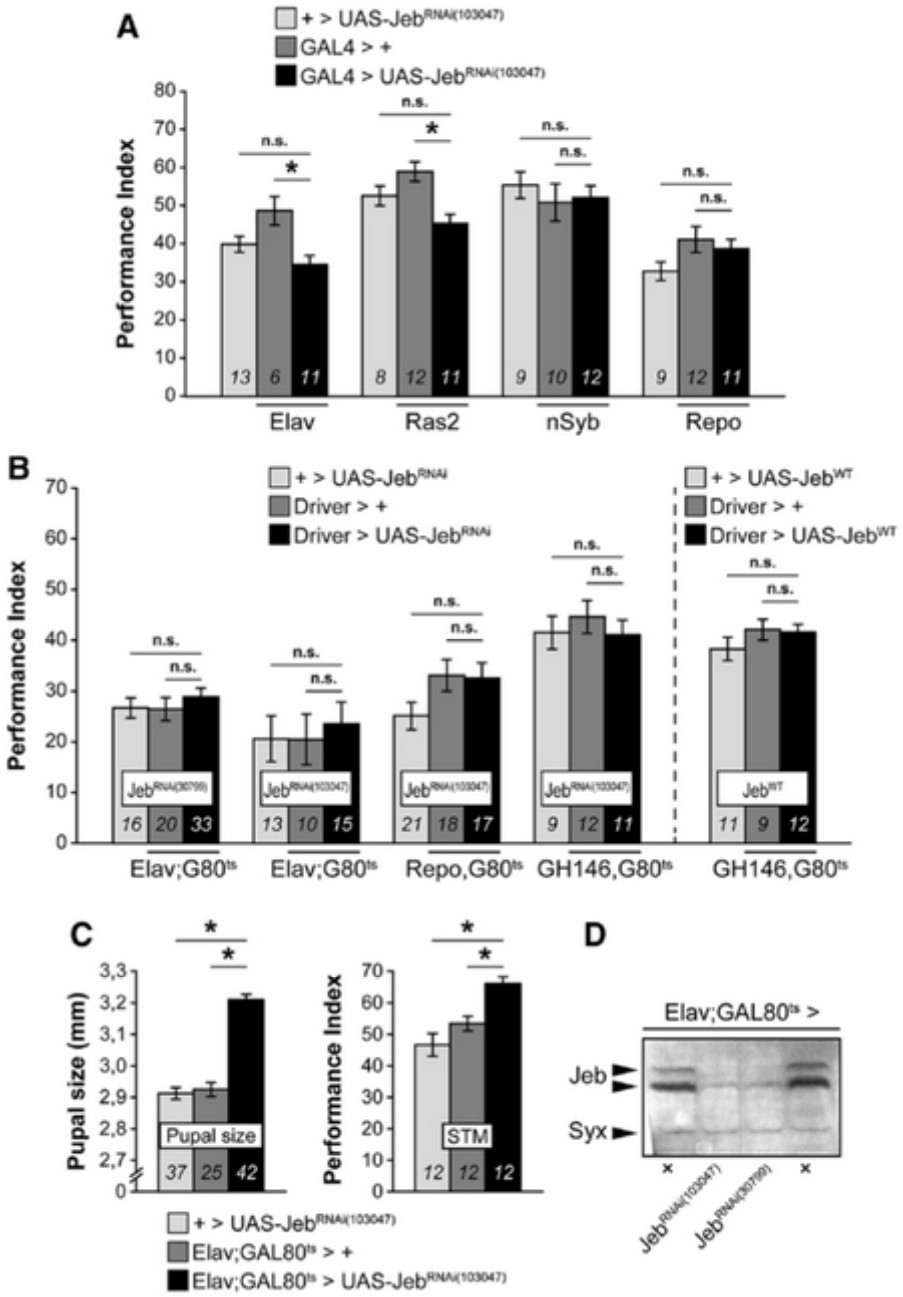

Figure 6. The dAlk-activating ligand Jeb is not involved in LTM. Mean PIs (bars)±SEMs (error bars) are shown. The number of experimental replicates (*n*) are indicated within the bars. *Significant differences denoted by horizontal line pairs. n.s. means not significant. ***A***, Attenuation of Jeb expression levels with the *JebRNAi(103047)* transgene (black bars) did not affect 24 h LTM performance compared with controls (light and dark gray bars) when the transgene was expressed pan-neuronally or in glial cells only using the indicated Gal4 drivers. ***B***, Attenuation of Jeb expression levels with the *JebRNAi(103047)* transgene restricted to the adult
CNS for 48 h before training also did not affect 24 h LTM when the transgene was expressed pan-neuronally, in glial cells or in projection neurons using the indicated G80 ts drivers. Lack of LTM effects was verified with pan-neuronal expression (Elav;Gal80ts) of a second independent *JebRNAi(30799)* transgene. Jeb overexpression (Jeb WT) in projection neurons (GH146,Gal80ts) also did not affect 24 h LTM. ***C***, Pan-neuronal Jeb attenuation with the *JebRNAi(103047)*

transgene yielded a substantial increase of pupal size compared with controls when the transgene was expressed throughout development and yielded a substantial increase of learning/
3 min memory (STM, 1 cycle of 3 CS/US pairings) when the transgene was expressed only during adulthood for 2 d before conditioning. ***D***, Representative semiquantitative immunoblot showing a dramatic reduction of endogenous Jeb levels upon pan-neuronal expression of both independent *JebRNAi* transgenes (UAS-*JebRNAi(103047)* and UAS-*JebRNAi(30799)*). Jeb protein (Jeb)was revealed with the anti-Jeb antibody (Jeb), and Syntaxin (Syx) was used as loading control.

conditioning, the pairing-dependent dAlk increase in controls (LSM unpaired w^{1118} vs paired w^{1118}: p= 2.3X 10^{-7}) was absent from the mutants (LSM unpaired mutant vs paired mutant: p=0.5769). Therefore, in $Alk^{MB06458}$ mutant homozygotes, MB dendritic levels of dAlk remain low even after conditioning (LSM paired w^{1118} vs paired mutant: p=3.5X10^{-7}), in effect mimicking its transgenic attenuation. Again, size and positioning cannot account for the effect, as the calycal areas quantified were identical (ANOVA:$F_{(3,53)}$=0.4121, p=0.7450) in controls and mutants (**Fig. *7E***, right). These results suggest that the conditioning-dependent modulation of dAlk levels in MB dendrites is conferred by the spatial arrangement of control sequences in the 3'UTRof its mRNA. Notably, dAlk retained its dendritic localization in the mutants, suggesting that the insertion does not disrupt signals targeting the mRNA to the calyces (**Fig. *7C***).

The attenuated conditioning-dependent dAlk levels in MB calyces predict that the Alk^{MB} mutants will present enhanced LTM. Indeed, 3 min memory (**Fig. *7F***; 3 US/CS) of controls, mutant heterozygotes, and homozygotes were indistinguishable (ANOVA: $F_{(2,32)}$=0.5853, p=0.5632). In contrast, mutant homozygotes exhibited substantially enhanced 24 h memory (**Fig. *7F***; spaced: ANOVA: $F_{(2,37)}$ =12.5306, p <0.0001; subsequent LSM vs controls p=3.9X10^{-5} and p=7.8X10^{-4}, respectively), which was PSD LTM specific, as it was not elicited by massed training (**Fig. *7F***; massed: ANOVA $F_{(2,31)}$= 0.1495, p=0.8618). Task-relevant sensory responses were normal in the mutants (**Fig. *7G***) (reactivity to shock: ANOVA: $F_{(1,21)}$=0.4616, p= 0.5047; octanol avoidance: ANOVA: $F_{(1,19)}$= 0.0846, p= 0.7745; benzaldehyde avoidance: ANOVA: $F_{(1,19)}$= 1.7238, p= 0.2057).

To ascertain that the elevated PSDLTM phenotype was consequent to disruption of the *dAlk* 3'UTR and not of a neighboring gene, we generated heteroallelics with the lethal (338) null Alk^{1} allele (**Fig. *7H***). Significantly, Alk^{1}/Alk^{MB} heteroallelics presented a substantial LTM enhancement over that of either Alk^{1} or Alk^{MB} heterozygotes (ANOVA: $F_{(3,39)}$= 18.5255, p < 0.0001; subsequent LSM Alk^{1}/Alk^{MB} vs Alk^{1}/+; p =1.9X 10^{-7}; vs $Alk^{MB06458}$/+: p =4.7X 10^{-7}), confirming that the mutations are allelic. Moreover, PSD-LTM in the heteroallelics was even higher than that of Alk^{MB} homozygotes (LSM $Alk^{1}/Alk^{MB06458}$ vs $Alk^{MB06458}$: p = 0.0092) as hypothesized, given that Alk^{1} is a null allele and conditioning-dependent upregulation of dAlk levels is blocked in Alk^{MB}. This is consistent with the notion that PSD-LTM formation is sensitive to the precise postconditioning levels of dAlk in MB dendrites.

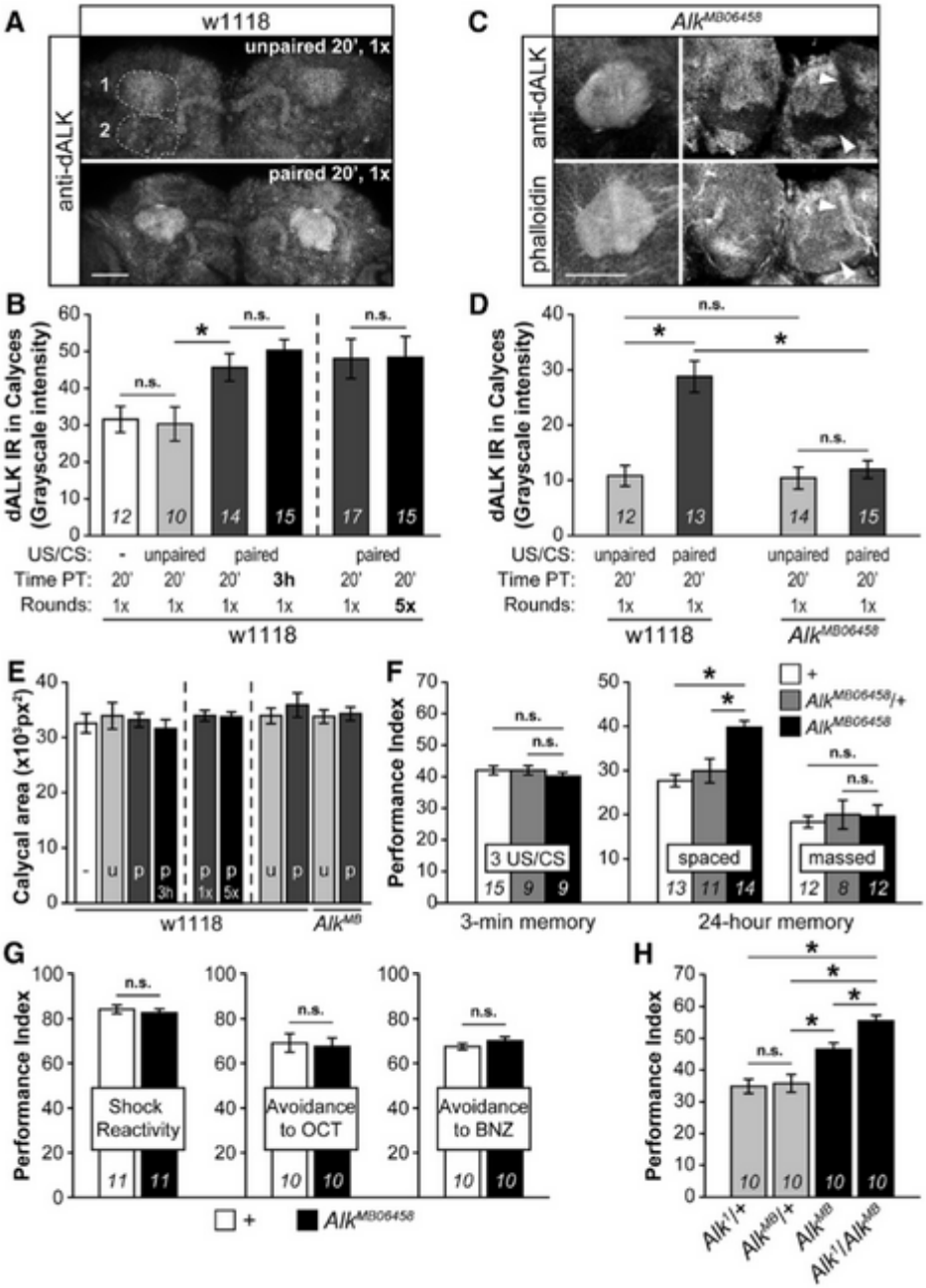

Figure 7. Dendritic dAlk levels in the MBs increase rapidly upon conditioning to constrain LTM. ***A***, Representative grayscale images of anti-dAlk immunofluorescence in control *w1118* flies. Scale bar, 50µm. Single confocal plane images of MB calyces were captured at the same section level corresponding to the middle part of the calyx, using constant optical acquisition settings, and examined in a single session to allow comparison between control (unpaired 20 min, 1 round, 1X) and experimental samples (paired 20 min, 1 round, 1X). ***B***, Semiquantitative analysis of dAlk immunoreactivity (IR) in the calyces of*w1118* control flies was achieved by subtracting from the mea ngrayscale intensity of the signal within a calyx (dashed circle 1, delimited by hand in ***A***), the mean grayscale intensity of the signal in an adjacent area (dashed circle 2, same size and shape as circle 1). The mean intensity differences±SEM for the indicated number (*n*) of calyces are shown. Control *w1118* flies were either trained with the typical conditioning protocol of 12 US/CS pairings (US/CS: paired) or trained with a modified protocol in which the US preceded the CS^+

without coincident pairing (US/CS: unpaired) or untrained (UC/CS:-). Flies were trained using either a single (1X) round or 5X spaced rounds of 12 US/CS pairings. Their brains were dissected and fixed either immediately (20′) or 3 h after training (Time PT, Time post-training). In control *w1118* flies, pairing the US with the CS^+ significantly increased calycal dAlk levels 20 min after conditioning, which apparently perdured at least for 3 h. Training flies either with 1Xround or with 5X spaced rounds did not alter increased calycal dAlk levels. In contrast, dAlk levels in flies submitted to unpaired stimuli (unpaired) were not different from in naive flies (-). ***C***, Single confocal plane images of a MB calyx (left) and lobes (right) in *AlkMB06458* homozygote fly brains stained with the anti-dAlk antibody (top row) and counterstained with rhodamine-conjugated phalloidin (bottom row) to mark the neuropil. In *AlkMB06458*, dAlk retained its calycal localization, remaining excluded from the lobes (arrowheads). Scale bar, 50μm. ***D***, Semiquantitative analysis of dAlk immunoreactivity (IR) in the calyces of *w1118* and *AlkMB06458* flies. The mean dAlk intensity differences (calculated as indicated above)±SEM for the indicated number of calyces (*n*) are shown. Differences in steady-state levels of dendritic dAlk were not detected in *AlkMB06458* mutants and *w1118* control flies (unpaired). However, in flies submitted to 1 round of conditioning (paired), the pairing-dependent increase of dendritic dAlk observed in *w1118* controls was absent in *AlkMB06458* homozygotes. Time PT, Time post-training. ***E***, Mean areas (in square pixels±SEM) of the calyces used in ***B*** and ***D*** to obtain the intensity measurements. No significant differences between calycal areas were detected that could explain the differences observed in dAlk intensities. Each bar corresponds to its equivalent in ***B*** and ***D***. -, Naive flies; u, unpaired; p, paired; 1X and 5X, number of rounds. Brains were all dissected/fixed 20 min after training, except where specified. ***F***, *AlkMB06458* homozygotes present enhanced LTM (spaced) but not 3 min memory (STM, 3 US/CS) or ARM (massed). Mean PIs (bars)±SEMs (error bars) are shown. The number of experimental replicates (*n*) are indicated within the bars. *Significant differences denoted by horizontal line pairs. n.s. means not significant. ***G***, Task-relevant olfactory and shock reactivity responses in *AlkMB06458* homozygotes (black bars) were indistinguishable from controls (white bars). ***H***, The dosage of dAlk protein in MB dendrites after conditioning calibrates the level of LTM performance. Mean PIs (bars)±SEMs (error bars) are shown. The number of experimental replicates (*n*) are indicated within the bars. *Significant differences denoted by horizontal line pairs. n.s. means not significant. *Alk1*/ *AlkMB06458* heteroallelics present even higher LTM than *AlkMB06458* homozygotes. The fact that heteroallelics present LTM elevation indicates that the mutations do not complement and are indeed allelic.

Discussion

Our findings reveal a novel role for dAlk in regulation of PSD-LTM formation in addition to its established role in learning (185). dAlk constrains both processes, but whereas learning attenuation requires its activity outside the MBs, suppression of PSD-LTM formation requires its elevation within the dendrites of α/β MB neurons. Moreover, although its activating ligand Jeb is required for learning attenuation, it is dispensable for PSD-LTM constraint.

Global pharmacological inhibition of dAlk activity resulted in both STM and LTM enhancement as expected (**Fig. 1**) because it addressed all neurons expressing this RTK. dAlk activity outside the MBs is known to be required for learning/3 min memory suppression (185) and these neurons are clearly affected by TAE684, as also are the MBs yielding enhanced PSDLTM. In contrast, dAlk levels were specifically abrogated within the

MBs where converging studies (341);(345);(347) established that STM and LTM engage different MB neuron types, the γ and the α/β, respectively. dAlk attenuation in γ MB neurons did not affect 3 min memory (185) or PSD-LTM, strongly suggesting that dAlk is not expressed therein.

The notion of memory suppression almost invariably refers to forgetting, broadly defined as a decay of memory that either actively dissipates in time or undergoes interference by additional learning of unrelated or irrelevant information (354);(355). Forgetting an odor/shock association in *Drosophila* (356) requires the small G-protein Rac (357), or dopamine (DA) signaling predominantly through the DAMB receptor (348), and its suppression appears as an enhancement of all types of 3–24 h memories. However, 24 h memory enhancement resulting from Rac attenuation appears distinct from PSD-LTM (357), and inhibition of DA signaling in the MB-afferent DAN neurons does not enhance 16–24 h memories (348). Hence, Rac and/or DA signaling inhibit recently acquired labile memories rather than consolidated forms. dAlk also acts during the labile stage of memory formation, but not its dissipation, and is specific to PSD-LTM, not 3 h memory or ARM (**Figs. 2*B*, 3*A***). Furthermore, dAlk is not required (**Fig. 2*A***) within the essential for forgetting dopaminergic neurons (356). Therefore, dAlk-mediated LTM inhibition is distinct from dissipation of labile memories.

A number of memory suppressor genes have been recently described in *Drosophila* (358) and mice (359), indicating that, although its exact role is unclear, memory restraint is evolutionarily conserved. Constraining memory may limit the conditioned associations processed toward the energetically demanding PSD-LTM (360), ensure the fidelity of associations that progress toward consolidation, or inhibit proactive or retroactive interference (354); (355); (356).

The role of all apparent memory suppressor proteins and miRNAs identified to date in *Drosophila* (361) has not been fully delineated, but some mechanistic aspects emerge. *Drosophila* memory suppressor miRNAs ostensibly regulate translation of postsynaptic proteins involved in MB excitability (362) hence, attenuation of their levels and the resultant hyperexcitability could underlie enhanced memory. Accordingly, loss of the apparent signal-tempering acetylcholine transporter DmSLC22A from MB neurons enhances their excitability and elevates memory. Interestingly, like dAlk, DmSLC22A is found in calycal microglomeruli. Therefore, in conjunction with our results, it appears that memory-constraining mechanisms depend on the level of postsynaptic proteins that limit the amplitude or duration of MB neuronal excitation. In contrast to other memory suppressor proteins and miRNAs (361), dAlk elevation in the MBs is not required for 3 h memory (**Fig. 3**) but appears specific to PSD-LTM. The temporal specificity of dAlk suggests that its activity may not constrain MB excitability, but rather LTM consolidation mechanisms, a hypothesis under investigation.

Conditioning-dependent dAlk elevation in MB dendrites appears to result via local translation regulated by the 3′UTR of its mRNA. This 3′UTR-conferred property is shared with multiple dendritic proteins (350), including another RTK involved in memory

formation, the BDNF receptor trkB (363). Similarly, 3'UTR sequences direct the mRNA of *Drosophila* CaMKII, a kinase also implicated in memory, to be translated in the postsynaptic zones of MB calyces (351). Significantly, the 3'UTR of dAlk mRNA contains more numerous regulatory elements than those on CaMKII transcripts, including several stabilizing AU-rich elements. The putative miRNA binding sites include those for miR- 305 and miR-932, both implicated in memory formation (361) and possibly in dAlk local translation. Translational regulation may also involve identified putative RBP binding sequences at the dAlk 3'UTR. Some, such as pumilio (pum) and the cytoplasmic polyadenylation element binding protein (CPEB) Orb2 (364), are translation suppressors with known function in memory. Whether others, such as Rox8, the ortholog of the stress granule-associated vertebrate protein TIA1, play a role in memory formation is currently unknown. Whether miRNAs and RBPs interact with dAlk mRNA upon conditioning to regulate its dendritic levels will be the focus of forthcoming work.

The PSD-LTM constraint depends on dAlk activity and the increased levels per se, as demonstrated by the elevated memory upon treatment with the inhibitor TAE684. How is calycal dAlk activated to constrain LTM formation since Jeb is dispensable for LTM attenuation (**Fig. 6*A***)? Presently, we cannot exclude the possibility that a yet unidentified ligand may activate dAlk upon spaced conditioning. However, another explanation we currently favor is that, upon spaced training, dAlk can autoactivate in response to its local elevation in the calyx. Level-dependent autoactivation has been reported for human ALK-positive cancers (326), or neurons transfected with ALK (365), a feature shared by almost all RTKs (366). Local elevation-dependent autoactivation of dAlk is in agreement with our own experimental data that acute dAlk elevation attenuates LTM (**Fig. 4*B***) and that conditioning elevates the endogenous protein in MB dendrites (**Fig. 7**). Moreover, dAlk autoactivation is consistent with the independence of dAlk-dependent PSD-LTM attenuation from Jeb (**Fig. 6**). The conditioning-dependent dAlk elevation and autoactivation in MB dendrites are likely considerably slower than acute activation by Jeb of extant dAlk outside the MBs required to constrain learning/3 min memory formation (185) (**Fig. 6*C***). Furthermore, pan-neuronal elevation of Jeb left PSD-LTM unaffected (**Fig. 6*B***), consistent with the notion that the two methods of dAlk activation, Jeb-dependent activation and autoactivation, are operant in spatially distinct neurons (outside and inside the MBs, respectively) and of distinct functional consequences.

Hence, we propose that conditioning results in local elevation of unliganded dAlk monomers in MB dendrites, raising the probability of encounter, lateral dimerization, autophosphorylation, and activation of the kinase domain at the postsynaptic plasma membrane. Unfortunately, an antibody specific to phosphorylated, hence activated, dAlk is not currently available; therefore, it is not possible to test this prediction *in situ*.

Downstream mechanisms engaged by dAlk to restrain LTM are still unknown. In our previous study (185), we described dAlk outside the MBs as an upstream activator of a dNf1-regulated Ras/ERK signaling pathway responsible for learning/STM attenuation. Interestingly, dAlk and dNf1 colocalize extensively in MB calyces (185), suggesting that

they could also interact to mediate PSD-LTM attenuation. However, unlike for dAlk abrogation, dNf1 loss results in PSD-LTM deficits restored by reexpression of the protein in α/β MB neurons under c739-Gal4 (367). Therefore, although possible that dAlk and dNf1 interact within these neurons, they are likely antagonistic with respect to PSD-LTM formation, a process potentially engaging and requiring suppression of Ras signaling, a hypothesis currently under investigation.

In conclusion, we have identified dAlk as a specific negative regulator of PSD-LTM formation. Thus far, dAlk appears unique among RTKs in that it constrains LTM formation, possibly acting as a memory filter. The nature of the specific signals engaged by dAlk and the downstream PSD-LTM-constraining mechanisms remains yet to be elucidated in future work.

IV. Bibliography

1. Kaufman TC. Short History and Description of Drosophila melanogaster Classical Genetics: Chromosome Aberrations, Forward Genetic Screens, and the Nature of Mutations Genetics. 2017;206(665-689).

2. Shingleton A. The regulation of organ size in Drosophila: physiology, plasticity, patterning and physical force. Organogenesis 2010 Apr-Jun;6(2):76-87.

3. Morgan T. LOCALIZATION OF THE HEREDITARY MATERIAL IN THE GERM CELLS. Proc Natl Acad Sci U S A 1915;1(7):420-9.

4. Benzer S. Behavioral mutants of Drosophila isolated by countercurrent distribution. Proc Natl Acad Sci U S A 1967;Sep;58(3):1112-9.

5. Konopka RJ BS. Clock mutants of Drosophila melanogaster. Proc Natl Acad Sci U S A 1971;Sep;68(9):2112-6.

6. Quinn W, Harris W, S. B. Conditioned behavior in Drosophila melanogaster. Proc Natl Acad Sci U S A 1974;71(3):708-12.

7. Dudai Y JY, Byers D, Quinn WG, Benzer S. dunce, a mutant of Drosophila deficient in learning. Proc Natl Acad Sci U S A. 1976;May;73(5):1684-8.

8. Livingstone MS, Sziber PP, Quinn WG. Loss of calcium/calmodulin responsiveness in adenylate cyclase of rutabaga, a Drosophila learning mutant. Cell. 1984;37:205-15.

9. Rubin GM SA. Genetic transformation of Drosophila with transposable element vectors. Science. 1982 Oct 22(218(4570)):348-53.

10. Adams MDea. The genome sequence of Drosophila melanogaster. Science 2000;287:2185-95

11. Ni JQ, R. Zhou, B. Czech, L. P. Liu, L. Holderbaum et al. A genome-scale shRNA resource for transgenic RNAi in Drosophila. Nat Methods. 2011; 8:405-7.

12. Golic KG LS. The FLP recombinase of yeast catalyzes site-specific recombination in the Drosophila genome. . Cell. 1989;59:499-509.

13. Caygill EE, Brand AH. The GAL4 System: A Versatile System for the Manipulation and Analysis of Gene Expression. Methods in molecular biology (Clifton, NJ. 2016;1478:33-52.

14. Bellen HJea. The BDGP gene disruption project: single transposon insertions associated with 40% of Drosophila genes. Genetics. 2004;167:761-81.

15. Groth AC, Fish, M., Nusse, R. & Calos, M. P. Construction of transgenic Drosophila by using the site-specific integrase from phage φC31. Genetics 2004; 166:1775-82

16. Sokolowski MB. Drosophila: genetics meets behaviour. Nature reviews. 2001;2(11):879-90.

17. HIRSCH J, ERLENMEYER-KIMLING L. Sign of taxis as a property of the genotype. Science. 1961;22(134(3482)):835-6.

18. Sokolowski MBeG, D., Wahlsten D. & Wimer, R. E.) Techniques for the Genetic Analysis of Brain and Behavior. Elsevier, Amsterdam. 1992;497

19. Young MW. The molecular control of circadian behavioral rhythms and their entrainment in Drosophila. Ann Rev Biochem. 1998 67:135-52.

20. Lowrey PaT, J. Mammalian circadian biology: elucidating genome-wide levels of temporal organization. Annu Rev Genom Hum Genet. 2004;5:407-41.

21. Young MW. Circadian rhythms. Marking time for a kingdom. Science. 2000;288:451-3.
22. Reiter L.T. P, L., Chien, S. and Gribskov, M. and Bier, E. A systematic analysis of human disease associated gene sequences in Drosophila melanogaster. Genome Res. 2001;11:1114-25.
23. Chien S, Reiter, L.T., Bier, E. and Gribskov, M. Homophila: human disease gene cognates in Drosophila. .Nucl Acids Res. 2002;30:149-51.
24. O'Kane C. Drosophila as a model organism for the study of neuropsychiatric disorders. Curr Top Behav Neurosci. 2011.
25. Benzer S. From the gene to behavior. JAMA. 1971;218:1015-22.
26. Min KT, and S. Benzer Spongecake and eggroll: two hereditary diseases in Drosophila resemble patterns of human brain degeneration. Curr Biol. 1997; 7:885-8.
27. Synofzik M, M. A. Gonzalez, C. M. Lourenco, M. Coutelier, T. B., Haack et al. PNPLA6 mutations cause Boucher- Neuhauser and Gordon Holmes syndromes as part of a broad neurodegenerative spectrum. Brain 2014;137:69-77.
28. Feany MB, and W. W. Bender. A Drosophila model of Parkinson's disease. Nature 2000 404:394-8.
29. Morales J, P. R. Hiesinger, A. J. Schroeder, K. Kume, P. Verstreken, al. e. Drosophila fragile X protein, DFXR, regulates neuronal morphology and function in the brain. Neuron. 2002 34:961-72.
30. Mutsuddi M, C. M. Marshall, K. A. Benzow, M. D. Koob, and I., Rebay. The spinocerebellar ataxia 8 noncoding RNA causes neurodegeneration and associates with staufen in Drosophila. Curr Biol 2004 14:302-8.
31. Dockendorff TC, H. S. Su, S. M. McBride, Z. Yang, C. H. Choi, al. e. Drosophila lacking dfmr1 activity show defects in circadian output and fail to maintain courtship interest. Neuron 2002;34:973-84.
32. McGurk L. BA, Bonini N.M. Drosophila as an In Vivo Model for Human Neurodegenerative Disease. Genetics. 2015; 201: 377-402.
33. Brand A, Perrimon N. Targeted gene expression as a means of altering cell fates and generating dominant phenotypes. Development 1993 118(2):401-15.
34. Pfeiffer B, Jenett A, Hammonds A, Ngo T, Misra S, Murphy C, et al. Tools for neuroanatomy and neurogenetics in Drosophila. Proc Natl Acad Sci U S A 2008;15(105(28)):9715-20.
35. Venken K, KL. S, NA. H, H. P, Y. H, M. E-H, et al. MiMIC: a highly versatile transposon insertion resource for engineering Drosophila melanogaster genes. Nat Methods. 2011;8(9):737-43.
36. AR. B, JL. L. CRISPR/Cas9 and genome editing in Drosophila. J Genet Genomics 2014;20(41(1)):7-19.
37. Bier E. Drosophila, the golden bug, emerges as a tool for human genetics. Nature reviews. 2005;6(1):9-23.
38. Freeman MR DJ. Glial cell biology in Drosophila and vertebrates. Trends Neurosci. 2006;29:82-90.
39. Reichert H. A tripartite organization of the urbilaterian brain: developmental genetic evidence from Drosophila. Brain Res Bull 2005;66:491-4.
40. Zhang D KH, Kidokoro Y. Activation of metabotropic glutamate receptors enhances synaptic transmission at the Drosophila neuromuscular junction. Neuropharmacology. 1999;38:645-57.

41. Mao Z DR. Eight different types of dopaminergic neurons innervate the Drosophila mushroom body neuropil: anatomical and physiological heterogeneity. Front Neural Circuits. 2009; 3(1).
42. McPartland J DMV, De Petrocellis L et al Cannabinoid receptors are absent in insects. J Comp Neurol. 2001;436:423-9.
43. Heisenberg M. Mushroom body memoir: from maps to models. Nature Reviews Neuroscience. 2003;4:266-75.
44. Crittenden JR SE, Han KA, Kalderon D, Davis RL. Tripartite mushroom body architecture revealed by antigenic markers. Learn Mem 1998;May-Jun;5(1-2):38-51.
45. Ito K AW, Suzuki K, Hiromi Y, Yamamoto D. The Drosophila mushroom body is a quadruple structure of clonal units each of which contains a virtually identical set of neurones and glial cells. Development. 1997;124:761-71.
46. Lee T LA, Luo L. Development of the Drosophila mushroom bodies: sequential generation of three distinct types of neurons from a neuroblast. Development. 1999;126:4065-76.
47. Kurusu M AT, Masuda-Nakagawa LM, Kawauchi H, Ito K, Furukubo-Tokunaga K. Embryonic and larval development of the Drosophila mushroom bodies: concentric layer subdivisions and the role of fasciclin II. Development 2002;129:409-19.
48. de Belle JS, M. H. Associative odor learning in Drosophila abolished by chemical ablation of mushroom bodies. Science. 1994;263:692-5.
49. Davis RL. Physiology and Biochemistry of Drosophila learning mutants. Physiological Reviews. 1996;76(2):299-317.
50. Zars T. Behavioral functions of the insect mushroom bodies. Curr Opin Neurobiol. 2000;10:790-5.
51. Pascual A PT. Localization of long-term memory within the Drosophila mushroom body. Science 2001;294:1115-7.
52. Dubnau J, Grady L, Kitamoto T, T. T. Disruption of neurotransmission in Drosophila mushroom body blocks retrieval but not acquisition of memory. . Nature 2001;411:476-80.
53. McGuire SE, Le PT, L DR. The role of Drosophila mushroom body signaling in olfactory memory. Science. 2001;293:1330-3.
54. Krashes MJ KA, Leung B, Armstrong JD, Waddell S. Sequential use of mushroom body neuron subsets during Drosophila odor memory processing. Neuron 2007;53:103-15.
55. Acevedo SF, Froudarakis EI, Kanellopoulos A, EM. S. Protection from premature habituation requires functional mushroom bodies in Drosophila. Learn Mem 2007;10;14(5):376-84.
56. Roussou IG PK, Savakis C, Skoulakis EMC. Drosophila Bruton's Tyrosine Kinase regulates habituation latency and facilitation in distinct mushroom body neurons. J Neurosci 2019;Sep 17.
57. Tanaka NK TH, Ito K. Neuronal assemblies of the Drosophila mushroom body. J Comp Neurol 2008;Jun 10; 508(5):711-55.
58. Crittenden JR, Skoulakis EMC, Han K-A, Kalderon D, Davis RL. Tripartite mushroom body architecture revealed by antigenic markers. Learning and Memory. 1998;5:38-51.
59. Venken KJ BH. Transgenesis upgrades for Drosophila melanogaster. . Development 2007;134:3571-84.
60. Geyer MA BD. Startle habituation and sensorimotor gating in schizophrenia and related animal models. Schizophr Bull 1987;13(4):643-68.

61. Thompson RF SW. Habituation: a model phenomenon for the study of neuronal substrates of behavior. Psychol Rev 1966;Jan;73(1):16-43.
62. Ramaswami M. Network plasticity in adaptive filtering and behavioral habituation. Neuron. 2014;82(6):1216-29.
63. Groves PM, Thomson RF. Habituation: A dual-process theory. Phychological Review. 1970;77:419-50.
64. Rankin CH, Abrams T, Barry RJ, Bhatnagar S, Clayton DF, Colombo J, et al. Habituation revisited: an updated and revised description of the behavioral characteristics of habituation. . Neurobiology Learn Mem. 2009;92(2):138-.
65. Poon CS YD. Nonassociative learning as gated neural integrator and differentiator in stimulus-response pathways. Behav Brain Funct 2006 Aug 8(2):29.
66. Braff DL, Grillon, C., and Geyer, M.A. Gating and habituation of the startle reflex in schizophrenic patients. . Arch Gen Psychiatry. 1992;49:206-15.
67. Jansiewicz E, Newschaffer C, Denckla M, Mostofsky S. Impaired habituation in children with attention deficit hyperactivity disorder. Cogn Behav Neurol. 2004;17(1):1-8.
68. McSweeney FK, Murphy, E.S., and Kowal, B.P. Regulation of drug taking by sensitization and habituation. . Exp Clin Psychopharmacol. 2005; 13
163-84.
69. Thompson RF, WA. S. Habituation: A model phenomenon for the study of neuronal substrates of behavior. . Psychological Review. 1966;3(1):16-43.
70. Pinsker H KI, Castellucci V, Kandel E. Habituation and dishabituation of the gill-withdrawal reflex in Aplysia. Science 1970 Mar 27;167(3926):1740-2.
71. Castellucci V, Pinsker H, Kupfermann I, ER. K. Neuronal mechanisms of habituation and dishabituation of the gill-withdrawal reflex in Aplysia. Science 1970;167:1745-8.
72. DL. G. Habituation in Aplysia: the Cheshire cat of neurobiology. Neurobiol Learn Mem 2009 2009;Sep;92(2):147-54.
73. Fischer TM, Jacobson,D.A., and Demorest-Hayes,K. Network processes involved in the mediation of short-term habituation in Aplysia:contribution
of intrinsic regulation of excitability and synaptic augmentation. . FrontIntegr Neurosci. 2014;8:15.
74. Rankin CH BC, Chiba CM. Caenorhabditis elegans: a new model system for the study of learning and memory. Behav Brain Res 1990;Feb 12;(37(1)):89-92.
75. Rankin CH, S BB. Factors affecting habituation and recovery from habituation in the nematode *Caenorhabtitis elegans*. Behavioral Neuroscience. 1992;106(2):239-49.
76. Rose JK, Rankin CH. Analyses of Habituation in *Caenorhabditis elegans*. Learning and Memory. 2001;8:63-9.
77. Giles AC RC. Behavioral and genetic characterization of habituation using Caenorhabditis elegans. Neurobiol Learn Mem. 2009 Sep;92(2):139-46.
78. Wong K EM, Bartels B, Elkhayat S, Tien D, Roy S, Goodspeed J, Suciu C, Tan J, Grimes C, Chung A, Rosenberg M, Gaikwad S, Denmark A, Jackson A, Kadri F, Chung KM, Stewart A, Gilder T, Beeson E, Zapolsky I, Wu N, Cachat J, Kalueff AV. Analyzing habituation responses to novelty in zebrafish (Danio rerio). Behav Brain Res 2010;Apr 2;208(2):450-7.
79. MacPhail RC ea. Locomotion in larval zebrafish: influence of time of day,
lighting and ethanol. . Neurotoxicology. 2009;930(1):52-8.
80. Eddins D ea. Zebrafish provide a sensitive model of persisting neurobehavioral

effects of developmental chlorpyrifos exposure: comparison with nicotine and pilocarpine effects and relationship to dopamine deficits. Neurotoxicol Teratol 2009.
81. LE. K. An altered electroretinogram transient associated with an unusual jump response in a mutant of Drosophila. Cell Mol Neurobiol 1983;Jun;3(2):143-9.
82. Engel JE WC. Altered habituation of an identified escape circuit in Drosophila memory mutants. J Neurosci 1996;May 15;16(10):3486-99.
83. Engel JE XX, Sokolowski MB, Wu CF. A cGMP-dependent protein kinase gene, foraging, modifies habituation-like response decrement of the giant fiber escape circuit in Drosophila. Learn Mem 2000;Sep-Oct;7(5):341-52.
84. Rees CT, Spatz H-C. Habituation of the landing response of Drosophila wild-type and mutants defective in olfactory learning. J Neurogenetics. 1989;5:105-18.
85. Asztalos Z, vonWegener J, Wustmann G, Dombradi V, Gausz J, Spatz H-C, et al. Protein Phosphatase 1-deficient mutant Drosophila is affected in habituationa and associative learning. J Neuroscience. 1993;13(3):924-30.
86. Corfas G, Dudai Y. Habituation and dishabituation of a cleaning reflex in normal and mutant Drosophila. J Neuroscience. 1989;9(1):56-62.
87. Asztalos Z, Baba K, Yamamoto D, T. The fickle mutation of a cytoplasmic tyrosine kinase effects sensitization but not dishabituation in Drosophila melanogaster. J Neurogenet. 2007;20(1-2):59-71.
88. Asztalos Z AN, Tully T. Olfactory jump reflex habituation in Drosophila and effects of classical conditioning mutations. J Neurogenet. 2007;Jan-Jun;21(1-2):1-18.
89. Cho W, Heberlein U, FW. W. Habituation of an odorant-induced startle response in Drosophila. Genes, Brain & Behavior. 2004;3:127-37.
90. Wolf FW EM, Lee S, Cho W, Heberlein U. GSK-3/Shaggy regulates olfactory habituation in Drosophila. Proc Natl Acad Sci U S A 2007;Mar 13;104(11):4653-7.
91. Devaud J-M, Keane J, Ferrus A. Blocking sensory inputs to identified antennal glomeruli selectively modifies odorant perception in *Drosophila*. J Neurobiol. 2003;56:1-12.
92. Das S, Sadanandappa MK, Dervan A, Larkin A, Lee JA, Sudhakaran IP, et al. Plasticity of local GABAergic interneurons drives olfactory habituation. Proc Natl Acad Sci U S A 2011;6;108(36):E646-54. .
93. Semelidou O AS, Skoulakis EM Temporally specific engagement of distinct neuronal circuits regulating olfactory habituation in Drosophila. eLife 2018;7:e39569.
94. Duerr JS, Quinn WG. Three Drosophila mutations that block associative learning also affect habituation and sensitization. Proc Natl Acad Sci USA. 1982;79:3646-50.
95. E. LB. Aging and habituation of the tarsal response in Drosophila melanogaster. Gerontology 1983;29(6):388-93.
96. Acevedo SF, Froudarakis EI, Kanellopoulos A, Skoulakis EMC. Protection from premature habituation requires functional mushroom bodies in Drosophila. Learn Mem. 2007;14(5):376-8.
97. KM OD. The inactive mutation leads to abnormal experience-dependent courtship modification in male Drosophila melanogaster. Behav Genet 1994 Jul;24(4):381-8.
98. Jin P, Griffith LC, Murphey RK. Presynaptic Calcium/Calmodulin-dependent Protein Kinase II regulates habituation of a simple reflex in Adult Drosophila. J Neuroscience. 1998;18(21):8955-64.
99. Lloyd DR, Medina,D.J.,Hawk,L.W.,Fosco,W.D.,andRichards,J.B. Habituation of reinforce effectiveness. . FrontIntegrNeurosci 2014;7:107.

100. Pilz PK SH. Habituation and sensitization of the acoustic startle response in rats: amplitude, threshold, and latency measures. Neurobiol Learn Mem 1996;Jul;66(1):67-79.
101. Simons-Weidenmaier NS WM, Plappert CF, Pilz PK, Schmid S. Synaptic depression and short-term habituation are located in the sensory part of the mammalian startle pathway. BMC Neurosci 2006;May 9;7(38).
102. Pilz PK AS, Rischawy AT, Plappert CF. Longterm-habituation of the startle response in mice is stimulus modality, but not context specific. Front Integr Neurosci. 2014 Jan 9;7(103).
103. Zaman T DOC, Smoka M, Narla C, Poulter MO, Schmid S. BK Channels Mediate Synaptic Plasticity Underlying Habituation in Rats. J Neurosci 2017;Apr 26;37(17):4540-51.
104. Wilson DA LC. Neurobiology of a simple memory. J Neurophysiol 2008;Jul;100 (1):2-7.
105. McNamara AM MP, Linster C, Wilson DA, Cleland TA. Distinct neural mechanisms mediate olfactory memory formation at different timescales. Learn Mem 2008;Feb 22;15(3):117-25.
106. Linster C MA, Singh CY, Wilson DA. Odor-specific habituation arises from interaction of afferent synaptic adaptation and intrinsic synaptic potentiation in olfactory cortex. Learn Mem 2009;Jun 24;16(7):452-9.
107. Typlt M, Mirkowski,M.,Azzopardi,E.,Ruth,P.,Pilz,P.K.,andSchmid,S. Habituation of reflexive and motivated behavior in mice with deficient BK channel function. . FrontIntegrNeurosci 2013;7(79).
108. Dutta A GY. Saliency mapping in the optic tectum and its relationship to habituation. Front Integr Neurosci 2014;Jan 16;8(1).
109. Dalton P WC. The nature and duration of adaptation following long-term odor exposure. Percept Psychophys 1996 Jul;58(5):781-92.
110. Wang L WV, Sardi H, Fraser C, Jacob TJ. The correlation between physiological and psychological responses to odour stimulation in human subjects. Clin Neurophysiol 2002;Apr;113(4):542-51.
111. Sobel N PV, Zhao Z, Desmond JE, Glover GH, Sullivan EV, Gabrieli JD. Time course of odorant-induced activation in the human primary olfactory cortex. J Neurophysiol 2000;Jan;83(1):537-51.
112. Stuck BA FV, Hummel T, Sommer JU. Subjective olfactory desensitization and recovery in humans. Chem Senses 2014;Feb;39(2):151-7. .
113. Mutschler I WB, Speck O, Schulze-Bonhage A, Hennig J, Seifritz E, Ball T. Time scales of auditory habituation in the amygdala and cerebral cortex. Cereb Cortex 2010;Nov;20(11):2531-9.
114. Phillips ML MN, Young AW, Williams L, Williams SC, Bullmore ET, Gray JA, Brammer MJ. Time courses of left and right amygdalar responses to fearful facial expressions. Hum Brain Mapp 2001; Apr;12(4):193-202.
115. Wright CI FH, Whalen PJ, McInerney SC, Shin LM, Rauch SL. Differential prefrontal cortex and amygdala habituation to repeatedly presented emotional stimuli. Neuroreport 2001;Feb 12;12(2):379-83.
116. Kindt KS QK, Giles AC, De S, Hendrey D, Nicastro I, Rankin CH, Schafer WR. Dopamine mediates context-dependent modulation of sensory plasticity in C. elegans. Neuron 2007 Aug 16;55(4):662-76.

117. Sanyal S WR, Kindt KS, Nuttley WM, Arvan R, Fitzmaurice P, Bigras E, Merz DC, Hébert TE, van der Kooy D, Schafer WR, Culotti JG, Van Tol HH. Dopamine modulates the plasticity of mechanosensory responses in Caenorhabditis elegans. EMBO J 2004; Jan 28;23(2):473-82.
118. SOKOLOV E. Higher nervous functions; the orienting reflex. Annu Rev Physiol 1963;25:545-80.
119. Castellucci VF KE. A quantal analysis of the synaptic depression underlying habituation of the gill-withdrawal reflex in Aplysia. Proc Natl Acad Sci U S A 1974;Dec;71(12)(12):5004-8.
120. Bailey CH, & Chen, M. . Long-term memory in Aplysia modulates the total number of varicosities of single identified sensory neurons. Proceedings of the National Academy of Sciences USA,. 1988;85: 2373-7.
121. Engel JE, Wu C-F. Altered habituation of an identified escape circuit in Drosophila memory mutants. J Neuroscience. 1996;16(10):3486-99.
122. Rankin CH. Context conditioningin Habituation in the nematode *Caenorabditis elegans*. Behavioral Neuroscience. 2000;114(3):496-505.
123. Sadanandappa MK, Blanco Redondo, B., Michels, B., Rodrigues, V.,, Gerber B, VijayRaghavan, K., Buchner, E., and Ramaswami, M. . Synapsin function in GABA-ergic interneurons is required for short-term olfactory habituation. J Neurosci 2013;33:16576-85.
124. Paranjpe P RV, VijayRaghavan K, Ramaswami M Gustatory habituation in Drosophila relies on rutabaga (adenylate cyclase)- dependent plasticity of GABAergic inhibitory neurons. . Learn Mem 2012;19:627-35.
125. Ardiel EL MT, Timbers TA, Lee KCY, Safaei J, Pelech SL3, Rankin CH. Insights into the roles of CMK-1 and OGT-1 in interstimulus interval-dependent habituation in Caenorhabditis elegans. Proc Biol Sci 2018;Nov 14;(285):1891.
126. De Luca MA. Habituation of the responsiveness of mesolimbic and mesocortical dopamine transmission to taste stimuli. FrontIntegrNeurosci 2014;8:21.
127. Manella LC, Alperin,S.,andLinster,C. . Stressors impair odor recognition memory via an olfactory bulb-dependent noradrenergic mechanism. Front IntegrNeurosci 2013;7:97.
128. Cevik MO. Habituation, sensitization, and Pavlovian conditioning. Front IntegrNeurosci 2014;8:13.
129. Cevik MÖ EA. The course of habituation of the proboscis extension reflex can be predicted by sucrose responsiveness in Drosophila. PLoS One 2012;7(6)(e39863).
130. van Os J, Kapur S. Schizophrenia. Lancet. 2009;374:635-45.
131. Gillberg C. Deficits in attention, motor control and perception: A brief review. Arch Dis Child. 2003;88:904-10.
132. Ludewig K, Geyer MA, FX. V. Deficits in prepulse inhibition and habituation in never-medicated, first-episode schizophrenia. . Biol Psychiatry. 2003;54(2):121-8.
133. Meincke U, Light GA, Geyer MA, Braff DL, Gouzoulis-Mayfrank E. Sensitization and habituation of the acoustic startle reflex in ptients with schizophrenia. Psychiatry Res. 2004;126(1):51-61.
134. Owen M, Sawa A, Mortensen PPdS--. Schizophrenia. Lancet. 2016;388(10039):86–97.
135. Akdag SJ, Nestor PG, O'Donnell BF, Niznikiewicz MA, Shenton ME, RW. M. The startle reflex in schizophrenia: habituation and personality correlates. Schizophr Res. 2003;64(2-3):165-73.

136. Barkus C, Sanderson DJ, Rawlins JN, Walton ME, Harrison PJ, DM. B. What causes aberrant salience in schizophrenia? A role for impaired short-term habituation and the GRIA1 (GluA1) AMPA receptor subunit. Mol Psychiatry 2014;19(10):1060-70.
137. Braff D, Grillon C, Geyer M. Gating and Habituation of the startle reflex in schizophrenic patients. Archives of General Psychiatry. 1992;49(3):206-15.
138. Braff DL, Geyer M, A,, Swerdlow NR. Human studies of prepulse inhibition of startle: Normal subjects, patient groups, and pharmacological studies. Psychopharmacology. 2001;156(2-3):234–58.
139. Ludewig K, Geyer MA, Vollenweider FX. Deficits in prepulse inhibition and habituation in never-medicated, first-episode schizophrenia. Biol Psychiatry. 2003;54(2):121-8.
140. Swerdlow NR, Weber M, Qu Y, Light GA, Braff DL. Realistic expectations of prepulse inhibition in translational models for schizophrenia research. Psychopharmacology 2008;199(3):331–88.
141. Braff D, Stone C, Callaway E, Geyer M, Glick I, L. B. Prestimulus effects on human startle reflex in normals and schizophrenics. Psychophysiology. 1978;15(4):339-43.
142. Lugtenberg D, M.R.F. Reijnders, M. Fenckova, E.K. Bijlsma, R. Bernier, B.W.M. van Bon, E. Smeets, A.T. Vulto-van Silfhout, D. Bosch, E.E. Eichler, H.C. Mefford, G.L. Carvill, E.M.H.F. Bongers, J.H. Schuurs-Hoeijmakers, C.A. Ruivenkamp, G.W.E. Santen, A.M.J.M. van den Maagdenberg, C.M.P.C.D. Peeters-Scholte, S. Kuenen, P. Verstreken, R. Pfundt, H. Yntema, P.F. de Vries, J.A. Veltman, A. Hoischen, C. Gilissen, B.B.A. de Vries, A. Schenck, T. Kleefstra, and L.E.L.M. Vissers, . De novo loss-of-function mutations in WAC cause a recognizable intellectual disability syndrome and learning deficits in Drosophila. . Eur J Hum Genet. 2016.
143. Stessman HAF, M.H. Willemsen, M. Fenckova, O. Penn, A. Hoischen, B. Xiong, T. Wang, K. Hoekzema, L. Vives, I. Vogel, H.G. Brunner, I. van der Burgt, C.W. Ockeloen, J.H. Schuurs-Hoeijmakers, J.S. Klein Wassink-Ruiter, C. Stumpel, S.J.C. Stevens, H.S. Vles, C.M. Marcelis, H. van Bokhoven, V. Cantagrel, L. Colleaux, M. Nicouleau, S. Lyonnet, R.A. Bernier, J. Gerdts, B.P. Coe, C. Romano, A. Alberti, L. Grillo, C. Scuderi, M. Nordenskjöld, M. Kvarnung, H. Guo, K. Xia, A. Piton, B. Gerard, D. Genevieve, B. Delobel, D. Lehalle, L. Perrin, F. Prieur, J. Thevenon, J. Gecz, M. Shaw, R. Pfundt, B. Keren, A. Jacquette, A. Schenck, E. Eichler, and T. Kleefstra, . Disruption of POGZ Is Associated with Intellectual Disability and Autism Spectrum Disorders. Am J Hum Genet. 2016;98(3):541-52.
144. Lugtenberg D, Reijnders MRF, Fenckova M, Bijlsma EK, Bernier R, van Bon BWM, et al. De novo loss-of-function mutations in WAC cause a recognizable intellectual disability syndrome and learning deficits in Drosophila. Eur J Hum Genet. 2016.
145. Stessman HAF, Willemsen MH, Fenckova M, Penn O, Hoischen A, Xiong B, et al. Disruption of POGZ Is Associated with Intellectual Disability and Autism Spectrum Disorders. Am J Hum Genet. 2016;98(3):541-52.
146. Kaartinen M PK, Himanen SL, Nevalainen J, Hietanen JK. Autonomic Arousal Response Habituation to Social Stimuli Among Children with Asd. J Autism Dev Disord 2016;Dec;46(12):3688-99.
147. Puts NA WE, Tommerdahl M, Mostofsky SH, Edden RA. Impaired tactile processing in children with autism spectrum disorder. J Neurophysiol 2014;May;111(9):1803-11.
148. Massa J ODI. Impaired visual habituation in adults with ADHD. J Atten Disord. 2012;16:553-61.

149. Consortium SWGotPG. Biological insights from 108 schizophrenia-associated genetic loci. Nature 2014;511:421- 7.
150. Gondo Y MT, Makino S, Fukumura R, Ishitsuka Y Mouse mutagenesis and disease models for neuropsychiatric disorders. In: Current topics in behavioral neurosciences. Springer, Heidelberg. 2011.
151. Chubb JE BN, Soares DC et al The DISC locus in psychiatric illness. Mol Psychiat 2008;13:36-64.
152. Millar JK PB, Mackie S et al DISC1 and PDE4B are interacting genetic factors in schizophrenia that regulate cAMP signaling. . Science. 2005;310:1187-91.
153. Ross CA MR, Reading SAJ et al Neurobiology of schizophrenia. Neuron. 2006;52::139-53.
154. Ryder PV FV. Schizophrenia: the "BLOC" may be in the endosomes. Sci Signal. 2009;2(93):pe66.
155. Dickman DK DG. The schizophrenia susceptibility gene dysbindin controls synaptic homeostasis. Science 2009;326:1127-31.
156. J. OKC. Drosophila as a Model Organism for the Study of Neuropsychiatric Disorders. Current Topics in Behavioral Neurosciences 2011;7.
157. McDiarmid T, Bernardos A, Rankin C. Habituation is altered in neuropsychiatric disorders-A comprehensive review with recommendations for experimental design and analysis. Neurosci Biobehav Rev. 2017;Sep;80:286-305.
158. Coppola G PF, Schoenen J. Habituation and migraine. Neurobiol Learn Mem. 2009 Sep;92(2):249-59.
159. Sinclair D OB, Razak KA, Siegel SJ, Schmid S. Sensory processing in autism spectrum disorders and Fragile X syndrome-From the clinic to animal models. Neurosci Biobehav Rev. 2017 May;76(Pt B)(235-253.).
160. Metaxakis A. OS, Klinakis A., Savakis C. Minos as a genetic and genomic tool in Drosophila melanogaster. Genetics 2005;171(2):571-81.
161. Loukeris TG AB, Livadaras I, Dialektaki G, Savakis C. Introduction of the transposable element Minos into the germ line of Drosophila melanogaster. Proc Natl Acad Sci U S A 1995;Oct 10(92(21)):9485-9.
162. Siniatchkin M, Kropp P, Gerber W-D. What kind of habituation is impaired in migraine patients? Cephalalgia. 2003;23:511-8.
163. Kalita J BS, MisraUK. Is lack of habituation of evoked potential a biological marker of migraine? . Clin J Pain 2014;30:724 -9.
164. D'Cruz A, Ragozzino M, Mosconi M, Shrestha S, Cook E, Sweeney J. Reduced behavioral flexibility in autism spectrum disorders. Neuropsychology. 2013;27(2):152-60.
165. Tei S, Fujino J, Hashimoto R, Itahashi T, Ohta H, Kanai C, et al. Inflexible daily behaviour is associated with the ability to control an automatic reaction in autism spectrum disorder. Sci Rep. 2018;8(1):8082.
166. Guven-Ozkan T DR. Functional neuroanatomy of Drosophila olfactory memory formation. Learn Mem 2014;21:519 -26.
167. Mattsson P, Vihinen M, Smith C. X-linked agammaglobulinemia (XLA): a genetic tyrosine kinase (Btk) disease. Bioessays. 1996 18((10)):825-34.
168. Gregory R, Kammermeyer K, Vincent Wr, W, SG. Primary sequence and developmental expression of a novel Drosophila melanogaster src gene. Mol Cell Biol 1987 7(6):2119-27.

169. Tsikala G, Karagogeos D, Strigini M. Btk-dependent epithelial cell rearrangements contribute to the invagination of nearby tubular structures in the posterior spiracles of Drosophila. Developmental biology. 2014;396(1):42-56.
170. Roulier E, Panzer S, SK. B. The Tec29 tyrosine kinase is Required during drosophila embryogenesis and interacts with Src64 in ring canal development. Mol Cell 1998;1(6):819-29.
171. Baba K, Takeshita A, Majima K, Ueda R, Kondo S, Juni N, et al. The Drosophila Bruton's Tyrosine Kinase (Btk) Homolog Is Required for Adult Survival and Male Genital Formation. Mol Cell Biol 1999;19(6):405-13.
172. Hamada-Kawaguchi N, Yamamoto D. Ovarian polarity and cell shape determination by Btk29A in Drosophila. 2017;55(8).
173. Sunouchi K, Koganezawa M, Yamamoto D. REQUIREMENT OF THE TEC FAMILY TYROSINE KINASE BTK29A FOR COURTSHIP MEMORY IN Drosophila MALES. Archives of insect biochemistry and physiology. 2016;91(3):165-74.
174. Aso Y, Grübel K, Busch S, Friedrich AB, Siwanowicz I, Tanimoto H. The mushroom body of adult Drosophila characterized by GAL4 drivers. J Neurogenet. 2009;23(1-2):156-72.
175. Gouzi JY BM, Roussou IG, Moressis A, Skoulakis EMC. The Drosophila Receptor Tyrosine Kinase Alk Constrains Long-Term Memory Formation. J Neurosci. 2018 Aug 29;38(35):7701-12.
176. Messaritou G LF, Franco M, Skoulakis EM A third functional isoform enriched in mushroom body neurons is encoded by the Drosophila 14-3-3ζ gene. FEBS letters. 2009;583:2934-8.
177. Gai Y LZ, Cervantes-Sandoval I, Davis RL. Drosophila SLC22A transporter is a memory suppressor gene that influences cholinergic neurotransmission to the mushroom bodies. . Neuron. 2016;90:581-95.
178. Shyu WH CT, Chiang MH, Cheng YC, Tsai YL, Fu TF, Wu T, Wu CL. Neural circuits for long-term water-reward memory processing in thirsty Drosophila. . Nat Commun. 2017; 8:15230.
179. McGuire SE LP, Osborn AJ, Matsumoto K, Davis RL Spatiotemporal rescue of memory dysfunction in Drosophila. . Science. 2003;302:1765-8.
180. Lee T LL. Mosaic analysis with a repressible cell marker for studies of gene function in neuronal morphogenesis. . Neuron 1999;22:451- 61.
181. Sokal RR, Rohlf FJ. Biometry The Principles and Practice of Statistics in Biological Research. 2nd ed. New York: W. H. Freeman; 1981.
182. Tillman B PJ, Satyanarayana G, Talbott M, Warner J Systematic review of infectious events with the Bruton tyrosine kinase inhibitor ibrutinib in the treatment of hematologic malignancies. . Eur J Haematol 2018;100:325-34.
183. Ysebaert L, Michallet A. Bruton's tyrosine kinase inhibitors: lessons learned from bench-to-bedside (first) studies. Curr Opin Oncol. 2014;26(5):463-8.
184. Hamada-Kawaguchi N, Nore B, Kuwada Y, Smith C, D. Y. Btk29A promotes Wnt4 signaling in the niche to terminate germ cell proliferation in Drosophila. Science 2014;17(343(6168)):294-7.
185. Gouzi JY MA, Walker JA, Apostolopoulou AA, Palmer RH, Bernards A, Skoulakis EM The receptor tyrosine kinase Alk controls neurofibromin functions in Drosophila growth and learning. PLoS Genet. 2011;7:e1002281.

186. Pavlopoulos E, Anezaki M, Skoulakis EMC. Neuralized is expressed in the α/β lobes of adult Drosophila Mushroom Bodies and facilitates olfactory Long-Term Memory formation. Proc Natl Acad Sci USA 2008;105(38):14674-9.
187. Kitamoto T. Conditional modification of Behavior in *Drosophila* by targeted expression of a Temperature-sensitive *shibire* allele in defined neurons. J Neurobiol. 2001;47(2):81-92.
188. Brisch R SA, Wolf R, Bielau H, Bernstein HG, Steiner J, Bogerts B,, Braun AK JZ, Kumaritlake J, Henneberg M, Gos T The role of dopamine in schizophrenia from a neurobiological and evolutionary perspective: old fashioned, but still in vogue. Front Psychiatry 2014;5:47.
189. Kesby J ED, McGrath J, Scott J Dopamine, psychosis and schizophrenia: the widening gap between basic and clinical neuroscience. Transl Psychiatry 2018;8(30.).
190. D R. CNS receptor partial agonists: a new approach to drug discovery. Primary Psychiatry. 2007;14:22-4.
191. Brunton L CB, Knollman B Goodman and Gilman's the pharmacological basis of therapeutics, Ed 12. New York: McGraw Hill. 2010.
192. Ries AS HT, Poeck B, Strauss R. Serotonin modulates adepression-like state in Drosophila responsive to lithium treatment. Nat Commun 2017;8(15738.).
193. Roth BL WKW, S Patel S, Lopez E The multiplicity of serotonin receptors: uselessly diverse molecules or an embarrasment of riches? Neuroscientist 2000;6:252-62.
194. Takemura SY AY, Hige T, Wong A, Lu Z, Xu CS, Rivlin PK, Hess H, Zhao, T PT, Berg S, Huang G, Katz W, Olbris DJ, Plaza S, Umayam L,, Aniceto R CL, Lauchie S, Ogundeyi O, et al. A connectome of a learning and memory center in the adult Drosophila brain. eLife 2017;6:e26975.
195. Yamazaki D HM, Abe T, Shimizu K, Minami-Ohtsubo M, Maeyama Y,, Horiuchi J TT. Two parallel pathways assign opposing odor valences during Drosophila memory formation. . Cell Rep 2018;22:2346-58.
196. Corneth OB KWR, Hendriks RW BTK signaling in B cell differentiation and autoimmunity. . Curr Top Microbiol Immunol 2016;393:67-105.
197. Rust MB MT. Relevance of presynaptic actin dynamics for synapse function and mouse behavior. . Exp Cell Res 2015;335:165-71.
198. Cognigni P FJ, Waddell S Do the right thing: neural network mechanisms of memory formation, expression and update in Drosophila. Curr Opin Neurobiol 2018;49:51-8.
199. Naheed M GB. Focus on clozapine. . Curr Med Res Opin 2001;17:223-9.
200. Fromer M, Roussos P, Sieberts S, Johnson J, Kavanagh D, Perumal T, et al. Gene expression elucidates functional impact of polygenic risk for schizophrenia. Nat Neurosci. 2016;doi: 10.1038/nn.4399.
201. Roussos PG ZC, Fullard JF, Karagiorga VE, Tsapakis EM, Petraki Z,, Siever LJ LT, Malhotra A, Spanaki C, Bitsios P. The relationship of common risk variants and polygenic risk for schizophrenia to sensorimotor gating. . Biol Psychiatry 2016;79:988 -96.
202. Sotiropoulos I, Galas MC, Silva JM, Skoulakis E, Wegmann S, Maina MB, et al. Atypical, non-standard functions of the microtubule associated Tau protein. Acta neuropathologica communications. 2017;5(1):91.
203. Wang Y, Mandelkow E. Tau in physiology and pathology. Nat Rev Neurosci. 2015;17(1):5-21.

204. Nishimura I, Yang Y, Lu B. PAR-1 kinase plays an initiator role in a temporally ordered phosphorylation process that confers tau toxicity in Drosophila. Cell. 2004;116(5):671-82.
205. Papanikolopoulou K, Skoulakis EM. The power and richness of modelling tauopathies in Drosophila. Mol Neurobiol. 2011;44(1):122-33.
206. Papanikolopoulou K, Skoulakis EM. Temporally distinct phosphorylations differentiate Tau-dependent learning deficits and premature mortality in Drosophila. Hum Mol Genet. 2015;24(7):2065-77.
207. Shulman JM, Feany MB. Genetic modifiers of tauopathy in Drosophila. Genetics. 2003;165(3):1233-42.
208. Chatterjee S, Sang TK, Lawless GM, Jackson GR. Dissociation of tau toxicity and phosphorylation: role of GSK-3beta, MARK and Cdk5 in a Drosophila model. Hum Mol Genet. 2009;18(1):164-77.
209. Heidary G, Fortini ME. Identification and characterization of the Drosophila tau homolog. Mech Dev. 2001;108(1-2):171-8.
210. Gistelinck M, Lambert JC, Callaerts P, Dermaut B, Dourlen P. Drosophila models of tauopathies: what have we learned? International journal of Alzheimer's disease. 2012;2012:970980.
211. Chen X, Li Y, Huang J, Cao D, Yang G, Liu W, et al. Study of tauopathies by comparing Drosophila and human tau in Drosophila. Cell Tissue Res. 2007;329(1):169-78.
212. Bolkan BJ, Kretzschmar D. Loss of Tau results in defects in photoreceptor development and progressive neuronal degeneration in Drosophila. Developmental neurobiology. 2014;74(12):1210-25.
213. Doerflinger H, Benton R, Shulman JM, St Johnston D. The role of PAR-1 in regulating the polarised microtubule cytoskeleton in the Drosophila follicular epithelium. Development. 2003;130(17):3965-75.
214. Burnouf S, Gronke S, Augustin H, Dols J, Gorsky MK, Werner J, et al. Deletion of endogenous Tau proteins is not detrimental in Drosophila. Scientific reports. 2016;6:23102.
215. Harada A, Oguchi K, Okabe S, Kuno J, Terada S, Ohshima T, et al. Altered microtubule organization in small-calibre axons of mice lacking tau protein. Nature. 1994;369(6480):488-91.
216. Zhukareva V, Vogelsberg-Ragaglia V, Van Deerlin VM, Bruce J, Shuck T, Grossman M, et al. Loss of brain tau defines novel sporadic and familial tauopathies with frontotemporal dementia. Ann Neurol. 2001;49(2):165-75.
217. Zhukareva V, Sundarraj S, Mann D, Sjogren M, Blenow K, Clark CM, et al. Selective reduction of soluble tau proteins in sporadic and familial frontotemporal dementias: an international follow-up study. Acta Neuropathol (Berl). 2003;105(5):469-76.
218. Mackenzie IR, Neumann M, Bigio EH, Cairns NJ, Alafuzoff I, Kril J, et al. Nomenclature for neuropathologic subtypes of frontotemporal lobar degeneration: consensus recommendations. Acta neuropathologica. 2009;117(1):15-8.
219. Papegaey A, Eddarkaoui S, Deramecourt V, Fernandez-Gomez FJ, Pantano P, Obriot H, et al. Reduced Tau protein expression is associated with frontotemporal degeneration with progranulin mutation. Acta neuropathologica communications. 2016;4(1):74.
220. Koolen DA, Vissers LE, Pfundt R, de Leeuw N, Knight SJ, Regan R, et al. A new chromosome 17q21.31 microdeletion syndrome associated with a common inversion polymorphism. Nat Genet. 2006;38(9):999-1001.

221. Shaw-Smith C, Pittman AM, Willatt L, Martin H, Rickman L, Gribble S, et al. Microdeletion encompassing MAPT at chromosome 17q21.3 is associated with developmental delay and learning disability. Nat Genet. 2006;38(9):1032-7.
222. Papanikolopoulou K, Kosmidis S, Grammenoudi S, Skoulakis EM. Phosphorylation differentiates tau-dependent neuronal toxicity and dysfunction. Biochem Soc Trans. 2010;38(4):981-7.
223. Sealey MA, Vourkou E, Cowan CM, Bossing T, Quraishe S, Grammenoudi S, et al. Distinct phenotypes of three-repeat and four-repeat human tau in a transgenic model of tauopathy. Neurobiol Dis. 2017;105:74-83.
224. Robinow S, White K. The locus elav of Drosophila melanogaster is expressed in neurons at all developmental stages. Developmental biology. 1988;126(2):294-303.
225. Messaritou G, Leptourgidou F, Franco M, Skoulakis EM. A third functional isoform enriched in mushroom body neurons is encoded by the Drosophila 14-3-3zeta gene. FEBS letters. 2009;583(17):2934-8.
226. McGuire SE, Mao Z, Davis RL. Spatiotemporal gene expression targeting with the TARGET and gene-switch systems in Drosophila. Sci STKE. 2004;2004(220):pl6.
227. Mershin A, Pavlopoulos E, Fitch O, Braden BC, Nanopoulos DV, Skoulakis EM. Learning and memory deficits upon TAU accumulation in Drosophila mushroom body neurons. Learn Mem. 2004;11(3):277-87.
228. Kosmidis S, Grammenoudi S, Papanikolopoulou K, Skoulakis EMC. Differential effects of Tau on the integrity and function of neurons essential for learning in Drosophila. J Neurosci. 2010;30:464-77.
229. Wisniewski JR, Zougman A, Nagaraj N, Mann M. Universal sample preparation method for proteome analysis. Nature methods. 2009;6(5):359-62.
230. Terzenidou ME, Segklia A, Kano T, Papastefanaki F, Karakostas A, Charalambous M, et al. Novel insights into SLC25A46-related pathologies in a genetic mouse model. PLoS Genet. 2017 13(4):e1006656.
231. Tyanova S, Temu T, Sinitcyn P, Carlson A, Hein MY, Geiger T, et al. The Perseus computational platform for comprehensive analysis of (prote)omics data. Nature methods. 2016;13(9):731-40.
232. Tyanova S, Temu T, Cox J. The MaxQuant computational platform for mass spectrometry-based shotgun proteomics. Nature protocols. 2016;11(12):2301-19.
233. Fahmy K, Akber M, Cai X, Koul A, Hayder A, Baumgartner S. alphaTubulin 67C and Ncd are essential for establishing a cortical microtubular network and formation of the Bicoid mRNA gradient in Drosophila. PloS one. 2014;9(11):e112053.
234. Buttgereit D, Leiss D, Michiels F, Renkawitz-Pohl R. During Drosophila embryogenesis the beta 1 tubulin gene is specifically expressed in the nervous system and the apodemes. Mech Dev. 1991;33(2):107-18.
235. Fulga TA, Elson-Schwab I, Khurana V, Steinhilb ML, Spires TL, Hyman BT, et al. Abnormal bundling and accumulation of F-actin mediates tau-induced neuronal degeneration in vivo. Nat Cell Biol. 2007;9(2):139-48.
236. Feuillette S, Miguel L, Frebourg T, Campion D, Lecourtois M. Drosophila models of human tauopathies indicate that Tau protein toxicity in vivo is mediated by soluble cytosolic phosphorylated forms of the protein. J Neurochem. 2010;113(4):895-903.
237. Gorsky MK, Burnouf S, Sofola-Adesakin O, Dols J, Augustin H, Weigelt CM, et al. Pseudo-acetylation of multiple sites on human Tau proteins alters Tau phosphorylation

and microtubule binding, and ameliorates amyloid beta toxicity. Scientific reports. 2017;7(1):9984.
238. Tully T, Quinn W. Classical conditioning and retention in normal and mutant Drosophila melanogaster. J Comp Physiol. 1985;157:263-77.
239. Pavlopoulos E, Anezaki M, Skoulakis EM. Neuralized is expressed in the alpha/beta lobes of adult Drosophila mushroom bodies and facilitates olfactory long-term memory formation. Proc Natl Acad Sci U S A. 2008;105(38):14674-9.
240. Placais PY, de Tredern E, Scheunemann L, Trannoy S, Goguel V, Han KA, et al. Upregulated energy metabolism in the Drosophila mushroom body is the trigger for long-term memory. Nat Commun. 2017;8:15510.
241. Cervantes-Sandoval I PA, Chakraborty M, Davis RL Reciprocal synapses between mushroom body and dopamine neurons form a positive feedback loop required for learning. . eLife 2017;6:e23789.
242. Bettencourt da Cruz A, Schwarzel M, Schulze S, Niyyati M, Heisenberg M, Kretzschmar D. Disruption of the MAP1B-related protein FUTSCH leads to changes in the neuronal cytoskeleton, axonal transport defects, and progressive neurodegeneration in Drosophila. Mol Biol Cell. 2005;16(5):2433-42.
243. Barlan K, Lu W, Gelfand VI. The microtubule-binding protein ensconsin is an essential cofactor of kinesin-1. Curr Biol. 2013;23(4):317-22.
244. Karpova N BY, Fouix S, Huitorel P, Debec A Jupiter, a new Drosophila protein associated with microtubules. Cell Motil Cytoskeleton. 2006;63:301-12.
245. Goldstein LS GS. Flying through the Drosophila cytoskeletal genome. J Cell Biol 2000;150:F63-F8.
246. Hubbert C, Guardiola A, Shao R, Kawaguchi Y, Ito A, Nixon A, et al. HDAC6 is a microtubule-associated deacetylase. Nature. 2002;417(6887):455-8.
247. Portran D, Schaedel L, Xu Z, Thery M, Nachury MV. Tubulin acetylation protects long-lived microtubules against mechanical ageing. Nature cell biology. 2017;19(4):391-8.
248. Martin DN, Baehrecke EH. Caspases function in autophagic programmed cell death in Drosophila. Development. 2004;131(2):275-84.
249. Frost B, Bardai FH, Feany MB. Lamin Dysfunction Mediates Neurodegeneration in Tauopathies. Curr Biol. 2016;26(1):129-36.
250. Henriquez JP, Cross D, Vial C, Maccioni RB. Subpopulations of tau interact with microtubules and actin filaments in various cell types. Cell Biochem Funct. 1995;13(4):239-50.
251. Kempf M, Clement A, Faissner A, Lee G, Brandt R. Tau binds to the distal axon early in development of polarity in a microtubule- and microfilament-dependent manner. J Neurosci. 1996;16(18):5583-92.
252. Davis RL. Olfactory memory formation in Drosophila: From Molecular to systems Neuroscience. Annu Rev Neurosci. 2005;28:275-302.
253. Matamoros AJ, Baas PW. Microtubules in health and degenerative disease of the nervous system. Brain Res Bull. 2016;126(Pt 3):217-25.
254. Tully T, Preat T, Boynton SC, Del Vecchio M. Genetic dissection of consolidated memory in Drosophila. Cell. 1994;79(1):35-47.
255. Krashes MJ, DasGupta S, Vreede A, White B, Armstrong JD, Waddell S. A neural circuit mechanism integrating motivational state with memory expression in Drosophila. Cell. 2009;139(2):416-27.

256. Aso Y, Grubel K, Busch S, Friedrich AB, Siwanowicz I, Tanimoto H. The mushroom body of adult Drosophila characterized by GAL4 drivers. J Neurogenet. 2009;23(1-2):156-72.
257. Gouzi JY, Moressis A, Walker JA, Apostolopoulou AA, Palmer RH, Bernards A, et al. The receptor tyrosine kinase Alk controls neurofibromin functions in Drosophila growth and learning. PLoS Genet. 2011;7(9):e1002281.
258. Isabel G, Pascual A, Preat T. Exclusive consolidated memory phases in Drosophila. Science. 2004;304(5673):1024-7.
259. Yu D, Akalal DB, Davis RL. Drosophila alpha/beta mushroom body neurons form a branch-specific, long-term cellular memory trace after spaced olfactory conditioning. Neuron. 2006;52(5):845-55.
260. Li W MT, Tani T, Watanabe T, Kaibuchi K, Goshima G. Reconstitution of dynamic microtubules with Drosophila XMAP215, EB1, and Sentin. J Cell Biol. 2012 Nov 26.199(5):849-62.
261. Pielage J CL, Fetter RD, Carlton PM, Sedat JW, DavisGW A presynaptic giant ankyrin stabilizes the NMJ through regulation of presynaptic microtubules and transsynaptic cell adhesion. Neuron. 2008;58:195-209.
262. Hudson AM CL. A subset of dynamic actin rearrangements in Drosophila requires the Arp2/3 complex. J Cell Biol 2002;156:677- 68.
263. Higham JP MB, Buhl E, Dawson JM, Ogier AS, Lunnon K, Hodge JJL. Alzheimer's disease associated genes ankyrin and tau cause shortened lifespan and memory loss in drosophila. Frontiers in cellular neuroscience. 2019;13(260).
264. Skoulakis EM, Grammenoudi S. Dunces and da Vincis: the genetics of learning and memory in Drosophila. Cell Mol Life Sci. 2006;63(9):975-88.
265. Papanikolopoulou K GS, Samiotaki M, SkoulakisEMC. Differential effects of 14-3-3 dimers on tau phosphorylation, stability and toxicity in vivo. Hum Mol Gen 2018;27:2244 - 61.
266. Tan Y, Yu D, Busto GU, Wilson C, Davis RL. Wnt signaling is required for long-term memory formation. Cell Rep. 2013;4(6):1082-9.
267. Comas D PF, Preat T Drosophila long-term memory formation involves regulation of cathepsin activity. . Nature 2004;430:460-3.
268. Walkinshaw E GY, Farkas C, Richter D, Nicholas E, Keleman K, Davis RL. Identification of genes that promote or inhibit olfactory memory formation in drosophila. . Genetics 2015;199:1173-82.
269. Kanellopoulos AK, Semelidou O, Kotini AG, Anezaki M, EM. S. Learning and memory deficits consequent to reduction of the fragile X mental retardation protein result from metabotropic glutamate receptor-mediated inhibition of cAMP signaling in Drosophila. J Neurosci. 2012;19;32(38):13111-24.
270. Copf T GV, Lampin-Saint-Amaux A, Scaplehorn N, Preat T Cytokine signaling through the JAK/STAT pathway is required for longterm memory in Drosophila. . Proc Natl Acad Sci U S A 2011;108:8059-806.
271. Colomb J BB. PKC in motorneurons underlies self-learning, a form of motor learning in Drosophila. Peer J 2016;4:e1971.
272. Khan MR LL, Perez-Sanchez C, Saraf A, Florens L, Slaughter BD, Unruh JR, Si K Amyloidogenic oligomerization transforms Drosophila Orb2 from a translation repressor to an activator. Cell 2015;163:1468 -83.

273. Philip N, Acevedo S, Skoulakis EMC. Conditional rescue of olfactory learning and memory defects in mutants of the 14-3-3z gene leonardo. J Neuroscience. 2001;21:8417-25.
274. Iqbal K, Gong CX, Liu F. Hyperphosphorylation-induced tau oligomers. Front Neurol 2013;15(4):112.
275. Hou Q JH, Zhang X, Guo C, Huang B, Wang P, Wang T, Wu K, Li J, Gong Z, Du L, Liu Y, Liu L, Chen C Nitric oxide metabolism controlled by formaldehyde dehydrogenase (fdh, homolog of mammalian GSNOR) plays a crucial role in visual pattern memory in drosophila.Nitric Oxide 2011;24:17-24.
276. Horiuchi J YD, Naganos S, Aigaki T, Saitoe M Protein kinase A inhibits a consolidated form of memory in drosophila. . Proc Natl Acad Sci U S A 2008;105:20976 - 81.
277. Goodwin SF DVM, Velinzon K, Hogel C, Russell SR, Tully T, Kaiser K Defective learning in mutants of the Drosophila gene for a regulatory subunit of cAMP-dependent protein kinase. J Neurosci. 1997; 17:8817-27.
278. Saumweber T WlA, Hallermann S, Diegelmann S, Michels B, Bucher D, Funk N, Reisch D, Krohne G, Wegener S, Buchner E, Gerber B. Behavioral and synaptic plasticity are impaired upon lack of the synaptic protein SAP47. . J Neurosci 2011;31:3508 -18.
279. Godenschwege TA, Reisch D, Diegelmann S, Eberle K, Funk N, Heisenberg M, et al. Flies lacking all synapsins are unexpectedly healthy but are impaired in complex behaviour. . European Journal of Neuroscience. 2004;20:611-22.
280. J. H. Recurrent loops: incorporating prediction error and semantic/ episodic theories into Drosophila associative memory models. Genes Brain Behav 2019 2019:e12567.
281. Le Guennec K, Quenez O, Nicolas G, Wallon D, Rousseau S, Richard AC, et al. 17q21.31 duplication causes prominent tau-related dementia with increased MAPT expression. Mol Psychiatry. 2016;22(8):1119-25.
282. Qiang L SX, Austin TO, Muralidharan H, Jean DC, Liu M, Yu W, Baas PW. Tau Does Not Stabilize Axonal Microtubules but Rather Enables Them to Have Long Labile Domains. Curr Biol 2018; Jul 9;28(13):2181-9.
283. Hempen B, Brion JP. Reduction of acetylated alpha-tubulin immunoreactivity in neurofibrillary tangle-bearing neurons in Alzheimer's disease. J Neuropathol Exp Neurol. 1996;55(9):964-72.
284. Xiong Y, Zhao K, Wu J, Xu Z, Jin S, Zhang YQ. HDAC6 mutations rescue human tau-induced microtubule defects in Drosophila. Proc Natl Acad Sci U S A. 2013;110(12):4604-9.
285. Apicco DJ, Ash PEA, Maziuk B, LeBlang C, Medalla M, Al Abdullatif A, et al. Reducing the RNA binding protein TIA1 protects against tau-mediated neurodegeneration in vivo. Nat Neurosci. 2018;21(1):72-80.
286. Koren R BR, Shohat T, Cohen D, Mor O, Mendelson E, Lustig Y. Presence of Antibodies against Sindbis Virus in the Israeli Population: A Nationwide Cross-Sectional Study. Viruses. 2019 Jun 11;11(6).
287. Meier S, Bell M, Lyons DN, Rodriguez-Rivera J, Ingram A, Fontaine SN, et al. Pathological Tau Promotes Neuronal Damage by Impairing Ribosomal Function and Decreasing Protein Synthesis. J Neurosci. 2016;36(3):1001-7.

288. Piao YS, Hayashi S, Wakabayashi K, Kakita A, Aida I, Yamada M, et al. Cerebellar cortical tau pathology in progressive supranuclear palsy and corticobasal degeneration. Acta neuropathologica. 2002;103(5):469-74.
289. Evans HT BJ, van Roijen M, Bodea LG, Götz J. Decreased synthesis of ribosomal proteins in tauopathy revealed by non-canonical amino acid labelling. EMBO J 2019; Jul 1;38(13:e101174.)
290. Kanellopoulos AK, Semelidou O, Kotini AG, Anezaki M, Skoulakis EM. Learning and memory deficits consequent to reduction of the fragile X mental retardation protein result from metabotropic glutamate receptor-mediated inhibition of cAMP signaling in Drosophila. J Neurosci. 2012;32(38):13111-24.
291. Akalal DB WC, Zong L, Tanaka NK, Ito K, Davis RL. Roles for Drosophila mushroom body neurons in olfactory learning and memory. Learn Mem 2006 13:659-68.
292. Ahmed T, Van der Jeugd A, Blum D, Galas MC, D'Hooge R, Buee L, et al. Cognition and hippocampal synaptic plasticity in mice with a homozygous tau deletion. Neurobiol Aging. 2014;35(11):2474-8.
293. Jara C AA, Cerpa W, Tapia-Rojas C, Quintanilla RA Genetic ablation of tau improves mitochondrial function and cognitive abilities in the hippocampus. Redox Biol 2018;18:279 -94.
294. Chee F, Mudher A, Newman TA, Cuttle M, Lovestone S, Shepherd D. Overexpression of tau results in defective synaptic transmission in Drosophila neuromuscular junctions. Biochem Soc Trans. 2006;34(Pt 1):88-90.
295. Levin LR, Han P-L, Hwang PM, Feinstein PG, Davis RL, Reed RR. The *Drosophila* learning and memory gene, *rutabaga*, encodes a Ca^{2+}/calmodulin-responsive adenylyl cyclase. Cell,. 1992;68:479-89.
296. Busto GU, Cervantes-Sandoval I, Davis RL. Olfactory Learning in Drosophila. Physiology. 2010;25:338-46.
297. Davis RL, Cherry J, Dauwalder B, Han P-L, Skoulakis EMC. The Cyclic AMP system and Drosophila learning. Mol Cell Biochem. 1995;149/150:271-8.
298. Tomchik SM DR. Dynamics of learning-related cAMP signaling and stimulus integration in the Drosophila olfactory pathway. Neuron. 2009;Nov 25;64(4):510-21.
299. RL. D. Physiology and biochemistry of Drosophila learning mutants. Physiol Rev. 1996 Apr;76(2):299-317.
300. Suárez-Rama JJ AM, Sobrino B, Amigo J, Brenlla J, Agra S, Paz E, Brión M, Carracedo Á, Páramo M, Costas J. Resequencing and association analysis of coding regions at twenty candidate genes suggest a role for rare risk variation at AKAP9 and protective variation at NRXN1 in schizophrenia susceptibility. J Psychiatr Res 2015;Jul-Aug;66-67:38-44.
301. Wray NR PM, Blackwood DH, Penninx BW, Gordon SD, Nyholt DR, Ripke S, MacIntyre DJ, McGhee KA, Maclean AW, Smit JH, Hottenga JJ, Willemsen G, Middeldorp CM, de Geus EJ, Lewis CM, McGuffin P, Hickie IB, van den Oord EJ, Liu JZ, Macgregor S, McEvoy BP, Byrne EM, Medland SE, Statham DJ, Henders AK, Heath AC, Montgomery GW, Martin NG, Boomsma DI, Madden PA, Sullivan PF. Genome-wide association study of major depressive disorder: new results, meta-analysis, and lessons learned. Mol Psychiatry 2012;Jan;17(1):36-48.
302. MR. K. A method for the isolation of longevity mutants in the nematode Caenorhabditis elegans and initial results. Mechanisms of Ageing and Development 1983;22(3-4):279-86.

303. Kenyon C CJ, Gensch E, Rudner A, Tabtiang R. A C.elegans mutant that lives twice as long as wild type. Nature. 1993;366(6454):461-4.
304. Clancy DJ GD, Harshman LG, Oldham S, Stocker H,, Hafen E ea. Extension of life-span by loss of CHICO, a Drosophila insulin receptor substrate protein. Science. 2001;292(5514):104-6.
305. Lopez-Otin C BM, Partridge L, Serrano M, Kroemer G. The hallmarks of aging. . Cell. 2013;153(6):1194-217.
306. Bygren LO KG, Edvinsson S. Longevity determined by paternal ancestors' nutrition during their slow growth period. Acta Biotheoretica. 2001;49(1):53-9.
307. Pembrey ME BL, Kaati G, Edvinsson S, Northstone, K SM, et al. Sex-specific, male-line transgenerational responses in humans. European Journal of Human Genetics: EJHG 2006;14(2):159-66.
308. Rechavi O H-ZeL, Anava S, Goh WS, Kerk SY, Hannon GJ, et al. Starvation-induced transgenerational inheritance of small RNAs in C. elegans. Cell. 2014;158(2):277-87.
309. Bass TM GR, Wong R, Martinez P, Partridge L, Piper MD. Optimization of dietary restriction protocols in Drosophila. The Journals of Gerontology Series A, Biological Sciences and Medical Sciences 2007;62(10):1071-81.
310. Metaxakis A PL. Dietary restriction extends lifespan in wild-derived populations of Drosophila melanogaster. PloS One. 2013;8(9):e74681.
311. Aldrich JC MK. Transgenerational inheritance of diet-induced genome rearrangements in Drosophila. . PLoS Genetics. 2015;11(4):e1005148.
312. Bacalini MG FS, Olivieri F, Pirazzini C, Giuliani C, Capri M, et al. . Present and future of anti-ageing epigenetic diets. . Mechanisms of Ageing and Development. 2014;136-137:101-15.
313. Chouliaras L vdHD, Kenis G, Draanen M, Hof PR, van Os J, et al. Histone deacetylase 2 in the mouse hippocampus: Attenuation of age-related increase by caloric restriction.Current Alzheimer Research. 2013;10(8):868-76.
314. Carone BR FL, Habib N, Shea JM, Hart CE, Li R, et al. Paternally induced transgenerational environmental reprogramming of metabolic gene expression in mammals. Cell. 2010;143(7):1084-96.
315. DeChiara TM RE, Efstratiadis A. Parental imprinting of the mouse insulin-like growth factor II gene. Cell. 1991;64(4):849-59.
316. Colman RJ AR, Johnson SC, Kastman EK, Kosmatka KJ, Beasley TM, et al. Caloric restriction delays disease onset and mortality in rhesus monkeys. Science. 2009;325((5937):201-4.
317. Fontana L PL. Promoting health and longevity through diet: From model organisms to humans. Cell. 2015;161(1):106-18.
318. Nelson VR SS, Nadeau JH. Transgenerational genetic effects of the paternal Y chromosome on daughters' phenotypes. Epigenomics. 2010;2(4):513-21.
319. Friberg U SA, Rice WR. X- and Y-chromosome linked paternal effects on a life-history trait. . Biology Letters. 2012;8(1):71-3.
320. Lyko F RB, Jaenisch R. DNA methylation in Drosophila melanogaster. Nature 2000;408(6812):538-40.
321. Golic KG GM, Pimpinelli S. Imprinted control of gene activity in Drosophila. Current Biology: CB. 1998;8(23):1273-6.

322. Grandison RC WR, Bass TM, Partridge L, Piper MDW. Effect of a standardised dietary restriction protocol on multiple laboratory strains of drosophila melanogaster. PloS One. 2009;4(1):e4067.
323. Spencer CC HC, Wright AR, Promislow DEL. Testing an 'aging gene' in long-lived Drosophila strains: Increased longevity depends on sex and genetic background. Aging Cell. 2003;2(2):123-30.
324. Lemos B AL, Hartl DL. Polymorphic Y chromosomes harbor cryptic variation with manifold functional consequences. . Science 2008;319(5859):91-3.
325. Greer EL MT, Ucar D, Hauswirth AG, Mancini E, Lim JP, et al. Transgenerational epigenetic inheritance of longevity in Caenorhabditis elegans. Nature. 2011;479((7373):365-71.
326. Hallberg B PR. Mechanistic insight into ALK receptor tyrosine kinase in human cancer biology. . Nat Rev Cancer 2013;13:685-700.
327. Guan J UG, Yamazaki Y, Wolfstetter G, Mendoza P, Pfeifer K,, Mohammed A HF, Zhang H, Hsu AW, Halenbeck R, Hallberg B,, RH P. FAM150A and FAM150B are activating ligands for anaplastic lymphoma kinase. Elife 2015;4(e09811).
328. Reshetnyak AV MP, Shi X, Mo ES, Mohanty J, Tome F, Bai H, Gunel, M LI, Schlessinger J Augmentor α and β (FAM150) are ligands of the receptor tyrosine kinases ALK and LTK: hierarchy and specificity of ligand-receptor interactions. Proc Natl Acad Sci U S A 2015;112 15862-7.
329. Loren CE SA, Grabbe C, Edeen PT, Thomas J, McKeown M, Hunter T, Palmer RH. Identification and characterization of DAlk: a novel Drosophila melanogaster RTK which drives ERK activation in vivo. . Genes Cells 2001;6:531-44.
330. Lasek AW LJ, Kliethermes CL, Berger KH, Joslyn G, Brush G, Xue L, Robertson M, Moore MS, Vranizan K, Morris SW, Schuckit MA, White RL, Heberlein U An evolutionary conserved role for anaplastic lymphoma kinase in behavioral responses to ethanol. PloS one. 2011;6:e22636.
331. Bai L SA. Anaplastic lymphoma kinase acts in the Drosophila mushroom body to negatively regulate sleep. PLoS Genet 2015;11:e1005611.
332. Weiss JB XC, Benice T, Xue L, Morris SW, Raber J Anaplastic lymphoma kinase and leukocyte tyrosine kinase: functions and genetic interactions in learning, memory and adult neurogenesis. . Pharmacol Biochem Behav 2012;100:566 -74.
333. de Belle JS HM. Associative odor learning in Drosophila abolished by chemical ablation of mushroom bodies. Science 1994;263:692-5.
334. Joiner WJ CA, White BH, Sehgal A Sleep in Drosophila is regulated by adult mushroom bodies. Nature. 2006;441:757-60.
335. Pitman JL MJ, Keegan KP, Allada R A dynamic role for the mushroom bodies in promoting sleep in Drosophila. . Nature 2006;441:753-6.
336. King I TL, Pflanz R, Voigt A, Lee S, Jackle H, Lu B, Heberlein U . Drosophila tao controls mushroom body development and ethanol stimulated behavior through par-1. J Neurosci 2011;31:1139 -48.
337. Tully T PT, Boynton SC, Del Vecchio M Genetic dissection of consolidated memory in Drosophila. Cell 7. 1994;9:35- 47.
338. Loren CE EC, Grabbe C, Hallberg B, Hunter T, PalmerRH A crucial role for the anaplastic lymphoma kinase receptor tyrosine kinase in gut development in Drosophila melanogaster. EMBO 2003;Rep 4:781-6.

339. Englund C LnC, Grabbe C, Varshney GK, Deleuil F, Hallberg B, Palmer, RH. Jeb signals through the alk receptor tyrosine kinase to drive visceral muscle fusion. . Nature. 2003;425:512-6.
340. McGuire SE MZ, Davis RL Spatiotemporal gene expression targeting with theTARGETand gene-switch systems in Drosophila. Sci STKE. 2004;2004:pl6.
341. Isabel G PA, Preat T. Exclusive consolidated memory phases in Drosophila. Science 2004;304:1024 -7.
342. Galkin AV MJ, Kim S, Hood TL, Li N, Li L, Xia G, Steensma R,, Chopiuk G JJ, Wan Y, Ding P, Liu Y, Sun F, Schultz PG, Gray NS,, M W. Identification of NVP-TAE684, a potent, selective, and efficacious inhibitor of NPM-ALK. . Proc Natl Acad Sci U S A 2007;104:270-5.
343. Englund C LnC, Grabbe C, Varshney GK, Deleuil F, Hallberg B, Palmer RH Jeb signals through the alk receptor tyrosine kinase to drive visceral muscle fusion. Nature 2003;425:512-6.
344. Liu X KW, Davis RL GABAA receptor RDL inhibits Drosophila olfactory associative learning. . Neuron 2007;56:1090 -102.
345. Pavlopoulos E AM, Skoulakis EM Neuralized is expressed in the alpha/beta lobes of adult Drosophila mushroom bodies and facilitates olfactory long-term memory formation. Proc Natl Acad Sci U S A. 2008;105.14674-9.
346. Knapek S SS, Tanimoto H. Bruchpilot, a synaptic active zone protein for anesthesia-resistant memory. J Neurosci 2011;31:3453-8.
347. Bouzaiane E TS, Scheunemann L, Plac¸ais PY, Preat T Two independent mushroom body output circuits retrieve the six discrete components of Drosophila aversive memory. Cell Rep 2015;11:1280 -92.
348. Berry JA C-SI, Nicholas EP, Davis RL Dopamine is required for learning and forgetting in Drosophila. Neuron 2012;74:530 -42.
349. Leiss F GC, Butcher NJ, Meinertzhagen IA, Tavosanis G Synaptic organization in the adult Drosophila mushroom body calyx. J Comp Neurol 2009;517:808-24.
350. Steward O SE. Protein synthesis at synaptic sites on dendrites. Annu Rev Neurosci 2001;24:299 -325.
351. Ashraf SI MA, Sclarsic SM, Kunes S Synaptic protein synthesis associated with memory is regulated by the RISC pathway in Drosophila. Cell 2006;124(191-205.).
352. Lewis BP BC, BartelDP Conserved seed pairing, often flanked by adenosines, indicates that thousands of human genes are microRNA targets. Cell. 2005; 120:15-20.
353. Paz I KI, Ares M Jr, Cline M, Mandel-Gutfreund Y RBPmap: a web server for mapping binding sites of RNA-binding proteins. Nucleic Acids Res. 2014; 42:W361-W7.
354. JT W. The psychology and neuroscience of forgetting. Annu Rev Psychol 2004;55:235-69.
355. Dewar MT CN, Sala SD. Forgetting due to retroactive interference: a fusion of Muller and Pilzecker's (1900) early insights into everyday forgetting and recent research on anterograde amnesia. Cortex 2007;43:616-34.
356. Davis RL ZY. The biology of forgetting: a perspective. Neuron 2017;95:490 -503.
357. Shuai Y LB, Hu Y, Wang L, Sun K, Zhong Y Forgetting is regulated through rac activity in Drosophila. Cell 2010;140:579 -89.
358. Walkinshaw E GY, Farkas C, Richter D, Nicholas E, Keleman K, Davis, RL. Identification of genes that promote or inhibit olfactory memory formation in Drosophila. Genetics 2015;199:1173-82.

359. Lee YS SA. The molecular and cellular biology of enhanced cognition. Nat Rev Neurosci 2009;10:126 -40.
360. Placais PY dTE, Scheunemann L, Trannoy S, Goguel V, Han KA,, Isabel G PT. Upregulated energy metabolism in the Drosophila mushroom body is the trigger for long-term memory. Nat Commun. 2017;8:15510.
361. Busto GU G-OT, Fulga TA, Van Vactor D, Davis RL. microRNAs that promote or inhibit memory formation in Drosophila melanogaster. Genetics. 2015; 200:569 -80.
362. Li W CM, Qin H, Fulga T, Van Vactor D, Dubnau J MicroRNA-276a functions in ellipsoid body and mushroom body neurons for naive and conditioned olfactory avoidance in Drosophila. J Neurosci 2013;33:5821-33.
363. Nagappan G LB. Activity-dependent modulation of the BDNF receptor TrkB: mechanisms and implications. . Trends Neurosci. 2005; 28:464-71.
364. Keleman K KtS, Alenius M, Dickson BJ Function of the Drosophila CPEB protein Orb2 in long-term courtship memory. Nat Neurosci 2007;10:1587-93.
365. Moog-Lutz C DJ, Gouzi JY, Frobert Y, Brunet-de Carvalho N, Bureau J,mCreminon C, VignyM Activation and inhibition of anaplastic lymphoma kinase receptor tyrosine kinase by monoclonal antibodies and absence of agonist activity of pleiotrophin. J Biol Chem 2005;280:26039-48.
366. Lemmon MA SJ. Cell signaling by receptor tyrosine kinases. Cell 2010;141:1117-34.
367. Buchanan ME DR. A distinct set of Drosophila brain neurons required for neurofibromatosis type 1-dependent learning and memory. J Neurosci 2010;30:10135-43.

Behavioral/Cognitive

Drosophila Bruton's Tyrosine Kinase Regulates Habituation Latency and Facilitation in Distinct Mushroom Body Neurons

Ilianna G. Roussou,[1,2] Katerina Papanikolopoulou,[1] Charalambos Savakis,[1,2] and Efthimios M. C. Skoulakis[1]
[1]Institute for Fundamental Biomedical Research, Biomedical Science Research Centre "Alexander Fleming," Vari 16672, Greece, and [2]School of Medicine, University of Crete, Heraklion, 71003, Greece

Habituation is the adaptive behavioral outcome of processes engaged in timely devaluation of non-reinforced repetitive stimuli, but the neuronal circuits and molecular mechanisms that underlie them are not well understood. To gain insights into these processes we developed and characterized a habituation assay to repetitive footshocks in mixed sex *Drosophila* groups and demonstrated that acute neurotransmission from adult α/β mushroom body (MB) neurons prevents premature stimulus devaluation. Herein we demonstrate that activity of the non-receptor tyrosine kinase dBtk protein is required within these neurons to prevent premature habituation. Significantly, we also demonstrate that the complementary process of timely habituation to the repetitive stimulation is facilitated by α'/β' MB neurons and also requires dBtk activity. Hence our results provide initial insights into molecular mechanisms engaged in footshock habituation within distinct MB neurons. Importantly, dBtk attenuation specifically within α'/β' neurons leads to defective habituation, which is readily reversible by administration of the antipsychotics clozapine and risperidone suggesting that the loss of the kinase may dysregulate monoamine receptors within these neurons, whose activity underlies the failure to habituate.

Key words: antipsychotics; Btk; *Drosophila*; habituation; mushroom bodies

Significance Statement

Habituation refers to processes underlying decisions to attend or ignore stimuli, which are pivotal to brain function as they underlie selective attention and learning, but the circuits involved and the molecular mechanisms engaged by the process therein are poorly understood. We demonstrate that habituation to repetitive footshock involves two phases mediated by distinct neurons of the *Drosophila* mushroom bodies and require the function of the dBtk non-receptor tyrosine kinase. Moreover, habituation failure upon dBtk abrogation in neurons where it is required to facilitate the process is readily reversible by antipsychotics, providing conceptual links to particular symptoms of schizophrenia in humans, also characterized by habituation defects and ameliorated by these pharmaceuticals.

Introduction

Habituation is a form of adaptive behavioral plasticity that permits animals to ignore repetitive or prolonged non-reinforced stimuli (Thompson and Spencer, 1966; Rankin et al., 2009). Timely devaluation of such stimuli is the behavioral output of largely undefined molecular processes, apparently engaging multiple cellular systems (Ramaswami, 2014). Because habituation underlies gated selective attention and discrimination between novel and pre-experienced stimuli (Gillberg, 2003), it represents a form of adaptive behavioral flexibility, reported defective in patients with migraines (Siniatchkin et al., 2003; Kalita et al.,

Received March 20, 2019; revised Aug. 19, 2019; accepted Aug. 21, 2019.

Author contributions: E.M.C.S. and I.G.R. designed research; I.G.R. and K.P. performed research; C.S. contributed unpublished reagents/analytic tools; I.G.R. and E.M.C.S. analyzed data; I.G.R., K.P., C.S., and E.M.C.S. wrote the paper.

This work was co-financed by the European Union (European Social Fund) and Greek national funds through the Operational Program "Education and Lifelong Learning" of the National Strategic Reference Framework 2007–2013, Research Funding Program: THALES- Investing in Knowledge Society through the European Social Fund, Project: "THALES–BSRC 'Alexander Fleming'–Development and employment of Minos-based genetic and functional genomic technologies in model organisms (MINOS)"–MIS: 376898; and by the project "Strategic Development of the Biomedical Research Institute 'Alexander Fleming'" (MIS 5002562), which is implemented under the "Action for the Strategic Development on the Research and Technological Sector", funded by the Operational Programme "Competitiveness, Entrepreneurship and Innovation" (NSRF 2014-2020) and co-financed by Greece and the European Union (European Regional Development Fund); and partly by Fondation Sante. We thank the Bloomington Drosophila Stock Center for strains and resources, Daisuke Yamamoto for mutant strains, Flybase for essential information, and Dr. A. Kanellopoulos for performing pilot experiments indicating that Btk mutants failed to habituate.

The authors declare no competing financial interests.

Correspondence should be addressed to Efthimios M. C. Skoulakis at skoulakis@fleming.gr.

https://doi.org/10.1523/JNEUROSCI.0633-19.2019

2014), attention deficit hyperactivity disorder (Jansiewicz et al., 2004; Massa and O'Desky, 2012), schizophrenia (SD; Braff et al., 2001; Meincke et al., 2004) and autism spectrum disorders (ASD; D'Cruz et al., 2013; Tei et al., 2018). Hence, defining molecular mechanisms that govern habituation is likely to contribute toward understanding the molecular etiology of these conditions.

To explore habituation mechanisms of CNS circuits in *Drosophila*, we developed a novel habituation paradigm to repetitive mild electric footshock (Acevedo et al., 2007). Habituation to repetitive footshock requires structurally and functionally intact mushroom bodies (MBs), neurons also essential for associative learning and memory (Guven-Ozkan and Davis, 2014). The MBs are comprised by ~2000 neurons per hemisphere subdivided into α/β, α'/β' and γ subtypes (Crittenden et al., 1998). Because neurotransmission from α/β MB neurons is required to suppress premature habituation, we proposed that physiologically, it blocks devaluation of the repetitive footshock stimuli, hence required for habituation latency (Acevedo et al., 2007). However, whether other intrinsic or extrinsic MB neurons are required to facilitate habituation remained unclear.

To address this question and to identify proteins governing habituation within the MBs, we have conducted a genetic screen for mutants that present defective habituation. Here we report on the role of one of the proteins identified in the screen, Bruton's tyrosine kinase (dBtk), which belongs to the Src non-receptor kinase superfamily and is associated with agammaglobulinemia in humans (Mattsson et al., 1996). The *Drosophila dBtk29A* (dBtk) gene encodes two proteins by alternative splicing, dBtk type 1 and dBtk type 2, with the latter considered orthologous to the human protein (Gregory et al., 1987). dBtk consists of conserved SH2, SH3 and kinase domains, whereas an N-terminal plekstrin homology (PH) domain characterizes the larger type 2 protein (Tsikala et al., 2014). dBtk is implicated in many essential functions in *Drosophila* (Gregory et al., 1987; Roulier et al., 1998; Baba et al., 1999; Hamada-Kawaguchi and Yamamoto, 2017), including regulation of the actin cytoskeleton (Tsikala et al., 2014). Although dBtk is highly expressed in the fly CNS, there is limited information regarding its functional role(s) therein (Asztalos et al., 2007; Sunouchi et al., 2016). Here we demonstrate acute differential roles for this kinase within distinct MB neuronal populations in the regulation of habituation dynamics to repeated footshock stimuli.

Materials and Methods

Drosophila *culture and strains*

Drosophila were cultured in standard wheat-flour-sugar food supplemented with soy flour and $CaCl_2$ (Acevedo et al., 2007) at 18°C or 25°C. All MiMIC insertions were from the Bloomington Stock Center (BDRC; Indiana University; Venken et al., 2011) and they were backcrossed to y^1w^1 for at least seven generations before use in behavioral experiments. MBGal80 (Krashes et al., 2007) was obtained from Ron Davis (Scripps Florida). The Btk-Gal4 (49182), dncGal4 (48571), and Btk RNAi stocks (35159 and 25791) were from BDRC. To generate the driver heterozygote controls for experiments with the RNAi-encoding transgenes, driver-bearing strains were crossed to their y^1v^1 (BDSC, 36303) background. The UAS-Btk lines (109-093 and 109-095) were from the Kyoto Stock Center (Kyoto Institute of Technology). VT44966-Gal4 (γ-driver) was from the Vienna *Drosophila* Resource Center (VDRC; Vienna Biocenter Core Facilities, 203571). The α'/β' Gal4 drivers VT030604 (VDRC, 200228) and c305a were a kind gift from S. Waddell (University of Oxford). The glial driver repo-Gal4, the pan-neuronal drivers elav-Gal4 and Ras2Gal4, and the mushroom body specific drivers 247-Gal4, leo-Gal4, c739-Gal4, c772-Gal4 were described previously (Aso et al., 2009; Gouzi et al., 2018). The Gal80^{ts} transgene was added to the driver-bearing chromosomes by recombination or standard crosses as indicated.

Description of Gal4 expression patterns used in this work.

Elav: pan-neuronal expression in all developmental stages (FlyBase ID: FBrf0237128)

Ras2: throughout the larval and adult CNS, enriched in the adult MBs (Gouzi et al., 2011)

repo: all glia (FlyBase ID: FBrf0237128)

leo: adult α, α', β, β', γ MB neurons (Messaritou et al., 2009)

247: adult α, α', β, β', γ MB neurons (RRID:BDSC_50742)

dnc: adult α, α', β, β', γ MB neurons, scattered neurons in subesophageal ganglion and ventral optic lobes (Gai et al., 2016)

c772: adult α, β, γ MB neurons, antennal lobe, medulla, tritocerebrum (Aso et al., 2009)

c739: adult α, β MB neurons, antennal lobe, medulla, restricted protocerebral neurons, inferior neuropils (Aso et al., 2009).

VT44966: γ MB neurons, wedge neurons, superior lateral protocerebrum, gnathal neurons, medial bundle (Shyu et al., 2017)

c305a: adult α', β' MB neurons, antennal nerve, medulla, restricted protocerebral neurons, inferior neuropil, gnathal neurons (Aso et al., 2009)

VT030604: adult α', β' MB neurons, gnathal neurons (Shyu et al., 2017)

Behavioral assays

All flies used in behavioral experiments were tested 3–5 d after emergence. All experiments were performed under dim red light at 25°C and 65–75% relative humidity. To obtain animals for behavioral experiments Gal4 driver homozygotes were crossed *en masse* to strains carrying either UAS-btk, UAS-btk-RNAi, or UAS-shi^{ts} transgenes. Animals expressing Gal80^{ts} (McGuire et al., 2003) were raised at 18°C until hatching and then placed at 30°C for 2 d before testing. Flies carrying UAS-shi^{ts} were reared at 18°C and the dynamin was inactivated by incubation at 32°C for 30 min before the behavioral experiment.

Electric footshock avoidance. Experiments were performed as described before (Acevedo et al., 2007). Briefly, ~70 flies were placed at the choice point of a T-maze to choose for 90 s between an electrified and an otherwise identical inert standard copper grid. In the electrified grid, 45 V shocks were delivered every 5.15 s, each lasting 1.2 s. The avoiding fraction (AF) was calculated by dividing the number of flies avoiding the shock by the total number of flies.

Habituation to electric footshock. Habituation to electric shock experiments were performed as described before (Acevedo et al., 2007). Briefly, for the training phase ~70 flies were sequestered in the upper arm of a standard T-maze lined with an electrifiable grid. They were exposed to 15 1.2 s electric shocks at 45 V with a 5.15 s interstimulus interval. Air was not drawn through the tube during training to avoid association of the shocks with air. After a 30 s rest and 30 s for transfer to the lower part of the maze, the flies were tested by choosing between an electrified and an inert grid. Therefore, the earliest measures of post-training responses are 1 min after the flies received the last training stimulus. Testing was performed at the same voltage (45 V) as for training. During the 90 s choice period, 17–18 1.2 s stimuli were delivered to the electrified arm of the maze. At the end of the choice period, the flies in each arm were trapped and counted, and the habituation fraction (HF) was calculated by dividing the number of flies preferring the shock by the total number of flies, as above. Finally, the habituation index (HI) was calculated as $(HF - AF) \times 100\%$ and therefore represents the change in footshock avoidance contingent upon prior footshock experience (habituation). Although the absolute avoidance score is variable, even for the same genotypes (Table 1), as expected for behavioral experiments performed over a significant time period, because the HI measures the relative change in avoidance within each genotype, it is not affected by such variability. In fact, failure to habituate, which is the primary phenotype reported herein, is a manifestation of maintained avoidance relative to that of naive flies of the same genotype.

Dishabituation. To distinguish habituation from fatigue or sensory adaptation, flies were dishabituated post-training with an 8 s puff [yeast odor (YO)] of air drawn at 500 ml/min over a 30% (w/v) aqueous solution of Brewer's yeast (Acros Organics) and then were submitted to testing.

Table 1. Collective avoidance indices and statistics

Genotype	Mean ± SEM	*t* Ratio	*p*
Fig. 1*C*. ANOVA: $F_{(2,58)} = 1.6020, p = 0.2106$			
c (control)	0.76 ± 0.03		
$btk^{M1}/+$	0.77 ± 0.05	0.106	0.9158
btk^{M1}/btk^{M1}	0.66 ± 0.07	1.5444	0.1281
Fig. 1*D*. ANOVA: $F_{(5,68)} = 0.8807, p = 0.4993$			
c (control)	0.61 ± 0.02		
$btk^{M2/M2}$	0.62 ± 0.04	−0.007	0.9945
$btk^{M1/M1}$	0.59 ± 0.05	0.4748	0.6365
$btk^{M1/ML}$	0.55 ± 0.05	1.0243	0.310
$btk^{M2/ML}$	0.53 ± 0.05	1.4211	0.1602
$btk^{ML}/+$	0.63 ± 0.03	−0.192	0.848
Fig. 1*E*. ANOVA: $F_{(3,60)} = 0.8603, p = 0.4670$			
0 μM	0.53 ± 0.03		
0.1 μM	0.49 ± 0.03	1.2032	0.2339
1 μM	0.55 ± 0.03	−0.291	0.7722
10 μM	0.49 ± 0.04	0.9707	0.3358
Fig. 1*F*. ANOVA: $F_{(3,62)} = 1.9514, p = 0.1312$			
c (control)	0.54 ± 0.04		
$btk^{M1/M1}$	0.67 ± 0.05	−1.737	0.0877
$btk^{M2/M2}$	0.51 ± 0.06	0.3651	0.7163
$btk^{ML}/+$	0.62 ± 0.06	−1.031	0.3066
Fig. 2*A*. ANOVA: $F_{(2,44)} = 1.3353, p = 0.2740$			
elavGAL4/+;UAS-btk^{RNA1}/$GAL80^{ts}$	0.59 ± 0.05		
elavGAL4/+;$GAL80^{ts}$/+	0.61 ± 0.04	−0.237	0.8139
UASbtk^{RNAi1}/+	0.49 ± 0.07	1.3101	0.1973
Fig. 2*B*. ANOVA: $F_{(2,35)} = 2.0785, p = 0.1412$			
elavGAL4/+;UAS-btk^{RNAi2}/$GAL80^{ts}$	0.66 ± 0.04		
elavGAL4/+;$GAL80^{ts}$/+	0.72 ± 0.03	−1.105	0.2771
UASbtk^{RNAi2}/+	0.78 ± 0.03	−2.006	0.0531
Fig. 2*C*. ANOVA: $F_{(2,30)} = 1.100\ p = 0.3468$			
elavGAL4/+;UAS-btk^{RNAi1}/$GAL80^{ts}$	0.73 ± 0.05		
elavGAL4/+;$GAL80^{ts}$/+	0.63 ± 0.03	1.4796	1.1502
UASbtk^{RNAi-1}/+	0.68 ± 0.05	0.7939	0.4340
Fig. 2*D*. ANOVA: $F_{(2,27)} = 0.1719, p = 0.8431$			
Ras2GAL4,$GAL80^{ts}$/+; UASbtk^{RNAi1}	0.67 ± 0.08		
Ras2GAL4, $GAL80^{ts}$/+	0.65 ± 0.05	0.1811	0.8578
UASBTK^{RNAi1}/+	0.70 ± 0.04	−0.386	0.703
Fig. 2*E*. ANOVA: $F_{(2,46)} = 2.1609, p = 0.1273$			
repoGAL4,$GAL80^{ts}$/UAS-btk^{RNAi1}	0.63 ± 0.05		
repoGAL4,$GAL80^{ts}$/+	0.73 ± 0.03	−2.075	0.044
UASbtk^{RNAi1}/+	0.67 ± 0.03	−0.955	0.3449
Fig. 2*F*. ANOVA: $F_{(2,47)} = 3.2093, p = 0.0498$			
elavGAL4/+;MBG80,$GAL80^{ts}$/UASbtk^{RNAi1}	0.71 ± 0.02		
elavGAL4/+; MBG80, $GAL80^{ts}$/+	0.63 ± 0.02	2.2266	0.031
UASbtk^{RNAi1}/+	0.71 ± 0.03	−0.085	0.932
Fig. 3*A*. ANOVA: $F_{(2,34)} = 0.5313, p = 0.5929$			
leoMBGAL4,$GAL80^{ts}$;UAS-btk^{RNAi1}/+	0.46 ± 0.09		
leoMB-GAL4, $GAL80^{ts}$/+	0.56 ± 0.07	−0.905	0.3723
UAS-btk^{RNAi1}/+	0.56 ± 0.07	−0.892	0.3788
Fig. 3*B*. ANOVA: $F_{(5,66)} = 2.7712, p = 0.0255$			
leoMBGAL4,btk^{M1}/+; GAL80ts/+ UN	0.65 ± 0.03		
leoMBGAL4,btk^{M1}/ btk^{M1}; GAL80ts/+ UN	0.50 ± 0.03	2.205	0.031
leoMBGAL4,btk^{M1}/ btk^{M1};GAL80ts,UASbtk^{S} UN	0.59 ± 0.05	0.9337	0.3541
leoMBGAL4,btk^{M1}/+; GAL80ts/+ IN	0.56 ± 0.04		
leoMBGAL4,btk^{M1}/ btk^{M1}; GAL80ts/+ IN	0.45 ± 0.04	−1.265	0.211
leoMBGAL4,btk^{M1}/btk^{M1};GAL80ts,UASbtk^{S} IN	0.62 ± 0.04	−0.914	0.364
Fig. 3*C*. ANOVA: $F_{(2,39)} = 0.5892, p = 0.5599$			
leoMBGAL4/+;UASbtk^{RNAi2}/$GAL80^{ts}$	0.65 ± 0.05		
leoMBGAL4/+;$GAL80^{ts}$/+	0.68 ± 0.03	−0.471	0.640
UAS-btk^{RNAi2}/+	0.61 ± 0.06	0.6403	0.5260
Fig. 3*D*. ANOVA: $F_{(2,42)} = 0.4747, p = 0.6256$			
247MBGAL4,$GAL80^{ts}$/UAS-btk^{RNAi1}	0.63 ± 0.03		
247MBGAL4,$GAL80^{ts}$/+	0.60 ± 0.02	0.9688	0.3385
UASbtk^{RNAi1}/+	0.61 ± 0.03	0.5817	0.5640

(*Table continues.*)

Table 1. Continued

Genotype	Mean ± SEM	*t* Ratio	*p*
Fig. 3*E*. ANOVA: $F_{(2,30)} = 0.2194, p = 0.8044$			
dncGAL4,$GAL80^{ts}$/ UASbtk^{RNAi1}	0.53 ± 0.02		
dncGAL4,$GAL80^{ts}$/+	0.51 ± 0.02	0.4624	0.6474
UASbtk^{RNAi1}/+	0.54 ± 0.03	−0.198	0.8443
Fig. 3F. ANOVA: $F_{(2,44)} = 1.1638, p = 0.3222$			
c772GAL4,$GAL80^{ts}$/ UASbtk^{RNAi1}	0.63 ± 0.03		
c772GAL4,$GAL80^{ts}$/+	0.54 ± 0.06	1.451	0.1542
UASbtk^{RNAi1}/+	0.57 ± 0.03	1.1173	0.2702
Fig. 3*G*. ANOVA: $F_{(2,43)} = 1.891, p = 0.1766$			
UASbtk^{RNAi-1}/c739GAL4,$GAL80^{ts}$	0.57 ± 0.05		
c739GAL4,$GAL80^{ts}$/+	0.46 ± 0.04	1.8657	0.0692
UASbtk^{RNAi1}/+	0.53 ± 0.04	0.6998	0.488
Fig. 3*H*. ANOVA: $F_{(2,47)} = 3.0762, p = 0.0559$			
γ lobeGAL4/+;UASbtk^{RNAi1}/$GAL80^{ts}$	0.58 ± 0.03		
γ lobe GAL4/+;$GAL80^{ts}$/+	0.49 ± 0.03	2.0924	0.0421
UASbtk^{RNAi1}/+	0.59 ± 0.03	−0.238	0.8133
Fig. 3*I*. ANOVA: $F_{(2,28)} = 1.0786, p = 0.3548$			
c305aGAL4/+;UASbtk^{RNAi1}/$GAL80^{ts}$	0.77 ± 0.03		
c305a GAL4/+;$GAL80^{ts}$/+	0.71 ± 0.02	1.3002	0.2049
UASbtk^{RNAi1}/+	0.77 ± 0.04	0.0361	0.9715
Fig. 3*J*. ANOVA: $F_{(2,49)} = 2.5477, p = 0.0156$			
VT030604GAL4/+, UASbtk^{RNAi1} 18°C	0.74 ± 0.03		
VT030604GAL4/+, UASbtk^{RNAi1} 25°C	0.67 ± 0.02	1.9623	0.0557
VT030604-GAL4/+, UAS-btk^{RNAi1} 18 > 30°C	0.78 ± 0.03	−0.972	0.3361
Fig. 3*K*. ANOVA: $F_{(1,25)} = 9.7589, p = 0.0046$			
c305aGAL4-UAS shi^{ts} UN	0.85 ± 0.03		
c305aGAL4-UAS shi^{ts} IN	0.75 ± 0.01	−3.124	**0.0046**
Fig. 4*A*. ANOVA: $F_{(5,104)} = 4.7413, p = 0.0006$			
control 6 sh	0.79 ± 0.04		
$btk^{M1/M1}$ 6 sh	0.63 ± 0.04	2.9535	**0.0039**
control 10 sh	0.69 ± 0.03		
$btk^{M1/M1}$ 10 sh	0.60 ± 0.04	1.6587	0.1003
control 15 sh	0.73 ± 0.02		
$btk^{M1/M1}$ 15 sh	0.58 ± 0.04	2.9818	**0.0036**
Fig. 4*B*. ANOVA: $F_{(8,156)} = 2.8880, p = 0.0051$			
UASbtk^{RNAi1}/elavGAL4;$GAL80^{ts}$ 6 sh	0.82 ± 0.02		
elavGAL4;$GAL80^{ts}$/+ 6 sh	0.66 ± 0.03	3.7031	**0.0003**
UAS-btk^{RNAi-1}/+ 6 sh	0.71 ± 0.04	2.5227	0.0127
UASbtk^{RNAi1}/elavGAL4;$GAL80^{ts}$ 10 sh	0.77 ± 0.02		
elavGAL4;$GAL80^{ts}$/+ 10 sh	0.66 ± 0.03	2.2533	0.0257
UAS btk^{RNAi1}/+ 10 sh	0.66 ± 0.06	2.0069	0.0466
UASbtk^{RNAi1}/elavGAL4;$GAL80^{ts}$ 15 sh	0.73 ± 0.04		
elavGAL4;$GAL80^{ts}$/+ 15 sh	0.74 ± 0.03	−0.171	0.8644
UASbtk^{RNAi-1}/+ 15 sh	0.70 ± 0.03	0.6554	0.5132
Fig. 4*C*. ANOVA: $F_{(2,28)} = 1.2620, p = 0.2999$			
0 μM	0.58 ± 0.05		
0.1 μM	0.64 ± 0.04	−0.832	0.4129
1 μM	0.68 ± 0.04	−1.588	0.1245
Fig. 4*D*. ANOVA: $F_{(2,30)} = 0.0147, p = 0.9854$			
Habituation,15 shocks	0.76 ± 0.02		
Y0 dishabituation	0.77 ± 0.02	−0.147	0.8839
AVD after yeast puff	0.77 ± 0.02	−0.147	0.8839
Fig. 4*E*. ANOVA: $F_{(2,30)} = 0.0147, p = 0.9854$			
$btk^{M1/M1}$ habituation 6 sh	0.68 ± 0.03		
$btk^{M1/M1}$ Dishabituation 6 sh	0.68 ± 0.03	0	1
$btk^{M1/M1}$ habituation 10 sh	0.73 ± 0.04		
$btk^{M1/M1}$ Dishabituation 10 sh	0.73 ± 0.03	0.0617	0.9511
$btk^{M1/M1}$ AVD after yeast puff	0.73 ± 0.04	−1.102	0.2772
Fig. 5*A*. ANOVA: $F_{(5,119)} = 3.8885\ p = 0.0027$			
leoGAL4/+;UASbtk^{RNAi1}/$GAL80^{ts}$ UN 6 sh	0.81 ± 0.02		
leoMBGAL4/+; UASbtk^{RNAi1}/$GAL80^{ts}$ IN 6 sh	0.78 ± 0.02	1.2528	0.2128
leoMBGAL4/+; UASbtk^{RNAi1}/$GAL80^{ts}$ IN 10 sh	0.82 ± 0.01		
leoMBGAL4/+; UASbtk^{RNAi1}/$GAL80^{ts}$ UN 10 sh	0.75 ± 0.02	3.053	**0.0052**
leoMBGAL4/+; UASbtk^{RNAi1}/$GAL80^{ts}$ IN 15 sh	0.82 ± 0.01		
leoMB-GAL4/+; UASbtk^{RNAi1}/$GAL80^{ts}$ UN 15 sh	0.75 ± 0.02	3.053	**0.0028**

(*Table continues.*)

Table 1. Continued

Genotype	Mean ± SEM	*t* Ratio	*p*
Fig. 5*B*. ANOVA: $F_{(5,77)} = 0.2798$, $p = 0.9227$			
leoG4,btk ^{M1}/btk ^{M1},G80ts,UAS*btk* ^{S} UN 6 sh	0.69 ± 0.03		
leoG4,btk ^{M1}/btk ^{M1},G80ts, UAS*btk* ^{S} *IN 6 sh*	0.71 ± 0.03	−0.391	0.6966
leoG4,btk ^{M1}/btk ^{M1},G80ts,UAS-btk ^{S} UN 10 sh	0.69 ± 0.03		
leoG4,btk ^{M1}/btk ^{M1},G80ts,UAS-btk ^{S} IN 10 sh	0.72 ± 0.03	−0.759	0.4505
leoG4,btk ^{M1}/btk ^{M1},G80ts,UAS-btk ^{S} UN 15 sh	0.69 ± 0.03		
leoG4,btk ^{M1}/btk ^{M1},G80ts,UAS-btk ^{S} IN 15 sh	0.72 ± 0.03	−0.759	0.4505
Fig. 5*C*. ANOVA: $F_{(5,77)} = 1.1341$, $p = 0.3503$			
UAS-*btk*^{RNAi1}/*c739-GAL4,GAL80*^{ts} *UN 6 sh*	0.73 ± 0.02		
UAS-*btk*^{RNAi1}/*c739-GAL4,GAL80*^{ts} *IN 6 sh*	0.72 ± 0.02	0.4393	0.6617
UAS-*btk*^{RNAi1}/*c739-GAL4,GAL80*^{ts} *UN 10 sh*	0.74 ± 1.01		
UAS-*btk*^{RNAi1}/*c739-GAL4,GAL80*^{ts} *IN 10 sh*	0.70 ± 0.02	1.2977	0.1985
UAS-*btk*^{RNAi1}/*c739-GAL4,GAL80*^{ts} *UN 15 sh*	0.74 ± 1.01		
UAS-*btk*^{RNAi1}/*c739-GAL4,GAL80*^{ts} *IN 15 sh*	0.70 ± 0.02	1.2977	0.1985
Fig. 5*D*. ANOVA: $F_{(5,82)} = 1.3274$ $p = 0.2614$			
c305aGAL4,GAL80^{ts}/UAS-*btk*^{RNAi1} *UN 6 sh*	0.78 ± 0.02		
c305aGAL4,GAL80^{ts}/UAS-*btk*^{RNAi1} *IN 6 sh*	0.74 ± 0.02	1.3687	0.1751
c305aGAL4,GAL80^{ts}/UAS-*btk*^{RNAi1} *UN 10 sh*	0.78 ± 0.02		
c305aGAL4,GAL80^{ts}/UAS-*btk*^{RNAi1} *IN 10 sh*	0.74 ± 0.02	1.5464	0.1261
c305aGAL4,GAL80^{ts}/UAS-*btk*^{RNAi1} *UN 15 sh*	0.78 ± 0.02		
c305aGAL4,GAL80^{ts}/UAS-*btk*^{RNAi1} *IN 15 sh*	0.74 ± 0.02	1.5222	1.1321
Fig. 6*A*. ANOVA: $F_{(2,28)} = 1.1989$, $p = 0.3176$			
0 μM	0.37 ± 0.04		
5 μM	0.45 ± 0.04	−1.45	0.1591
10 μM	0.43 ± 0.03	−1.139	0.2652
Fig. 6*B*. ANOVA: $F_{(2,30)} = 0.8493$, $p = 0.4384$			
0 μM	0.50 ± 0.05		
5 μM	0.54 ± 0.05	−0.624	0.5376
10 μM	0.46 ± 0.03	0.5694	0.5736
Fig. 6*C*. ANOVA: $F_{(3,44)} = 1.3657$, $p = 0.2667$			
0 μM	0.50 ± 0.03		
0.1 μM	0.57 ± 0.06	−1.432	0.1598
1 μM	0.56 ± 0.02	−1.373	0.1772
10 μM	0.50 ± 0.03	−0.063	0.9502
Fig. 6*D*. ANOVA: $F_{(2,26)} = 8.8963$, $p = 0.0013$*			
0 μM	0.71 ± 0.03		
5 μM	0.53 ± 0.07	2.7508	**0.0111**
10 μM	0.78 ± 0.03	−1.216	0.0243
Fig. 6*E*. ANOVA: $F_{(2,27)} = 1.3673$, $p = 0.2732$			
c305aGAL4/+;UAS-*btk*^{RNAi1}/*GAL80*^{ts}	0.66 ± 0.04		
c305aGAL4/+;UAS-*btk*^{RNAi1}/*GAL80*^{ts} *Clz*	0.73 ± 0.03	−1.54	0.1361
c305-GAL4/+;UAS-*btk*$^{RNAi-1}$/*GAL80*^{ts} *Ris*	0.72 ± 0.03	−1.26	0.2193
Fig. 6F. ANOVA: $F_{(2,26)} = 2.2671$, $p = 0.1254$			
c739GAL4/+;UAS-*btk*^{RNAi1}/*GAL80*^{ts}	0.66 ± 0.04		
c739GAL4/+;UAS-*btk*^{RNAi1}/*GAL80*^{ts} *Clz*	0.73 ± 0.03	1.6255	0.1171
c739GAL4/+;UAS-*btk*^{RNAi1}/*GAL80*^{ts} *Ris*	0.72 ± 0.03	−0.378	0.7085
Fig. 6*G*. ANOVA: $F_{(5,95)} = 1.8751$, $p = 0.1065$			
btk $^{M1/M1}$ 6 sh	0.44 ± 0.05		
btk $^{M1/M1}$ Clz 6 sh	0.43 ± 0.02	0.3073	0.7593
btk $^{M1/M1}$ 10 sh	0.43 ± 0.05		
btk $^{M1/M1}$ Clz 10 sh	0.45 ± 0.03	−0.352	0.726
btk $^{M1/M1}$ 15 sh	0.20 ± 0.04		
btk $^{M1/M1}$ Clz 15 sh	0.43 ± 0.03	−2.527	0.0133
Fig. 6H. ANOVA: $F_{(5,73)} = 28.6620$, $p < 0.0001$*			
btk $^{M1/M1}$ 6 sh	0.35 ± 0.03		
btk $^{M1/M1}$ Ris 6 sh	0.63 ± 0.03	−6.509	**1.1×10^{-8}**
btk $^{M1/M1}$ 10 sh	0.36 ± 0.02		
btk $^{M1/M1}$ Ris 10 sh	0.64 ± 0.04	−6.91	**2.1×10^{-9}**
btk $^{M1/M1}$ 15 sh	0.38 ± 0.03		
btk $^{M1/M1}$ Ris 15 sh	0.68 ± 0.04	−6.64	**6.3×10^{-9}**
Fig. 6*I*. ANOVA: $F_{(3,52)} = 0.5727$, $p = 0.6356$			
0 μM 6 sh	0.76 ± 0.03		
10 μM 6 sh	0.72 ± 0.03	0.952	0.3458
0 μM 15 sh	0.78 ± 0.0.02		
10 μM 15 sh	0.73 ± 0.04	0.8233	0.4143

(*Table continues.*)

Table 1. Continued

Genotype	Mean ± SEM	*t* Ratio	*p*
Fig. 6*I*. ANOVA: $F_{(3,53)} = 65.5164$, $p < 0.0001$*			
0 μM 6 sh	0.78 ± 0.01		
10 μM 6 sh	0.85 ± 0.00	−10.26	**7×10^{-14}**
0 μM 15 sh	0.79 ± 0.01		
10 μM 15 sh	0.84 ± 0.00	−9.555	**7×10^{-13}**

Avoidance of 45 V footshocks are shown for all genotypes per figure as indicated. Initial ANOVA: values are shown as well as individual statistical comparisons with the respective controls. Significant differences uncovered are highlighted in bold.

Olfactory habituation. Olfactory habituation experiments were performed as detailed in Semelidou et al. (2018). Avoidance of the aversive odorant 3-octanol (OCT) carried in an airstream of 500 ml/min in one arm of a standard T-maze versus air was assessed and an index (AF) was calculated. For the "training phase", ~70 flies were exposed in the upper arm of a standard T-maze to OCT for 4 min. After a 30 s rest period, the flies were lowered to the center of the maze for testing their osmotactic response by a choice of air versus OCT. At the end of the 90 s choice period the flies in each arm were trapped counted and HF and HI were calculated as described.

Pharmaceutical treatments

The Btk inhibitor Ibrutinib (Selleck Chemicals) and the antipsychotic drugs clozapine (Sigma-Aldrich) and risperidone (Tocris Bioscience) were diluted in DMSO and mixed at the indicated final concentrations in Brewer's yeast (Acros Organics) aqueous paste. The concentration ranges used bracketed analogous concentrations as used for humans. Ibrutinib was used at 0.1, 1, and 10 μM; clozapine at 5 and 10 μM; and risperidone at 0.1, 1, and 10 μM. Flies were starved for 5 h in empty vials at 25°C before exposure to drug or vehicle-only containing yeast paste for 14–16 h. The following day, flies were transferred in normal food vials, trained, and tested as detailed for footshock habituation.

Western blots

Five adult female heads 1–3 d post-eclosion were homogenized in 1× Laemmli buffer (50 mM Tris, pH 6.8, 100 mM DTT, 5% 2-mercaptoethanol, 2% SDS, 10% glycerol, and 0,01% bromophenol blue). The lysates were boiled for 5 min at 95°C, centrifuged at 10,000 × *g* for 5 min and separated by SDS-PAGE. Proteins were transferred to a PVDF membrane at 120 V for 80 min and probed with anti-dBtk antibody (Tsikala et al., 2014) at 1:4000 and anti-syntaxin (Syn) antibody (8C3; Developmental Studies Hybridoma Bank) at 1:3000. Rat and mouse HRP-conjugated antibodies were applied at 1:5000 and proteins were visualized with chemiluminescence (ECL Plus, GE Healthcare). Signals were measured with Bio-Rad Molecular Imager Chemidoc XRS+.

Confocal microscopy

BtkGal4 flies were crossed to UAS-mCD8-GFP (Lee and Luo, 1999) and progeny were used to examine the expression pattern of dBtk in the adult brain. Flies were dissected in cold PBS, fixed in 4% paraformaldehyde for 15 min, and imaged by laser-scanning confocal microscopy (Leica, TCS SP8). Images were captured using a 40 ×/1.3 NA oil objective after 488 nm excitation and digital image resolution was set at 1024 × 1024. Image stacks were collected at 0.75 μm intervals to cover the entire brain. The images were converted to grayscale, inverted in Adobe Photoshop 3, and shown as maximum intensity projections derived from confocal stacks.

Statistical analysis and experimental design

For all experiments, controls and genetically matched experimental genotypes were tested in the same session in a balanced experimental design. The order of training and testing was randomized. When two genetic controls were used, we required an experimental result to be significantly different from both genetic controls. Untransformed (raw) data were analyzed parametrically with the JMP 7 statistical software package (SAS Institute). If significant, initial ANOVA tests were followed by planned comparisons [least square mean (LSM) contrast analyses] if they indicated significant differences among the genotypes and the level of significance was adjusted for the experiment-wise error rate as suggested by Sokal and Rohlf (1981).

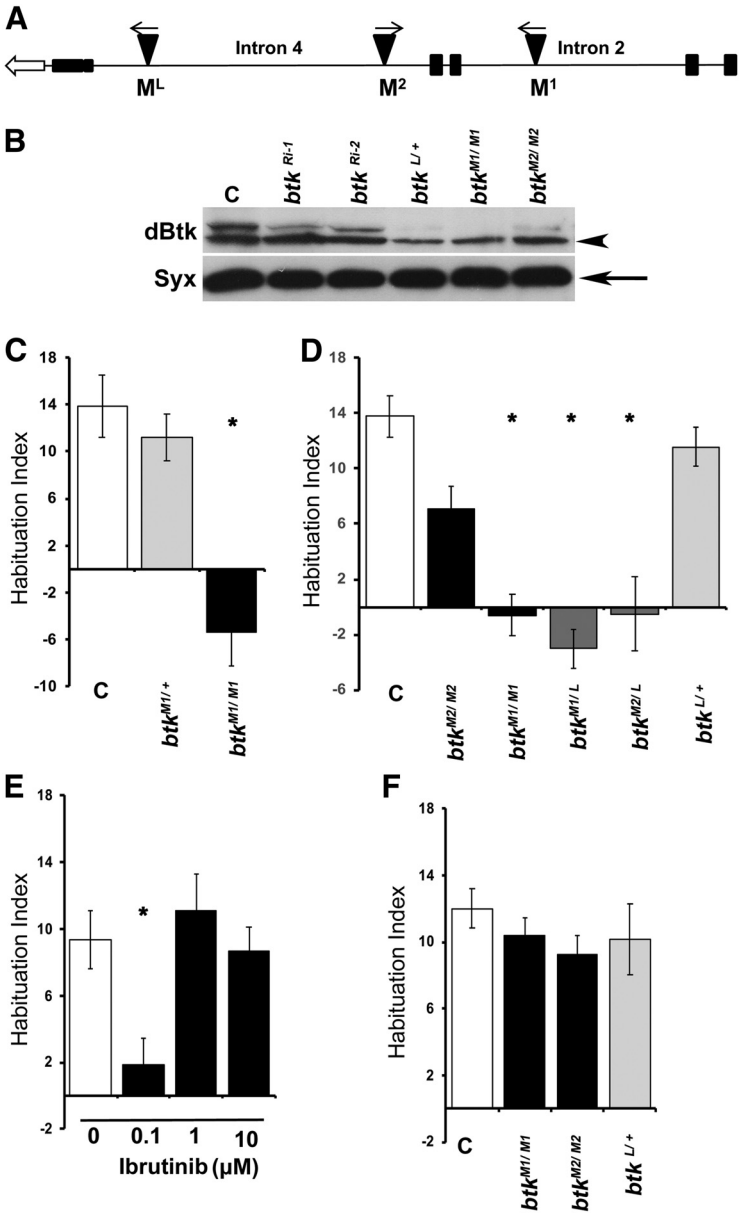

Figure 1. dBtk is essential for footshock habituation. ***A***, A schematic of the *Btk29A* (*dBtk*) genomic area where the transposon insertions used in this study reside. The open arrow demonstrates the direction of transcription. Filled boxes correspond to exons, whereas lines correspond to the indicated introns. The triangles show the MiMIC insertions. M^1, The homozygous viable MI01270; M^2, the homozygous viable MI02160; M^L, the lethal insertion MI02966. ***B***, Western blot analysis of head lysates from five 3- to 5-d-old female *btk* mutants and pan-neuronally expressing RNAis as indicated. The arrowhead points to a band which migrates as predicted for the long (type 2) dBtk protein, whereas the arrow points to the apparent short (type 1) isoform (Hamada-Kawaguchi et al., 2014). The following strains were used: C, Control (y^1w^*); $btk^{Ri\text{-}1}$, pan-neuronal expression under Elav-Gal4 of the BDSC 35159 RNAi-encoding transgene; $btk^{Ri\text{-}2}$, pan-neuronal expression under Elav-Gal4 of the BDSC 25791 RNAi-encoding transgene; $btk^{L/+}$, heterozygotes for the lethal (MI02966) insertion; $btk^{M1/M1}$, homozygotes for the M^1 (MI01270) insertion; $btk^{M2/M2}$, homozygotes for the M^2 MI02160) insertion. The anti-dBtk antibody (Btk) recognizes two bands, the upper one of which is reduced the most in all mutants and RNAi-expressing animals, with the lower one also reduced, albeit to a lesser degree. Syntaxin 1 (Syx) is used as a loading control. ***C–F***, Habituation indices quantify the difference in footshock avoidance following exposure to 15 stimuli from that of same genotype naive flies and are shown as the mean ± SEM for the indicated number of repetitions (*n*). Stars indicate significant differences from controls as indicated in the text. ***C***, Homozygous $btk^{M1/M1}$ mutants perform significantly different from mutant heterozygotes and y^1w^* controls (***C***). $n \geq 16$ for all groups. ***D***, Complementation of the habituation failure among *dBtk* insertion mutants. Although the performance of btk^L heterozygotes was not significantly different from that of the y^1w^*controls (***C***), hetero-allelics of this lethal insertion over both viable M1 and M2 insertions presented significant habituation deficits. $n \geq 9$ for all groups. ***E***, The Btk inhibitor Ibrutinib induces habituation deficits in y^1w^* control flies in a dose-specific manner. 0 represents y^1w^*animals fed the DMSO vehicle and compared with their performance; 0.1 μM Ibrutinib induced a significant deficit, but higher doses did not. $n \geq 9$ for all groups. ***F***, *dBtk* mutants do not present habituation deficits to 4 min exposure of the aversive odorant OCT. $n \geq 12$ for all groups.

Results

dBtk mutants are defective in footshock habituation

In the footshock habituation paradigm (Acevedo et al., 2007), flies avoid the initial 2–8 repetitive stimuli, but their response declines rapidly to an asymptotic baseline as predicted (Rankin et al., 2009), after 10–11 stimuli. This pre-exposure-dependent attenuated avoidance after 15 footshocks relative to that of naive animals is quantified as a positive change in the HI of control flies in Figure 1*C* (open bar). Failure to establish habituation does not attenuate shock avoidance after shock pre-exposure and therefore yields the zero or negative difference from the naive response reported by the HI. Because the HI measures the relative change in avoidance within each genotype, it is not dependent on absolute 45 V avoidance levels, which can be variable (Table 1).

Viable MiMIC (Venken et al., 2011) insertion mutants (34172-$dBtk^{M1}$) in intron 2 of the *dBtk* gene (Fig. 1*A*), resulting in reduction of both protein isoforms in adult heads (Fig. 1*B*), did not attenuate shock avoidance following exposure to 15 stimuli, in contrast to controls and heterozygotes, indicating failure to habituate (Fig. 1*C*, $btk^{M1/M1}$; ANOVA: $F_{(2,58)} = 16.7450$, $p < 0.0001$; subsequent LSM: $p = 1.2 \times 10^{-6}$ vs control). Mutants for a different insertion (34284-btk^{M2}) in intron 4 (Fig. 1*A*), which has a milder effect on dBtk levels (Fig. 1*B*), habituated to the footshocks, albeit not to the same degree as controls (Fig. 1*D*, $btk^{M2/M2}$; ANOVA: $F_{(5,68)} = 13.3566$, $p < 0.0001$; subsequent LSM: $p = 0.0144$ vs control). In agreement with the behavior of $dBtk^{M1}/+$ (Fig. 1*C*, $dBtk^{M1}/+$; ANOVA: $F_{(2,58)} = 16.7450$, $p < 0.0001$; subsequent LSM: $p = 0.4960$ vs control), heterozygotes for a lethal insertion (37042-btk^L) in intron 4 (Fig. 1*A*) presented normal habituation (Fig. 1*D*, $btk^L/+$; ANOVA: $F_{(5,68)} = 13.3566$, $p < 0.0001$; subsequent LSM: $p = 0.4495$ vs control). It should be noted that although the shock AF is intrinsic to calculation of the HI, AFs for all genotypes used herein are collectively presented on Table 1.

To ascertain that the habituation defect is indeed consequent of reduction in dBtk levels and not unrelated mutations on the chromosome, we examined hetero-allelic combinations of these independently isolated mutations. Significantly, hetero-allelics of the lethal btk^L with both viable btk^{M1} and btk^{M2} insertions failed to habituate to 15 footshocks (Fig. 1*D*; ANOVA: $F_{(5,68)} = 13.3566$, $p < 0.0001$; subsequent LSM: $p = 1.2 \times 10^{-7}$ $btk^{M1/L}$

vs control and $p = 1.1 \times 10^{-6}$ $btk^{M2/L}$ vs control), indicating that indeed reduced dBtk in the CNS does not support normal footshock habituation.

Because the human ortholog is implicated in cancers (Tillman et al., 2018) and the kinase domain is highly conserved (Gregory et al., 1987), covalent Btk inhibitors have been developed (Ysebaert and Michallet, 2014) and are available. Hence, dBtk activity was inhibited by feeding the commonly used inhibitor ibrutinib to control flies. Compared with vehicle treated animals, ibrutinib treatment resulted in strong abrogation of footshock habituation at low (Fig. 1*E*; 0.1 μM, ANOVA: $F_{(3,60)} = 5.4217$, $p = 0.0024$; subsequent LSM: $p = 0.0012$ vs 0 μM), but not high concentrations (Fig. 1*E*; ANOVA: $F_{(3,60)} = 5.4217$, $p = 0.0024$; subsequent LSM: $p = 0.5368$, 1 vs 0 μM, and $p = 0.7965$ 10 vs 0 μM). The reason for this sharp concentration optimum is unclear at the moment, but at higher concentrations it may affect activities of potentially related proteins with opposing effects on habituation to footshock. Nevertheless, the results are consistent with the genetic evidence and strengthen the conclusion that dBtk kinase activity is required for habituation to repeated footshocks. Because, *dBtk* mutants were found to habituate prematurely in an olfactory jump reflex assay (Asztalos et al., 2007), we tested whether dBtk reduction resulted in deficient olfactory avoidance habituation (Semelidou et al., 2018). However, dBtk abrogation did not affect habituation to aversive odor (OCT) exposure (Semelidou et al., 2018), suggesting that the protein is specifically required for habituation to footshocks (Fig. 1*F*; ANOVA: $F_{(3,62)} = 0.8339$, $p = 0.4806$).

To independently validate these results, we used the TARGET system (McGuire et al., 2003) to abrogate the protein in adult animals by transgene-mediated RNA-interference (RNAi). In fact, adult-specific pan-neuronal (Fig. 2*A*; ANOVA: $F_{(2,44)} = 6.1651$, $p = 0.0045$; subsequent LSM: $p = 0.0016$ and $p = 0.018$ vs controls, respectively), dBtk attenuation recapitulated the footshock habituation failure of the mutants and also did not compromise habituation to the aversive odorant octanol (Fig. 2*C*; ANOVA: $F_{(2,30)} = 1.3588$, $p = 0.2734$). The latter supports the notion that dBtk functions specifically in footshock habituation. Identical results were obtained with the second RNAi-mediating transgene (Fig. 2*B*; ANOVA: $F_{(2,35)} = 11.8202$, $p < 0.0001$; subsequent LSM: $p = 0.00068$ and $p = 0.00014$ vs controls, respectively) and a different pan-neuronal driver (Gouzi et al., 2011), Ras2Gal4 (Fig. 2*D*; ANOVA: $F_{(2,27)} = 11.2630$, $p = 0.0003$; subsequent LSM: $p = 0.0002$ and $p = 0.0008$ vs controls, respectively). Therefore, the failed habituation phenotype of *dBtk* mutants is not developmental in origin, but reflects an acute requirement for dBtk activity to facilitate habituation. Significantly, its abrogation in glia (Fig. 2*E*; ANOVA: $F_{(2,46)} = 0.2643$, $p = 0.7690$), or constitutively sparing the MBs from dBtk attenuation under MBGal80 (Fig. 2*F*; ANOVA: $F_{(2,47)} = 0.0326$, $p = 0.9679$; Krashes et al., 2007), did not affect habituation, suggesting that activity of the kinase is required within these neurons. Therefore, the habituation failure is not a consequence merely of the presence of the RNAi encoding transgenes, or drivers, but their induction not in glia, but within MB neurons, as suggested by Figure 2*F* and reported (Fig. 2*G*) expression of dBtk in these neurons.

dBtk functions within α'/β' mushroom body neurons to facilitate footshock habituation

Neurotransmission from the α/β MB neurons is essential to prevent premature footshock habituation (Acevedo et al., 2007), but apparently not to facilitate its onset. So, we wondered where within the adult CNS is dBtk activity required for facilitation of footshock habituation. Initially, to unequivocally establish that dBtk activity solely within the MBs is essential for facilitation of footshock habituation, we attenuated it therein with the strong pan-MB driver Leo-Gal4 (Messaritou et al., 2009). This abolished footshock habituation (Fig. 3*A*; ANOVA: $F_{(2,34)} = 12.6248$, $p < 0.0001$; subsequent LSM: $p = 0.0001$ and $p = 0.0002$ vs controls, respectively) and the result was independently validated with another RNAi transgene (Fig. 3*C*; ANOVA: $F_{(2,39)} = 60{,}9160$, $p < 0.0001$; subsequent LSM: $p = 1.76 \times 10^{-12}$ and $p = 6.55 \times 10^{-10}$ vs controls, respectively), establishing the necessity of dBtk within the MBs for the process. This conclusion was strengthened by reinstating dBtk specifically within the MBs of adult btk^{M1} homozygotes, which fully reversed their deficient habituation (Fig. 3*B*; ANOVA: $F_{(5,66)} = 18.3727$, $p < 0.0001$; subsequent LSM: $p = 6 \times 10^{-6}$ leoMB-GAL4, btk^{M1}/ btk^{M1}; GAL80ts/+ induced vs leoMB-GAL4,btk^{M1}/+; GAL80ts/+ induced and $p = 0.1918$ leoMB-GAL4,btk^{M1}/ btk^{M1}; GAL80ts,UAS-$btk^{\text{short isoform}}$ induced vs leoMB-GAL4,btk^{M1}/+; GAL80ts/+ induced). The transgene encodes the predominately neuronal type 1 short dBtk isoform (Tsikala et al., 2014), containing all conserved domains except the N-terminal PH. However, if the UAS-$btk^{\text{short isoform}}$ was not induced in adult animals the mutant phenotype persisted (Fig. 3*B*; uninduced LSM: uninduced leoG4,btk^{M1}/btk^{M1}; $G80^{ts}$/UASbtk $p = 0.0367$ vs leoG4,btk^{M1}/btk^{M1}; $G80^{ts}$/+ and $p < 0.0001$ with leoG4,btk^{M1}/+; $G80^{ts}$/+ controls, respectively). The acute requirement for dBtk within adult MBs for footshock habituation was further supported by attenuating its levels under the pan-MB drivers 247-Gal4 (Fig. 3*D*; ANOVA: $F_{(2,42)} = 11.0752$, $p = 0.0001$; subsequent LSM: $p = 0.0032$ and $p = 4 \times 10^{-5}$ vs controls, respectively) and dnc-Gal4 (Fig. 3*E*; ANOVA: $F_{(2,30)} = 12.4333$, $p = 0.0001$; subsequent LSM: $p = 0.0012$ and $p = 0.0001$ vs controls, respectively), both of which precipitated pronounced habituation defects.

Given the role of neurotransmission from MB α/β neurons in preventing premature habituation (Acevedo et al., 2007), we wondered whether dBtk acts within these neurons to inhibit this process and consequently facilitate habituation. Thus, dBtk was attenuated within α/β neurons under the c772 (Fig. 3*F*; ANOVA: $F_{(2,44)} = 0.6731$, $p = 0.5156$) and c739 (Fig. 3*G*; ANOVA: $F_{(2,43)} = 1.1146$, $p = 0.3378$) drivers in $\alpha\beta$ cortex or core neurons, respectively (Pavlopoulos et al., 2008), but habituation was not altered, eliminating this hypothesis. In addition, dBtk attenuation within γ neurons also did not affect footshock habituation (Fig. 3*H*; ANOVA: $F_{(2,47)} = 0.0266$, $p = 0.9737$). Significantly however, dBtk abrogation within α'/β' MB neurons [Fig. 3*I*; ANOVA: $F_{(3,44)} = 22.5186$, $p < 0.0001$; subsequent LSM: induced (IN) $p < 0.0001$ vs both controls] abolished footshock habituation. In contrast, if the RNAi-mediating transgene remained uninduced, habituation was indistinguishable from controls (Fig. 3*I*; LSM: uninduced (UN) $p = 0.0891$ and $p = 0.3397$ vs the controls, respectively). Therefore, dBtk is not developmentally, but rather acutely required within α'/β' MB neurons to facilitate footshock habituation.

To verify this conclusion independently, we used a "split-Gal4" driver expressed specifically in α'/β' MB neurons and varied the expression of the RNAi-mediating transgene ($btk^{Ri\text{-}1}$) based on the optimum temperature for Gal4-mediated transcription (McGuire et al., 2004). Raising and maintaining the flies at 18°C, should not yield appreciable $btk^{Ri\text{-}1}$ expression and presented normal habituation within the range of controls (Fig. 1). In contrast, animals raised at 18°C, but kept at 30°C for 48 h before training to achieve maximal $btk^{Ri\text{-}1}$ expression failed to

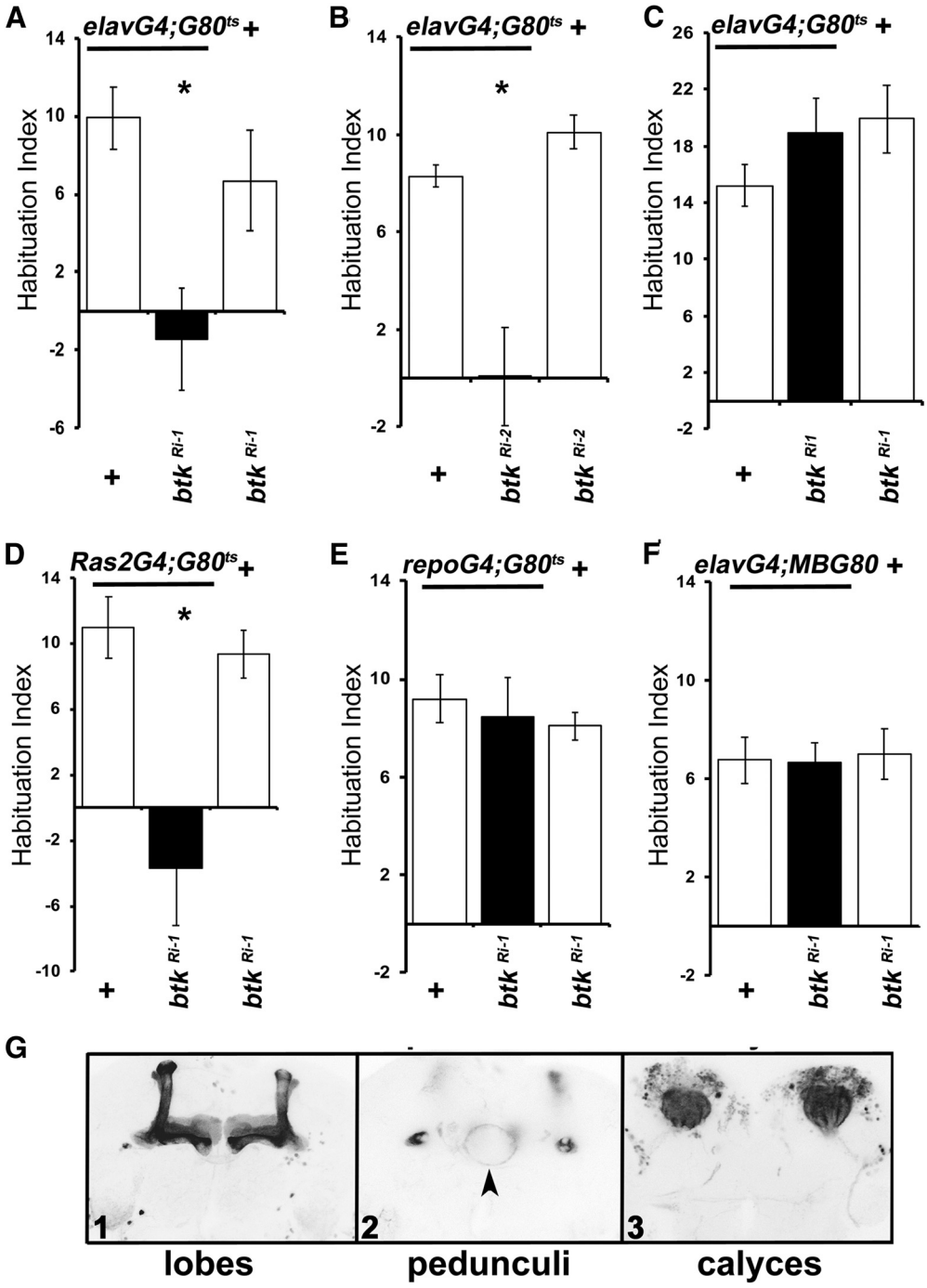

Figure 2. Adult-specific abrogation of dBtk results in deficient footshock habituation. HIs quantifying the difference in footshock avoidance following exposure to 15 stimuli from that of same genotype naive flies are shown as the mean ± SEM for the indicated number of repetitions (*n*). All panels show the performance of animals expressing a *dbtk* RNAi-encoding transgene ($btk^{Ri-1}/+$) under the indicated driver (black bar), the driver heterozygotes (left open bars), and the RNAi-mediating transgene heterozygotes (+, right open bars). driver/+, Progeny from the cross of the w^{1118} background driver with 36303 y^1v^1, whereas for the $btk^{Ri-1}/+$, the y^1v^1 background of btk^{Ri-1} was crossed to w^{1118} so that the two controls have equivalent backgrounds as the experimentals. Asterisks indicate significant differences from controls as detailed in the text. ***A***, Adult limited pan-neuronal expression of btk^{Ri-1} eliminates habituation to 15 footshocks. $n \geq 11$ for all groups. ***B***, Adult-limited pan-neuronal expression of an independent RNAi-mediating transgene (btk^{Ri-2}), also results in habituation defects. $n \geq 9$ for all groups. ***C***, Adult-limited pan-neuronal expression of btk^{Ri-1} does not yield defects in habituation to 4 min of OCT exposure. $n \geq 9$ for all groups. ***D***, Flies expressing btk^{Ri-1} under the pan-neuronal Ras2Gal4,Gal80 ^{ts} driver present adult-specific habituation defects compared with controls. $n \geq 9$ for all groups. ***E***, Adult limited btk^{Ri-1} expression in glia did not precipitate deficits. $n \geq 14$ for all groups. ***F***, Pan-neuronal expression of btk^{Ri-1}, but at the exclusion of the MBs did not yield deficits in shock habituation. $n \geq 12$ for all groups. ***G***, dBtk is preferentially distributed within the MBs evidenced by mcD8-GFP expression under the control of the btkG4 driver (BDSC, 49182). The arrowhead indicates faint expression in the ring neurons of the ellipsoid body at the level of the pedunculi.

habituate (Fig. 3*J*; ANOVA: $F_{(2,55)} = 4.8324$, $p = 0.0118$; subsequent LSM: $p = 0.0032$ vs 18°C). Footshock habituation in animals raised and kept at 25°C was not abolished, but was highly suppressed compared with the performance of animals kept at 18°C (Fig. 3*J*; ANOVA: $F_{(2,55)} = 4.8324$, $p = 0.0118$; subsequent LSM: $p = 0.0546$ vs 18°C). These results demonstrate that dBtk function in α'/β' neurons is indeed essential to facilitate footshock habituation. This is not specific to dBtk, as conditionally

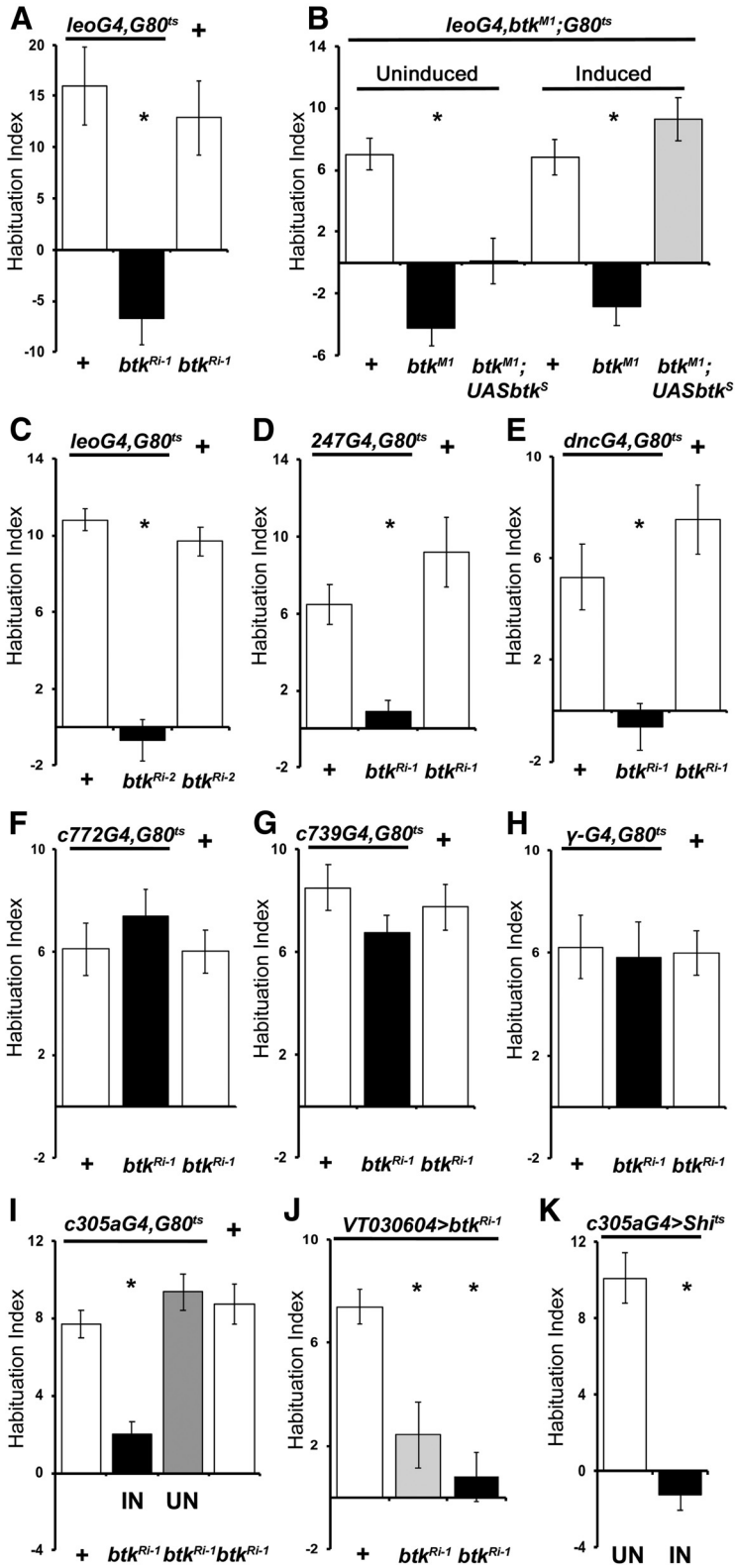

Figure 3. dBtk is acutely required within the α'/β' mushroom body neurons to facilitate habituation to footshock. Habituation indices quantifying the difference in footshock avoidance following exposure to 15 stimuli from that of same genotype naive flies are shown as the mean ± SEM for the indicated number of repetitions (n). All panels show the performance of animals expressing a *dbtk* RNAi-encoding transgene ($btk^{Ri-1}/+$) under the indicated driver (black bar), the driver heterozygotes (left open bars), and the RNAi-mediating transgene heterozygotes (+, right open bars). driver/+, Progeny from the cross of the w^{1118} background driver with 36303 y^1v^1, whereas for the $btk^{Ri-1}/+$, the y^1v^1 background btk^{Ri-1} was crossed to w^{1118} so that the two controls have equivalent backgrounds as the experimental. Asterisks indicate significant differences from controls as detailed in the text. ***A***, Adult limited pan-MB expression of btk^{Ri-1} eliminates habituation to 15 footshocks. $n \geq 11$ for all groups. ***B***, Rescue of the habituation deficit of $btk^{M1/M1}$ by adult-limited expression of a dBtk transgene in the MBs. Uninduced (left side) transgene-bearing flies (gray bar) behave significantly different from controls, much like non-transgene bearing mutants homozygotes ($p = 0.0014$ and $p = 2.2 \times 10^{-6}$, respectively). In contrast, a 2 d induction of the transgene (gray bar right side) completely reversed the deficient habituation ($p = 0.1918$ vs $p = 6 \times 10^{-6}$ for mutant homozygotes compare to controls; open bar). $n \geq 8$ for all groups. ***C***, Adult limited pan-MB expression of the independent btk^{Ri-2} transgene precipitates defective shock habituation compared with both controls. $n \geq 10$ for all groups. ***D***, Adult specific expression of btk^{Ri-1} under the independent pan-MB 247Gal4 driver results in abrogated shock habituation compared with controls. $n \geq 14$ for all groups. ***E***, A third MB-restricted driver (dncGal4) yields adult-specific shock habituation deficits when driving UAS-btk^{Ri-1}. $n \geq 9$ for all groups. ***F***, Adult-limited btk^{Ri-1} expression in α/β MB neurons does not precipitate habituation deficits. $n \geq 11$ for all groups. ***G***, Adult-specific btk^{Ri-1} expression in α/β MB neurons under the independent c739Gal4 driver does not compromise shock habituation. $n \geq 13$ for all groups. ***H***, Adult-specific btk^{Ri-1} expression in γ MB neurons under VT030604 also does not compromise shock habituation. $n \geq 14$ for all groups. ***I***, Adult-specific IN of btk^{Ri-1} expression in α'/β' MB neurons abrogates shock habituation, whereas the uninduced transgene (UN) does not. $n \geq 9$ for all groups. ***J***, Expression of btk^{Ri-1} driven by the α'/β'-specific VT030604 driver present aberrant habituation (black bar) when induced for 2 d compared to their uninduced siblings. However, when flies were raised at 25°C (gray bar), they presented an ameliorated deficit compared with those raised at 18°C and uninduced. $n \geq 14$ for all groups. ***K***, Expression of shi^{ts} in α'/β' MB neurons compromises habituation under the restrictive conditions (black bar) compared with animals kept under permissive temperature ($p = 9 \times 10^{-8}$). $n \geq 11$ for all groups.

blocking neurotransmission from α'/β' neurons with the thermosensitive transgenic dynamin Shi^{ts} (Kitamoto, 2001), under c305a-Gal4 completely blocked habituation (Fig. 3*K*; ANOVA: $F_{(1,25)} = 56.7690$, $p < 0.0001$; subsequent LSM: $p = 9 \times 10^{-8}$). This is despite the small but significant shock avoidance reduction in the "induced" (IN) versus the "uninduced" (UN) state (Table 1), which does not contribute to the phenotype because of the normalization afforded by the calculation of the HI.

The collective results demonstrate two important points. Neurotransmission from α'/β' MB neurons facilitates footshock habituation, whereas activation of their α/β counterparts suppresses it (Acevedo et al., 2007).

dBtk is also required within α/β neurons to maintain stimulus responsiveness

Three main reasons prompted us to investigate dBtk function in α/β neurons. The protein appears present in these neurons (Fig. 2*G*), *dbtk* mutants habituate prematurely their olfactory jump reflex (Asztalos et al., 2007) and neurotransmission

←

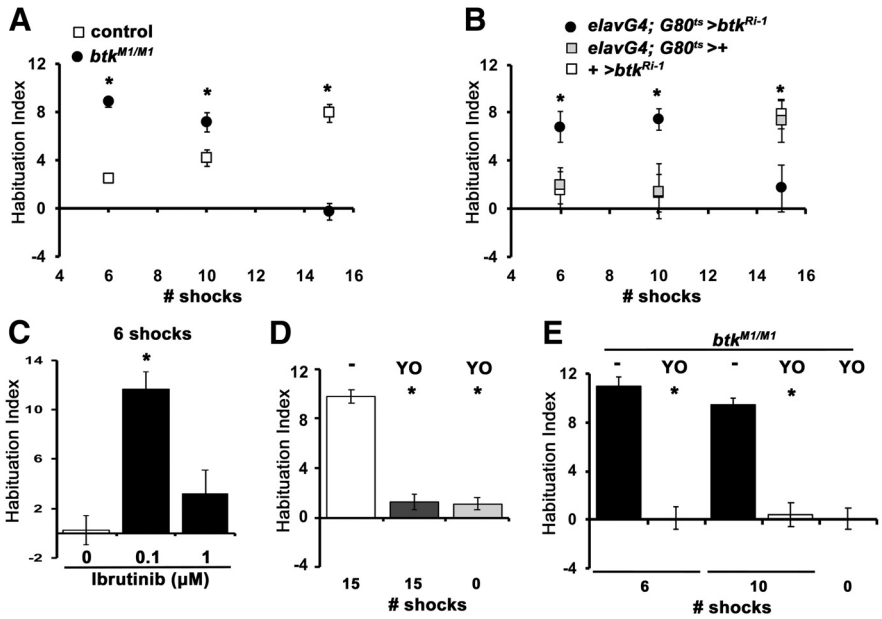

Figure 4. dBtk is acutely required within α/β MB neurons to inhibit premature habituation to footshock. Habituation indices quantifying the difference in footshock avoidance following exposure to the indicated number of stimuli from that of same genotype naive flies are shown as the mean ± SEM for the indicated number of repetitions (*n*). Filled circles represent the mean performance of animals with abrogated dBtk, whole open squares the respective controls. Stars indicate significant differences from controls as detailed in the text. ***A***, Footshock habituation of controls (y^1w^*) and $btk^{M1/M1}$ mutants after prior experience of 6, 10, and 15 shocks. The performance of controls is significantly different from that of the mutants after 6, 10, and 15 footshocks. $n > 13$ for all groups. ***B***, Adult-limited pan-neuronal expression of btk^{Ri-1} recapitulates both the premature habituation after 6 and 10 shocks and the habituation failure after 15 stimuli. So that the controls have similar genetic backgrounds, progeny from the cross of the w^{1118} background ElavGal4;Gal80^{ts} with 36303 y^1v^1, whereas for the $btk^{Ri-1}/+$, the y^1v^1 background btk^{Ri-1} was crossed to w^{1118}. $n \geq 11$ for all groups. ***C***, Ibrutinib promotes premature habituation after 6 shocks at 0.1 μM, but not at 1 μM relative to the performance of vehicle-treated y^1w^* animals. $n \geq 8$ for all groups. ***D***, Dishabituation in y^1w^* flies after 8 s of YO puff. White bar, Habituation after 15 shocks; dark gray bar, dishabituation with YO after experiencing 15 shocks; light gray bar, the effect on avoidance of YO on naive flies before testing their shock avoidance. YO exposure has significant effects on reversing the habituated response, but YO exposure of naive flies does not affect their shock avoidance (0). $n \geq 10$ for all groups. ***E***, The reduced avoidance of $btk^{M1/M1}$ mutants after 6 and 10 footshocks is *bona fide* premature habituation because it is reversible (dishabituated) by a single puff of YO after the respective footshocks as indicated. Black bars denote habituation without YO and the open bars after odor presentation. 0 denotes shock avoidance of naive flies after YO exposure. YO exposure results in significant dishabituation after 6 and 10 shocks. $n \geq 8$ for all groups.

from α/β neurons is essential for mediating responsiveness to footshocks and prevent premature habituation (Acevedo et al., 2007). Therefore, we wondered whether dBtk is also involved in maintenance of stimulus responsiveness within α/β neurons. Surprisingly, in contrast to controls subjected to the same number of stimuli, btk^{M1} mutants habituated prematurely after 6 and 10 footshocks (Fig. 4*A*; ANOVA: $F_{(5,104)} = 34.9318$, $p < 0.0001$; subsequent LSM: 6 shocks $p = 4 \times 10^{-10}$, 10 shocks $p = 0.0027$ vs controls), but failed to habituate to 15 shocks (LSM: $p = 9 \times 10^{-16}$ vs controls). The deficits were phenocopied by acute pan-neuronal dBtk abrogation (Fig. 4*B*; ANOVA: $F_{(8,156)} = 3.8010$, $p = 0.0004$; subsequent LSM: 6 shocks $p = 0.0088$ and $p = 0.0193$, 10 shocks $p = 0.0121$ and $p = 0.0259$, 15 shocks $p = 0.0057$ and $p = 0.0125$ vs controls, respectively) and induced upon inhibition of dBtk activity with Ibrutinib in control flies with a similar dose–response as for failed habituation to 15 stimuli (Fig. 4*C*; ANOVA: $F_{(2,28)} = 10.1984$, $p = 0.0005$; subsequent LSM: $p = 0.0002$, 0.1 vs 0 μM and $p = 0.2240$, 1 vs 0 μM). Therefore, as for habituation failure to 15 shocks, the premature avoidance attenuation of the mutants is also not developmental in origin. If the attenuated avoidance is indeed habituation, it should be dishabituated (Rankin et al., 2009). We used an 8 s puff of YO, which has been shown effective for habituation to aversive odors (Paranjpe et al., 2012; Semelidou et al., 2018). In fact, the premature footshock avoidance attenuation was reversed by post-training exposure to YO (Fig. 4*E*; ANOVA: $F_{(4,43)} = 45.5267$, $p < 0.0001$; subsequent LSM: 6 shocks $p = 1.1 \times 10^{-11}$, 10 shocks $p = 1.5 \times 10^{-9}$, AVD after YO $p = 1.9 \times 10^{-9}$), which also suffices to dishabituate control flies after typical habituation to 15 shock stimuli (Fig. 4*D*; ANOVA: $F_{(2,30)} = 84.8182$, $p < 0.0001$; subsequent LSM: YO dishabituation, $p = 9.28 \times 10^{-12}$; AVD, $p = 6.27 \times 10^{-12}$). Because control flies do not habituate to six shocks (Fig. 4*A*,*B*), dishabituation after six shocks was not performed as unnecessary.

Further confirmation that both aberrant habituation phenotypes result from dBtk attenuation and not another mutation on the btk^{M1} chromosome was obtained by adult-specific pan-MB abrogation of the protein under Leo-Gal4. This also yielded both premature habituation to 6 and 10 footshocks and failure to habituate to 15 stimuli and significantly both deficits were absent if the attenuating transgene was uninduced (Fig. 5*A*; ANOVA: $F_{(5,119)} = 8.6993$ $p < 0.0001$; subsequent LSM, 6 shocks, $p = 0.0002$; 10 shocks, $p = 0.0304$; 15 shocks, $p = 1 \times 10^{-5}$ vs uninduced). Importantly, expression of the dBtk-encoding transgene (UAS-btk^S) under Leo-Gal4 in btk^{M1} homozygotes fully restored both, the ability to prevent premature habituation to 6 and 10 footshocks and to facilitate habituation after 15 stimuli, but not if the transgene remained uninduced (Fig. 5*B*; ANOVA: $F_{(5,77)} = 13.3452$ $p < 0.0001$; subsequent LSM, 6 shocks, $p = 0.0036$; 10 shocks, $p = 0.0161$; 15 shocks, $p = 6 \times 10^{-10}$ vs uninduced). This is consistent with the notion that dBtk functions to maintain habituation latency within α/β MB neurons and to facilitate footshock habituation within their α'/β' counterparts.

To confirm the independent function of dBtk in both preventing premature habituation in α/β and facilitating it in α'/β' neurons, the protein was selectively abrogated therein. Significantly, animals with abrogated dBtk in adult α/β neurons under c739Gal4 habituated prematurely to 6 and 10 stimuli (Fig. 5*C*; ANOVA: $F_{(5,77)} = 17.1806$, $p < 0.0001$; subsequent LSM: 6 shocks $p = 8.9 \times 10^{-6}$, 10 shocks $p = 2.9 \times 10^{-8}$, 15 shocks $p = 0.9504$ vs control), whereas attenuation in α'/β' neurons under c305aGal4 did not affect habituation latency, but blocked habituation to 15 shocks (Fig. 5*D*; ANOVA: $F_{(5.82)} = 12.2529$, $p < 0.0001$; subsequent LSM: 6 shocks $p = 0.3433$, 10 shocks $p = 0.777$, 15 shocks $p = 3.7 \times 10^{-7}$ vs control).

Therefore, dBtk has two functionally distinct and apparently independent neuronal type-specific roles. It engages mechanisms that maintain latency, thus preventing premature habituation within α/β neurons and potentially distinct mechanisms that facilitate habituation in their α'/β' counterparts. Alternatively, upon activation of these neurons by the footshock stimuli, dBtk

may mediate neurotransmission from both types, which in the case of α/β neurons is required to maintain the value of the stimulus and prevent premature habituation (Acevedo et al., 2007) and α'/β' neurons to facilitate it (Fig. 3*I*,*K*). Moreover, since *btk* mutants present habituation deficits specifically to footshock, but not odor stimuli, it is possible that the kinase is involved in second messenger pathways transducing dopaminergic signals that apparently communicate footshock information to the MBs and result in their activation (Cervantes-Sandoval et al., 2017; Horiuchi, 2019).

Antipsychotics rescue the deficient habituation of dBtk mutants

We assumed that the inability to habituate upon dBtk attenuation may result from persistent neurotransmission from α'/β'. This could be due to excess dopaminergic signaling or inability of the mutants to downregulate the response to dopaminergic input. To differentiate between these possibilities, we initially sought to inhibit dopaminergic inputs pharmacologically. Interestingly, excess dopaminergic signaling has been linked with schizophrenia in humans (Brisch et al., 2014; Kesby et al., 2018), a condition also associated with habituation failures and defects (Gillberg, 2003; Ludewig et al., 2003; Barkus et al., 2014; McDiarmid et al., 2017). In fact, pharmaceuticals used to treat this condition are thought to act mostly as monoamine receptor antagonists including dopaminergic ones (Robinson, 2007; Brunton et al., 2010).

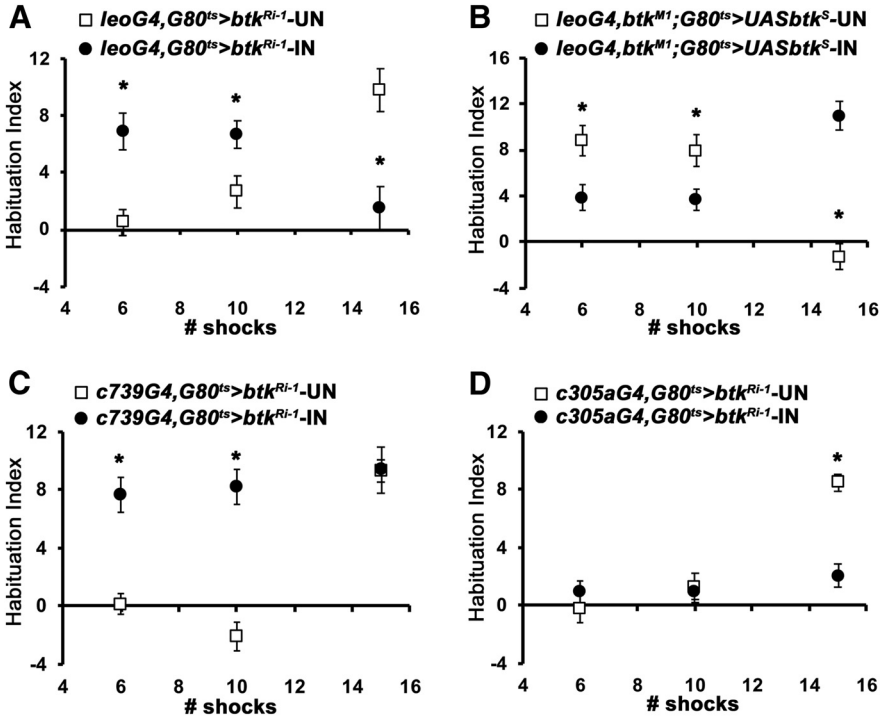

Figure 5. Differential roles for dBtk in latency and habituation in α/β and α'/β' MB neurons. Habituation indices quantifying the difference in footshock avoidance following exposure to the indicated number of stimuli from that of same genotype naive flies are shown as the mean ± SEM for the indicated number of repetitions (*n*). Filled circles represent the mean performance of animals with abrogated dBtk; whole open squares, the respective controls. Asterisks indicate significant differences from controls as detailed in the text. ***A***, Adult-limited pan-MB expression of $btk^{Ri\text{-}1}$ (IN) yields premature habituation after 6 and 10 stimuli and failed habituation after 15 shocks compared to in-genotype controls of siblings with the transgene silent (UN). $n > 18$ for all groups. ***B***, The complementary experiment of adult-limited pan-MB expression of UAS-btk^s rescued (IN) the premature habituation after 6 and 10 stimuli, as well as the habituation deficit after 15 footshocks compared to siblings not expressing the transgene (UN). $n \geq 12$ for all groups. ***C***, Adult-limited expression of $btk^{Ri\text{-}1}$in α/β MB neurons (IN) recapitulates the premature habituation after 6 and 10 shocks but not the failed habituation after 15 stimuli, compared to siblings not expressing the transgene (UN). $n \geq 10$ for all groups. ***D***, Adult-limited expression of $btk^{Ri\text{-}1}$in α'/β' MB neurons (IN) recapitulates the failed habituation to 15 footshocks, but not the premature habituation to 6 or 10 stimuli compared to siblings not expressing the transgene (UN). $n \geq 11$ for all groups.

Therefore, to investigate whether monoamine receptors are involved, we sought to antagonize them in the *btk* mutants, with the typical tricyclic antipsychotic clozapine, thought to primarily address dopamine, but also serotonin receptors and the atypical benzisothiazole risperidone, which is thought to be a more pronounced serotonergic antagonist, but also efficaciously antagonizes additional monoamine receptors (Brunton et al., 2010). Interestingly, administration of clozapine for 16–18 h before habituation training reversed in a dose-dependent manner the inability of btk^{M1} homozygotes (Fig. 6*A*; ANOVA: $F_{(2,28)} = 11.6054$, $p = 0.0002$; subsequent LSM: 5 μM $p = 0.0041$, 10 μM $p = 0.0001$ vs 0 μM) and $btk^{M1/M2}$ hetero-allelics (Fig. 6*B*; ANOVA: $F_{(2,30)} = 4.7128$, $p = 0.0172$; subsequent LSM: 5 μM $p = 0.0648$, 10 μM $p = 0.0048$ vs 0 μM) to habituate to 15 footshocks. A similar treatment with risperidone also reversed the defective habituation of btk^{M1} homozygotes, although at the high concentration of 10 μM, the effect of the drug appeared reduced (Fig. 6*C*; ANOVA: $F_{(3,44)} = 9.0647$, $p = 0.0001$; subsequent LSM: 0.1 μM $p = 0.0005$, 1 μM $p = 1.2 \times 10^{-5}$, 10 μM $p = 0.0066$ vs 0 μM). Assuming that clozapine antagonizes dopamine receptors, dBtk loss appears to affect their levels or activity. Since phenotypic reversal was elicited by risperidone, at least at the lower concentrations and serotonergic neurotransmission has not been reported to mediate footshock information to the MBs, it is likely that this drug also addresses dopaminergic receptors.

Importantly, clozapine treatment also reversed the defective footshock habituation of animals with pan-MB RNAi-mediated dBtk abrogation (Fig. 6*D*; ANOVA: $F_{(2,26)} = 5.2147$, $p = 0.0132$; subsequent LSM: 5 μM $p = 0.0531$, 10 μM $p = 0.0038$ vs 0 μM) suggesting that the drug reaches these neurons and mediates the observed phenotypic reversal upon acute dBtk attenuation therein. Significantly, both pharmaceuticals reversed the habituation defect to 15 shocks in animals with dBtk abrogation specifically in α'/β' MB neurons (Fig. 6*E*; ANOVA: $F_{(2,27)} = 19.1763$, $p < 0.0001$; subsequent LSM: 10 μM clozapine $p < 0.0001$, 10 μM risperidone $p < 0.0001$ vs untreated-0). As expected, dBtk attenuation in α/β neurons did not yield deficient habituation, and the drugs did not affect normal habituation to 15 footshocks (Fig. 6*F*; ANOVA: $F_{(2,26)} = 1.5268$, $p = 0.2376$). These results confirm that the habituation failure is specifically driven by dBtk attenuation within the α'/β' neurons and likely results from consequent excess or elevated signaling from one or more monoamine receptors within these neurons. In fact, Dop1R2 (Crittenden et al., 1998) and 5HT1B have been reported to be expressed in these neurons (Ries et al., 2017). Moreover, dBtk abrogation in α/β neurons did not affect habituation to 15 shocks, further suggest-

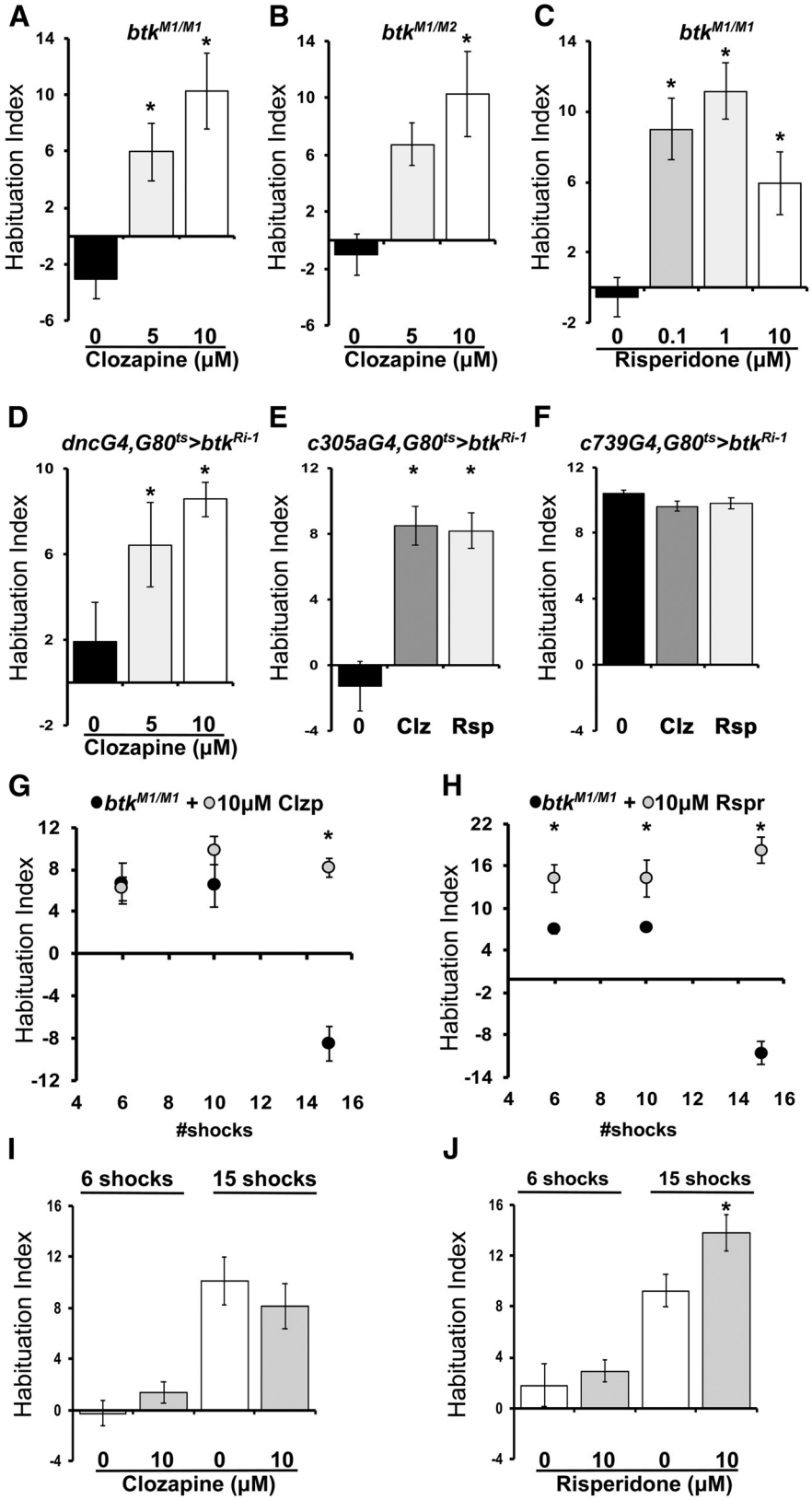

Figure 6. Antipsychotics selectively rescue the defective habituation of *btk* mutants. Habituation indices quantifying the difference in footshock avoidance following exposure to the indicated number of stimuli from that of same genotype naive flies are shown as the mean ± SEM for the indicated number of repetitions (*n*). Asterisks indicate significant differences from controls as detailed in the text. ***A***, Clozapine restores the defective habituation of btk^{M1} homozygotes. Compared with vehicle-treated mutants that do not habituate to 15 footshocks (0), habituation was significantly improved after treatment with 5 and 10 μM clozapine. $n \geq 9$. ***B***, Clozapine restores the defective habituation of $btk^{M1/M2}$ hetero-allelics, which present a strong habituation defect if treated only with vehicle (0). Clozapine at 5 and 10 μM restored habituation to 15 footshocks. $n \geq 8$ for all groups. ***C***, Risperidone restores the defective habituation of btk^{M1} homozygotes. The strong habituation defect to 15 shocks of vehicle-treated mutant homozygotes was reversed after treatment with 0.1, 1, and 10 μM risperidone. $n \geq 9$ for all groups. ***D***, The habituation defect precipitated by adult-limited pan-MB abrogation of dBtk is barely reversible by 5 μM, but restored with 10 μM clozapine compared with vehicle-treated animals (0). $n \geq 8$ for all groups. ***E***, Clozapine (10 μM) and risperidone (10 μM) restore the defective habituation phenotype precipitated by adult-limited abrogation of dBtk in α'/β' neurons. $n \geq 9$ for all groups. ***F***, Clozapine (10 μM) and risperidone (10 μM) do not affect the performance of flies where adult-limited abrogation of dBtk in α/β neurons. $n \geq 9$ for all groups. ***I***, Clozapine (10 μM) in control flies does not induce premature habituation after 6 shocks, or a change in habituation after 15 such stimuli relative to vehicle (0)-treated controls. $n \geq 9$ for all groups. ***J***, Risperidone (10 μM) in control flies does not induce premature habituation after 6 shocks, but yields elevated habituation after 15 such stimuli relative to vehicle (0)-treated controls. $n \geq 9$ for all groups. ***G***, Clozapine selectively restores the defective, but not the premature habituation of btk^{M1} homozygotes. Clozapine did not change the premature habituation to 6 or 10 stimuli, but reversed the habituation failure after 15 footshocks. $n \geq 10$ for all groups. ***H***, Risperidone restores the defective habituation, but also enhances the premature habituation of btk^{M1} homozygotes. Risperidone rescued the habituation defect after 15 stimuli, but also resulted in significantly higher habituation scores after 6 and 10 footshocks. $n \geq 10$ for all groups.

ing that the drugs specifically address consequences of dBtk abrogation within their α'/β' counterparts.

As *btk* mutants present both impaired latency and failed habituation, we wondered whether the antipsychotics can reverse both phenotypes. Interestingly, 10 μM clozapine did not alter the premature habituation of btk^{M1} homozygotes, but potently reversed their failure to habituate (Fig. 6*G*; ANOVA: $F_{(5,95)} = 7.8245$, $p < 0.0001$; subsequent LSM: 6 shocks $p = 0.8085$, 10 shocks $p = 0.1382$, 15 shocks $p = 7.3 \times 10^{-7}$ vs control). Risperidone also potently suppressed the habituation failure in the mutants (Fig. 6*H*; ANOVA: $F_{(5,73)} = 39.2195$, $p < 0.0001$; subsequent LSM: 6 shocks $p = 0.00014$, 10 shocks $p = 0.0017$, 15 shocks $p = 1 \times 10^{-19}$ vs control), but interestingly it increased significantly the shock avoidance of the mutants (Table 1), suggesting that it may actually induce hyperactivity, increased locomotion or enhance the aversion of the 45 V shock. In agreement, whereas 10 μM clozapine did not affect avoidance (Table 1), or habituation to 6 or 15 stimuli in control flies (Fig. 6*I*; ANOVA: $F_{(3,52)} = 14.7186$, $p < 0.0001$; subsequent LSM: 6 shocks $p = 0.3096$, 15 shocks $p = 0.3398$ vs control), risperidone (10 μM) consistently elevated 45 V avoidance in control flies (Table 1). However, this did not affect habituation to 6 shocks in control an-

imals, but appeared to mildly enhance habituation after 15 stimuli (Fig. 6*F*; ANOVA: $F_{(3,53)} = 16.9637$, $p < 0.0001$; subsequent LSM: 6 shocks $p = 0.5796$, 15 shocks $p = 0.0205$ vs control). Collectively these results suggest distinct mechanisms of action for the two antipsychotics in *Drosophila*, in agreement with their proposed activities in vertebrates. In fact, risperidone is a potent serotonin and dopamine antagonist, but unlike clozapine presents measurable activities against adrenergic and histamine receptors (PDSD Ki database; Roth et al., 2000), which may underlie the increase in avoidance or locomotion upon its administration.

Discussion

The response dynamics to repeated footshocks define two phases. Avoidance is initially maintained for 8–10 stimuli, followed by its rapid attenuation to an apparently asymptotic habituated response by the 15th stimulus (Acevedo et al., 2007; Figs. 4*A*,*B*, 5*A*,*B*, controls). Neurotransmission from α/β MB neurons is required to maintain stimulus responsiveness in the initial latency phase (Acevedo et al., 2007) and significantly we now demonstrate that synaptic activity from their α'/β' counterparts is essential to facilitate the subsequent habituation phase (Fig. 2*K*). Therefore, the two habituation phases are mediated by distinct MB neurons.

Because neurotransmission from different MB neurons is required both to prevent and to induce the habituated response, it is likely that it engages distinct α/β and α'/β' MB output neurons (MBONs; Takemura et al., 2017). We hypothesize that these potentially antagonistic signals are relayed to neurons driving the choice to avoid or ignore the footshocks in a manner akin to neurons toggling attractive and aversive odor responses in *Drosophila* (Yamazaki et al., 2018). It is unclear at the moment how the activities of the two types of MB neurons are coordinated upon repeated stimulation as indicated by the response dynamics (Acevedo et al., 2007; Fig. 3*A*,*C*–*F*). However, the current data predict that synaptic transmission from α/β neurons requisite for maintenance of habituation latency precedes α'/β' activation, which facilitates habituation onset. Nevertheless, how neurotransmission from α/β neurons is attenuated after a relatively set number of stimuli and why it precedes activation of α'/β' neurons is unclear at the moment. Significantly, abrogation of dBtk in adult α/β neurons yielded strong latency attenuation (Fig. 3*E*), whereas loss from α'/β' neurons did not affect latency, but eliminated habituation (Fig. 3*F*). Therefore, although α/β and α'/β' activities may be coordinated, they appear independent.

Importantly, we describe the first mutant with specific defects in footshock habituation and demonstrate that dBtk activity is acutely required in adult MBs for both phases (Figs. 1*B*,*C*, 3*A*), in accord with its apparent expression within α/β and α'/β' neurons. The premature habituation upon dBtk abrogation suggests reduced or dysregulated neurotransmission from α/β neurons (Acevedo et al., 2007; Fig. 2*K*), whereas the habituation defect is consistent with attenuated neurotransmission from their α'/β' counterparts. As Btk is involved in regulation of actin cytoskeleton dynamics (Corneth et al., 2016) and given the involvement of cortical actin in neurotransmitter release (Rust and Maritzen, 2015), the kinase may modulate directly or indirectly the responsiveness to afferent signaling and subsequent neurotransmission to MBONs from both types of MB neurons. In agreement with this notion, dBtk loss specifically from α/β and α'/β' neurons phenotypically mimics Shibire^{ts}-dependent silencing of their synaptic output (Figs. 3*I*–*K*, 5*C*,*D*).

Alternatively, dBtk may be involved in footshock signal reception at least by the α'/β' neurons, which specifically respond to the dopamine and serotonin receptor antagonists clozapine and risperidone upon attenuation of the kinase. Given that footshock signals are relayed to the MBs by dopamine (Cognigni et al., 2018) and these neurons contain at least one dopamine (Crittenden et al., 1998) and serotonin (Ries et al., 2017) receptors, dBtk loss may alter the number or activity of these receptors within these neurons. Interestingly, mammalian Btk is implicated in regulation of G-protein-coupled receptor (GPCR) signaling (Corneth et al., 2016) and importantly, clozapine and risperidone address and antagonize primarily the typical serotonin and dopamine GPCRs (Naheed and Green, 2001; Brunton et al., 2010). This is in accord with the notion that in α'/β' neurons dBtk negatively regulates dopamine and/or serotonin receptor signaling or levels. It follows that dBtk loss would increase the levels or activity of one or more of these receptors, altering MB activation threshold and reducing synaptic transmission to efferents mediating the habituated response. Clozapine and risperidone-mediated antagonism of this putative α'/β' overactivation upon repetitive footshock may restore regulated neurotransmission mediating normal habituation. In contrast, in α/β neurons, which do not appear to respond to dopamine or serotonin receptor antagonism, dBtk may regulate neurotransmitter release via its modulation of actin dynamics (Corneth et al., 2016). Impaired neurotransmission from α/β neurons may also underlie the reduced latency to suppress the olfactory jump response of *btk* mutants (Asztalos et al., 2007).

Therefore, we propose that dBtk may differentially regulate neuronal activities in α/β and α'/β' neurons. In α/β by positively regulating neurotransmitter release, which is impaired upon dBtk loss, leading to shortened latency and premature habituation. In contrast, in α'/β' neurons dBtk could have primarily a postsynaptic role, by negatively regulating the number or downstream signaling of dopamine and/or serotonin receptors. Elevated intra-α'/β' monoamine receptor signaling upon dBtk loss may lead to dysregulation of downstream synaptic activity and functional silencing of neurotransmission required to facilitate footshock habituation onset. Ongoing experiments aim to test these hypotheses.

It is intriguing that schizophrenia patients also present habituation defects manifested as failures in prepulse inhibition (Braff et al., 2001; Akdag et al., 2003; Ludewig et al., 2003; Meincke et al., 2004; van Os and Kapur, 2009), where a weak prestimulus inhibits the reaction to a following strong startling stimulus. These defects are thought to reflect inability to devalue inconsequential stimuli (Braff et al., 2001; Swerdlow et al., 2008) and can be reversed with antipsychotics including clozapine and risperidone implicating excessive or dysregulated dopaminergic and/or serotonergic signaling similar to *btk* mutants. Recent genome-wide association studies (GWASs) suggested linkage of polymorphisms in a number of genes to schizophrenia and other neuropsychiatric disorders (Schizophrenia Working Group of the Psychiatric Genomics Consortium, 2014; Fromer et al., 2016; Roussos et al., 2016), but human Btk was not among them. Nevertheless, given that habituation deficits in flies and humans are reversible with antipsychotics, it is possible that mutations in *Drosophila* orthologs of genes linked to schizophrenia by GWAS may also present defective footshock habituation and provide expedient experimental validation of their effects on signaling within and between CNS neurons.

References

Acevedo SF, Froudarakis EI, Kanellopoulos A, Skoulakis EM (2007) Protection from premature habituation requires functional mushroom bodies in *Drosophila*. Learn Mem 14:376–384.

Akdag SJ, Nestor PG, O'Donnell BF, Niznikiewicz MA, Shenton ME, McCarley RW (2003) The startle reflex in schizophrenia: habituation and personality correlates. Schizophr Res 64:165–173.

Aso Y, Grübel K, Busch S, Friedrich AB, Siwanowicz I, Tanimoto H (2009) The mushroom body of adult *Drosophila* characterized by GAL4 drivers. J Neurogenet 23:156–172.

Asztalos Z, Baba K, Yamamoto D, Tully T (2007) The fickle mutation of a cytoplasmic tyrosine kinase effects sensitization but not dishabituation in *Drosophila melanogaster*. J Neurogenet 21:59–71.

Baba K, Takeshita A, Majima K, Ueda R, Kondo S, Juni N, Yamamoto D (1999) The *Drosophila* Bruton's tyrosine kinase (Btk) homolog is required for adult survival and male genital formation. Mol Cell Biol 19:4405–4413.

Barkus C, Sanderson DJ, Rawlins JN, Walton ME, Harrison PJ, Bannerman DM (2014) What causes aberrant salience in schizophrenia? A role for impaired short-term habituation and the GRIA1 (GluA1) AMPA receptor subunit. Mol Psychiatry 19:1060–1070.

Braff DL, Geyer MA, Swerdlow NR (2001) Human studies of prepulse inhibition of startle: normal subjects, patient groups, and pharmacological studies. Psychopharmacology 156:234–258.

Brisch R, Saniotis A, Wolf R, Bielau H, Bernstein HG, Steiner J, Bogerts B, Braun AK, Jankowski Z, Kumaritlake J, Henneberg M, Gos T (2014) The role of dopamine in schizophrenia from a neurobiological and evolutionary perspective: old fashioned, but still in vogue. Front Psychiatry 5:47.

Brunton L, Chabner B, Knollman B (2010) Goodman and Gilman's the pharmacological basis of therapeutics, Ed 12. New York: McGraw Hill.

Cervantes-Sandoval I, Phan A, Chakraborty M, Davis RL (2017) Reciprocal synapses between mushroom body and dopamine neurons form a positive feedback loop required for learning. eLife 6:e23789.

Cognigni P, Felsenberg J, Waddell S (2018) Do the right thing: neural network mechanisms of memory formation, expression and update in *Drosophila*. Curr Opin Neurobiol 49:51–58.

Schizophrenia Working Group of the Psychiatric Genomics Consortium (2014) Biological insights from 108 schizophrenia-associated genetic loci. Nature 511:421–427.

Corneth OB, Klein Wolterink RG, Hendriks RW (2016) BTK signaling in B cell differentiation and autoimmunity. Curr Top Microbiol Immunol 393:67–105.

Crittenden JR, Skoulakis EM, Han KA, Kalderon D, Davis RL (1998) Tripartite mushroom body architecture revealed by antigenic markers. Learn Mem 5:38–51.

D'Cruz AM, Ragozzino ME, Mosconi MW, Shrestha S, Cook EH, Sweeney JA (2013) Reduced behavioral flexibility in autism spectrum disorders. Neuropsychology 27:152–160.

Fromer M, Roussos P, Sieberts SK, Johnson JS, Kavanagh DH, Perumal TM, Ruderfer DM, Oh EC, Topol A, Shah HR, Klei LL, Kramer R, Pinto D, Gümüş ZH, Cicek AE, Dang KK, Browne A, Lu C, Xie L, Readhead B, et al. (2016) Gene expression elucidates functional impact of polygenic risk for schizophrenia. Nat Neurosci 19:1442–1453.

Gai Y, Liu Z, Cervantes-Sandoval I, Davis RL (2016) *Drosophila* SLC22A transporter is a memory suppressor gene that influences cholinergic neurotransmission to the mushroom bodies. Neuron 90:581–595.

Gillberg C (2003) Deficits in attention, motor control and perception: a brief review. Arch Dis Child 88:904–910.

Gouzi JY, Moressis A, Walker JA, Apostolopoulou AA, Palmer RH, Bernards A, Skoulakis EM (2011) The receptor tyrosine kinase Alk controls neurofibromin functions in *Drosophila* growth and learning. PLoS Genet 7:e1002281.

Gouzi JY, Bouraimi M, Roussou IG, Moressis A, Skoulakis EMC (2018) The *Drosophila* Receptor Tyrosine Kinase Alk Constrains Long-Term Memory Formation. J Neurosci. 38:7701–7712.

Gregory RJ, Kammermeyer KL, Vincent WS 3rd, Wadsworth SG (1987) Primary sequence and developmental expression of a novel *Drosophila melanogaster src* gene. Mol Cell Biol 7:2119–2127.

Guven-Ozkan T, Davis RL (2014) Functional neuroanatomy of *Drosophila* olfactory memory formation. Learn Mem 21:519–526.

Hamada-Kawaguchi N, Yamamoto D (2017) Ovarian polarity and cell shape determination by Btk29A in *Drosophila*. Genesis 55:e23042.

Hamada-Kawaguchi N, Nore BF, Kuwada Y, Smith CI, Yamamoto D (2014) Btk29A promotes Wnt4 signaling in the niche to terminate germ cell proliferation in *Drosophila*. Science 343:294–297.

Horiuchi J (2019) Recurrent loops: incorporating prediction error and semantic/episodic theories into *Drosophila* associative memory models. Genes Brain Behav 2019:e12567.

Jansiewicz EM, Newschaffer CJ, Denckla MB, Mostofsky SH (2004) Impaired habituation in children with attention deficit hyperactivity disorder. Cogn Behav Neurol 17:1–8.

Kalita J, Bhoi SK, Misra UK (2014) Is lack of habituation of evoked potential a biological marker of migraine? Clin J Pain 30:724–729.

Kesby J, Eyles D, McGrath J, Scott J (2018) Dopamine, psychosis and schizophrenia: the widening gap between basic and clinical neuroscience. Transl Psychiatry 8:30.

Kitamoto T (2001) Conditional modification of behavior in *Drosophila* by targeted expression of a temperature-sensitive *shibire* allele in defined neurons. J Neurobiol 47:81–92.

Krashes MJ, Keene AC, Leung B, Armstrong JD, Waddell S (2007) Sequential use of mushroom body neuron subsets during *Drosophila* odor memory processing. Neuron 53:103–115.

Lee T, Luo L (1999) Mosaic analysis with a repressible cell marker for studies of gene function in neuronal morphogenesis. Neuron 22:451–461.

Ludewig K, Geyer MA, Vollenweider FX (2003) Deficits in prepulse inhibition and habituation in never-medicated, first-episode schizophrenia. Biol Psychiatry 54:121–128.

Massa J, O'Desky IH (2012) Impaired visual habituation in adults with ADHD. J Atten Disord 16:553–561.

Mattsson P, Vihinen M, Smith C (1996)) X-linked agammaglobulinemia (XLA): a genetic tyrosine kinase (Btk) disease. Bioessays 18:825–834.

McDiarmid TA, Bernardos AC, Rankin CH (2017) Habituation is altered in neuropsychiatric disorders: a comprehensive review with recommendations for experimental design and analysis. Neurosci Biobehav Rev 80: 286–305.

McGuire SE, Le PT, Osborn AJ, Matsumoto K, Davis RL (2003) Spatiotemporal rescue of memory dysfunction in *Drosophila*. Science 302:1765–1768.

McGuire S, Roman G, Davis R (2004) Gene expression systems in *Drosophila*: a synthesis of time and space. Trends Genet 20:384–391.

Meincke U, Light GA, Geyer MA, Braff DL, Gouzoulis-Mayfrank E (2004) Sensitization and habituation of the acoustic startle reflex in patients with schizophrenia. Psychiatry Res 126:51–61.

Messaritou G, Leptourgidou F, Franco M, Skoulakis EM (2009) A third functional isoform enriched in mushroom body neurons is encoded by the *Drosophila* 14–3-3zeta gene. FEBS Lett 583:2934–2938.

Naheed M, Green B (2001) Focus on clozapine. Curr Med Res Opin 17:223–229.

Paranjpe P, Rodrigues V, VijayRaghavan K, Ramaswami M (2012) Gustatory habituation in *Drosophila* relies on rutabaga (adenylate cyclase)-dependent plasticity of GABAergic inhibitory neurons. Learn Mem 19: 627–635.

Pavlopoulos E, Anezaki M, Skoulakis EM (2008) Neuralized is expressed in the α/β lobes of adult *Drosophila* mushroom bodies and facilitates olfactory long-term memory formation. Proc Natl Acad Sci U S A 105:14674–14679.

Ramaswami M (2014) Network plasticity in adaptive filtering and behavioral habituation. Neuron 82:1216–1229.

Rankin C, Abrams T, Barry R, Bhatnagar S, Clayton D, Colombo J, Coppola G, Geyer M, Glanzman D, Marsland S, McSweeney F, Wilson D, Wu CF, Thompson R (2009) Habituation revisited: an updated and revised description of the behavioral characteristics of habituation. Neurobiol Learn Mem 92:135–138.

Ries AS, Hermanns T, Poeck B, Strauss R (2017) Serotonin modulates a depression-like state in *Drosophila* responsive to lithium treatment. Nat Commun 8:15738.

Robinson D (2007) CNS receptor partial agonists: a new approach to drug discovery. Primary Psychiatry 14:22–24.

Roth BL, WK Kroeze WK, S Patel S, Lopez E (2000) The multiplicity of serotonin receptors: uselessly diverse molecules or an embarrasment of riches? Neuroscientist 6:252–262.

Roulier E, Panzer S, Beckendorf SK (1998) The Tec29 tyrosine kinase is required during *Drosophila* embryogenesis and interacts with Src64 in ring canal development. Mol Cell 1:819–829.

Roussos PG, Zouraraki C, Fullard JF, Karagiorga VE, Tsapakis EM, Petraki Z, Siever LJ, Lencz T, Malhotra A, Spanaki C, Bitsios P (2016) The relationship of common risk variants and polygenic risk for schizophrenia to sensorimotor gating. Biol Psychiatry 79:988–996.

Rust MB, Maritzen T (2015) Relevance of presynaptic actin dynamics for synapse function and mouse behavior. Exp Cell Res 335:165–171.

Semelidou O, Acevedo S, Skoulakis EM (2018) Temporally specific engagement of distinct neuronal circuits regulating olfactory habituation in *Drosophila*. eLife 7:e39569.

Shyu WH, Chiu TH, Chiang MH, Cheng YC, Tsai YL, Fu TF, Wu T, Wu CL (2017) Neural circuits for long-term water-reward memory processing in thirsty *Drosophila*. Nat Commun 8:15230.

Siniatchkin M, Kropp P, Gerber WD (2003) What kind of habituation is impaired in migraine patients? Cephalalgia 23:511–518.

Sokal RR, Rohlf FJ (1981) Biometry the principles and practice of statistics in biological research, Ed 2. New York: WH Freeman.

Sunouchi K, Koganezawa M, Yamamoto D (2016) Requirement of the Tec family tyrosine kinase Btk29a for courtship memory in *Drosophila* males. Arch Insect Biochem Physiol 91:165–174.

Swerdlow NR, Weber M, Qu Y, Light GA, Braff DL (2008) Realistic expectations of prepulse inhibition in translational models for schizophrenia research. Psychopharmacology 199:331–388.

Takemura SY, Aso Y, Hige T, Wong A, Lu Z, Xu CS, Rivlin PK, Hess H, Zhao T, Parag T, Berg S, Huang G, Katz W, Olbris DJ, Plaza S, Umayam L, Aniceto R, Chang LA, Lauchie S, Ogundeyi O, et al. (2017) A connectome of a learning and memory center in the adult *Drosophila* brain. eLife 6:e26975.

Tei S, Fujino J, Hashimoto R, Itahashi T, Ohta H, Kanai C, Kubota M, Nakamura M, Kato N, Takahashi H (2018) Inflexible daily behaviour is associated with the ability to control an automatic reaction in autism spectrum disorder. Sci Rep 8:8082.

Thompson R, Spencer W (1966) Habituation: a model phenomenon for the study of neuronal substrates of behavior. Psychol Rev 73:16–43.

Tillman B, Pauff J, Satyanarayana G, Talbott M, Warner J (2018) Systematic review of infectious events with the Bruton tyrosine kinase inhibitor ibrutinib in the treatment of hematologic malignancies. Eur J Haematol 100:325–334.

Tsikala G, Karagogeos D, Strigini M (2014) Btk-dependent epithelial cell rearrangements contribute to the invagination of nearby tubular structures in the posterior spiracles of *Drosophila*. Dev Biol 396:42–56.

van Os J, Kapur S (2009) Schizophrenia. Lancet 374:635–645.

Venken KJ, Schulze KL, Haelterman NA, Pan H, He Y, Evans-Holm M, Carlson JW, Levis RW, Spradling AC, Hoskins RA, Bellen HJ (2011) MiMIC: a highly versatile transposon insertion resource for engineering *Drosophila* melanogaster genes. Nat Methods 8:737–743.

Yamazaki D, Hiroi M, Abe T, Shimizu K, Minami-Ohtsubo M, Maeyama Y, Horiuchi J, Tabata T (2018) Two parallel pathways assign opposing odor valences during *Drosophila* memory formation. Cell Rep 22:2346–2358.

Ysebaert L, Michallet AS (2014) Bruton's tyrosine kinase inhibitors: lessons learned from bench-to-bedside (first) studies. Curr Opin Oncol 26:463–468.

Cellular/Molecular

Drosophila Tau Negatively Regulates Translation and Olfactory Long-Term Memory, But Facilitates Footshock Habituation and Cytoskeletal Homeostasis

Katerina Papanikolopoulou,[1*] Ilianna G. Roussou,[1*] Jean Y. Gouzi,[1*] Martina Samiotaki,[2] George Panayotou,[2] Luca Turin,[1] and Efthimios M.C. Skoulakis[1]

[1]Institute for Fundamental Biomedical Research, and [2]Institute for Bioinnovation, Biomedical Sciences Research Centre "Alexander Fleming," 16672 Vari, Greece

Although the involvement of pathological tau in neurodegenerative dementias is indisputable, its physiological roles have remained elusive in part because its abrogation has been reported without overt phenotypes in mice and *Drosophila*. This was addressed using the recently described *Drosophila tau*^{KO} and Mi{MIC} mutants and focused on molecular and behavioral analyses. Initially, we show that *Drosophila* tau (dTau) loss precipitates dynamic cytoskeletal changes in the adult *Drosophila* CNS and translation upregulation. Significantly, we demonstrate for the first time distinct roles for dTau in adult mushroom body (MB)-dependent neuroplasticity as its downregulation within $\alpha'\beta'$ neurons impairs habituation. In accord with its negative regulation of translation, dTau loss specifically enhances protein synthesis-dependent long-term memory (PSD-LTM), but not anesthesia-resistant memory. In contrast, elevation of the protein in the MBs yielded premature habituation and depressed PSD-LTM. Therefore, tau loss in *Drosophila* dynamically alters brain cytoskeletal dynamics and profoundly affects neuronal proteostasis and plasticity.

Key words: *Drosophila*; habituation; memory; proteome; tau

Significance Statement

We demonstrate that despite modest sequence divergence, the *Drosophila* tau (dTau) is a true vertebrate tau ortholog as it interacts with the neuronal microtubule and actin cytoskeleton. Novel physiological roles for dTau in regulation of translation, long-term memory, and footshock habituation are also revealed. These emerging insights on tau physiological functions are invaluable for understanding the molecular pathways and processes perturbed in tauopathies.

Introduction

Tau is a microtubule-associated protein (MAP), a neuronal protein enriched in axons. Through its interaction with tubulin, tau is involved in the regulation of neuronal polarity, axon outgrowth, and axonal transport mediated by kinesin and dynein motor proteins. Apart from its axonal function, several studies indicate alternative cellular functions of tau proteins at the synapse and in the nucleus, as well as interactions with the plasma membrane and the actin cytoskeleton (Sotiropoulos et al., 2017).

Under pathological conditions, tau undergoes post-translational modifications that trigger its pathogenicity (Wang and Mandelkow, 2016). The prevalence of tauopathies and the current lack of prevention or treatment mandate elucidation of the physiological functions of tau, which are requisite to understanding the molecular etiology of its pathogenicity. Transgenic expression of human tau isoforms in *Drosophila* has contributed to identification of novel tau phosphorylation sites (Nishimura et al., 2004; Papanikolopoulou and Skoulakis, 2011, 2015) and molecular pathways contributing to neuronal dysfunction and toxicity (Shulman and Feany, 2003; Chatterjee et al., 2009). However, the physiological function of the endogenous *Drosophila* protein has not been fully elucidated.

Drosophila possesses a single *tau* gene encoding multiple transcripts and potential protein isoforms ostensibly via alternative splicing (http://flybase.org/reports/FBgn0266579). It contains the characteristic conserved tubulin binding repeats with 46%

Received Feb. 18, 2019; revised July 24, 2019; accepted Aug. 7, 2019.

Author contributions: K.P., I.G.R., J.Y.G., G.P., L.T., and E.M.C.S. designed research; K.P., I.G.R., J.Y.G., and M.S. performed research; K.P., I.G.R., J.Y.G., M.S., and E.M.C.S. analyzed data; K.P. and E.M.C.S. wrote the paper.

This research was supported by a grant from the Stavros Niarchos Foundation to the Biomedical Sciences Research Center "Alexander Fleming," as part of the initiative of the Foundation to support the Greek research center ecosystem. We thank L. Partridge, C.S. Lopes, and the Bloomington Stock Center for fly strains. We also thank S. Baumgartner, D. Buttgereit, N. Lowe, and DSHB for antibodies. Finally, we thank Babis Savakis for comments on the manuscript and helpful suggestions.

*K.P., I.G.R., and J.Y.G. contributed equally to this work.

The authors declare no competing financial interests.

Correspondence should be addressed to Katerina Papanikolopoulou at papanikolopoulou@fleming.gr.

https://doi.org/10.1523/JNEUROSCI.0391-19.2019

identity and 66% similarity to the corresponding human tau sequences (Heidary and Fortini, 2001). Despite the similarity, the presence of unique and divergent sequences outside the repeats, and the presence of an apparent fifth repeat (Gistelinck et al., 2012) have led to questions as to whether the fly protein functions as a physiological tau ortholog (Chen et al., 2007).

Drosophila tau (dTau) is expressed in the developing and adult CNS, prominently in photoreceptors (Heidary and Fortini, 2001), cell bodies, and neuropils of the visual system and the central brain (Bolkan and Kretzschmar, 2014). Functional regulation by phosphorylation seems conserved in flies, since dTau possesses multiple SKXGS motifs and has been shown to be phosphorylated (Doerflinger et al., 2003; Burnouf et al., 2016). Examination of its physiological functions was attempted with the generation of a knock-out (*tau*^{KO}) mutant lacking exons 2–6 including the tubulin-binding repeats (Burnouf et al., 2016). However, obvious phenotypes were not reported for these mutants, and apparently this was not a consequence of the upregulation of other microtubule-associated proteins, as in mice (Harada et al., 1994), furthering the notion that dTau may not be an ortholog of the vertebrate protein. This prompted us to determine whether dTau loss affects the neuronal cytoskeleton, as would be expected if functionally conserved with its vertebrate homolog.

Reduced tau characterizes humans with variants of frontotemporal lobar degeneration with granulin (*GRN*) mutations (Zhukareva et al., 2001, 2003; Mackenzie et al., 2009; Papegaey et al., 2016). In addition, a deletion encompassing the *tau* gene is linked to mental retardation, although it also removes adjacent genes (Koolen et al., 2006; Shaw-Smith et al., 2006), making assignment of the pathological phenotype to tau loss difficult. Therefore, we also investigated whether dTau loss also precipitates phenotypes in learning and memory as upon human tau expression in the fly CNS (Papanikolopoulou et al., 2010; Papanikolopoulou and Skoulakis, 2015; Sealey et al., 2017).

Materials and Methods

Drosophila culture and strains. Flies were cultured on standard wheat-flour-sugar food supplemented with soy flour and $CaCl_2$, at 25°C in 50–70% relative humidity in a 12 h light/dark cycle. *tau*^{KO} mutant flies (Burnouf et al., 2016) were a gift from Dr. L. Partridge (Max Planck Institute for Biology of Aging, Cologne, Germany). The mutant was backcrossed into the resident Cantonised-*w*^{1118}control isogenic background for six generations. The transposon insertion mutant Mi{MIC}tau[MI03440] was obtained from the Bloomington Stock Center (catalog #BL37602), and Mi{PT-GFSTF.0}tau[MI03440-GFSTF.0] (catalog #BL60199) was a gift from Dr. Carla Sofia Lopes, Universidade do Porto (Porto, Portugal). The Gal4 driver lines used in this work were as follows: elav[C155]-Gal4 (Robinow and White, 1988), LeoMB-Gal4 (Messaritou et al., 2009), dnc-Gal4 (BL48571; Aso et al., 2009), and MB247-Gal4 and c739-Gal4 (Zars et al., 2000). The Gal4 α'/β' c305a driver was a gift of Dr. S. Waddell (University of Oxford, Oxford, UK). The c739-Gal4; TubGal80^{ts} line was from Dr. G. Roman (University of Mississippi, Oxford, MS). The TubGal80^{ts} transgene (McGuire et al., 2004) was introduced into all other Gal4 strains through standard genetic crosses.

To generate *UAS-Flag-dtau* a NotI/XbaI fragment containing the RA *dtau* cDNA (Mershin et al., 2004) was subcloned into pUAST-FLAG vector (Kosmidis et al., 2010). The *dtau* RNA interference (RNAi) target region was selected to be a 632 bp BglII-BamHI fragment from the entire *dtau* cDNA to target all tau splice forms. UAS-dTauRNAi was designed as a genomic-cDNA hybrid consisting of the BglII-BamHI fragment cloned into pUAST vector in forward and reverse orientations. Germline transformants were obtained in the Canton S-*w*^{1118} genetic background using standard methods. A second *dtau* RNAi line was obtained from the Bloomington Stock Center (catalog #BDSC-40875).

Proteomic analysis. Three to four biological and two technical replicas from each genotype (*w*^{1118} vs backcrossed *tau*^{KO} and Elav-Gal4; TubGal80^{ts} > + vs Elav-Gal4; TubGal80^{ts} >dtauRNAi induced for 3 d at 30°C) were used for this experiment. Briefly, 10 fly brains per genotype were dissected in PBS and, after removal of the optic lobes, were lysed by boiling for 3 min in 50 μl of a solution containing 4% SDS, 100 mM fresh DTT, and 10 mM Tris, pH 7.6. The lysates were processed according to the filter-aided sample preparation (FASP) protocol using spin filter devices with 10 kDa cutoff (catalog # VN01H02, Sartorius; Wiśniewski et al., 2009). Proteins were subsequently subjected to alkylation and trypsin digestion (1 μg trypsin/ LysC mix mass spectrometry grade; Promega). Peptide products were analyzed by nano-LC-MS/MS (liquid chromatography with tandem mass spectrometry) using a LTQ Orbitrap XL mass spectrometer (Thermo Fisher Scientific) coupled to a nano-LC high-performance liquid chromatography (RSLCnano, Thermo Fisher Scientific) as described in the study by Terzenidou et al. (2017).

The raw files were analyzed using MaxQuant 1.5.3.30 (Tyanova et al., 2016a) against the complete Uniprot proteome of *Drosophila melanogaster* (Downloaded 1 April 2016/42,456 entries) and a common contaminants database by the Andromeda search engine. Protein abundance was calculated on the basis of the normalized spectral protein intensity as label-free quantitation (LFQ intensity). The statistical analysis was performed with Perseus (version 1.5.3.2) using a two-sample *t* test with a false discovery rate (FDR) value of 0.05 (Tyanova et al., 2016b).

Western blot analyses. Single female fly heads at 1–3 d posteclosion were homogenized in 1× Laemmli buffer (50 mM Tris, pH 6.8, 100 mM DTT, 5% 2-mercaptoethanol, 2% SDS, 10% glycerol, and 0,01% bromophenol blue). Proteins were transferred to PVDF membrane and probed with the following monoclonal antibodies: N2 7A1 Armadillo [Developmental Studies Hybridoma Bank (DSHB)] at 1:200, E7 β-tubulin 97EF (DSHB) at 1:250, ADL84.12 Lamin Dm0 (DSHB) at 1:100, acetyl-α-tubulin (Cell Signaling Technology) at 1:2000, FLAGM2 (Sigma-Aldrich) at 1:1000, and 8C3 syntaxin (DSHB) at 1:3000. Anti-αTub84B+D guinea pig polyclonal antibody (1:300) was a gift from Stefan Baumgartner (Lund University, Sweden) (Fahmy et al., 2014), rabbit polyclonal anti-βTub56D (1:1000) was from Dr. Detlev Buttgereit (Philipps Universität Marburg, Germany) (Buttgereit et al., 1991) and rabbit polyclonal anti-dTau was from Dr. Nick Lowe (Cambridge University, UK) (1:2000). Appropriate HRP-conjugated secondary antibodies were applied at 1:5000. Proteins were visualized with chemiluminescence (ECL Plus, GE Healthcare), and signals were quantified by densitometry with the Image Lab 5.2 program (Bio-Rad). Results were plotted as mean ± SEM values from two or three independent experiments. The data were analyzed by standard parametric statistics (*t* tests) as indicated in the text.

Confocal microscopy. The protein-trap *Drosophila* strain Mi{PT-GFSTF.0}tau[MI03440-GFSTF.0] was used to examine the expression pattern of dTau in the adult brain. Flies were dissected in cold PBS, fixed in 4% paraformaldehyde for 15 min, and imaged by laser-scanning confocal microscopy (TCS SP8, Leica). F-actin levels were determined in adult fly brains from three independent experiments as described previously (Fulga et al., 2007; Kotoula et al., 2017).

F-actin and microtubule precipitation assay. Total F-actin has been isolated as in (Fulga et al., 2007). Briefly four brains from each genotype (1- to 3-d-old flies) were dissected in cold PBS and transferred in 25 μl of homogenization buffer (100 mM Na_2HPO_4–NaH_2PO_4 at pH 7.2, 2 mM ATP, 2 mM $MgCl_2$), supplemented with phosphatase (Sigma-Aldrich) and protease (Thermo Fisher Scientific) inhibitor cocktails. After homogenization, Invitrogen biotinylated phalloidin (Thermo Fisher Scientific) was added to a final concentration of 0.15 units per brain followed by precipitation with streptavidin-coupled Invitrogen Dynabeads (Thermo Fisher Scientific). The precipitated material and supernatant were probed for dTau (1:2000) and actin (1:1000; Sigma-Aldrich). To control for nonspecific binding, the same protocol was followed without the addition of biotinylated phalloidin to the lysate. Microtubule-binding experiments were based on established methods (Feuillette et al., 2010; Gorsky et al., 2017). Briefly, Taxol-stabilized microtubules have been isolated from head extracts by ultracentrifugation at 100,000 ×

g for 1 h. Soluble and insoluble fractions were probed with E7 and acetyl-α-tubulin.

Puromycin assay. The protocol was adapted from the studies by Belozerov et al. (2014) and Deliu et al. (2017). Briefly, flies were starved for 4 h and transferred onto 5% sucrose-1% low-melting agarose supplemented with 600 μM puromycin (Santa Cruz Biotechnology) for 16 h. Six female fly heads were homogenized in 20 μl of buffer containing 20 mM Tris-HCl pH 8.0, 137 mM NaCl, 1 mM EDTA, 25% glycerol, 1% NP-40, and a protease inhibitor cocktail (Thermo Fisher Scientific). Samples were run on SDS 10% PAGE gels, proteins were transferred to PVDF membrane and probed sequentially with anti-puromycin (Millipore) at 1:2000 and anti-syntaxin (8C3, DSHB) at 1:3000. Anti-mouse HRP-conjugated secondary antibody was applied at 1:5000. Proteins were visualized with chemiluminescence (ECL Plus, GE Healthcare), and signals corresponding to the molecular weight region 30–125 kDa were quantified by densitometry with Image Lab 5.2 (Bio-Rad). Results were plotted as mean ± SEM values from two independent experiments. The data were analyzed by standard parametric statistics (*t* tests), as indicated in the text.

Behavioral analyses. All experiments were performed in mixed sex populations. Animals bearing TubG80^{ts} were raised at 18°C until adulthood, and transgenes were induced maximally by placing 2- to 5-d-old flies at 30°C for 72 h. Flies were kept at the training temperature (25°C) for 30 min before the behavioral assays. Other flies or mutants were raised at 25°C throughout development, adulthood, and behavioral testing. Olfactory memory in the negatively reinforced paradigm coupling aversive odors as conditioned stimuli (CS) with the electric shock unconditioned stimulus (US; Tully and Quinn, 1985) was performed essentially as described previously (Pavlopoulos et al., 2008). The aversive odors used were benzaldehyde and 3-octanol, diluted in isopropylmyristate (Fluka). Electric foot shock avoidance and habituation to electric shock experiments were performed under the conditions described in the study by Acevedo et al. (2007). Each genotype was tested in yoked experiments whereby estimation of the avoidance was immediately followed by habituation training and testing of the same genotype. Hence, all data consist of yoked pairs per genotype. The avoidance fraction was calculated by dividing the number of naive flies preferring shock by the total number of flies. After exposure of the flies to several 1.2 s electric shocks at 45 V, the habituation fraction was calculated by dividing the number of flies preferring shock by the total number of flies. Finally, the habituation index was calculated by subtracting the avoidance fraction from the habituation fraction and multiplying by 100. Cycloheximide treatment has been performed as in the study by Plaçais et al. (2017). Briefly, flies were treated with 35 mM CXM (cycloheximide) in 5% sucrose for 16 h before training at 30°C. After training and until memory test, flies were kept on regular food.

Learning experiments described in Figure 4 were performed as in the study by Cervantes-Sandoval et al. (2016). Briefly, training for 3 min learning experiments consisted of 1 single session of 12 US/CS pairings of 90 V electric shocks (US) with one odor (CS^+) over 1 min, followed after a 30 s purge with air, by the presentation of the second odor (CS^-) without shocks for 1 min. Training for reversal learning consisted of a standard conditioning protocol (CS^+ = OCT, CS^- = BNZ; reciprocal, CS^+ = BNZ, CS^- = OCT) followed by 1 min of air and then the reverse odor–shock contingency (CS^+ = BNZ, CS^- = OCT; reciprocal, CS^+ = OCT, CS^- = BNZ). Testing was performed immediately after reversal training.

Experimental design and statistical analysis. For all experiments, controls and experimental genotypes were tested in the same session in balanced design. The order of training and testing these genotypes was randomized. We required an experimental result to be significantly different from both genetic controls. Data are shown as the mean ± SEM. Data were analyzed parametrically with the JMP 7.1 statistical software package (SAS Institute) as described previously (Gouzi et al., 2018). Following initial ANOVA, planned multiple comparisons were performed, using a p value = 0.05. The level of significance was adjusted for the experimentwise error rate. Detailed results of all ANOVA and planned comparisons using the Least Squares Means (LSM) approach are reported in the text.

Results

dTau loss alters microtubule polymerization and stability

Because the *Drosophila* genome contains only one homolog of the tau/MAP2/MAP4 family (Heidary and Fortini, 2001), and given the involvement of tau in multiple vital functions (Sotiropoulos et al., 2017), it was highly surprising that null mutants of the protein were viable in *Drosophila* (Burnouf et al., 2016). Potential explanations for this could be that, unlike its apparent vertebrate homologs, dTau is not involved in essential cytoskeletal functions, or that, like in mice, its activities are compensated at least in part by other MAPs (Harada et al., 1994; Bettencourt da Cruz et al., 2005; Barlan et al., 2013). If dTau acted like its vertebrate homolog, then its absence should affect the cytoskeleton and/or the levels of other microtubule-associated proteins, perhaps in compensation for its absence.

To address this hypothesis, we adopted a comparative proteomic approach using LC-MS/MS and label-free quantitation in protein extracts from the brains of null tau^{KO} (Fig. 1*A*; Burnouf et al., 2016) versus control (WT) flies (Table 1). As expected, dTau was present in the CNS of WT flies and absent in the mutants. In agreement with a previous report (Burnouf et al., 2016), dTau loss did not affect the levels of Futsch and Ensconsin, the known fly homologs of MAP1 and MAP7, respectively, or those of Map205 (Table 1). Since *Drosophila* does not contain a MAP2 homolog, these are the MAPs that could presumably compensate dTau loss and account for the viability of the mutants as suggested for tau loss in mice (Harada et al., 1994; Bettencourt da Cruz et al., 2005; Barlan et al., 2013). Furthermore, although the centrosomal MAP60 was elevated, previous studies suggested that it cannot functionally replace dTau (Bolkan and Kretzschmar, 2014). The atypical MAP Jupiter (Karpova et al., 2006) was found significantly reduced in tau^{KO} animals. In addition, the spectraplakin Short Stop (Shot), a large actin-microtubule linker molecule, which could in principle functionally overlap tau for microtubule stabilization (Alves-Silva et al., 2012), remained unaltered upon dTau deletion (Table 1). Only the highly divergent Mapmodulin (Goldstein and Gunawardena, 2000) was highly upregulated in the mutant. However, Mapmodulin is leucine rich, unlike the proline rich-dTau, and this, along with its divergent sequence, strongly suggests that it is rather unlikely to functionally compensate for loss of the latter. Hence, there is no obvious upregulation of one of the major *Drosophila* MAPs under chronic dTau loss (Table 1), similar to that reported to account for the viability and lack of gross mutant phenotypes in tau^{KO} mice (Harada et al., 1994). Therefore, functional compensation of tau loss by MAP upregulation may characterize vertebrates, but divergent molecular mechanisms appear able to overcome the deficit in *Drosophila*.

However, dTau depletion resulted in significant reductions in both α- and β-tubulin and, interestingly, elevation in the major microtubule-associated motor proteins (Table 1). We aimed to validate independently the reduction of tubulins in tau^{KO} and a second Mi{MIC} transposon insertion mutant (tau^{MI}) by Western blots. Both mutants are null as they lack the 50 and 75 kDa dTau isoforms (Fig. 1*A*), and both harbored reduced levels of both tubulin (Tub) isoforms in head lysates (Fig. 1*B*; for tau^{KO} and tau^{MI}, respectively, βTub97EF $p = 0.004$, $p = 0.009$, $n = 4$, βTub56D $p < 0.0001$, $n = 6$ and $n = 8$, αTub84D $p = 0.0003$, $n = 5$ and $n = 7$), in agreement with the results in Table 1. Given the lack of obvious phenotypes despite the significant reduction, we wondered whether tubulin attenuation affected its partitioning between monomer and polymer pools.

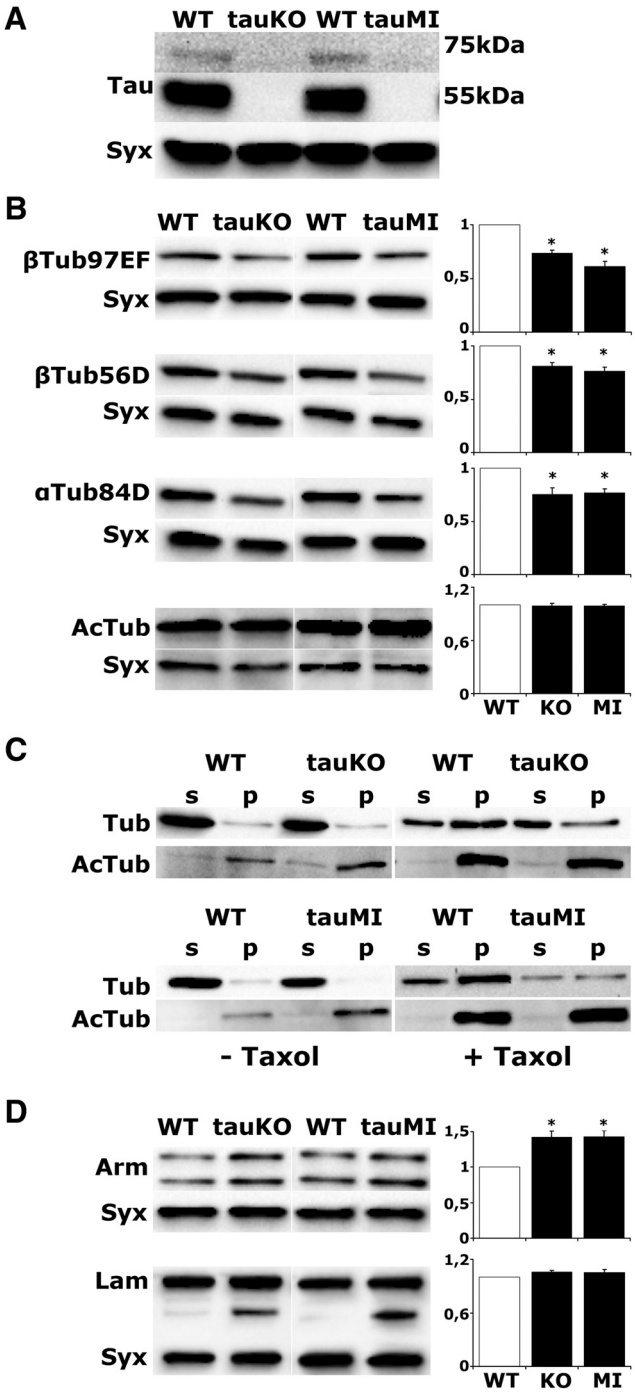

Figure 1. dTau loss precipitates changes in microtubule cytoskeleton. ***A***, Western blot analysis of head lysates from WT, tau^{KO}, and tau^{MI} flies probed with anti-dTau. ***B***, ***D***, Representative blots of head lysates probed with the indicated antibodies. For quantifications, levels of the indicated protein in the mutants were normalized using the syntaxin (Syx) loading control and are shown as a ratio of their mean ± SEM values relative to their respective level in WT flies, which is arbitrarily set to 1. Stars indicate significant differences ($p < 0.05$) from control (open bars) for tau^{KO} and tau^{MI}. ***C***, Endogenous microtubules were purified from fly head lysates in the absence or presence of Taxol. p, Pellet fraction; s, supernatant fraction. Fractions were analyzed by Western blotting using antibodies against total tubulin (Tub) and acetylated tubulin (AcTub).

Table 1. Differentially regulated cytoskeletal proteins upon dTau deletion

Gene	Identifier	Log 2 fold change	*p* Value
tau	FBgn0266579	−7.66922013	0*
futsch	FBgn0259108	−0.098929167	0.23816
Map205	FBgn0002645	0.172052622	0.163753
Map60	FBgn0010342	0.447441737	0.012972*
Jupiter	FBgn0051363	−0.281016827	0.013477*
ens	FBgn0264693	−0.176790555	0.411188
Mapmodulin	FBgn0034282	0.385273457	0.00035*
βTub56D	FBgn0003887	−0.467973868	0.000265*
βTub97EF	FBgn0003890	−0,399647633	0.004722*
αTub84D	FBgn0003885	−0.209974686	0.01011*
HDAC6	FBgn0026428	−0.393520594	0.014513*
Dhc64C	FBgn0261797	0.173733711	0.00421*
Dlic	FBgn0030276	0.268746932	0.001894*
BicD	FBgn0000183	0.389154911	0.013152*
Klc	FBgn0010235	0.258972645	0.008748*
Khc	FBgn0001308	0.284088135	0.000915*
Klp10A	FBgn0030268	0.30295078	0.000371*
Mtor	FBgn0013756	0.234465	0.000624*
CLIP-190	FBgn0020503	0.197493394	0.001698*
shot	FBgn0013733	0.026000439	0.729461
Actin-5C	FBgn0000042	0.101068815	0.097274
Arm	FBgn0000117	0.287528	0.005765*
α-Cat	FBgn0010215	0.194383144	0.008364*
sqh	FBgn0003514	0.302096923	0.011639*
sn	FBgn0003447	0.478138049	0.000003*
cpb	FBgn0011570	0.188986699	0.013467*
tsr	FBgn0011726	0.160349607	0.000611*
cpa	FBgn0034577	0.211062511	0.00578*
zip	FBgn0265434	0.229537	0.018528*
vib	FBgn0267975	−0.180737	0.015157*
flr	FBgn0260049	0.207514842	0.000992*
Lam	FBgn0002525	0.170005878	0.016684*

Selected proteins, *p* values, and average log2 fold differences from three biological and two technical replicas have been calculated as described in Materials and Methods. The log2 fold change becomes positive when mutant > control and negative when control > mutant. The *t* test was performed with a permutation-based FDR (0.05) calculation, and the *p* value determines the statistical significance (*$p < 0.05$). Proteins are functionally grouped into Drosophila MAP family proteins, tubulin and microtubule-associated proteins, actin, and actin associated proteins.

Neuronal-specific dTau reduction has been reported to affect microtubule morphology and density, resulting in fewer, but larger axonal microtubules (Bolkan and Kretzschmar, 2014). A hallmark of long-lived, stably polymerized microtubules is tubulin acetylation, which is negatively regulated by the tubulin-histone deacetylase HDAC6 (Hubbert et al., 2002). Importantly, HDAC6 levels were reduced in tau^{KO} flies (Table 1), suggesting that tubulin acetylation could be elevated in the mutants. As total tubulin acetylation did not differ among genotypes (Fig. 1*B*; for tau^{KO} and tau^{MI}, respectively, AcTub $p = 0.678$, $p = 0.875$, $n = 4$), it raised the possibility that it is the nonacetylated tubulin, which is lower in the mutants and is reflected in the reduced α- and β-tubulin isoforms (Fig. 1*B*).

To validate this notion, we extracted intact microtubules from the same number of *Drosophila* heads in the presence of the microtubule-stabilizing paclitaxel (Taxol; Feuillette et al., 2010). Microtubules were then sedimented by ultracentrifugation, and the pellet and supernatant fractions were probed for total and acetylated tubulin. In the absence of the microtubule-stabilizing Taxol, polymerized acetylated tubulin appeared more abundant in the mutants. However, the addition of Taxol revealed a significant increase in pelleted tubulin in control, but not the mutant lysates, while the fraction of acetylated tubulin remained equivalent (Fig. 1*C*). Together, the data indicate that whereas total polymerized tubulin is reduced in the mutants, its acetylation appears unaltered. Because acetylation enhances flexibility and confers resilience against mechanical stresses (Portran et al., 2017), the data suggest that the microtubule lattice in dTau mutants is likely less rigid. Collectively, the results underscore the

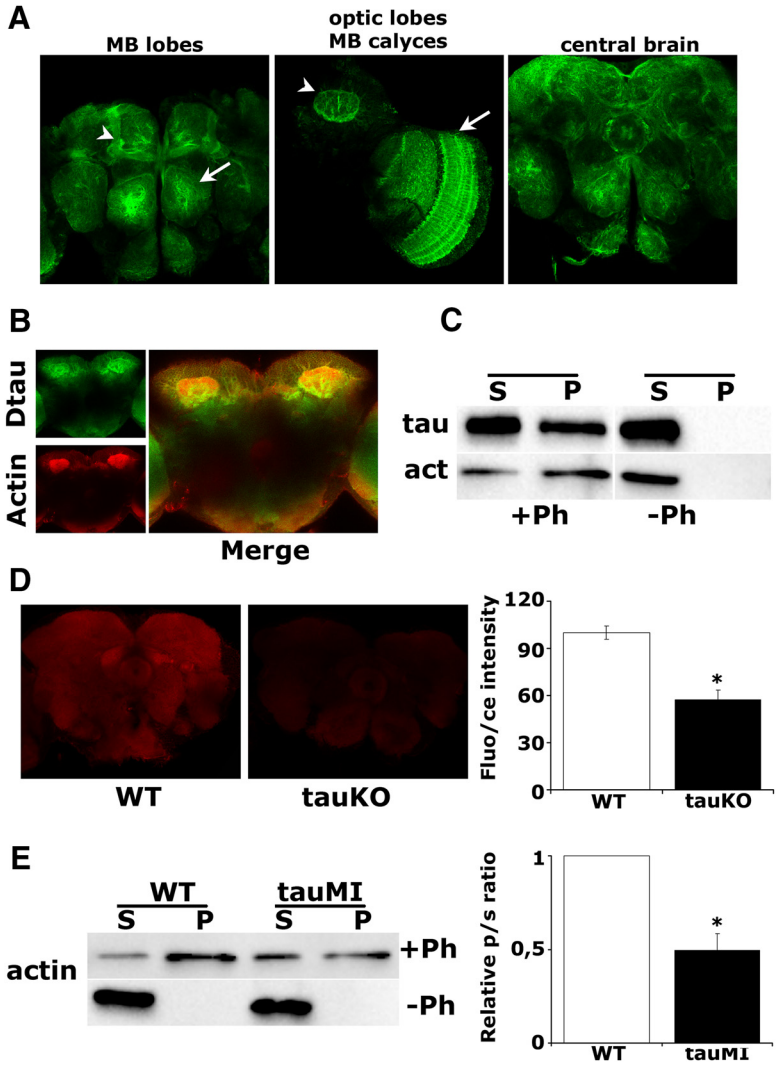

Figure 2. dTau loss affects the actin cytoskeleton. ***A***, Expression pattern of a GFP::dTau protein-trap in the adult brain at the level of the MB lobes (arrowhead) and antennal lobe (arrow; left), MB calyx (arrowhead) and optic lobe (arrow), (middle), and the central brain (right). ***B***, Prominent colocalization of rhodamine-phalloidin-stained F-actin with the GFP::dTau fusion protein in adult MBs. ***C***, Coprecipitation of phalloidin-bound F-actin and dTau from WT fly brains. ***D***, Confocal images in the central fly brain following rhodamine-phalloidin staining of whole-mount brains from WT and tau^{KO} flies (arrow, ellipsoid body). The mean relative fluorescence intensities ± SEM are shown as a percentage of control. ***E***, Phalloidin-bound F-actin was isolated from fresh brain extracts of WT and tau^{MI} mutants, and its levels were assessed by probing for actin. The ratio of precipitated actin in the pellet (p) to the actin in the supernatant (s) was used for quantification and was significantly different in the mutant, as indicated by the star.

essential role of dTau in microtubule cytoskeleton dynamics, supporting its functional role as a true ortholog of its vertebrate counterpart.

Loss of dTau destabilizes F-actin

Although significant changes in the ubiquitous actin 5C levels were not detected, dTau loss resulted in elevation of both α-catenin and β-catenin (Armadillo-Arm) and a number of other major actin-binding proteins, as well as the nucleoskeletal protein Lamin (Table 1). These results were selectively verified for Arm and Lamin due to reagent availability (Fig. 1*D*; for tau^{KO} and tau^{MI}, respectively: Arm, $p = 0.007$, $p = 0.001$, $n = 5$; Lam, $p = 0.231$, $p = 0.817$, $n = 4$). Notably, although the full-length 75 kDa Lamin was present in equal quantities in both mutants and controls, a 45–50 kDa band, representing a cleavage product (Martin and Baehrecke, 2004), was detected only in the tau^{KO} and tau^{MI} flies, which is suggestive of excess Lamin degradation. In accord with these results, transgenic tau elevation by the expression of human tau in the fly CNS promotes F-actin stabilization leading to disruption of the Lamin nucleoskeleton and reduction of Lamin levels in flies (Fulga et al., 2007; Frost et al., 2016).

Given the broad upregulation of actin-binding proteins (Table 1) and its interaction with tau (Henríquez et al., 1995; Kempf et al., 1996), we investigated whether the actin cytoskeleton is altered upon dTau loss. We capitalized on a protein-trap fly strain expressing a GFP::dTau fusion protein, which recapitulated the distribution of dTau in the visual system and central brain, including the mushroom bodies (MBs; Fig. 2*A*). The MBs are bilateral clusters of neurons in the dorsal posterior cortex of the brain, which is essential for olfactory learning and memory in *Drosophila* (Davis, 2005). Notably, the GFP-marked dTau colocalized with rhodamine-phalloidin within these neurons (Fig. 2*B*). In accord, total F-actin isolated from brain lysates with biotinylated phalloidin coprecipitated a significant amount of dTau (Fig. 2*C*). Because dTau was absent from the pellet if phalloidin was omitted, this validates the specificity of dTau interaction with polymerized filamentous actin.

Furthermore, immunofluorescence microscopy of tau^{KO} mutant brains revealed a substantial decrease in total F-actin levels (Fig. 2*D*; $p < 0.0001$, $n = 10$). This was independently verified in tau^{MI} flies, where pelleted, phalloidin-bound F-actin levels were also significantly reduced ($p = 0.01$, $n = 3$), while total actin was unaltered (Fig. 2*E*, Table 1). Collectively therefore, dTau promotes actin polymerization and cytoskeletal dynamics *in vivo*. It follows that the upregulation of actin-binding proteins upon dTau loss (Table 1) is likely a reflection of homeostatic compensatory responses consequent to decreased F-actin levels (Fig. 2*D*,*E*).

dTau is a negative regulator of translation and protein synthesis-dependent long-term memory

Because cytoskeletal proteins are essential for multiple neuronal properties, including plasticity and metabolism (Matamoros and Baas, 2016), in conjunction with its presence within the MBs, neurons essential for learning and memory in the fly, prompted us to investigate whether dTau loss affects behavioral plasticity.

To examine whether dTau is involved in associative learning and memory, we used the olfactory classical conditioning paradigm and examined controls and mutants immediately after training to assess 3 min memory/learning and 24 h later to probe consolidated memories (Fig. 3*A*,*B*). Two forms of consolidated memories can be assayed in *Drosophila*, the protein synthesis-dependent long-term memory (PSD-LTM), induced after multi-

ple rounds of spaced training and the protein synthesis-independent anesthesia-resistant memory (ARM), elicited after repeated massed training cycles (Tully et al., 1994). Whereas 3 min memory was not affected (tau^{KO}, ANOVA: $F_{(2,29)} = 0.1721$, $p = 0.8428$; tau^{MI}, ANOVA: $F_{(2,31)} = 0.7133$, $p = 0.4984$), both mutants surprisingly presented enhanced LTM (tau^{KO}, ANOVA: $F_{(2,31)} = 11.2031$, $p = 0.0002$; subsequent LSM: $p = 7.4 \times 10^{-5}$ vs WT; tau^{M}, ANOVA: $F_{(2,31)} = 23.8424$, $p < 0.0001$; subsequent LSM: $p = 9.6 \times 10^{-7}$ vs WT). In contrast, ARM remained at control levels (tau^{KO}, ANOVA: $F_{(2,29)} = 1.9692$, $p = 0.1591$; tau^{MI}, ANOVA: $F_{(2,31)} = 1.7708$, $p = 0.1881$).

To determine whether the enhanced 24 h performance is indeed PSD-LTM, we took advantage of its requirement for *de novo* protein synthesis (Tully et al., 1994) and fed control and mutant flies with the protein synthesis inhibitor CXM. CXM-fed mutants did not present elevated 24 h spaced training-induced memory (ANOVA: $F_{(3,31)} = 35.9177$, $p < 0.0001$; subsequent LSM: $p = 0.2981$, tau^{MI} + CXM vs WT + CXM), but their performance was reduced equally with the expected (Krashes et al., 2009) PSD-LTM reduction of drug-fed controls (Fig. 3*C*). Therefore, the enhanced memory of the mutants (ANOVA: $F_{(3,31)} = 35.9177$, $p < 0.0001$; subsequent LSM: $p = 1.6 \times 10^{-4}$, tau^{MI}-CXM vs WT-CXM) is the PSD-LTM form of consolidated memory.

To confirm these surprising results independently and to determine whether they are a consequence of altered development upon dTau loss, we used RNAi and the TARGET system (McGuire et al., 2004). Adult-specific pan-neuronal RNAi-mediated abrogation of dTau in the CNS reduced its level by ~65% (Fig. 3*D*; $p < 0.0001$, $n = 4$). As shown in Figure 3*E*, this did not alter learning, but resulted in strong PSD-LTM enhancement (Fig. 3*F*; Elav, ANOVA: $F_{(2,31)} = 23.2665$, $p < 0.0001$; subsequent LSM: $p = 6.4 \times 10^{-5}$ and $p = 2.5 \times 10^{-7}$ vs controls, respectively). Hence, the elevated memory is not developmental in origin, but reflects an acute requirement for dTau-engaging processes to limit negatively reinforced olfactory PSD-LTM.

Given their essential role for LTM (Davis, 2005), we limited dTau abrogation to adult MBs (Fig. 3*F*). The LeoMB and dnc-Gal4 are pan-mushroom body drivers (Aso et al., 2009; Messaritou et al., 2009), MB247-Gal4 drives expression mainly in α/β and γ neurons, whereas c305α and

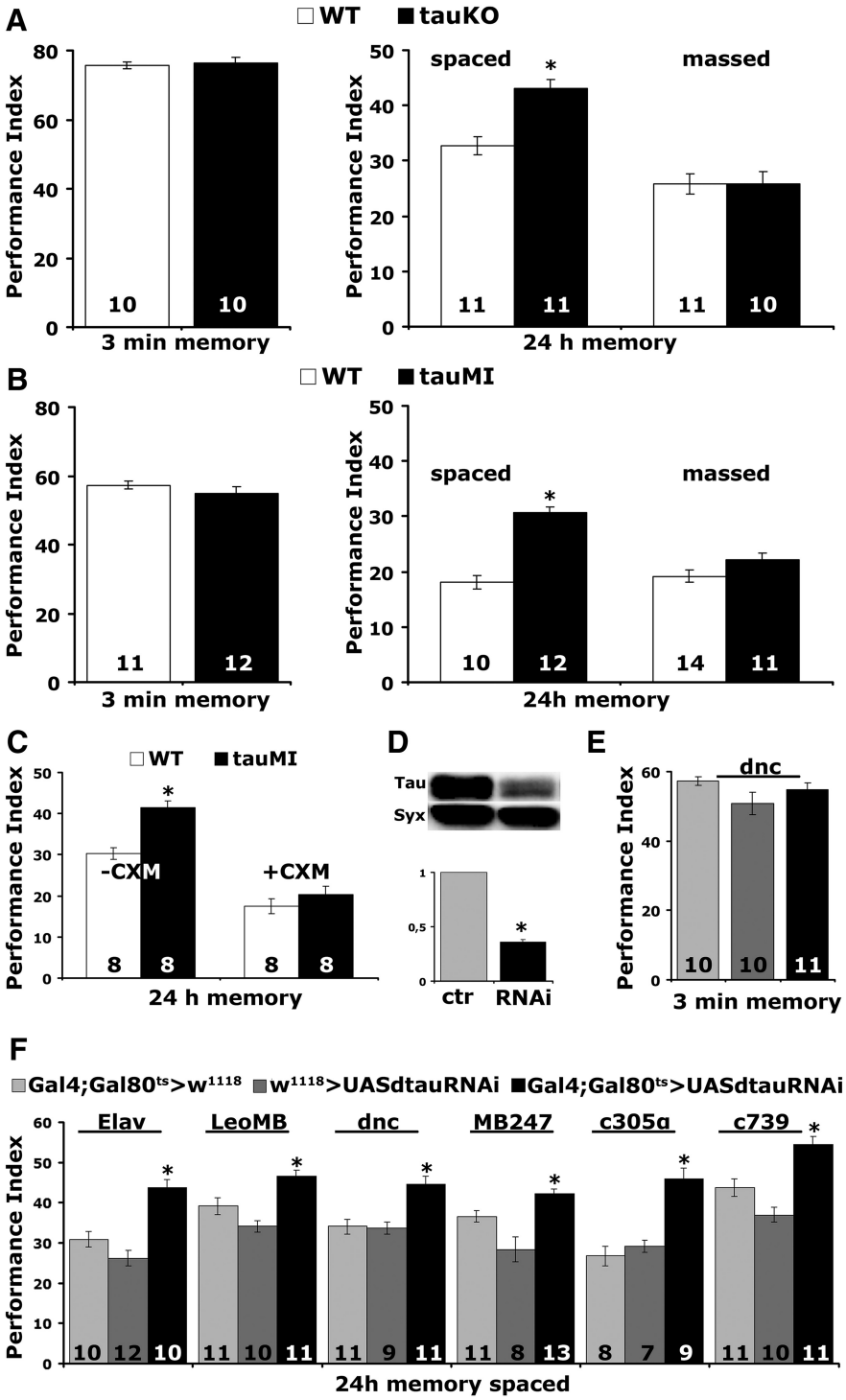

Figure 3. dTau abrogation affects long term memory. ***A***, ***B***, tau^{KO} and tau^{MI} mutants present enhanced LTM (*$p < 0.0001$), whereas 3 min memory and ARM are not affected ($p > 0.05$). The number of experimental replicates (n) is indicated within the bars. ***C***, CXM administration eliminated the enhanced LTM of tau^{MI} flies (*$p < 0.0001$). ***D***, Representative Western blot of head lysates from flies expressing UAS-dtauRNAi with Elav-Gal4 using an anti-dTau antibody. The genotype of control animals was Elav-Gal4/+. Compared with its levels in control animals, dTau was significantly reduced. For the quantification, tau levels were normalized using the syntaxin (Syx) loading control and shown as a ratio of their mean ± SEM values relative to its respective levels in control flies, which was set to 1. The star indicates significant differences from the control indicative of reduced dTau levels (*$p < 0.0001$). ***E***, Three minute memory is not affected after the downregulation of dTau in the adult MBs using dnc compared with driver and transgene heterozygotes. ***F***, Enhanced LTM performance upon abrogation of dTau during adulthood using Elav (*$p < 0.0001$), LeoMB (*$p = 0.0027$), MB247 (*$p = 0.0199$), dnc (*$p = 0.0001$), c305α (*$p = 0.00001$), and c739 (*$p = 0.0005$).

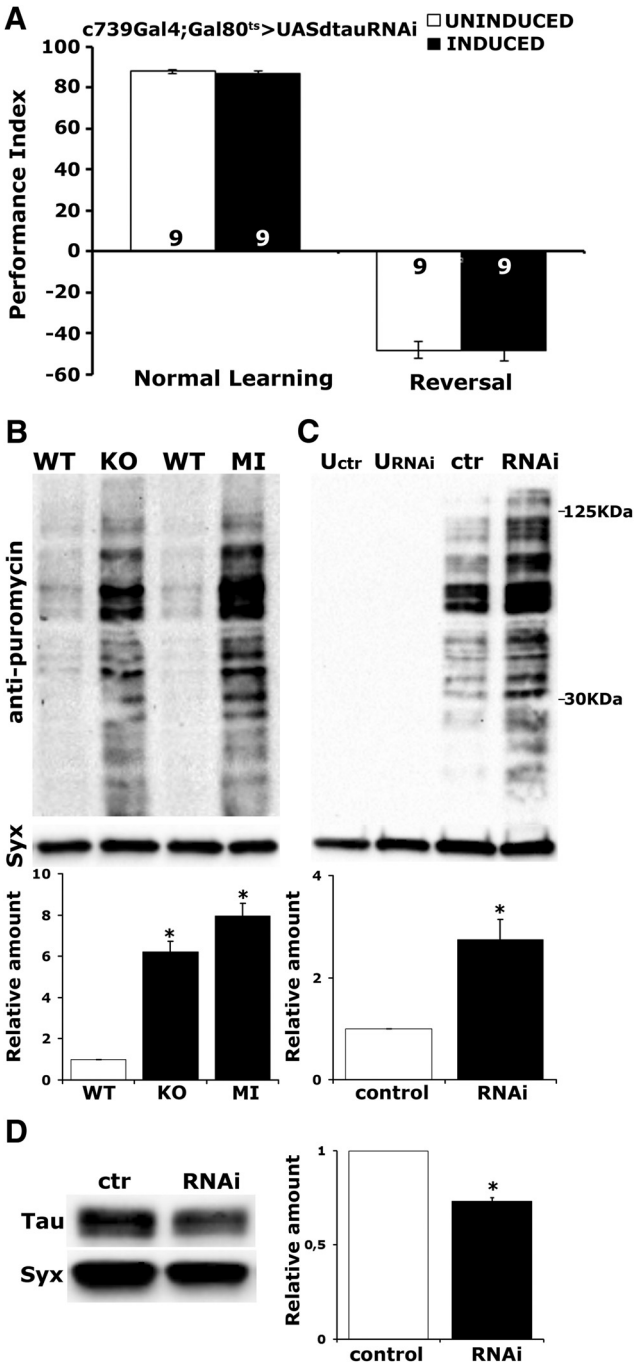

Figure 4. dTau is not required for forgetting of olfactory memories, and its abrogation increases protein synthesis levels. ***A***, Flies expressing dTauRNAi within $\alpha\beta$ MB neurons under c739-Gal4;TubGal80ts performed at levels similar to the control group when they were trained with a reversed contingency. Both groups expressed considerable memory to the more recent learning event. No significant difference in 3 min memory was observed between the experimental and control groups when using the typical learning protocol. Animals were raised at 18°C and shifted to 30°C for 3 d, while uninduced animals were kept at 18°C for these 3 d and were used as controls. The number of experimental replicates (*n*) is indicated within the bars. ***B***, To measure protein synthesis levels flies were treated with 600 μM puromycin for 16 h. Representative blots of head lysates from WT, *tau*^{KO}, and *tau*^{MI} flies probed with either anti-puromycin or anti-syntaxin (Syx). For quantifications, levels of the signal corresponding to molecular weight region 30–125 Da in the mutants were normalized using the Syx loading control and are shown as a ratio of their mean ± SEM values relative to their respective level in WT flies, which is arbitrarily set to 1. Stars indicate significant differences ($p < 0.0001$) from control (open bars) for *tau*^{KO} and *tau*^{MI}. ***C***, Representative Western blot of head lysates from flies expressing UAS-dtauRNAi using Elav-Gal4;TubG80^{ts} and probed with anti-puromycin antibody. Animals were raised at 18°C and shifted to 30°C for 3 d, while uninduced animals (U) were kept at 18°C for these 3 d. The genotype of control animals was Elav-Gal4;TubG80^{ts}/+. For the quantification, levels of the signal corresponding to molecular weight region 30–125 kDa were normalized using the Syx loading control and are shown as a ratio of their mean ± SEM values relative to their respective level in control flies, which is arbitrarily set to 1. The star indicates significant differences ($p = 0.0044$) from control (open bar), indicative of increased protein synthesis upon dTau loss. ***D***, Representative Western blot of head lysates from flies expressing UAS-dtauRNAi with Elav-Gal4;TubG80^{ts} using an anti-dTau antibody. The genotype of control animals was Elav-Gal4;TubG80^{ts}/+ shifted to 30°C for 3 d. Compared with its levels in control animals, dTau was significantly reduced. For the quantification, tau levels were normalized using the Syx loading control and are shown as a ratio of their mean ± SEM values relative to respective levels in control flies, which was set to 1. The star indicates significant differences from the control indicative of reduced dTau levels (*$p < 0.0001$).

c739 are restricted to α'/β' and α/β, respectively (Aso et al., 2009). To verify that pan-MB dTau attenuation under dnc-Gal4 did not result in enhanced learning, we limited the number of odor/shock pairings from 6 to 3, conditions conducive to revealing such properties (Pavlopoulos et al., 2008; Gouzi et al., 2011). However, enhanced learning was not detectable even under such limited training (Fig. 3*E*; ANOVA: $F_{(2,30)} = 1.9220$, $p = 0.1651$), but, in contrast, PSD-LTM was significantly enhanced (LeoMB, ANOVA: $F_{(2,31)} = 14.6273$, $p < 0.0001$; subsequent LSM: $p = 0.0027$ and $p = 9.5 \times 10^{-6}$ vs controls, respectively; dnc, ANOVA: $F_{(2,30)} = 12.8673$, $p < 0.0001$; subsequent LSM: $p = 0.0001$ and $p = 0.0002$ vs controls respectively; MB247, ANOVA: $F_{(2,31)} = 14.8900$, $p < 0.0001$; subsequent LSM: $p = 0.0199$ and $p = 7.2 \times 10^{-6}$ vs controls, respectively) under these drivers (Fig. 3*F*). These results were confirmed with an independent RNAi-mediating transgene (dTau levels for control set to 1, pan-neuronally expressed dtauRNAi40875 = 0.674 ± 0.0497, $p < 0.0001$, $n = 6$), which also yielded elevated PSD-LTM (dnc >+ = 23.32 ± 1.51; dtauRNAi40875 >+ = 27.72 ± 1.10; dnc >dtauRNAi40875 = 32.36 ± 1.26; $n = 9$; ANOVA: $F_{(2,23)} = 12.4614$, $p = 0.0003$; subsequent LSM: $p = 6.2 \times 10^{-5}$ and $p = 0.0224$ vs controls respectively) under dnc-Gal4;TubG80^{ts}.

Significantly, the attenuation of dTau within α'/β' and α/β MB neurons (Fig. 3*F*, c305α and c739, respectively), yielded strong PSD-LTM memory improvement (c305α, ANOVA: $F_{(2,23)} = 18.8052$, $p < 0.0001$; subsequent LSM: $p = 0.00001$ and $p = 0.00011$ vs controls, respectively; c739, ANOVA: $F_{(2,31)} = 20.0470$, $p < 0.0001$; subsequent LSM: $p = 0.0005$ and $p = 8 \times 10^{-7}$ vs controls, respectively). Both subtypes of neurons are known to be essential for 24 h memory with apparently distinct roles in olfactory memory processing (Isabel et al., 2004; Yu et al., 2006; Krashes et al., 2007; Gouzi et al., 2018). Output from the α'/β' neurons is required for olfactory memory acquisition and stabilization (Krashes et al., 2007), whereas neurotransmission from the α/β neurons is required for its retrieval (Dubnau et al., 2001; McGuire et al., 2001; Pascual and Préat, 2001; Akalal et al., 2006). Collectively, the data strongly indicate that dTau acts as a negative regulator of PSD-LTM within MB neurons in accord with cumulative evidence on the role of these neurons in the process (McGuire et al., 2001; Krashes et al., 2007).

The CXM treatment experiment in Figure 3*C* suggested that elevated memory upon dTau loss could be due to improved consolidation, whereas the equivalent performance of control and dTauRNAi flies immediately after training with a limited number of US/CS pairings (Fig. 3*E*) indicated that the increased memory observed at later time points was not due to improved acquisition. However, the enhanced memory observed upon the attenuation of dTau could also arise from decreased forgetting (Cervantes-Sandoval et al., 2016). To test whether forgetting is

defective upon dTau attenuation, we performed reversal learning in which we trained flies to associate an aversive odor to footschock and 1 min later to the opposite contingency. Control flies typically avoid the odor most recently associated with shock, whereas flies with decreased forgetting keep the memory of the initial contingency (Cervantes-Sandoval et al., 2016). As shown in Figure 4*A*, dTau attenuation within $\alpha\beta$ MB neurons yielded equal learning as the in-genotype controls both in the typical learning paradigm (learning, ANOVA: $F_{(1,17)} = 0.7532$, $p = 0.3983$) and upon reverse training (reversal, ANOVA: $F_{(1,17)} = 0.0067$, $p = 0.9356$). The reversal Performance Indexes are negative because the performance was scored as if the initial contingency was the correct choice. This would be expected to be positive if dTau loss impaired forgetting, in essence eliminating the effect of the second contingency in favor of the initial odor shock pairing. Therefore, the increased memory upon dTau loss is unlikely to be due to impaired forgetting.

The proteomic results suggested an elevation of proteins essential for translation in the mutant (Table 2), and this included a number of proteins involved in memory formation or recall (Table 3), in accord with the PSD-LTM dependence on translation. To independently confirm that protein synthesis is in fact elevated upon dTau loss, we used a functional assay, that of puromycin incorporation. Puromycin acts as an aminoacyl-tRNA analog becoming incorporated into nascent peptides causing termination (Nathans, 1964), but also labeling newly synthesized proteins, whose levels are readily measured with an anti-puromycin antibody.

In agreement with the proteomic results, protein synthesis levels were significantly elevated in both mutants relative to control (WT) flies (Fig. 4*B*; for tau^{KO} and tau^{MI}, respectively, $p = 0.00004$, $p = 0.00002$; $n = 4$). Moreover, qualitatively similar elevation of puromycin incorporation was obtained upon adult-specific pan-neuronal dTau abrogation (Fig. 4*C*; $p = 0.0044$, $n = 4$), suggesting rather acute effects on translation. It is also worth noting that protein synthesis increases in response to temperature elevation as expected [Fig. 4*C*, uninduced control (lane 1) vs control induced flies (lane 3)]. Given the dependence of PSD-LTM on translation, this protein synthesis upregulation could account, at least in part, for the enhanced memory in the mutants. The collective results in Tables 2 and 3, and Figure 4 support a role for dTau as an acute negative regulator of protein synthesis in the CNS.

Interestingly, acute abrogation of dTau yielded a memory enhancement similar to that in the null mutants. Therefore, we wondered whether the proteomic profiles would be similar or diverge, an indication of compensatory mechanisms dynamics in these situations of acute or chronic dTau attenuation. Therefore, proteomic profiling was performed after acute pan-neuronal dTau attenuation, which, as shown in Figure 4*D*, leads to 30% reduction of dTau expression levels ($p < 0.0001$, $n = 6$).

In accord with the results from chronic dTau reduction in the mutants, proteomic changes were also uncovered upon acute dTau attenuation. Although they represented the three main protein groups, cytoskeletal (Table 1), translation linked (Table 2), and neuronal function linked (Table 3), which were also altered in the mutants, few were in common (Tables 4, 5). For example, although tubulin levels and HDAC6 appeared unaltered upon acute attenuation, nevertheless proteins critical for the dynamics and function of the microtubule cytoskeleton were altered. These include the microtubule tip-localizing protein Eb1, which is critical for accelerating their dynamics (Li et al., 2012); the synaptic microtubule stabilization protein Ank2 (Pielage et al., 2008),

Table 2. Upregulation of proteins that function in translation upon dTau loss

Gene	Identifier	Log 2 fold change	*p* Value
RpL3	FBgn0020910	0.29769754	0.015227*
RpL4	FBgn0003279	0.28274552	0.017456*
RpL10	FBgn0024733	0.38811628	0.019366*
RpL10Ab	FBgn0036213	0.41334375	0.010486*
RpL11	FBgn0013325	0.47628427	0.008492*
RpL12	FBgn0034968	0.22205798	0.008651*
RpL13	FBgn0011272	0.42983913	0.005514*
RpL18A	FBgn0010409	0.46355637	0.000564*
RpL23	FBgn0010078	0.44537226	0.022022*
RpL26	FBgn0036825	0.33991647	0.020167*
RpL30	FBgn0086710	0.33723116	0.011247*
RpLP2	FBgn0003274	0.38862832	0.005669*
RpS2	FBgn0004867	0.32947826	0.000604*
RpS3	FBgn0002622	0.33969498	0.002684*
RpS3A	FBgn0017545	0.29286544	0.014919*
RpS4	FBgn0011284	0.44215218	0.000334*
RpS6	FBgn0261592	0.35850573	0.013199*
RpS7	FBgn0039757	0.34377821	0.008244*
RpS8	FBgn0039713	0.28432178	0.007677*
RpS10b	FBgn0261593	0.30869754	0.020561*
RpS11	FBgn0033699	0.47895050	0.001293*
RpS12	FBgn0260441	0.45860616	0.005995*
RpS13	FBgn0010265	0.35336463	0.012484*
RpS14b	FBgn0004404	0.37592173	0.000738*
RpS15Aa	FBgn0010198	0.3678902	0.00019*
RpS16	FBgn0034743	0.36565614	0.00736*
RpS17	FBgn0005533	0.34326967	0.011799*
RpS18	FBgn0010411	0.34453487	0.003018*
RpS23	FBgn0033912	0.30110852	0.005235*
RpS27	FBgn0039300	0.3223815	0.010737*
Rbp2	FBgn0262734	0.26778308	0.002853*
sta	FBgn0003517	0.32786949	0.005807*
Ef1beta	FBgn0028737	0.23767066	0.015910*
Elf	FBgn0020443	0.31957237	0.002937*
eEF1delta	FBgn0032198	0.20101547	0.007045*
eIF2gamma	FBgn0263740	0.33932988	0.009390*
eIF-3p66	FBgn0040227	0.36954904	0.005558*
eIF3-S5–1	FBgn0037270	0.43084621	0.005214*
eIF3-S8	FBgn0034258	0.38344447	0.000346*
eIF3-S9	FBgn0034237	0.25910266	0.005049*
eIF3-S10	FBgn0037249	0.37967841	0.001322*
eIF4G	FBgn0023213	0.31082757	0.011195*
eRF1	FBgn0036974	0.34124954	0.002162*
bel	FBgn0263231	0.37415822	0.000987*
bol	FBgn0011206	0.36492339	0.000232*
glo	FBgn0259139	0.31756496	0.002210*
Trip1	FBgn0015834	0.41510550	0.000583*
Tango7	FBgn0033902	0.37924329	0.003916*
AGO1	FBgn0262739	0.20476087	0.011386*
U2af50	FBgn0005411	0.25440500	0.017200*
Dp1	FBgn0027835	0.27406081	0.009374*
Fmr1	FBgn0028734	0.32938814	0.000069*
Hrb27C	FBgn0004838	0.29338336	0.000018*
Hrb98DE	FBgn0001215	0.18872627	0.002404*
kra	FBgn0250753	0.36629526	0.005815*
Not1	FBgn0085436	0.27462665	0.002692*
Not3	FBgn0033029	0.33431784	0.011705*
pAbp	FBgn0265297	0.32483967	0.000818*
tyf	FBgn0026083	1.42353360	0.000399*

Average log2 fold differences and *p* values for the indicated proteins calculated from three biological and two technical replicas. As the log2 fold changes denote, all listed proteins were upregulated in the tau^{KO} mutant. The *t* tests were performed with a permutation-based FDR (0.05) calculation, and the *p* value determines the statistical significance of the difference (*significant *p* value <0.05).

Table 3. Differentially regulated proteins upon dTau deletion that affect memory formation

Gene	Identifier	Log2 fold change	*p* Value	References
A2bp1	FBgn0052062	0.242381	0.01749*	1
arm	FBgn0000117	0.287528	0.00576*	2
cer	FBgn0034443	0.352768	0.0016*	3
emb	FBgn0020497	0.187307	0.005865*	4
Fmr1	FBgn0028734	0.329388	0.00007*	5
Hop	FBgn0024352	0.358213	0.0002*	6
lig	FBgn0020279	0.360493	0.0066*	4
Pdk	FBgn0017558	0.392657	0000001*	4
Pkc53E	FBgn0003091	0.207134	0.0022*	7
CG4612	FBgn0035016	0.332883	0.00988*	8
Ugt	FBgn0014075	0.248749	0.0097*	4
Ugt35b	FBgn0026314	4.02456	0*	4

Selected proteins, *p* values, and average log2 fold differencess (four biological and three technical replicas) have been calculated as described in Materials and Methods. As the log2 fold change denotes all proteins are upregulated in the tau^{KO} mutant. The *t* test was performed with a permutation-based FDR (0.05) calculation, and the *p* value determines the statistical significance (*p value <0.05). References: 1, Guven-Ozkan et al. (2016); 2, Tan et al. (2013); 3, Comas et al. (2004); 4, Walkinshaw et al. (2015); 5, Kanellopoulos et al. (2012); 6, Copf et al. (2011); 7, Colomb and Brembs (2016); and 8, Khan et al. (2015). The two proteins highlighted in gray are family members of a protein identified in 4.

Table 4. Differentially regulated proteins involved in cytoskeleton organization and translation upon acute pan-neuronal dTau downregulation

	Identifier	Log 2 fold change	*p* Value
14-3-3ζ	FBgn0004907	−0.250421	0.023824*
Ank2	FBgn0261788	−0.16070	0.040059*
Eb1	FBgn0027066	−0.269836	0.038913*
dgt3	FBgn0034569	1.62118	0.031084*
Klp35D	FBgn0267002	−0.490059	0.016159*
Mtor	FBgn0013756	−0.376771	0.040521*
mud	FBgn0002873	2.61944	0.010824*
Pka-C1	FBgn0000273	−0.229651	0.009899*
Pka-R1	FBgn0259243	−0.217834	0.006967*
Rab11	FBgn0015790	−0.172639	0.018478*
Rbp	FBgn0262483	−0.173228	0.012758*
Strip	FBgn0035437	−0.457799	0.016759*
Arp2	FBgn0011742	−0.410359	0.009826*
bt	FBgn0005666	0.361831	0.034574*
btsz	FBgn0266756	−1.04969	0.049232*
didum	FBgn0261397	1.17976	0.001963*
mtm	FBgn0025742	−1.24456	0.034627*
SelR	FBgn0267376	−0.198595	0.039084*
vib	FBgn0267975	2.51317	0.001071*
WASp	FBgn0024273	−0.415598	0.003013*
zip	FBgn0265434	−0.16072	0.019419*
RpLP2	FBgn0003274	−0.22082	0.016296*
RpL9	FBgn0015756	0.363787	0.014304*
Ef1β	FBgn0028737	−0.18861	0.025385*
eIF-4B	FBgn0020660	1.22347	0.017551*
Elf	FBgn0020443	0.783829	0.029138*
EF2	FBgn0000559	−0.36835	0.001801*
eIF-2α	FBgn0261609	−0.16968	0.027685*
LeuRs	FBgn0053123	−1.95364	0.016296*
Fmr1	FBgn0028734	−0.8741	0.028043*
Dp1	FBgn0027835	−0.19861	0.03618*
U2af50	FBgn0005411	0.37609	0.024622*
qkr54B	FBgn0022987	0.619797	0.049061*
nito	FBgn0027548	−0.99659	0.045671*
La	FBgn0011638	0.505715	0.028674*
CG4612	FBgn0035016	−0.32493	0.011309*

Selected proteins, *p* values, and average log2 fold differences from four biological and two technical replicas have been calculated as described in Materials and Methods. Control animals are Elav-Gal4;TubG80^{ts} > + vs Elav-Gal4; TubG80^{ts} > dtauRNAi induced for 3 d at 30°C. The log2 fold change becomes positive when RNAi > control and negative when control > RNAi. The *t* test was performed with a permutation-based FDR (0.05) calculation, and the *p* value determines the statistical significance (*$p < 0.05$). In bold are proteins whose levels were also found to be changed in the mutant (Tables 1, 2).

which is downregulated upon acute dTau loss; and Arp2, an actin-related protein within the Arp2/3 complex, which is the basic actin nucleator in eukaryotes (Hudson and Cooley, 2002). In support of these results, Ank2 was recently suggested to interact with human tau expressed in *Drosophila* (Higham et al., 2019).

Similarly, few of the proteins involved in translation and memory formation such as Fmr1, lig, and CG4612 (Table 5), are shared between chronic and acute dTau attenuation. These similarities, but also the intriguing differences, suggest dynamic proteostatic adjustments of cytoskeletal and translation-linked proteins upon acute dTau loss, which evolve into steady-state long-term compensatory changes to support neuronal structure and function in the mutant. It is interesting that proteins such as 14-3-3ζ and the catalytic and regulatory subunits of protein kinase A, known to be involved in *Drosophila* learning and memory (Skoulakis and Grammenoudi, 2006), are significantly changed upon acute but not chronic dTau attenuation (Tables 3, 5; Walkinshaw et al., 2015). 14-3-3ζ has recently been reported to interact with human tau expressed pan-neuronally in *Drosophila* in support of this (Papanikolopoulou et al., 2018). This suggests that the molecular mechanisms underlying PSD-LTM enhancement upon acute and chronic dTau loss are also dynamically proteostatically adjusted, although the net effect may be similar. This is in accord with the notion that PSD-LTM formation or attenuation may result from the engagement of distinct, possibly parallel molecular pathways.

dTau is required for footshock habituation

Apart from their established roles in olfactory learning and memory (Heisenberg, 2003), MBs are also involved in habituation to repeated footshocks (Acevedo et al., 2007). Habituation is a form of nonassociative plasticity manifested as a response attenuation to repetitive inconsequential stimuli. To investigate whether dTau is involved in mechanisms underlying habituation, both tau^{KO} and tau^{MI} mutants and their genetic background controls (w^{1118} and y^1w^1, respectively) were subjected to the established footshock habituation protocol (Acevedo et al., 2007) of repeated 45 V electric shocks (Fig. 5*A*,*B*).

All genotypes avoided electric shock normally when naive (tau^{KO}, ANOVA: $F_{(2,34)} = 5.5093$, $p = 0.0088$; tau^{MI}, ANOVA: $F_{(2,40)} = 1.8286$, $p < 0.1745$), and the controls presented habituated responses after exposure to 15 such stimuli (Fig. 5*A*,*B*), as expected (Acevedo et al., 2007). In contrast, both dTau mutants failed to habituate to 15, 45 V shocks (tau^{KO}, ANOVA: $F_{(2,34)} = 58.5474$, $p < 0.0001$; subsequent LSM: $p = 3 \times 10^{-10}$ vs WT, tau^{MI}, ANOVA: $F_{(2,40)} = 11.0184$, $p = 0.0002$; subsequent LSM: $p = 7.9 \times 10^{-5}$ vs WT), indicating an inability to devalue inconsequential stimuli. The habituation deficit was not sensitive to CXM in the mutants (Fig. 5*C*; ANOVA: $F_{(3,68)} = 30.4059$, $p < 0.0001$; subsequent LSM: $p = 5 \times 10^{-7}$, tau^{MI}-CXM vs WT-CXM and ANOVA: $F_{(3,68)} = 30.4059$, $p < 0.0001$; subsequent LSM: $p = 8 \times 10^{-11}$, tau^{MI} + CXM vs WT + CXM), indicating that failure to habituate is not the result of elevated protein synthesis. Hence, dTau appears to physiologically engage neuronal mechanisms necessary to devalue the repeated footshock stimulation and to facilitate habituation.

To confirm that the habituation defect maps to the adult MBs, we used the same Gal4 drivers as described above to conditionally attenuate dTau via RNAi (Fig. 5*D*). Habituation deficits were uncovered upon pan-neuronal (Elav, ANOVA: $F_{(2,39)} = 18.8294$, $p < 0.0001$; subsequent LSM: $p = 1.3 \times 10^{-5}$ and $p = 2.2 \times 10^{-6}$

Table 5. Differentially regulated proteins upon acute dTau loss that affect memory formation

Gene	Identifier	Log 2 fold change	*p* Value	References
Fmr1	FBgn0028734	−0.874096	0.028043*	1
lig	FBgn0020279	−1.006	0.032011*	2
14-3-3zeta	FBgn0004907	−0.250421	0.023824*	3
Ank2	FBgn0261788	−0.1607	0.040059*	4
CG4612	FBgn0035016	−0.324925	0.011309*	5
SLC22A	FBgn0037140	−0.850807	0.006731*	6
Fdh	FBgn0011768	0.29288	0.007593*	7
Pka-C1	FBgn0000273	−0.229651	0.009899*	8
Pka-R1	FBgn0259243	−0.217834	0.006967*	9
Sap47	FBgn0013334	−0.802852	0.003545*	10
Syn	FBgn0004575	−0.150291	0.005463*	11

Selected proteins, *p* value, and average log2 fold differences (four biological and three technical replicas) have been calculated as described in Materials and Methods. Control animals are Elav-Gal4;TubGal80ts >+ vs Elav-Gal4; TubGal80ts >dtauRNAi induced for 3 d at 30°C. The log2 fold change becomes positive when RNAi > control and negative when control > RNAi. The *t* test was performed with a permutation-based FDR (0.05) calculation, and the *p* value determines the statistical significance (*$p < 0.05$). In bold are proteins whose levels were also found to be changed in the mutant (Table 3). References: 1, Kanellopoulos et al. (2012); 2, Walkinshaw et al. (2015); 3, Philip et al. (2001); 4, Iqbal et al. (2013); 5, Khan et al. (2015); 6, Gai et al. (2016); 7, Hou et al. (2011); 8, Horiuchi et al. (2008); 9, Goodwin et al. (1997); 10, Saumweber et al. (2011); and 11, Godenschwege et al. (2004).

vs controls, respectively) and adult MB limited attenuation (LeoMB, ANOVA: $F_{(2,39)} = 8.0835$, $p = 0.0012$; subsequent LSM: $p = 0.0004$ and $p = 0.0058$ vs controls, respectively; dnc, ANOVA: $F_{(2,29)} = 16.7159$, $p < 0.0001$; subsequent LSM: $p = 2.2 \times 10^{-5}$ and $p = 4.3 \times 10^{-5}$ vs controls respectively; MB247, ANOVA: $F_{(2,30)} = 11.5623$, $p = 0.0002$; subsequent LSM: $p = 0.0004$ and $p = 0.0002$ vs controls, respectively). These results were recapitulated with an independent RNAi-mediating transgene driven pan-MB under dncGal4 (dnc-Gal4;TubG80^{ts} >+ = 12.23 ± 1.34; dtauRNAi40875 >+ = 8.71 ± 1.88; dnc-Gal4; TubG80^{ts} >dtauRNAi40875 = 1.99 ± 1.65; $n = 14$, ANOVA: $F_{(2,42)} = 9.8512$, $p = 0.0003$; subsequent LSM: $p = 0.0001$ and $p = 0.0056$ vs controls, respectively).

Interestingly, dTau attenuation restricted to $\alpha'\beta'$ neurons precipitated pronounced habituation defects (c305α, ANOVA: $F_{(2,28)} = 72.8606$, $p < 0.0001$; subsequent LSM: $p = 1.16 \times 10^{-10}$ and $p = 2.63 \times 10^{-11}$ vs controls, respectively), in agreement with an accompanying report (Roussou et al., 2019). In contrast, habituation was normal if abrogation was limited to c739-Gal4-marked neurons (c739, ANOVA: $F_{(2,43)} = 0.5378$, $p = 0.5881$). Collectively, the results indicate a distinct role for dTau specifically within the α'/β' neurons in molecular mechanisms that facilitate footshock habituation, in addition to its role in limiting PSD-LTM within these and their α/β counterparts.

dTau elevation in adult MBs suppresses memory and results in premature habituation

Because LTM and footshock habituation appear sensitive to dTau levels within the MBs, we hypothesized that their elevation within these neurons may lead to the opposite phenotypes, akin to those observed upon overexpression of human tau (Sealey et al., 2017). In humans, duplication of the *tau* gene and, hence, presumably elevation of the protein levels, causes prominent neurofibrillary tangle pathology leading to early-onset dementia with an Alzheimer's disease (AD) clinical phenotype (Le Guennec et al., 2016).

To elevate dTau, a UAS-Flag-dTau transgene was expressed specifically throughout the adult MBs under the pan-mushroom body driver dnc-Gal4;TubG80^{ts} (Fig. 6*E*). The increase in dTau within the MBs did not affect learning (Fig. 6*A*; ANOVA: $F_{(2,33)} = 0.9706$, $p = 0.3901$) or the protein synthesis-independent ARM (Fig. 6*B*; massed, ANOVA: $F_{(2,23)} = 1.9193$, $p = 0.1716$), but PSD-LTM (Fig. 6*B* spaced) was deficient (ANOVA: $F_{(2,28)} = 13.7758$, $p < 0.0001$; subsequent LSM: $p = 4.1 \times 10^{-5}$ and $p = 0.0003$ vs controls, respectively). In accord with the hypothesis that elevated translation is, at least in part, responsible for the increased PSD-LTM, adult-specific pan-neuronal accumulation of dTau resulted in an acute translation decrease (Fig. 6*I*; $p = 0.0026$, $n = 4$). Therefore, processes required for PSD-LTM are sensitive to dTau levels in a manner akin to that recently described for dAlk (Gouzi et al., 2018) and in accord with the interpretation that dTau participates in processes that limit LTM formation, storage, or recall.

Interestingly, dTau elevation did not affect habituation (Fig. 6*C*) to 15 footshocks (ANOVA: $F_{(2,27)} = 0.7958$, $p = 0.4623$), but onset of the habituated response was premature (Fig. 6*D*) as it occurred after only two stimuli (ANOVA: $F_{(2,39)} = 33.1018$, $p < 0.0001$; subsequent LSM: $p = 3.2 \times 10^{-6}$ and $p = 1.9 \times 10^{-9}$ vs controls, respectively). Because silencing neurotransmission from α/β MB neurons results in premature habituation (Acevedo et al., 2007), we overexpressed dTau specifically in these neurons under c739-Gal4. Although this resulted in deficient (Fig. 6*F*) PSD-LTM (ANOVA: $F_{(2,31)} = 18.0720$, $p < 0.0001$; subsequent LSM: $p = 8.9 \times 10^{-6}$ and $p = 4 \times 10^{-5}$ vs controls, respectively), it yielded normal habituation to 15 footshocks (ANOVA: $F_{(2,43)} = 0.5105$, $p = 0.6040$) and did not result in premature habituation after two footshocks (ANOVA: $F_{(2,43)} = 0.9059$, $p = 0.4121$; Fig. 6*G*,*H*). This suggests that its overaccumulation does not inhibit neurotransmission and that dTau is strongly implicated in a dosage-dependent manner in processes mediating footshock habituation within the MBs.

Discussion

Although our phenotypic search was not exhaustive, our results demonstrate, to our knowledge for the first time, robust mutant phenotypes upon dTau loss. In agreement with prior reports, we also find that both *tau*^{KO} and *tau*^{MI} mutants are viable and fertile (data not shown).

Proteostatic changes upon chronic and acute dTau loss

Significant changes in the adult CNS cytoskeletal proteome were uncovered by comparative proteomics and appear to underlie a global proteostatic adjustment to dTau abrogation. We have modeled two scenarios of dTau abrogation, chronic dTau loss as seen in the mutants, and a milder acute attenuation in the adult CNS. Although both situations elicited broad changes with certain proteins altered in common, they yielded differential proteomic signatures (Tables 1-5). Chronic changes appear to have resolved into a proteostatic steady state, presumably to minimize the effects of dTau loss. This is reflected, for example, by compensatory changes in HDAC levels, which stabilize the microtubule cytoskeleton, despite the ostensibly chronic reduction in tubulin (Fig. 1*B*, Table 1). On the other hand, acute dTau attenuation revealed the initial response of the CNS proteome to the insult, which included the downregulation of many tau interacting proteins (Table 4). We suggest that, with time, this acute proteostatic flux resolves to a steady state reflective of the level of dTau attenuation, and ongoing experiments are addressing this hypothesis.

Interestingly, the steady-state levels of all three tubulins were significantly reduced (Table 1), in accord with the notion that tau is essential for the maintenance of long labile domains of microtubules (Qiang et al., 2018) and may also be reflected in the acute downregulation of proteins such as labile end-organizing protein Eb1 (Li et al., 2012). dTau loss-dependent reduction of labile

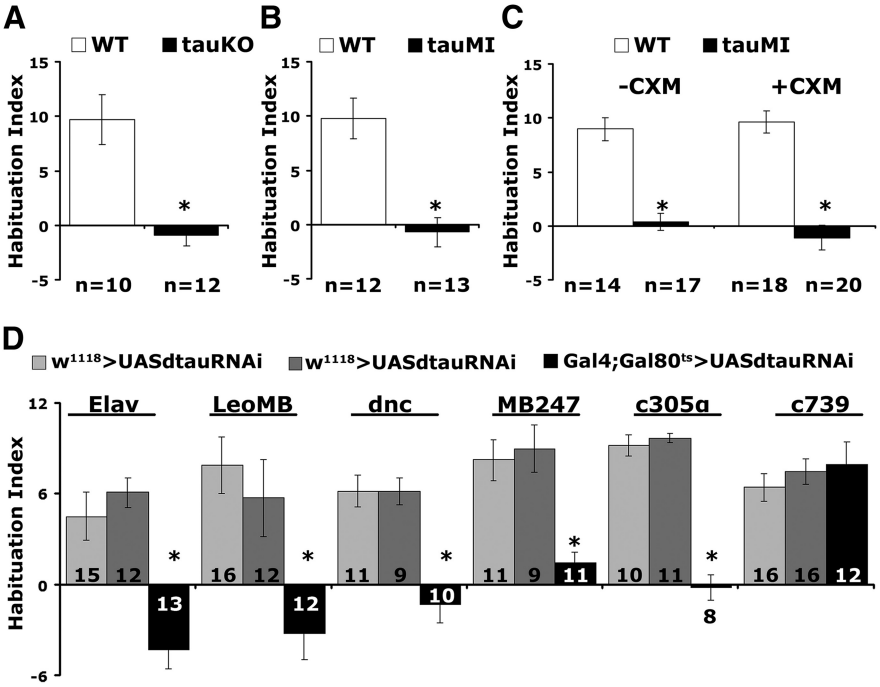

Figure 5. dTau abrogation impairs habituation. ***A***, ***B***, *tau*^{MI} and *tau*^{KO} mutants present strong habituation deficits (*$p < 0.0001$). The number of experimental replicates (*n*) is indicated below the graphs. ***C***, CXM administration did not affect the defective habituation of *tau*^{MI} flies. ***D***, Deficient habituation upon dTau abrogation in adult animals using Elav (*$p < 0.0001$), LeoMB (*$p = 0.0004$), MB247 (*$p = 0.0004$), dnc (*$p < 0.0001$), and c305α (*$p < 0.0001$) drivers, but not under c739 ($p = 0.3269$). The number of experimental replicates (*n*) is indicated within the bars.

domain length is in effect reducing microtubule mass and hence the number of tubulins. The relative increase in acetylated tubulin (Fig. 1*B*,*C*) is consistent with the reduction in labile domains, which are expected to be underacetylated (Qiang et al., 2018). A potential consequence of the increased microtubule stability is the significant elevation in the subunits of both anterograde and retrograde moving motor proteins (Table 1).

Cytoskeletal homeostasis upon chronic dTau loss also benefits from the reduction in HDAC (Table 1), which may mediate the increase in acetylated tubulin and also account for the proposed reduction in the labile domains. Although how dTau loss affects HDAC levels is unclear at the moment, levels of HDAC are sensitive to tau dosage as HDAC6 is elevated in AD brains and tubulin acetylation is reduced in neurofibrillary tangle-bearing neurons (Hempen and Brion, 1996). Consistent with these observations, increased tubulin acetylation rescues human tau overexpression-induced defects in *Drosophila* (Xiong et al., 2013; Mao et al., 2017).

The functional role for dTau as a major regulator of cytoskeletal dynamics *in vivo* is also illustrated by the upregulation of the steady-state levels of actin binding proteins (Table 1), likely in response to the negative effects on actin polymerization upon dTau loss. Our data demonstrate that F-actin interacts directly with and is stabilized by dTau within the fly CNS (Fig. 2*B*–*E*). In congruence, perturbation of actin dynamics has also been reported upon pan-neuronal expression of human tau isoforms in *Drosophila* (Fulga et al., 2007) and may underlie some of the resultant neuropathologies. Therefore, our collective data strongly support the notion that dTau is a true MAP impacting the microtubule and actin cytoskeleton and, despite the sequence diversity, is an apparent ortholog of its vertebrate counterpart.

dTau translation regulation and neuroplasticity

Chronic, but surprisingly also acute, dTau abrogation resulted in the upregulation of translation-linked proteins (Tables 2, 4), strongly indicating that dTau is a negative regulator of translation (Fig. 4*B*). Congruently, vertebrate tau is a negative regulator of translation (Apicco et al., 2018) and was also recently reported to act as a negative regulator of ribosomal protein levels in mouse brains (Koren et al., 2019). Importantly, the fly brain comparative proteomics provide further validation of these results in a different system, as clearly dTau loss results in the broad elevation of proteins involved in regulation, initiation, and termination of translation, as well as most cellular ribosomal proteins (Tables 2, 4). In addition, tau is known to bind to ribosomes in the brain and to impair their function in reducing protein synthesis (Meier et al., 2016), an effect also observed in human tauopathy brains (Piao et al., 2002). Finally, this agrees with quantitative proteomics in a mouse model of tauopathy, which revealed a decrease in protein synthesis, specifically in neurons with high levels of pathological tau (Evans et al., 2019). This effect was recapitulated by acute dTau overexpression (Fig. 6*I*), demonstrating the sensitivity of translation to tau levels.

Interestingly, translational upregulation may be partially selective, because under chronic or acute dTau attenuation the levels of most MAPs, tubulins, HDACs, and other abundant proteins were not elevated, but rather reduced (Tables 1, 4). Consistent with this notion, the level of translational regulator dFmr1, whose loss results in LTM deficits (Kanellopoulos et al., 2012), is also elevated (Table 2), suggesting that dTau may be implicated in translational selectivity mechanisms. The elevation of proteins potentially involved in PSD-LTM in mutant brains (Tables 3, 5; Godenschwege et al., 2004; Hou et al., 2011; Iqbal et al., 2013) and probably within MB neurons, likely underlies, at least in part, the enhanced memory, in agreement with its CXM sensitivity (Fig. 3*C*). The enhanced 24 h memory is not ARM (Fig. 3*A*,*B*), or impaired forgetting (Fig. 4*A*). Furthermore, dTau is required within α/β and α'/β' neurons involved in recall and memory consolidation, respectively (Dubnau et al., 2001; McGuire et al., 2001; Pascual and Préat, 2001; Akalal et al., 2006; Krashes et al., 2007). Collectively then, the enhanced 24 h memory upon dTau abrogation is most likely due to enhanced consolidation of true PSD-LTM.

In contrast to PSD-LTM, the defective footshock habituation upon dTau loss is CXM insensitive, arguing that it is not consequent of excessive protein synthesis (Fig. 5). Is it possible that failure to devalue the electric footshock US results in better acquisition, resulting in better learning that eventually forms enhanced memory? This is unlikely because abrogation of dTau in the MBs did not result in better performance after limited training with three odor/shock pairings (Fig. 3*E*). Moreover, limiting dTau abrogation to the α'/β' MB neurons resulted in enhanced PSD-LTM, as well as failure to devalue the shock stimulus, demonstrating that these effects are cell autonomous. Neurotrans-

mission from these neurons is required for olfactory memory acquisition and stabilization (Krashes et al., 2007), but also to facilitate shock habituation (Roussou et al., 2019). Therefore, it is unlikely that dTau is implicated in a common mechanism affecting both processes, because the enhanced PSD-LTM mediated by these neurons (Fig. 3*F*) suggests increased neurotransmission, although failure to habituate its impairment.

A parsimonious explanation for this paradox would be that dTau functions in distinct mechanisms regulating conditional neurotransmitter traffic and release within these neurons, which is in line with the changes in actin binding proteins, and microtubule motor and associated proteins uncovered by the proteomics (Tables 1, 4). Changes upon dTau abrogation may selectively deregulate neurotransmitter levels and their regulated release, which are known to depend on presynaptic microtubule and cortical actin dynamics (Rust and Maritzen, 2015; Bodaleo and Gonzalez-Billault, 2016). This may selectively enhance neurotransmission upon associative (memory), but not upon nonassociative (habituation) stimulation. This is in line with the observation that dTau abrogation in $\alpha\beta$ neurons, where neurotransmission is essential for LTM retrieval (Dubnau et al., 2001; McGuire et al., 2001; Pascual and Préat, 2001; Akalal et al., 2006), also enhances LTM (Fig. 3*F*). Interestingly, tau-null mice were also recently reported to perform better than WT littermates in a spatial navigation task (Ahmed et al., 2014) and showed enhanced exploration and recognition memory (Jara et al., 2018). Given these collective results, the effects of dTau loss on *Drosophila* PSD-LTM and the molecular targets offered by our comparative proteomic data, potential physiological roles for dTau in these processes are currently under investigation.

Overexpression of human tau in the adult *Drosophila* CNS precipitates significant impairment in LTM, but not ARM (Sealey et al., 2017). This effect was recapitulated by adult-specific pan-neuronal or MB limited overexpression of dTau (Fig. 6). Again, relatively acute dTau elevation precipitated the complementary phenotype of premature habituation. Blocked neurotransmission from the MBs results in premature footshock habituation (Acevedo et al., 2007), which is similar to that observed upon dTau overexpression. Therefore, we hypothesize that excess dTau in the MBs might reduce neurotransmitter availability in

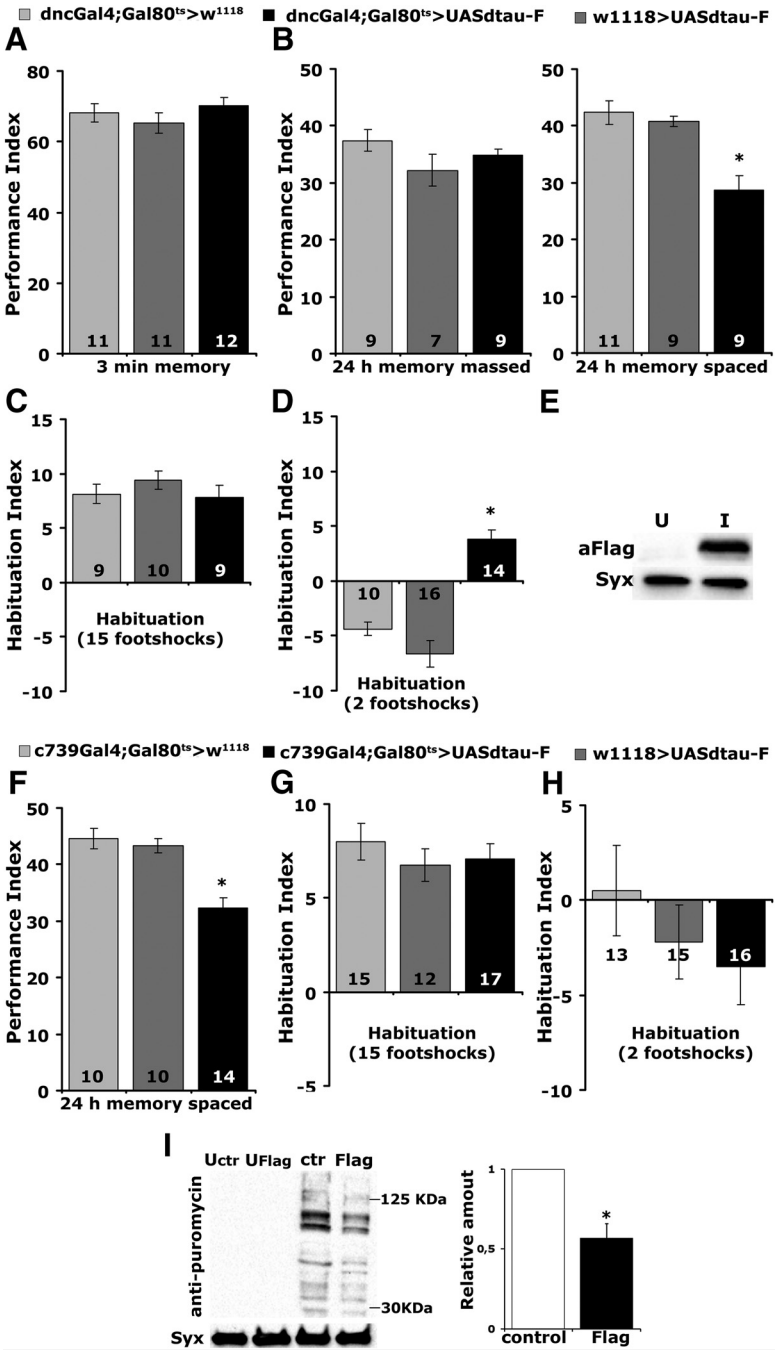

Figure 6. dTau elevation within the adult MBs leads to premature habituation and LTM deficits with a concomitant decrease in protein synthesis levels. ***A***, ***A–D***, Adult-specific expression of UAS-Flag dTau within the MBs under dnc-Gal4 results (***A***), normal 3 min memory (***B***), normal ARM after massed training but LTM deficits after spaced training (*$p < 0.0001$), normal habituation following 15-stimulus training (***C***), and premature habituation (*$p < 0.0001$) following 2-stimulus training (***D***). The number of experimental replicates (*n*) is indicated within the bars. ***E***, Representative Western blot demonstrating accumulation of Flag-dTau in adult MBs using LeoMB-Gal4;TubG80^{ts} of animals raised at 18°C and shifted to 30°C for 2 d (I), while uninduced animals (U) were kept at 18°C for these 2 d. dTau was revealed with an anti-Flag antibody. Syntaxin (Syx) was used as a loading control. ***F–H***, Adult-specific expression of UAS-Flag dTau within $\alpha\beta$ neurons under c739 yields significant LTM deficits (*$p < 0.0001$) compared with controls (***F***), and results in normal habituation following 15-stimuli (***G***) or 2-stimuli (***H***) training. The number of experimental replicates (*n*) is indicated within the bars. ***I***, Representative Western blot of head lysates from flies expressing UAS-Flag-dTau using Elav-Gal4;TubG80^{ts} and probed with anti-puromycin antibody. Animals were raised at 18°C and shifted to 30°C for 3 d, while uninduced animals (U) were kept at 18°C for these 3 d. The genotype of control animals was Elav-Gal4;Gal80^{ts}/+. Flies were treated with 600 μM puromycin for 16 h. For the quantification, levels of the signal corresponding to molecular weight region 30–125 kDa were normalized using the Syx loading control and are shown as a ratio of their mean ± SEM values relative to their respective level in control flies, which is arbitrarily set to 1. The star indicates significant differences ($p = 0.0026$) from control (open bar), indicative of decreased protein synthesis upon dTau loss.

accord with data from the larval neuromuscular junction (Chee et al., 2005).

In conclusion, it is apparent that dTau contributes in a dosage-dependent manner to a broad number of distinct processes involved in CNS function. Although it is a challenge of future work to understand how dTau can alter neuronal plasticity, the emerging insights into its physiological functions are expected to enhance our understanding of the molecular and cellular pathways perturbed in the various tauopathies.

References

Acevedo SF, Froudarakis EI, Kanellopoulos A, Skoulakis EM (2007) Protection from premature habituation requires functional mushroom bodies in Drosophila. Learn Mem 14:376–384.

Ahmed T, Van der Jeugd A, Blum D, Galas MC, D'Hooge R, Buee L, Balschun D (2014) Cognition and hippocampal synaptic plasticity in mice with a homozygous tau deletion. Neurobiol Aging 35:2474–2478.

Akalal DB, Wilson CF, Zong L, Tanaka NK, Ito K, Davis RL (2006) Roles for Drosophila mushroom body neurons in olfactory learning and memory. Learn Mem 13:659–668.

Alves-Silva J, Sánchez-Soriano N, Beaven R, Klein M, Parkin J, Millard TH, Bellen HJ, Venken KJ, Ballestrem C, Kammerer RA, Prokop A (2012) Spectraplakins promote microtubule-mediated axonal growth by functioning as structural microtubule-associated proteins and EB1-dependent +TIPs (tip interacting proteins). J Neurosci 32:9143–9158.

Apicco DJ, Ash PEA, Maziuk B, LeBlang C, Medalla M, Al Abdullatif A, Ferragud A, Botelho E, Ballance HI, Dhawan U, Boudeau S, Cruz AL, Kashy D, Wong A, Goldberg LR, Yazdani N, Zhang C, Ung CY, Tripodis Y, Kanaan NM, et al (2018) Reducing the RNA binding protein TIA1 protects against tau-mediated neurodegeneration in vivo. Nat Neurosci 21:72–80.

Aso Y, Grübel K, Busch S, Friedrich AB, Siwanowicz I, Tanimoto H (2009) The mushroom body of adult Drosophila characterized by GAL4 drivers. J Neurogenet 23:156–172.

Barlan K, Lu W, Gelfand VI (2013) The microtubule-binding protein ensconsin is an essential cofactor of kinesin-1. Curr Biol 23:317–322.

Belozerov VE, Ratkovic S, McNeill H, Hilliker AJ, McDermott JC (2014) In vivo interaction proteomics reveal a novel p38 mitogen-activated protein kinase/Rack1 pathway regulating proteostasis in Drosophila muscle. Mol Cell Biol 34:474–484.

Bettencourt da Cruz A, Schwärzel M, Schulze S, Niyyati M, Heisenberg M, Kretzschmar D (2005) Disruption of the MAP1B-related protein FUTSCH leads to changes in the neuronal cytoskeleton, axonal transport defects, and progressive neurodegeneration in Drosophila. Mol Biol Cell 16:2433–2442.

Bodaleo FJ, Gonzalez-Billault C (2016) The presynaptic microtubule cytoskeleton in physiological and pathological conditions: lessons from Drosophila fragile X syndrome and hereditary spastic paraplegias. Front Mol Neurosci 9:60.

Bolkan BJ, Kretzschmar D (2014) Loss of tau results in defects in photoreceptor development and progressive neuronal degeneration in drosophila. Dev Neurobiol 74:1210–1225.

Burnouf S, Grönke S, Augustin H, Dols J, Gorsky MK, Werner J, Kerr F, Alic N, Martinez P, Partridge L (2016) Deletion of endogenous tau proteins is not detrimental in drosophila. Sci Rep 6:23102.

Buttgereit D, Leiss D, Michiels F, Renkawitz-Pohl R (1991) During Drosophila embryogenesis the beta 1 tubulin gene is specifically expressed in the nervous system and the apodemes. Mech Dev 33:107–118.

Cervantes-Sandoval I, Chakraborty M, MacMullen C, Davis RL (2016) Scribble scaffolds a signalosome for active forgetting. Neuron 90:1230–1242.

Chatterjee S, Sang TK, Lawless GM, Jackson GR (2009) Dissociation of tau toxicity and phosphorylation: role of GSK-3beta, MARK and Cdk5 in a Drosophila model. Hum Mol Genet 18:164–177.

Chee FC, Mudher A, Cuttle MF, Newman TA, MacKay D, Lovestone S, Shepherd D (2005) Overexpression of tau results in defective synaptic transmission in Drosophila neuromuscular junctions. Neurobiol Dis 20:918–928.

Chen X, Li Y, Huang J, Cao D, Yang G, Liu W, Lu H, Guo A (2007) Study of tauopathies by comparing Drosophila and human tau in drosophila. Cell Tissue Res 329:169–178.

Colomb J, Brembs B (2016) PKC in motorneurons underlies self-learning, a form of motor learning in Drosophila. Peer J 4:e1971.

Comas D, Petit F, Preat T (2004) Drosophila long-term memory formation involves regulation of cathepsin activity. Nature 430:460–463.

Copf T, Goguel V, Lampin-Saint-Amaux A, Scaplehorn N, Preat T (2011) Cytokine signaling through the JAK/STAT pathway is required for long-term memory in Drosophila. Proc Natl Acad Sci U S A 108:8059–8064.

Davis RL (2005) Olfactory memory formation in drosophila: from molecular to systems neuroscience. Annu Rev Neurosci 28:275–302.

Deliu LP, Ghosh A, Grewal SS (2017) Investigation of protein synthesis in Drosophila larvae using puromycin labelling. Biol Open 6:1229–1234.

Doerflinger H, Benton R, Shulman JM, St Johnston D (2003) The role of PAR-1 in regulating the polarised microtubule cytoskeleton in the Drosophila follicular epithelium. Development 130:3965–3975.

Dubnau J, Grady L, Kitamoto T, Tully T (2001) Disruption of neurotransmission in Drosophila mushroom body blocks retrieval but not acquisition of memory. Nature 411:476–480.

Evans HT, Benetatos J, van Roijen M, Bodea LG, Götz J (2019) Decreased synthesis of ribosomal proteins in tauopathy revealed by non-canonical amino acid labelling. EMBO J 38:e101174.

Fahmy K, Akber M, Cai X, Koul A, Hayder A, Baumgartner S (2014) αTubulin 67C and Ncd are essential for establishing a cortical microtubular network and formation of the Bicoid mRNA gradient in drosophila. PLoS One 9:e112053.

Feuillette S, Miguel L, Frébourg T, Campion D, Lecourtois M (2010) Drosophila models of human tauopathies indicate that tau protein toxicity in vivo is mediated by soluble cytosolic phosphorylated forms of the protein. J Neurochem 113:895–903.

Frost B, Bardai FH, Feany MB (2016) Lamin dysfunction mediates neurodegeneration in tauopathies. Curr Biol 26:129–136.

Fulga TA, Elson-Schwab I, Khurana V, Steinhilb ML, Spires TL, Hyman BT, Feany MB (2007) Abnormal bundling and accumulation of F-actin mediates tau-induced neuronal degeneration in vivo. Nat Cell Biol 9:139–148.

Gai Y, Liu Z, Cervantes-Sandoval I, Davis RL (2016) Drosophila SLC22A transporter is a memory suppressor gene that influences cholinergic neurotransmission to the mushroom bodies. Neuron 90:581–595.

Gistelinck M, Lambert JC, Callaerts P, Dermaut B, Dourlen P (2012) Drosophila models of tauopathies: what have we learned? Int J Alzheimers Dis 2012:970980.

Godenschwege TA, Reisch D, Diegelmann S, Eberle K, Funk N, Heisenberg M, Hoppe V, Hoppe J, Klagges BR, Martin JR, Nikitina EA, Putz G, Reifegerste R, Reisch N, Rister J, Schaupp M, Scholz H, Schwärzel M, Werner U, Zars TD, et al (2004) Flies lacking all synapsins are unexpectedly healthy but are impaired in complex behaviour. Eur J Neurosci 20:611–622.

Goldstein LS, Gunawardena S (2000) Flying through the Drosophila cytoskeletal genome. J Cell Biol 150:F63–F68.

Goodwin SF, Del Vecchio M, Velinzon K, Hogel C, Russell SR, Tully T, Kaiser K (1997) Defective learning in mutants of the *Drosophila* gene for a regulatory subunit of cAMP-dependent protein kinase. J Neurosci 17:8817–8827.

Gorsky MK, Burnouf S, Sofola-Adesakin O, Dols J, Augustin H, Weigelt CM, Grönke S, Partridge L (2017) Pseudo-acetylation of multiple sites on human tau proteins alters tau phosphorylation and microtubule binding, and ameliorates amyloid beta toxicity. Sci Rep 7:9984.

Gouzi JY, Moressis A, Walker JA, Apostolopoulou AA, Palmer RH, Bernards A, Skoulakis EM (2011) The receptor tyrosine kinase Alk controls neurofibromin functions in Drosophila growth and learning. PLoS Genet 7:e1002281.

Gouzi JY, Bouraimi M, Roussou IG, Moressis A, Skoulakis EMC (2018) The *Drosophila* receptor tyrosine kinase alk constrains long-term memory formation. J Neurosci 38:7701–7712.

Guven-Ozkan T, Busto GU, Schutte SS, Cervantes-Sandoval I, O'Dowd DK, Davis RL (2016) MiR-980 is a memory suppressor MicroRNA that regulates the autism-susceptibility gene A2bp1. Cell Rep 14:1698–1709.

Harada A, Oguchi K, Okabe S, Kuno J, Terada S, Ohshima T, Sato-Yoshitake R, Takei Y, Noda T, Hirokawa N (1994) Altered microtubule organization in small-calibre axons of mice lacking tau protein. Nature 369:488–491.

Heidary G, Fortini ME (2001) Identification and characterization of the Drosophila tau homolog. Mech Dev 108:171–178.

Heisenberg M (2003) Mushroom body memoir: from maps to models. Nat Rev Neurosci 4:266–275.

Hempen B, Brion JP (1996) Reduction of acetylated alpha-tubulin immunoreactivity in neurofibrillary tangle-bearing neurons in Alzheimer's disease. J Neuropathol Exp Neurol 55:964–972.

Henríquez JP, Cross D, Vial C, Maccioni RB (1995) Subpopulations of tau interact with microtubules and actin filaments in various cell types. Cell Biochem Funct 13:239–250.

Higham JP, Malik BR, Buhl E, Dawson JM, Ogier AS, Lunnon K, Hodge JJL (2019) Alzheimer's disease associated genes ankyrin and tau cause shortened lifespan and memory loss in drosophila. Front Cell Neurosci 13:260.

Horiuchi J, Yamazaki D, Naganos S, Aigaki T, Saitoe M (2008) Protein kinase A inhibits a consolidated form of memory in drosophila. Proc Natl Acad Sci U S A 105:20976–20981.

Hou Q, Jiang H, Zhang X, Guo C, Huang B, Wang P, Wang T, Wu K, Li J, Gong Z, Du L, Liu Y, Liu L, Chen C (2011) Nitric oxide metabolism controlled by formaldehyde dehydrogenase (fdh, homolog of mammalian GSNOR) plays a crucial role in visual pattern memory in drosophila. Nitric Oxide 24:17–24.

Hubbert C, Guardiola A, Shao R, Kawaguchi Y, Ito A, Nixon A, Yoshida M, Wang XF, Yao TP (2002) HDAC6 is a microtubule-associated deacetylase. Nature 417:455–458.

Hudson AM, Cooley L (2002) A subset of dynamic actin rearrangements in Drosophila requires the Arp2/3 complex. J Cell Biol 156:677–687.

Iqbal Z, Vandeweyer G, van der Voet M, Waryah AM, Zahoor MY, Besseling JA, Roca LT, Vulto-van Silfhout AT, Nijhof B, Kramer JM, Van der Aa N, Ansar M, Peeters H, Helsmoortel C, Gilissen C, Vissers LE, Veltman JA, de Brouwer AP, Frank Kooy R, Riazuddin S, et al (2013) Homozygous and heterozygous disruptions of ANK3: at the crossroads of neurodevelopmental and psychiatric disorders. Hum Mol Genet 22:1960–1970.

Isabel G, Pascual A, Preat T (2004) Exclusive consolidated memory phases in drosophila. Science 304:1024–1027.

Jara C, Aránguiz A, Cerpa W, Tapia-Rojas C, Quintanilla RA (2018) Genetic ablation of tau improves mitochondrial function and cognitive abilities in the hippocampus. Redox Biol 18:279–294.

Kanellopoulos AK, Semelidou O, Kotini AG, Anezaki M, Skoulakis EM (2012) Learning and memory deficits consequent to reduction of the fragile X mental retardation protein result from metabotropic glutamate receptor-mediated inhibition of cAMP signaling in *Drosophila*. J Neurosci 32:13111–13124.

Karpova N, Bobinnec Y, Fouix S, Huitorel P, Debec A (2006) Jupiter, a new Drosophila protein associated with microtubules. Cell Motil Cytoskeleton 63:301–312.

Kempf M, Clement A, Faissner A, Lee G, Brandt R (1996) Tau binds to the distal axon early in development of polarity in a microtubule- and microfilament-dependent manner. J Neurosci 16:5583–5592.

Khan MR, Li L, Pérez-Sánchez C, Saraf A, Florens L, Slaughter BD, Unruh JR, Si K (2015) Amyloidogenic oligomerization transforms Drosophila Orb2 from a translation repressor to an activator. Cell 163:1468–1483.

Koolen DA, Vissers LE, Pfundt R, de Leeuw N, Knight SJ, Regan R, Kooy RF, Reyniers E, Romano C, Fichera M, Schinzel A, Baumer A, Anderlid BM, Schoumans J, Knoers NV, van Kessel AG, Sistermans EA, Veltman JA, Brunner HG, de Vries BB (2006) A new chromosome 17q21.31 microdeletion syndrome associated with a common inversion polymorphism. Nat Genet 38:999–1001.

Koren SA, Hamm MJ, Meier SE, Weiss BE, Nation GK, Chishti EA, Arango JP, Chen J, Zhu H, Blalock EM, Abisambra JF (2019) Tau drives translational selectivity by interacting with ribosomal proteins. Acta Neuropathol 137:571–583.

Kosmidis S, Grammenoudi S, Papanikolopoulou K, Skoulakis EM (2010) Differential effects of tau on the integrity and function of neurons essential for learning in *Drosophila*. J Neurosci 30:464–477.

Kotoula V, Moressis A, Semelidou O, Skoulakis EMC (2017) Drk-mediated signaling to rho kinase is required for anesthesia-resistant memory in *Drosophila*. Proc Natl Acad Sci U S A 114:10984–10989.

Krashes MJ, Keene AC, Leung B, Armstrong JD, Waddell S (2007) Sequential use of mushroom body neuron subsets during Drosophila odor memory processing. Neuron 53:103–115.

Krashes MJ, DasGupta S, Vreede A, White B, Armstrong JD, Waddell S (2009) A neural circuit mechanism integrating motivational state with memory expression in drosophila. Cell 139:416–427.

Le Guennec K, Quenez O, Nicolas G, Wallon D, Rousseau S, Richard AC, Alexander J, Paschou P, Charbonnier C, Bellenguez C, Grenier-Boley B, Lechner D, Bihoreau MT, Olaso R, Boland A, Meyer V, Deleuze JF, Amouyel P, Munter HM, Bourque G, et al (2016) 17q21.31 duplication causes prominent tau-related dementia with increased MAPT expression. Mol Psychiatry 22:1119–1125.

Li W, Moriwaki T, Tani T, Watanabe T, Kaibuchi K, Goshima G (2012) Reconstitution of dynamic microtubules with Drosophila XMAP215, EB1, and Sentin. J Cell Biol 199:849–862.

Mackenzie IR, Neumann M, Bigio EH, Cairns NJ, Alafuzoff I, Kril J, Kovacs GG, Ghetti B, Halliday G, Holm IE, Ince PG, Kamphorst W, Revesz T, Rozemuller AJ, Kumar-Singh S, Akiyama H, Baborie A, Spina S, Dickson DW, Trojanowski JQ, et al (2009) Nomenclature for neuropathologic subtypes of frontotemporal lobar degeneration: consensus recommendations. Acta Neuropathol 117:15–18.

Mao CX, Wen X, Jin S, Zhang YQ (2017) Increased acetylation of microtubules rescues human tau-induced microtubule defects and neuromuscular junction abnormalities in drosophila. Dis Model Mech 10:1245–1252.

Martin DN, Baehrecke EH (2004) Caspases function in autophagic programmed cell death in Drosophila. Development 131:275–284.

Matamoros AJ, Baas PW (2016) Microtubules in health and degenerative disease of the nervous system. Brain Res Bull 126:217–225.

McGuire SE, Le PT, Davis RL (2001) The role of Drosophila mushroom body signaling in olfactory memory. Science 293:1330–1333.

McGuire SE, Mao Z, Davis RL (2004) Spatiotemporal gene expression targeting with the TARGET and gene-switch systems in Drosophila. Sci STKE 2004:pl6.

Meier S, Bell M, Lyons DN, Rodriguez-Rivera J, Ingram A, Fontaine SN, Mechas E, Chen J, Wolozin B, LeVine H 3rd, Zhu H, Abisambra JF (2016) Pathological tau promotes neuronal damage by impairing ribosomal function and decreasing protein synthesis. J Neurosci 36:1001–1007.

Mershin A, Pavlopoulos E, Fitch O, Braden BC, Nanopoulos DV, Skoulakis EM (2004) Learning and memory deficits upon TAU accumulation in Drosophila mushroom body neurons. Learn Mem 11:277–287.

Messaritou G, Leptourgidou F, Franco M, Skoulakis EM (2009) A third functional isoform enriched in mushroom body neurons is encoded by the Drosophila 14-3-3zeta gene. FEBS Lett 583:2934–2938.

Nathans D (1964) Puromycin inhibition of protein synthesis: incorporation of puromycin into peptide chains. Proc Natl Acad Sci U S A 51:585–592.

Nishimura I, Yang Y, Lu B (2004) PAR-1 kinase plays an initiator role in a temporally ordered phosphorylation process that confers tau toxicity in drosophila. Cell 116:671–682.

Papanikolopoulou K, Skoulakis EM (2011) The power and richness of modelling tauopathies in drosophila. Mol Neurobiol 44:122–133.

Papanikolopoulou K, Skoulakis EM (2015) Temporally distinct phosphorylations differentiate tau-dependent learning deficits and premature mortality in drosophila. Hum Mol Gen 24:2065–2077.

Papanikolopoulou K, Kosmidis S, Grammenoudi S, Skoulakis EM (2010) Phosphorylation differentiates tau-dependent neuronal toxicity and dysfunction. Biochem Soc Trans 38:981–987.

Papanikolopoulou K, Grammenoudi S, Samiotaki M, Skoulakis EMC (2018) Differential effects of 14-3-3 dimers on tau phosphorylation, stability and toxicity in vivo. Hum Mol Gen 27:2244–2261.

Papegaey A, Eddarkaoui S, Deramecourt V, Fernandez-Gomez FJ, Pantano P, Obriot H, Machala C, Anquetil V, Camuzat A, Brice A, Maurage CA, Le Ber I, Duyckaerts C, Buée L, Sergeant N, Buée-Scherrer V (2016) Reduced tau protein expression is associated with frontotemporal degeneration with progranulin mutation. Acta Neuropathol Commun 4:74.

Pascual A, Préat T (2001) Localization of long-term memory within the Drosophila mushroom body. Science 294:1115–1117.

Pavlopoulos E, Anezaki M, Skoulakis EM (2008) Neuralized is expressed in the alpha/beta lobes of adult Drosophila mushroom bodies and facilitates olfactory long-term memory formation. Proc Natl Acad Sci U S A 105:14674–14679.

Philip N, Acevedo SF, Skoulakis EM (2001) Conditional rescue of olfactory learning and memory defects in mutants of the 14-3-3z gene leonardo. J Neurosci 21:8417–8425.

Piao YS, Hayashi S, Wakabayashi K, Kakita A, Aida I, Yamada M, Takahashi H (2002) Cerebellar cortical tau pathology in progressive supranuclear palsy and corticobasal degeneration. Acta Neuropathol 103:469–474.

Pielage J, Cheng L, Fetter RD, Carlton PM, Sedat JW, Davis GW (2008) A presynaptic giant ankyrin stabilizes the NMJ through regulation of

presynaptic microtubules and transsynaptic cell adhesion. Neuron 58:195–209.

Plaçais PY, de Tredern É, Scheunemann L, Trannoy S, Goguel V, Han KA, Isabel G, Preat T (2017) Upregulated energy metabolism in the Drosophila mushroom body is the trigger for long-term memory. Nat Commun 8:15510.

Portran D, Schaedel L, Xu Z, Théry M, Nachury MV (2017) Tubulin acetylation protects long-lived microtubules against mechanical ageing. Nat Cell Biol 19:391–398.

Qiang L, Sun X, Austin T, Muralidharan H, Jean DC, Liu M, Yu W, Baas PW (2018) Tau does not stabilize axonal microtubules but rather enables them to have long labile domains. Curr Biol 28:2181–2189.e4.

Robinow S, White K (1988) The locus elav of Drosophila melanogaster is expressed in neurons at all developmental stages. Dev Biol 126:294–303.

Roussou IG, Papanikolopoulou K, Savakis C, Skoulakis E (2019) Drosophila Bruton's Tyrosine Kinase regulates habituation latency and facilitation in distinct mushroom body neurons. J Neurosci, in press.

Rust MB, Maritzen T (2015) Relevance of presynaptic actin dynamics for synapse function and mouse behavior. Exp Cell Res 335:165–171.

Saumweber T, Weyhersmüller A, Hallermann S, Diegelmann S, Michels B, Bucher D, Funk N, Reisch D, Krohne G, Wegener S, Buchner E, Gerber B (2011) Behavioral and synaptic plasticity are impaired upon lack of the synaptic protein SAP47. J Neurosci 31:3508–3518.

Sealey MA, Vourkou E, Cowan CM, Bossing T, Quraishe S, Grammenoudi S, Skoulakis EMC, Mudher A (2017) Distinct phenotypes of three-repeat and four-repeat human tau in a transgenic model of tauopathy. Neurobiol Dis 105:74–83.

Shaw-Smith C, Pittman AM, Willatt L, Martin H, Rickman L, Gribble S, Curley R, Cumming S, Dunn C, Kalaitzopoulos D, Porter K, Prigmore E, Krepischi-Santos AC, Varela MC, Koiffmann CP, Lees AJ, Rosenberg C, Firth HV, de Silva R, Carter NP (2006) Microdeletion encompassing MAPT at chromosome 17q21.3 is associated with developmental delay and learning disability. Nat Genet 38:1032–1037.

Shulman JM, Feany MB (2003) Genetic modifiers of tauopathy in drosophila. Genetics 165:1233–1242.

Skoulakis EM, Grammenoudi S (2006) Dunces and da vincis: the genetics of learning and memory in Drosophila. Cell Mol Life Sci 63:975–988.

Sotiropoulos I, Galas MC, Silva JM, Skoulakis E, Wegmann S, Maina MB, Blum D, Sayas CL, Mandelkow EM, Mandelkow E, Spillantini MG, Sousa N, Avila J, Medina M, Mudher A, Buee L (2017) Atypical, non-standard functions of the microtubule associated tau protein. Acta Neuropathol Commun 5:91.

Tan Y, Yu D, Busto GU, Wilson C, Davis RL (2013) Wnt signaling is required for long-term memory formation. Cell Rep 4:1082–1089.

Terzenidou ME, Segklia A, Kano T, Papastefanaki F, Karakostas A, Charalambous M, Ioakeimidis F, Papadaki M, Kloukina I, Chrysanthou-Piterou M, Samiotaki M, Panayotou G, Matsas R, Douni E (2017) Novel insights into SLC25A46-related pathologies in a genetic mouse model. PLoS Genet 13:e1006656.

Tully T, Quinn WG (1985) Classical conditioning and retention in normal and mutant Drosophila melanogaster. J Comp Physiol A Neuroethol Sens Neural Behav Physiol 157:263–277.

Tully T, Preat T, Boynton SC, Del Vecchio M (1994) Genetic dissection of consolidated memory in drosophila. Cell 79:35–47.

Tyanova S, Temu T, Cox J (2016a) The MaxQuant computational platform for mass spectrometry-based shotgun proteomics. Nat Protoc 11: 2301–2319.

Tyanova S, Temu T, Sinitcyn P, Carlson A, Hein MY, Geiger T, Mann M, Cox J (2016b) The perseus computational platform for comprehensive analysis of (prote)omics data. Nat Methods 13:731–740.

Walkinshaw E, Gai Y, Farkas C, Richter D, Nicholas E, Keleman K, Davis RL (2015) Identification of genes that promote or inhibit olfactory memory formation in drosophila. Genetics 199:1173–1182.

Wang Y, Mandelkow E (2016) Tau in physiology and pathology. Nat Rev Neurosci 17:5–21.

Wiśniewski JR, Zougman A, Nagaraj N, Mann M (2009) Universal sample preparation method for proteome analysis. Nat Methods 6:359–362.

Xiong Y, Zhao K, Wu J, Xu Z, Jin S, Zhang YQ (2013) HDAC6 mutations rescue human tau-induced microtubule defects in Drosophila. Proc Natl Acad Sci U S A 110:4604–4609.

Yu D, Akalal DB, Davis RL (2006) Drosophila alpha/beta mushroom body neurons form a branch-specific, long-term cellular memory trace after spaced olfactory conditioning. Neuron 52:845–855.

Zars T, Wolf R, Davis R, Heisenberg M (2000) Tissue-specific expression of a type I adenylyl cyclase rescues the rutabaga mutant memory defect: in search of the engram. Learn Mem 7:18–31.

Zhukareva V, Vogelsberg-Ragaglia V, Van Deerlin VM, Bruce J, Shuck T, Grossman M, Clark CM, Arnold SE, Masliah E, Galasko D, Trojanowski JQ, Lee VM (2001) Loss of brain tau defines novel sporadic and familial tauopathies with frontotemporal dementia. Ann Neurol 49:165–175.

Zhukareva V, Sundarraj S, Mann D, Sjogren M, Blenow K, Clark CM, McKeel DW, Goate A, Lippa CF, Vonsattel JP, Growdon JH, Trojanowski JQ, Lee VM (2003) Selective reduction of soluble tau proteins in sporadic and familial frontotemporal dementias: an international follow-up study. Acta Neuropathol 105:469–476.

Nutrition and Healthy Aging 4 (2016) 47–54
DOI 10.3233/NHA-160012
IOS Press

Research Report

Stage dependent nutritional regulation of transgenerational longevity

Ilianna G. Roussou[a], Charalambos Savakis[a], Nektarios Tavernarakis[b,*] and Athanasios Metaxakis[c,*]
[a]*B.S.R.C. Alexander Fleming, Vari, Athens, Greece*
[b]*Institute of Molecular Biology and Biotechnology, Foundation for Research and Technology-Hellas, Heraklion, Crete, Greece; Department of Basic Sciences, Faculty of Medicine, University of Crete, Heraklion, Crete, Greece*
[c]*Institute of Molecular Biology and Biotechnology, Foundation for Research and Technology – Hellas, Heraklion, Crete, Greece*

Abstract.
BACKGROUND: Statistical analyses in human populations have associated limited food availability during development with increased longevity of next generations. In support, recent findings in *Caenorhabditis elegans* revealed nutritional effects on transgenerational longevity.
OBJECTIVES: In this study we tested the effect of nutrition on longevity of future generations in *Drosophila* and whether this is sex-specific.
METHODS: We reared male larvae and adults of *Drosophila* under different food conditions and performed lifespan analyses in F2 generation.
RESULTS: Grandsons of males which experienced starvation through larval stages were long-lived and grandsons of well fed larvae were short lived, in two *Drosophila* strains. In one strain, the nutritional effect on transgenerational longevity was transmitted through male line. Interestingly, we find that dietary restriction in adult males is the main nutritional condition affecting lifespan of grandsons.
CONCLUSIONS: Our findings suggest that nutritional regulation of transgenerational longevity is evolutionarily conserved and developmental stage – dependent in *Drosophila*.

Keywords: Aging, dietary restriction, drosophila, epigenetic regulation, lifespan, longevity, starvation, transgenerational inheritance

Abbreviations

IIS	Insulin/insulin like signaling
Igf	Insulin growth factor

*Corresponding author: Dr. Athanasios Metaxakis, or Prof. Nektarios Tavernarakis, Institute of Molecular Biology and Biotechnology, Foundation for Research and Technology – Hellas, Nikolaou Plastira 100, 70013, Heraklion, Greece. Tel.: +30 2810 391147; Fax: +30 2810 391067; E-mails: thanos_metaxakis@imbb.forth.gr. (A. Metaxakis), tavernarakis@imbb.forth.gr (N. Tavernarakis).

1. Introduction

Discovery of single genetic mutations that increase lifespan in animal model systems established aging research as one of the most fascinating and rapidly evolving scientific fields. Such mutations were rapidly linked to reduced insulin-insulin like signaling pathway (IIS) [1–3] and since then, several genes, signaling pathways, dietary interventions and drugs, often converging into common lifespan-extending mechanisms, have been shown to affect aging [4]. Importantly, most of these lifespan-extending factors seem to have an evolutionarily conserved anti-aging

ISSN 2451-9480/16/$35.00

role, thus making their manipulation a promising method to delay aging and increase healthy lifespan in humans. However, recent findings offer new insights on longevity regulation; nutritional state can have a transgenerational impact on future generations' longevity.

As such, statistical analyses of human famines indicate food availability as a transgenerational regulator of longevity. Historical data analyses linking food availability and mortality of several generations (Överkalix study), revealed a strong association of longevity with ancestors' diet during the slow growth period (SGP) in mid childhood (9–12 years) [5, 6]. Specifically, the grandsons, but not the granddaughters, of paternal grandfathers who had experienced low food supply during the SGP exhibited lower mortality rates. Similarly, paternal grandmother's food supply had some tendency to be linked with reduced granddaughters', but not grandsons', mortality. In summary, this study showed for the first time that food supply during a specific period of human development can affect mortality of next generations. Importantly, recent findings have associated starvation with transgenerational longevity in *Caenorhabditis elegans* [7], thus showing for the first time experimentally that nutrition can regulate longevity of future generations.

2. Materials and methods

We used two laboratory-adapted strains, Canton Special (CS) and white Dahomey (w^{Dah}), maintained on a 12 hours lights on/12 hours dark cycle at 25°C. Standard food contained: 65 gram/lt cornmeal, 23 gram/lt sugar, 10 gram/lt agar, 56 gram/lt dry yeast, 16 ml/lt nipagin (10% in ethanol), 4 ml/lt propionic acid. Larvae were reared in food with different yeast concentrations as follows: Flies laid eggs in sugar-agar petri dishes (5 gram agar, 40 ml apple juice and 5 ml propionic acid per 100 ml). Eggs were washed in PBS and 100 ul of eggs were placed in bottles with varying concentrations of yeast. These corresponded to 10% (starvation conditions), 50%, 100% and 200% of standard yeast concentration used in our laboratory (0.1, 0.5, 1.0 and 2.0 food respectively). Adult males (F0) were selected from each bottle and were massively crossed with virgin females reared under standard food (normally fed females). From their progeny we selected both virgin males (F1 males) and females (F1 females). These were separately crossed with normally fed females or males respectively. We then selected virgin males (F2 males) of these crosses and performed lifespan analysis under standard food.

First, we analyzed lifespans of F2 males, derived from the male offspring of F0 males that were reared under different yeast concentrations (*F2 parental males*) and secondly we analyzed lifespans of F2 males derived from the daughters of these F0 males (*F2 maternal males*). F2 males were put in plastic vials in groups of twenty. For each food condition we analyzed at least 13 plastic vials and totally at least 260 flies. To measure lifespan, flies were transferred to new vials three times per week at which time deaths were scored.

Lifespan data were analyzed using ANOVA, with Graph Pad Prism 5.03 software (Graph Pad Prism Software Inc.). Multiple comparisons among strains were performed with one-way ANOVA with Dunnett's Multiple Comparison test. Regression analysis was performed in Graph Pad Prism 5.03 software (Graph Pad Prism Software Inc.). Survivorship data were analyzed in Excel using the Log Rank test.

3. Results and discussion

To test whether nutritional regulation of transgenerational longevity is a general, evolutionarily conserved rule underlying aging regulation in animals, we simulated the Överkalix study in flies, a powerful model organism for aging research. We reared larvae of a *Drosophila melanogaster* control, laboratory-adapted Canton Special (CS) strain under food conditions containing four yeast concentrations, 10%, 50%, 100% and 200% of standard fly food used in our laboratory (0.1, 0.5, 1.0 and 2.0). Yeast concentration alone sufficiently recapitulates the effect of food availability on flies' lifespan [8] and lifespan of wild derived *Drosophila* strains is shown to respond to these yeast concentrations with a typical tent-shaped response, with the lowest one (0.1) representing starvation conditions. F0 males were classified in four groups based on rearing food conditions (groups F0 0.1, 0.5, 1.0 and 2.0) and massively crossed with females reared under standard food (1.0- normally fed). F1 males and females were crossed with normally fed flies and lifespan analysis was carried out in F2 virgin males. These were named as F2 (paternal) or F2 (maternal) depending on whether they derived from male or female offspring of the F0 males reared under different food conditions. They were also categorized as groups F2 0.1, 0.5, 1.0 and 2.0, based on the food rearing conditions of their ancestors.

First, we measured lifespan of F2 males whose paternal grandfathers had experienced starvation through larval stages. *F2 (paternal) 0.1* flies had the longest and *2.0 flies* the shortest lifespan (Fig. 1A). Mean, median and maximum lifespan values were significantly influenced by paternal grandparents' diet (for mean lifespan: $p = 0.0008$, $F = 6.52$, $R^2 = 0.2736$, for median lifespan: $p = 0.022$, $F = 5.53$, $R^2 = 0.2421$, for maximum lifespan: $p = 0.019$, $F = 3.6$, $R^2 = 0.172$, one-way ANOVA) and *F2 (paternal) 0.1* group had significantly higher mean and median lifespan values compared to the *F2 parental 2.0 males* (Fig. 1B).

To test if the above observations are caused by sex specific transgenerational mechanisms we performed similar analysis on maternal grandsons. The effects of ancestor's diet during larval stages were even more robust on longevity of maternal grandsons (Fig. 1A and 1B). *F2 (maternal) 0.1* flies had the longest and *2.0 flies* the shortest lifespan. Again, mean, median and maximum lifespan values were significantly influenced by maternal grandparents' diet and significantly correlated with shortage of food during development (for mean lifespan: $p = 0.0001$, $F = 21.72$, $R^2 = 0.5422$, for median lifespan: $p = 0.0001$, $F = 22.06$, $R^2 = 0.5461$, for maximum lifespan: $p = 0.0011$, $F = 6.143$, $R^2 = 0.2510$, one-way ANOVA). Concluding, the poorest feeding conditions that we used (10% of standard yeast concentration, which corresponds to starvation conditions) to rear larvae of F0 males induced a significant lengthening of lifespan in F2 male offspring. Conversely, rich nutrients conditions had a robust shortening effect on longevity.

To further verify the nutritional effect on transgenerational longevity we repeated lifespan analysis in another laboratory adapted *Drosophila* strain, white Dahomey (w^{Dah}). *F2 (paternal) 0.1* flies lived longer compared to the other three F2 (paternal) groups (Fig. 2A). No statistically significant differences were observed among lifespans of F2 (paternal) 0.5, 1.0 and 2.0 flies ($p > 0.05$, log rank test). Feeding through larval stages significantly affected mean and median, but not maximum lifespan (for mean lifespan: $p = 0.0189$, $F = 3.611$, $R^2 = 0.1671$, for median lifespan: $p = 0.0279$, $F = 3.275$, $R^2 = 0.1539$, for maximum lifespan: $p = 0.0898$, $F = 2.28$, $R^2 = 0.1124$, one-way ANOVA) and *F2 (paternal) 0.1* group had significantly higher mean and median lifespan values (Fig. 2B). Interestingly though, feeding through larval stages did not exert lifespan effects on F2 maternal grandsons ($p > 0.05$, log rank test, for mean lifespan: $p = 0.84$, $F = 0.2785$, $R^2 = 0.014$, for median lifespan: $p = 0.87$, $F = 0.2263$, $R^2 = 0.011980$, for maximum lifespan: $p = 0.8307$, $F = 0.2924$, $R^2 = 0.0154$, one-way ANOVA). Thus, we conclude that starvation-induced transgenerational effects on longevity passed only through male line in w^{Dah} strain (Fig. 2A and B).

We then subjected adult F0 males belonging to the CS strain into different food regimes, to test if nutritional effects on transgenerational longevity are exclusively generated through larval developmental stages. As depicted in Fig. 3A, in both experiments with F2 paternal and maternal grandsons, dietary restriction induced the highest lifespan-extending effect on males grandsons' longevity ($p < 0.05$, log rank test). Although *F2 (maternal) 0.1* flies were equally long lived as *F2 (maternal) 0.5* flies (*F2 maternal 0.1 vs. 0.5* flies $p > 0.05$, log rank test), in F2 paternal flies only dietary restriction induced enhanced longevity in F2 (*F2 paternal 0.1 vs. 0.5* flies $p < 1.48 \times 10^{-9}$, log rank test). Nutrition through adulthood significantly affected lifespan values (For F2 paternal males, median lifespan: $p = 0.0105$, $F = 4.05$, $R^2 = 0.1555$, for maximum lifespan: $p = 10^{-4}$, $F = 9.668$, $R^2 = 0.3053$. For F2 maternal males, mean lifespan: $p = 0.0247$, $F = 3.397$, $R^2 = 0.1665$, median lifespan: $p = 0.089$, $F = 2.295$, $R^2 = 0.1189$, maximum lifespan: $p = 0.0742$, $F = 2.449$, $R^2 = 0.1259$, one-way ANOVA) (Fig. 3B). Hence, adult specific nutritional effects can also induce enhanced transgenerational longevity; however, it is dietary restriction and not starvation that has the major impact on future generations' lifespan.

Lifespan response to dietary restriction fits in a polynomial equation, but response of F2 males' lifespan to F0 larval feeding conditions did not fit in such a model. The former has been previously shown to fit a third-order polynomial (cubic) model, described by the equation: $Y = B0 + B1*X + B2*X^2 + B3*X^3$ [9]. Non-linear regression analysis showed that goodness of fit was low for all models tested (For w^{Dah} strain; first order polynomial: $R^2 = 0.08639$ and 0.03723, second order polynomial: $R^2 = 0.1234$ and 0.1403, third order polynomial: $R^2 = 0.1556$ and 0.1539, fourth order polynomial: $R^2 = 0.1556$ and 0.1539, for mean and median lifespans respectively). Hence, transgenerational influence of larval feeding on F2 male offspring's lifespan does not fit a polynomial equation and does not mimic the pattern of lifespan response to dietary restriction.

Nutritional state can affect future generations through specific mechanisms; diet can generate transgenerationally heritable rDNA rearrangements in

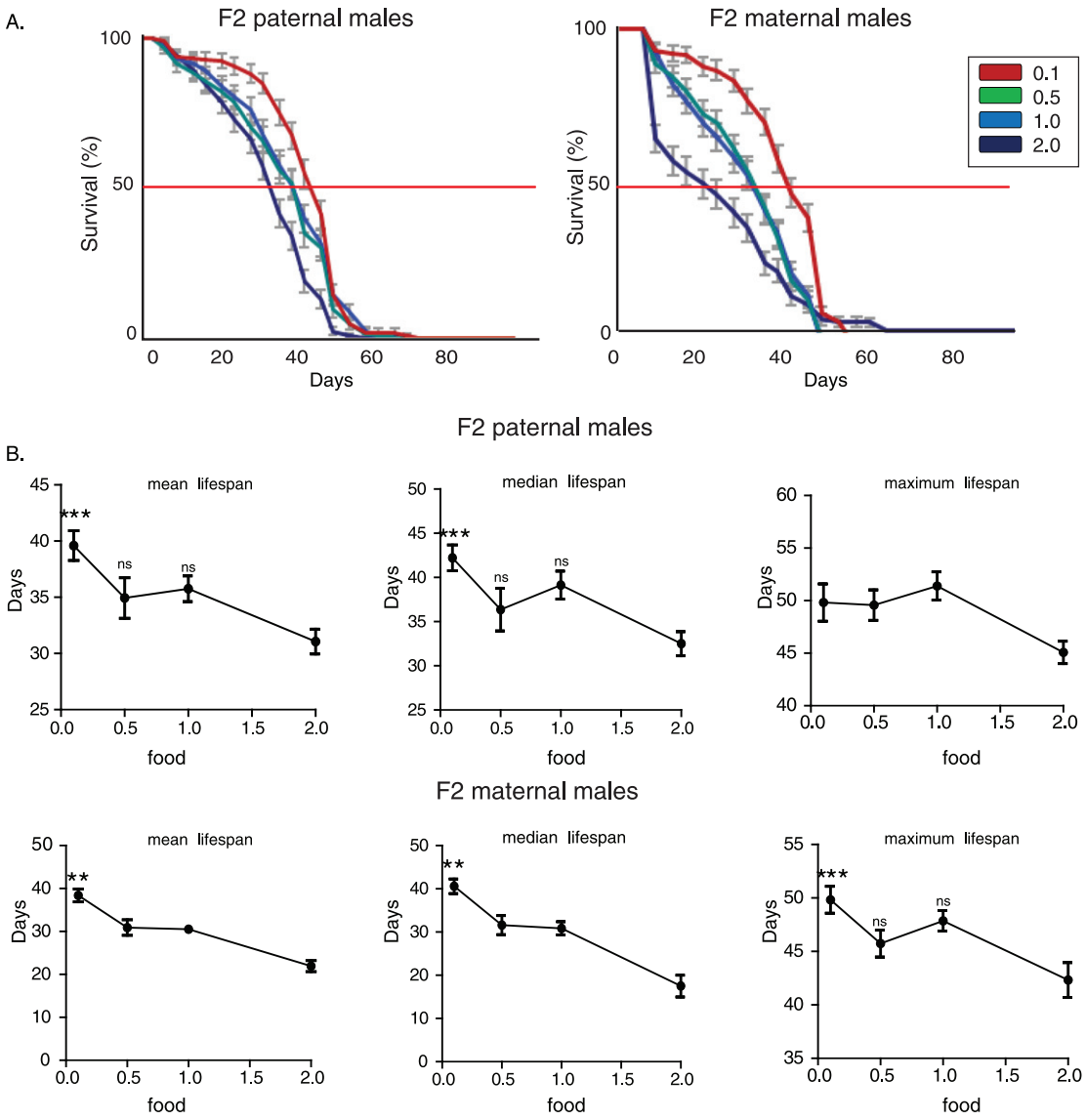

Fig. 1. Starvation-induced transgenerational effect on longevity is evolutionarily conserved in *Drosophila melanogaster*. A) Lifespan curves of F2 males (CS strain) from paternal and maternal grandfathers exposed to different dietary conditions. F2 virgin males whose paternal grandfathers had experienced starvation through larval stages (*F2 paternal 0.1 males*) were long-lived compared to the other groups. *F2 (paternal) 0.1 vs. 0.5*: $p < 1.2 \times 10^{-4}$, *F2 (paternal) 0.1 vs. 1.0*: $p < 0.014$ and *F2 (paternal) 0.1 vs. 2.0*: $p < 1.7 \times 10^{-21}$, log rank test. Also, F2 virgin males whose paternal grandfathers were fed under the richest conditions through larval stages (*F2 paternal 2.0 males*) were the shortest lived compared to the other groups. *F2 (paternal) 2.0 vs. 1.0:* $p < 1.7 \times 10^{-9}$, *F2 (paternal) 2.0 vs. 0.5*: $p < 5.7 \times 10^{-7}$, log rank test. F2 virgin males whose maternal grandfathers had experienced starvation through larval stages (*F2 maternal 0.1 males*) were also long-lived compared to the other groups. *F2 (maternal) 0.1 vs. 0.5*: $p < 7 \times 10^{-14}$, *F2 (maternal) 0.1 vs. 1.0*: $p < 1.6 \times 10^{-14}$ and *F2 (paternal) 0.1 vs. 2.0*: $p < 1 \times 10^{-40}$, log rank test. On the contrary, the richest conditions of larval feeding (*F2 maternal 2.0 males*) led to significant lifespan reduction. *F2 (paternal) 2.0 vs. 1.0:* $p < 1.3 \times 10^{-11}$, *F2 (paternal) 2.0 vs. 0.5*: $p < 7 \times 10^{-12}$, log rank test. Lifespan data shown are from a single trial. For each lifespan experiment $n > 260$. Error bars indicate SEM. B) Mean, median and maximum lifespan of F2 males from paternal and maternal grandfathers exposed to different dietary conditions. Grandparents' feeding affected mean, median but not maximum lifespan in F2 paternal flies (the mean lifespan of the longest-lived 10% of flies); *F2 (paternal) 0.1 vs. 2.0*: $p < 0.001$, $q = 4{,}404$ and $p < 0.001$, $q = 3.912$, for mean and median lifespan respectively. Ancestor's feeding affected more pronouncedly lifespan values in maternal grandsons (*F2 maternal 0.1 vs. 0.5*: $p < 0.01$, $q = 3{,}739$ and $p < 0.01$, $q = 3{,}204$ for mean and median lifespan respectively, *F2 maternal 0.1 vs. 1.0*: $p < 0.001$, $q = 3{,}929$ and $p < 0.01$, $q = 3{,}465$ for mean and median lifespan respectively, *F2 maternal 0.1 vs. 2.0*: $p < 0.001$, $q = 8{,}067$, $p < 0.001$, $q = 8.081$ and $p < 0.001$, $q = 4.100$ for mean, median and maximum lifespan. One-way ANOVA with Dunnett's multiple comparison against *F2 0.1 flies*. For each lifespan experiment $n > 13$, $^{**}p < 0.01$, $^{***}p < 0.001$. Error bars indicate SEM.

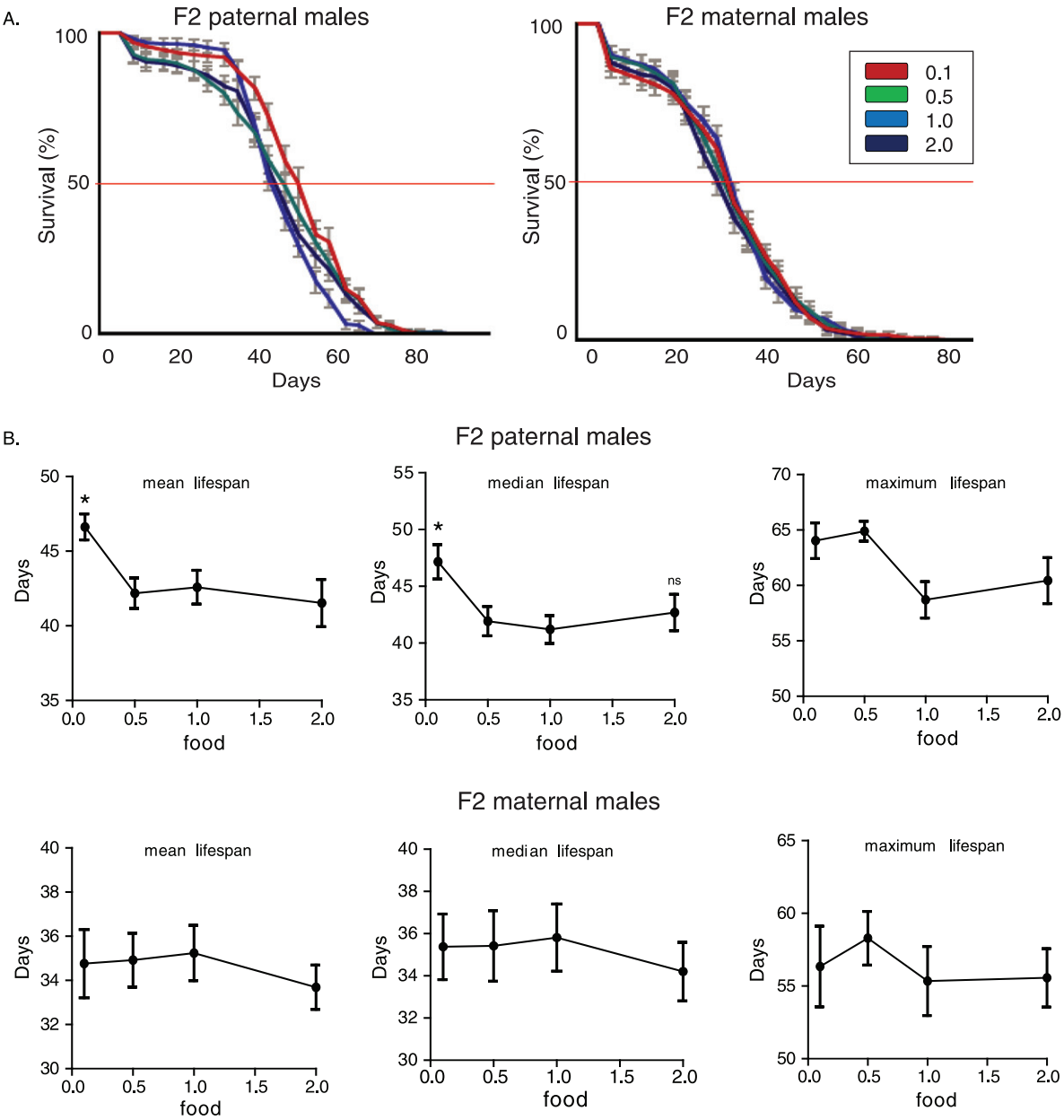

Fig. 2. Nutritional regulation of transgenerational longevity in w^{Dah} strain is sex-specific. A) Lifespan curves of F2 males from paternal and maternal grandfathers subjected to different dietary regimes through larval stages. F2 virgin males whose paternal grandfathers had experienced starvation through larval stages (*F2 paternal 0.1 males*) were long-lived compared to the other groups. *F2 (paternal) 0.1 vs. 0.5*: $p < 0.042$, *F2 (paternal) 0.1 vs. 1.0*: $p < 4 \times 10^{-6}$ and *F2 (paternal) 0.1 vs. 2.0*: $p < 0.0025$, log rank test. Lifespan curves did not differ significantly in F2 virgin males whose maternal grandfathers were reared under different food conditions (*F2 maternal males*) ($p > 0.05$, log rank test). Lifespan data shown are from a single trial. For each lifespan experiment $n > 260$. Error bars indicate SEM. B) Mean, median and maximum lifespan of F2 males from paternal and maternal grandfathers exposed to different dietary conditions. Mean and median, but not maximum, lifespans were significantly increased in *F2 parental males*. *F2 (paternal) 0.1 vs. 0.5*: $p < 0.05$, $q = 2.54$, $p < 0.05$, $q = 2.49$ and $p > 0.05$, $q = 0.356$, *F2 (paternal) 0.1 vs. 1.0*: $p < 0.05$, $q = 2.54$, $p < 0.05$, $q = 2.89$ and $p > 0.05$, $q = 1.696$, *F2 (paternal) 0.1 vs. 2.0*: $p < 0.05$, $q = 3$, $p > 0.05$, $q = 2.203$ and $p > 0.05$, $q = 1.548$, for mean, median and maximum lifespan respectively. However, ancestor's diet during larval stages did not significantly affect lifespan of *F2 maternal males*. One-way ANOVA with Dunnett's multiple comparison against *F2 0.1 flies*. For each lifespan experiment $n > 13$, $^*p < 0.05$. Error bars indicate SEM.

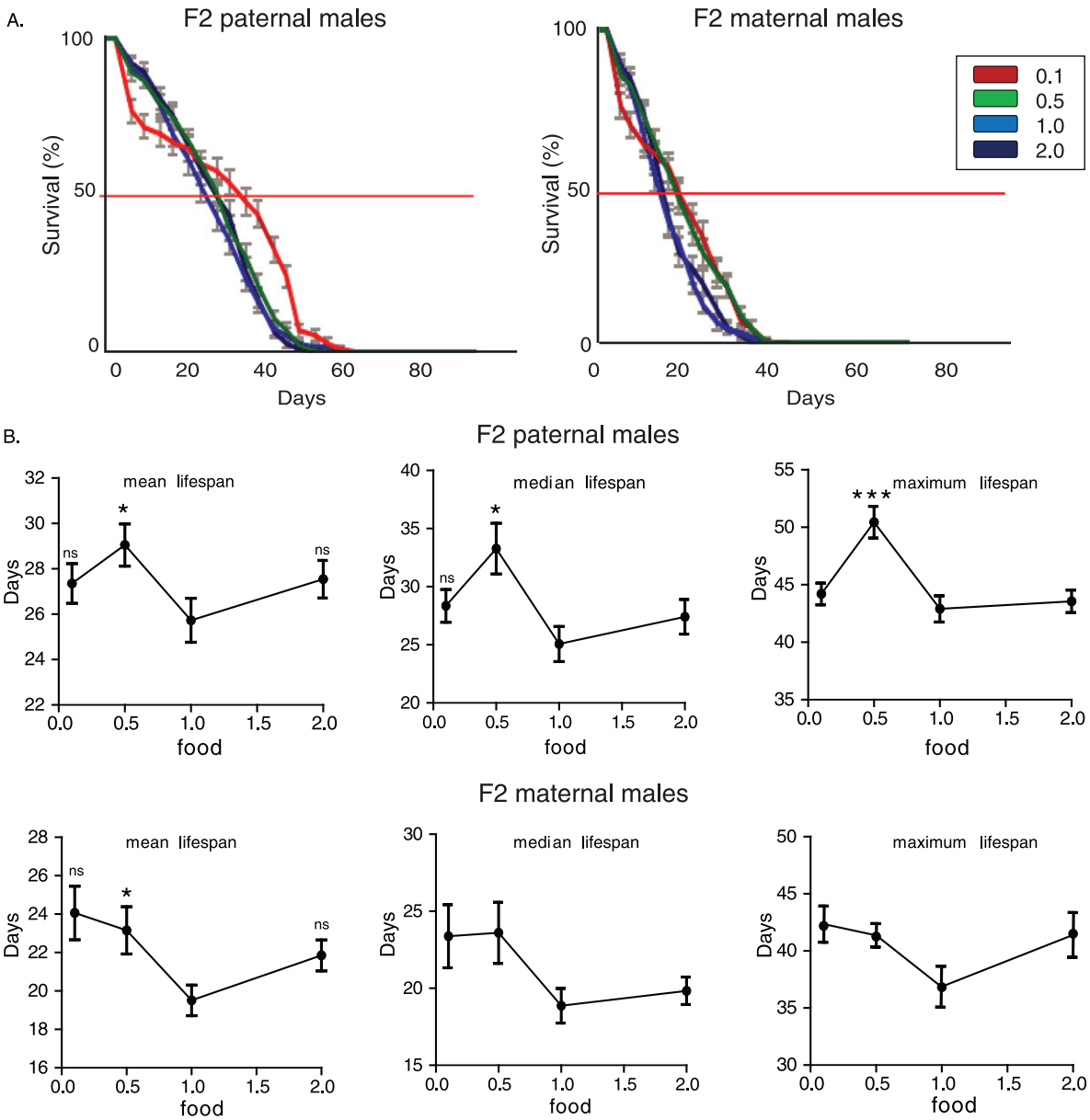

Fig. 3. Dietary restriction during adulthood induces transgenerational effects on longevity. A) Lifespan curves of F2 males from paternal and maternal grandfathers subjected to different dietary regimes through adult stages. F2 virgin males whose paternal grandfathers had experienced starvation through adult stages lived longer; *F2 (paternal) 0.1 vs.. 0.5*: $p < 1.47 \times 10^{-9}$, *F2 (paternal) 0.1 vs.. 1.0*: $p < 3.6 \times 10^{-10}$ and *F2 (paternal) 0.1 vs.. 2.0*: $p < 3 \times 10^{-12}$, log rank test. In F2 maternal males, dietary restriction and starvation of F0 males induced similar effects; *F2 (maternal) 0.5 vs. 0.1*: $p > 0.9$, *F2 (maternal) 0.5 vs. 1.0*: $p < 8 \times 10^{-7}$, *F2 (maternal) 0.5 vs. 2.0*: $p < 0.0049$, *F2 (maternal) 0.1 vs. 1.0*: $p < 1 \times 10^{-6}$, *F2 (maternal) 0.1 vs. 2.0*: $p < 0.0049$, log rank test. Lifespan data shown are from a single trial. For each lifespan experiment $n > 260$. Error bars indicate SEM. B) Mean, median and maximum lifespan of F2 males from paternal and maternal grandfathers exposed to different dietary conditions during adulthood. *F2 (paternal) 0.5 vs. 0.1*: $p < 0.001$, $q = 4.097$, for maximum lifespan, *F2 (paternal) 0.5 vs. 1.0*: $p < 0.05$, $q = 2.512$, $p < 0.01$, $q = 3.326$, $p < 0.001$, $q = 4.6$ for mean, median and maximum lifespan, *F2 (paternal) 0.5 vs. 2.0*: $p < 0.05$, $q = 2.456$ and $p < 0.001$, $q = 4.34$, for median and maximum lifespan. *F2 (maternal) 0.5 vs. 1.0*: $p < 0.05$, $q = 2.457$ for mean lifespan, *F2 (maternal) 0.1 vs. 1.0*: $p < 0.05$, $q = 2.95$, for mean lifespan, one-way ANOVA with Dunnett's multiple comparison against *F2 0.5 flies*. For each lifespan experiment $n > 13$, $^{*}p < 0.05$, $^{***}p < 0.001$. Error bars indicate SEM.

flies [10], caloric restriction can induce histone modification, as also DNA methylation [10–12] and parental diet can affect cholesterol and lipid metabolism in offspring, through DNA methylation in mammals [11]. Interestingly, IIS pathway and nutritional alterations have similar effects on rDNA in flies, thus making IIS pathway a putative mediator of starvation-induced transgenerational phenomena. In support, insulin growth factor (Igf) gene can be regulated by DNA methylation and parental imprinting [13, 14]. IIS pathway downregulation and dietary restriction are the most reliable ways to extend lifespan in yeast, worms, flies and mammals, but also to improve health, even in aged humans [15, 16]. For this, we predict that nutritional effects at specific developmental stages in flies and humans might change activity of genes affecting nutrient-sensing pathways, such as IIS, which, in turn, affect lifespan in future generations.

It has been suggested that Y- and X-chromosomes might control epigenetic effects by altering the chromatin structure on other chromosomes [16, 17]. *Drosophila* genes can be methylated [18] and imprinted [19]. Moreover, the Y chromosome alters expression of several X-linked and autosomal genes affecting, among others, lipid and mitochondrial metabolism [20]. Such trans-chromosomal epigenetic effects imposed by the Y chromosome could explain the sex-specific lifespan increase observed in F2 males of the w^{Dah}. However, in CS flies transgenerational lifespan increase was not affected by female interference in F1. *Drosophila* strains, including w^{Dah} and CS, have been previously reported to differ regarding the nutritional range affecting longevity and sex-specific factors differentially influence lifespan extending factors X genotype interactions among strains [21, 22]. Identification of the molecular mechanisms underlying nutritional effects on transgenerational longevity in flies is a prerequisite to understand sex-specific transgenerational lifespan increase of w^{Dah}.

In worms, specific heritable chromatin modifications, affecting epigenetics, are shown to induce transgenerational inheritance of longevity [23]. Furthermore, a recent study showed that starvation can transgenerationally increase longevity through expression and transmittance of small RNAs. Interestingly, these RNA molecules target metabolism-related genes [24]. In conclusion, dietary conditions seem to alter activity of metabolic pathways through DNA methylation, histone modifications or small regulatory RNAs molecules production. We hypothesize that such alterations underlie transgenerational longevity effects of starvation.

Interestingly, despite starvation during larval stages being the effector of transgenerational lifespan increase in F2, dietary restriction seem to be the equivalent effector during adulthood. In the case of F2 maternal males, starvation had a similar lifespan effect to dietary restriction. Hence, we could presume that, during adulthood, the range of nutrients shortage, which suffices for generation of transgenerational longevity effects, differs through development. In adults, a narrower reduction in nutrients might be necessary for generation of longevity effects in future generations.

Here for the first time we show that *Drosophila* lifespan can be transgenerationally regulated. We found that starvation during development can transgenerationally increase lifespan in flies, as it has been previously reported in humans and worms. We assume that this is an evolutionarily conserved mechanism of lifespan regulation in animals. Moreover, our findings revealed a sex-specific mode for this regulation in one of the strains tested, similarly to what has been observed in humans. This implicates common mechanisms underlying lifespan extension in flies and humans. Therefore, we believe that *Drosophila* is suitable as an experimental platform to study epigenetic alterations that increase life expectancy and identify genes that regulate human aging. Reversibility and chemical manipulation of epigenetic alterations make them promising tools for the development of anti-aging treatments in humans. Our findings pave the way for further studies towards elucidating the molecular mechanisms by which limited nutrition increases transgenerational longevity, and assessing whether it enhances healthspan in addition to lifespan.

Acknowledgments

AM is supported by a standard Marie Curie intra-European individual fellowship.

References

[1] Klass MR. A method for the isolation of longevity mutants in the nematode Caenorhabditis elegans and initial results. Mechanisms of Ageing and Development. 1983;22(3-4): 279-86.

[2] Kenyon C, Chang J, Gensch E, Rudner A, Tabtiang R. A C. elegans mutant that lives twice as long as wild type. Nature. 1993;366(6454):461-4.

[3] Clancy DJ, Gems D, Harshman LG, Oldham S, Stocker H, Hafen E, et al. Extension of life-span by loss of CHICO, a Drosophila insulin receptor substrate protein. Science. 2001;292(5514):104-6.

[4] Lopez-Otin C, Blasco MA, Partridge L, Serrano M, Kroemer G. The hallmarks of aging. Cell. 2013;153(6):1194-217.

[5] Bygren LO, Kaati G, Edvinsson S. Longevity determined by paternal ancestors' nutrition during their slow growth period. Acta Biotheoretica. 2001;49(1):53-9.

[6] Pembrey ME, Bygren LO, Kaati G, Edvinsson S, Northstone K, Sjostrom M, et al. Sex-specific, male-line transgenerational responses in humans. European Journal of Human Genetics: EJHG. 2006;14(2):159-66.

[7] Rechavi O, Houri-Ze'evi L, Anava S, Goh WS, Kerk SY, Hannon GJ, et al. Starvation-induced transgenerational inheritance of small RNAs in C. elegans. Cell. 2014; 158(2):277-87.

[8] Bass TM, Grandison RC, Wong R, Martinez P, Partridge L, Piper MD. Optimization of dietary restriction protocols in Drosophila. The Journals of Gerontology Series A, Biological Sciences and Medical Sciences. 2007;62(10):1071-81.

[9] Metaxakis A, Partridge L. Dietary restriction extends lifespan in wild-derived populations of Drosophila melanogaster. PloS One. 2013;8(9):e74681.

[10] Aldrich JC, Maggert KA. Transgenerational inheritance of diet-induced genome rearrangements in Drosophila. PLoS Genetics. 2015;11(4):e1005148.

[11] Bacalini MG, Friso S, Olivieri F, Pirazzini C, Giuliani C, Capri M, et al. Present and future of anti-ageing epigenetic diets. Mechanisms of Ageing and Development. 2014;136-137:101-15.

[12] Chouliaras L, van den Hove DL, Kenis G, Draanen M, Hof PR, van Os J, et al. Histone deacetylase 2 in the mouse hippocampus: Attenuation of age-related increase by caloric restriction. Current Alzheimer Research. 2013;10(8):868-76.

[13] Carone BR, Fauquier L, Habib N, Shea JM, Hart CE, Li R, et al. Paternally induced transgenerational environmental reprogramming of metabolic gene expression in mammals. Cell. 2010;143(7):1084-96.

[14] DeChiara TM, Robertson EJ, Efstratiadis A. Parental imprinting of the mouse insulin-like growth factor II gene. Cell. 1991;64(4):849-59.

[15] Colman RJ, Anderson RM, Johnson SC, Kastman EK, Kosmatka KJ, Beasley TM, et al. Caloric restriction delays disease onset and mortality in rhesus monkeys. Science. 2009;325(5937):201-4.

[16] Fontana L, Partridge L. Promoting health and longevity through diet: From model organisms to humans. Cell. 2015;161(1):106-18.

[17] Nelson VR, Spiezio SH, Nadeau JH. Transgenerational genetic effects of the paternal Y chromosome on daughters' phenotypes. Epigenomics. 2010;2(4):513-21.

[18] Friberg U, Stewart AD, Rice WR. X- and Y-chromosome linked paternal effects on a life-history trait. Biology Letters. 2012;8(1):71-3.

[19] Lyko F, Ramsahoye BH, Jaenisch R. DNA methylation in Drosophila melanogaster. Nature. 2000;408(6812):538-40.

[20] Golic KG, Golic MM, Pimpinelli S. Imprinted control of gene activity in Drosophila. Current Biology: CB. 1998;8(23):1273-6.

[21] Grandison RC, Wong R, Bass TM, Partridge L, Piper MDW. Effect of a standardised dietary restriction protocol on multiple laboratory strains of drosophila melanogaster. PloS One. 2009;4(1):e4067.

[22] Spencer CC, Howell CE, Wright AR, Promislow DEL. Testing an 'aging gene' in long-lived Drosophila strains: Increased longevity depends on sex and genetic background. Aging Cell. 2003;2(2):123-30.

[23] Lemos B, Araripe LO, Hartl DL. Polymorphic Y chromosomes harbor cryptic variation with manifold functional consequences. Science. 2008;319(5859):91-3.

[24] Greer EL, Maures TJ, Ucar D, Hauswirth AG, Mancini E, Lim JP, et al. Transgenerational epigenetic inheritance of longevity in Caenorhabditis elegans. Nature. 2011; 479(7373):365-71.

Behavioral/Cognitive

The *Drosophila* Receptor Tyrosine Kinase Alk Constrains Long-Term Memory Formation

Jean Y. Gouzi, Mikela Bouraimi, Ilianna G. Roussou, Anastasios Moressis, and Efthimios M.C. Skoulakis
Division of Neuroscience, Biomedical Sciences Research Center Alexander Fleming, Vari, 16672, Greece

In addition to mechanisms promoting protein-synthesis-dependent long-term memory (PSD-LTM), the process appears to also be specifically constrained. We present evidence that the highly conserved receptor tyrosine kinase dAlk is a novel PSD-LTM attenuator in *Drosophila*. Reduction of dAlk levels in adult α/β mushroom body (MB) neurons during conditioning elevates LTM, whereas its overexpression impairs it. Unlike other memory suppressor proteins and miRNAs, dAlk within the MBs constrains PSD-LTM specifically but constrains learning outside the MBs as previously shown. Dendritic dAlk levels rise rapidly in MB neurons upon conditioning, a process apparently controlled by the 3′UTR of its mRNA, and interruption of the 3′UTR leads to enhanced LTM. Because its activating ligand Jeb is dispensable for LTM attenuation, we propose that postconditioning elevation of dAlk within α/β dendrites results in its autoactivation and constrains formation of the energy costly PSD-LTM, acting as a novel memory filter.

Key words: Alk; *Drosophila*; memory constraint; mushroom bodies; PSD-LTM

Significance Statement

In addition to the widely studied molecular mechanisms promoting protein-synthesis-dependent long-term memory (PSD-LTM), recent discoveries indicate that the process is also specifically constrained. We describe a role in PSD-LTM constraint for the first receptor tyrosine kinase (RTK) involved in olfactory memory in *Drosophila*. Unlike other memory suppressor proteins and miRNAs, dAlk limits specifically PSD-LTM formation as it does not affect 3 h, or anesthesia-resistant memory. Significantly, we show conditioning-dependent dAlk elevation within the mushroom body dendrites and propose that its local abundance may activate its kinase activity, to mediate imposition of PSD-LTM constraints through yet unknown mechanisms.

Introduction

Since its identification, the receptor tyrosine kinase (RTK) anaplastic lymphoma kinase (ALK) has emerged as a key player in the physiology and pathology of the CNS (Hallberg and Palmer, 2013). ALK belongs to the insulin receptor subfamily of monomeric RTKs. It features a large extracellular ligand-binding domain, a short transmembrane-spanning region, and an intracellular tyrosine kinase (TK) domain. Upon activation by its recently identified ALKAL ligands (Guan et al., 2015; Reshetnyak et al., 2015), ALK initiates the activation of several intracellular signaling pathways, including the canonical Ras/ERK cascade. Unsurprisingly, ALK has been linked to multiple human cancers (Hallberg and Palmer, 2013) characterized by constitutive kinase activation due to point mutations, chromosomal translocations, or overexpression by gene amplification, which confer ligand independence. However, the normal role of ALK in the CNS remains poorly documented.

ALK is highly conserved in vertebrates, *Caenorhabditis elegans* and *Drosophila melanogaster* (Lorén et al., 2001; Hallberg and Palmer, 2013). *Drosophila* Alk (dAlk) and its secreted activating ligand Jelly Belly (Jeb) are essential for gut muscle differentiation, axon targeting in the retina, organ and body size growth control, and synapse growth at the larval neuromuscular junction (Hallberg and Palmer, 2013). Recent studies indicate that dAlk activity regulates ethanol sensitivity (Lasek et al., 2011), sleep (Bai and Sehgal, 2015), and learning/short-term memory (STM) (Gouzi et al., 2011) in adult flies. Jeb or dAlk overexpression precipitates associative olfactory learning deficits, whereas genetic or pharmacological inhibition of dAlk kinase activity enhances learning

Received March 26, 2018; revised June 21, 2018; accepted July 3, 2018.

Author contributions: J.Y.G. and E.M.C.S. edited the paper; J.Y.G., A.M., and E.M.C.S. designed research; J.Y.G., M.B., I.G.R., and A.M. performed research; J.Y.G., A.M., and E.M.C.S. analyzed data; J.Y.G. and E.M.C.S. wrote the paper.

This work was supported by Fondation Santé. We thank Seth Tomchik (Scripps Research Institute) for sharing Gal4 strains; Ruth H. Palmer (University of Gothenburg) for fly stocks and reagents, and providing critical assistance in manuscript preparation; the Developmental Hybridoma Studies Bank for antibodies; the Bloomington *Drosophila* Stock Center and the Vienna *Drosophila* RNAi Center for resources; and Flybase for essential information.

We declare no competing financial interests.

Correspondence should be addressed to Dr. Efthimios M. C. Skoulakis, Division of Neuroscience, Biomedical Sciences Research Center Alexander Fleming, Vari, 16672, Greece. E-mail: skoulakis@fleming.gr.

M. Bouraimi's present address: G. d'Annunzio University, Medical School of Chieti, Chieti, Italy.

A. Moressis' present address: Laboratory of Neural Circuits and Computations, Friedrich Miescher Institute for Biomedical Research, 4058 Basel, Switzerland.

DOI:10.1523/JNEUROSCI.0784-18.2018

 0270-6474/18/387701-12$15.00/0

performance (Gouzi et al., 2011). dAlk-dependent learning, spatial memory, and novel object recognition inhibition were subsequently confirmed in mice also (Weiss et al., 2012).

dAlk is widely expressed in the adult brain (Gouzi et al., 2011), accumulating preferentially in the dendrites of the mushroom bodies (MBs), neuroanatomical structures essential for olfactory learning and memory (de Belle and Heisenberg, 1994), sleep (Joiner et al., 2006; Pitman et al., 2006), and ethanol sensitivity (King et al., 2011). However, whereas dAlk-dependent regulation of sleep and ethanol sensitivity require its expression within the MBs (Lasek et al., 2011; Bai and Sehgal, 2015), regulation of learning does not (Gouzi et al., 2011). However, dAlk is present within MBs; and because these neurons are also essential for intermediate/middle-term memory (MTM), anesthesia-resistant memory (ARM), and protein-synthesis-dependent long-term memory (PSD-LTM) (Tully et al., 1994; Guven-Ozkan and Davis, 2014), we hypothesized that dAlk could serve one or more of these forms of labile and consolidated olfactory memories.

Materials and Methods

Drosophila culture and strains. Drosophila were cultured on standard wheat-flour-sugar food supplemented with soy flour and $CaCl_2$, at 25°C in 50%–70% relative humidity in a 12 h light/dark cycle (Gouzi et al., 2011). Alk^1 mutants (Lorén et al., 2003) were a kind gift from R. H. Palmer (University of Gothenburg, Gothenburg, Sweden). $Alk^{MB06458}$ flies were obtained from the Bloomington Stock Center (BL25509). Transgenic fly strains used in this work were as follows: UAS-Alk^{WT} (Lorén et al., 2001), UAS-Alk^{RNAi} (v11446 and v107083, Vienna Drosophila Resource Centre), UAS-*Jeb* (Englund et al., 2003), UAS-Jeb^{RNAi} (v30799 and v103047, Vienna Drosophila Resource Centre), UAS-*mCD8::GFP* (Lee and Luo, 1999), and TubGal80^{ts} (McGuire et al., 2004). The Gal4 driver lines used in this work were as follows: Alk(38)-Gal4 (Gouzi et al., 2011), repo-Gal4 (BL715), nSyb-Gal4, Ras2-Gal4, Elav[C155]-Gal4 (BL458), TH-Gal4, MB247-Gal4, c739-Gal4, OK107-Gal4 (BL854), LeoMB-Gal4 (Messaritou et al., 2009), 17d-Gal4 (BL51631), NP1131-Gal4, and 1471-Gal4 (BL9465; Isabel et al., 2004). The c739-Gal4,TubGal80^{ts} line was obtained from G. Roman (University of Mississippi, Oxford, MS). The GH146-Gal4, TubGal80^{ts} line was from M. Ramaswami (Trinity College Dublin, Dublin, Ireland). The MB-specific Gal80 (MBGal80), which drives expression predominantly in the MBs, was introduced into the Elav-Gal4 strain through standard genetic crosses. All strains were backcrossed into the resident Cantonised-w^{1118} control isogenic strain for six generations to normalize their genetic background.

Drug feeding. The selective Alk inhibitor NPV-TAE684 (Galkin et al., 2007) was dissolved in DMSO, and serial dilutions of stock solutions were prepared following the previously described method (Gouzi et al., 2011). Briefly, the solution was mixed into 10 ml Brewers-yeast paste and was fed for 16 h to flies previously starved for 6–8 h and transferred into normal fly-food vials 1 h before behavioral conditioning.

Western blot analysis. For detection of Jeb levels, 10 adult heads or 5 larval CNSs were homogenized in standard Laemmli buffer supplemented with protease and phosphatase inhibitors. Extract equivalent to one adult head was loaded per lane on 10% acrylamide gels, transferred to PVDF membranes, and probed with primary antibodies, which were used at 1:1000 for guinea-pig anti-JEB (Englund et al., 2003) and at 1:2000 for mouse anti-Syntaxin (8C3, Developmental Studies Hybridoma Bank), which was used to normalize sample loading.

Immunohistochemical analysis and confocal imaging. Whole-mount adult brains were dissected in cold PBS, fixed in 4% PFA for 20 min, and permeabilized using 1% Triton X-100 in PBS. The primary antibodies used were as follows: rabbit anti-dALK (1:1000) (Lorén et al., 2001), guinea-pig anti-JEB (1:1000) (Englund et al., 2003), mouse anti-DLG1 (1:1000) (4F3), and mouse anti-ChAT (1:1000) (4B1) (both from the Developmental Studies Hybridoma Bank, University of Iowa). The following secondary antibodies were used: goat anti-mouse, or anti-rabbit conjugated with AlexaFluor secondary antibodies (1:400, all from Invitrogen). Confocal laser microscopy was performed using a TCS SP5 Confocal system (Leica Microsystems) equipped with the LAS AF image acquisition analysis software suite (Leica Microsystems). To quantify dAlk expression levels in the MBs, we used an adapted semiquantitative immunofluorescence protocol detailed previously (Liu et al., 2007). Whole-mount brains were dissected and prepared as described above and were stained with a rabbit anti-dALK antibody and counterstained with rhodamine-conjugated phalloidin (Invitrogen; 1:100) to mark the neuropil. Single confocal plane images of MB calyces were captured at the same section level corresponding to the middle part of the calyx and using constant optical acquisition settings (laser power, gain, pinhole, offset, zoom) and examined within a single session to allow comparison between control and experimental samples. dAlk expression levels in the calyces were estimated by subtracting from the measured mean grayscale intensity of a ROI (delimited by hand around a calyx), the measured mean grayscale intensity of an identical area adjacent to the calyx (background region). Fluorescence intensities were measured with ImageJ 1.51k software (National Institutes of Health).

Behavioral analyses and conditioning. Olfactory learning and memory in the Pavlovian negatively reinforced conditioning paradigm, coupling aversive odors as conditioned stimuli (CS^+ and CS^-) with the electric shock unconditioned stimulus (US), were performed essentially as described previously, for 3 min/learning (Gouzi et al., 2011) and for 24 h memory/LTM (Pavlopoulos et al., 2008). Briefly, all experiments were performed in a genotype-balanced manner, with the experimenter blind to genotype and under dim red light, at 25°C and 70% humidity. Groups of ~75, 2- to 3-d-old flies were transferred to fresh vials 1 h before training and then trained in a T-maze apparatus. The aversive odors used were benzaldehyde and 3-octanol, diluted in isopropyl myristate (Fluka). Training for 3 min/learning or 3 h/mid-term memory experiments consisted of 1 single session of 12 US/CS pairings of 90 V electric shocks (US) with one odor (CS^+) over 1 min, followed after a 30 s purge with air, by the presentation of the second odor (CS^-) without shocks for 1 min. For 24 h memory, animals were subjected to five such training sessions, either massed together or spaced by a 15 min rest interval. For testing, flies were allowed to choose between the two odors presented in the two arms of the T-maze apparatus for 1.5 min. Performance was measured by calculating a performance index (PI) as follows: the fraction of flies that avoided the shock-associated odor (CS^+) minus the fraction that avoided the control odor (CS^-) represented half of the PI. One PI was calculated as the average of the half-learning indexes for each of the two groups of flies trained to complementary conditioning stimuli. To validate consolidated LTM, flies were placed for 16 h at 25°C in empty vials containing a piece of Whatman filter paper (2 × 2 cm) soaked with 200 μl of 5% sucrose solution (Fisher Scientific) containing 35 mM cycloheximide (Sigma-Aldrich). Flies were then transferred to standard food vials 30 min before training. After training, flies were kept in standard food vials for 24 h at 18°C until testing. To assess 10 min and 3 h ARMs, flies were cold-shocked in prechilled glass vials on ice for 2 min after a single round of training. Complete anesthesia and recovery were controlled. After a 2 min recovery, they were transferred back to vials at 25°C in the dark and maintained until testing. For 10 min short-term ARM (ST-ARM), trained flies were cold-shocked immediately after training as described previously (Knapek et al., 2011; Bouzaiane et al., 2015). For 3 h middle-term ARM (MT-ARM), trained flies were cold-shocked 2 h after training, as described by Bouzaiane et al. (2015). Task-relevant sensory behavioral responses, such as odor avoidance and electric shock avoidance, were controlled and performed as described previously in detail (Gouzi et al., 2011).

Experimental design and statistical analysis. For all experiments, controls and experimental genotypes were tested in the same session in balanced design. The order of training and testing these genotypes was randomized. We required an experimental result to be significantly different from both genetic controls. Data are shown as mean ± SEM. The final number of experiments per genotype is listed on the bars in all figures and represents data collected from at least two broods of the given genotypes.

Untransformed (raw) data were analyzed parametrically with the JMP 7.1 statistical software package (SAS Institute) as described previously (Gouzi et al., 2011). Following initial ANOVA, planned comparison con-

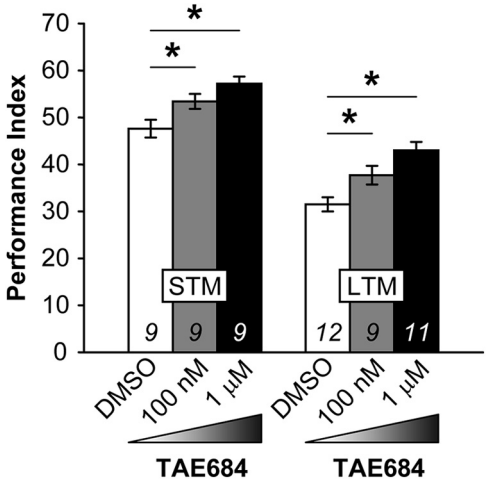

Figure 1. Pharmacological inhibition of dAlk activity enhances STM and LTM. Mean PIs (bars) ± SEMs (error bars) are shown. The number of experimental replicates (*n*) are indicated within the bars. *Significant differences denoted by horizontal line pairs. Left, TAE684 administration 100 nM or 1 μM to w^{1118} flies enhanced their learning/3 min STM performance in a high-resolution limited training protocol (1 cycle of 3 CS/US pairings). Right, TAE684 administration to w^{1118} flies enhanced their 24 h LTM performance. LTM performance was obtained using the typical spaced training protocol of 5 cycles of 12 CS/US pairings, each cycle separated (spaced) by a 15 min rest interval.

trast analyses (LSM) were performed between the experimental group (in black throughout all figures) and its genetic or treatment controls, using $\alpha = 0.05$. The level of significance was adjusted for the experimentwise error rate. Detailed results of all ANOVA and planned comparisons are reported in the text.

Results

Pharmacological inhibition of dAlk enhances both STM and LTM

To investigate whether dAlk plays a role in negatively reinforced associative olfactory memory, we administered the dAlk selective kinase inhibitor TAE684 (Galkin et al., 2007) to control (w^{1118}) flies (Fig. 1). In agreement with published data (Gouzi et al., 2011), 100 nM and 1 μM TAE684 enhanced 3 min memory by ~12% and 20%, respectively, (STM: ANOVA $F_{(2,26)} = 8.3362$, $p = 0.0018$; subsequent LSM: $p = 0.0208$ and $p = 0.0005$ for 100 nM and 1 μM, respectively, vs vehicle-fed w^{1118} controls), but significantly it also precipitated a very robust increase in 24 h memory of ~20% and 36% (LTM: ANOVA $F_{(2,31)} = 11.6696$, $p = 0.0002$; subsequent LSM: $p = 0.0194$ and $p = 4.2 \times 10^{-5}$ for 100 nM and 1 μM, respectively, vs vehicle). Together, these initial pharmacological results strongly suggest that dAlk inhibits olfactory memory in *Drosophila* in addition to its established role in inhibition of learning/3 min memory in the context of Nf1-regulated pathway(s) (Gouzi et al., 2011).

Downregulation of dAlk specifically within MB neurons enhances LTM

To validate this memory enhancement genetically, we attenuated dAlk in cells endogenously expressing the RTK by RNAi-mediated abrogation with $Alk^{RNAi(11446)}$ under Alk(38)-Gal4 (Gouzi et al., 2011). Consistent with the TAE684 results, dAlk abrogation in Alk-expressing cells (Fig. 2*A*) elevated 24 h memory (Alk(38)-Gal4: ANOVA: $F_{(2,31)} = 12.8918$, $p < 0.0001$; subsequent LSM vs controls: $p = 0.0011$ and $p = 4.5 \times 10^{-5}$, respectively), suggesting that the RTK mediates long-term memory attenuation. Task-relevant sensory responses were known to be normal (Gouzi et al., 2011).

To determine the neurons requiring dAlk function to constrain 24 h memory, we abrogated the RTK in defined brain cell types (Fig. 2*A*, top). Attenuating dAlk in glia did not affect 24 h memory (Repo-Gal4: ANOVA: $F_{(2,23)} = 1.9385$, $p = 1688$). In contrast, pan-neuronal dAlk abrogation (nSyb-Gal4: ANOVA: $F_{(2,31)} = 12.9304$, $p < 0.0001$; subsequent LSM vs controls: $p = 0.0026$ and $p = 3 \times 10^{-5}$, respectively; and Elav-Gal4: ANOVA: $F_{(2,39)} = 19.9132$, $p < 0.0001$; subsequent LSM vs controls: $p = 0.0003$ and $p = 3.8 \times 10^{-7}$) enhanced 24 h memory, mimicking the results with Alk(38)-Gal4, but not if MB neurons were spared (Elav-Gal4; MBGal80: ANOVA: $F_{(2,39)} = 0.9212$, $p = 0.4070$). Hence, dAlk within MB neurons appears necessary for the 24 h memory enhancement. Dopaminergic neurons (TH-Gal4: ANOVA: $F_{(2,31)} = 0.9152$, $p = 0.4117$) were not required, minimizing the possibility that enhanced memory is the consequence of attenuated forgetting (Berry et al., 2012).

To determine which MB neurons require dAlk for memory suppression, several specific drivers were used (Fig. 2*A*, bottom). dAlk abrogation under the panMB drivers MB247-Gal4, OK107-Gal4, and LeoMB-Gal4 (Messaritou et al., 2009), and c739-Gal4, 17d-Gal4 marking α/β neurons, yielded significantly elevated 24 h memory (MB247-Gal4: ANOVA: $F_{(2,23)} = 13.9858$, $p = 0.0001$; subsequent LSM vs controls: $p = 3.4 \times 10^{-4}$ and $p = 1.2 \times 10^{-4}$, respectively; OK107-Gal4: ANOVA: $F_{(2,31)} = 23.3012$, $p < 0.0001$; subsequent LSM: $p = 0.0172$ and $p = 1.8 \times 10^{-7}$ vs controls, respectively; LeoMB-Gal4: ANOVA: $F_{(2,39)} = 10.9654$, $p = 0.0002$; subsequent LSM: $p = 0.0034$ and $p = 6.1 \times 10^{-5}$ vs controls, respectively; c739-Gal4: ANOVA: $F_{(2,23)} = 31.3183$, $p < 0.0001$; subsequent LSM: $p = 2.6 \times 10^{-5}$ and $p = 1.8 \times 10^{-7}$ vs controls, respectively; 17d-Gal4: ANOVA: $F_{(2,38)} = 11.7483$, $p < 0.0001$; subsequent LSM: $p = 0.0257$ and $p = 2.4 \times 10^{-5}$ vs controls, respectively). In contrast, attenuation within γ neurons did not affect memory (NP1131-Gal4: ANOVA: $F_{(2,31)} = 4.4173$, $p = 0.0212$; 1471-Gal4: ANOVA: $F_{(2,23)} = 1.0385$, $p = 0.3715$). The stronger memory improvement yielded by c739-Gal4 compared with 17d-Gal4 is consistent with previous reports (Akalal et al., 2006) that, although both mark MB α/β lobes, c739-Gal4 is expressed higher and in more than twice the number of Kenyon cells compared with 17d-GAL4. These results demonstrate that dAlk is required specifically in α/β neurons, known to be essential for 24 h memory (Isabel et al., 2004; Yu et al., 2006; Pavlopoulos et al., 2008). These results were further validated (Fig. 2*B*, spaced) with an independent RNAi-mediating transgene (UAS-$Alk^{RNAi(107083)}$) (Gouzi et al., 2011), which also yielded elevated 24 h memory after spaced conditioning under LeoMB-Gal4 and c739-Gal4 (LeoMB-Gal4 spaced: ANOVA: $F_{(2,31)} = 14.6651$, $p < 0.0001$; subsequent LSM vs controls: $p = 0.0005$ and $p = 1.9 \times 10^{-5}$, respectively; and c739-Gal4 spaced: ANOVA: $F_{(2,31)} = 13.8101$, $p < 0.0001$; subsequent LSM vs controls: $p = 0.0007$ and $p = 2 \times 10^{-5}$).

Two forms of consolidated memory are detectable 24 h after training: PSD-LTM, formed after spaced training; and ARM, formed after massed training, which does not depend on *de novo* protein synthesis (Tully et al., 1994; Isabel et al., 2004). Significantly, MB-specific dAlk downregulation did not affect ARM (Fig. 2*B*, massed), suggesting that the 24 h memory enhancement is PSD-LTM-specific (LeoMB-Gal4 massed: ANOVA: $F_{(2,25)} = 0.8317$, $p = 0.4480$; and c739-Gal4 massed: ANOVA: $F_{(2,23)} = 0.9291$, $p = 0.4105$). Consistently, inhibition of protein synthesis before spaced training with cycloheximide (Tully et al., 1994) eliminated the 24 h memory enhancement (Fig. 2*B*, spaced +

CXM: c739-Gal4: ANOVA: $F_{(2,23)} = 0.4472$, $p = 0.6454$), demonstrating that it consists entirely of bona fide PSD-LTM.

Downregulation of dAlk in the MBs enhances PSD-LTM specifically

Are earlier memories affected by dAlk attenuation in α/β MB neurons? To increase resolution and assess all memory forms concurrently, we used 1 training cycle of 12 US/CS pairings. Under these conditions (Fig. 3*A*), dAlk abrogation did not affect 10 min memory (STM, 10 min cold shock: ANOVA: $F_{(1,15)} = 0.2659$, $p = 0.6142$) as expected (Gouzi et al., 2011), or labile short-term ARM (Knapek et al., 2011; Bouzaiane et al., 2015) (10 min + cold shock: ANOVA: $F_{(1,15)} = 0.0717$, $p = 0.7928$). Moreover, 3 h middle-term memory (MTM) (3 h − cold shock: ANOVA: $F_{(1,15)} = 0.3578$, $p = 0.5593$) and labile middle-term ARM (3 h + cold shock: ANOVA: $F_{(1,15)} = 0.0313$, $p = 0.8622$) remained unaffected (Fig. 3*A*). However, a mild enhancement was detectable at 6 h after training (ANOVA: $F_{(1,15)} = 8.6609$, $p = 0.0107$), which was striking at 12 h (ANOVA: $F_{(1,15)} = 17.1629$, $p = 0.0010$) and 24 h (24 h-CXM: ANOVA: $F_{(1,15)} = 19.2126$, $p = 0.0006$). Even after one training cycle, the resultant 24 h memory was also bona fide PSD-LTM and not long-term ARM (Bouzaiane et al., 2015), as it was eliminated by cycloheximide treatment (24 h + CXM: ANOVA: $F_{(1,15)} = 0.1461$, $p = 0.7081$) (Fig. 3*A*).

Because 10 min memory was maximal under the intense 12 US/CS training conditions, enhanced learning may not have been visible due to ceiling effect. Hence, to verify that dAlk attenuation within the MBs did not result in enhanced learning, we limited the number of US/CS pairings from 12 to 3 (Fig. 3*B*). Nevertheless, enhanced learning was not detectable even under limited training (3 US/CS: ANOVA: $F_{(1,15)} = 1.9861$, $p = 0.1806$; 6 US/CS: ANOVA: $F_{(1,15)} = 0.5248$, $p = 0.4808$; 12 US/CS: ANOVA: $F_{(1,15)} = 0.0428$, $p = 0.8392$). In conclusion, a single training cycle upon dAlk abrogation in α/β MB lobes elicits bona fide PSD-LTM, which is not consequent of enhanced learning per se.

dAlk levels constrain PSD-LTM in adult MBs

To ascertain that dAlk plays an acute role in PSD-LTM, we modulated dAlk levels specifically in the adult CNS (McGuire et al., 2004). Adult-restricted dAlk abrogation (Fig. 4*A*) yielded significant memory elevation whether it was pan-neuronal (Elav;Gal80^{ts}: ANOVA: $F_{(2,31)} = 35.5212$, $p <$

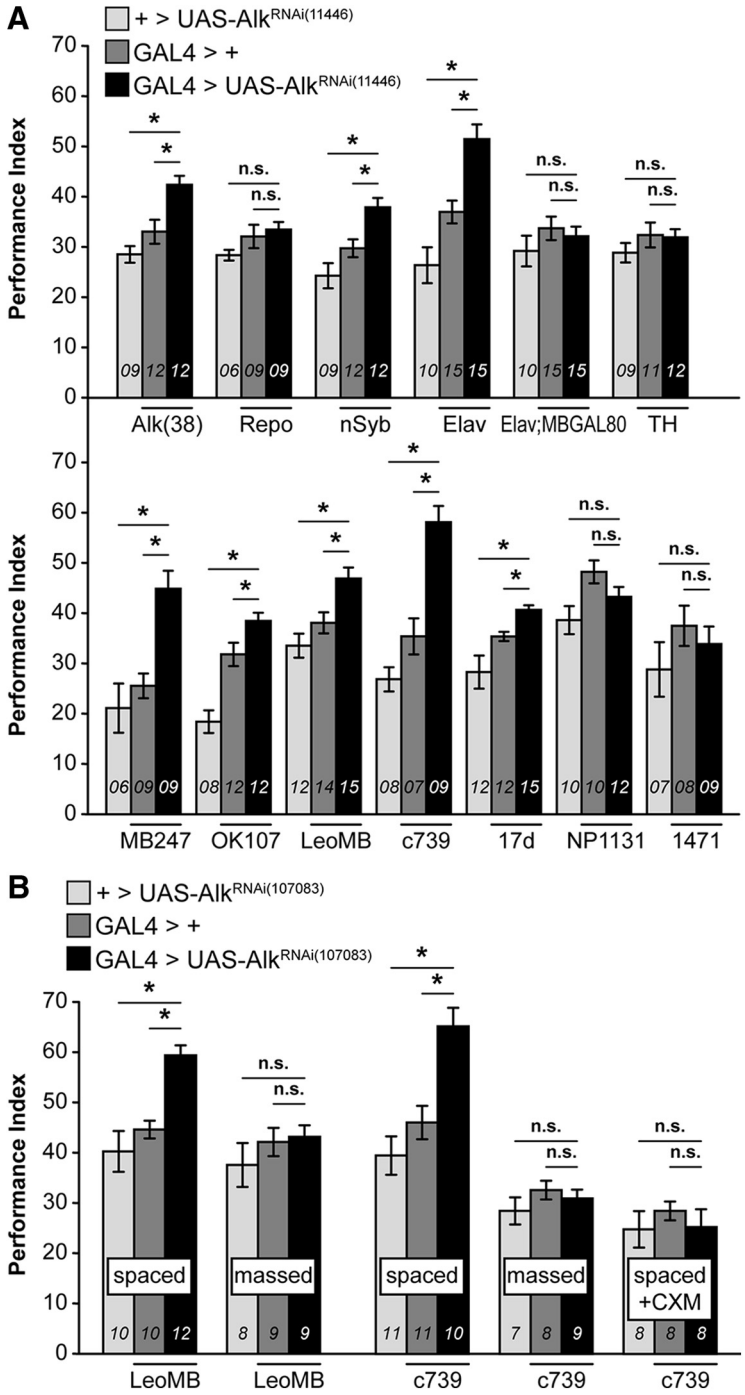

Figure 2. Downregulation of dAlk in intrinsic α/β MB neurons enhances PSD-LTM. Mean PIs (bars) ± SEMs (error bars) are shown. The number of experimental replicates (*n*) are indicated within the bars. Mean PIs are shown after typical spaced training of 5 cycles of 12 CS/US pairings, unless indicated otherwise. *Significant differences denoted by horizontal line pairs. n.s. means not significant. ***A***, GAL4 screen performed with expression of a UAS-*Alk*^{RNAi} transgene in defined GAL4-marked neuronal subsets of the fly brain. Neuronal and glial GAL4 drivers (top) and MB GAL4 drivers (bottom) represent LTM PI of flies expressing the UAS-*Alk*$^{RNAi(11446)}$ transgene driven by the indicated GAL4 (dark bars) and relevant genetic controls (light and dark gray bars). Significant LTM enhancement was revealed for Alk(38), nSyb, Elav, MB247, OK107, LeoMB, c739, and 17d driven dAlk abrogation. ***B***, Validation of the specificity of the 24 h memory enhancement with the independent RNAi-mediating transgene UAS-*Alk*$^{RNAi(107083)}$. Attenuation of dAlk specifically in LeoMB and c739 marked MB neurons (black bars) improved 24 h memory performance after spaced training (spaced) and phenocopied the effect previously observed with *Alk*$^{RNAi(11446)}$. In contrast, 24 h memory performance observed after massed training (massed) or cycloheximide treatment (35 mM, spaced + CXM) was not enhanced, demonstrating that the enhanced memory consists entirely of bona fide PSD-LTM.

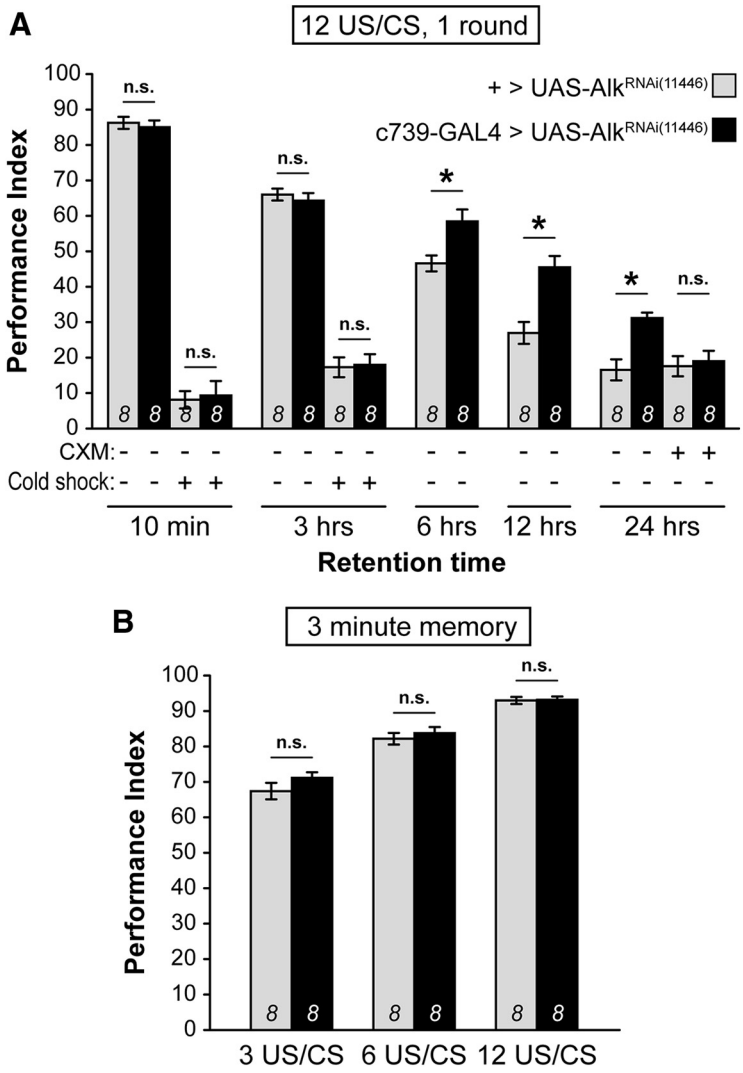

Figure 3. Downregulation of dAlk in the MBs enhances PSD-LTM specifically. Mean PIs (bars) ± SEMs (error bars) are shown. The number of experimental replicates (*n*) are indicated within the bars. *Significant differences denoted by horizontal line pairs. n.s. means not significant. ***A***, After a single round of 12 US/CS conditioning, memory retention was significantly enhanced at 6, 12, and 24 h upon attenuation of dAlk levels within c739-marked MB neurons (black bars) compared with the indicated relevant control (light gray bars). The improvement of 24 h memory consisted of bona fide PSD-LTM, as treatment with the protein synthesis inhibitor CXM totally eliminated the improvement. In contrast, 10 min and 3 h memories were not improved upon dAlk attenuation. ARM immediately after training (10 min + cold shock) and ARM after 3 h (3 h + cold shock) were also not elevated. ***B***, Learning (3 min memory) was not significantly improved in flies with attenuated dAlk expression in c739-marked MB neurons (black bars) compared with control (light gray bars) under any US/CS pairing protocol (3, 6, 12 US/CS).

0.0001; LSM vs controls: $p = 8 \times 10^{-7}$ and $p = 1.1 \times 10^{-8}$, respectively), pan-MB (Leo;Gal80^{ts}: ANOVA: $F_{(2,38)} = 8.1033$, $p = 0.0012$; subsequent LSM vs controls: $p = 0.0038$ and $p = 0.0008$), or specifically in α/β neurons (c739;Gal80^{ts}: ANOVA: $F_{(2,31)} = 15.7468$, $p < 0.0001$; LSM vs controls: $p = 0.0005$ and $p = 1 \times 10^{-5}$). Hence, dAlk attenuation within α/β MB neurons appears sufficient for the 24 h PSD-LTM elevation, and developmental alterations within MBs cannot account for the enhancement. Although still formally possible, it is highly unlikely that adult-specific attenuation of dAlk outside of the MBs could lead to LTM enhancement as constitutive attenuation of dAlk under Elav-Gal4; MB-Gal80 did not elevate it (Fig. 2*A*).

Collectively, dAlk appears to constrain PSD-LTM formation and its abrogation enhances it, even after minimal training. It follows then that acute dAlk elevation within α/β neurons could suppress PSD-LTM. Notably, increasing the levels of dAlk in adult neurons marked by commonly used drivers resulted in lethality within 24 h but was circumvented by reducing transgene induction to 8 h. Acute adult-specific overexpression of dAlk precipitated a highly significant LTM deficit (Fig. 4*B*), whether pan-neuronal (Elav;Gal80^{ts}: ANOVA: $F_{(2,23)} = 19.2806$, $p < 0.0001$; subsequent LSM vs controls: $p = 3.9 \times 10^{-6}$ and $p = 0.0031$), pan-MB (LeoMB; Gal80^{ts}: ANOVA: $F_{(2,23)} = 6.6558$, $p = 0.0058$; LSM vs controls: $p = 0.0037$ and $p = 0.0048$, respectively), or only in α/β neurons (c739;Gal80^{ts}: ANOVA: $F_{(2,23)} = 30.1603$, $p < 0.0001$; LSM vs controls: $p = 1.3 \times 10^{-7}$ and $p = 0.0021$). This deficit seems specific to LTM as sensory responses under Elav were normal (Gouzi et al., 2011), the flies were viable, normal externally, without apparent locomotor deficits (data not shown), and both their ARM after massed training and 3 min memory (Fig. 4*B*, massed and STM) were normal (massed: ANOVA: $F_{(2,23)} = 0.7627$, $p = 0.4789$; STM: ANOVA: $F_{(2,23)} = 0.6109$, $p = 0.5522$). Thus, the deficit is not consequent of disabled or unfit flies, and increased dAlk levels impair LTM, whereas its attenuation improves it.

We used the fact that 8 h of *dAlk*^{WT} induction suffice to yield deficits, to dissect the requirement for this RTK in PSD-LTM formation, consolidation, or retrieval (Tully et al., 1994) (Fig. 4*C*). Inducing *dAlk*^{WT} in adult MB neurons 8 h before conditioning manifested in deficient LTM ([$t_{-8\ h}$-t_0]: ANOVA: $F_{(2,23)} = 30.1603$, $p < 0.0001$; LSM vs controls: $p = 1.3 \times 10^{-7}$ and $p = 0.0021$, respectively). However, elevating dAlk for 8 h post-training or 8 h pre-testing did not result in LTM deficits ([t_0-$t_{+8\ h}$]: ANOVA: $F_{(2,31)} = 3.8911$, $p = 0.0318$; [$t_{+16\ h}$-$t_{+24\ h}$]: ANOVA: $F_{(2,23)} = 4.6712$, $p = 0.0210$). Therefore, to constrain PSD-LTM formation, dAlk activity is required during conditioning; therefore, it acts specifically as a negative regulator of its formation, not of its consolidation or retrieval.

dAlk is confined to the dendritic postsynaptic active zones of Kenyon cells

Is the distribution of dAlk within the MBs consistent with its proposed role in LTM inhibition? As shown in Figure 5*A1*, intense anti-dAlk staining was observed in the calyces and absent in other parts of MB neurons, such as the pedunculus and the lobes (Fig. 5*A2–A4*) in a manner reminiscent of another memory suppressor protein in *Drosophila*, SLC22A (Gai et al., 2016).

Further examination at higher magnification and single optical sections revealed that dAlk is broadly distributed throughout the calyces (Fig. 5*B2*) in contrast to its ligand Jeb, whose distribution appeared discrete, punctate, and granular (Fig. 5*B1*), proximal to dAlk, but without obvious colocalization (Fig. 5*B3*). Indeed, dAlk appeared to surround areas of Jeb immunoreactivity (Fig. 5*B4*), whose size and morphology are characteristic of MB calycal microglomeruli (Leiss et al., 2009). These postsynap-

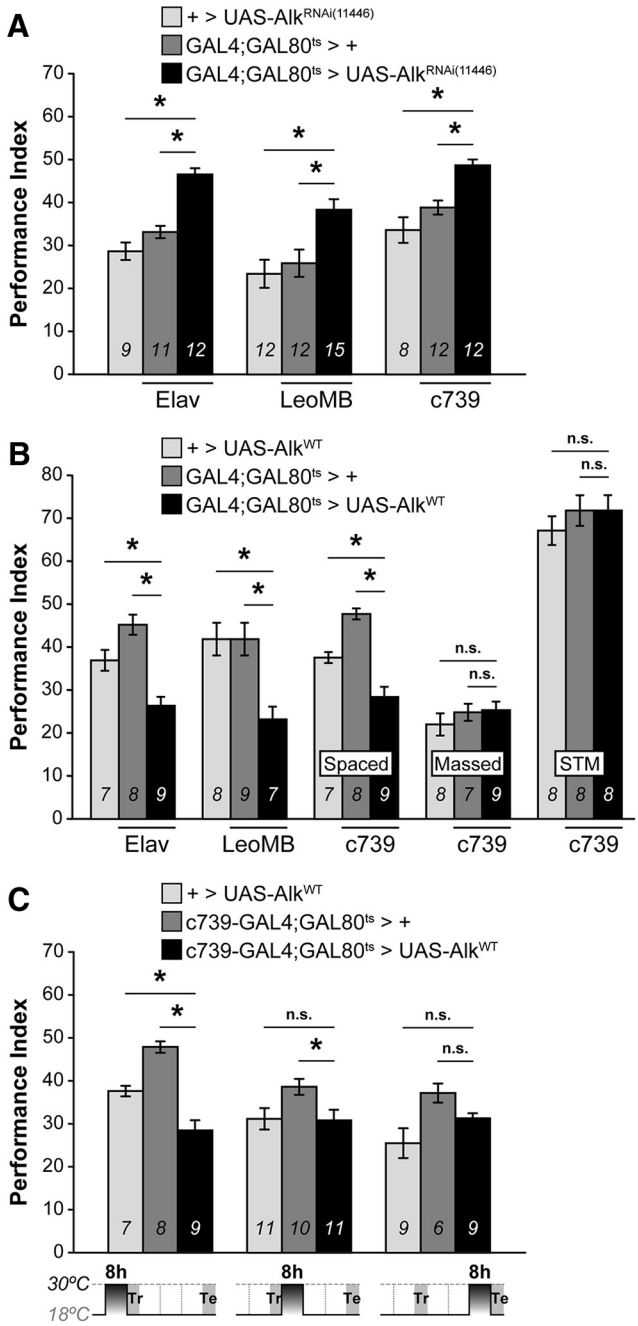

Figure 4. dAlk levels in the adult MBs during conditioning enhance or constrain LTM performance. Mean PIs (bars) ± SEMs (error bars) are shown. The number of experimental replicates (*n*) are indicated within the bars. *Significant differences denoted by horizontal line pairs. n.s. means not significant. ***A***, Attenuation of dAlk expression levels with the *dAlk*$^{RNAi(11446)}$ transgene restricted specifically to the adult CNS for 48 h before training yielded significant LTM increase (black bars) compared with controls (light and dark gray bars) when the transgene was expressed pan-neuronally (Elav;G80^{ts}), in all MB neurons (LeoMB;G80^{ts}) and more specifically in α/β MB neurons (c739;G80^{ts}). ***B***, Conversely, adult-specific overexpression of the wild-type dAlk^{WT} transgene using the same indicated G80^{ts} drivers elicited significant LTM deficits. In contrast, ARM and learning/3 min memory (Massed and STM) were not affected. ***C***, Induction of dAlk^{WT} expression in adult c739;G80^{ts} MB neurons for 8 h before conditioning ($t_{-8\,h}$-t_0) resulted in deficient LTM; but in contrast, it left LTM intact if the transgene was induced for 8 h immediately following conditioning (t_0-$t_{+8\,h}$), or 8 h before testing ($t_{+16\,h}$-$t_{+24\,h}$), as indicated in the diagram below.

tic microstructures are formed by the claw-like dendritic specializations of the KCs, and presynaptically by the enlarged terminal specializations/boutons of projection neurons (PNs). This notion was validated with typical presynaptic and postsynaptic MB markers (Fig. 5*C*). dAlk is extensively colocalized with the postsynaptic active zone marker DLG (discs large), whereas Jeb colocalized within characteristic large puncta with ChAT (Choline Acetyl Transferase), a PN presynaptic marker (Leiss et al., 2009). Thus, dAlk and Jeb are components of the calycal PN-MB synapses, sites of structural plasticity underlying olfactory learning and memory.

The dAlk-activating ligand Jeb does not affect LTM

Based on the complementarity of dAlk and Jeb patterns in MB calyces, we predicted that reducing Jeb levels would phenocopy dAlk attenuation and enhance PSD-LTM. However, developmental (Fig. 6*A*) or adult-specific (Fig. 6*B*) downregulation of Jeb by pan-neuronal (Elav, Ras2, and nSyb), glial (Repo), or PN-specific (GH146) expression of two different *Jeb*^{RNAi} transgenes did not enhance LTM (Fig. 6*A*; *Jeb*$^{RNAi(103047)}$: Elav-Gal4: ANOVA: $F_{(2,29)} = 6.6866$, $p = 0.0044$; LSM vs controls: $p = 0.0011$ and $p = 0.0988$, respectively; Ras2-Gal4: ANOVA: $F_{(2,30)} = 8.7923$, $p = 0.0011$; LSM vs controls: $p = 0.0002$ and $p = 0.0563$, respectively; nSyb-Gal4: ANOVA: $F_{(2,30)} = 0.3647$, $p = 0.6976$; Repo-Gal4: ANOVA: $F_{(2,31)} = 2.1992$, $p = 0.1291$; Fig. 6*B*; *Jeb*$^{RNAi(103047)}$: Elav-Gal80^{ts}: ANOVA: $F_{(2,37)} = 0.1693$, $p = 0.8449$; Repo-Gal80^{ts}: ANOVA: $F_{(2,55)} = 2.5336$, $p = 0.0890$; GH146-Gal80^{ts}: ANOVA: $F_{(2,31)} = 0.4709$, $p = 0.6291$; Fig. 6*B*; *Jeb*$^{RNAi(30799)}$: Elav-Gal80^{ts}: ANOVA: $F_{(2,68)} = 0.5738$, $p = 0.5662$). Jeb overexpression also did not alter LTM (Fig. 6*B*, *Jeb*^{WT}: GH146-Gal80^{ts}: ANOVA: $F_{(2,31)} = 1.1982$, $p = 0.3162$). We are certain that the tools used for Jeb abrogation are functional because they dramatically reduce its level (Fig. 6*D*) and recapitulated established Jeb-dependent phenotypes (Gouzi et al., 2011) of increased pupal size (Elav-Gal80^{ts}: ANOVA: $F_{(2,103)} = 85.3173$, $p < 0.0001$; LSM vs controls: $p = 5.9 \times 10^{-17}$ and $p = 1.3 \times 10^{-20}$, respectively) and enhanced 3 min memory (Elav-Gal80^{ts}: ANOVA: $F_{(2,35)} = 13.0861$, $p < 0.0001$; LSM vs controls: $p = 0.0026$ and $p = 1.6 \times 10^{-5}$, respectively) (Fig. 6*C*). Therefore, the dAlk-dependent LTM inhibition is Jeb independent.

dAlk levels increase rapidly in KC dendrites upon conditioning

Because excessive dAlk in the MBs suppressed LTM, we wondered whether, under physiological conditions, its levels change within these neurons consequent to conditioning. Therefore, we used a well-established quantification protocol (Liu et al., 2007) to monitor dAlk levels in MB calyces after conditioning with 1 round of 12 US/CS, which is sufficient to trigger elevated LTM upon its attenuation (Fig. 3*A*). Given the time required to condition and sacrifice the flies, we monitored its levels at 20 min and 3 h after conditioning.

Significantly, dAlk levels were substantially elevated in conditioned flies (US/CS paired), in contrast to animals after sham conditioning (US/CS unpaired) with the US preceding the CS without coincidence (Fig. 7*A*). Quantification of dAlk levels (Fig. 7*B*, left) revealed that US/CS pairing resulted in a significant ~1.5-fold elevation (ANOVA: $F_{(3,50)} = 7.9802$, $p = 0.0002$; LSM 20′ paired vs 20′ unpaired: $p = 0.005$; and $p = 0.0003$ for 3 h paired vs 20′ unpaired). Because each group of flies experienced both stimuli, this result indicates that dendritic dAlk elevation emerges specifically upon stimulus pairing. In confirmation, dAlk levels after sham training were found equivalent to those in naive flies (LSM 20′ naive vs 20′ unpaired: $p = 0.8114$). This difference cannot be attributed to positioning or to the size of the flies because female flies of similar age were used for all quantifications and the calycal areas quantified were statistically identical

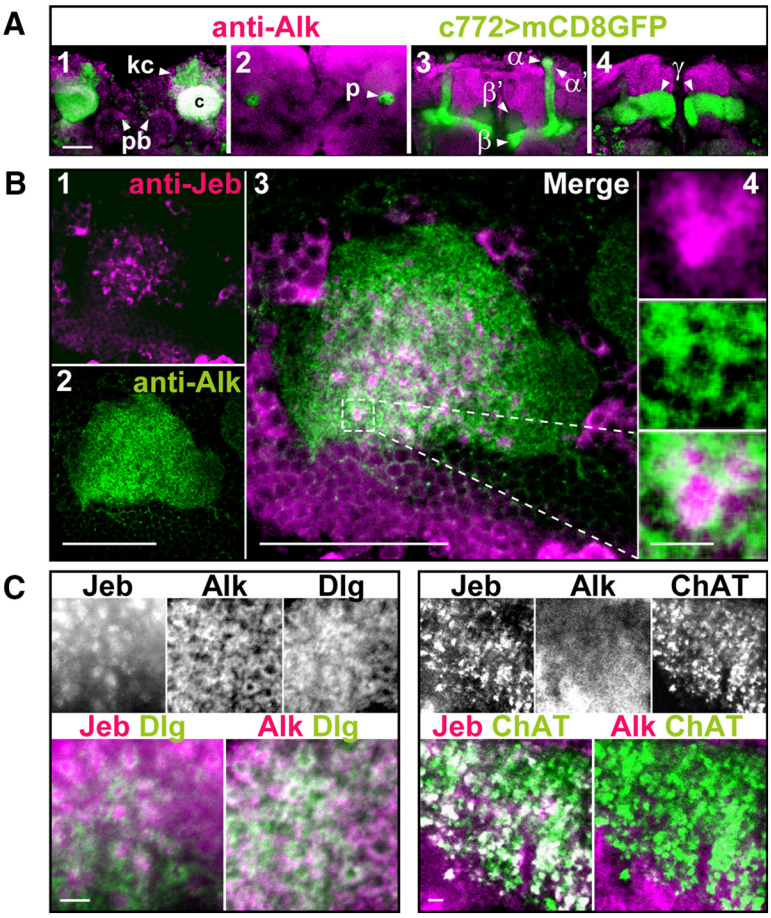

Figure 5. dAlk and its ligand Jeb are enriched in synapses of projection neurons and Kenyon cells. ***A***, dAlk is enriched in MB calyces but is absent in the MB lobes. Confocal images of single optical sections of the fly brain from posterior to anterior (***A1–A4***) were acquired at the level of MB calyces (***A1***), pedunculus (***A2***), α/β lobes (***A3***), and γ lobe (***A4***). Confocal images were acquired at the same section levels with identical settings. dAlk was visualized with an anti-dAlk antibody (purple). Fly brain structures were marked with a membrane GFP (green) encoded by the mCD8:GFP transgene expressed with the neuronal c772-GAL4 driver. White represents colocalization of dAlk and GFP immunofluorescence. dAlk protein accumulates within the dendrites (***A1***: calyces, c) and cell bodies (***A1***: Kenyon cells, kc, arrowhead) of MB neurons and in the protocerebral bridge (***A1***: pb, arrowheads). It is also expressed widely in the neuropil, above background. In contrast, MB axons (***A2***: pedunculus, p, arrowhead) (***A3***: α, α', β, and β' lobes, arrowheads) (***A4***: γ lobes, arrowheads) are devoid of dAlk staining. Scale bar, 50 μm. ***B***, dAlk and Jeb display a complementary pattern of expression within MB calyces. Confocal images of a single optical transverse section of an MB calyx were acquired using identical settings and at the same section level corresponding approximately to its middle section (***B1–B3***). Jeb protein was visualized with an anti-Jeb antibody (***B1***, purple), and dAlk protein was visualized with an anti-dAlk antibody (***B2***, green). Scale bar, 50 μm. Colocalization of Jeb and dAlk immunofluorescence (***B3***, merge, white) is shown at the same magnification. Scale bar, 50 μm. Inset, Higher magnification of the hatched box, showing in a single synaptic microglomerulus (***B4***), from top to bottom, Jeb, dAlk, and their complementary pattern. Scale bar, 10 μm. ***C***, dAlk is expressed at the postsynaptic dendritic active zones of the MB calyces, whereas Jeb is expressed presynaptically in the synaptic buttons of apparent projection neurons. Confocal images of single optical sections of MB calyces were acquired at similar levels, using identical settings and displaying triple staining of Jeb, dAlk, and membrane GFP. Scale bars, 10 μm. Left, White represents signals of anti-Jeb, anti-dAlk, and anti-Dlg, a marker of the postsynaptic active zones. Colored images represent lack of colocalization of Jeb (purple) and Dlg (green), and colocalization (white) of dAlk (purple) and Dlg (green). Right, White represents signals of anti-Jeb, anti-dAlk, and anti-ChAT, a marker of presynaptic terminal buttons. Colored images represent complete colocalization of Jeb (purple) and ChAT (green), and lack of colocalization (white) between dAlk (purple) and ChAT (green).

(ANOVA $F_{(3,50)} = 0.3589$, $p = 0.7829$) in the 51 individuals evaluated (Fig. 7*E*, left). Finally, dAlk levels were not found further elevated upon increasing the number of conditioning rounds from 1× to 5× (spaced conditioning) (Fig. 7*B*, right, ANOVA $F_{(1,31)} = 0.0000$, $p = 0.9976$). Therefore, the first round of conditioning appears sufficient for dAlk to attain maximal accumulation levels in the early phase of memory encoding. This is consistent with the notion that dAlk elevation attenuates or blocks PSD-LTM formation upon a single round of conditioning, and congruent with PSD-LTM formation with a single round of conditioning when dAlk was abrogated (Fig. 3*A*).

Importantly, dAlk elevation in MB dendrites was detected 20 min after conditioning and remained elevated for at least 3 h (Fig. 7*B*; LSM 3 h paired vs 20′ paired: $p = 0.3305$). The short time required for a rather large transmembrane protein to increase its dendritic levels fits the temporal requirement for locally translated proteins (Steward and Schuman, 2001). Considering the role of dAlk in PSD-LTM formation, its restricted dendritic distribution, and its rapid increase upon US/CS pairing, we suggest that its mRNA is likely transported to dendrites and translated upon conditioning. Furthermore, we hypothesized that dendritic targeting and local translation of dAlk mRNA may be conferred by sequences in its 3′UTR, as for several other synaptic proteins (Steward and Schuman, 2001; Ashraf et al., 2006). Inspection of the dAlk 3′UTR with TargetScanFly 6.2 (Lewis et al., 2005) and RBPmap 1.1 (Paz et al., 2014) revealed that it contains numerous elements potentially controlling mRNA stability and translation, such as AU-rich elements and cytoplasmic polyadenylation elements, but also sites for RNA binding proteins (RBPs). Disruption of the spatial arrangement of such sequences could reduce or eliminate its translation and keep local dAlk levels low, in effect mimicking its attenuation.

To test this possibility, we capitalized on flies carrying a P-element insertion in the 3′UTR of *dAlk* ($Alk^{MB06458}$), which disrupts the spatial continuity of the putative translational control sequences. These mutants present increased responses to ethanol, are otherwise normal, and their total dAlk levels remain comparable with controls (Lasek et al., 2011). Consistent with these observations, we did not detect differences in the steady-state levels of dendritic dAlk in mutants and controls (Fig. 7*D*, unpaired) (ANOVA: $F_{(3,53)} = 18.2206$, $p < 0.0001$; LSM unpaired w^{1118} vs unpaired mutant: $p = 0.9219$). However, after conditioning, the pairing-dependent dAlk increase in controls (LSM unpaired w^{1118} vs paired w^{1118}: $p = 2.3 \times 10^{-7}$) was absent from the mutants (LSM unpaired mutant vs paired mutant: $p = 0.5769$). Therefore, in $Alk^{MB06458}$ mutant homozygotes, MB dendritic levels of dAlk remain low even after conditioning (LSM paired w^{1118} vs paired mutant: $p = 3.5 \times 10^{-7}$), in effect mimicking its transgenic attenuation. Again, size and positioning cannot account for the effect, as the calycal areas quantified were identical (ANOVA: $F_{(3,53)} = 0.4121$, $p = 0.7450$) in controls and mutants (Fig. 7*E*, right). These results suggest that the conditioning-dependent modulation of dAlk levels

in MB dendrites is conferred by the spatial arrangement of control sequences in the 3′UTR of its mRNA. Notably, dAlk retained its dendritic localization in the mutants, suggesting that the insertion does not disrupt signals targeting the mRNA to the calyces (Fig. 7*C*).

The attenuated conditioning-dependent dAlk levels in MB calyces predict that the Alk^{MB} mutants will present enhanced LTM. Indeed, 3 min memory (Fig. 7*F*; 3 US/CS) of controls, mutant heterozygotes, and homozygotes were indistinguishable (ANOVA: $F_{(2,32)} = 0.5853$, $p = 0.5632$). In contrast, mutant homozygotes exhibited substantially enhanced 24 h memory (Fig. 7*F*; spaced: ANOVA: $F_{(2,37)} = 12.5306$, $p < 0.0001$; subsequent LSM vs controls $p = 3.9 \times 10^{-5}$ and $p = 7.8 \times 10^{-4}$, respectively), which was PSD-LTM specific, as it was not elicited by massed training (Fig. 7*F*; massed: ANOVA $F_{(2,31)} = 0.1495$, $p = 0.8618$). Task-relevant sensory responses were normal in the mutants (Fig. 7*G*) (reactivity to shock: ANOVA: $F_{(1,21)} = 0.4616$, $p = 0.5047$; octanol avoidance: ANOVA: $F_{(1,19)} = 0.0846$, $p = 0.7745$; benzaldehyde avoidance: ANOVA: $F_{(1,19)} = 1.7238$, $p = 0.2057$).

To ascertain that the elevated PSD-LTM phenotype was consequent to disruption of the *dAlk* 3′UTR and not of a neighboring gene, we generated heteroallelics with the lethal (Lorén et al., 2003) null Alk^1 allele (Fig. 7*H*). Significantly, Alk^1/Alk^{MB} heteroallelics presented a substantial LTM enhancement over that of either Alk^1 or Alk^{MB} heterozygotes (ANOVA: $F_{(3,39)} = 18.5255$, $p < 0.0001$; subsequent LSM Alk^1/Alk^{MB} vs $Alk^1/+$: $p = 1.9 \times 10^{-7}$; vs $Alk^{MB06458}/+$: $p = 4.7 \times 10^{-7}$), confirming that the mutations are allelic. Moreover, PSD-LTM in the heteroallelics was even higher than that of Alk^{MB} homozygotes (LSM $Alk^1/Alk^{MB06458}$ vs $Alk^{MB06458}$: $p = 0.0092$) as hypothesized, given that Alk^1 is a null allele and conditioning-dependent upregulation of dAlk levels is blocked in Alk^{MB}. This is consistent with the notion that PSD-LTM formation is sensitive to the precise postconditioning levels of dAlk in MB dendrites.

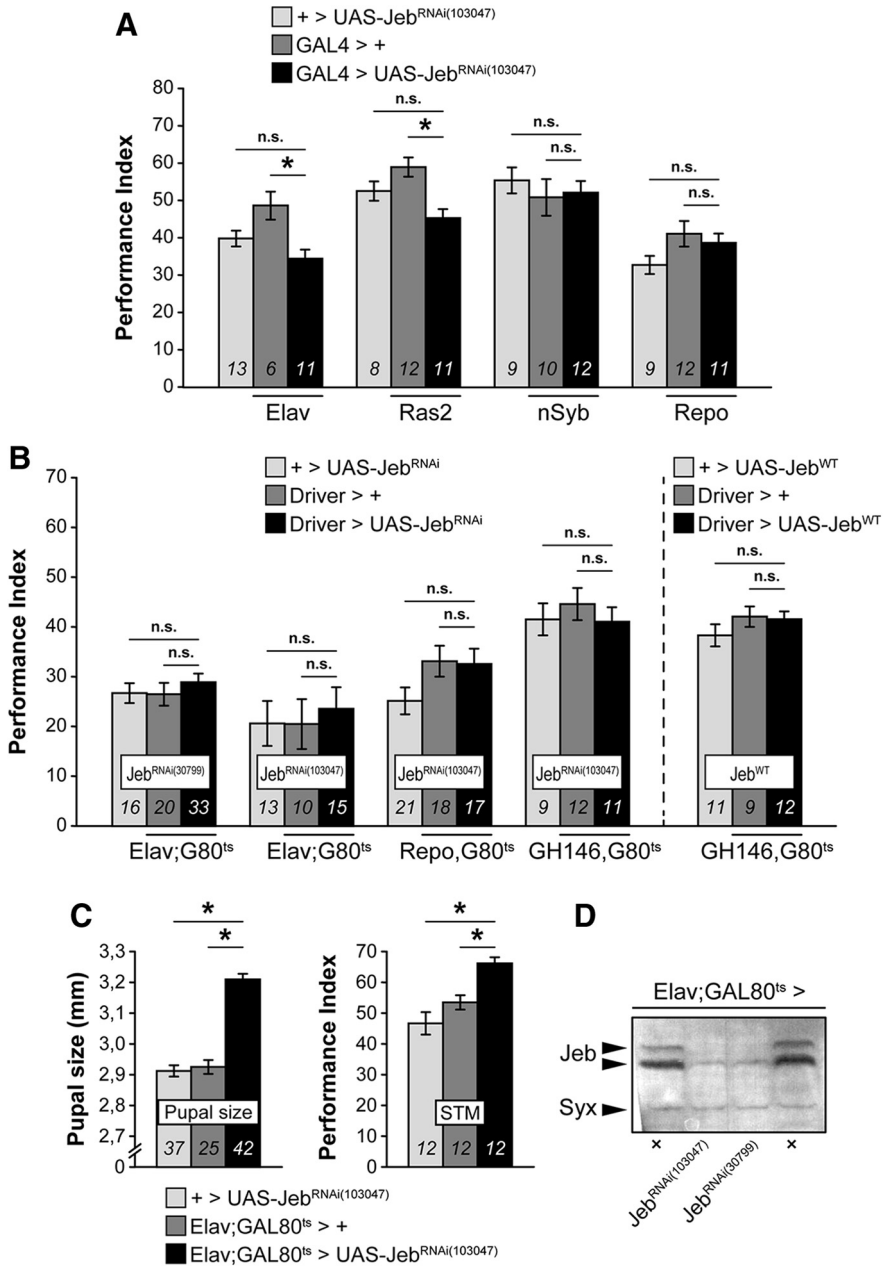

Figure 6. The dAlk-activating ligand Jeb is not involved in LTM. Mean PIs (bars) ± SEMs (error bars) are shown. The number of experimental replicates (*n*) are indicated within the bars. *Significant differences denoted by horizontal line pairs. n.s. means not significant. ***A***, Attenuation of Jeb expression levels with the $Jeb^{RNAi(103047)}$ transgene (black bars) did not affect 24 h LTM performance compared with controls (light and dark gray bars) when the transgene was expressed pan-neuronally or in glial cells only using the indicated Gal4 drivers. ***B***, Attenuation of Jeb expression levels with the $Jeb^{RNAi(103047)}$ transgene restricted to the adult CNS for 48 h before training also did not affect 24 h LTM when the transgene was expressed pan-neuronally, in glial cells or in projection neurons using the indicated $G80^{ts}$ drivers. Lack of LTM effects was verified with pan-neuronal expression (Elav;$Gal80^{ts}$) of a second independent $Jeb^{RNAi(30799)}$ transgene. Jeb overexpression (Jeb^{WT}) in projection neurons (GH146,$Gal80^{ts}$) also did not affect 24 h LTM. ***C***, Pan-neuronal Jeb attenuation with the $Jeb^{RNAi(103047)}$ transgene yielded a substantial increase of pupal size compared with controls when the transgene was expressed throughout development and yielded a substantial increase of learning/3 min memory (STM, 1 cycle of 3 CS/US pairings) when the transgene was expressed only during adulthood for 2 d before conditioning. ***D***, Representative semiquantitative immunoblot showing a dramatic reduction of endogenous Jeb levels upon pan-neuronal expression of both independent Jeb^{RNAi} transgenes (UAS-$Jeb^{RNAi(103047)}$ and UAS-$Jeb^{RNAi(30799)}$). Jeb protein (Jeb) was revealed with the anti-Jeb antibody (Jeb), and Syntaxin (Syx) was used as loading control.

Discussion

Our findings reveal a novel role for dAlk in regulation of PSD-LTM formation in addition to its established role in learning (Gouzi et al., 2011). dAlk constrains both processes, but whereas learning attenuation requires its activity outside the MBs, suppression of PSD-LTM formation requires its elevation within the dendrites of α/β MB neurons. Moreover, although its activating ligand Jeb is required for learning attenuation, it is dispensable for PSD-LTM constraint.

Global pharmacological inhibition of dAlk activity resulted in both STM and LTM enhancement as expected (Fig. 1) because it addressed all neurons expressing this RTK. dAlk activity outside the MBs is known to be required for learning/3 min memory

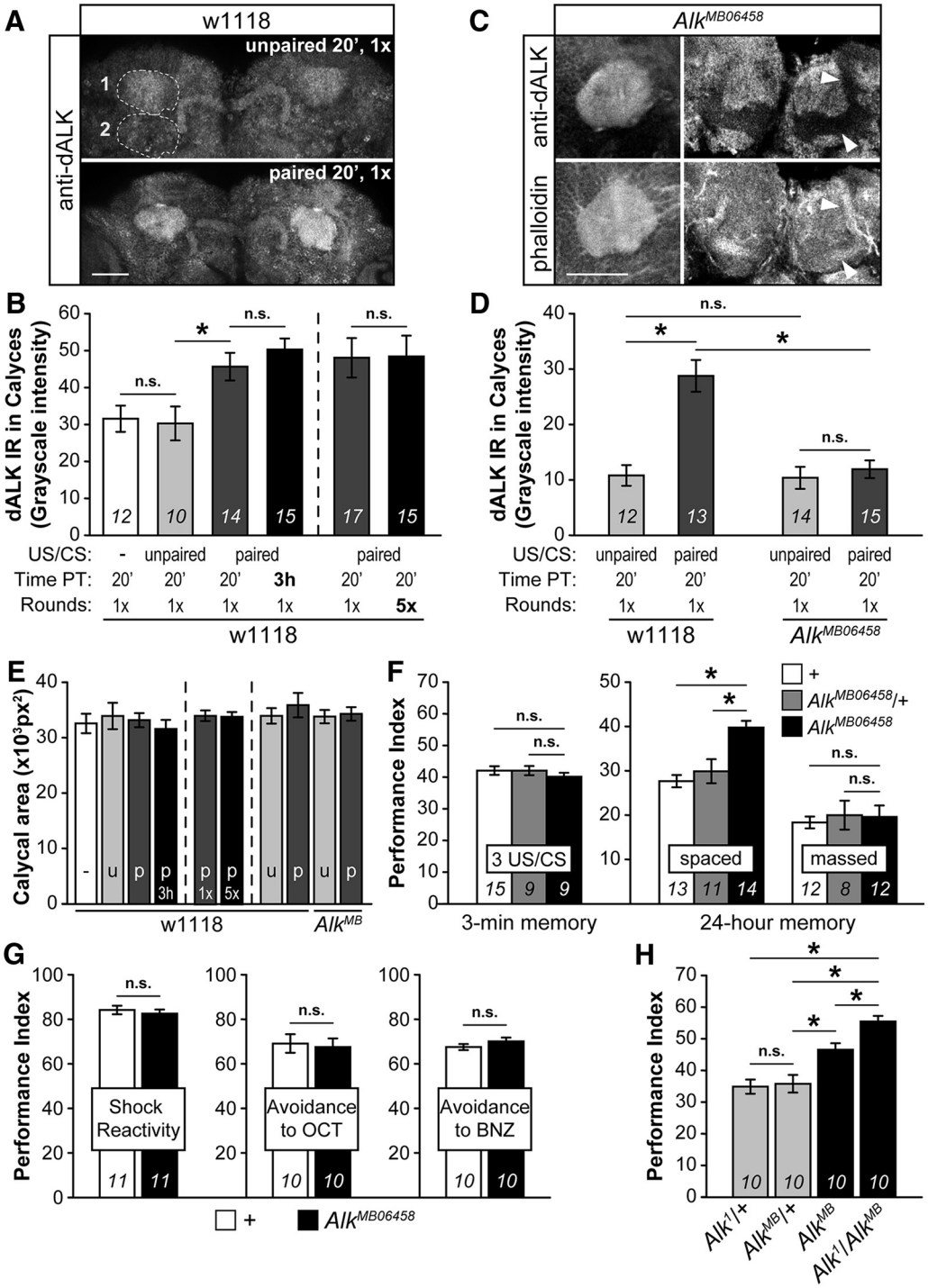

Figure 7. Dendritic dAlk levels in the MBs increase rapidly upon conditioning to constrain LTM. ***A***, Representative grayscale images of anti-dAlk immunofluorescence in control w^{1118} flies. Scale bar, 50 μm. Single confocal plane images of MB calyces were captured at the same section level corresponding to the middle part of the calyx, using constant optical acquisition settings, and examined in a single session to allow comparison between control (unpaired 20 min, 1 round, 1×) and experimental samples (paired 20 min, 1 round, 1×). ***B***, Semiquantitative analysis of dAlk immunoreactivity (IR) in the calyces of w^{1118} control flies was achieved by subtracting from the mean grayscale intensity of the signal within a calyx (dashed circle 1, delimited by hand in ***A***), the mean grayscale intensity of the signal in an adjacent area (dashed circle 2, same size and shape as circle 1). The mean intensity differences ± SEM for the indicated number (*n*) of calyces are shown. Control w^{1118} flies were either trained with the typical conditioning protocol of 12 US/CS pairings (US/CS: paired) or trained with a modified protocol in which the US preceded the CS^+ without coincident pairing (US/CS: unpaired) or untrained (UC/CS: −). Flies were trained using either a single (1×) round or 5× spaced rounds of 12 US/CS pairings. Their brains were dissected and fixed either immediately (20′) or 3 h after training (Time PT, Time post-training). In control w^{1118} flies, pairing the US with the CS^+ significantly increased calycal dAlk levels 20 min after conditioning, which apparently perdured at least for 3 h. Training flies either with 1× round or with 5× spaced rounds did not alter increased calycal dAlk levels. In contrast, dAlk levels in flies submitted to unpaired stimuli (unpaired) were not different from in naive flies (−). ***C***, Single confocal plane images of a MB calyx (left) and lobes (right) in $Alk^{MB06458}$ homozygote fly brains stained with the anti-dAlk antibody (top row) and counterstained with rhodamine-conjugated phalloidin (bottom row) to mark the neuropil. In $Alk^{MB06458}$, dAlk retained its calycal localization, remaining excluded from the lobes (arrowheads). Scale bar, 50 μm. ***D***, Semiquantitative analysis of dAlk immunoreactivity (IR) in the calyces of w^{1118} and $Alk^{MB06458}$ flies. The mean dAlk intensity differences (calculated as indicated above) ± SEM for the indicated number of calyces (*n*) are shown. Differences in steady-state levels of dendritic dAlk were not detected in $Alk^{MB06458}$ mutants and w^{1118} control flies (unpaired). However, in flies submitted to 1 round of conditioning (paired), the pairing-dependent increase of dendritic dAlk observed in w^{1118} controls was absent in (*Figure legend continues.*)

suppression (Gouzi et al., 2011), and these neurons are clearly affected by TAE684, as also are the MBs yielding enhanced PSD-LTM. In contrast, dAlk levels were specifically abrogated within the MBs where converging studies (Isabel et al., 2004; Yu et al., 2006; Pavlopoulos et al., 2008; Bouzaiane et al., 2015) established that STM and LTM engage different MB neuron types, the γ and the α/β, respectively. dAlk attenuation in γ MB neurons did not affect 3 min memory (Gouzi et al., 2011) or PSD-LTM, strongly suggesting that dAlk is not expressed therein.

The notion of memory suppression almost invariably refers to forgetting, broadly defined as a decay of memory that either actively dissipates in time or undergoes interference by additional learning of unrelated or irrelevant information (Wixted, 2004; Dewar et al., 2007). Forgetting an odor/shock association in *Drosophila* (Davis and Zhong, 2017) requires the small G-protein Rac (Shuai et al., 2010), or dopamine (DA) signaling predominantly through the DAMB receptor (Berry et al., 2012), and its suppression appears as an enhancement of all types of 3–24 h memories. However, 24 h memory enhancement resulting from Rac attenuation appears distinct from PSD-LTM (Shuai et al., 2010), and inhibition of DA signaling in the MB-afferent DAN neurons does not enhance 16–24 h memories (Berry et al., 2012). Hence, Rac and/or DA signaling inhibit recently acquired labile memories rather than consolidated forms. dAlk also acts during the labile stage of memory formation, but not its dissipation, and is specific to PSD-LTM, not 3 h memory or ARM (Figs. 2*B*, 3*A*). Furthermore, dAlk is not required (Fig. 2*A*) within the essential for forgetting dopaminergic neurons (Davis and Zhong, 2017). Therefore, dAlk-mediated LTM inhibition is distinct from dissipation of labile memories.

A number of memory suppressor genes have been recently described in *Drosophila* (Walkinshaw et al., 2015) and mice (Lee and Silva, 2009), indicating that, although its exact role is unclear, memory restraint is evolutionarily conserved. Constraining memory may limit the conditioned associations processed toward the energetically demanding PSD-LTM (Plaçais et al., 2017), ensure the fidelity of associations that progress toward consolidation, or inhibit proactive or retroactive interference (Wixted, 2004; Dewar et al., 2007; Davis and Zhong, 2017).

The role of all apparent memory suppressor proteins and miRNAs identified to date in *Drosophila* (Busto et al., 2015; Walkinshaw et al., 2015) has not been fully delineated, but some mechanistic aspects emerge. *Drosophila* memory suppressor miRNAs ostensibly regulate translation of postsynaptic proteins involved in MB excitability (Li et al., 2013; Guven-Ozkan et al., 2016); hence, attenuation of their levels and the resultant hyperexcitability could underlie enhanced memory. Accordingly, loss of the apparent signal-tempering acetylcholine transporter DmSLC22A from MB neurons enhances their excitability and elevates memory (Gai et al., 2016). Interestingly, like dAlk, DmSLC22A is found in calycal microglomeruli (Gai et al., 2016). Therefore, in conjunction with our results, it appears that memory-constraining mechanisms depend on the level of postsynaptic proteins that limit the amplitude or duration of MB neuronal excitation. In contrast to other memory suppressor proteins and miRNAs (Busto et al., 2015, 2017; Walkinshaw et al., 2015), dAlk elevation in the MBs is not required for 3 h memory (Fig. 3) but appears specific to PSD-LTM. The temporal specificity of dAlk suggests that its activity may not constrain MB excitability, but rather LTM consolidation mechanisms, a hypothesis under investigation.

Conditioning-dependent dAlk elevation in MB dendrites appears to result via local translation regulated by the 3′UTR of its mRNA. This 3′UTR-conferred property is shared with multiple dendritic proteins (Steward and Schuman, 2001), including another RTK involved in memory formation, the BDNF receptor trkB (Nagappan and Lu, 2005). Similarly, 3′UTR sequences direct the mRNA of *Drosophila* CaMKII, a kinase also implicated in memory, to be translated in the postsynaptic zones of MB calyces (Ashraf et al., 2006). Significantly, the 3′UTR of dAlk mRNA contains more numerous regulatory elements than those on CaMKII transcripts, including several stabilizing AU-rich elements. The putative miRNA binding sites include those for miR-305 and miR-932, both implicated in memory formation (Cristino et al., 2014; Busto et al., 2015) and possibly in dAlk local translation. Translational regulation may also involve identified putative RBP binding sequences at the dAlk 3′UTR. Some, such as pumilio (pum) and the cytoplasmic polyadenylation element binding protein (CPEB) Orb2 (Dubnau et al., 2003; Keleman et al., 2007), are translation suppressors with known function in memory. Whether others, such as Rox8, the ortholog of the stress granule-associated vertebrate protein TIA1, play a role in memory formation is currently unknown. Whether miRNAs and RBPs interact with dAlk mRNA upon conditioning to regulate its dendritic levels will be the focus of forthcoming work.

The PSD-LTM constraint depends on dAlk activity and the increased levels per se, as demonstrated by the elevated memory upon treatment with the inhibitor TAE684. How is calycal dAlk activated to constrain LTM formation since Jeb is dispensable for LTM attenuation (Fig. 6*A*)? Presently, we cannot exclude the possibility that a yet unidentified ligand may activate dAlk upon spaced conditioning. However, another explanation we currently favor is that, upon spaced training, dAlk can autoactivate in response to its local elevation in the calyx. Level-dependent autoactivation has been reported for human ALK-positive cancers (Hallberg and Palmer, 2013), or neurons transfected with ALK (Moog-Lutz et al., 2005), a feature shared by almost all RTKs (Lemmon and Schlessinger, 2010). Local elevation-dependent autoactivation of dAlk is in agreement with our own experimental data that acute dAlk elevation attenuates LTM (Fig. 4*B*) and that conditioning elevates the endogenous protein in MB dendrites (Fig. 7). Moreover, dAlk autoactivation is consistent with the independence of dAlk-dependent PSD-LTM attenuation from Jeb (Fig. 6). The conditioning-dependent dAlk elevation and autoactivation in MB dendrites are likely considerably slower than acute activation by Jeb of extant dAlk outside the MBs required to constrain learning/3 min memory formation (Gouzi et

←

(*Figure legend continued.*) $Alk^{MB06458}$ homozygotes. Time PT, Time post-training. ***E***, Mean areas (in square pixels ± SEM) of the calyces used in ***B*** and ***D*** to obtain the intensity measurements. No significant differences between calycal areas were detected that could explain the differences observed in dAlk intensities. Each bar corresponds to its equivalent in ***B*** and ***D***. −, Naive flies; u, unpaired; p, paired; 1× and 5×, number of rounds. Brains were all dissected/fixed 20 min after training, except where specified. ***F***, $Alk^{MB06458}$ homozygotes present enhanced LTM (spaced) but not 3 min memory (STM, 3 US/CS) or ARM (massed). Mean PIs (bars) ± SEMs (error bars) are shown. The number of experimental replicates (*n*) are indicated within the bars. *Significant differences denoted by horizontal line pairs. n.s. means not significant. ***G***, Task-relevant olfactory and shock reactivity responses in $Alk^{MB06458}$ homozygotes (black bars) were indistinguishable from controls (white bars). ***H***, The dosage of dAlk protein in MB dendrites after conditioning calibrates the level of LTM performance. Mean PIs (bars) ± SEMs (error bars) are shown. The number of experimental replicates (*n*) are indicated within the bars. *Significant differences denoted by horizontal line pairs. n.s. means not significant. $Alk^{1}/Alk^{MB06458}$ heteroallelics present even higher LTM than $Alk^{MB06458}$ homozygotes. The fact that heteroallelics present LTM elevation indicates that the mutations do not complement and are indeed allelic.

al., 2011) (Fig. 6*C*). Furthermore, pan-neuronal elevation of Jeb left PSD-LTM unaffected (Fig. 6*B*), consistent with the notion that the two methods of dAlk activation, Jeb-dependent activation and autoactivation, are operant in spatially distinct neurons (outside and inside the MBs, respectively) and of distinct functional consequences.

Hence, we propose that conditioning results in local elevation of unliganded dAlk monomers in MB dendrites, raising the probability of encounter, lateral dimerization, autophosphorylation, and activation of the kinase domain at the postsynaptic plasma membrane. Unfortunately, an antibody specific to phosphorylated, hence activated, dAlk is not currently available; therefore, it is not possible to test this prediction *in situ*.

Downstream mechanisms engaged by dAlk to restrain LTM are still unknown. In our previous study (Gouzi et al., 2011), we described dAlk outside the MBs as an upstream activator of a dNf1-regulated Ras/ERK signaling pathway responsible for learning/STM attenuation. Interestingly, dAlk and dNf1 colocalize extensively in MB calyces (Gouzi et al., 2011), suggesting that they could also interact to mediate PSD-LTM attenuation. However, unlike for dAlk abrogation, dNf1 loss results in PSD-LTM deficits restored by reexpression of the protein in α/β MB neurons under c739-Gal4 (Buchanan and Davis, 2010). Therefore, although possible that dAlk and dNf1 interact within these neurons, they are likely antagonistic with respect to PSD-LTM formation, a process potentially engaging and requiring suppression of Ras signaling, a hypothesis currently under investigation.

In conclusion, we have identified dAlk as a specific negative regulator of PSD-LTM formation. Thus far, dAlk appears unique among RTKs in that it constrains LTM formation, possibly acting as a memory filter. The nature of the specific signals engaged by dAlk and the downstream PSD-LTM-constraining mechanisms remains yet to be elucidated in future work.

References

Akalal DB, Wilson CF, Zong L, Tanaka NK, Ito K, Davis RL (2006) Roles for *Drosophila* mushroom body neurons in olfactory learning and memory. Learn Mem 13:659–668. CrossRef Medline

Ashraf SI, McLoon AL, Sclarsic SM, Kunes S (2006) Synaptic protein synthesis associated with memory is regulated by the RISC pathway in *Drosophila*. Cell 124:191–205. CrossRef Medline

Bai L, Sehgal A (2015) Anaplastic lymphoma kinase acts in the *Drosophila* mushroom body to negatively regulate sleep. PLoS Genet 11:e1005611. CrossRef Medline

Berry JA, Cervantes-Sandoval I, Nicholas EP, Davis RL (2012) Dopamine is required for learning and forgetting in *Drosophila*. Neuron 74:530–542. CrossRef Medline

Bouzaiane E, Trannoy S, Scheunemann L, Plaçais PY, Preat T (2015) Two independent mushroom body output circuits retrieve the six discrete components of *Drosophila* aversive memory. Cell Rep 11:1280–1292. CrossRef Medline

Buchanan ME, Davis RL (2010) A distinct set of *Drosophila* brain neurons required for neurofibromatosis type 1-dependent learning and memory. J Neurosci 30:10135–10143. CrossRef Medline

Busto GU, Guven-Ozkan T, Fulga TA, Van Vactor D, Davis RL (2015) microRNAs that promote or inhibit memory formation in *Drosophila melanogaster*. Genetics 200:569–580. CrossRef Medline

Busto GU, Guven-Ozkan T, Davis RL (2017) MicroRNA function in *Drosophila* memory formation. Curr Opin Neurobiol 43:15–24. CrossRef Medline

Cristino AS, Barchuk AR, Freitas FC, Narayanan RK, Biergans SD, Zhao Z, Simoes ZL, Reinhard J, Claudianos C (2014) Neuroligin-associated microRNA-932 targets actin and regulates memory in the honeybee. Nat Commun 5:5529. CrossRef Medline

Davis RL, Zhong Y (2017) The biology of forgetting: a perspective. Neuron 95:490–503. CrossRef Medline

de Belle JS, Heisenberg M (1994) Associative odor learning in *Drosophila* abolished by chemical ablation of mushroom bodies. Science 263:692–695. CrossRef Medline

Dewar MT, Cowan N, Sala SD (2007) Forgetting due to retroactive interference: a fusion of Müller and Pilzecker's (1900) early insights into everyday forgetting and recent research on anterograde amnesia. Cortex 43:616–634. CrossRef Medline

Dubnau J, Chiang AS, Grady L, Barditch J, Gossweiler S, McNeil J, Smith P, Buldoc F, Scott R, Certa U, Broger C, Tully T (2003) The staufen/pumilio pathway is involved in *Drosophila* long-term memory. Curr Biol 13:286–296. CrossRef Medline

Englund C, Lorén CE, Grabbe C, Varshney GK, Deleuil F, Hallberg B, Palmer RH (2003) Jeb signals through the alk receptor tyrosine kinase to drive visceral muscle fusion. Nature 425:512–516. CrossRef Medline

Gai Y, Liu Z, Cervantes-Sandoval I, Davis RL (2016) *Drosophila* SLC22A transporter is a memory suppressor gene that influences cholinergic neurotransmission to the mushroom bodies. Neuron 90:581–595. CrossRef Medline

Galkin AV, Melnick JS, Kim S, Hood TL, Li N, Li L, Xia G, Steensma R, Chopiuk G, Jiang J, Wan Y, Ding P, Liu Y, Sun F, Schultz PG, Gray NS, Warmuth M (2007) Identification of NVP-TAE684, a potent, selective, and efficacious inhibitor of NPM-ALK. Proc Natl Acad Sci U S A 104:270–275. CrossRef Medline

Gouzi JY, Moressis A, Walker JA, Apostolopoulou AA, Palmer RH, Bernards A, Skoulakis EM (2011) The receptor tyrosine kinase Alk controls neurofibromin functions in *Drosophila* growth and learning. PLoS Genet 7:e1002281. CrossRef Medline

Guan J, Umapathy G, Yamazaki Y, Wolfstetter G, Mendoza P, Pfeifer K, Mohammed A, Hugosson F, Zhang H, Hsu AW, Halenbeck R, Hallberg B, Palmer RH (2015) FAM150A and FAM150B are activating ligands for anaplastic lymphoma kinase. Elife 4:e09811. CrossRef Medline

Guven-Ozkan T, Davis RL (2014) Functional neuroanatomy of *Drosophila* olfactory memory formation. Learn Mem 21:519–526. CrossRef Medline

Guven-Ozkan T, Busto GU, Schutte SS, Cervantes-Sandoval I, O'Dowd DK, Davis RL (2016) MiR-980 is a memory suppressor MicroRNA that regulates the autism-susceptibility gene A2bp1. Cell Rep 14:1698–1709. CrossRef Medline

Hallberg B, Palmer RH (2013) Mechanistic insight into ALK receptor tyrosine kinase in human cancer biology. Nat Rev Cancer 13:685–700. CrossRef Medline

Isabel G, Pascual A, Preat T (2004) Exclusive consolidated memory phases in *Drosophila*. Science 304:1024–1027. CrossRef Medline

Joiner WJ, Crocker A, White BH, Sehgal A (2006) Sleep in *Drosophila* is regulated by adult mushroom bodies. Nature 441:757–760. CrossRef Medline

Keleman K, Krüttner S, Alenius M, Dickson BJ (2007) Function of the *Drosophila* CPEB protein Orb2 in long-term courtship memory. Nat Neurosci 10:1587–1593. CrossRef Medline

King I, Tsai LT, Pflanz R, Voigt A, Lee S, Jäckle H, Lu B, Heberlein U (2011) *Drosophila* tao controls mushroom body development and ethanol-stimulated behavior through par-1. J Neurosci 31:1139–1148. CrossRef Medline

Knapek S, Sigrist S, Tanimoto H (2011) Bruchpilot, a synaptic active zone protein for anesthesia-resistant memory. J Neurosci 31:3453–3458. CrossRef Medline

Lasek AW, Lim J, Kliethermes CL, Berger KH, Joslyn G, Brush G, Xue L, Robertson M, Moore MS, Vranizan K, Morris SW, Schuckit MA, White RL, Heberlein U (2011) An evolutionary conserved role for anaplastic lymphoma kinase in behavioral responses to ethanol. PLoS One 6:e22636. CrossRef Medline

Lee T, Luo L (1999) Mosaic analysis with a repressible cell marker for studies of gene function in neuronal morphogenesis. Neuron 22:451–461. CrossRef Medline

Lee YS, Silva AJ (2009) The molecular and cellular biology of enhanced cognition. Nat Rev Neurosci 10:126–140. CrossRef Medline

Leiss F, Groh C, Butcher NJ, Meinertzhagen IA, Tavosanis G (2009) Synaptic organization in the adult *Drosophila* mushroom body calyx. J Comp Neurol 517:808–824. CrossRef Medline

Lemmon MA, Schlessinger J (2010) Cell signaling by receptor tyrosine kinases. Cell 141:1117–1134. CrossRef Medline

Lewis BP, Burge CB, Bartel DP (2005) Conserved seed pairing, often flanked by adenosines, indicates that thousands of human genes are microRNA targets. Cell 120:15–20. CrossRef Medline

Li W, Cressy M, Qin H, Fulga T, Van Vactor D, Dubnau J (2013) MicroRNA-276a functions in ellipsoid body and mushroom body neurons for naive and conditioned olfactory avoidance in *Drosophila*. J Neurosci 33:5821–5833. CrossRef Medline

Liu X, Krause WC, Davis RL (2007) GABAA receptor RDL inhibits *Drosophila* olfactory associative learning. Neuron 56:1090–1102. CrossRef Medline

Lorén CE, Scully A, Grabbe C, Edeen PT, Thomas J, McKeown M, Hunter T, Palmer RH (2001) Identification and characterization of DAlk: a novel *Drosophila melanogaster* RTK which drives ERK activation in vivo. Genes Cells 6:531–544. CrossRef Medline

Lorén CE, Englund C, Grabbe C, Hallberg B, Hunter T, Palmer RH (2003) A crucial role for the anaplastic lymphoma kinase receptor tyrosine kinase in gut development in *Drosophila melanogaster*. EMBO Rep 4:781–786. CrossRef Medline

McGuire SE, Mao Z, Davis RL (2004) Spatiotemporal gene expression targeting with the TARGET and gene-switch systems in *Drosophila*. Sci STKE 2004:pl6. CrossRef Medline

Messaritou G, Leptourgidou F, Franco M, Skoulakis EM (2009) A third functional isoform enriched in mushroom body neurons is encoded by the *Drosophila 14-3-3ζ* gene. FEBS Lett 583:2934–2938. CrossRef Medline

Moog-Lutz C, Degoutin J, Gouzi JY, Frobert Y, Brunet-de Carvalho N, Bureau J, Créminon C, Vigny M (2005) Activation and inhibition of anaplastic lymphoma kinase receptor tyrosine kinase by monoclonal antibodies and absence of agonist activity of pleiotrophin. J Biol Chem 280:26039–26048. CrossRef Medline

Nagappan G, Lu B (2005) Activity-dependent modulation of the BDNF receptor TrkB: mechanisms and implications. Trends Neurosci 28:464–471. CrossRef Medline

Pavlopoulos E, Anezaki M, Skoulakis EM (2008) Neuralized is expressed in the alpha/beta lobes of adult *Drosophila* mushroom bodies and facilitates olfactory long-term memory formation. Proc Natl Acad Sci U S A 105: 14674–14679. CrossRef Medline

Paz I, Kosti I, Ares M Jr, Cline M, Mandel-Gutfreund Y (2014) RBPmap: a web server for mapping binding sites of RNA-binding proteins. Nucleic Acids Res 42:W361–W367. CrossRef Medline

Pitman JL, McGill JJ, Keegan KP, Allada R (2006) A dynamic role for the mushroom bodies in promoting sleep in *Drosophila*. Nature 441:753–756. CrossRef Medline

Plaçais PY, de Tredern É, Scheunemann L, Trannoy S, Goguel V, Han KA, Isabel G, Preat T (2017) Upregulated energy metabolism in the *Drosophila* mushroom body is the trigger for long-term memory. Nat Commun 8:15510. CrossRef Medline

Reshetnyak AV, Murray PB, Shi X, Mo ES, Mohanty J, Tome F, Bai H, Gunel M, Lax I, Schlessinger J (2015) Augmentor α and β (FAM150) are ligands of the receptor tyrosine kinases ALK and LTK: hierarchy and specificity of ligand-receptor interactions. Proc Natl Acad Sci U S A 112: 15862–15867. CrossRef Medline

Shuai Y, Lu B, Hu Y, Wang L, Sun K, Zhong Y (2010) Forgetting is regulated through rac activity in *Drosophila*. Cell 140:579–589. CrossRef Medline

Steward O, Schuman EM (2001) Protein synthesis at synaptic sites on dendrites. Annu Rev Neurosci 24:299–325. CrossRef Medline

Tully T, Preat T, Boynton SC, Del Vecchio M (1994) Genetic dissection of consolidated memory in *Drosophila*. Cell 79:35–47. CrossRef Medline

Walkinshaw E, Gai Y, Farkas C, Richter D, Nicholas E, Keleman K, Davis RL (2015) Identification of genes that promote or inhibit olfactory memory formation in *Drosophila*. Genetics 199:1173–1182. CrossRef Medline

Weiss JB, Xue C, Benice T, Xue L, Morris SW, Raber J (2012) Anaplastic lymphoma kinase and leukocyte tyrosine kinase: functions and genetic interactions in learning, memory and adult neurogenesis. Pharmacol Biochem Behav 100:566–574. CrossRef Medline

Wixted JT (2004) The psychology and neuroscience of forgetting. Annu Rev Psychol 55:235–269. CrossRef Medline

Yu D, Akalal DB, Davis RL (2006) *Drosophila* α/β mushroom body neurons form a branch-specific, long-term cellular memory trace after spaced olfactory conditioning. Neuron 52:845–855. CrossRef Medline